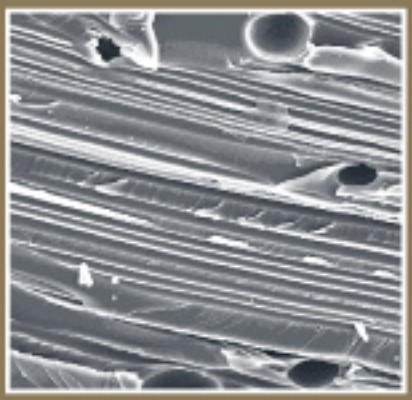
WOODHEAD PUBLISHING IN MATERIALS



Durability of composites for civil structural applications

Edited by Vistasp M. Karbhari

CRC

WP

Durability of composites for civil structural applications

Related titles:

Corrosion of reinforcement in concrete: Monitoring, prevention and rehabilitation techniques (EFC 38)
(ISBN 978-1-84569-210-0)
Corrosion of metal within reinforced concrete is one of the most important problems facing the construction industry. Key research on this topic is summarised in this latest volume of 24 chapters from the prestigious European Federation of Corrosion. The book begins by reviewing findings from various experiments designed to test the corrosion rate of metals induced by a range of factors. Later chapters discuss techniques for monitoring and testing for corrosion. Important methods of prevention, including inhibitors and protective coatings are evaluated. The book concludes with the discussion of electrochemical methods for protection and rehabilitation procedures for susceptible structures.

Composites forming technologies
(ISBN 978-1-84569-033-5)
When forming composite materials with textiles there is always a degree of error when draping a fabric over the mould and adding the resin. The fabric can deform or shift in the mould before the resin is added or whilst it is being poured in. Such problems can cause weaknesses in the composite leading to failure or even rendering the composite useless. In order to counteract this it is necessary to be able to model the draping of different textiles to fully understand the issues that may arise and how to prevent them from occurring in the future. *Composites forming technologies* brings together the research of leading experts in the area to give a comprehensive understanding of modelling and simulation within composites forming and design.

Durability of concrete and cement composites
(ISBN 978-1-85573-940-6)
Concrete and other cement-based composites are by far the most widely used man-made construction materials in the world. However, major problems of infrastructure deterioration have been caused by unanticipated premature degradation of these materials. This book provides an up-to-date review of several of the main forms of degradation, examining what is known about their causes and control. Trends in modelling and prediction of service-life are also examined.

Details of these and other Woodhead Publishing materials books, as well as materials books from Maney Publishing, can be obtained by:

- visiting www.woodheadpublishing.com
- contacting Customer Services (e-mail: sales@woodhead-publishing.com; fax: +44 (0) 1223 893694; tel.: +44 (0) 1223 891358 ext. 130; address: Woodhead Publishing Ltd, Abington Hall, Abington, Cambridge CB21 6AH, England)

Maney currently publishes 16 peer-reviewed materials science and engineering journals. For further information visit www.maney.co.uk/journals.

Durability of composites for civil structural applications

Edited by
Vistasp M. Karbhari

Woodhead Publishing and Maney Publishing
on behalf of
The Institute of Materials, Minerals & Mining

CRC Press
Boca Raton Boston New York Washington, DC

WOODHEAD PUBLISHING LIMITED
Cambridge England

Woodhead Publishing Limited and Maney Publishing Limited on behalf of
The Institute of Materials, Minerals & Mining

Published by Woodhead Publishing Limited, Abington Hall, Abington
Cambridge CB21 6AH, England
www.woodheadpublishing.com

Published in North America by CRC Press LLC, 6000 Broken Sound Parkway, NW,
Suite 300, Boca Raton, FL 33487, USA

First published 2007 by Woodhead Publishing Limited and CRC Press LLC
© 2007, Woodhead Publishing Limited
The authors have asserted their moral rights.

This book contains information obtained from authentic and highly regarded sources. Reprinted material is quoted with permission, and sources are indicated. Reasonable efforts have been made to publish reliable data and information, but the authors and the publishers cannot assume responsibility for the validity of all materials. Neither the authors nor the publishers, nor anyone else associated with this publication, shall be liable for any loss, damage or liability directly or indirectly caused or alleged to be caused by this book.

Neither this book nor any part may be reproduced or transmitted in any form or by any means, electronic or mechanical, including photocopying, microfilming and recording, or by any information storage or retrieval system, without permission in writing from Woodhead Publishing Limited.

The consent of Woodhead Publishing Limited does not extend to copying for general distribution, for promotion, for creating new works, or for resale. Specific permission must be obtained in writing from Woodhead Publishing Limited for such copying.

Trademark notice: Product or corporate names may be trademarks or registered trademarks, and are used only for identification and explanation, without intent to infringe.

British Library Cataloguing in Publication Data
A catalogue record for this book is available from the British Library.

Library of Congress Cataloging in Publication Data
A catalog record for this book is available from the Library of Congress.

Woodhead Publishing ISBN 978-1-84569-035-9 (book)
Woodhead Publishing ISBN 978-1-84569-356-5 (e-book)
CRC Press ISBN 978-0-8493-9109-5
CRC Press order number: WP9109

The publishers' policy is to use permanent paper from mills that operate a sustainable forestry policy, and which has been manufactured from pulp which is processed using acid-free and elementary chlorine-free practices. Furthermore, the publishers ensure that the text paper and cover board used have met acceptable environmental accreditation standards.

Typeset by Replika Press Pvt Ltd, India
Printed by TJ International Limited, Padstow, Cornwall, England

Contents

Contributor contact details *xi*

1 Introduction: the use of composites in civil structural applications 1

V. M. Karbhari, University of California San Diego, USA

1.1 Introduction 1
1.2 Application in civil infrastructure 2
1.3 Durability 3
1.4 Myths and mysteries 5
1.5 References 10

Part I Aspects of composite durability

2 Fabrication, quality and service-life issues for composites in civil engineering 13

V. M. Karbhari, University of California San Diego, USA

2.1 Introduction 13
2.2 Fabrication processes 16
2.3 Quality control during manufacture 25
2.4 Exposure environments 26
2.5 References 29

3 Durability of composites in aqueous environments 31

C. Helbling and V. M. Karbhari, University of California San Diego, USA

3.1 Introduction 31
3.2 Influence of moisture at the constituent level 32
3.3 Mass uptake profiles 41
3.4 Effect of moisture on mechanical and physical properties 50
3.5 Synergistic effects of stress and hygrothermal exposure 58
3.6 Summary and conclusions 66
3.7 References 66

4 Durability of composites in sub-zero and freeze–thaw conditions 72

V. M. Karbhari, University of California San Diego, USA

4.1 Introduction 72
4.2 Overall effects 72
4.3 Consideration of hygrothermal effects 75
4.4 References 77

5 Durability of composites exposed to ultraviolet radiation 80

J. W. Chin, National Institute of Standards and Technology (NIST), USA

5.1 Introduction 80
5.2 Ultraviolet radiation effects on polymers 80
5.3 Ultraviolet radiation effects on fibre-reinforced polymer composites 83
5.4 Testing methodologies 89
5.5 Mitigation strategies 92
5.6 References 94

6 Durability of composites exposed to elevated temperature and fire 98

A. P. Mouritz, Royal Melbourne Institute of Technology, Australia

6.1 Introduction 98
6.2 Combustion of polymer composites 99
6.3 Fire reaction properties of polymer composites 102
6.4 Fire-resistant polymer composites 111
6.5 Structural properties of polymer composites in fire 115
6.6 Fire protection coatings for polymer composites 118
6.7 Fire safety regulations 119
6.8 Future fire-resistant composite materials 120
6.9 Acknowledgements 121
6.10 References 121

7 Durability of composites under fatigue loads 126

A. Zhou, N. Post, R. Pingry, J. Cain, J. J. Lesko and S. W. Case, Virginia Polytechnic Institute and State University, USA

7.1 Introduction 126
7.2 Fatigue behavior of civil engineering composites 127
7.3 Predictive/descriptive modeling of fatigue 136
7.4 Reliability-based design for fatigue 142
7.5 Conclusions 146
7.6 References 147

8 Creep and time-dependent response of composites 150
L. S. Lee, Louisiana Tech University, USA
8.1 Introduction 150
8.2 Creep and relaxation 152
8.3 Modelling long-term behaviour 155
8.4 Accelerated aging 158
8.5 Synergistic effects on the time-dependent response 160
8.6 Effects at the structural level 163
8.7 Future trends 167
8.8 References 168

9 Durability of composites in relation to wear and erosion 170
A. P. Mouritz, Royal Melbourne Institute of Technology, Australia
9.1 Introduction 170
9.2 Gouging and abrasion wear 172
9.3 Erosive wear 180
9.4 Conclusions and future trends 183
9.5 References 185

Part II Applications and monitoring of composites in civil engineering

10 Fibre-reinforced polymer composite structures and structural components: current applications and durability issues 189
L.C. Hollaway, University of Surrey, UK
10.1 Introduction 189
10.2 'All-composite' structures 192
10.3 'All-composite' bridges 196
10.4 External strengthening 199
10.5 Seismic retrofit 204
10.6 Tendons 206
10.7 Rebars – exposure to concrete environments 208
10.8 Bridge decks 212
10.9 Girders and profiles 217
10.10 Observations 220
10.11 Acknowledgements 222
10.12 References 222

11 Reinforcement of concrete using fiber-reinforced polymer composites 225

B. Benmokrane, M. Robert and T. Youssef, University of Sherbrooke, Canada

11.1 Introduction 225
11.2 Durability concerns 226
11.3 Principal environments affecting fiber-reinforced polymer internal reinforcement durability 227
11.4 Design and application recommendations 240
11.5 Conclusions and future trends 241
11.6 References 242

12 Durability of external fiber-reinforced polymer strengthening systems 247

J. J. Myers, University of Missouri-Rolla, USA

12.1 Introduction 247
12.2 Definition and types of environments 248
12.3 Retrofit and external strengthening of flexural members 248
12.4 Seismic retrofit and external strengthening of columns 256
12.5 Design and use recommendations 259
12.6 Future trends and research needs for the durability of external fiber-reinforced polymer strengthening systems 274
12.7 Sources of further information and advice 276
12.8 References 279

13 Rehabilitation of concrete structures using fibre-reinforced polymer composites: identifying potential defects 284

H. Kaiser and V. M. Karbhari, University of California San Diego, USA; and C. Sikorsky, California Department of Transportation, USA

13.1 Introduction 284
13.2 Defects in composite materials 286
13.3 Defects occurring during rehabilitation 289
13.4 Effect of defects 299
13.5 Use of non-destructive evaluation/non-destructive testing 302
13.6 Future trends 321
13.7 References 322

14 Structural health monitoring and field evaluation of composite durability 324

A. A. Mufti, University of Manitoba, Canada; and L. A. Bisby, Queen's University, Canada

14.1 Introduction 324
14.2 The need for structural health monitoring 326
14.3 Civionics 328
14.4 Field applications and service-life determination 331
14.5 Future trends 350
14.6 Sources of further information and advice 351
14.7 References 351

Index 355

x

Contributor contact details

(* = main contact)

Editor

and Chapters 1, 2 and 4 (author); Chapters 3 and 13 (co-author)

Professor Vistasp M. Karbhari
University of California San Diego
Department of Structural Engineering
Jacobs School of Engineering
University of California, San Diego
9500 Gilman Drive
MC 0085
La Jolla
CA 92093-0085
USA

E-mail: vkarbhari@ucsd.edu

Chapter 3

C. Helbling and V. M. Karbhari*
University of California San Diego
Department of Structural Engineering
Jacobs School of Engineering
University of California, San Diego
9500 Gilman Drive
MC 0085
La Jolla
CA 92093-0085
USA

E-mail: vkarbhari@ucsd.edu

Chapter 5

J. W. Chin
National Institute of Standards and Technology (NIST)
Materials and Construction Research Division
Polymeric Materials Group
100 Bureau Drive, Stop 8615
Building 226, Room B350
Gaithersburg
MD 20899
USA

E-mail: joannie.chin@nist.gov

Chapter 6

A. P. Mouritz
Sir Lawrence Wackett Centre for Aerospace Design Technology
School of Aerospace, Mechanical and Manufacturing Engineering
Royal Melbourne Institute of Technology
GPO Box 2476V
Melbourne
Victoria 3001
Australia

E-mail: adrian.mouritz@rmit.edu.au

Chapter 7

A. Zhou*
Assistant Professor
Department of Engineering Technology
William States Lee College of Engineering
University of North Carolina at Charlotte
9201 University City Boulevard
Charlotte, NC 28223-0001
USA

E-mail: azhou3@uncc.edu

N. Post, R. Pingry, J. Cain, J. J. Lesko and S. W. Case
120D Patton Hall, MC-0219
Department of Engineering Science and Mechanics
Virginia Polytechnic Institute and State University
Blacksburg
VA 24061-0219
USA

Chapter 8

L. S. Lee
Louisiana Tech University
College of Engineering and Science
Bogard Hall 248
600 West Arizona
Ruston
LA 71272
USA

E-mail: lukelee@latech.edu

Chapter 9

A. P. Mouritz
Sir Lawrence Wackett Centre for Aerospace Design Technology
School of Aerospace, Mechanical and Manufacturing Engineering
Royal Melbourne Institute of Technology
GPO Box 2476V
Melbourne
Victoria 3001
Australia

E-mail: adrian.mouritz@rmit.edu.au

Chapter 10

L. C. Hollaway
School of Engineering
University of Surrey
Guildford
Surrey
GU2 7XH
UK

E-mail: l.hollaway@surrey.ac.uk

Chapter 11

B. Benmokrane*, M. Robert and T. Youssef
NSERC Research in Innovative FRP Composite Materials for Infrastructure
Department of Civil Engineering
University of Sherbrooke
Sherbrooke
Quebec
J1K 2R1
Canada

E-mail:
Brahim.Benmokrane@USherbrooke.ca

Chapter 12

J. J. Myers
Associate Professor
UMR-UTC Interim Director
Architectural Engineering Program Coordinator
University of Missouri-Rolla
325 Butler Carlton Hall
1870 Miner Circle
Rolla
MO 65409-0030
USA

E-mail: jmyers@umr.edu

Chapter 13

H. Kaiser and V. M. Karbhari*
University of California San Diego
Department of Structural Engineering
Jacobs School of Engineering
University of California, San Diego
9500 Gilman Drive
MC 0085
La Jolla
CA 92093-0085
USA

E-mail: vkarbhari@ucsd.edu

C. Sikorsky
California Department of Transportation
Engineering Services Center
1801 30th Street
MS 9
Sacramento
CA 95816
USA

Chapter 14

A. A. Mufti*
ISIS Canada Research Network
Agricultural and Civil Engineering Building
University of Manitoba
A250 – 96 Dafoe Road
Winnipeg
Manitoba
R3T 2N2
Canada

E-mail: muftia@cc.umanitoba.ca

L. A. Bisby
Department of Civil Engineering
99 University Avenue, Ellis Hall
Queen's University
Kingston
Ontario
K7L 3N6
Canada

E-mail: bisby@civil.queensu.ca

1

Introduction: the use of composites in civil structural applications

V. M. KARBHARI,
University of California San Diego, USA

1.1 Introduction

The infrastructure of constructed facilities for the transportation and housing of people, goods and services, which was largely expanded in the period between 1950 and the early 1970s, is now reaching a critical age with increasing signs of deterioration and reduced functionality. Deficiencies in the existing bridge inventory, for example, range from those related to wear, environmental deterioration and aging of structural components, to increased traffic demands and changing patterns; and from insufficient detailing at the time of construction/original design, to the use of substandard materials in initial construction, to inadequate maintenance and rehabilitation measures taken through the life of the structure. These deficiencies are not limited to bridge and other transportation-related structures alone, but are endemic to the built environment, ranging from residential housing and industrial/commercial structures to pipelines used for the distribution of water and sewage. This deterioration and the inability to provide the required services have a tremendous impact on society in terms of socio-economic losses resulting from delays, accidents and irregularity in supply.

Conventional materials such as steel, concrete and wood have a number of advantages, not least of which is the relatively low cost of materials and construction. However, it is clear that conventional materials and technologies, although suitable in many cases and with a history of good applicability, lack longevity in some cases, and in others are susceptible to rapid deterioration, emphasizing the need for better grades of these materials or newer technologies to supplement those used conventionally. It should also be noted that in a number of cases design alternatives are constrained by the current limitations of the materials used, e.g. the length of the clear span of a bridge due to weight constraints, or the size of a column due to restrictions on design and minimum dimensions needed. Similarly, the use of conventional materials is often either not possible in cases of retrofit, or may be deemed ineffective in terms of functionality. In other cases, constraints such as dead load restrict

the widening of current structures or the carriage of higher amounts of traffic over existing lifelines. In all such (and other) cases, there is a critical need for the use of new and emerging materials and technologies, with the end goal of facilitating functionality and efficiency.

1.2 Application in civil infrastructure

Since the beginning of mankind, the human race has attempted to create new materials with enhanced properties for the construction of structural systems. The use of combinations of materials to provide both ease of use and enhanced performance – as in the application of straw reinforcement in mud by the ancient Israelites (800 BC), or in the combination of different orientations of veneer to form plywood – has a long history. The concept of combining materials to create a new system having some of the advantages of each of the constituents can be seen in reinforced concrete. The use of fiber-reinforced polymer (FRP) composites takes this one step further enabling the synergistic combination of reinforcing fibers, with appropriate fillers/additives, in a polymeric resin matrix. The fibrous reinforcement carries load in predetermined directions (indicated by fiber orientation) and the polymer acts as a medium to transfer stresses between adjoining fibers through adhesion, and also provides toughness and protection for the material. The combination of the matrix phase with the fiber reinforcement thus creates a new material that is conceptually analogous to steel rebar-reinforced concrete although the reinforcing fractions vary considerably (i.e. reinforced concrete in general rarely contains more than 5% reinforcement, whereas in FRP composites the reinforcing volume fraction can range from 25 to 70% depending on the process used); the matrix has both tensile and compression capabilities (unlike cement which is strong only in compression) and, unlike concrete, polymeric resins used in the civil infrastructure area impart a high degree of toughness and damage tolerance as well. These materials provide the designer with a wide palette of materials choices to fit the specific requirements of the structure and show immense potential for adding to the current palette of materials being used in civil infrastructure.

The attractiveness of FRP composites as construction materials derives from a set of advantages that include: high specific stiffness and specific strength characteristics; low weight, corrosion resistance and potentially high durability; the mechanical properties can be tailored using characteristics of anisotropic materials; the ability to have low conductivity and to act as an insulator (in the case of glass fiber-reinforced composites), and to be electromagnetically transparent. In addition the wide variety of manufacturing processes available enables these materials to be fabricated both in the field under highly uncontrolled environments (such as in the case of wet layup used in external strengthening applications) and to very precise dimensional

tolerances under highly controlled factory conditions (such as in the case of autoclave-cured composites).

The ease of application of FRP composites makes them extremely attractive for use in civil infrastructure applications, especially in cases where dead weight, space or time restrictions exist. Although FRP composites can have strength levels significantly higher than those of steel, and can be formed of constituents such as carbon fibers that have moduli equal to, or greater than, the modulus of steel, it is important to note that the limit of use is often dictated by strain limitations. FRP composites in general behave in a linear elastic fashion to failure, without any significant yielding or plastic deformation-induced ductility as seen in steel or reinforced concrete. In addition, it should be noted that unlike reinforcing steel, some fibers, such as carbon fibers, are anisotropic, having different properties in the longitudinal (i.e. along the length of the fiber) and transverse directions. For example, although the tensile modulus for T300 carbon fibers in the longitudinal direction is 230 GPa, in the transverse direction it is only about 40 GPa, a fact that must be considered when designing with fibers or fabrics that have to conform to tight radii and corners. In the case of aramid fibers, the fiber structure itself tends to fibrillate on the compression side, again emphasizing the need for special consideration in design. This anisotropy is also apparent in relation to the different coefficients of thermal expansion in the longitudinal and transverse directions.

1.3 Durability

FRP composites are increasingly being used in civil infrastructure in a range of applications such as: reinforcing rods and tendons; wraps for seismic retrofit of columns; externally bonded reinforcement for strengthening of walls, beams and slabs; composite bridge decks; and even hybrid (FRP composite in combination with conventional materials) and all-composite structural systems. Since FRP composites are still relatively unknown to the practicing civil engineer and infrastructure systems planner, there are heightened concerns related to the overall durability of these materials, especially as related to their capacity for sustained performance under harsh and changing environmental conditions under load.

Although FRP composites have been successfully used in the industrial, automotive, marine and aerospace sectors, there are critical differences in loading, environment and even the types of materials and processes used in these applications as compared with the materials–process–load combinations likely to be used in civil infrastructure. These materials also have a fairly successful record of use in pipelines, underground storage tanks, building facades and architectural components. Anecdotal evidence provides substantial reason to believe that if appropriately designed and fabricated, these systems

can provide longer lifetimes and lower maintenance costs than equivalent structures fabricated from conventional materials. However, actual data on durability are sparse, not well documented, and in cases where they are available – they are not easily accessible to the civil engineer.[1]

This lack of data and the need for a high level of safety have, in the past, lead to the use of high factors of safety in design such as 4–6 in the marine industry and as high as 8–10 (as prescribed in BS 4994[2]) and 10–12 (in ASME-RTP-1[3]) in the area of tanks and pipes. In addition, there is a wealth of contradictory data published in a variety of sources that tends to confuse the practicing engineer. The reasons for the apparent contradictions on durability are related to the reporting of data without sufficient detail of the actual materials used, the use of different forms of materials and processing techniques, and even changes in the materials systems with time (especially as related to resin formulations that are specified only by generic names). A recent 'gap analysis' conducted under the aegis of the Civil Engineering Research Foundation, the Federal Highway Administration and the Market Development Alliance pinpointed critical gaps in durability data that needed to be filled and recommended a three-part strategy for addressing the overall consideration of durability of FRP composites for use in civil infrastructure.[1]

The determination of the long-term durability of FRP composites used in civil infrastructure, and the development of a methodology that is capable of addressing the intricacies of this material in an environment that is not always well defined, are critical to the further use and widespread acceptance of FRP composites in civil infrastructure. In addition, because of the relative immaturity of the methodologies used for rehabilitation and of the specific materials and forms being used, there is a need for the development and implementation of efficient and relatively easy non-destructive health evaluation tools that can assist in systems identification and monitoring of the structures over extended periods of time. This will not only provide a greater degree of comfort to the users/owners of bridge systems but will also provide useful information on the integrity and durability of the rehabilitated component/system in the field over the period of time under consideration, thereby providing useful data to the designer for the selection of materials allowables and pertinent factors for design.

This book provides a basic introduction to aspects of durability pertaining to the use of FRP materials in civil infrastructure. It should be noted that although the term 'durability' is widely used, its meaning and implications are often ambiguous. Often it is erroneously taken to refer only to the weathering/degradation of a material, whereas in reality this is only a small aspect of the overall phenomenon. FRP composites (and their constituents) can be affected by a variety of factors (including those related to the natural and surrounding environment), and the actual effect of each of these factors, or combinations thereof, can be substantially affected by the presence or

absence of defects or other damage to the composite (or constituents thereof). A variety of different constituent materials are commercially available and the appropriate combination of these constituents allows for the development of an FRP composite system that provides the performance attributes for its intended use. In order to ensure that the term and its implications are completely understood it is important to realize that the durability of a material or structure should be defined as its 'ability to resist cracking, oxidation, chemical degradation, delamination, wear and/or the effects of foreign object damage for a specified period of time, under the appropriate load conditions, under specified environmental conditions'. The use of durability data in design can efficiently be realized not merely through the determination of factors of safety (which could in many cases be actually called factors of ignorance) but through the application of sound design principles and the implementation of damage tolerance whereby levels of performance can be guaranteed through relationships between performance levels and damage/degradation accrued over specified periods of time. In this sense, damage tolerance is defined as 'the ability of a material or structure to resist failure and continue performing at prescribed levels of performance in the presence of flaws, cracks or other forms of damage/degradation for a specified period of time under specified environmental conditions'.

1.4 Myths and mysteries

In considering the use of FRP materials in civil infrastructure it is important to point out, at the outset, that there are a number of myths regarding FRP composites, chief among which are that:

- composites are a panacea for the deterioration of civil infrastructure;
- composites do not degrade and are not affected by environmental influences;
- the performance attributes of FRP composites used in civil infrastructure, at present, are comparable with those of aerospace-grade, prepreg-based autoclave-cured composites;
- due to stress-rupture considerations glass fiber-reinforced composites should only be used in architectural applications;
- carbon fiber-reinforced composites are not degradable and have infinite life;
- all composites have well-documented databases;
- variations in field conditions, incoming raw materials or manufacturing processes do not cause any changes in properties and performance.

Rather than being a panacea for the existing issues related to the deterioration of conventional materials used in civil infrastructure, FRP composites do provide alternatives for rehabilitation and renewal not possible with

conventional materials. However, these materials can degrade at the level of the fiber, polymer and/or interface under specific circumstances. It must be remembered that the resin matrix allows moisture adsorption and this can lead to a variety of mechanisms, some of which result in deterioration of the polymer and, in some cases, the reinforcing fiber. Although glass fiber-reinforced composites are susceptible to creep- and stress-rupture, in general their use under sustained loads is possible as long as the stress levels do not exceed 25–30% of the ultimate. This has been shown to advantage in the resiliency of glass fiber-reinforced pipes and underground storage tanks which have withstood very aggressive environments through the use of appropriate factors of safety.[4] Although carbon fibers are generally considered to be inert to most environmental influences likely to be faced in civil infrastructure applications, the inertness does not apply to the fiber–matrix bond and the matrix itself, both of which can in fact be significantly deteriorated by environmental exposure. As emphasized in a recent study[1] significant gaps exist in the durability database for FRP composites used in civil infrastructure, even for environmental conditions such as moisture and alkalinity, due to reasons ranging from an actual lack of data on specific systems to difficulty in accessing data from investigations conducted in industry and government laboratories.

Furthermore, it is important to understand that since FRP composites are formed through the combination of micron-sized fibers in polymer matrices the actual performance and longevity of the material is intrinsically controlled by the microstructure, which is in turn controlled by the choice of constituent materials and form, interphase development and the processing route taken. Minor changes in any of these aspects can result in significant changes, not just in short-term performance but also in the overall durability of the FRP composite, which depends on factors such as bonding, void content, degree of cure and level of process-induced residual stresses.

Results from the aerospace industry are often used to argue that if FRP composites are accepted for use in such high-precision applications with very low tolerance for failure, then their use in civil infrastructure (often considered ‘low-tech’ in comparison) should pose absolutely no problem. It should, however, be remembered that the use of FRP composites in aerospace applications has been based on extensive materials testing for the purposes of qualification followed by strict adherence to prescribed specifications for autoclave-based fabrication in highly controlled factory environments. These materials and processes are unlikely to find significant application in civil infrastructure due to cost and processing-specific aspects. Civil applications are more likely to: (a) use processes such as wet layup, pultrusion and resin infusion than autoclave molding; (b) use fiber and resin as separate constituents rather than in the form of preimpregnated material; and (c) use resin systems such as polyesters, vinylesters, phenolics and lower temperature cure epoxies

rather than the higher temperature curable epoxies and thermoplastics. Furthermore, in cases of rehabilitation, there is likely to be extensive use of processes under ambient conditions in the field, rather than fabrication in factory-controlled environments. Even in the case of prefabricated elements, adhesive bonding to substrates has to be conducted under field conditions with little control, if any, of humidity and/or temperature. Thus, the civil engineering environment not only brings with it new challenges for the control of quality and uniformity of FRP composites, but also makes it difficult (if not impossible) to use the well-established databases generated by DoD (Department of Defense)-sponsored research (such as those for commonly used carbon/epoxy systems designated as AS4/3501-6 or T300/5208) for more than comparative baseline and trend analysis purposes. Furthermore, aerospace-grade FRP composites are to a large degree extensively inspected at routine intervals within carefully controlled environments, whereas inspection and maintenance requirements in civil infrastructure are neither as regulated nor as thorough.

Despite the significant changes in material specifications and process methods, FRP composites have been shown to have very good long-term response when used in applications such as underground storage tanks, pressure vessels and corrosion-resistant equipment. In addition, their successful use in marine vessels over extended periods of time has been extensively documented. Yet, data from laboratory studies consistently shows significant levels of degradation in the same classes of materials when subjected to moisture/humidity, temperature and stress. The mystery of the apparent dichotomy between 'real-world' applications and laboratory data, which is often forgotten in discussions related to the use of FRP composites in civil infrastructure, can be explained in terms of the use of appropriate 'knock-down' or safety factors.

Within the aerospace industry, FRP composite materials usage is typically predicated through the establishment of design allowables through extensive programs of specification and qualification. This ensures that failure does not take place in unexpected periods of time and enables the use of a damage tolerance philosophy. The most commonly used basis levels are the A-basis and the B-basis, and in order to obtain a reasonable evaluation of materials variability, the determination of these values is based on a minimum of 30 specimens from at least 5 batches of a material per environmental condition and direction. In some rare cases, S-basis allowables may be used wherein a minimum expected value is specified. Whereas the method for the establishment of the A- and B-basis values provides a very good method for the selection of materials allowables, it must be noted that qualification programs are extremely expensive and are based on the use of a limited number of materials, in carefully monitored applications wherein cost concerns (as related to qualification) are not the primary drivers. Furthermore, due to the levels of

safety factors used in the aerospace world (which can approach 1 in some cases, such as fairings) there is a need for a very high level of specification, qualification and testing. Although very rigorous, the method does not allow for ease of replacement of material constituents, and even minor modifications to qualified material systems can only be made after extensive testing.

Since FRP composites for most layups show linear-elastic response to failure, and in the case of carbon fiber reinforcements not only have fairly low strain levels (9000–10 000 microstrain) but are also very sensitive to defects, strain is often used as the controlling factor for determination of factors of safety rather than load or stress. For the case of a material with an ultimate strain of about 9500 microstrain (i.e. 0.95%), a level of 4500 microstrain is generally taken to be the design limit, with the drop from ultimate representing limitations for hole and defect tolerance. A factor of 1.5 when applied to the design ultimate would thus give a design allowable limit of 3000 microstrain with the factor of uncertainty representing load regime and path (as defined by layup and orientation).

Although FRP composites have been used extensively in naval and marine applications there is still a lack of design rules[5] and an incomplete understanding of the complex scaling laws for anisotropic materials; this results in the use of very conservative safety factors that are often far higher than those used in similar applications using metals.[6] For the most part their use is predicated through the adoption of a factor of safety of 4–6 for strength[7–9] based on the combined effects of stress-rupture and fatigue. It should be noted that although hulls face a greater degree of loading than a number of thin-skin FRP composite elements in other application areas, hulls in general are not subjected to sustained loading, but rather to impact and slamming loads of short and intermittent duration.[8] If the structure has to be designed to carry impact loads, safety factors of as high as 10 are often used.[10] In almost all cases, durability for long-term use is dependent on the use of an appropriate gel-coat without which there is a realistic fear of premature degradation through surface blistering which can lead to further deterioration and delamination of the FRP composites, especially those fabricated using orthophthalic polyesters.

FRP composites, primarily using glass fiber reinforcements, have a history of successful use in underground storage tanks, corrosion-resistant equipment and pressure vessels. Because of a high level of regulatory activity this area has, perhaps, the highest development of standards for design and use. The US standard – ASME RTP-1[3]– for reinforced thermoset plastic corrosion-resistant equipment, provides for the use of factors based on whether design is conducted through the application of rules (Subpart 3A) or through stress analysis (Subpart 3B). When design rules are used a design factor of 10 is specified for the determination of minimum thickness of shells subject to internal pressure, and a factor of 5 is specified for determination of minimum

moment of inertia for stiffening rings. In cases where design is carried out using specific methods of stress analysis, minimum strength ratios of between 8 and 10 are used for the inner surface and interior layer depending on the design method and type of non-destructive testing used.[3] For vessels designated for critical service the factor is required to be multiplied by 1.25. For all other layers in the laminate the minimum strength ratio is required to be 1.6 for vessels not in critical service and 2 for vessels in critical service. The British standard BS 4994, for the design and construction of vessels and tanks in reinforced plastics,[2] requires a minimum design factor of 8. It is noted that the Foreword to this standard explains that the factor was increased to 8 from the previous value of 6 specified in the 1973 edition 'because experience has shown that the overall strain limitation does not permit lower values than 8'. Under the provisions of the ASME Boiler and Pressure Vessel Code[11] two methods based on 'class' of design are allowable for qualification of design adequacy. Under Class-I design, which specifies qualification through pressure testing of a prototype, the minimum qualification pressure is set at 6 times the design pressure. The maximum design pressure is limited to: 1034 kPa (150 psi) for vessels fabricated using bag molding, centrifugal casting or contact molding; 10 342 kPa (1500 psi) for filament-wound vessels; and 20 685 kPa (3000 psi) for filament-wound vessels with polar boss openings. For the latter case a minimum factor of safety of 5 is allowable. Specific conditions are also set for cycling and temperature conditions. Under Class-II design, stress analysis is required using either specific design rules or discontinuity analysis. If the specified design rules are used the membrane strains are restricted to 0.001 and the thickness is required to exceed 6 mm (0.25 in) with a design factor of 5 applied to the modulus parameter. In the case of discontinuity analysis the minimum buckling pressure is required to be at least 5 times the design external pressure and the average shear stress between the vessel and overlays/joints is restricted to 1379 kPa (200 psi).

In all these examples it should be noted that stresses are kept to a very low level through the use of fairly high factors of safety. This results in large thicknesses for parts with significant tolerance for degradation and a very long period of time for moisture/solvent saturation or even through-thickness infiltration, ensuring that structures can be made such that durability is not a concern over the period of design service-life. However, in most cases this is through the use of excessive conservatism grounded in the lack of a comprehensive understanding of the deterioration science basis related to a specific material system and of the operative environment to be faced by that system through its intended service-life. Since civil infrastructure components and systems are extremely cost-sensitive, the use of excessive 'factors of ignorance' would be counter-productive to their widespread use and acceptance.

This book is intended to provide a basic understanding of durability as related to FRP materials used in civil infrastructure and is intended to bridge

the gap between the FRP specialist and the end user in the civil/construction area. Thus the chapters provide broad descriptions of mechanisms of deterioration such as through exposure to moisture, temperature excursions (including fire), ultraviolet radiation, fatigue, creep and wear. In addition, specific applications areas such as rebar and rehabilitation are addressed due to the increasing use of FRP materials in these areas. Since deterioration, and degradation, of materials and structures carries with it an inherently negative connotation, it is important to note that although the chapters highlight potential problems, rather than solutions, FRP composites have a history of long and successful use in other application areas. It is in this vein that a chapter on structural health monitoring has also been included in the book, since it is only through the monitoring of FRP components and systems used in civil infrastructure that the true longevity of this class of materials can be assessed.

1.5 References

1 Karbhari, V.M., Chin, J.W., Hunston, D., Benmokrane, B., Juska, T., Morgan, R., Lesko, J.J., Sorathia, U. and Reynaud (2003), 'Durability Gap Analysis for Fiber-Reinforced Polymer Composites in Civil Infrastructure,' *ASCE Journal of Composites in Construction*, **7**(3), 238–247.

2 BS 4994 (1987), Specification for Design and Construction of Vessels and Tanks in Reinforced Plastics, British Standards Institution, London.

3 ASME-RTP-1d-1998 (1998), Addenda to ASME-RTP-1-1995 edition, Reinforced Thermoset Plastic Corrosion Resistant Equipment, ASME, New York.

4 Karbhari, V.M. and Li, Y. (2001), 'Safety Factors and Materials Design Allowables for FRP Composites – Application to Civil Infrastructure,' Proceedings of the 33rd International SAMPE Technical Conference, Seattle WA, 4–8 November.

5 Mouritz, A.P., Gellert, E., Burchill, P. and Challis, K. (2001), 'Review of Advanced Composite Structures for Naval Ships and Vessels,' *Composite Structures*, **53**, 21–41.

6 Evans, T.W., Swann, R.F. and Troffer, M.A. (1991), 'The Submarine Perspective,' Proceedings of the National Conference on the Use of Composite Materials in Load-Bearing Marine Structures, Arlington, VA, 25–26 September, National Academy Press, Washington, DC, pp. 11–17.

7 Gibbs and Cox, Inc. (1960), *Marine Design Manual for Fiberglass Reinforced Plastics*, McGraw Hill, New York.

8 Puccini, G. (1993), 'Environmental aspects' in *Composite Materials in Maritime Structures*, Vol. 1, Eds R.A. Shenoi and J.F. Wellicome, pp. 44–85, Cambridge University Press, Cambridge, UK.

9 Cable, C.W. (1991), 'The Effect of Defects in Glass-Reinforced Plastics,' *Marine Technology*, **28**(2), 91.

10 Chalmers, D.W. (1988), 'The Properties and Uses of Marine Structural Materials,' *Marine Structures*, **1**, 47–70.

11 ASME Boiler and Pressure Vessel Code (2001), Section, X, Fibre-Reinforced Plastic Pressure Vessels, ASME, New York.

Part I

Aspects of composite durability

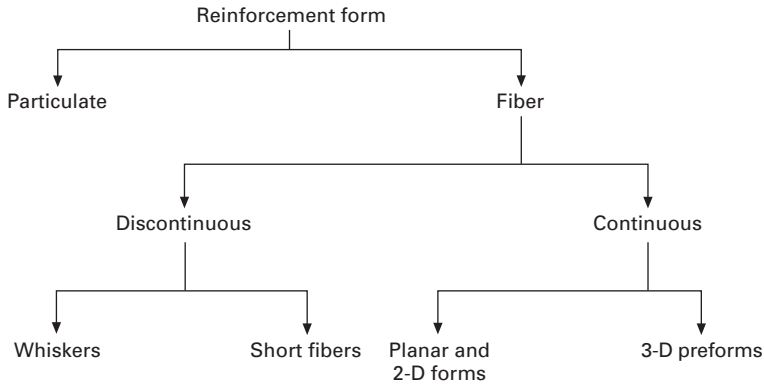
2

Fabrication, quality and service-life issues for composites in civil engineering

V. M. KARBHARI,
University of California San Diego, USA

2.1 Introduction

In the context of the present discussion, a composite material is defined as a macroscopic combination of two or more distinct materials having a finite interface between them. One of the constituents is the reinforcement, or reinforcing phase, while the other is the matrix phase. The major, or at least clearly apparent, difference between a material such as a plastic and a composite is thus that the composite consists of both reinforcement (fibers for example) and a matrix (which could be the polymer used to form the plastic itself). Composite materials are generically classified at two different levels. The first, and more generic, is related to the matrix phase. It is noted that the matrix serves a number of functions besides being the binder to hold the reinforcing phase together. It provides environmental and damage protection to the reinforcing phase, toughness and multi-functional non-mechanical properties to the composite and enables the material to be formed into shapes. The common types of composites are ceramic matrix composites (CMC), metal matrix composites (MMC) and polymer matrix composites (PMC). In the context of this book the latter class will be discussed and will be referred to as fiber-reinforced polymers (FRPs) following the commonly used terminology in civil construction. The second method of classification, shown schematically in Fig. 2.1, is based on the form of reinforcement used. For the reinforcing phase to provide a useful enhancement in the properties provided by the matrix phase alone a minimum fiber volume fraction, generally not lower than 10%, is required. This can, however, be in a variety of forms. Particulate reinforcements are those whose dimensions are all roughly equal. These are used for non-structural applications, and are often termed as 'fillers', such as for the enhancement of fire resistance, electro-magnetic shielding, thermal conductivity, fracture toughness, etc. In contrast, fiber reinforcement is a term used to denote a phase having one dimension substantially larger than the others. Discontinuous fiber reinforcements have low aspect ratios (ratio of length to diameter). Whiskers are extremely short, generally in the



2.1 Classification based on form of reinforcing phase.

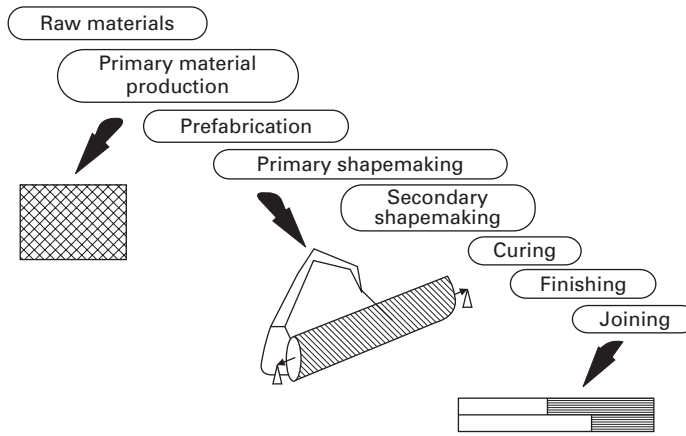
form of single crystals with almost no crystalline defects; their diameters usually fall in the range of 1–25 μm, and have aspect ratios less than 100. Short fibers are fibers with aspect ratios between 100 and 250 and are of the same material as used in continuous reinforcement. Continuous fiber-reinforced composites contain reinforcements having lengths much greater than their cross-sectional dimensions. Although the fiber length does not necessarily have to be comparable in dimension to the part being fabricated it is essential that the length is such that any further increase in length will not change properties such as modulus or strength. These reinforcements are usually used in the form of bundles called rovings and tows, and in the form of fabrics wherein a number of bundles are woven, knitted or braided in specific patterns. In some cases the reinforcement is specially formed using textile processes into a three-dimensional formwork. This allows the entire skeleton of reinforcement to be formed prior to the introduction of the resin and could be considered, albeit on a much smaller dimensional scale, as analogous to the steel reinforcement cages that are tied prior to pouring of concrete.

The ability to combine the phases macroscopically provides immense opportunities for the tailoring of materials. This in fact enables the true creation of 'materials by design' since properties and performance can be designed through selection and proportion of constituent materials, orientation of the reinforcing phase and layup of different layers in a laminated structure. Thus, depending on the set of requirements it is possible to create a range of materials from those that are homogeneous and isotropic to those that are heterogenous and anisotropic, as well as all combinations in between. A composite, if conceptualized in the correct fashion is a designer's dream, whereas in the hands of a novice it could well become a nightmare.

Results from the aerospace industry are often used to argue that if FRP composites could be accepted for use in such high-precision applications with very low tolerance for failure, then their use in civil infrastructure

(often considered 'low-tech' in comparison) should pose absolutely no problem. It should, however, be remembered that the use of FRP composites in aerospace applications has been predicated on extensive materials testing for the purposes of qualification followed by strict adherence to prescribed specifications for autoclave-based fabrication in highly controlled factory environments. These materials and processes are unlikely to find significant application in civil infrastructure due to cost and processing-specific aspects. Civil applications, currently, are more likely to: (a) use processes such as wet layup, pultrusion and resin infusion than autoclave molding; (b) use fiber and resin as separate constituents rather than in the form of preimpregnated material; (c) use resin systems such as polyesters, vinylesters, phenolics and lower temperature cure epoxies rather than the higher temperature curable epoxies and thermoplastics. Furthermore, in cases of rehabilitation, there is likely to be extensive use of processes under ambient conditions in the field, rather than fabrication in factory-controlled environments. Even in the case of prefabricated elements, adhesive bonding to substrates has to be conducted under field conditions with little control, if any, of humidity and/or temperature. Thus, the civil engineering environment not only brings with it new challenges for the control of quality and uniformity of FRP composites, but also makes it difficult (if not impossible) to use the well-established databases generated by DoD (Department of Defense)-sponsored research (such as those for commonly used carbon/epoxy systems designated as AS4/3501-6 or T300/5208) for more than comparative baseline and trend analysis purposes. Furthermore, aerospace-grade FRP composites are to a large degree extensively inspected at routine intervals within carefully controlled environments, whereas inspection and maintenance requirements in civil infrastructure are neither as regulated nor as thorough.

In considering the durability of FRP materials, manufacturing methods for composite structures need to be considered as important as aspects of materials selection, configuration design and development, since the successful integration of fibrous reinforcement and matrix materials to create a composite is largely dependent on the processing method used. This is especially true with thermoset resin-based composites where the material is itself formed at the same time as the structure. The selection of a manufacturing process is, in general, much more critical for composites than for most conventional engineering materials. This is because each process is limited in the shapes and microstructures that can be created, as well as in the material combinations that can be utilized. As with more traditional materials, manufacturing processes for composites consist of a series of steps or stages, as shown in Fig. 2.2. Within each step there are a number of choices, including in some cases the possibility of skipping a step. Obviously, process economics and reliability are tied to the number of steps needed within a process to move from the raw materials stage to the finished product.



2.2 The materials transformation process.

2.2 Fabrication processes

The successful integration of fibrous reinforcement and matrix materials to create a composite is largely dependent on the choice of processing method. There are a large number of processing methods available and each process has specific attributes. In general, the fabrication scheme for any composite structure can be outlined using eight generic steps as outlined below.

1. Design – stress and geometric envelope.
2. Materials selection.
3. Arrangement (orientation and configuration) of the reinforcment.
4. Assembly of the reinforcement and resin system.
5. Application of heat and pressure as appropriate to cure the composite.
6. Finishing processes.
7. Assembly.
8. Quality control and non-destructive inspection.

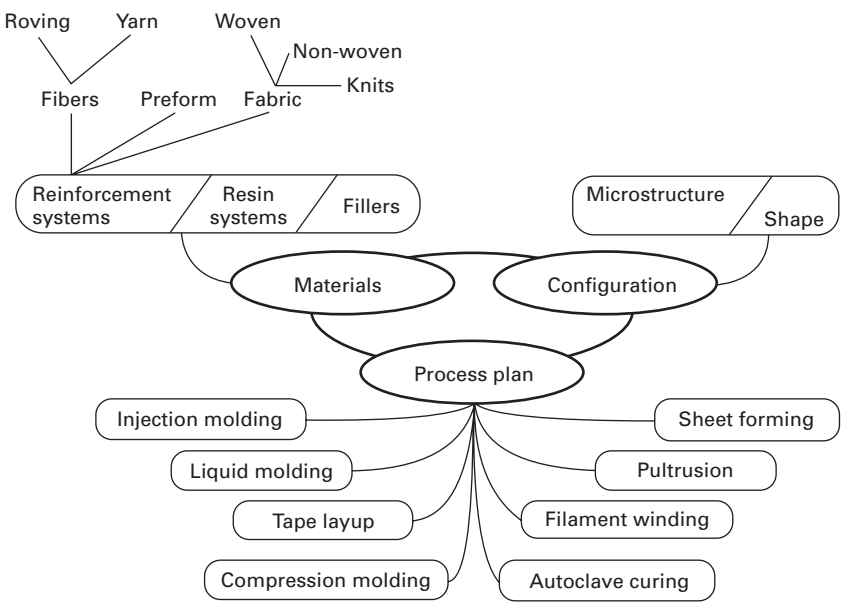
In an ideal scenario a process should be such that it has the attributes given below.

1. High productivity – i.e. short cycle times, low manpower requirements, low requirements for capital expenditure and minimum permanent use of space.
2. Minimal conversion cost – minimum cost spent on processing stages used to combine the fiber and matrix in order to form the composite.
3. Maximum tailorability – maximum ability to tailor the performance of the composite through materials and configurational choices.
4. Maximum geometrical flexibility – the ability to mold parts of varying dimensions and shapes with the ability to include cores, inserts, etc.

5. Minimal finishing – near-net-shape and net-shape processes are preferred since operations such as deflashing, trimming, etc. are reduced.
6. Quality control – each step in the process should be capable of being controlled on-line, without causing significant changes to the process.

The tailorability of composites for specific applications is one of the biggest advantages of the material, and simultaneously one of its most perplexing challenges. The wide choice of materials combinations, processing methods and shapes possible, presents bewildering problems of selection. In the isotropic world of traditional materials it was possible to use tables, charts and simple formulae to check the validity of a concept, thereby relegating the need for specialists to the final stage before prototyping. This is not possible in composites, where every decision made during the product development process is intricately linked to the three interacting decision areas of materials, configuration, and process plan (Fig. 2.3), with a decision to select one automatically resulting in a narrowing of choices for the other two (Wilkins and Karbhari, 1991).

Each of the elements in Fig. 2.3 presents a spectrum of choices. The configuration of a composite is unique in that it includes both shape and microstructure, either or both of which could be varied to attain a specific attribute. Unlike manufacturing methods for metals the processes related to the fabrication of composites have limitations based on shape, microstructure and materials. Theoretically, any combination of the three aspects should be



2.3 Interacting decision areas.

possible. Yet, the development is a complex process and requires the simultaneous consideration of parameters such as component geometry, production volume, reinforcement and matrix types and relative volumes, tooling requirements, and process and market economics.

In this section we briefly review aspects related to processes pertinent to the fabrication of components or systems related to civil infrastructure. Thus not all composite processing methods are covered, neither is this a comprehensive review of composite processing techniques.

2.2.1 Classification of methods

In general, processes can be divided into direct (i.e. those that utilize the reinforcement and resin directly without any preprocessing changes) and those that are indirect (i.e. those requiring that the reinforcing and matrix phases are first preprocessed into a form suitable for processing). The preparation of prepreg (preimpregnated material), injection molding pellets and sheet molding compound are examples of preprocessed material forms used in indirect methods. Table 2.1 provides a list of processes belonging to each group. Processes such as filament winding and pultrusion appear in both categories since they can be used with reinforcement both in the form of dry roving, tape or fabric (direct) or as prepreg (indirect). Although quality assurance is generally higher through the use of an indirect method the costs can be substantially higher with the resulting control on dimensions or other aspects sometimes being at a much higher level than routinely required in infrastructure rehabilitation.

2.2.2 Wet layup

Wet layup is probably the oldest and most commonly used composite process. Fabric is cut to the appropriate size and is placed on a mold layer by layer, resin being applied to each layer by pouring, brushing/rolling or spraying, prior to placement of the next layer. Entrapped air is removed from the fibrous assembly and resin impregnation of the reinforcement is achieved through the manual application of pressure using rollers/squeegees. The process

Table 2.1 Classification of processes

Direct methods	Indirect methods
Wet layup	Compression molding
Spray up	Pultrusion
Pultrusion	Autoclave molding of prepreg
Filament winding	Filament winding
Liquid molding	Injection molding

is extremely flexible and can be used over a wide range of sizes and shapes. Since tooling is generally simple and low cost, and there is no need for specialized equipment, capital costs are low. Foam cores, inserts and attachments can easily be built into the part. Often a vacuum bag is used to apply further pressure on the impregnated assembly leading to a higher level of fabric compaction with lower void content. A wide range of thermosets can be used in this process under both ambient and heated conditions with impregnation being more uniform and easier when the resin viscosity is low. Volume fractions achievable are based on the level of compaction achieved with levels just reaching 35% without the use of a vacuum bag and up to 55% being obtained with a vacuum bag under specific conditions. Although the manual nature of the process lends it flexibility, and to an extent lower cost, it also results in greater variability from part to part and even within the same part. The process is widely used to fabricate jackets/wraps directly onto columns for the purpose of seismic retrofit/strengthening (Fig. 2.4), and for placement of fabric strips onto concrete as a mode of external strengthening (Fig. 2.5).

2.2.3 Spray up

The spray up process is one in which resin and chopped fibers are applied simultaneously onto the mold surface. A specially designed spray head impels



2.4 Use of wet layup for installation of a fiber-reinforced polymer jacket for seismic retrofit of columns.



2.5 External bonding of fabric onto deck soffits for strengthening using wet layup.

catalyzed resin in a spray into which chopped fibers are introduced in lengths of 25–75 mm. The fibers are carried by the force of the spray onto the mandrel surface, to which pressure is applied through rollers and sometimes even a vacuum bag. The process enables greater flexibility of shape than wet layup and has a very high rate of production (up to 90.9 kg (2000 lbs) of material per hour) but limits reinforcement to random architectures only. As with the wet layup process ambient conditions are normally used although elevated temperatures can be used for cure and post-cure. In some cases, spray up is combined with the wet layup process to enable the use of fabric architectures as needed in conjunction with the lower cost and higher bulk of the random sprayed architecture. Fiber volume fractions are necessarily lower than those achieved by wet layup and there can be significant variation in content and even uniformity within the same part. Because the reinforcement is sprayed in the chopped form it is often difficult to maintain smooth and uniform surfaces and even appropriate levels of dimensional tolerance. Due to the random nature of the reinforcement the process does not provide reinforcement in an optimal orientation (hoop). However, the process is relatively cheap, easy to use and is analogous to shotcreting. It has found application both in the retrofit of columns where the demand is very small and for rehabilitation of slabs (Seim *et al.*, 2001; Ross *et al.*, 2004).

2.2.4 Injection molding

Injection molding is an automated process with very high versatility for production of large runs of relatively complex shapes with a high degree of dimensional accuracy. Although the process is commonly used with thermoplastic resins it can also be used with thermosets. Essentially, injection molding is a high-pressure process in which precompounded molding pellets,

consisting of short fibers and encapsulating resin, are fed through a hopper to a screw or ram device. This mechanism conveys the charge through the barrel while subjecting it to strong shearing action that results in a viscous homogeneous mix. The mix is then injected into the mold where it is allowed to cure. Since the mold is closed, complex-shaped parts can be fabricated very rapidly as long as flow of the filled resin can be achieved through the mold. Due to surface effects, fibers next to the mold surface have a preferential alignment parallel to the surface, whereas the orientation away from the surface is random, giving rise to a skin–core morphology. Fiber loadings are generally fairly low and parts are usually for non-structural or secondary structural applications. A number of ancillary structures such as rails, barriers and fittings are routinely made using injection molding.

2.2.5 Compression molding

Compression molding is a widely used process in the industrial and automotive sectors. Essentially the process consists of the application of pressure to a specially prepared 'charge' (which is a preblended mixture of reinforcement, resin and filler) between two tool surfaces causing squeeze- and shear-flow of the material to fill the mold cavity, which is then cured at elevated temperature within the tool. The process takes place between a pair of heated matched metal dies, mimicking steel stamping. The most common 'blank' is sheet-molding compound (SMC), which has polyester as the most prevalent resin. SMC is made in rolls, which are then stored in a freezer to retard the progression of cure. Although most compression-molded parts use a random arrangement of fibers (which is an optimal form for squeeze-flow from a 'charge'), SMC is also available in unidirectional, biaxial (±45°), directional-discontinuous and combined forms enabling a wide range of potential architectures. Since it is a closed-mold process parts can be fairly complex with a very high degree of dimensional tolerance. Fiber volume fraction is generally not very high and most parts are for secondary structural applications.

2.2.6 Autoclave molding

Autoclave molding is widely used in the aerospace industry for the production of high quality, prepreg-based parts. The preimpregnated laminae are laid onto the tool surface, on top of which a peel ply, bleeder ply and vacuum bag are placed. The entire assembly, once sealed, is placed in an autoclave (a combination of an oven and pressure chamber) for cure. The use of the autoclave enables excellent control of pressure and temperature with appropriate ramps and dwells. The vacuum serves to assist in ply consolidation while continuously removing volatiles that may form during the molding operation to reduce the incidence of porosity. The combination of the vacuum and the

pressure acting on the assembly serves to apply uniform pressure over the part surface resulting in a very high quality laminate with fiber volume fractions at 60–70% and a very high level of dimensional control. The process results in perhaps the highest quality laminates with lowest void content but requires substantial capital investment in the autoclave itself. The process provides very high levels of uniformity, dimensional tolerance and quality, and hence could easily be used for the manufacture of prefabricated jackets to be adhesively bonded in the field. However, costs – due to the need for an autoclave and for prepreg – are likely to make this prohibitively expensive unless there is a requirement for the level of quality control and dimensional tolerance needed. It should be noted that the control of incoming materials that is afforded by prepreg can also be attained with the use of prepreg tow as elucidated in Section 2.2.7.

2.2.7 Filament winding

Filament winding is used for the fabrication of parts that are generally axisymmetric in nature, or that entail the placement of reinforcement around a mandrel that is rotated. In the simplest form of the process, reinforcement in tow or bundle form is fed through a wet bath wherein it is impregnated with resin and is then wound onto a rotating mandrel. Once the desired architecture and layup thickness are achieved the part is bagged and then cured. In variations of the process, preimpregnated tow or tape is wound onto the mandrel, and the part is then cured. The process can be used with both thermosetting and thermoplastic resins and provides excellent dimensional control and repeatability. In principle labor content is fairly low and there is a high efficiency in the materials transformation process. Fiber architecture can be changed, within limits, from one layer to the next, and even within the same layer, with orientations as low as ±2° and as high as ±88° being possible. Although the process is best suited to axisymmetric parts, complicated contours such as those on aircraft inlet ducts can be achieved through the use of special heads and the use of multiple tows, as in the use of fiber placement machines. This process is ideal for accurate and uniform placement of tow (either through a wet bath or in prepreg form) around a column and has already been adapted in two forms: wet winding of tow and prepreg winding – both using carbon fibers – wherein the winder itself rotates around the column on a ring-like stage (Fig. 2.6) (Karbhari, 2001). The method has also been used to fabricate shells used as hybrid girders for FRP bridge systems wherein the thin carbon/epoxy filament shell is placed in the field between supports and then pumped full of a high-slump concrete slurry (Karbhari *et al*., 2000).



2.6 Automated winding of prepreg tow for seismic retrofit of columns.

2.2.8 Pultrusion

The pultrusion process is similar to extrusion in that continuous lengths of constant cross-section can be formed although the reinforcement and resin is pulled through a die rather than being pushed through it as in the extrusion of plastics. In the generic form of the process impregnated fabric is shaped and pulled through a heated die which not only provides final shape, but also causes the composite to reach an adequate level of cure. The process is amenable to the use of dry roving and fabric, which are impregnated in wet baths prior to being shaped, as well as prepreg. Final compaction is conducted within the die which also controls dimensional tolerance. Because the reinforcement has to be pulled through the die a high percentage of it has to be in the axial direction. Since the process is highly automated it provides a very high level of uniformity and can lead to the highest level of materials efficiency. The only drawback to the process is the constraint for constant cross-sections, although innovative die designs have been demonstrated to allow changes – albeit at a very slow rate of pulling making the process analogous to sequential stamping. As in the case of compression molding the process uses a fairly high filler content both to reduce material cost and more importantly to control shrinkage and to reduce frictional resistance in the

die. This process has been used extensively for the fabrication of structural profiles including I-beams and channel sections, framework for temporary buildings, gantries, bridge girders and deck sections.

2.2.9 Liquid molding

Liquid molding refers to the family of processes in which a skeleton of dry reinforcement, the preform, is first placed in a tool, which is closed prior to injection of resin into the tool under pressure, after which the composite is cured under ambient or elevated temperature conditions. Resin transfer molding (RTM), structural reaction injection molding (SRIM) and resin infusion are the most commonly used subsets of this process (Steenkamer *et al.*, 1993). In RTM a two-sided tool is used resulting in fairly complex net-shape or near-net-shape parts with high fiber volume fractions and a high level of dimensional tolerance. The resin infusion version generally uses a one-sided tool with a specially designed silicone or other bag on the other surface with resin being pulled into the preform by the application of vacuum. This enables fabrication of larger parts without the need for large presses for the movement of two-sided tooling. Overall since the processes separate the stages of reinforcement placement, and infusion, extreme levels of architectural tailoring can be achieved at lower cost without excessive expenditure on equipment. Successful molding is highly dependent on flow, necessitating a good understanding of preform permeability and flow phenomena especially under non-isothermal conditions. Void content and wet-out are highly dependent on flow. The coupling of preform fabrication from both structural and infusion perspectives brings with it challenges related to concurrent design for load and processing. Due to the requirement for low viscosity to enable good infusion of resin into the preform the processes are almost completely restricted to thermosetting polymer systems although some recent work has shown the feasibility of using cyclic oligomers. This set of processes can be used very efficiently for the fabrication of shells that can be adhesively bonded in the field for seismic retrofit of columns. The use of resin infusion also provides a method by which the jacket can be directly infused onto the column. In addition, the method has also been used for fabrication of bridge decks (Karbhari, 2003), pilings and other structural elements.

2.2.10 Process selection

It is emphasized that whereas it may be possible to fabricate a component using a variety of processes, the choice of the optimum process will depend on aspects such as size, shape complexity, type and level of reinforcement loading, speed required, number of parts to be fabricated, level of dimensional tolerance and part-to-part uniformity required. A variety of process

discriminators are discussed by Karbhari and Wilkins (1992), Krolewski (1989) and Gutowski *et al*. (1991). The reader is, however, cautioned that selection is not generic and depends largely on the specifics of the application and the capabilities of the fabricator in question. Thus, although wet layup is generally considered to be capable of far lower product quality than prepreg-based autoclave cure, the process when used by an expert crew can result in very high quality comparable parts without the capital expenditure of an autoclave.

2.3 Quality control during manufacture

Quality assurance and quality control are important aspects in the processing of composites, both as related to the resulting performance characteristics and to the overall integrity and durability of the resulting components. In so far as civil structures are concerned this takes on added importance because the components are likely to be expected to withstand harsh and varying environmental exposure conditions over extended periods of time (75+ years, for example, in the case of new bridge structures) without the same level of inspection and maintenance used in the aerospace industry. Furthermore, in a number of cases, the FRP is likely to be fabricated on site, in the form of externally bonded reinforcement, for example, resulting in a greater degree of uncertainty during fabrication. Achieving a reliable standard of product necessitates use of good quality assurance procedures, a high level of training for personnel, appropriate levels of oversight of the processing operations and control of the processing environment. It is noted that in some cases this will be easier since the primary fabrication is done under controlled conditions in a factory, whereas in others control is inherently difficult due to field-driven conditions. Examples of process specifications and quality control procedures for rehabilitation are given by Mirmiran *et al*. (2004).

At the minimum, quality control is needed at the levels of:

- incoming raw material;
- storage of constituents;
- mixing of resin components;
- processing;
- post-processing, prior to installation in the field;
- during and after installation.

Aspects that could be checked include the type of fiber and fabric, the number of layers of fabric and details of layup orientation, resin constituents and stoichiometry, rheology and cure kinetics, and final properties as determined primarily through assessment of physical and mechanical characteristics. A range of tests can be conducted both during processing and on the final components; further details can be found in the published literature (Geier,

1994; ASM International, 2001; ASTM, 2002) and are hence not repeated here. Nonetheless it is important to note that defects traceable to incoming material, or related to processing, can have a substantial effect on the durability and reliability of FRP materials and components fabricated from these materials.

2.4 Exposure environments

While FRP materials have a fairly successful record of use in pipelines, underground storage tanks, building facades and architectural components – and anecdotal evidence provides substantial reason to believe that if appropriately designed and fabricated, these systems can provide longer lifetimes and lower maintenance costs than equivalent structures fabricated from conventional materials – it must be remembered that the FRP systems used in civil infrastructure have critical differences in loading, environment and even in the types of materials and processes used as compared with the materials–process–load combinations commonly seen in aerospace applications.

In general, FRP materials and components thereof used in civil infrastructure are exposed to a variety of environments that may act individually or may be synergistic in nature. Environmental factors that are often considered more critical to the long-term performance of external strengthening systems include moisture/solution, alkaline environment, thermal effects, fatigue, creep/relaxation, ultraviolet exposure, fire and synergistic effects.

Although the term 'durability' is widely used, its meaning and implications are often ambiguous. In order to ensure that the term 'durability' and its implications are completely understood, the durability of a material or structure is defined as 'its ability to resist cracking, oxidation, chemical degradation, delamination, wear, and/or the effects of foreign object damage for a specified period of time, under the appropriate load conditions, under specified environmental conditions'. In this vein, damage tolerance is defined as 'the ability of a material or structure to resist failure and continue performing at prescribed levels of performance in the presence of flaws, cracks or other forms of damage/degradation for a specified period of time under specified environmental conditions'. The most common of these environmental conditions and a brief summary of the effects of each are provided below, following the discussion provided by Karbhari *et al.* (2003).

2.4.1 Moisture/solution

Exposure to moisture/solution includes effects from direct exposure to rain, humidity, moisture or diffused solutions through other substrates, in addition to immersion in aqueous solutions, as in the case of external column jackets used for bridge columns in flood plains, structures used in harbors, or bridge

decks that could have ponding or overflow in times of heavy rain. Moisture diffuses into all organic polymers, leading to changes in thermophysical, mechanical and chemical characteristics. The primary effect of the absorption is on the resin itself through hydrolysis, plasticization, saponification and other mechanisms that cause both reversible and irreversible changes in the polymer structure. In some cases, the moisture wicks along the fiber–matrix interphase and has been shown to cause deleterious effects to the fiber–matrix bond, resulting in a loss of integrity at that level. Moisture and chemicals have also been shown, in the case of aramid and glass fibers, to cause degradation at the fiber level. In the case of glass fibers, degradation is initiated by moisture extracting ions from the fiber, thereby altering its structure. Aramid fibers absorb moisture, which can result in accelerated fibrillation under specific conditions. Solutions such as sodium hydroxide and hydrochloric acid are known to cause dramatic accelerated hydrolysis of Kevlar® 49 yarn, especially in combination with temperature and stress. It is, however, possible to protect these fibers to a significant degree from rapid attack through the selection of appropriate resin systems and processing conditions, and the application of gel coats and protective coatings. Since most FRP composites in civil infrastructure will come in contact with moisture and various solutions, either due to natural causes or location, or due to design or accident, it is essential that both the short- and long-term effects of these solutions are well understood and documented.

2.4.2 Alkaline environment

Although FRP composites can come in contact with alkaline media through interaction with a variety of sources – including alkaline chemicals, soil (or solutions diffusing through soil) and concrete – the main concern at the present time stems from the potential effects of degradation due to concrete pore water solution, which is known to have a hydrogen ion concentration level as high as 13.5. A large body of research exists on the degradation of bare glass fibers in contact with, or in, alkaline solutions, especially those derived from concrete, and there is no doubt that bare glass fibers in this environment are severely degraded due to a combination of mechanisms ranging from pitting, hydroxylation, hydrolysis and leaching. Although the presence of resins in FRP composites around individual filaments can be expected to protect the fibers from such attack, the alkaline solutions can accelerate the degradation of bond and of some resins themselves, especially if not fully cured.

2.4.3 Thermal effects

Thermal effects include response changes due to temperatures above the cure temperature, freezing and freeze–thaw conditions, and temperature

variations and cycles. It is acknowledged at the outset that not all thermal exposure is deleterious since in a number of cases it can actually result in much needed post-cure of FRP components, although exposure to temperatures above that of processing can result in severe deterioration of the bulk resin and the fiber–matrix interface. It is noted that resins and adhesives soften over a temperature range, which causes an increase in viscoelastic response, a consequent reduction in elastic mechanical performance levels and, in a number of cases, an increased susceptibility to moisture absorption. Prior research, materials testing and anecdotal data have shown that, in general, subzero temperature exposure can result in matrix hardening, matrix microcracking and fiber–matrix bond degradation, whereas freeze–thaw in the presence of salt can result in accelerated degradation due to the formation and expansion of salt deposits in addition to effects of moisture-induced swelling and drying.

2.4.4 Creep/relaxation

For any practical civil infrastructure composite, the creep/stress relaxation properties are dominated by the resin matrix-dependent properties, rather than fiber or interfacial properties. Undercured resins are susceptible to significant creep and possible microcrack initiation during the early stages of service environment exposure. Absorbed moisture and higher service environment exposure temperatures both enhance creep susceptibility, which is ultimately diminished by enhanced further cure. In most cases, at the level of a structure or component, creep and stress relaxation can be guarded against or reduced significantly by taking advantage of the fact that the creep and stress relaxation response is likely to be resin dominated for most practical civil infrastructure applications. Thus appropriate selection and processing of resins, and the designed placement of fibers can solve a large part of the challenge.

2.4.5 Fatigue

Fatigue, which is generally defined as ‘the physical phenomenon that causes a material or component to fail after the application of an applied condition or conditions (cycles) even though the level of that condition is not high enough to cause failure on the first cycle of application’, is an important consideration for the durability and safety of civil infrastructure. The loading may be mechanical (due to vehicle traffic, for example), thermal (from variations in temperature) or chemical (from seasonal road treatments, oxidation, NO_x effects, water, etc.).

2.4.6 Ultraviolet radiation

Ultraviolet radiation that reaches the Earth's surface constitutes about 6% of the total solar radiant flux and has wavelengths between 290 and 400 nm. Since most polymers have bond dissociation energies on the order of the 290–400 nm wavelengths in the ultraviolet region, they are greatly affected by exposure to this portion of the solar spectrum. The effects of ultraviolet exposure, or photodegradation, are usually confined to the top few microns of the surface. However, in some cases, degradation at the surface of a polymeric component has been shown to affect mechanical properties disproportionately, as flaws that result from surface photodegradation can serve as stress concentrators and initiate fracture at stress levels much lower than those for unexposed specimens. The effect of ultraviolet radiation is also compounded by the action of temperature, moisture, wind-borne abrasives, freeze–thaw and other environmental components.

2.4.7 Fire

A significant concern in any application of organic matrix-based composites is the possibility that an accidental (or deliberate) fire may ignite the composite material. This may result in the spread of flame on the composite surface, and may also release heat and generate potentially toxic smoke. The fibers displace polymer resin, making less fuel available to the fire. When the outermost layers of a composite lose their resin due to heat-induced gasification, they act as an insulating layer, slowing heat penetration and evolution of gases from the depth of the composite. It must be recognized that fire-related issues associated with composite materials are more severe in confined spaces (such as tunnels and buildings) as opposed to open spaces (such as roads and bridges). The effect of fire is initially exhibited by the heating up of the composite surface. Over the depth of composite material heated up to temperatures past the glass transition temperature, the composite exhibits a corresponding loss of modulus. Below the temperature of chemical degradation, this loss in modulus is reversible. Further increase in temperature, such as above 450°F for glass/vinylester, results in the degradation of the chemical structure of the resin. This thermal damage results in irreversible loss in load-bearing characteristics.

2.5 References

ASM International, *ASM Handbook*, Vol 21, *Composites*, ASM International, Materials Park, OH, 2001.

ASTM (American Society for Testing and Materials), *MIL-17*, *The Composite Materials Handbook*, Vols 1–5, ASTM, West Conshohocken, PA, 2002.

Geier, M.H., *Quality Handbook for Composite Materials*, Kluwer Academic Publishers, Dordrecht, 1994.

Gutowski, T., Henderson, R. and Shipp, C., 'Manufacturing Costs for Advanced Composites Aerospace Parts,' *SAMPE Journal*, 1991, **27**(3), 37–43.

Karbhari, V.M., 'Materials Considerations in FRP Rehabilitation of Concrete Structures,' Invited paper for a Special Issue on Fracture Mechanics in Concrete Repair/Strengthening, *ASCE Journal of Materials in Civil Engineering*, 2001, **13**(2), 90–97.

Karbhari, V.M., 'FRP Bridge Decks – From Design and Characterization to Field Implementation,' Proceedings of the European Bridge Engineering Conference – Lightweight Bridge Decks, Rotterdam, Netherlands, 27–28 March 2003.

Karbhari, V.M. and Wilkins, D.J., 'The Use of Decision Support Systems for the Efficient Selection and Design of Composites and Their Products,' *International Journal of Materials and Product Technology*, 1992, **7**(2), 125–149.

Karbhari, V.M., Seible, F., Burgueno, R., Davol, A., Wernli, M. and Zhao, L., 'Structural Characterization of Fiber-Reinforced Composite Short- and Medium-Span Bridge Systems,' *Applied Composite Materials*, 2000, **7**(2/3), 151–182.

Karbhari, V.M., Chin, J.W., Hunston, D., Benmokrane, B., Juska, T., Morgan, R., Lesko, J.J., Sorathia, U. and Reynaud, D., 'Durability Gap Analysis for FRP Composites in Civil Infrastructure,' *ASCE Journal of Composites for Construction*, 2003, **7**(3), 238–247.

Krolewski, S.M., 'Study of the Application of Automation to Composites Manufacture,' MTL-TR-89-47, US Army Materials Technology Laboratory, Watertown, MA, 1989.

Mirmiran, A., Shahawy, M., Nanni, A. and Karbhari, V.M., 'Bonded Repair and Retrofit of Concrete Structures Using FRP Composites: Recommended Construction Specifications and Process Control Manual,' NCHRP 514, Transportation Research Board of the National Academies, Washington, DC, 2004.

Ross, S., Boyd, A., Johnson, M., Sexmith, R. and Banthia, N., 'Potential Retrofit Methods for Concrete Channel Beam Bridges Using Glass Fiber Reinforced Polymer,' *ASCE Journal of Bridge Engineering*, 2004, **9**(1), 66–74.

Seim, W., Hormann, M., Karbhari, V.M. and Seible, F., 'External FRP Poststrengthening of Scaled Concrete Slabs,' *ASCE Journal of Composites in Construction*, 2001, **5**(2), 67–75.

Steenkamer, D.A., Wilkins, D.J. and Karbhari, V.M. 'Resin Transfer Molding: Part I Materials and Preforming,' *Processing of Advanced Materials*, 1993, **3**(2), 89–105.

Wilkins, D.J. and Karbhari, V.M., 'Concurrent Engineering for Composites,' *International Journal of Materials and Product Technology*, 1991, **6**(3), 257–268.

3

Durability of composites in aqueous environments

C. HELBLING and V. M. KARBHARI,
University of California San Diego, USA

3.1 Introduction

Fiber-reinforced polymer (FRP) composites have a long history of use in marine vessels, piping, corrosion equipment, and underground storage tanks, and anecdotal evidence and limited testing shows that they can be successfully engineered to have long service lives in contact with moisture and aqueous solutions. It is, however, a misnomer that FRP composites and polymers are 'waterproof' since moisture diffuses into all organic polymers, leading to changes in thermophysical, mechanical, and chemical characteristics. The primary effect of the absorption is on the resin itself – through hydrolysis, plasticization, saponification, and other mechanisms which cause both reversible and irreversible changes in the polymer structure. In some cases, the moisture wicks along the fiber–matrix interphase and has been shown to cause deleterious effects to the fiber–matrix bond, resulting in loss of integrity at that level. Moisture and chemicals have also been shown, in the case of aramid and glass fibers, to cause degradation at the fiber level. In the case of glass fibers, degradation is initiated by moisture-extracting ions from the fiber, thereby altering its structure. These ions combine with water to form bases, which etch and pit the fiber surface, resulting in flaws that significantly degrade strength and can result in premature fracture and failure of the fibers. Basic solutions, when in direct contact with glass fibers, can cause significant pitting and leaching, often resulting in the fiber losing its core over a short period of time with the outer sheath being reactive, accelerating the leaching process. Aramid fibers absorb moisture, which can result in accelerated fibrillation under specific conditions. Solutions such as sodium hydroxide and hydrochloric acid are known to cause dramatic accelerated hydrolysis of Kevlar 49 yarn, especially in combination with temperature and stress. Carbon fibers are largely inert to the influences of aqueous solutions likely to be found in civil infrastructure. However, just as with glass and aramid fibers, the bond between the fiber and the resin can be deteriorated by exposure. In light of this aspect, and the current preponderance of the use of

glass fiber for civil infrastructure applications, the emphasis in this chapter will be on the effects of aqueous environments on glass fiber-reinforced polymers (GFRPs).

It is, however, possible to protect these fibers to a significant degree from rapid attack through the selection of appropriate resin systems, processing conditions, and the application of gel coats and protective coatings. In general, degradation is significantly retarded if the resin (and resulting composite) is completely cured prior to use in a service environment, and has not undergone microcracking or any other form of physical/mechanical deterioration. It should be noted that there is a degree of concern related to the use of ambient cure systems such as polyesters and vinyl-esters in structural applications, prior to their having achieved full cure. The efficacy of application of gel coats and protective coatings has been shown by the marine industry in the prevention of blistering, jackstraw, matrix degradation, and fiber attack. However, it should be noted that a gel coat serves the same purpose, and under the same principles, as a rust preventive coating, and damage to the coating can result in rapid deterioration of the substrate material.

Most effects of moisture- and solution-related deterioration/degradation are on the strength of a composite, with changes in modulus, in most cases, being very small, generally of the order of 10% over a period of 10–15 years. However, it is noted that once the interphase or the fiber itself is sufficiently degraded, changes in modulus (of the composite) can be fairly large. Keeping in mind aspects of stress-rupture, factors of safety of 4–6 for boats and 8–10 for storage tanks have been routinely used by industry in the past. FRP composite components used in civil infrastructure are likely to be exposed to rain, humidity, moisture, or solutions diffused through other substrates (such as concrete). In some cases components may even be immersed in aqueous media as in the case of column jackets used for bridge columns in flood plains, structures used in harbors, or bridge decks that may undergo ponding or overflow in times of heavy rain or due to melt of heavy snowfall. The determination of the effect of such exposure on the FRP components, especially over prolonged periods of exposure and over extended periods of overall exposure, is of critical importance.

3.2 Influence of moisture at the constituent level

The study of the degradation mechanisms of GFRP composites encapsulates chemical as well as physical aspects of ageing. Physical ageing refers to the reversible alteration of the material properties. The property changes are essentially temperature dependent and usually dramatic but can be recovered upon drying. Chemical ageing occurs with longer exposure duration and mainly involves irreversible degradation of the resin and the fiber, as well as the fiber/matrix interface at the molecular level.

Even though a lot of research has been concentrated on the study of the effects of moisture on composite properties, the mechanisms of water-induced degradation, which mainly include a reversible process known as plasticization and an irreversible process that involves chemical reaction, are still not comprehensively understood. Hence, there is a research emphasis on the study of the maximum absorption capacity of composites (Harper and Naeem, 1989; Chateauminois *et al*., 1993; Ghorbel and Valentin, 1993; Mensitieri *et al*., 1995; Sridharan *et al*., 1998; Chin *et al*., 1999), the mobility of water molecules within composites (Diamant *et al*., 1981), the reversibility of wet/dry cycles (Illinger and Schneider, 1980), the damage induced by the adsorption of moisture and the effect of this damage on later absorption rates and magnitudes (Apicella *et al*., 1983; Harper and Naeem, 1989; Ghorbel and Valentin, 1993; Chin *et al*., 2001a), the effect of moisture on the fiber/matrix interfaces (Vaughan *et al*., 1984; Wagner and Lustiger, 1994), the effect of temperature on sorption profiles (Apicella *et al*., 1983; Harper and Naeem, 1989; Hamada *et al.*, 1994; Chin *et al*., 1999; Liao *et al.*, 1999, Chin *et al*., 2001a), and, finally, the effect of applied stresses (Fahmy and Hurt, 1980; Springer *et al.*, 1980; Marom and Broutman, 1981; Marshall *et al*., 1982, Kasturiarachchi and Pritchard, 1983; Neumann and Marom, 1985, 1986, 1987; Henson and Weitsman, 1986; Karbhari *et al.*, 2007) on the moisture absorption behavior over short and long time scales.

3.2.1 Effects on the resin component

The role of the polymer matrix is three-fold, i.e. it is used to protect fibers against environmental attack, it serves as a load-transfer medium and it also acts as an energy-dissipation outlet for arresting crack propagation. Hence, it is of crucial importance to determine the effects of water on the resin properties since the absorption of water molecules in the resin will cause a slow but significant degradation of the composite properties, as will be developed next.

While an incomplete cross-linking of the resin as well as the presence of a large number of ester links induces low heat stability and greater susceptibility to moisture-related degradation (Apicella *et al.*, 1983), such as hydrolysis and leaching out of low-molecular-weight elements, the addition of styrene monomer, as is done in polyesters and vinyl-esters, in the resin mixture can help improve the hydrolytic stability by increasing the polymer's hydrophobicity (Karbhari *et al.*, 1998).

Vinyl-ester resins are very stable chemically in aqueous environments and less susceptible to hydrolysis relative to unsaturated polyester resins because of their terminal ester functional groups that are shielded by methyl groups (Chin *et al.*, 2001a). Ganem *et al*. (1994) demonstrated for instance that vinyl-esters are at least one order of magnitude more hydrolytically

stable than unsaturated polyesters as a result of the especially low reactivity of their methacrylate groups. They also showed that the copolymerization of unsaturated esters with styrene improves stability by decreasing water equilibrium concentration and increasing steric hindrance (steric shielding effect of polystyryl groups) around the ester groups. Finally, they noticed that the presence of a hydroxyl group in the β position of the ester in vinyl-esters decreases significantly their hydrolytic stability. Moreover, Chin *et al.* (1999, 2001a) showed that vinyl-ester resins absorb less moisture as compared with isophthalic polyester resins in water at 22°C. Apicella *et al.* (1983) observed the opposite at 20°C; however, the isophthalic polyester resin exhibited a lower hydrolytic stability, undergoing significant weight loss during exposure, as compared with the vinyl-ester resin. In contrast, according to a study by Ghorbel and Valentin (1993), results suggested that vinyl-esters have lower chemical and thermal stability than polyesters since they experienced greater hydrolysis and plasticization. They showed that vinyl-ester resins have a higher moisture saturation level as compared with polyester resins due to the presence of moderately (esters and ethers) and strongly (alcohols) polar groups, and a lower glass transition temperature ($T_{g,vinyl\text{-}ester}$ = 114°C; $T_{g,polyester}$ = 138.5°C), which is attributed to their higher molecular mobility and generally incomplete curing. Apicella *et al.* (1983) also observed that vinyl-ester resins have a lower T_g as compared with isophthalic and bisphenol polyesters prepared by hand lay-up and post-cured at 100°C. On the other hand, Chin *et al.* showed contradictory results with the vinyl-ester resins having similar T_g in the results of Chin *et al.* 2001a but a lower T_g in those of Chin *et al.* 1999, as compared with the isophthalic polyester resins produced by molding and post-cured at 150°C. In another study on pultruded composites, however, Chin *et al.* (2001b) observed that the vinyl-esters had a much higher T_g than the polyesters.

It is generally accepted that sorbed moisture can act as a plasticizer, hydrolyser, and post-curing promoting agent, increasing or decreasing the mechanical integrity of the ester matrix to a degree dependent upon the exposure temperature (Apicella *et al.*, 1983). At first, water penetration in thermosetting polymers causes physical ageing known as plasticization. Plasticization results in an increase in molecular mobility because of small water molecules occupying positions between the large polymer chains. This increases the intermolecular distance, thereby decreasing intermolecular cohesive forces. This reversible process primarily results in a decrease in T_g due to the higher molecular mobility (Ghorbel and Valentin, 1993). Additionally, plasticization is generally accompanied by an increase of the glassy modulus in the temperature interval T_α–T_β, which is known as antiplasticization (Pascault *et al.*, 2002). In the case of long exposure in water, chemical ageing simultaneously occurs through hydrolysis, with chemical attack on the ester linkages of the resin, which are the reactive groups mostly involved in the

breakdown and leaching observed in polyester and vinyl-ester systems (Apicella *et al*., 1983). Hydrolysis irreversibly affects the chemical structure of the resin and causes a decrease in its T_g (Ghorbel and Valentin, 1993). The hydrolysis of ester groups results in the formation of carboxyl and hydroxyl groups (Chin *et al*., 2001b) with the former carboxyl groups being able to autocatalyze further decomposition (Magnus *et al*., 1966). It has also been shown that the loss of hydrolyzed, low-molecular-weight elements, which serve as resin flexibilizers, results in an embrittlement of the matrix, and thus, in an increase in T_g (Apicella *et al*., 1983). However, chemical ageing can also occur in the form of post-curing causing T_g to increase. Indeed, ageing in water can lead to further reaction (previously inhibited by the presence of oxygen in air) of residual styrene monomer and anhydrides with radicals fixed in the network (Mensitieri *et al*., 1995; Karbhari and Zhang, 2002), increasing the amount of cross-linking of the polymer network.

As shown in some experiments conducted by Ghorbel and Valentin (1993), ageing of neat vinyl-ester and polyester resins in water at elevated temperatures was primarily governed by plasticization. Hydrolysis became significant for longer exposure time (4000 h) only. In addition, for both resin types, the exponential decrease of T_g was correlated to the increasing molecular mobility with advanced hydrothermal ageing. Ageing of the glass/polyester and glass/vinyl-ester composites was similarly initially governed by plasticization (<2500 h) and ultimately, for longer durations (>3000 h), by hydrolysis. However, the presence of fibers and interfaces enhanced the hydrothermal ageing (plasticization and hydrolysis) of the matrix accelerating the decrease in T_g. Furthermore, chemical ageing of the vinyl-ester composites through hydrolysis was ultimately counterbalanced by post-curing effects (>550 h) resulting in a substantial final increase in T_g. In a similar study (Chin *et al*., 2001b) to that mentioned above, immersion of vinyl-ester and isopolyesters composites in water at room temperature and up to 60°C resulted in a rather strong initial increase in T_g followed by a slower decrease. The immersion of the vinyl-ester composites at 80°C followed the same trend, while the immersion of the isopolyester composites at 80°C caused a continuous increase in T_g. It was postulated that the initial increase in T_g was associated with dissolution of low-molecular-weight elements, while the final decrease was related to chain scission in the main network chains. On the other hand, the continuous increase in T_g observed at 80°C for isopolyesters was associated with progressive embrittlement of the resin through loss of resin flexibilizers. In contrast, Nguyen *et al*. (1998) showed that even though an immersion in water substantially reduced the T_g of an epoxy resin, temperature did not have any effect on the decrease.

Ghorbel and Valentin (1993) have shown that the immersion of unsaturated polyester resins and composites in water at 60°C primarily results in a loss

in styrene, with additional formation of phenols for the polyester composites owing to hydrolysis. The immersion of vinyl-ester resins and composites on the other hand induces hydrolysis and post-curing reactions, with an additional dehydration reaction for the vinyl-ester composites. Prian and Barkatt (1999) demonstrated that the immersion of E-glass/vinyl-ester composites in water at 80°C results in the depolymerization of the vinyl-ester resin. This depolymerization proceeds with the cleavage of the unsaturated part of the polymeric chain leading to the loss of acrylic acid from the matrix.

Prian and Barkatt (1999) also provided a detailed analysis of the degradation mechanisms occurring upon prolonged exposure of E-glass/vinyl-ester composites to deionized water with explanations as to why the interfacial region undergoes more rapid attack as compared with the bulk. They showed that the pH at the internal fiber/matrix interfaces eventually increases due to selective leaching of alkaline components by water from the silicate glass fibers, leading to enhanced nucleophilic attack on the fibers. The elevated pH also causes enhanced matrix hydrolysis and extraction of acrylic acid from the resin. The accelerated fiber dissolution is then followed by interfacial debonding, which by opening new routes for water penetration, promotes further hydrolytic depolymerization of the matrix and the formation of microcracks. Moreover, as temperature increases, the degradation becomes more severe and the induction period for the sudden increase in the dissolution rate of silica from glass fibers decreases.

The thermal degradation of various polyvinyl esters was studied by Simon and Rybar (1992). They showed that the degradation of polyvinyl acetate (PVAc), polyvinyl propionate, polyvinyl butyrate, and polyvinyl valerate followed the model of gradual zip propagation, while the degradation of polyvinyl caproate (PVCa) followed the model of immediate zip growth. In all cases, the initiation step of the zip reaction was not autocatalytic. The thermal degradation of all polyvinyl esters occurred by zip elimination of acids, polyene sequences being formed along the polymer backbone. In the model of immediate zip growth, the zip growth occurred at a very high propagation rate with the propagation rate being much higher than the initiation rate, while in the model of gradual zip growth, the rates of initiation and propagation were comparable. In both models, it was assumed that the zip growth ceased only at the ends of the sequences or at the monomeric units, which had already been degraded. The decomposition of PVAc had already been extensively studied (Barrales-Rienda *et al.*, 1989) and it was shown that its degradation is autocatalytic and via a non-radical process. It was also observed that the participation of the autocatalytic mechanism decreases as the length of the *n*-acyl portion increases. Some disagreement still exists, however, on whether the initiation reaction with the elimination of acetic acid occurs at random or not. For polyvinyl chloride (PVC), on the other hand, the thermal stability of the polyvinyl esters was found to decrease as

the length of the *n*-acyl substituents increased, due to a decrease in the energy of activation for the initiation reaction (Simon and Rybar, 1992).

Vinyl-ester resins have been largely used in composite structures for fluid storage and transportation; and in the naval, nuclear, and chemical industry due their good resistance to hygrothermal degradation (Liétard *et al*., 2000). It is noted that the use of non-fully cured and stabilized composite systems can result in the alteration of their residual physical and mechanical properties during environmental ageing. It is also noted that it has been demonstrated that post-cure directly affects the residual styrene content and degree of cross-linking of the resin by favoring further polymerization reactions, and further suggested that free residual styrene evaporates from the resin during post-cure or gets consumed in the formation of oligomers but does not participate in the creation of further cross-linking. Thus, it is either the increase in cross-linking or the disappearance of free styrene acting as a plasticizer during post-cure that improves the composite mechanical properties. As a consequence, the absence of post-cure could significantly affect the long-term ageing behavior of polymer composites and its influence should, therefore, be studied.

Liétard *et al*. (2000) studied the effect of post-cure on the ageing behavior of a vinyl-ester resin and unidirectional glass/vinyl-ester composite at ambient conditions. First, it was found that depending on the time of processing, significant changes in T_g were obtained for the vinyl-ester resin cured under ambient conditions, i.e. T_g = 92–117°C. Moreover, following processing, the T_g was found to vary with time under the influence of ambient temperature (23°C) and relative humidity (50% R.H.). Directly after processing, two distinct glass transition phases were found to exist within the resin; however, the first phase, attributed to the vinyl-ester network being plasticized by residual styrene, slowly disappeared with time (T_{g1} = 60–70°C, T_{g2} = 114–116°C). Similar changes were observed for the composites, underlying the fact that a partially cured network is not stable even under ambient conditions, which makes its structure and properties very sensitive to processing/storage conditions. Thus, post-cure of the vinyl-ester network seems to be required in order to stabilize the resin and to achieve reproducible properties for the manufactured composites. Post-cure of the composites for 5 h at 90°C involved the evaporation of residual styrene as well as the consumption of residual styrene in the formation of polystyrene and/or in further polymerization reactions of the vinyl-ester resin. Post-cure also led to the disappearance of the first glass transition phase.

3.2.2 Effects on glass fibers

It is well known that polymeric resins are sensitive to moisture; however, it should not be overlooked that glass fibers can undergo degradation by moisture

too. Two main approaches exist to explain the stress corrosion of glass fibers by water (Metcalfe and Schmitz, 1972), which can both be related to the Griffith–Irwin–Orowan equation:

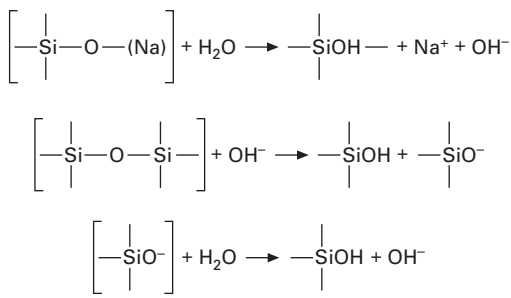
$$S = \sqrt{\frac{2E\gamma}{\pi c}} \qquad [3.1]$$

where S is the fracture stress, $2c$ is the sharp crack length, E is the material elastic modulus, γ is the surface energy, and c is the theoretical cohesive strength. One approach postulates that moisture adsorption causes a decrease in the surface energy of glass fibers, thereby reducing the cohesive strength of the material. The second approach attributes the loss of strength of glass fibers in a moisture environment to the slow growth of cracks until a critical size is reached that leads to failure.

The first corrosion mechanism for glass was proposed by Charles (1958) based on a study on soda-lime glass rods. He showed that the corrosion of glass was temperature dependent with an activation energy of about 20 kcal, which corresponded to the activation energy for self-diffusion of sodium ions in glass. He then postulated a mechanism for stress corrosion involving terminal groups in the silica network. According to this mechanism, selective leaching of alkaline components from the silicate glass causes the concentration of OH^- ions in the aqueous medium to rise. The hydroxide ions break up the silica network without being consumed, thus, the rate of dissolution of the silicate glass is expected to rise with time. Figure 3.1 details the autocatalytic mechanism that underlies the continued attack on the silica network. Based on these reaction processes, and assuming a stress-accelerated corrosion rate, Charles developed a relationship between the applied stress and the time to grow a flaw of critical size as

$$| V_x |_T = k_l \sigma^n + k \qquad [3.2]$$

$$\log t = n \log \frac{1}{\sigma_A} - \log k \qquad [3.3]$$



3.1 Reaction processes for the corrosion mechanism of silicate glass.

where $| V_x |_T$ is the corrosion rate, t is the time to grow a flaw of critical size, k and k_1 are constants, σ is the actual stress at the root of the flaw, n is an integer, and σ_A is the applied stress.

Another theory was developed by Schmitz and Metcalfe (1966) to show how pre-existing structural flaws serve as sites for hydrolysis and ion exchange reactions, ultimately leading to fiber failure. Their results from static tensile fatigue tests at 100% R.H. on E-glass filaments were in disagreement with Charles' theory, since they showed that the relationship between applied stress and log(time to failure) was not linear and that the growth of existing flaws was not continuous. The autocatalytic attack on the silica network proposed by Charles was assumed to be correct; however, modifications were made to his theory to explain the mechanism of stress corrosion. They showed that incubation and flaw growth by corrosion constitute the two stages preceding fracture and that stress corrosion occurs at so-called C-type flaws located on the glass surfaces. During the incubation period, water reacts with cations in the C-flaws leading to hydrolysis and to an increased concentration of hydroxyl ions, thereby increasing pH. The incubation period continues until the pH reaches the level necessary for corrosion to occur. This stage, which extends to 95% (or more) of the total static fatigue process duration, thus occupies most of the life of the fiber. During this period, no strength loss is experienced. Once the critical pH is reached, subsequent corrosion (originating at C-flaws) of the surrounding silica network takes place until a critical size flaw has formed, when fracture ensues.

In a later study on the mechanism of stress corrosion for E-glass filaments, a thorough investigation of the ion exchange involved during immersion of E-glass in various environments, going from an acidic to an alkaline solution, was performed (Metcalfe and Schmitz, 1972). The ion exchange was found to occur at the glass surface between sodium ions in the glass and hydrions from the surrounding atmosphere according to the following equation: $SiONa + H^+ \rightarrow SiOH + Na^+$. The ion exchange was believed to occur in all E-type glasses; however, only glasses containing 5% alkali (e.g. sodium or potassium oxides) could build enough stress to cause spontaneous cracking in the absence of externally applied stress. The reduction in molecular volume at the glass surface caused by this ion exchange generates high tensile stresses, which account for strength loss of glass filaments and spontaneous cracking. The superficial tensile stresses that are created are balanced by compression stresses in the core of the filament and, hence, will begin decreasing as the continued hydrolysis reduces the stress difference. Thus, the three main observations made were that: first, the continuation of the ion exchange could lead to a reversal of the initial strength loss; secondly, the maximum strength loss is related to the alkali metal content of the glass; and finally, the filaments could crack spontaneously before the residual strength has reached zero. An incubation period was also shown to precede strength loss in static

fatigue tests, suggesting that theories involving slow crack growth are not valid for glass filaments. As a reminder, the two main flaws involved in the stress corrosion process are the A-type flaws (most severe compared with B- and C-flaws) as well as flaws formed by ion exchange and originating on the pristine glass surface. Thus, although the ion exchange will generate a tensile stress field creating high stress concentration – thereby ultimately affecting the filament strength – the original and unchanged A-type flaws will control strength during the incubation period. Delay in ion exchange can be caused by low stresses or low hydrion concentration and could lead to a reversal of strength or to a static fatigue limit. The effect of water on the strength of stress-free fibers immersed at 96°C was therefore studied, and a significant strength loss resulted from the exposure. There was evidence of sodium ion diffusion during water immersion, with a typical activation energy of 20 kcal/g. Simulated static fatigue tests on E-glass under a stress of 80% of the average tensile strength were also conducted, and it was shown that increasing pH resulted in an increase in the filament lifetime, reflecting the power of the ion exchange reaction in controlling failure.

Michalske and Freiman (1983) have also proposed a molecular model for stress corrosion of glasses in which the silicate network (Si–O–Si bond) is destroyed by water molecules. A comprehensive review of the adsorption of water onto various oxides (including silicate glasses), and the subsequent degradation of glass plates and filaments by water through moisture-assisted crack propagation, was provided by Bascom (1974). Failure is anticipated to begin with the formation of superficial flaws or cracks on glass that will start propagating under an applied stress. The stage of crack growth at which catastrophic failure occurs will depend on the specimen dimensions and the manner in which load is applied. The condition $\delta E_c > \delta\sigma + \delta W$, corresponding to an elastic strain energy due to an applied stress (δE_c) exceeding the energy needed to create a new surface ($\delta\sigma$) plus the energy expended in plastic deformation (δW), will cause a crack to propagate. The decrease in fiber reinforcement strength due to moisture was usually related to a reduction in surface energy due to the adsorption of moisture onto the glass fiber surfaces as the crack propagated. This resulted in an alteration of the bond strength at the crack tip, thereby reducing $\delta\sigma$ by reducing the cohesive energy. An alternative mechanism involved the embrittlement of the material by water around the crack tip, thus reducing δW. Two other ways in which moisture could assist failure included the surface corrosion of glass fibers by water and the condensation of water into the crack tip which, by exerting enough capillary pressure, could open flaws.

3.2.3 Effects on the interphase

The effect of moisture at the fiber/matrix interface is two-fold (Bradley and Grant, 1995). First, moisture can chemically reduce the bond strength between

the fibers and the matrix, by reacting with sizing/coupling agents and wicking along the interfaces. The other effect is through the matrix swelling that generally accompanies moisture sorption. Residual stresses that develop in the matrix during cure of the resin (shrinkage) and cooling down of the composite after cure (for $T < T_g$) are typically tensile parallel to fibers and compressive at interfaces, due to the greater coefficient of thermal expansion of the polymer matrix as compared with that of the glass fibers. Thus, the moisture-related swelling of the resin will reduce these residual stresses and relax the interfacial compressive stresses, thereby reducing the interfacial shear strength of the composites. It is also worth noting that the rapid cure and cooling down of composites during pultrusion result in high resin shrinkage and subsequent microcracking in resin-rich pockets within the composites (Phifer *et al.*, 2000), which can become sites for accelerated degradation.

3.3 Mass uptake profiles

Moisture may penetrate into a polymer resin/composite either by diffusion or capillarity. The generally accepted mechanism for moisture penetration in polymers is an activated sorption–diffusion process (Mensitieri *et al.*, 1995). The water molecules are first dissolved into the polymer surface and, at the same time as they diffuse through the bulk, start forming a solution with the polymer. The sorption phenomenon involving absorption and adsorption will be explained later. The diffusion mechanism occurs by the direct transport of water molecules in holes of the polymer matrix via random molecular motion (Crank and Park, 1968) and is driven by concentration gradient, whereas the capillarity mechanism involves flow of water molecules along the fiber/matrix interface caused by surface tension. This latter mechanism depends on the relative magnitude of the cohesion forces between water molecules and the adhesion forces of water molecules to the glass fiber surface. The capillarity mechanism becomes active after debonding, and thus depends on the bond strength of the fiber/matrix interface (Marom and Broutman, 1981). However, moisture attack at the fiber/matrix interface does not necessarily involve hydrolytic attack of the glass fiber reinforcement, since the accumulation of water at hydroscopic sites can produce an osmotic pressure sufficient to cause debonding (Bascom, 1974). A third mechanism of moisture penetration into the polymer matrix is through cracks and voids.

The diffusion behavior of moisture in amorphous polymers, such as the thermoset resins predominantly used in civil infrastructure applications, can be classified as follows (Chin *et al.*, 1999):

1. *Case I or Fickian*: rate of moisture diffusion is much less than polymer segment mobility.

2. *Case II*: rate of diffusion is much greater than polymer segment mobility and strongly dependent on swelling kinetics.
3. *Non-Fickian*: rate of diffusion is comparable with polymer segment mobility.

It has been shown for instance that moisture sorption can be Fickian by direct diffusion through the polymeric matrix (Menges and Gitschner, 1980), non-Fickian by diffusion through existing voids or cracks in the matrix, or capillary by wicking along fiber/matrix interfaces (Loos and Springer, 1981).

It is important before going further to clarify the terms 'absorption' and 'adsorption', which are often misused in the literature, but, however, refer to two completely different phenomena. Absorption is a capillary moisture uptake through existing pores, voids or other defects in the polymer structure (Chin *et al.*, 1999). Thus, it does not result in matrix plasticization and generates only very little heat or swelling. Absorbed moisture can be referred to as 'mobile water' and is easily desorbed. On the other hand, adsorption is a process by which a solution is formed through physical interactions between the polar water molecules and polar groups in the polymer. Hence, the concentration of water that permeates into the cross-linked resin will depend on the free energy of mixing of the polymer/solvent system. The extensive hydrogen bonding capability of vinyl-esters (OH groups) with water, for instance, can have significant effect on their moisture saturation content. Adsorbed moisture can be referred to as 'bound water' and is, therefore, less easily desorbed. The adsorption process generates heat and significant swelling, and promotes plasticization. The adsorption of water molecules can occur in the polymer structure or onto the glass fiber surfaces through hydrogen bonds, ultimately promoting debonding (Sonawala and Spontak, 1996).

The Fickian diffusion model is derived from the one-dimensional form of Fick's second law:

$$\frac{\partial C}{\partial t} = -D\,\frac{\partial^2 C}{\partial x^2} \qquad [3.4]$$

where C is the concentration of penetrant (i.e. water), D is the diffusion coefficient of the penetrant into a medium (i.e. polymer matrix), t is time, and x refers to position. The resolution of this equation using appropriate boundary conditions for diffusion into a semi-infinite solid yields (Marsh *et al.*, 1984; Pascault *et al.*, 2002)

$$\frac{C}{C_\infty} = 1 - \frac{8}{\pi^2}\sum_{n=0}^{\infty}\frac{1}{(2n+1)}\exp\left(-\frac{\pi^2(2n+1)^2 Dt}{l^2}\right) \qquad [3.5]$$

where C is the moisture concentration at time t, C_∞ is the equilibrium moisture concentration, D is the diffusion coefficient for moisture, which is assumed to be concentration independent although this does not always hold true (Marshall *et al.*, 1982), l is the specimen thickness and n is an integer. The

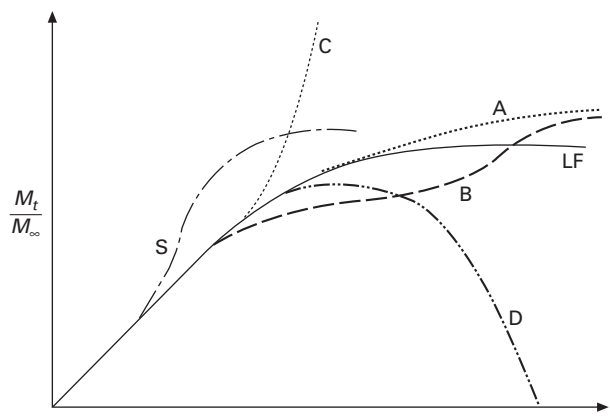
previous equation can be solved for short times ($M_t \leq 0.5M_\infty$ or $d^2 < 20Dt$) and yields the following:

$$\frac{C}{C_\infty} = \frac{M_t}{M_\infty} = \frac{4}{l}\sqrt{\frac{Dt}{\pi}} \qquad [3.6]$$

where M_t is the relative moisture uptake at time t and M_∞ is the relative moisture uptake at equilibrium. The Fickian diffusion behavior of a material can be confirmed if the following characteristics are observed (Chin *et al.*, 1999):

- both uptake and desorption plots of M_t/M_∞ versus $t^{1/2}$ are initially linear;
- the initial linear region extends at least up to $M_t/M_\infty = 0.6$ (case of uptake);
- above the linear region, curves are concave against abscissa;
- the uptake curves of M_t/M_∞ versus $t^{1/2}/l$ coincide regardless of specimen thickness.

While Fickian response is often assumed, in reality various types of sorption curves can be obtained for the immersion of polymer resins and composites in moist environments, with the most frequent ones being shown in Fig. 3.2 (Weitsman, 1995). The curve LF represents a linear Fickian diffusion behavior. However, composites usually exhibit one of the other profiles. A, B, and S represent anomalous weight gain due to the inherent viscoelastic nature of the polymer matrix, with A corresponding to a pseudo-Fickian behavior with a continuous gradual increase in weight, B corresponding to a two-stage diffusion due to relaxation effects (diffusion speed and relaxation rate are comparable), and S corresponding to a moving diffusion front. Finally, C and D represent profiles where the departure from LF is due to irreversible degradation of the material, with profile C resulting from damage growth



3.2 Typical range of uptake response.

due to possible debonding or delamination, and D resulting from physical or chemical breakdown such as hydrolysis.

Thermoset resins and glass fiber-reinforced composite systems usually follow a Fickian diffusion behavior (case A or LF) as long as no permanent damage has occurred. The initial linear increase of the moisture sorption curve is driven by water diffusion and the first maximum reached is explained by the fast diffusion of small water molecules overcoming the slow desorption of low-molecular-weight elements (Apicella *et al.*, 1982). The initial rate of moisture sorption as well as the moisture content at the first saturation level are dependent upon the material (resin and reinforcement composition), the temperature of exposure, and the environment (Springer *et al.*, 1980). Moisture equilibrium is attained in cured thermoset resins when the elastic expansion of the polymer network exerts sufficient pressure on the composite system to increase the chemical potential of the sorbed water to such an extent that no further sorption will occur. On standing (under no load or under constant strain), however, the elastic force is allowed to slowly relax, thereby decreasing the chemical potential of the sorbed moisture. This results in a new and higher equilibrium being reached (case B). After reaching saturation, polyester and vinyl-ester composite systems usually exhibit non-Fickian behavior with subsequent weight loss or regain. The mass loss (case D) sometimes observed for resin and/or composite systems at longer exposure times is attributed to chemical degradation (e.g. leaching, hydrolysis), whereas the final weight regain (case C) often observed in composite systems is mainly related to physical damage such as matrix microcracks and fiber/matrix debonding. For instance, the prolonged exposure of polymeric composite systems in aqueous media, especially glass/polyesters, can lead to the formation of microcracks and voids, resulting in an increase in the exposed surface area causing an increase in the effective dissolution rate of silica from glass fibers (Prian and Barkatt, 1999).

This opening of new routes for moisture absorption is associated with the sudden increased moisture content often observed after saturation. Polyester systems can also experience mass loss due to hydrolysis and resin dissolution. On the other hand, the weight decrease usually observed in vinyl-ester systems after saturation is attributed to the leaching out of low-molecular-weight elements (Harper and Naeem, 1989; Ghorbel and Valentin, 1993; Chu and Karbhari, 2005).

The chemical structure and morphology of a polymer is also known to affect moisture uptake (Chin *et al.*, 1999). In particular, a high concentration of polar functional groups can promote increased sorption of a polar penetrant such as water due to a greater sorption affinity. Chin *et al.* (1999) have shown, for instance, that indeed epoxy resins, which have a significant concentration of hydrophilic hydroxyl groups located along their backbone, absorb substantially more water than their vinyl-ester and polyester counterparts,

which contain less polar ester groups. The moisture sensitivity of resins can also be affected by variations in the distribution of cross-link density. Hence, Jacobs and Jones (1993) showed that in unsaturated polyester resins, the regions with lower cross-link density are most sensitive to plasticization effects, because of the tendency of the more polar components (e.g. acidic and hydroxyl end-groups) to segregate in the least cross-linked areas resulting in greater moisture sorption. The regions of high and low cross-link density formed as a result of the free radical cure of the polymer resin.

3.3.1 Influence of fibers

Neat polymer resins and FRP composites usually have different sorption behaviors and saturation moisture contents. The reason for the latter is that composites usually absorb a higher amount of moisture due to their additional fibers and fiber/matrix interfaces creating additional paths for moisture diffusion through debonding (Apicella *et al.*, 1983; Ghorbel and Valentin, 1993). The diffusion coefficient of moisture for composites is surprisingly significantly lower than that for neat resins, at least up to a certain temperature. This is probably related to the rather high fiber content of these composites, since the polymer resin is mostly responsible for moisture absorption, and/or to the difference in sample geometry for the composites (circular) and resins (rectangular) in Ghorbel and Valentin (1993), which could affect the diffusion rate.

Indeed, in their study on the role of absorbed water on the physico-chemical properties of glass-reinforced vinyl-ester and polyester composites, Ghorbel and Valentin (1993) found that neat resins and composites have very different sorption behaviors. The water uptake of both resin systems followed a Fickian diffusion behavior described by

$$M = M_m \left[1 - \frac{8}{\pi^2} \sum_{n=0}^{+\infty} \frac{1}{2n+1} \exp\left(\frac{-Dt}{e^2} \pi^2 (2n+1)^2 \right) \right] \qquad [3.7]$$

while that of the composites followed a Langmuir law described by

$$M = M_m \left[1 - \frac{\beta^*}{\alpha^* + \beta^*} \exp(-\beta^* t) - \frac{\beta^*}{\alpha^* + \beta^*} \frac{8}{\pi^2} \times \sum_{n=0}^{+\infty} \frac{1}{2n+1} \exp\left(\frac{-Dt}{e^2} \pi^2 (2n+1)^2 \right) \right] \qquad [3.8]$$

where M_m is the maximum moisture content; α^* is the probability that a water molecule will pass from the combined state to a free state, β^* is the probability that a water molecule will pass from the free state to a combined

state, and *e* is the sample thickness. Additionally, a weight loss and subsequent weight regain were observed for the vinyl-ester composites. The weight loss was attributed to molecular extraction from the resin, while the weight regain was related to the formation of microcracks and debonding allowing additional water to be absorbed. Overall, the composites absorbed more water than the neat resins probably due to the presence of voids and fiber/matrix debonding.

Similarly, Phifer *et al*. (2000) observed that vinyl-ester resins immersed in water from 25 to 84°C followed a Fickian uptake behavior with a maximum moisture content of 1.1% and an activation energy of 9.2 kcal/mol. However, pultruded E-glass/vinyl-ester composites exhibited a non-Fickian diffusion behavior at all temperatures from 18 to 80°C with no equilibrium value reached after 80 days of immersion. It also appeared that higher saturation moisture contents would be attained with increasing temperature at and above 55°C. Thus, even though the saturation content of the resin was temperature independent, it seemed that the saturation content of the composite would be dependent upon temperature. Since the moisture content of the composites was found to be higher than a simple estimation combining the rule of mixture with the resin results, it was speculated that the glass fibers, interface, and matrix cracks were influencing the moisture absorption.

3.3.2 Influence of other parameters

The influence of different fabric orientations (uniaxial, biaxial, and triaxial) on the moisture absorption of E-glass/vinyl-ester composites in deionized water at 23°C was studied by Karbhari *et al*. (1998). Increasing the number of base fabric orientations resulted in an increased level of moisture absorption, which was attributed to absorption along interfaces with increased directionality due to the increased number of cross-over points. Furthermore, all specimens appeared to have concentration-dependent diffusion coefficients as evidenced by their two-plateau profiles, which could be due to relaxation effects. Hence, even though the sorption curves could be assumed to be roughly Fickian, they were better described by the Langmuir diffusion model.

Commercial glass fibers are usually supplied with sizing that helps prevent damage to the brittle fibers. Standard sizing materials include resins (or film formers) which provide protection to fibers, lubricants which ease processing, and anti-static agents to prevent charge build-up (Gorowara, 2001). Other materials include various coupling agents (surface-active materials) to enhance the composite performance. The influence of coupling agents on the composite moisture uptake, and therefore durability, can be significant since fibers used in thermosetting polymer composites may have up to 2 wt.% of sizing.

Because E-glass typically contains substantial amounts of alkaline (MgO and CaO) and alkaline earth (Na_2O and K_2O) oxides, which are hydroscopic, water is expected to have a greater affinity towards the surface of untreated

E-glass fibers (Nguyen *et al.*, 1998). Appropriate sizing can, thus, help reduce the amount of absorbed moisture at the interface, and therefore prevent interfacial degradation caused by internal matrix swelling stresses and by direct chemical attack by water (Zhang *et al.*, 2003).

Suri *et al*. (2001) investigated the effect of various coupling agents (concentrations of 0.01, 0.4, and 1% for the methacryl silane solution) on the rate of moisture uptake and moisture saturation level of E-glass/vinyl-ester composites immersed in water at 90°C. They observed that the higher concentrations of silane coupling agent resulted in lower moisture absorption, which was attributed to the stronger resistance of the interfaces to chemical attack by water. Indeed, the specimens treated with 0.01% methacryl silane developed long cracks propagating along the fiber/matrix interface after 480 h of immersion, whereas specimens treated with 0.4 and 1% developed some cracks limited only to an area around the fibers. The interface rupture was associated with matrix swelling and a weak fiber coupling agent–matrix bond. Similarly, Nguyen *et al*. (1998) observed an enhanced hydrolytic stability for silane-treated unidirectional glass/epoxy composite specimens as compared with the untreated specimens. They found that almost no water entered the interface of the silane-treated specimens, while about 10 mono-layers of water built up at the interface of the untreated specimens after 100 h of exposure in water at 24°C. This was attributed to the negative value of the work of adhesion of this later system in water, which suggested that the bond strength between the glass surface and epoxy was weaker than that of the glass surface and water. Hence, the strength of the interactions between the resin and fiber reinforcement is crucial in governing the composite hydrolytic stability.

Liétard *et al*. (2000) examined the effect of post-cure on the moisture absorption behavior of a vinyl-ester resin and unidirectional glass/vinyl-ester composite immersed in deionized water for up to 1000 h at 60 and 90°C. The apparent moisture content (M_a), net moisture content (M_n), and weight loss ($M_i = M_n - M_a$) were determined as a function of exposure time. The resin and composite were characterized by dynamic mechanical thermal analysis (DMTA; T_g = peak of tanδ), differential scanning calorimetry (DSC; comparison of enthalpies for various reactions), and Fourier transform infrared spectroscopy (FTIR; analysis of the absorption bands characteristic of vibrational modes associated with principal functional groups). It was observed that post-cure did not have a significant effect on the net absorption behavior of the resin, only slightly reducing the absorbed moisture content; however, it did influence weight loss, with a substantially lower weight loss as compared with that of the non-post-cured resin. The weight loss was attributed to the extraction of free molecules of the catalyst and initiator and to the loss of free residual styrene. Temperature, on the other hand, significantly increased both the net absorbed moisture content and weight loss. Immersion of the

vinyl-ester resin in hot water was also followed by the progressive disappearance of the first glass transition phase, as well as by a decrease in the T_g of the second glass transition phase, with, however, full recovery after re-drying. This was characteristic of a reversible change due to plasticization of the resin by water. Similar changes were observed for the hygrothermally aged glass/vinyl-ester composites. These results tended to show that the vinyl-ester resin was chemically stable even for hygrothermal ageing at elevated temperatures up to 1000 h, since the damage introduced to the resin by water was reversible and attributed to plasticization. Moreover, as it was observed with the non-post-cured resin, hygrothermal ageing favored 'post-curing' (i.e. continuation of the polymerization reactions) similar to that obtained after post-cure (5 h in air at 90°C), leading to the disappearance of prepolymer chains and free residual styrene. Thus, with increasing exposure time, the difference between the net weight gain of the post-cured and non-post-cured resin diminished.

The water uptake of most polyester and vinyl-ester resin and composite systems exhibits Fickian diffusion behavior when they are immersed in water at room temperature. However, deviation from Fickian behavior is often observed after the first saturation level is reached when immersed at elevated temperatures. This deviation is related to the permanent physical (e.g. formation of microcracks) and chemical (e.g. resin hydrolysis) degradation of the composites and, therefore, becomes more pronounced as the exposure temperature increases. For example, Apicella *et al*. (1983) showed that the dramatically altered behavior of hand laid-up glass/polyester composites observed at 90°C ($T_{g,composites} > 113$°C) was associated with the formation of disc-shaped cracks on the matrix, resin losses, and additional massive fiber debonding and delamination. The observed dissolution of the isopolyester resin at elevated temperatures was in accordance with Abeysinghe *et al*. (1982). In a similar work, Hamada *et al*. (1994) noticed that continuous-strand mat E-glass/polyester composites immersed in water at 80 and 95°C followed a Fickian diffusion behavior at an early immersion time. However, after 100 h at 80°C and 30 h at 95°C, a considerable increase was observed in the net weight gain. This departure from the initial Fickian behavior was attributed to additional moisture being absorbed due to fiber/matrix debonding as well as debonding within fiber bundles. Following debonding, however, some composite mass was lost due to the hydrolysis of the interface resin. Infrared measurements showed that swelling and extraction of polymer occurred after 100 h in water at 80°C as evidenced by the increased absorbance due to the C–H bond, and hydrolysis of the interface occurred after 3000 h as evidenced by the increased absorbance due to the carboxylate group. However, almost immediate matrix and interface hydrolysis occurred after immersion at 95°C. Correspondingly, Harper and Naeem (1989) observed some deviations from Fickian behavior occurring at high temperatures on glass-reinforced

vinyl-ester and polyester laminates. The deviation was related to the leaching out of soluble oxides from the glass fibers (weight loss) and to the formation of surface microcracks (weight gain). Finally, as noticed by Liao *et al*. (1999), increasing water temperature from 25 to 75°C drastically changed the sorption behavior of pultruded E-glass/vinyl-ester composite laminates. At room temperature, the composites followed Fickian behavior, whereas at 75°C, the weight started decreasing after 200 h of immersion, which was attributed to hydrolysis. It can also be pointed out that the 90°-coupons absorbed a higher amount of moisture as compared with the 0°-coupons.

Apicella *et al*. (1982) observed that increasing temperature from 20 to 60°C did not have a noticeable influence on the maximum moisture content of glass/polyester composites; however, the rate of moisture uptake was increased. This observation was in contradiction with that of Harper and Naeem (1989), who showed a temperature dependence of the moisture saturation content. In contrast with the observations obtained at 60°C and below, higher rates of moisture uptake as well as much higher maximum moisture levels were reached at 90°C; these were attributed to possible microcavitational damage (Apicella *et al.*, 1982). Furthermore, the subsequent weight loss observed both at 60 and 90°C tended to indicate that unreacted components or partially bonded groups were desorbed easily and preferentially to the debonded and water-coated fibers. In similar studies by Sridharan (1987), it was observed that the moisture saturation level of E-glass/vinyl-ester composites immersed in distilled water at 25, 50, and 80°C reached approximately 0.4%, irrespective of temperature. As expected, the time to reach equilibrium decreased as temperature increased (600, 400, and 300 h at 25, 50, and 80°C, respectively). Some weight loss was also evidenced, about 0.07%, due to leaching out from the resin. Surprisingly, however, the authors did not notice any change in the chemical structure of the hygrothermally conditioned resin nor formation of any new chemical species using FTIR. Finally, the rather low moisture content combined with the small decrease in T_g (drop of 6°C) following immersion in water suggested that plasticization of the matrix by water was very small.

3.3.3 Influence of fluid type

Experiments were conducted over a 3-month period by Bradley and Grant (1995) on unidirectional E-glass/vinyl-ester composite laminates immersed in distilled water, seawater, and seawater at 20.7 MPa to compare the relative absorption in the different waters and to determine the effect of hydrostatic pressure. They observed that the saturation level in distilled water was slightly higher than in seawater presumably due to salt and/or trace elements being absorbed less readily. The hydrostatic pressure, however, only barely affected moisture absorption, which was attributed to the greater driving force for

moisture absorption under pressure being compensated by the reduction in free volume of the matrix. About 75% of the saturation moisture gain was achieved after 1 week, reaching 1 and 0.6% after 3 months for glass/vinyl-ester systems 411 and 510, respectively. The weight gain was reported as a percentage of matrix weight and was compared with the weight after processing, since no drying procedure was used.

The effect of an immersion in distilled water or exposure to various relative humidities (40, 60, 100% R.H.) at different temperatures (23 and 50°C for water; 32, 50 and 65°C for humid air) on the moisture absorption of E-glass/polyester composites was investigated by Loos *et al*. (1980). The results indicated that the weight change was affected by exposure time, temperature, and composition of the environment, and the influence of each of these parameters was assessed by evaluating the apparent maximum moisture content and apparent diffusivity. It was found that the apparent moisture content was dependent upon the relative humidity – increasing with increasing relative humidity – but relatively insensitive to temperature, while the apparent diffusivity was dependent upon the relative humidity as well as strongly affected by temperature – increasing with increasing relative humidity and temperature. A comparison between experimental and estimated weight gain values using Fick's law and the apparent diffusivity showed that they agreed well until the apparent maximum moisture content was reached, after which deviation was observed especially at high temperatures and humidities. Subsequent weight gain occurred owing to the development of microcracks in high-temperature moist environments. This ingress of moisture in the material caused the loss of resin particles resulting in further weight loss. In addition, it is the ratio between these two phenomena that would dictate whether the final weight change would increase or decrease. Similarly, Jacobs and Jones (1993) observed that the equilibrium moisture content of an unsaturated polyester resin increased, as expected, with increasing relative humidity (0, 46, 75, 96 and 100% R.H.).

An interesting review of weather data from six worldwide locations was published by Collings (1986). The author reported the effect of the respective climate conditions (temperature, relative humidity) of these locations on the diffusion coefficient and moisture saturation level of epoxy composites, and suggested a 'universal' constant humidity of 84% R.H. that might simulate the moisture levels typical of the natural climates, to which the polymer composites are most likely to be exposed.

3.4 Effect of moisture on mechanical and physical properties

The presence of moisture significantly affects the mechanical properties of FRP composites – and in particular their tensile, flexural, and short-beam

shear characteristics – as a result of the degradation of the matrix, fibers, and interfaces.

3.4.1 Effect on resins

Polymer matrices undergo severe degradation when immersed in water at elevated temperatures. Experiments conducted on polyester resins at 90°C (Apicella *et al.*, 1983) showed for instance that local autocatalyzed hydrolysis led to the formation of randomly distributed disc-shaped cracks, which further embrittled the matrix. The cracks acted as nuclei for stress concentrations and caused brittle fracture under tensile loading. A study on a bisphenol polyester resin (Apicella *et al.*, 1982) showed that ageing in water, especially at elevated temperatures, induced an increase in T_g and elastic modulus as well as an increase in brittleness. The desorption of low-molecular-weight segments from the matrix was found to be predominantly responsible for the embrittlement of the matrix and, together with residual curing, resulted in an increase in T_g. On the other hand, the increase in T_g sometimes observed in epoxy resin systems after immersion in an aqueous medium is generally related to the formation of strong intermolecular hydrogen bonding, which stiffens the network (Mensitieri *et al.*, 1995). The tendency for moisture sorption by hydrogen bonding is attributed to the presence of a large amount of unreacted secondary amines in the cured epoxy resins. Conversely, another study on an unsaturated polyester resin (Jacobs and Jones, 1993) showed that an increase in moisture equilibrium content (due to a higher relative humidity exposure) resulted in a decrease in T_g. The authors explained that the initial slope of the T_g/M_∞ curves represented plasticization effects by individual water molecules, while at higher moisture contents clustering of water molecules occurred with a smaller effect on T_g. Hence, the higher plasticization efficiency at lower moisture concentrations indicated that direct interaction of water with polymer chains was more important than the additional free volume created when clustering of water molecules occurred.

Durability experiments performed on vinyl-ester and isophthalic polyester resins in water at 60 and 90°C showed that the T_g of both resins increased with immersion time, although in a non-uniform manner (Chin *et al.*, 2001a). The increase was associated with hydrolytic degradation of the resin and subsequent dissolution of low-molecular-weight segments in accordance with Apicella *et al.*, (1982). An overall decrease in ultimate tensile strength was also observed for both resin systems at all test temperatures (22, 60, and 90°C), with a greater degradation in strength at the higher temperatures. However, it should be noted that immersion of the vinyl-ester resin in room-temperature water for about 60 weeks did not significantly reduce its tensile properties.

In view of the changes occurring in the strength and T_g of resins immersed in water at various temperatures, models have been developed to try to correlate the degradation in their mechanical and physical properties. For instance, Chamis *et al.* (1981) demonstrated the relationship between the mechanical properties of a resin in the wet state and its properties in the dry state as

$$\frac{\text{Property, wet, test temperature}}{\text{Property, dry, room temperature}} \sim \sqrt{\frac{T_{g,w} - T}{T_{g,d} - T_0}} \qquad [3.9]$$

where T is the test temperature (K), $T_0 = 273$ K, and $T_{g,d}$ and $T_{g,w}$ are the glass transition temperatures (K) in the dry and wet state, respectively, measured by DMTA and determined using the storage modulus, E'. Another model was developed by Kambour (1983) in the domain where the material is ductile, which related the yield stress σ to T_g by a constant C_k, as

$$\sigma = C_k(T_g - T) \qquad [3.10]$$

As a consequence, since plasticization leads to a decrease in T_g, it also leads to a decrease in σ. This effect becomes important when the material is not far from its T_g and subjected to loads (Pascault *et al.*, 2002), since water absorption can induce yielding.

3.4.2 Effect of FRP systems

The mechanical properties of composites are generally less sensitive to hygrothermal ageing as compared with those of resins because of the presence and strong influence of fibers. However, they are affected by fiber debonding favored by hydrolysis of the matrix and delamination (Apicella *et al.*, 1983). Additionally, tensile properties, for instance, can be influenced both by plasticization of the matrix due to water sorption and by an increase in stiffness due to loss of low-molecular-weight substances from the matrix (Apicella *et al.*, 1983; Mensitieri *et al.*, 1995). As a consequence of moisture-related degradation of the fibers, matrix, and interface, substantial reductions in longitudinal (Phifer *et al.*, 2000) and transverse tensile strength (Bradley and Grant, 1995), compressive strength (Collings *et al.*, 1993), short-beam shear strength (Nguyen *et al.*, 1998), and flexural strength (McClurg and Vaughan, 1998) are often observed.

An investigation of the retention strength of hygrothermally aged pultruded cross-ply E-glass/vinyl-ester composite laminates was conducted by Phifer *et al.* (2000). The specimens were exposed to tap water at temperatures of 18, 35, 45, 55, 65, and 80°C for up to 80 days. Fracture analysis of the tension specimens showed a change in the failure mechanisms. While unaged composite specimens were characterized by a sudden and extensive

delamination upon failure, specimens aged at 80°C for 80 days failed suddenly with little or no delamination because of the significant debonding, fiber damage in the form of cracks and chips, and resin microcracking present in the composites. On the other hand, specimens aged for shorter times developed a continuous delamination and fiber breakage, with progressive failure from the outer surfaces into the inner core. The tensile strength values were scattered, which may be attributed to the non-uniformity in the concentration of microcracking in the aged composites. Hence, some specimens exhibited extensive microcracking in resin-rich areas, while others did not. However, a clear decrease in the composite tensile strength with increasing immersion time and temperature was evidenced. A 4-day exposure in water at 45 and 80°C yielded a retention strength of 85 and 65%, respectively, whereas an 80-day exposure resulted in retention strengths of 65 and 35%, respectively. Some amount of recovery was obtained after re-drying the specimens, with a higher recovery in strength with respect to the wet strength at the lower immersion temperatures. Finally, an Arrhenius analysis was utilized to assess any change in the degradation mechanisms during stress corrosion of the polymer composites. Two different approaches were used: one proposed by Phani and Bose (1987) and the other one proposed by Heitman and Lindstrom (1964). A definite change in the activation energy was observed at 45 and 35°C, respectively, using Phani and Bose's analysis and Heitman and Lindstrom' first model. However, using a modification of Heitman and Lindstrom's model to address diffusion limitations, the knee for the activation energy was found to occur at 55°C. Thus, it was concluded that a change in the activation energy of the wet remaining tensile strength of E-glass/vinyl-ester composites immersed in water from 18 to 80°C was taking place between 35 and 55°C, with a higher activation energy at the higher immersion temperatures. This suggested that time/temperature superposition was not a valid technique for accelerated ageing of this composite system due to a change in the degradation mechanisms around 45°C.

Karbhari *et al*. (1998) studied the short-term environmental effect (1 year) of deionized water on the tensile properties of uniaxial, biaxial, and triaxial E-glass/vinyl-ester composites. It was shown that water exposure significantly affected their tensile strength, and to a lesser extent, their tensile modulus. The tensile strength of immersed specimens was found to decrease initially, then increase due to post-cure effects, and finally decrease again with a maximum degradation in residual strength for the uniaxial specimens. Thus, two competing mechanisms were occurring during ageing, namely post-cure as well as resin and bond degradation by water. As expected, the amount of degradation in the residual tensile strength was greater at 62°C than at 23°C; however, similar failure mechanisms were observed at both temperatures.

Apicella *et al*. (1982) showed that glass/polyester composites immersed for 15 days in water experienced a reduction in elastic modulus with increasing

test temperature due to greater plasticization effects, and an increase in the elongation at break up to 60°C followed by a decrease at 90°C, which was correlated with an increase in T_g at the higher temperatures. In another study (Apicella *et al*., 1983), they confirmed that the short-term exposure of glass/polyester composite laminates to water at 20°C resulted in a decrease of the elastic modulus due to plasticization, while exposure to water at 90°C led to an increase in the elastic modulus and T_g due to embrittlement of the matrix. The latter increase was explained by the effect of the resin loss (dissolution of low-molecular-weight elements) overcoming the effect of water plasticization.

According to experiments conducted by Boller (1956) on glass/polyester composite laminates, the composite tensile strength decreased by about 30% following a 1-year immersion in water at 73°F. This decrease was accompanied by a slight increase in tensile modulus. On the other hand, tensile tests performed by Liao *et al*. (1999) on E-glass/vinyl-ester composite specimens aged in room-temperature water showed a substantial decrease in tensile modulus (23%) and tensile strength (29%) after 9120 h of immersion.

In another study, Liao and Tan (2001) studied the *in situ* tensile strength of unidirectional E-glass fibers in an epoxy matrix model immersed in water at 25°C to assess the influence of the resin on the fiber property degradation. They concluded that under stress-free ageing in water, it was the synergistic action of moisture-induced tensile stresses and subsequent stress corrosion by water that played an important role in the strength degradation of the glass fibers in the composites and, consequently, strength degradation of the composites. Tensile stresses could be introduced to the fibers due to the higher coefficient of moisture expansion of epoxy resins, and water could also accelerate the strength reduction by its well-known corrosive action. The fiber strength degradation was obvious after 500 h of immersion, at which point moisture saturation was reached. After 500 h of immersion, however, the degradation rate diminished because of fiber/matrix debonding causing the tensile stresses in fibers to be relaxed.

A study by Suri *et al*. (2001) demonstrated the importance of an appropriate coupling agent to the tensile and fracture properties of E-glass/vinyl-ester composite laminates immersed in water at 90°C. They showed that the lowest concentration of methacryl silane for the coupling agent resulted in the least amount of degradation in tensile strength despite the presence of interfacial macrocracks; the 0.01 and 1% treated specimens showing a 15 and 30% strength loss, respectively, after 480 h of immersion. They also observed that the tensile strength was more sensitive to water content and coupling agent formulation than the Young's modulus. The modulus was found to decrease slightly with increasing water content; however, there was no clear effect of the coupling agent formulation. A comparison of stress–strain curves also showed that the ultimate strain of the composites decreased significantly

with increasing water content. Mode II fracture tests performed in a three-point flexure configuration showed for all specimens an unstable crack propagation through the interface. The stable interlaminar fracture propagation of the 0.01% treated composite after 480 h of immersion was related to the presence of macrocracks that slowed down crack propagation, the initial fracture toughness being higher than the propagation one. The mode II interlaminar fracture toughness, G_{II}, was calculated using

$$G_{II} = \frac{9P^2Ca^2}{2B(2L^3 + 3a^3)} \qquad [3.11]$$

where P is the maximum load, C is the load point compliance, a is the crack length, B is the specimen width, and L is the half-span of the bending supports. The fracture toughness values were found to decrease with increasing immersion time, thus with increasing moisture-related crack size and density. Finally, a comparison of load-displacement curves for all materials showed that load and displacement significantly decreased at long immersion times ($t = 480$ h) with a greater loss as the methacryl silane concentration decreased. This explained the decrease in fracture toughness that may be related to increasing interfacial damage by water. Hence, even though an increasing concentration of methacryl silane in the coupling agent had opposite effects on the retention strength and fracture toughness of the composites, it improved the resistance of the overall composite to degradation by water by limiting interfacial damage.

Bradley and Grant (1995) examined the effect of an immersion in distilled water, seawater, and seawater at 20.7 MPa on the transverse tensile strength of two vinyl-ester resin systems (numbers 411 and 510) reinforced with unidirectional E-glass fibers. The glass/vinyl-ester system that absorbed the least amount of water (510) also experienced the least amount of degradation in its transverse tensile strength, with a 20% reduction after 3 months of immersion. It is also worth noting that the transverse tensile strength was essentially the same for the immersion in distilled water, seawater, or seawater under hydrostatic pressure.

The effects of moisture and elevated temperatures on the longitudinal flexural properties of unidirectional pultruded E-glass/vinyl-ester composites were investigated by Sridharan *et al.* (1998). The composites were aged in dry air or in distilled water at 25, 50, and 80°C. The longitudinal flexural strength of the composites was found to be relatively unaffected by immersions at 25 and 50°C; however, it was substantially decreased at 80°C with a 23% drop after 1500 h. As evidenced by electron microscopy, interfacial debonding occurred at 80°C after 63 days allowing moisture to come into direct contact with the glass fibers. The fibers then underwent stress corrosion, i.e. growth of existing flaws leading to superficial crack formation and growth, and ultimately failure. Thus, it was the combined degradation of the interface

and fibers that led to the loss of load-bearing capacity of the composites. Furthermore, analysis of fracture modes showed that failure of the composites always occurred in tension due to fiber fracture, since the phenomenon of stress corrosion was enhanced under tensile stresses. Unlike flexural strength, the flexural modulus was found to decrease with increasing immersion time at all temperatures, with a greater reduction at high temperatures and short times, followed by a plateau. For instance, the composites aged at 80°C experienced a 14% drop in modulus after 1500 h of immersion. Additionally, the properties of the neat vinyl-ester resin were investigated, and it was shown that the temperature and moisture effects on the neat resin were not as pronounced as on the composites. For instance, the flexural modulus of the neat resin continuously decreased at 50 and 80°C reaching about 92% of its original value after 1350 h of immersion. However, the drop in flexural strength was much greater, reaching about 80% of its original value at both temperatures. Finally, a comparison of the composite flexural modulus and strength at 80°C under dry and wet conditions showed that moisture had the most detrimental effect on the retention strength of the composites. The flexural modulus was reduced by 5% after 1680 h in the hot, dry environment as compared with a reduction of 17% in hot water due to the absorbed moisture content. On the other hand, the flexural strength increased by 9% during the same period in hot, dry air due to an increased degree of cross-linking of the resin as compared with a 20% drop in hot water.

Similarly, the influence of ageing in deionized water at 25 and 75°C on the flexural properties of pultruded E-glass/vinyl-ester composite laminates was investigated by Liao *et al*. (1999). They observed that the flexural modulus of the 0°-coupons remained essentially the same after ageing in water, even at 75°C with only a 10% drop. However, the flexural strength did show some amount of degradation with a 5 and 40% decrease, respectively, after 3900 h at 25°C and 2400 h at 75°C. The failure process under flexural loading was also analyzed, i.e. failure started with the formation of transverse matrix cracks on the tensile side of the specimens, followed by failure of fibers and finally initiation and propagation of delamination. Moreover, scanning electron microscopy (SEM) of the fractured 0°-fibers suggested a strong link between the fiber strength degradation – related to the fracture mirror surface and the composite flexural strength degradation. However, now considering 90°-specimens, the significant difference between the reduction in fiber strength (only a few percent) and composite flexural strength (40%), comparing an immersion in water at 25 and 75°C, implied that the matrix or more likely the fiber/matrix interface played an important role in the accelerated degradation process observed at 75°C. The degraded interfacial bonding was evidenced by the smooth fiber surfaces of the failed aged 90°-specimens.

The rate of degradation in the flexural properties of pultruded unidirectional glass/epoxy, glass/vinyl-ester, and glass/polyester composites immersed in

water at 93°C for up to 3 weeks was characterized by McClurg and Vaughan (1998). The flexural strength of the glass/epoxy and glass/vinyl-ester composites exhibited an exponential decay with exposure time. The most significant decrease in flexural strength occurred within the first week of immersion. Using an exponential decay model, it was predicted that the minimum flexural strength of the glass/epoxy and glass/vinyl-ester composites would attain 47 and 55% of the original strength of each material, respectively. The same general trend was observed for the glass/polyester composite system; however, the exponential decay model did not correlate as well in this case. It appeared that the polyester resin weakened during the hot–wet exposure because of its T_g being lower than the exposure temperature. This resulted in a change in the failure mechanism, for exposure times greater than 2 weeks, characterized by fiber and resin buckling under the loading nose. This failure mode differed from that required by ASTM D790-03 (2003) and, hence, may explain the deviation from the exponential decay model at longer exposure times. Thus, the severity in the degradation of the flexural strength was dependent upon the glass/resin system used. As for the flexural modulus, it was affected by temperature and moisture to a lesser extent than the flexural strength. The modulus of elasticity of the glass/epoxy composites initially decreased and then tended to recover at longer exposure times, that of the glass/vinyl-ester composites remained relatively constant, while that of the glass/polyester composites showed a marked decrease. Additionally, some weight loss was observed in all composite systems after 5–7 days of immersion due to exposure to moisture or moisture/temperature, and may be attributed to the dissolution of the binder material at the fiber/matrix interface. Finally, a direct correlation between the change in specimen width and the change in weight was observed.

Hamada *et al*. (1994) studied the short-term effect (4000 h) of an immersion in water at high temperatures on the bending modulus of E-glass/polyester composites to clarify the change in degradation mechanisms occurring above 80°C. They found that the modulus initially decreased with immersion time due to a reduction in the matrix rigidity, before reaching a plateau, with a lower final value for the 95°C immersion as compared with the 80°C immersion. The initial decrease at 80°C was related to swelling of the polymer matrix and fiber/matrix debonding, while the initial decrease at 95°C was also due to debonding but primarily related to degradation of the interface through hydrolysis. For longer immersion times (3000 h), the modulus of the specimens immersed at 80°C finally leveled off to the same value as that of the specimens immersed at 95°C, retaining about 75% of its original value. This final decrease corresponded to the occurrence of interface hydrolysis in the composites immersed at 80°C. Thus, both chemical degradation (resin and interface hydrolysis) and physical degradation (swelling and debonding) had an effect on the reduction in bending modulus. Conversely, experiments

conducted by Boller (1956) showed a decrease in the flexural modulus of glass/polyester composite laminates following a 1-year immersion in water at 73°F.

3.5 Synergistic effects of stress and hygrothermal exposure

GFRP composites are known to fail when subjected to long-continued loads at stresses less than the ultimate strength of the material. Therefore, the study of the effects of an applied stress in the form of sustained loading, creep, or stress-rupture combined with an immersion in an aqueous medium is necessary in order to understand and to be able to predict the mechanical response of GFRP composites under actual service conditions.

The diffusion of water in a polymer-matrix/fiber composite is highly anisotropic, being faster in the fiber direction than in the transverse direction because of the capillary effect. Fahmy and Hurt (1980) utilized the free volume concept in order to account for the effect of stress on the diffusion of water in resins. The free volume of a polymer corresponds to the difference between its specific volume and the actual volume of its molecules, and is widely accepted to be equal to 1/40 at a temperature below T_g. Considering a uniform pressure or uniaxial stress around the fibers, $\sigma = -P$, they demonstrated that

$$D_\sigma \approx D_0 \, \mathrm{e}^{\frac{6 \text{ to } 10\sigma}{G}} \qquad [3.12]$$

where D_σ and D_0 are the diffusion coefficients in the presence and absence of stress, respectively, G is the material shear modulus and σ is the applied stress. In addition, experiments were conducted on a bent epoxy bar, and results showed that the excess curvature in the wet bent specimen as compared with the dry bent specimen was correlated to the difference in water pick-up on both sides. Indeed, more water was absorbed on the tension side than on the compression side.

The main penetration mechanism of water into a polymer matrix is diffusion, i.e. the transport of water molecules through holes in the polymer structure (Marom, 1985). Thus, the water mobility will depend on the size of these holes, which in turn depends on the free volume of the matrix. An analogous model to that presented by Fahmy and Hurt (1980) was proposed by Neumann and Marom (1985) to account for the effect of external stress on the diffusion coefficient of moisture in bulk resins and unidirectional reinforced composites. This model was derived using the Doolittle equation (linking mobility to free volume) and the calculation of Fahmy and Hurt (1980) presented above. It attributed the effect of external loading on the diffusion coefficient to a change in the free volume of the polymer matrix, which is equal to its volume strain.

$$\ln \frac{D_\sigma}{D_0} = a\left(\frac{1}{v_{f0}} - \frac{1}{v_{f\sigma}}\right) \qquad \text{Bulk resin} \qquad [3.13a]$$

$$v_{f\sigma} = v_{f0}\left(1 + \frac{\sigma}{4G}\right) \qquad [3.13b]$$

Thus, the ratio of the moisture diffusion coefficient in composites in a stressed and unstressed state is expressed as a function of the matrix volume strain, $(\Delta V/V_0)_m$, itself a function of stress level, fiber volume fraction, and angle between the applied stress and the fiber direction:

$$\ln \frac{D_\sigma}{D_0} = b\left(\frac{1}{v_{fo}} - \frac{1}{\left(\frac{\Delta V}{V_0}\right)_m + v_{fo}}\right) \qquad \text{Unidirectional composite} \qquad [3.14]$$

where a and b are proportion constants, v_{f0} is the free volume fraction under no stress, and $v_{f\sigma}$ is the free volume fraction under stress. Thus, changes in the free volume of the resin due to external loading will affect the diffusion mechanism. However, since external loading also enhances debonding and, hence, capillarity flow along fibers, the capillarity mechanism is expected to be dependent upon the normal component of the applied stress. Finally, in order to account for edge effects, specific correction factors can be added to the diffusion coefficient of the resins and composites (Marom and Broutman, 1981).

Numerous papers have been published on the effect of various sustained stresses on the sorption behaviors and mechanical properties of carbon/epoxy composites, thus it is worth reporting a few of their results. For instance, Neumann and Marom (1987) studied the effect of a tensile load on the moisture diffusion parameters of carbon/epoxy composites and reported that an increasing stress level resulted in an increased rate of moisture uptake and moisture saturation content, therefore increasing the diffusion coefficient. On the other hand, Henson and Weitsman (1986) investigated the effect of transverse tensile stresses on the sorption of water vapor (97% R.H., 40°C) in epoxy resins and unidirectional graphite/epoxy composites. An interesting observation was that the amplitude of data scatter for moisture uptake increased with increasing stress level. However, the increased stress level unquestionably resulted in an increase in moisture uptake, with a rather linear increase of the maximum moisture content with increasing applied stress for the composites. For both resins and composites, external stresses affected the diffusion process and the sorption behaviors departed from classical Fickian diffusion, which was attributed to the time-dependent response of the resin and to the introduction of damage in the composite via debonding and coalescence into continuous cracks. Finally, it was shown that in epoxy

resins stresses appeared to raise the moisture saturation levels, while in epoxy composites stresses appeared to affect the entire sorption process accentuating asymmetries between the absorption and desorption behavior.

Among the few publications available to date on the effect of static bending stresses on the water absorption characteristics of GFRP composites, are the works by Kasturiarachchi and Pritchard (1983), Marshall *et al*. (1982), and Karbhari *et al*. (2007). Kasturiarachchi and Pritchard (1983) tested unidirectional glass/epoxy laminates under flexural loading at 95% R.H. and 80°C. As they showed, bending stresses did not have a significant effect on the water absorption magnitude or on the diffusion coefficient of moisture, because of the opposing effects of tension and compression stresses on water diffusivity. Still, surface damage such as fiber buckling and fiber rupture with tearing of the laminate surface was observed on the compressive side of the samples subjected to the highest bending stresses (≥30% of ultimate strain). However, it should be noted that the diffusion experiments under four-point bending were conducted over a 45-day period only, therefore it cannot be concluded as such that bending stresses do not have any long-term effect on moisture absorption. Furthermore, as the authors themselves pointed out, their short-term values for the diffusion coefficient are not fully consistent because of the difficulty in assessing M_∞ and because of edge effects. Finally, bending stresses did indeed cause significant damage as shown by the delamination, cracking, and fiber buckling observed. In fact, a different conclusion was drawn by Marshall *et al*. (1982), who observed that the water content of glass/vinyl-ester composites placed in water at 20°C under four-point bending was unaffected by a stress of 70 MPa on the compressive side but was enhanced on the tension side due to an increased diffusion coefficient. Therefore, the diffusion coefficient was globally enhanced by flexural stresses.

Meyer *et al*. (1999) reported that glass/polyurethane composites subjected to a constant tensile strain or a nearly constant tensile stress in water had their tensile strength and modulus considerably decreased as well as their weight gain increased with increasing strain/stress level. Immersion in distilled water for 300 h under no load reduced the composite strength by 2–8%, while loading under 50% of the original ultimate strength reduced the composite strength by 12–16%, depending on the type of loading. The two loading methods (constant tensile strain test and constant tensile load or 'spring load' test) showed similar degrees of degradation, suggesting that the initial strain-induced damage (e.g. matrix microcracking, debonding, and fiber fracture) combined with the immersion in water controlled the property degradation. For the constant stress application, the creep strain (or residual strain, probably due to polymer-phase molecular motion and not to damage) also increased with increasing applied load; however, it did not significantly affect the reduction in tensile properties.

The individual and combined effects of hygrothermal ageing at elevated temperatures and sustained loading under constant flexural deformation or stress were studied by Liétard *et al.* (2000). Unidirectional glass/vinyl-ester composites with and without post-cure were immersed in deionized water for up to 1000 h at 60 and 90°C and tested under three-point bending. The flexural properties – i.e. flexural modulus, strength, and strain – were shown to degrade upon prolonged exposure in water, with a more pronounced decrease for the 90°C immersion. However, a significant initial increase in properties was observed for the non-post-cured composites immersed at 60°C; on the other hand, a substantial decrease in the properties of the post-cured composites immersed at 90°C was observed. After 1000 h of exposure, however, the difference between the properties of the post-cured and the non-post-cured composites disappeared. Thus, it was concluded that two phenomena were competing: a 'post-curing' effect due to the immersion in water coupled with a water degradation effect, especially at the fiber/matrix interface. This competition occurred mainly for short exposure times, since for longer times the degradation effect overcame the 'post-curing' effect. Thus, although the absence of post-cure resulted in higher weight loss for the composites, which was attributed to hydrolysis and/or loss of low-molecular-weight elements from the matrix, it did not affect their long-term residual mechanical properties, since the hydrothermal ageing had partially similar effects (i.e. continuation of polymerization reactions) on the composites as the post-cure step. Additionally, some composite specimens (with and without post-cure) were subjected to a constant flexural stress of 335 MPa (corresponding to 50% of the strength of post-cured composite at 60°C) while immersed in water at 60°C. The post-cured composites exhibited a much longer time to failure (96 h versus 55 min), whereas the non-post-cured composites had a greater strain at rupture, indicating a higher ductility due to a greater mobility of the polymer chains. Some experiments were also carried out under constant deformation and, because of stress relaxation effects, the degradation mechanisms were very slow. For instance, non-post-cured composites subjected to 80% flexural strain and immersed in water at 60 and 90°C did not fail after 19 months of exposure. Thus, even though experiments under constant deformation are convenient, they are not very useful for prediction.

Creep experiments under tension and three-point bending were performed by Lagrange *et al.* (1991) on unidirectional E-glass/polyester laminates to assess the influence of a static stress on the kinetics of water diffusion. The weight change was found to be clearly dependent upon the composition of the environment and the nature and intensity of external loading. A lower moisture saturation content was recorded for immersion in seawater versus distilled water and an increase in temperature from 5 to 40°C resulted in an increased rate of moisture uptake as well as an increased moisture content at saturation. The creep tensile and bending experiments also showed that the

rate of moisture uptake and moisture saturation content depended upon the load, even though the moisture absorption was more enhanced by an increased load under tensile stress than under bending stress, which would be in accordance with the results reported by Marshall *et al*. (1982). However, the diffusion coefficient seemed independent of the nature and level of load applied. In another study conducted by Boller (1956) on the tensile and flexure creep behavior of glass/epoxy and glass/polyester laminates immersed in water at 73°F, it was observed that the creep strain increased with increasing time and load applied, and that failure occurred much sooner in specimens immersed in water as compared with those exposed to air. Both the creep data also showed that the value of the ratio of strain at failure to elastic strain decreased with increasing stress level. Additionally, the tensile creep behavior could be expressed fairly accurately by an equation of the form

$$\varepsilon = \varepsilon_0(1 + t^n) \qquad [3.15]$$

where ε is the total strain under constant stress, ε_0 is the initial strain and n is a dimensionless exponent. As mentioned in a work by Worley and Findley (1950), n and ε_0 can be used to compare materials. Indeed, the present results also indicated that n was dependent upon the composite material and the composition of the environment, while ε_0 was a function of the applied steady stress. Finally, Hojo and Tsuda (1979) performed tensile creep-rupture tests on vinyl-ester resins and E-glass/vinyl-ester composites in water at 50°C to investigate the effects of water and stress on their time-dependent degradation behavior and mechanism. At an early stage of immersion under no load, the tensile strength held an initial level, and then decreased linearly with increasing immersion time. Moreover, the creep-rupture tests showed a linear logarithmic decrease of the applied stress versus time to rupture and a linear increase of the elongation at rupture with decreasing stress ratio (applied creep stress/initial tensile strength). A comparison between the creep-rupture and immersion test data suggested a similar degradation behavior, hence it was concluded that when immersion in water is considered, conventional immersion tests under no load might be sufficient in order to estimate the properties of composites subjected to stress for long periods, which is in disagreement with the conclusions from Liétard *et al.* (2000).

The detrimental effect of an immersion in water on the stress-rupture behavior of glass/epoxy and glass/polyester composite laminates loaded in tension, flexure, and shear was studied by Boller (1956). The stress-rupture data demonstrated that all the specimens placed in water failed under a much lower applied stress level than the specimens in air, if similar failure times were considered, for all three loading cases. As expected, the stress at rupture was found to logarithmically decrease with increasing time to failure, and the rate of decrease was greater in water than in air. A different conclusion, however, was drawn by Lyons and Phillips (1981), who conducted tensile

dead-load tests on chopped-strand mat/isopolyester composites in air and water under 70% or more of the ultimate reinforcement stress. The scatter in their results was such that no significant changes in stress-rupture behavior were detected between the samples loaded under constant stress in air, the samples either preloaded at 50% nominal tensile strength for 10 days in air or unloaded intermittently during testing in air, and finally the samples loaded under constant stress while immersed in water. However, although preloaded samples were expected to fail at similar times to samples under steady load in air, the former exhibited fewer resin cracks. This was attributed to the resin being allowed to creep because of the more gradual loading. Even an immersion in water had no deleterious effect on the failure times. Finally, the fracture surfaces of samples loaded in air were analyzed and showed that resin cracks originated at points of fiber debonding (due to the applied stress), and subsequently propagated to the specimen surfaces. This constituted the first step in damage accumulation. The fracture was then thought to spread by intermittent load transfer between adjacent fiber bundles, followed by environmental stress-cracking of the glass fibers under the influence of atmospheric moisture, finally followed by further increments in resin cracking.

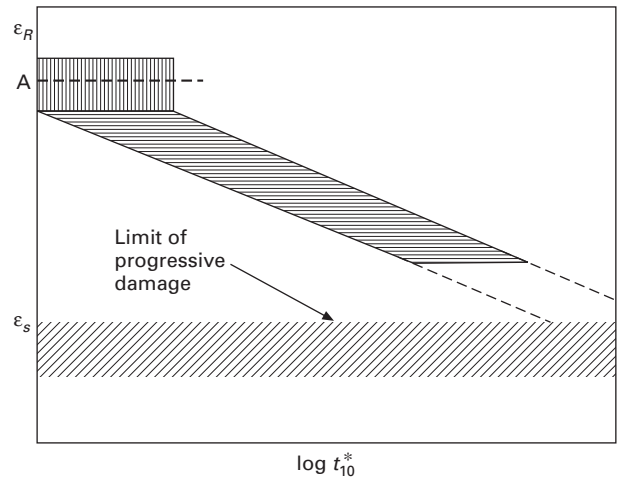
It has been observed that certain composite laminates (e.g. glass/polyesters) behave differently during environmental stress-rupture in water at stresses above and below 50% of the ultimate tensile unit load (UTUL). For instance, White and Phillips (1985) discussed the effect of various load levels on the mechanism of environmental creep-rupture of bi-directional glass/polyester laminates immersed in seawater at 20 and 60°C under tension. They observed that below 50% UTUL, the samples tested in air did not fail, while the samples immersed in water did fail; however, the failure times were apparently insensitive to the load level. Thus, chemical effects were predominant, in particular the effect of temperature. Between 50 and 85% UTUL, the influence of water was apparent through stress-induced pitting of fibers at cross-over points. The cross-over points were preferential sites for absorbed water and, therefore, pitting attack and debonding in stressed laminates, since water had rapid access to these points through cracks formed along the transverse rovings. Multi-filament fracture was also evidenced and caused high local stress concentration, encouraging the formation of roving cracks. The time dependence for growth of these defects can arise from load transfer in the vicinity of broken fibers by creep of the resin and from the enlargement of fiber pits. Finally, above 85% UTUL, the accumulation of damage in the composites through resin creep was such that the time to failure was not significantly influenced by a change in the environment (e.g. temperature) anymore.

The stress-rupture mechanism of E-glass/polyester composite laminates immersed in water at various temperatures under tension was investigated by Pritchard and Speake (1988), who also concluded that temperature is a

determining factor for failure. The authors developed a four-stage failure process for the composites subjected to a tension load to account for the order of occurrence of cracks and debonding, which influenced the possible migration paths of water. An interesting observation was that transverse cracking occurred only at 30°C and not at higher temperatures, since the matrix was presumably allowed to creep at higher temperatures, relieving stresses and, thereby, avoiding extensive debonding and microcracking. Indeed, stress relief in the matrix becomes easier as the exposure water temperature approaches or surpasses the T_g of the resin. Another important observation was that the rupture times at 45°C were greater than those at 30 and 60°C, irrespective of the load level. This was attributed to the competing effects of diffusion rate (i.e. greater absorption and moisture-related property degradation at high temperatures) and matrix toughness (lesser amount of debonding and microcracking at high temperatures).

Using a mechanical approach, Chateauminois *et al*. (1993) examined the stress-rupture behaviors of unidirectional glass/epoxy composites under three-point bending when immersed in distilled water at 30, 50, 70, and 90°C. It was shown that hygrothermally induced defects resulted in a temperature-dependent decrease of the static fatigue properties, which was associated with a decrease of the monotonic properties. Furthermore, they showed that the nucleation of these defects was irreversible because of the non-recoverable strength and strain to failure upon re-drying. In addition, the lowering of the endurance properties at 90°C was associated with a transition from a progressive to a non-progressive damage, as will be explained later. The *in-situ* analysis of the tensile side of specimens aged at 90°C showed that first there was delocalized multiplication of broken fibers and that, second, the stress concentration at the vicinity of the broken fiber ends often resulted in the nucleation of matrix cracks. Hence, the damage evolution was governed by the local tolerance of the composite to these first nucleated defects, and the initial loss in stiffness during this first stage – attributed to fiber breakage and viscoelastic relaxation of the matrix – then tended to stabilize. In a second stage, there was drastic tensile failure of the composite characterized by a sudden drop in stiffness without any previous macroscopic damage. The difference in behavior between aged and unaged specimens was that for unaged specimens the second stage consisted of the progressive propagation of localized damage (i.e. matrix cracking, fiber cracking, and interfacial shear failure at crack tip) characterized by an important but progressive loss in stiffness. Thus, to correlate the damage evolution with properties of composite constituents, stress-rupture data were reported in damage maps (Chateauminois *et al.*, 1993).

A schematic of this map for static bending fatigue in air is presented in Fig. 3.3 and features a horizontal band centered around A (strain level inducing 10% stiffness loss) and a sloping band terminating at ε_S (resistance to crack



3.3 Schematic of damage map for static bending fatigue in air. ε_R is maximum strain.

propagation from the first defects created during loading). The top horizontal band corresponds to a non-progressive damage and a failure characterized by delayed fiber breakage, while the sloping band corresponds to the progressive propagation of localized damage in the form of matrix cracking and interfacial shear failure. An exposure to water would then result in a decrease in the value of A as well as in a shift to shorter times of the sloping band. As for ε_S, it would be affected by both the beneficial effects of debonding on crack propagation and of the network plasticization on the intrinsic resistance of the matrix to cracking.

The environmental stress corrosion of unidirectional E-glass/epoxy, vinyl-ester, and polyester composites in water under a constant bending strain was investigated by van den Ende and van den Dolder (1991). It was shown that the quality of the adhesion between the fibers and the matrix is crucial in determining the type of fracture occurring under load. A good fiber/matrix adhesion resulted in brittle fracture with a smooth fracture surface since the cracks would propagate through the fibers, unlike a poorer interfacial bond that resulted in brush-like fracture with numerous fiber pull-outs due to the deviation of cracks along the fiber/matrix interface. As the applied strain increased, the fracture initiation time became shorter, hence, the effects of physical water diffusion and/or chemical attack by water became of less importance. This result was consistent with the observations made by White and Phillips (1985) through stress-rupture experiments, which showed that under high strains the failure time is environment independent, while at intermediate strains it is stress and environment dependent. However, water diffusion will have an influence on the environmental stress corrosion once

water starts accumulating along the interfaces, since it will affect the interfacial bond, thereby reducing the total composite failure time.

3.6 Summary and conclusions

Although both resins and E-glass fibers are susceptible to deterioration as a result of hygrothermal exposure, careful selection of materials, quality control during processing, and use of appropriate coatings can result in FRP materials and components that show significantly enhanced durability over conventional materials under these exposure conditions. Based on the current state of knowledge, albeit incomplete, the following overall aspects are emphasized following recommendations made by Karbhari *et al*., 2003):

- Since the polymeric resin plays a critical role in protecting the fiber and slowing the diffusion process, preference should be given to the use of appropriate epoxies and vinyl-esters.
- In order to decrease the possibility of rapid movement of moisture and chemicals in solution into the bulk composite and towards the fiber surface, it is critical that an appropriate thickness of resin-rich surface exist in FRP composites used in this environment, with the resin layer remaining uncracked through the period of intended use. This effect can be augmented through the use of gel coats and surface scrim layers.
- Acknowledging the impact of undercure on increase in moisture susceptibility of resins, it is recommended that the resin and FRP composite be fully cured prior to use in the field.
- It is emphasized that testing over short periods of time followed by extrapolation of results, especially for ambient temperature cure systems, can lead to erroneous results.
- Due to the effect of moisture on T_g, composites must be cured such that the T_g achieved is significantly higher than the maximum service temperature (a minimum level of 30°C above maximum service temperature is recommended).
- Taking into account effects of degradation and damage tolerance requirements and the lack of sufficient data at present, the stress level in the composite should be limited under sustained factored loads to less than 25% of guaranteed design strength for GFRP, 30% for aramid fiber-reinforced polymer (AFRP), and 40% of guaranteed design strength for carbon fiber-reinforced polymer (CFRP). These values can be modified upwards if substantial validated data can be generated.

3.7 References

Abeysinghe, H.P., Edwards, W., Pritchard, G. and Swampillai, G.J. 'Degradation of cross-linked resins in water and electrolyte solutions', *Polymer*, **23**, 1785 (1982).

Apicella, A., Migliaresi, C., Nicodemo, C., Nicolais, L., Iaccarino, L. and Roccotelli, S. 'Water sorption and mechanical properties of a glass-reinforced polyester resin', *Composites*, **13**, 406–410 (1982).

Apicella, A., Migliaresi, C., Nicolais, L., Iaccarino, L. and Roccotelli, S. 'The water ageing of unsaturated polyester-based composites: influence of resin chemical structure', *Composites*, **14**(4), 387–392 (1983).

ASTM D790-03 Standard test methods for flexural properties of unreinforced and reinforced plastics and electrical insulating materials, Philadelphia, PA, 2003.

Barrales-Rienda, J.M., Sanchez Chaves, M., Mazon-Arechederra, J.M. and Fernandez-Martin, F. 'Polymer precursors of polyacetylene. Thermal degradation of poly(vinyl esters). Part II-effect of the n-acyl chain length on the autocatalytic thermal degradation of a homologous series of poly(vinyl n-alkyl esters) (PV -n-AEs)', *Polymer Degradation and Stability*, **23**(3), 279–298 (1989).

Bascom, W.D. 'The surface chemistry of moisture-induced composite failure', *Interfaces in Polymer Matrix Composites*, E.P. Plueddemann Ed., Chapter 3, pp. 79–108, Academic Press, New York (1974).

Boller, K.H. 'Effect of long-term loading on glass fiber-reinforced plastic laminates', *Plastics Technology*, **2**(12), 808–821 (1956).

Bradley, W.L. and Grant, T.S. 'The effect of moisture absorption on the interfacial strength of polymeric matrix composites', *Journal of Materials Science*, **30**, 5537–5542 (1995).

Chamis, C.C., Lark, R.F. and Sinclair, J.H. 'Integrated theory for predicting the hygrothermomechanical response of advanced composite structural components', American Society for Testing and Materials, *Advanced Composite Materials – Environmental Effects*, ASTM STP 658 (1981).

Charles, R.J. 'Static fatigue of glass Part I', *Journal of Applied Physics*, **29**(11), 1549–1560 (1958).

Chateauminois, A., Chabert, B., Soulier, J.P. and Vincent, L. 'Effects of hygrothermal aging on the durability of glass/epoxy composites, physico-chemical analysis and damage mapping in static fatigue', *Proceedings of the 9th International Conference on Composite Materials (ICCM/9)*, pp. 593–600 (1993).

Chin, J.W., Nguyen, T. and Aouadi, K. 'Sorption and diffusion of water, salt water, and concrete pore solution in composite matrices', *Journal of Applied Polymer Science*, **71**, 483–492 (1999).

Chin, J.W., Aouadi, K., Haight, M.R., Hughes, W.L. and Nguyen, T. 'Effects of water, salt solution and simulated concrete pore solution on the properties of composite matrix resins used in civil engineering applications', *Polymer Composites*, **22**(2), 282–297 (2001a).

Chin, J.W., Hughes, W.L. and Signor, A. 'Elevated temperature aging of glass fiber reinforced vinyl ester and isophthalic polyester composites in water, salt water and concrete pore solution', *American Society for Composites*, *Proceedings of the 16th Technical Conference*, pp. 1–12 (2001b).

Chu, W. and Karbhari, V.M. 'Effect of water sorption on performance of pultruded E-glass/vinylester composites,' *ASCE Journal of Materials in Civil Engineering*, **17**(1), 63–71 (2005).

Collings, T.A. 'The effect of observed climatic conditions on the moisture equilibrium level of fibre-reinforced plastics', *Composites*, **17**(1), 33–41 (1986).

Collings, T.A., Harvey, R.J. and Dalziel, A.W. 'The use of elevated temperature in the structural testing of FRP components for simulating the effects of hot and wet environmental exposure', *Composites*, **24**(8), 625–634 (1993).

Crank, J. and Park, G.S. *Diffusion in Polymers*, Academic Press, New York (1968).

Diamant, Y., Marom, G. and Broutman, L.J. 'The effect of network structure on moisture absorption of epoxy resins', *Journal of Applied Polymer Science*, **26**, 3015–3025 (1981).

Fahmy, A.A. and Hurt, J.C. 'Stress dependence of water diffusion in epoxy resin', *Polymer Composites*, **1**(2), 77–80 (1980).

Ganem, M., Mortaigne, B., Bellenger, V. and Verdu, J. 'Hydrolytic ageing of vinyl ester materials, Part 1. Ageing of prepolymers and model compounds', *Polymer Networks Blends*, **4**(2), 87–92 (1994).

Ghorbel, I. and Valentin, D. 'Hydrothermal effects on the physico-chemical properties of pure and glass fiber reinforced polyester and vinylester resins', *Polymer Composites*, **14**(4), 324–334 (1993).

Gorowara, R.L. 'Interphase formation and environmental degradation in glass fiber/vinyl ester composites', PhD Thesis, University of Delaware (2001).

Hamada, H., Maekawa, Z.I., Ikuta, N., Kiyosumi, K., Tanimoto, T. and Morii, T. 'Chemical and physical degradation of glass fiber reinforced cross-linked polyester immersed in hot water', *American Society for Composites*, *Proceedings of the 9th Technical Conference on Composite Materials*, pp. 1009–1016 (1994).

Harper, J.F. and Naeem, M. 'The moisture absorption of glass fibre reinforced vinylester and polyester composites', *Materials & Design*, **10**(6), 297–300 (1989).

Heitman, R.E. and Lindstrom, R.S. 'A method for predicting the strength degradation in an underground environment of polyester fiberglass laminates', *Proceedings of the 19th Annual Technical and Management Conference of the Society of the Plastics Industry*, *Reinforced Plastics Division*, 4-F, pp. 1–9 (1964).

Henson, M.C. and Weitsman, Y. 'Stress effects on moisture transport in an epoxy resin and its composite', *Proceedings of the 3rd Japan–U.S. Conference on Composite Materials*, pp. 775–783 (1986).

Hojo, H. and Tsuda, K. 'Effects of chemical environments and stress on corrosion behaviors of glass fiber reinforced plastics and vinyl ester resin', *Proceedings of the 34th Annual Technical Conference of SPI*, section 13-B, pp. 1–6 (1979).

Illinger, J.L. and Schneider, N.S. 'Water vapor transport in an epoxy resin based on TGMDA and DICY', *Polymer Engineering and Science*, **20**(4), 310–314 (1980).

Jacobs, P.M. and Jones, F.R. 'Influence of heterogeneous crosslink density on the thermomechanical and hygrothermal properties of an unsaturated polyester resin: 2. Hygrothermal studies', *Polymer*, **34**(10), 2122–2127 (1993).

Kambour, R.P. 'Correlations of the dry crazing resistance of glassy polymers with other physical properties', *Polymer Communications*, **24**(10), 292–296 (1983).

Karbhari, V.M. and Zhang, S. 'E-Glass/vinylester composites in aqueous environments – I: experimental results,' *Applied Composite Materials*, **10**, 19–48 (2002).

Karbhari, V.M., Zhao, L., Murphy, K. and Kabalnova, L. 'Environmental durability of glass fiber reinforced composites – short term effects', *Proceedings of the 1st International Conference on the Durability of Fibre Reinforced Polymer Composites for Construction (CDCC'98)* pp. 513–524 (1998).

Karbhari, V.M., Chin, J.W., Hunston, D., Benmokrane, B., Juska, T., Morgan, R., Lesko, J.J., Sorathia, V. and Reynaud, D. 'Durability gap analysis for FRP composites in civil infrastructure,' *ASCE Journal of Composites for Construction*, **7**(3), 238–247 (2003).

Karbhari, V.M., Stachowski, C. and Wu, L. 'Durability of pultruded E-glass/vinylester under combined hygrothermal exposure and sustained bending' *ASCE Journal of Materials in Civil Engineering* (2007, in press).

Kasturiarachchi, K.A. and Pritchard, G. 'Water absorption of glass/epoxy laminates under bending stresses', *Composites*, **14**(3), 244–250 (1983).

Lagrange, A., Melennec, C. and Jacquemet, R. 'Influence of various stress conditions of the moisture diffusion of composites in distilled water and in natural sea-water', *Durability of Polymer Based Composite Systems for Structural Applications*, A.H. Cardon and G. Verchery Eds, pp. 385–392, Elsevier Applied Sciences, Amsterdam (1991).

Liao, K. and Tan, E.Y.M. 'In situ tensile strength degradation of glass fiber in polymer composite', *Scripta Materialia*, **44**, 785–789 (2001).

Liao, K., Schultheisz, C.R. and Hunston, D.L. 'Effects of environmental aging on the properties of pultruded GFRP', *Composites Engineering Part B*, **30B**(5), 485–493 (1999).

Liétard, V., Krawczak, P. and Pabiot, J. 'Influence de la post-cuisson sur le comportement à long terme en fissuration sous tension dans l'eau de composites verre/vinylester', *European Polymer Journal*, **36**, 555–570 (2000).

Loos, A.C. and Springer, G.S. *Environmental Effects on Composite Materials*, G.S. Springer Ed., Vol. 1, p. 34, Technomic Publishing Co., Lancaster, PA (1981).

Loos, A.C., Springer, G.S., Sanders, B.A. and Tung, R.W. 'Moisture absorption of polyester-E glass composites', *Journal of Composite Materials*, **14**, 142–154 (1980).

Lyons, K.B. and Phillips, M.G. 'Creep-rupture and damage mechanisms in glass-reinforced plastics', *Composites*, **12**(4), 265–271 (1981).

Magnus, G., Dunleavy, R.A. and Critchfield, F.E. 'Stability of urethane elastomers in water, dry air, and moist air environments', *Rubber Chemistry and Technology*, **39**(4), 1328–1337 (1966).

Marom, G. 'The role of water transport in composite materials', *Polymer Permeability*, J. Comyn Ed., Vol. **9**, pp. 341–374, Elsevier Applied Sciences, Amsterdam (1985).

Marom, G. and Broutman, L.J. 'Moisture penetration into composites under external stress', *Polymer Composites*, **2**(3), 132–136 (1981).

Marsh, L.L., Lasky, R., Seraphim, D.P. and Springer, G.S. 'Moisture solubility and diffusion in epoxy and epoxy-glass composites', *Journal of Research and Development*, **28**(6), 655–661 (1984).

Marshall, J.M., Marshall, G.P. and Pinzelli, R.F. 'The diffusion of liquids into resins and composites', *Polymer Composites*, **3**(3), 131–137 (1982).

McClurg, J.A. and Vaughan, J.G. 'Characterization of degradation for pultruded glass reinforced composite materials when immersed in high temperature water', *Proceedings of the 43rd International SAMPE Symposium*, pp. 2134–2143 (1998).

Menges, G. and Gitschner, H.W. 'Sorption behavior of glass-fiber reinforced composites and the influence of diffusing media on deformation and failure behavior', *Proceedings of the 3rd International Conference on Composite Materials (ICCM–3)*, pp. 25–48 (1980).

Mensitieri, G., Del Nobile, M.A., Apicella, A. and Nicolais, L. 'Moisture-matrix interactions in polymer based composite materials', *Revue de l'Institut Français du Pétrole*, **50**(4), 551–571 (1995).

Metcalfe, A.G. and Schmitz, G.K. 'Mechanism of stress corrosion in E glass filaments', *Glass Technology*, **13**(1), 5–16 (1972).

Meyer, L.J., Henshaw, J.M., Houston, D.Q. and Hagerman, E.M. 'The effects of stressed environmental exposure on the durability of automotive composite materials', *Polymers and Polymer Composites*, **7**(4), 269–281 (1999).

Michalske, T.A. and Freiman, S.W. 'A molecular mechanism for stress corrosion in vitreous silica', *Journal of the American Ceramic Society*, **66**(4), 284–288 (1983).

Neumann, S. and Marom, G. 'Stress dependence of the coefficient of moisture diffusion in composite materials', *Polymer Composites*, **6**(1), 9–12 (1985).

Neumann, S. and Marom, G. 'Free-volume dependent moisture diffusion under stress in composite materials', *Journal of Materials Science*, **21**, 26–30 (1986).

Neumann, S. and Marom, G. 'Prediction of moisture diffusion parameters in composite materials under stress', *Journal of Composite Materials*, **21**, 68–80 (1987).

Nguyen, T., Byrd, E., Alshed, D., Aouadi, K. and Chin, J. 'Water at the polymer/substrate interface and its role in the durability of polymer/glass fiber composites', *Proceedings of the 1st International Conference on the Durability of Fibre Reinforced Polymer Composites for Construction (CDCC'98)*, pp. 451–462 (1998).

Pascault, J.-P., Sautereau, H., Verdu, J. and Williams, R.J.J. *Thermosetting Polymers*, Marcel Dekker, New York (2002).

Phani, K.K. and Bose, N.R. 'Temperature dependence of hydrothermal ageing of CSM-laminate during water immersion', *Composite Science and Technology*, **29**, 79–87 (1987).

Phifer, S.P., Verghese, K.N.E. and Lesko, J.J. 'Remaining strength of hygrothermally aged pultruded vinyl ester E-glass laminates', *Proceedings of the 3rd International Conference on the Advanced Composite Materials in Bridges and Structures (ACMBS MCAPC)*, pp. 29–36 (2000).

Prian, L. and Barkatt, A. 'Degradation mechanisms of fiber-reinforced plastics and its implication to prediction of long-term behavior', *Journal of Materials Science*, **34**, 3977–3989 (1999).

Pritchard, G. and Speake, S.D. 'Effects of temperature on stress-rupture times in glass/polyester laminates', *Composites*, **19**(1), 29–35 (1988).

Schmitz, G.K. and Metcalfe, A.G. 'Stress corrosion of E-glass fibres', *Industrial and Engineering Chemistry Product Research and Development*, **5**(1), 1 (1966).

Simon, P. and Rybar, M. 'Kinetics of polymer degradation involving the splitting off of small molecules: Part 8. Thermal degradation of polyvinyl esters', *Polymer Degradation and Stability*, **38**, 255–259 (1992).

Sonawala, S.P. and Spontak, R.J. 'Degradation kinetics of glass-reinforced polyesters in chemical environments, Part II Organic solvents', *Journal of Materials Science*, **31**, 4757–4765 (1996).

Springer, G.S., Sanders, B.A. and Tung, R.W. 'Environmental effects on glass fiber reinforced polyester and vinylester composites', *Journal of Composite Materials*, **14**, 213–232 (1980).

Sridharan, S. 'Environmental durability of E-glass/vinylester composites in hot-moist conditions', PhD Thesis, Georgia Institute of Technology (1987).

Sridharan, S., Zureick, A.-H. and Muzzy, J.D. 'Effect of hot-wet environments on E-glass/vinylester composites', *ANTEC*, 2255–2259 (1998).

Suri, C., Hamada, H. and Fujihara, K. 'Influence of aging and surface treatment on the mode II fracture behavior in a glass/vinylester composite', *Composite Interfaces*, **8**(2), 135–149 (2001).

van den Ende, C.A.M. and Van den Dolder, A. 'Comparison of environmental stress corrosion cracking in different glass fibre reinforced thermoset composites', *Durability of Polymer Based Composite Systems for Structural Applications*, A.H. Cardon and G. Verchery Eds, pp. 408–417, Elsevier Applied Sciences, Amsterdam (1991).

Vaughan, D.J., Peek, R.C. and Creech, M.H. 'The importance of the interface on water absorption in glass reinforced epoxy composites', *Proceedings of the 39th Annual Conference, Reinforced Plastics/Composites Institute, The Society of the Plastics Industry*, pp. 1–4 (1984).

Wagner, H.D. and Lustiger, A. 'Effect of water on the mechanical adhesion of the glass/epoxy interface', *Composites*, **25**(7), 613–616 (1994).

Weitsman, Y.J. 'Effects of fluids on polymeric composites – a review', Contract Report for Office of Naval Research, No. N00014–90–J–1556 (1995).

White, R.J. and Phillips, M.G. 'Environmental stress-rupture mechanisms in glass fibre/polyester laminates', *Proceedings of the 5th International Conference on Composite Materials (ICCM-V)*, pp. 1089–1099 (1985).

Worley, W.J. and Findley, W.N. 'The effect of temperature on the creep and recovery of a melamine-glass fabric laminate', *ASTM Proceedings*, **50**, 1399–1412 (1950).

Zhang, J.S., Karbhari, V.M., Isley, F. and Neuner, J. 'Fiber sizing based enhancement of materials durability for seismic retrofit,' *ASCE Journal of Composites for Construction*, **7**(3), 194–199 (2003).

4

Durability of composites in sub-zero and freeze–thaw conditions

V. M. KARBHARI,
University of California San Diego, USA

4.1 Introduction

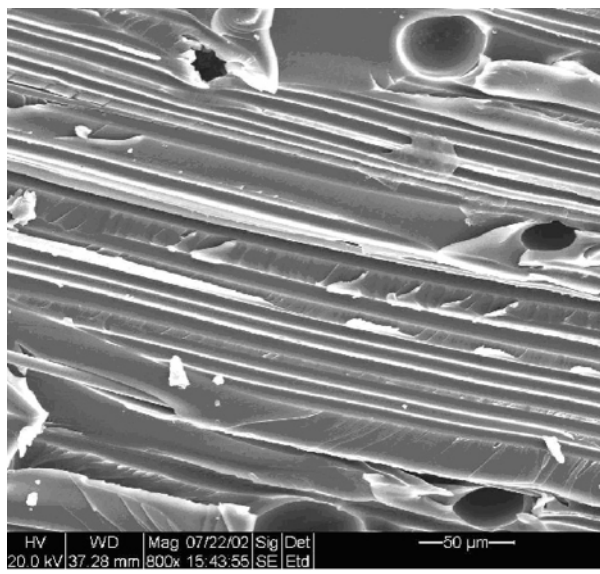
While the effects of elevated temperature are routinely considered in the selection of fiber-reinforced polymer (FRP) materials for specific applications, and a substantial body of knowledge exists regarding materials response at temperatures close to or exceeding the glass transition temperature, the effects of cold regions environments are not as well understood. Although the term 'cold regions' is generally related to geographical areas 'with appreciable frozen ground and a substantial fraction of the annual precipitation falling as snow' (Grant, 2000), the terminology lexically refers to areas within which the ambient temperature is such that it has a significant effect on the environment and human activities. Bates and Bilello (1966) delineate 'cold regions' as being those that have: (a) air temperatures below 0°C and –18°C with a 50% likelihood annually; (b) mean annual snow depth; (c) ice cover on navigable rivers; and (d) isolines based on permanence, depth and continuity of frozen ground. In a number of cases this has been taken to mean areas with an average temperature of 0°C during the coldest months, with a 0.3 m depth of frost penetration for at least 1 year in 10 and about 100 days of ice in a year on navigable waters, which translates to a large area on the North American continent having an environment that can either be described as 'cold regions' or close to it. With the increasing use of FRP composites in civil infrastructure the consideration of exposure to freeze and 'freeze–thaw' conditions is hence important. In addition, keeping in mind that polymeric resins (and the resulting FRP composites) absorb moisture in varying quantities, the effects of these colder conditions on the material with absorbed water is also important.

4.2 Overall effects

At the outset it is, perhaps, important to review the thermal characteristics of the constituents used in FRPs since a number of effects are directly related to the incompatibility between the coefficients of thermal expansion of fibers

and resins. In general polymeric resins have coefficients of thermal expansion at least an order of magnitude greater than those of the glass fiber. A decrease in temperature, which in the case of isotropic materials would cause the material to shrink, results in the formation of residual stresses at the interface between the resin and the fiber since the contraction in the bulk resin is constrained by the stiffer E-glass fibers. In the case of carbon fibers the effects are even more pronounced since the fiber is itself anisotropic having a positive coefficient of thermal expansion in the transverse direction and a negative coefficient of thermal expansion in the longitudinal direction, which often results in clean debonding of the fibers from the surrounding matrix (Dutta and Taylor, 1989; Rivera and Karbhari, 2002; Abanilla *et al*., 2006). This is most often seen after thermal cycling, such as through repeated freeze–thaw exposures, as seen in Fig. 4.1. In addition the exposure to cold temperatures generally results in an increased embrittlement of the resin, causing an increase in effective stiffness, but a decrease in damage tolerance.

The effect of cold winter and cold regions-type climates, especially as related to freeze–thaw effects on the overall integrity of the retrofit system, is one such concern, especially in light of data in the composites literature that show that sub-zero (not cryogenic) temperatures akin to those seen in winter in North America, and freeze–thaw exposure, can result in significant changes in thermomechanical response (Gerasimov and Bulmanis, 1988; Lord and Dutta, 1988; Kuz'min *et al*., 1989; Karbhari and Pope, 1993;



4.1 Resin surfaces after freeze–thaw cycling showing clean debonding from fibers.

Zheng and Morgan, 1993; GangaRao *et al*., 1995). Unidirectional tensile strengths have been shown to decrease at low temperatures in the –10 to –40°C range, whereas the off-axis and transverse strengths may increase due to matrix hardening, and increasing cycles at low temperature have been shown to accentuate residual stresses resulting in increased severity and density of matrix cracks (Dutta, 1989). The apparent increase in matrix brittleness and decrease in tensile strength was also noted by Gadke (1985). Kuz'min *et al*. (1989) reported an increase in ultimate tensile strength of 6457 wound fiber glass tubular specimens, but a decrease for a reinforced organoplastic. Although, in general, testing at cryogenic levels has shown that static performance improves whereas dynamic performance degrades, linear interpolation of results obtained in the 20°C to –196°C range should not be used, since it has been established that the temperature dependency of composite strength is not only nonlinear but may also be nonmonotonic (Milkovich *et al*., 1986).

Exposure to freeze–thaw, in addition to causing progression of damage within the FRP material itself as a result of the cyclic expansion and contraction of the entrapped water, can also significantly affect the bond between laminae as well as the bond between the FRP and the concrete substrate. Howie (1995) exposed carbon/epoxy-confined concrete cylinders to freeze–thaw cycles between 20 and –18°C for a period of 45 days and reported a decrease in compression strength of about 5% and significant reductions in overall stiffness. Soudki and Green (1997) exposed a very limited number of carbon/epoxy-wrapped concrete cylinders to 50 freeze–thaw cycles between 18°C (for 8 hours in water) and –18°C (for 16 hours), and concluded that the exposure caused a more catastrophic failure, with specimens showing evidence of microcracking. The single-layer wrap samples showed a 17% loss in axial compressive strength caused by this level of exposure. In a series of limited tests conducted on carbon/epoxy- and glass/epoxy-confined concrete exposed to a total of 300 cycles of freeze–thaw in a salt solution (35 g NaCl in 1 L water) between 4 and –18°C at a rate of 6 cycles/day, it was reported that the glass/fiber epoxy-confined concrete specimens showed a reduction of 28% in compression strength over the unexposed specimens; whereas, the carbon fiber/epoxy-confined concrete specimens showed a reduction of 19% (Toutanji and Rey, 1998; Toutanji and Balaguru, 1999). The authors further reported that if the edge areas (top and bottom) that showed visible effects of exposure were removed, the reduction for the glass/epoxy-confined concrete specimens was between 4 and 12%; whereas, for the carbon/epoxy specimens it was between 4 and 15%, depending on areal weight of fabric used. Callery *et al*. (2000) described an extensive program of environmental effects on FRP composite- and Rockguard-wrapped concrete cylinders, including freeze–thaw cycling between 20 and –18°C for up to 250 cycles but provided no data on response except that failures were more volatile after exposure and

there was relatively little effect on axial or radial deformation levels. Karbhari *et al*. (2000) cycled carbon/epoxy-confined concrete cylinders between 22.5 and –20°C 201 times without prior moisture exposure and noted there was insignificant change in levels of ultimate strength, although a decrease in hoop strain levels was seen. It was noted, however, that 'dry' freeze–thaw cycling did result in substantial matrix microcracking that in the presence of moisture, could result in significantly accelerated degradation in overall response.

While all composite components used in civil infrastructure systems exposed to cold regions-type environments need to be assessed for effects of freeze and freeze–thaw, the effects are likely to be of more consequence in cases where the FRP composite is directly exposed to the environment itself. Thus, the effect on FRP rebar and embedded tendons, for example, can be expected to be less since the FRP is surrounded by concrete. Only preliminary, and limited, studies have been conducted on the effects on different FRP deck systems, and results although varying do show effects of cold temperatures and especially differentials between the top and bottom surfaces of the decks, as well as emphasizing the importance of connections (Dutta *et al.*, 2007; Prachasaree *et al.*, 2007; Shahrooz *et al.*, 2007). The effects can, however, be significant in the case of thin overlays/wraps such as those that are used in seismic retrofit and strengthening through external bonding of the FRP onto the concrete substrate, and need to be considered when designing FRP schemes for these applications.

4.3 Consideration of hygrothermal effects

Hygrothermal conditions are known to cause degradation in a composite through changes such as: plasticization, hydrolysis and saponification of the resin: fiber–matrix debonding and matrix microcracking in the composite; and in the case of glass fibers, even pitting, etching and cracking of the fiber itself. Although the comprehensive mechanistic modeling of all these effects for the purposes of durability/life prediction has still not been completely achieved, in most cases fairly precise predictions can be made through the judicious use of equations based on micromechanics and semi-empirical approaches based on extensive prior testing. In this section, equations related to the prediction of the effects of cold, and of moisture absorption, are briefly outlined. No attempt is made to review the large number of potential approaches for the modeling of both effects – rather only those equations that provide a basic overview of the approach are presented.

Based on the analysis of a number of sets of experimental data of different polymers over a range of temperatures extending into the cold regions regime, Dutta (1989) showed that the elastic modulus of a resin system could be approximated as

$$E_{m(T)} = E_{m(To)} + K(T_o - T) \quad [4.1]$$

where: $T_o > T$ (in °C); $E_{m(To)}$ is the reference modulus of the resin system at a specified temperature, T_o; $E_{m(T)}$ is the modulus at the lower temperature, representative of a subzero environment; and K is an empirical constant of the order of 20 MPa/°C. Considering the effects of modulus on strength through an empirical formulation based in part on the use of the concept of the maximum critical fiber stress, Rosen (1964) and Dutta (1992, 1994) proposed a relationship of the form

$$\frac{\sigma_T}{\sigma_{To}} = \left[\frac{E_{m(T)}}{E_{m(To)}}\right]^{-0.5n} \quad [4.2]$$

where σ_T is the tensile strength at the cold regions (sub-zero in °C) temperature under consideration, σ_{To} is the tensile strength at the reference temperature, and n is an exponent between 0.8 and 1.2, usually taken to be 1 for the resin, or higher – such as 1.1 (Dutta, 1992) – when a composite is fabricated using a process that could result in fiber waviness.

The absorption of moisture, from the environment or from an aqueous solution, is known to result in a depression of the glass transition temperature. Chamis (1987) suggested that the effect of moisture absorption, measured by gain in weight of a resin sample, on glass transition temperature could be determined as

$$T_{gw} = (0.005\, M_r^2 - 0.10 M_r + 1.0) T_{go} \quad [4.3]$$

where M_r is the weight percentage of moisture in the resin (usually measured as the percentage weight gain as a result of exposure), T_{go} is the glass transition temperature at the reference condition and T_{gw} is the glass transition temperature for 'wet' matrix material at the moisture content M_r. Chamis (1987) and Chamis and Sinclair (1982) postulated that the effect of moisture on matrix properties could be determined through use of a factor F_m expressed as

$$F_m = \frac{P}{P_o} = \left[\frac{T_{gw} - T}{T_{go} - T_o}\right]^{0.5} \quad [4.4]$$

where F_m is the matrix property retention ratio, P is the matrix property after hygrothermal exposure, P_o is the reference matrix property prior to hygrothermal exposure, T is the temperature at which P is to be predicted, T_{go} is the glass transition temperature under reference dry conditions and T_o is the test temperature at which P_o was measured. Assuming that moisture absorption occurs through the matrix and that it is not absorbed by the fiber, the property retention ratio is applied only to matrix properties as

$$E_{m(h)} = F_m E_m \quad \text{and} \quad \sigma_{m(h)} = F_m \sigma_m \quad [4.5]$$

where E_m and σ_m are the matrix modulus and tensile strength, respectively, and the subscript (h) represents hygrothermal exposure. Thus the longitudinal modulus of a unidirectional composite with fiber volume fraction, V_f, after hygrothermal exposure can be expressed as

$$E_{11} = E_f V_f + F_m E_m V_m \quad [4.6]$$

where V_m is the matrix volume fraction.

Exposure to moisture resulting in high levels of moisture absorption, accompanied by temperature changes and/or cycling, including freeze–thaw cycling, is known to cause matrix microcracking and fiber-matrix debonding, both of which potentially result in degradation of the tensile strength of a composite. Approximating this effect through the determination of an effective void fraction, V_v, the strength of a composite can be determined as

$$\sigma = \{1 - [4V_v/(1 - V_f)\pi]^{1/2}\}\ \sigma_{ref} \quad [4.7]$$

where σ_{ref} is the reference strength, often determined after accounting for property changes through low temperature and moisture absorption, as through equations [4.2] and [4.5], for example.

4.4 References

Abanilla, M.A., Li, Y. and Karbhari, V.M. 'Durability characterization of wet layup graphite/epoxy composites used in external strengthening,' *Composites B*, **37**(2/3), 2006, 200–212.

Bates, R.E. and Bilello, M.A. 'Defining the cold regions of the northern hemisphere,' US CRREL Report TR–178, 1966.

Callery, K., Green, M.F. and Archibald, J.F. 'Environmental effects on the behaviour of wrapped concrete cylinders,' in *Proceedings of the 3rd International Conference on Advanced Composite Materials in Bridges and Structures*, Ottawa, Canada, 2000, pp. 759–766.

Chamis, C.C. 'Simplified composite micromechanics equations for mechanical, thermal, and moisture-related properties,' in *Engineers Guide to Composite Materials*, eds J.W. Weeton *et al*., ASM International, Materials Park, OH, 1987, pp. 3–8 to 3–24.

Chamis, C.C. and Sinclair, J.H. 'Durability/life of fiber composites in hygrothermomechanical environments,' in *ASTM STP 787*, ed. I.M. Daniel, 1982, pp. 498–512.

Dutta, P.K. 'A theory of strength degradation of unidirectional fiber composites at low temperature,' in *Proceedings of the Advanced Materials Conference II*, ed. F.W. Smith, Golden, Colorado, 1989, pp. 647–662.

Dutta, P.K. 'Tensile strength of unidirectional fiber composites at low temperatures,' *Proceedings of the 6th US–Japan Conference on Composite Materials*, Orlando, FL, 1992, pp. 782–792.

Dutta, P.K. 'Low-temperature compressive strength of glass-fiber-reinforced polymer composites,' *Journal of Offshore Mechanics and Arctic Engineering*, **116**, 1994, 167–172, 201.

Dutta, P.K. and Taylor, S. 'A fractographic analysis of graphite-epoxy composites subjected

to low temperature thermal cycling,' in *Proceedings of the International Symposium for Testing and Failure Analysis*, Los Angeles, CA, 1989, pp. 429–435.

Dutta, P.K., Lopez-Anido, R. and Kwon S.C. 'Fatigue durability of FRP composite bridge decks at extreme temperatures,' *International Journal of Materials and Product Technology*, **28**, (1/2), 2007, 198–217.

Gadke, M. 'Response of statically tested unnotched specimens: Mechanical properties and damage mechanisms of carbon fiber-reinforced composites,' DFVLR Report No. DFVLR-FB85-45, Institut fur Strukturmechanik, Braunschweig, West Germany, 1985.

GangaRao, H.V.S., Vijay, P.V. and Dutta, P.K. 'Durability of composites in infrastructure,' *Proceedings of Corrosion '95*, Paper No. 550, 1995, pp. 1–8.

Gerasimov, A.A. and Bulmanis, V.N. 'Effect of static loads and of factors of cold climate on the deformability, strength, and life of polyester wound glass-reinforced plastic,' *Mekhanika Kompzitnykh Materialov*, **5**, 1988, 862–867.

Grant, S.A. 'Physical and chemical factors affecting contaminant hydrology in cold environments,' ERDC/CRREl Report TR-00-21, December 2000.

Howie, I. 'A study on the use of composite wraps for the rehabilitation of deteriorated concrete columns,' MS thesis, Department of Civil Engineering, University of Delaware, Newark, DE, 1995.

Karbhari, V.M. and Pope, G. 'Effect of cold region type environment on impact and flexure properties of glass/vinylester composites,' *ASCE Journal of Cold Regions Engineering*, **8**(1), 1993, 1–20.

Karbhari, V.M., Rivera, J. and Dutta, P.K. 'Effect of short-term freeze–thaw cycling on composite confined concrete,' *ASCE Journal of Composites for Construction*, **4**(4), 2000, 191–197.

Kuz'min, S.A., Bulmanis, V.N. and Struchkov, A.S. 'Experimental investigation of the strength and deformability of wound fiberglasses and organoplastic under low climatic temperatures,' *Mekhanika Kompozitnykh Materialov*, **1**(Jan/Feb), 1989, 57–61.

Lord, H.W. and Dutta, P.K. 'On the design of polymer composite structures for cold regions applications,' *Journal of Reinforced Plastics and Compos*ites, **7**, 1988, 435–458.

Milkovich, S.H., Herakovich, C.T. and Sykes, G.F. 'Space radiation effects on the thermomechanical behavior of graphite-epoxy components,' *Journal of Composite Materials*, **6**, 1986, 579–593.

Prachasaree, W., GangaRao, H.V.S., Laosiriphong, K., Shekar, V. and Whitlock, J. 'Theoretical and experimental analysis of FRP bridge deck under cold temperatures,' *International Journal of Materials and Product Technology*, **28**, (1/2), 2007, 103–122.

Rivera, J. and Karbhari, V.M. 'Cold temperature and simultaneous aqueous environment related degradation of carbon/vinylester composites,' *Composites B*, **33**(1), 2002, 17–24.

Rosen, B.W. 'Mechanics of composite strengthening,' in *Fiber Composite Materials*, American Society of Metals, Metals Park, OH, 1964.

Shahrooz, B.M., Neumann, A.R. and Reising, R.M.W. 'Durability of FRP composite bridge decks – construction and temperature effects,' *International Journal of Materials and Product Technology*, **28**, (1/2), 2007, 66–88.

Soudki, K.A. and Green, M.F. 'Freeze–thaw response of CFRP wrapped concrete,' *Concrete International*, **19**(8), 1997, 64–67.

Toutanji, H.A. and Balaguru, P. 'Effects of freeze–thaw exposure on performance of concrete columns strengthened with advanced composites,' *ACI Materials Journal*, **96**(5), 1999, 605–610.

Toutanji, H.A. and Rey, F. 'Performance of concrete columns strengthened with advanced composites subjected to freeze–thaw conditions,' *Proceedings of the International Conference on Durability of Fibre Reinforced Polymer (FRP) Composites for Construction*, Sherbrooke, Canada, 1998, pp. 351–360.

Zheng, Q. and Morgan, R.J. 'Synergistic thermal-moisture damage mechanisms of epoxies and their carbon fiber composites,' *Journal of Composite Materials*, **27**(15), 1993, 1465–1478.

5

Durability of composites exposed to ultraviolet radiation

J. W. CHIN,
National Institute of Standards and Technology (NIST), USA

5.1 Introduction

In recent years, fiber-reinforced polymer (FRP) composites have become increasingly important in outdoor applications. The polymeric matrix of an FRP composite, like other polymeric systems, is subject to degradation caused by solar ultraviolet (UV) radiation, hot/cold cycling, moisture (liquid and vapor) and environmental pollutants, in a process known as 'weathering'. UV radiation is considered to be the most critical weathering element because it initiates photochemical reactions that lead to irreversible material degradation, yet many of its effects on FRP composites are not fully understood. Since the polymeric matrix binds and transfers load to the reinforcing fibers, damage to this critical component can be detrimental to the overall mechanical properties of the FRP composite and limit its service life. This chapter will describe the effects of UV radiation on polymeric materials in general, and FRP matrix composites specifically. A brief overview of UV exposure testing and UV mitigation strategies will also be provided.

5.2 Ultraviolet radiation effects on polymers

Commercial polymers are susceptible to photodegradation initiated by the UV component of solar radiation. While a pure polymer may not contain chemical groups (chromophores) that absorb in the UV-visible region of the electromagnetic spectrum, it may contain impurities, residual catalyst, thermal oxidation byproducts and additives that do. The polymeric matrix of an FRP composite is prone to the same photochemical damage as unreinforced bulk polymers and polymer coatings. To understand the effects of UV radiation on FRP composites, it is necessary to have a general understanding of the effects of UV radiation on polymeric materials.

The spectral range of solar radiation that reaches the Earth is from approximately 295 nm in the UV region to >2500 nm in the near infrared. The contribution of UV radiation to the total solar global radiation is 5–6%

depending on latitude, altitude, season, time of day, atmospheric conditions, cloud cover and angle of incidence.[1] The remainder of the photolytically active solar radiation is composed of visible (52%) and infrared (42%) radiation. The UV wavelengths observed on the Earth's surface range from approximately 295 to 400 nm, with radiation below approximately 295 nm effectively eliminated by stratospheric ozone.[2] UV radiation between 280 and 315 nm is commonly called UVB radiation while the radiation between 315 and 400 nm is called UVA radiation.

A number of commercial polymers have bond dissociation energies corresponding to the photon wavelengths in the 295–400 nm range, and are greatly affected by exposure to this portion of the solar spectrum.[1] The lower the wavelength of the incident radiation, the higher the photon energies and quantum efficiencies, and the more potentially active it is in initiating bond breakage in polymeric materials. Any decrease in the stratospheric ozone column thickness could lead to an incremental increase in the photoactive UVB radiation flux and a corresponding decrease in the performance and lifetime of polymeric systems used in outdoor applications.

One important point that is often overlooked in the study of UV effects on polymeric materials is that only wavelengths that are *absorbed* by a material can cause damage, regardless of their intensity. The spectral radiation absorbed by a polymeric material depends on the spectral absorption characteristics of the material as well as the spectral emission properties of the UV source. For example, in polyesters it has been observed that the 330 nm wavelength has the greatest effect, whereas some epoxies have been observed to absorb strongly throughout the entire UV radiation range.[3]

Of the radiation that is absorbed, only a percentage of the absorbed wavelengths are effective in initiating damage. The actual dosage that initiates damage in a material can be calculated via the total effective dosage model, as follows:

$$D_{tot}(t) = \int_0^t \int_{\lambda_{min}}^{\lambda_{max}} E_o(\lambda, t)(1 - 10^{-A(\lambda,t)})\phi(\lambda)\mathrm{d}\lambda\mathrm{d}t$$

where $D_{tot}(t)$ is the total effective dosage, $E_o(\lambda, t)$ is the spectral irradiance, $A(\lambda, t)$ is the spectral absorbance of the sample, $\phi(\lambda)$ is the spectral quantum yield of the material, and λ_{min} and λ_{max} are the minimum and maximum photolytically effective wavelengths, respectively. For a polymeric material, the quantum yield represents the photolytic efficiency of a given wavelength in producing a chemical change and is primarily a function of its physical and chemical structure, as well as environmental factors such as moisture and temperature.[4]

When UV radiation is absorbed by a polymeric material in the presence of oxygen, a complex series of photochemical reactions is initiated that leads

to chemical changes in the material, including the generation of oxygen-containing functional groups such as carbonyl (C=O), carboxyl (COOH) and/or peroxide (O–O). Other chemical reactions that may occur in UV-irradiated polymers include chain scission, side group abstraction, branching, crosslinking and rearrangement processes, depending on the structure of the particular polymer involved.[5] In-depth reviews of photodegradation mechanisms have been compiled by Ranby and Rabek[6] and Guillet[7] for a wide variety of polymers.

The earliest effect on a polymer subjected to UV exposure can be found at the molecular level. Chemical changes in an epoxy composite matrix resin were observed by Monney *et al.*[8,9] following irradiation with a xenon arc lamp. After aging for 1000 h, specimens showed a decrease in the infrared methyl and methylene peak intensities between 2800 and 3000 cm^{-1}, disappearance of aromatic ring peaks (1608, 1510 and 1458 cm^{-1}) and disappearance of C–O stretching peaks (1232 and 1045 cm^{-1}). The C=O stretching peak at 1730 cm^{-1} underwent considerable broadening, which is indicative of the formation of other carbonyl-containing compounds. Energy dispersive x-ray analysis revealed an increase in the oxygen/carbon ratio of the surface regions from 0.6 to between 1.8 and 2.0. Additional information on the oxidative photodegradation of epoxy and polyester matrix resins can be found in references 10 and 11, respectively.

The early stages of UV damage are also readily apparent in the polymer surface morphology. Gu *et al.*[12,13] have utilized atomic force microscopy (AFM) as a non-destructive method to follow changes in the nano-scale surface morphology of UV-exposed polymers, where craters, protuberances and cracks could be observed early in the degradation process. The use of laser scanning confocal microscopy (LSCM) for characterizing the changes in local surface morphology as well as the thickness of UV-exposed polymer films is also described in detail in reference 14.

In an accelerated UV exposure study involving cast films of non-UV-stabilized vinyl ester and isophthalic polyester irradiated with a 1000 W xenon arc source for 1200 h, Chin *et al.*[15] reported changes in the surface topography using AFM. Both vinyl ester and isopolyester specimens showed a substantial degree of cratering and cracking after 1200 h of UV exposure. No changes in the glass transition temperatures (T_g) of the exposed specimens were observed following the exposure period, as measured by dynamic mechanical thermal analysis. Increases in surface oxygen concentration were observed via x-ray photoelectron spectroscopy, indicative of the formation of new oxygen-containing functional groups.

Due to the fact that absorption of UV radiation diminishes rapidly with depth, these photochemical reactions are generally limited to the topmost several microns to 1 mm.[16] For a number of different polymers, Nagai *et al.*[17] observed a severely degraded layer about 0.2 μm deep, followed by an

exponentially decreasing level of damage into the bulk. This degraded top layer is postulated to partially shield the remainder of the polymer from UV damage, as it may have a higher UV-visible absorbance relative to the non-degraded material.

Chemical and morphological changes induced by UV exposure are precursors to changes in the bulk physical, mechanical and optical properties of the polymer,[5] ranging from changes in gloss and color – which are primarily aesthetic – to extensive mechanical property degradation that severely impacts the service life of the polymeric component.[18] The first signs of UV macrodamage usually appear as gloss loss, chalking and yellowing. Gloss loss and chalking are phenomena related to the surface erosion that occurs as fragmented polymer chains are removed from the surface of the polymer. For some polymers, yellowing is the result of unreacted double bonds in incompletely cured resins being photo-oxidized to colored products, or to the formation of conjugated double bonds.[2] The intensity of the yellowing is dependent on the chemical structure of the resin and the type/concentration of UV stabilizers employed. Polymers containing styrene crosslinks, such as vinyl ester and isophthalic polyester, are particularly prone to UV-induced yellowing.[2,11]

After prolonged periods of exposure, more severe damage in the form of surface crazing and cracking may occur.[1] Cracking is often the result of chain scission reactions initiated by UV exposure, in which the fragments resulting from chain scission occupy more volume than the original polymers, causing stresses that lead to crack formation. If the degradation products are volatile or gaseous, pore and pit formation may also occur.[5]

The surface morphological features resulting from UV exposure described above can potentially serve as sites for moisture sorption and fracture initiation that contribute to the degradation of mechanical properties. It has been postulated that a ductile to brittle transition occurs in UV-exposed polymer surfaces, and decreases in impact strength, tensile strength and elongation have been observed following prolonged UV exposure.[16] Signor *et al.*[19] carried out UV exposure studies on non-reinforced vinyl ester matrix resins using a xenon arc lamp source and observed decreases in toughness and strain to failure, and increases in surface hardness and modulus, following 4000 h of UV exposure.

5.3 Ultraviolet radiation effects on fibre-reinforced polymer composites

As with any polymeric system, the durability, performance and rate of degradation of FRP composites are significantly influenced by material composition and the environmental/climatic conditions to which they are exposed. In general, the variability in weathering behavior due to temporal

changes in temperature, rainfall/relative humidity and UV radiation is not fully understood.[18]

UV-induced degradation in FRP composites typically follows the sequence detailed below:

- loss of surface gloss;
- surface discoloration;
- chalking;
- flaking of surface resin;
- pitting;
- microcracking;
- blistering;
- severe loss of resin from outer surface, fibers not yet visible;
- severe loss of resin from outer surface, fibers visible (also known as 'blooming');
- fibers visible and loosened from surface;
- delamination of topmost ply.

As with unreinforced polymers, UV radiation primarily affects the surface and appearance-related properties in the initial stages. Commonly observed initial effects are similar to those observed in unreinforced polymers and include gloss loss, chalking and discoloration (particularly yellowing).[18]

If the polymeric matrix is prone to UV-induced chain scission reactions, the molecular mass or chain length of the surface polymers will decrease, followed by water erosion of the low molecular mass fragments. With additional exposure, the scission/erosion cycle continues until the top layer of fiber reinforcement becomes visible, at which point damage is considered to be severe. This process is commonly referred to as fiber 'blooming'. If the structure of the polymer favors crosslinking reactions, then the increased crosslink density of the surface material may lead to embrittlement and microcracking of the matrix resin.[18] One explanation for this phenomenon is that UV degradation products occupy greater free volume and therefore embrittle and stiffen the polymeric matrix.[5,20]

As damage progresses into the bulk, impact strength, tensile strength and elongation may also decrease as the polymeric matrix resin and fiber–matrix interphase region degrades.[21] This deterioration of mechanical properties could be due to ductile/brittle transitions, embrittlement or microcracking of the matrix resin as described above,[18] or to the ingress of moisture into surface microcracks, followed by diffusion of this moisture into the interior of the matrix and the fiber–matrix interphase.[20] In fact, it is believed that the most deleterious effects of UV radiation on FRP composites are not due to direct photolytic UV damage, which is limited to the surface regions, but to the increased propensity for moisture ingress into damaged regions in the surface of the composites.

The effect of UV radiation on polymeric materials can also be compounded by other environmental factors. As discussed earlier, the combined action of UV radiation and water can lead to surface erosion, resulting in ablation of the resin-rich layer above the reinforcing fiber and eventually causing the fibers to be exposed.[2] In any chemical process, elevated temperatures accelerate the photochemical reactions initiated by UV radiation and hence potential degradation. Cyclic exposure to high and low temperatures may cause microcracking or fatigue damage.[21] Mechanical stress has also been shown to greatly accelerate photodegradation effects on the properties of FRP composites.[20]

Overall, the published literature on the effect of UV radiation on the mechanical properties of FRP composites reports mixed results and there are diverse conclusions about the UV weatherability of FRP materials. In some cases, only minor changes in mechanical properties have been observed following either laboratory or field UV exposure. In general, it has been observed that UV radiation effects on mechanical properties are generally less apparent in thicker specimens,[3] whereas thinner specimens exhibit larger changes in mechanical properties. Transverse properties, which are dominated by the matrix, are observed to be more greatly affected than axial properties.[20] Other studies report much more substantial changes in physical and mechanical properties. Both outcomes are discussed in the selected studies highlighted below.

Roylance and Roylance[22,23] exposed glass/epoxy composites without any protective coatings in the Panama Canal Zone, Puerto Rico, Arizona, Massachusetts, Australia and an accelerated outdoor test site in Arizona. Following a 24 month exposure, significant resin loss and surface fiber exposure were observed on the exposed side of the laminates. Although a great deal of scatter was present in the test results, a downward trend in tensile and flexural strength was noted.

In a study by Kato *et al.*[24] aramid, glass and carbon fiber-reinforced polymer rods were exposed to up to 1250 cycles of UV radiation (1 cycle = 102 min at 52% relative humidity (RH) followed by 18 min at >90% at a dose rate of 0.2 MJ m^{-2} h^{-1} at 26 °C). Aramid fiber-reinforced rods exhibited up to 13% decrease in tensile strength following exposure, glass fiber-reinforced rods showed up to 8% reduction in tensile strength and carbon fiber-reinforced rods showed no reduction in tensile strength throughout the exposure period. Aramid, glass and carbon fibers, as well as dogbone-shaped specimens of matrix resins, were also exposed to 1000 h of UV radiation. Aramid fibers showed an almost 55% decrease in tensile strength, glass fibers showed a 20% decrease and carbon fibers showed no decrease whatsoever. These results parallel the results of the tensile tests on the fiber-reinforced rods. Little or no decrease in the tensile strengths of the neat resin dogbones was observed.

In a study of glass/epoxy and graphite/epoxy laminates exposed in an accelerated UV weathering device for 6 months, Liau and Tseng[25] reported surface erosion in the form of resin spalling and cracking, as well as decreases in tensile strength. It was postulated that surface damage induced by UV radiation could serve to initiate crack growth and subsequent damage.

Choi *et al.*[26] exposed unreinforced and short glass fiber-reinforced thermoplastic polyester outdoors in Perth, Western Australia for 11 months, after which no changes in yield strength were reported for either the unreinforced or the glass-reinforced specimens. However, fracture toughness of the naturally weathered specimens decreased relative to the controls, with the unreinforced materials exhibiting the larger decrease (~33%).

Kumar *et al.*[27] reported that exposure of carbon fiber-reinforced epoxy to UV radiation and moisture resulted in severe erosion of the epoxy matrix, resulting in a 29% decrease in transverse tensile strength after 1000 h of exposure. Longitudinal fiber-dominated properties were not significantly affected in the time period of study, although it was speculated that eventually severe matrix erosion would limit effective load transfer to reinforcing fibers and would eventually lead to the degradation of the even longitudinal fiber-dominated properties.

Segovia *et al.*[28] observed that glass fiber/polyester composites exhibited 15 and 20% decreases in elastic modulus and tensile strength, respectively, following 7000 h of an accelerated laboratory UV exposure. Break energy and strain at break exhibited losses ranging from 20 to 56 %. Degradation was observed primarily in the surface resin, whereas the glass fiber reinforcement appeared to remain intact.

Pang *et al.*[29] reported on glass/epoxy composites that were exposed in an artificial UV chamber for 48 h. Following UV exposure, no visual changes were observed in the specimens, but the deflection at maximum impact load increased substantially and the load carrying capacity was reduced. Compressive buckling load values were also lower for the UV-exposed specimens. Scanning electron microscopy (SEM) analysis revealed delamination, interfacial debonding and matrix cracking in the UV exposed specimens. It was concluded that UV exposure greatly reduced the toughness and cracking resistance of the matrix and rendered the glass/epoxy laminates more vulnerable to impact and compressive loading.

A number of researchers reported that exposure to sunlight produced color changes and surface degradation, but found little effect on mechanical properties within the study period. Trabocco and Stander[30] carried out a study on graphite/epoxy composites that were exposed at outdoor sites in Panama and Warminster, Pennsylvania in a state of flexural stress (tensile strain on the exposure side of the specimens was estimated to be 0.004). Half of the specimens were primed with an epoxy-polyamide material and coated with a 625 μm thick polyurethane coating. Very little degradation in compressive

strength, shear strength or modulus of the exposed laminates was found following the exposure period. Visual examination of exposed laminates revealed major surface degradation, where the resin on the tensile face of the exposed laminate had been completely eroded. Loose fibers on the tension surfaces were observed, as well as delamination of some of the outer plies. Protective coatings appeared to be beneficial in protecting composites from mechanical property degradation due to UV effects, but did not completely prevent UV degradation from occurring.

Physical properties of pultruded glass/vinyl ester and glass/isopolyester profiles were evaluated by Bogner and Borja[31] following 10 000 h of accelerated laboratory UV exposure and Florida exposure. Following 10 000 h of exposure in a fluorescent UV device, flexural strength and flexural modulus of both types of FRP were reduced by between 0 and 4% relative to unexposed controls. Following 10 000 h of Florida exposure, the isopolyester composite retained its performance, but the vinyl ester lost ~ 28% of its initial strength and modulus. In both cases, signs of gloss loss, chalking and surface erosion were evident.

Phelps and Long[32] exposed unidirectional graphite/epoxy coupons to UV radiation in a solar simulator for 4 weeks, after which the flexural properties of specimens were tested by stressing the UV-exposed sides in tension. The flexural properties of the UV-exposed specimens were not significantly different from those of the unexposed controls. Changes in surface morphology were observed in the form of surface resin spalling. It was postulated that this surface erosion may eventually lead to changes in mechanical properties of the coupons after longer exposures.

Larsson[33] carried out tensile experiments on aramid fiber-reinforced epoxy composites following UV exposure and observed that only the one-ply laminates exhibited substantial losses in tensile strength (23% loss after 1000 h and 43% loss after 2000 h). No changes in tensile modulus were observed for any specimens, regardless of exposure time or laminate thickness. It was postulated that because UV radiation damage is mainly a surface phenomenon, any influence on mechanical properties is more pronounced for thinner specimens. For specimens >25 mm thick, no mechanical property degradation was observed. Giori and Yamauchi[34] reported on graphite/epoxy systems exposed to mercury arc radiation) for 210, 480, 720 and 960 equivalent sun hours while stored under vacuum. Although surface damage was apparent in the epoxy laminate, no changes in mechanical properties were observed after 960 h of UV exposure.

Monney *et al.*[35] reported on glass/epoxy tubular structures that were subjected to photo-oxidation in a weathering chamber (75 Wm^{-2} for 920 h) in northeast France for up to 2 years and in southeast France for up to 2 years. The yield points, rupture stress, elongation at failure and elastic modulus of the tubes remained essentially unchanged following the exposure period.

In a follow-on study,[36] the authors exposed the tubular structures to a xenon arc weathering device as well as to the same outdoor environment. During the artificial aging, the matrix eroded to the point where fibers were exposed; these fibers were later observed to be detached from the remainder of the laminate. It was concluded that initial exposure to UV radiation causes a thin photo-oxidation layer to be formed. This layer is then ablated through the loss of volatile, low molecular mass fragments, exposing a fresh surface that then undergoes photo-oxidation, thus re-starting the cycle. Chemical modification and ablation of the composite surfaces were observed following UV exposure; however, no changes in mechanical properties were observed after 2000 h.

Outdoor exposure experiments were carried out on glass-reinforced epoxy composites in cold, moderate and warm/humid climates for periods of 0.5, 1, 2 and 5 years, followed by treatment with γ-radiation. In another set of experiments, γ-radiation treatments preceded the outdoor exposures. Both the modulus and the bending strength of the specimens were unchanged following various periods of exposure in all three outdoor environments. It was proposed that both physical and chemical transformations occur in the epoxy binder during the outdoor exposure experiments, and that the resulting laminate properties are determined by the superposition of post-curing phenomena and matrix degradation. It was suggested that UV exposure could actually improve short-term properties due to post-curing, but eventually matrix degradation occurs which could subsequently lead to deterioration in mechanical properties.[37]

Polyaramid/epoxy, carbon/epoxy and glass/epoxy specimens were exposed for 10 years in Batumi, Russia, a warm and humid environment. After 6–10 years of outdoor exposure, the interlayer shear strength had decreased significantly (up to 50% in some cases) in the outer layers of the laminate, while the inner layers retained almost all of their initial interlayer shear strength. Tensile fatigue life is also known to have a high sensitivity to surface defects and was also observed to decrease after 2 years of outdoor exposure. The tensile strengths, bending strengths and both the Young's and shear modulus were only slightly decreased after outdoor exposure, with the exception of certain grades of polyaramid and glass-reinforced laminates. Visual inspection of the laminates revealed matrix resin degradation that in some cases caused the fibers to be exposed.[38]

In a field study conducted by the Army Corps of Engineers, 10-year-old polyvinyl chloride (PVC) sheet pile installations have shown no signs of significant degradation. Very little degradation in tensile and flexural properties was observed, although there was a minor degree of degradation in impact strength. Surface discoloration and increase in surface hardness were also reported.[39]

5.4 Testing methodologies

In general, UV exposure tests for polymeric materials can be grouped into three categories:

- Outdoor testing (real time): specimens are exposed outdoors to solar radiation at a fixed angle relative to the horizontal and in a fixed direction.
- Accelerated outdoor testing: Fresnel lens mirrors are used to concentrate solar radiation onto the test specimen.
- Accelerated laboratory testing: specimens are exposed to UV radiation from a variety of UV light sources, filters are often employed to remove wavelengths that fall outside of the solar spectral range of interest.

The test methods that are listed in this section are primarily taken from ASTM International and are active at the time of writing. International Organization for Standardization (ISO) equivalences for any ASTM standard are also noted.

5.4.1 General

- ASTM G113 'Terminology Relating to Natural and Artificial Weathering Tests of Nonmetallic Materials'.
- ASTM G141 'Standard Guide for Addressing Variability in Exposure Testing on Nonmetallic Materials'.

5.4.2 Outdoor testing

- ASTM D1435 'Standard Practice for Outdoor Weathering of Plastics' (equivalent to ISO 877.2-1991, method A).
- ASTM G7 'Practice for Atmospheric Environmental Exposure Testing of Nonmetallic Materials' (equivalent to ISO 877).

5.4.3 Accelerated outdoor testing

- ASTM D4364 'Standard Practice for Performing Outdoor Accelerated Weathering Tests of Plastics Using Concentrated Sunlight' (equivalent to ISO 877.2-1991).
- ASTM G90 'Standard Practice for Performing Accelerated Outdoor Weathering of Nonmetallic Materials Using Concentrated Natural Sunlight'.

5.4.4 Accelerated laboratory testing

- ASTM D822 'Standard Practice for Filtered Open-Flame Carbon-Arc Exposures of Paint and Related Coatings'.

- ASTM D1499 'Standard Practice for Filtered Open Flame Carbon Arc Exposures of Plastics' (equivalent to ISO 4892-4).
- ASTM D2565 'Standard Practice for Xenon-Arc Exposure of Plastics Intended for Outdoor Applications' (equivalent to ISO 4894-2).
- ASTM D3361 'Standard Practice for Unfiltered Open-Flame Carbon-Arc Exposures of Paint and Related Coatings'.
- ASTM D4329 'Standard Practice for Fluorescent UV Exposure of Plastics' (equivalent to ISO 4892-3).
- ASTM D4459 'Standard Practice for Xenon-Arc Exposure of Plastics Intended for Indoor Applications'.
- ASTM D4587 'Standard Practice for Fluorescent UV-Condensation Exposures of Paint and Related Coatings' (equivalent to ISO 11507: 1997).
- ASTM D5031 'Standard Practice for Enclosed Carbon-Arc Exposure Tests of Paint and Related Coatings'.
- ASTM D6360 'Standard Practice for Enclosed Carbon Arc Exposures of Plastics'.
- ASTM D6695 'Standard Practice for Xenon-Arc Exposures of Paint and Related Coatings'.
- ASTM G151 'Standard Practice for Exposing Nonmetallic Materials in Accelerated Test Devices that Use Laboratory Light Sources' (equivalent to ISO 4892-1).
- ASTM G152 'Standard Practice for Operating Open Flame Carbon Arc Light Apparatus for Exposure of Nonmetallic Materials' (equivalent to ISO 4892-4).
- ASTM G153 'Standard Practice for Operating Enclosed Carbon Arc Light Apparatus for Exposure of Nonmetallic Materials'.
- ASTM G154 'Standard Practice for Operating Fluorescent Light Apparatus for UV Exposure of Nonmetallic Materials' (equivalent to ISO 4892-3 and ISO DIS 11507).
- ASTM G155 'Standard Practice for Operating Xenon Arc Light Apparatus for Exposure of Nonmetallic Materials' (equivalent to ISO 4892-2, ISO 11341, ISO 105 B02, ISO 105 B04, ISO 105 B05 and ISO 105 B06).
- ASTM G156 'Standard Practice for Selecting and Characterizing Weathering Reference Materials Used to Monitor Consistency of Conditions in an Exposure Test'.
- ASTM G169 'Standard Guide for Application of Basic Statistical Methods to Weathering Tests'.
- ASTM G178 'Standard Practice for Determining the Activation Spectrum of a Material (Wavelength Sensitivity to an Exposure Source) Using the Sharp Cut-On Filter or Spectrographic Technique'.

UV testing of FRP composites should be undertaken with caution, whether the testing is carried out outdoors or in a laboratory weathering device, due

to the variability and uncertainty associated with the current testing methodology.[40] Outdoor test results (real time or accelerated) are influenced by fluctuations in temperature, moisture and UV irradiance. The intensity of UV irradiance changes with the test location, sample orientation, the season in which the testing is carried out and climatological variations. Results of testing in outdoor environments are seldom reproducible, due to the highly variable nature of the weather and associated climactic factors. Test results from the same material at different exposure sites, times of the year or time periods are seldom comparable.

There are also a number of systematic errors associated with current commercial laboratory weathering devices that make it difficult to compare results between nominally identical devices. In accelerated laboratory testing, the repeatability of results for a given laboratory weathering device has been found to be reasonably good; however, reproducibility between nominally identical test devices has been shown to be poor.[41] The variability encountered between nominally identical test devices can be due to manufacturing variations in spectral radiance and flux of the light sources, variations in UV transmission characteristics of the filters, variations in the aging characteristics of the lamps and filters, and non-uniform irradiance in the exposure chambers.[42] Thus, extreme caution should be used when comparing results from different test devices or even from the same device obtained at different time periods.

This variability in both laboratory and outdoor exposure testing makes it extremely difficult to obtain accurate correlations between laboratory and outdoor exposure results. In an accelerated aging experiment carried out on composite gel coats using a variety of laboratory weathering devices, Crump[43] reported results that were compared to south Florida exposure for southern exposure panels at 45 °C. Total exposure in the laboratory weathering devices ranged from 250 to 4000 h, compared with 34 months in the outdoor exposure. Overall, there was only moderate statistical correlation between the results from the laboratory weathering devices and outdoor exposure, and between the various laboratory weathering devices.

ASTM G151 states that:

> No laboratory exposure test can be specified as a total simulation of actual use conditions in outdoor environments … The relative durability of materials in actual use conditions can be very different in different locations because of differences in UV radiation, time of wetness, relative humidity, temperature, pollutants, and other factors. Therefore, even if results from a specific exposure test conducted according to this practice are found to be useful for comparing the relative durability of materials exposed in a particular exterior environment, it cannot be assumed that they will be useful for determining relative durability of the same materials for a different environment.

The use of reliability-based methods makes it possible to predict weathering service lifetimes even when the scatter in the data is high. This methodology has been used successfully in the electronics, medical, nuclear and aerospace communities. In support of this new methodology, a number of new concepts have been proposed for the collection of data, including precise quantification of temperature, time-of-wetness and spectral UV radiation (in outdoor and accelerated laboratory testing). In particular, the calculation of total effective UV dosage, i.e. the actual amount of UV radiation that induces photochemical reactions in a material, takes into account the fact that not all UV radiation is absorbed, and that not all absorbed UV radiation causes a photochemical event to occur. This is in contrast to the conventional methodology which attempts to correlate total UV irradiance or total UV dosage with observed changes in properties.[44]

5.5 Mitigation strategies

UV-induced polymer photodegradation can be inhibited or delayed by introducing stabilizers into the polymer matrix or into a coating applied to the surface of the FRP component. Stabilizer concentrations employed are typically 0.05–2% by mass and their presence can significantly lengthen the lifetime of a polymer product.[1] To be effective, stabilizers need to be: (a) photostable, soluble or dispersible in the polymer matrix; (b) non-volatile and non-leaching; and (c) compatible with the polymer and other additives.[1] Combinations of stabilizers are also often used, to protect against more than one mechanism or to provide synergistic protection. For example, UV absorbers do not usually provide adequate UV protection unless paired with hindered amine light stabilizers (HALS).[21]

UV stabilizers function in various ways. Some control the amount of radiation that reaches the polymer, and others inhibit chemical reactions initiated by the absorption of the radiation. The primary methods of UV stabilization involve:

- Absorbing or blocking UV radiation before it can reach the chromophore(s) in the polymer matrix.
- Deactivating or quenching the excited species generated by the UV radiation and converting them into stable, non-reactive forms.
- Scavenging reactive free radicals generated by UV radiation and converting them into stable, non-reactive forms.[1,21]

A detailed discussion of the UV stabilization of polymers can be found in reference 6. A brief overview of these main categories of UV stabilizers is given below.

UV blockers/absorbers are compounds that function by restricting UV penetration into the topmost surface regions of a polymer, and are effective

only if the compound has a larger absorption coefficient than the polymer for the wavelengths of interest. The greatest effectiveness is found when the blocker/absorber is concentrated on the surface, as in an applied coating or film on the polymeric component.[45]

Carbon black absorbs strongly in the UV and visible regions, and also may have radical scavenging and excited-state quenching capabilities as well, due to its aromatic ring character.[1] Photostable forms of TiO_2 are also effective in absorbing UV radiation in coatings[46,47]. In general, the level of UV protection provided by inorganic fillers increases as the size of the particles decrease. Organic UV stabilizers are aromatic organic compounds that competitively absorb UV radiation and dissipate it as heat. The most commonly used UV absorbers are 2-hydroxy-benzophenone and 2-hydroxy-benzotriazole derivatives. Hydroxyphenyltriazine derivatives are also commonly used in engineering thermoplastics.[6]

George *et al*.[48] exposed UV-stabilized glass/epoxy laminates (seven-ply) and neat (unreinforced) resin slabs to a bank of 275 W sunlamps with a total irradiance of 0.004 W cm^{-2}. Following a 12 month exposure, surface layers of unstabilized resin on the composite were depleted, causing the fibers to be exposed. UV stabilizers were partly effective in limiting photo-oxidation. The optimal UV protection was postulated to be achieved by concentrating the UV stabilizers in the topmost layers of resin, as stabilizers dispersed into the bulk would first have to diffuse to the surface to be effective.

Excited-state quenchers de-activate excited molecular species generated by the action of UV radiation by transferring energy to an acceptor molecule, which then dissipates the energy harmlessly, as either heat or fluorescent/phosphorescent emissions. One subgroup of excited-state quenchers decomposes hydroperoxides, which are aggressive agents in photodegradation. Common excited-state quenchers and hydroperoxide decomposers are metal chelates, phosphite esters, dithiocarbamates, mercaptobenzothizaoles and metal complexes of sulfur-containing compounds.[49]

Radical scavengers trap free radicals that propagate oxidative reactions, thus breaking the oxidation chain. One commonly used type of radical scavenger is the class of HALS, used alone or with a UV absorber. Upon exposure to UV radiation, the parent HALS compound is first oxidized to a nitroxyl radical, which is then capable of competing with oxygen to scavenge free radicals. In the process, the nitroxyl radicals are regenerated, thus prolonging the lifetime of the stabilizer.[50] HALS are also believed to promote hydroperoxide decomposition and inhibit the catalytic effects of metal impurities in polymers. If residual acids are present in the polymer system, then the HALS are deactivated via the formation of amine salts and are rendered ineffective.[1]

A common practice in outdoor applications of FRP composites is the use of a gel coat or other resin-rich surface coating to shield the surface of the

FRP from direct UV exposure. Gel coats are polymeric coatings that can be composed of the same resin as the FRP matrix resin or a different resin, and can be reinforced or non-reinforced, pigmented or non-pigmented.[20,21] Reinforced gel coats typically utilize glass fiber mats, or polyester or acrylic fiber mats as the reinforcing agent.[2]

It must be noted that the use of a polymeric protective coating does not prevent UV-induced damage from occurring. As indicated earlier, gel coats themselves are polymers and are therefore susceptible to UV damage. They function as a sacrificial layer to delay the effects of UV exposure by lengthening the time period before photo-induced damage reaches the FRP surface. The gel coat or protective coating itself will eventually be degraded by UV radiation and will need to be maintained or replaced. Gel coat deterioration during weathering typically manifests itself as a change in gloss and/or changes in color.[43] Periodic inspections of the protective coating should be performed to ensure that the composite surface is not visible. Repair generally involves the application of a fresh gel coat or resin layer.

A study of polyester gel coats was carried out by applying UV-stabilized gel coats to glass/polyester panels and exposing them in laboratory weathering devices and in outdoor exposure conditions in Arizona.[21] Both chalking and degree of surface discoloration were minimized with hydroxyphenylbenzotriazole or hydroxybenzophenone when combined with HALS. By itself, HALS did not provide sufficient photo-oxidation protection.

Conventional coatings are also used to protect FRP installations from UV degradation. Epoxy paint was used to protect an FRP bridge superstructure installed in upstate New York[51] from UV degradation. Unfortunately, the authors did not report as to whether this coating served its function by protecting the superstructure from UV radiation damage. In another FRP bridge installed in Idaho, UV protective coatings (unspecified) were reported to perform adequately after 18 months in service. The only visible signs of degradation were chalking; none of the underlying FRP was exposed.[52]

5.6 References

1 N.D. Searle, 'Environmental Effects on Polymeric Materials', *Plastics and the Environment*, A.L. Andrady, ed. (John Wiley and Sons, New York, 2003).
2 A. Davis and D. Sims, *Weathering of Polymers* (Applied Science Publishers, London, 1983).
3 L.C. Hollaway, *Polymers and Polymer Composites in Construction* (Thomas Telford Ltd, London, 1990).
4 J.W. Martin, 'Quantitative characterization of spectral ultraviolet radiation-induced photodegradation in coating systems exposed in the laboratory and the field', *Progress in Organic Coatings*, **23**, 49 (1993).
5 H. Kaczmarek, 'Changes in polymer morphology caused by u.v. irradiation, 1. Surface Damage', *Polymer*, **37**(2), 189 (2002).

6 B. Ranby and J.F. Rabek, *Photodegradation, Photo-oxidation and Photostabilization of Polymers: Principles and Applications* (John Wiley and Sons, New York, 1975).
7 J. Guillet, *Polymer Photophysics and Photochemistry* (Cambridge University Press, 1985).
8 L. Monney, R. Belali, J. Vebrel, C. Dubois, and A. Chambaudet, 'Photochemical degradation study of an epoxy material by IR-ATR spectroscopy', *Polymer Degradation and Stability*, **62**, 353 (1998).
9 L. Monney, N. Rouge, C. Dubois, and A. Chambaudet, 'Photochemical degradation study of an epoxy material by x-ray analysis', *Polymer Degradation and Stability*, **62**, 367 (1998).
10 G. Zhang, W.G. Pitt, S.R. Goates, and N.L. Owen, 'Studies on oxidative photodegradation of epoxy resins by IR-ATR spectroscopy', *Journal of Applied Polymer Science*, **54**, 419 (1994).
11 S.Z. Jian, J. Lucki, J.F. Rabek, and B. Ranby, 'Photooxidation and photostabilisation of unsaturated cross-linked polyesters', *ACS Symposium Series, Proceedings of the 187th Meeting of the American Chemical Society* (ACS, Washington, DC, 1985).
12 X.H. Gu, T. Nguyen, L.P. Sung, M.R. VanLandingham, M.J. Fasolka, J.W. Martin, Y.C. Jean, D. Guyen, N.K. Chang, and T.Y. Wu, 'Advanced techniques for nanocharacterization of polymeric coatings surfaces', *JCT Research*, **1**(3), 191 (2004).
13 X.H. Gu, T. Nguyen, M. Oudina, D. Martin, B. Kidah, J. Jasmin, A. Rezig, L.P. Sung, E. Byrd, and J.W. Martin, 'Microstructure and morphology of amine-cured epoxy coatings before and after outdoor exposures – an AFM study', *JCT Research*, **2**(7), 547 (2005).
14 L.P. Sung, J. Jasmin, X.H. Gu, T. Nguyen, and J.W. Martin, 'Use of laser scanning confocal microscopy for characterizing changes in film thickness and local surface morphology of UV-exposed polymer coatings', *JCT Research*, **1**(4), 267 (2004).
15 J.W. Chin, T. Nguyen, and K. Aouadi, 'Effects of environmental exposure on fiber-reinforced plastic (FRP) materials used in construction', *Journal of Composites Technology and Research*, **19**(4), 205 (1997).
16 G.E. Schoolenberg and P. Vink, 'Ultra-violet degradation of polypropylene: 1. Degradation profile and thickness of the embrittled surface layer', *Polymer*, **32**(3), 432 (1991).
17 N. Nagai, T. Matsunobe, and T. Imai, 'Infrared analysis of depth profiles in UV-photochemical degradation of polymers', *Polymer Degradation and Stability*, **88**, 224 (2005).
18 M.S. Jones, 'Effects of UV radiation on building materials', *Proceedings of Workshop on UV Radiation and its Effects*, New Zealand, 2002.
19 A.W. Signor, M.R. VanLandingham, and J.W. Chin, 'Effects of ultraviolet radiation exposure on vinyl ester resins: characterization of chemical, physical and mechanical damage', *Polymer Degradation and Stability*, **79**(2), 359 (2003).
20 G. Wypych, *Handbook of Material Weathering*, 2nd Edition (Chemtec Publishing, Toronto, 1995).
21 C. Capanescu and C. Cincu, 'Evaluation of UV inhibitors in polyester gelcoats', *Advances in Polymer Technology*, **22**(4), 365 (2003).
22 D. Roylance and M. Roylance, 'Influence of outdoor weathering on dynamic mechanical properties of glass/epoxy laminate', *Environmental Effects on Advanced Composite Materials*, ASTM STP 602, p. 85 (ASTM, Philadelphia, PA, 1976).
23 D. Roylance and M. Roylance, 'Degradation of fiber-reinforced epoxy composites

by outdoor weathering', *Proceedings of the International Conference on Environmental Degradation of Engineering Materials*, Blacksburg, VA, 1977.
24 Y. Kato, T. Mishimura, and T. Uomoto, 'The effect of ultraviolet rays to FRP rods', *Proceedings of the 1st International Conference on Durability of Fibre Reinforced Polymer (FRP) Composites for Construction*, B. Benmokrane and H. Rahman, eds, pp. 487–497, 1998.
25 W.B. Liau and F.P. Tseng, 'The effect of long-term ultraviolet light irradiation on polymer matrix composites', *Polymer Composites*, **19**(4), 440 (1998).
26 N.S. Choi, K. Takahashi, D. Oschmann, J. Karger-Kocsis, and K. Friedrich, 'Influence of weathering on unreinforced and short glass fibre reinforced thermoplastic polyester', *Journal of Materials Science*, **33**, 2529 (1998).
27 B.G. Kumar, R.P. Singh, and T. Nakamura, 'Degradation of carbon fiber-reinforced epoxy composites by ultraviolet radiation and condensation', *Journal of Composite Materials*, **36**, 2713 (1992).
28 F. Segovia, C. Ferrer, M.D. Salvador, and V. Amigo, 'Influence of processing variables on mechanical characteristics of sunlight aged polyester-glass fibre composites', *Polymer Degradation and Stability*, **71**, 179 (2001).
29 S.-S. Pang, G. Li, J.E. Helms, and S.I. Ibekwe, 'Influence of ultraviolet radiation on the low velocity impact response of laminated beams', *Composites: Part B*, **32**, 521 (2001).
30 R.E. Trabocco and M. Stander, 'Effect of natural weathering on the mechanical properties of graphite/epoxy composite materials', *Environmental Effects on Advanced Composite Materials*, ASTM STP 602 (ASTM, Philadelphia, PA, 1976).
31 B.R. Bogner and P.P. Borja, 'Ultraviolet light resistance of pultruded composites', *Proceedings of the European Pultrusion Technology Association Conference*, June 1994.
32 H.R. Phelps and E.R. Long, Jr, 'Property changes of a graphite/epoxy composite exposed to nonionizing space parameters', *Journal of Composite Materials*, **14**, 334 (1980).
33 F. Larsson, 'The effect of ultraviolet light on mechanical properties of Kevlar 49 composites', *Environmental Effects on Composite Materials*, vol. 3, G. Springer, ed., p. 132 (Technomic Publishing Company, Basel, Switzerland, 1988).
34 C. Giori and T. Yamauchi, 'Effects of ultraviolet and electron radiations on graphite-reinforced polysulfone and epoxy resins', *Journal of Applied Polymer Science*, **29**, 237 (1984).
35 L. Monney, C. Dubois, D. Perreux, A. Burtheret, and A. Chambaudet, 'Mechanical behavior of an epoxy-glass composite under photo-oxidation', *Polymer Degradation and Stability*, **63**, 219 (1999).
36 C. Dubois, L. Monney, N. Bonnet, and A. Chambaudet, 'Degradation of an epoxy-glass fiber laminate under photo-oxidation/leaching complementary constraints', *Composites*, *Part A: Applied Science and Manufacturing*, **30**, 361 (1999).
37 O.V. Startsev, A.S. Krotov, and P.D. Golub, 'Effect of climatic and radiation aging on properties of VPS-7 glass fiber reinforced epoxy composite', *Polymer Degradation and Stability*, **63**, 353 (1999).
38 O.V. Startsev, A.S. Krotov, and L.T. Startseva, 'Interlayer shear strength of polymer composite materials during long term climactic aging', *Polymer Degradation and Stability*, **63**, 183 (1999).
39 P.K. Dutta, and U. Vaidya, 'A study of the long-term applications of vinyl sheet piles', ERDS/CRREL Letter Report, August 2003.

40 J.W. Martin, 'Repeatability and reproducibility of field exposure results', *Service Life Prediction: Methodology and Metrologies*, ACS Symposium Series 805 (American Chemical Society, Washington, DC, 2001).
41 R.M. Fischer, W.D. Ketola, and W.P. Murray, 'Inherent variability in accelerated weathering devices', *Progress in Organic Coatings*, **19**, 165 (1991).
42 J.W. Martin, J.W. Chin, E. Byrd, E. Embree, and K.M. Kraft, 'An integrating sphere-based ultraviolet exposure chamber for the photodegradation of polymeric materials', *Polymer Degradation and Stability*, **63**(2), 297 (1999).
43 L.S. Crump, 'Evaluating the durability of gel coats using outdoor and accelerated weathering techniques: a correlation study', *Proceedings from the Composites Institute's 51st Annual Conference and Exposition*, session 22-B, p. 1 February 1996.
44 J.W. Martin, S.C. Saunders, F.L. Floyd, and J.P. Wineberg, *Federation Series on Coatings Technology: Methodologies for Predicting Service Life of Coatings Systems* (Federation of Societies for Coatings Technology, Whitpain Township, PA, 1996).
45 J.E. Pickett, 'Calculation of the efficiency of ultraviolet screeners in plastics', *Journal of Applied Polymer Science*, **33**, 525 (1987).
46 T.A. Skowronski, J.F. Rabek, and B. Ranby, 'The role of commercial pigments in the photodegradation of poly(vinyl chloride) (PVC)', *Polymer Degradation and Stability*, **8**, 37 (1984).
47 R.E. Day, 'The role of titanium dioxide pigments in the degradation and stabilisation of polymers in the plastics industry', *Polymer Degradation and Stability*, **29**, 73 (1990).
48 G.A. George, R.E. Sacher, and J.F. Sprouse, 'Photo-oxidation and photoprotection of the surface resin of a glass fiber-epoxy composite', *Journal of Applied Polymer Science*, **21**, 2241 (1977).
49 J.R. White and A. Turnbull, 'Weathering of polymers: mechanisms of degradation and stabilization, testing strategies and modelling', *Journal of Materials Science*, **29**(3), 584 (1994).
50 B. Felder, R. Schumacher, and F. Sitek, 'Hindered amine light stabilizers: a mechanistic study', *Photodegradation and Photostabilization of Coatings*, ACS Symposium Series 151 (American Chemical Society, Washington, DC, 1981).
51 S. Alampalli, J. O'Connor, and A.P. Yannotti, 'Design, fabrication, construction, and testing of an FRP superstructure', Special Report FHWA/NY/SR-00/134, Transportation Research and Development Bureau, New York Department of Transportation, 2000.
52 J.M. Rodriguez, N.M. Carlson, L.L. Torres, L.G. Blackwood, and T.S. Yoder, 'INEEL tests on composite bridge – final report', Report prepared for the US Department of Energy/US Department of Transportation/Federal Highway Administration, under contract DE –AC07-941D13223, July 1999.

6

Durability of composites exposed to elevated temperature and fire

A. P. MOURITZ,
Royal Melbourne Institute of Technology, Australia

6.1 Introduction

An important durability property of polymer matrix composites when used in civil infrastructure is fire resistance. The use of polymer composites has grown considerably over the last three decades, and the current annual consumption of these materials in buildings, bridges and other infrastructure applications in the United States is about 350 000 tons. The composites most commonly used in infrastructure are reinforced with fibreglass due to its relatively low cost and high strength. The organic matrix to fibreglass composites is usually a polyester, vinyl ester or general-purpose epoxy, again due to low cost and good mechanical properties. More expensive carbon fibre composites are used in exceptional circumstances, usually when high stiffness and fatigue endurance are required for the reinforcement of highly loaded bridge sections.

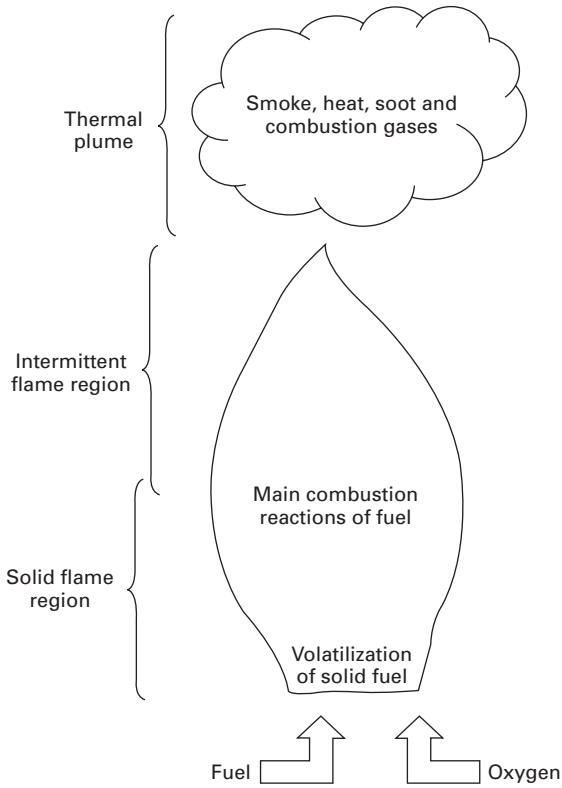
An important consideration in the use of polymer composites is the threat of fire from arson, terrorist attack, accidents and natural events; for example, fires on bridges can be caused by arson, the ignition of spilt fuel in a motor vehicle accident or by flame spread from a bush fire. Such fires can heat the surface of a composite structure to over 100°C within a few seconds and to over 400°C within several minutes. When composites are exposed to high temperature (typically over 100°C) the polymer matrix will soften, and this can cause distortion, buckling and failure of load-bearing structures. Pyrolysis of the matrix occurs above 250–400°C with the release of heat, smoke and toxic fumes. The composites used in civil infrastructure pose an unusually high hazard because the polymers most often used (ie. polyesters, vinyl esters, epoxies) are highly flammable and release copious amounts of heat, smoke and fumes when they smoulder and burn. The need to use low-cost materials in many infrastructure applications precludes the use of expensive flame-retardant polymers or fire-protective coatings. Therefore, an appreciation by civil engineers of the fire properties of polymer composites is important in the safe design and durability assessment of structures.

The fire performance of polymer composites used in civil infrastructure is described in this chapter. An overview is given of the main thermal decomposition mechanisms and combustion reactions of composite materials. The fire reaction properties of composites are described, including time-to-ignition, heat release rate, flame spread rate, smoke density and smoke toxicity. Degradation of the load-bearing properties of structural composite materials at elevated temperature and in fire is also described. Methods for improving the fire resistance of composites are discussed, including flame-retardant polymers, thermal barrier films and intumescent coatings. The chapter concludes with an assessment of the current fire safety standards for composites used in civil infrastructure, and the need to establish uniform, international regulations. The chapter also concludes with an overview of future developments in highly flame-retardant composites using inorganic polymers and nanopolymer composites. Examples are given throughout the chapter of the fire properties of the composites used in civil structures, with special attention given to fibreglass laminates with a polyester, vinyl ester, epoxy or phenolic matrix. Unless otherwise stated, this chapter is confined to describing the fire performance of thermoset polymer composites containing glass or carbon fibres. The fire durability of thermoplastic composites or composites containing organic fibres (eg. aramid, ultra-high molecular weight polyethylene) is not considered in detail because their use in civil construction is very low.

6.2 Combustion of polymer composites

The combustion of composites in fire is a complex process that is controlled by many factors, with the most important being the fuel source, the oxygen content and temperature of the flame, and the chemical composition and mass fraction of the polymer matrix. The most common type of fire involving civil structures is called a 'turbulent fire', in which the flame consists of three zones known as the solid region, the intermittent region and the thermal plume (Fig. 6.1) (see, for example, references 1 and 2). The solid flame region is where most of the combustion reactions that sustain a fire occur. The temperature in this zone reaches 830–900°C for most solid fuel fires (e.g. bushfire, house furnishings) and 1150–1250°C for liquid hydrocarbon and natural gas fires. Above the solid flame zone is the intermittent region where a small percentage of the combustion reactions occur, and the temperature drops continuously up this region towards the flame tip. The average temperature at the flame tip is about 400°C, although it fluctuates between ~300 and 600°C. Above the flame is the thermal plume which consists of hot smoke, soot, combustion gases and possibly toxic fumes.

A composite material in the vicinity of a fire can be rapidly heated by thermal radiation and/or convection of hot gas. It is common practice by fire scientists to describe the intensity of thermal radiation by heat flux rather



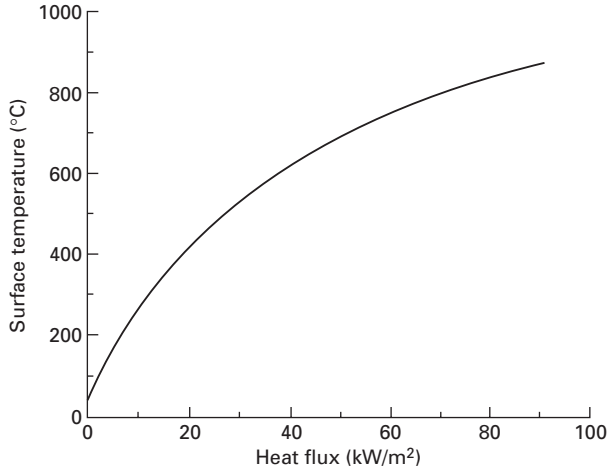
6.1 Schematic of a turbulent flame.

than by temperature. Heat flux is defined as the amount of thermal energy radiated over a solid surface, and has the unit of W/m^2. There is an approximate relationship between fire type and heat flux, and examples are:

- small smouldering fire: 2–10 kW/m^2;
- trash can fire: 10–50 kW/m^2;
- room fire: 50–100 kW/m^2;
- hydrocarbon fire: 100–150 kW/m^2;
- gas-jet fire: 150–300 kW/m^2.

Figure 6.2 shows the relationship between incident heat flux and maximum surface temperature for a fibreglass composite used in civil construction.

A composite material can undergo changes to its physical, chemical and mechanical condition in a fire. The first changes occur at the heat distortion and glass transition temperatures of the matrix, which are usually in the range of 80–180°C. The load-bearing properties are severely degraded within this temperature range. Decomposition of the polymers used in civil composite structures occurs between 300 and 500°C (see, for example, references 3 to



6.2 Relationship between heat flux and temperature at the surface of a fibreglass composite.

5). The decomposition process for most polymers yields solid carbonaceous char and gaseous volatiles. The chemical composition and amount of the volatiles is dependent on the polymer matrix, oxygen content and temperature, although the majority of the gases are flammable hydrocarbons. Highly flammable polymers – including the polyesters, vinyl esters and general-purpose epoxies used in civil composite materials – generate a large amount of volatiles and retain only a small amount of their mass (less than 10–20%) as char. The hydrocarbon volatiles provide a rich source of fuel to sustain and grow a fire. Fire-resistant polymers, such as phenolic and flame-retardant resins, yield a higher amount of char at the expense of volatiles, and therefore contribute less to the growth of fire.

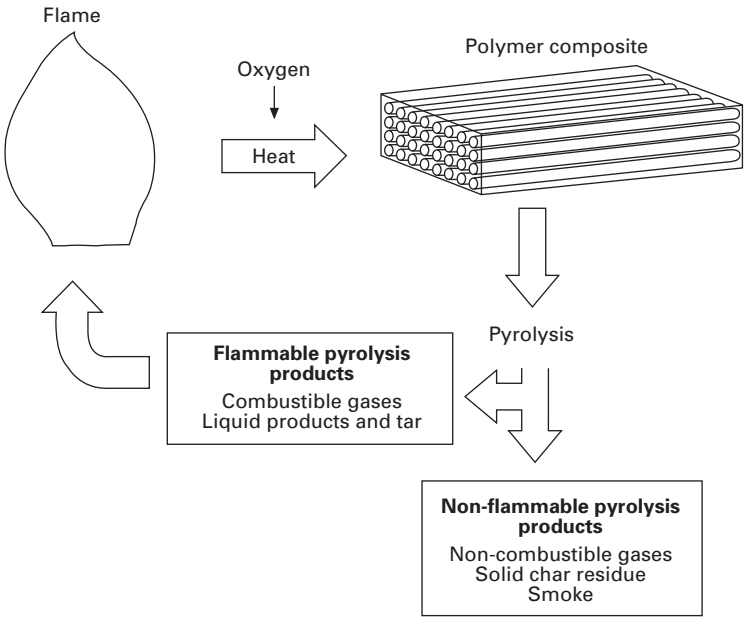
The hydrocarbon volatiles diffuse from the decomposing polymer matrix into the flame where they undergo a series of combustion reactions that generate heat that sustains the fire. Combustion of the volatiles occurs in the solid and (to a lesser extent) intermittent zones of a turbulent flame, and this produces highly reactive $H^{\bullet}$ radicals. This radical combines with oxygen in the flame to produce hydroxyl radicals ($OH^{\bullet}$) via the generalised reaction sequence:

$$H^{\bullet} + O_2 \rightarrow OH^{\bullet} + O^{\bullet} \quad [6.1]$$

$$O^{\bullet} + H_2 \rightarrow OH^{\bullet} + H^{\bullet} \quad [6.2]$$

These reactions are exothermic and therefore result in increased flame temperature, although the main exothermic reaction that generates most of the thermal energy in a flame is:

$$OH^{\bullet} + CO \rightarrow CO_2 + H^{\bullet} \quad [6.3]$$



6.3 The combustion cycle of polymer composites.

The $H^{\bullet}$ radicals produced in reactions [6.2] and [6.3] feedback into reaction [6.1], and thereby the combustion process becomes a self-sustaining process when sufficient oxygen is available. This is known as the combustion cycle of organic polymers, and is illustrated in Fig. 6.3. The cycle stops only when the fuel source has been exhausted, which is usually when the organic matrix has completely decomposed, or the oxygen is depleted to a low level.

6.3 Fire reaction properties of polymer composites

The flammability and fire hazard of composite materials are determined by their fire reaction properties. Reaction properties that describe the flammability of a material include the time-to-ignition, limiting oxygen index (LOI), heat release rate (HRR) and flame spread rate. Properties that determine the fire hazard of a material are smoke density and smoke toxicity. This section describes the fire reaction properties for composite materials used in civil construction.

6.3.1 Time-to-ignition of polymer composites

Time-to-ignition is an important fire reaction property because it defines how quickly flaming combustion of a material will occur when exposed to a heat source.[6] The organic resins used in civil composite structures (e.g.

polyesters, vinyl esters, epoxies) can ignite within a short time of being exposed to a flame. Ignition usually occurs when the surface of a composite is heated to about the pyrolysis temperature of the polymer matrix, which is somewhere in the range of 250–400°C for most organic resins. As mentioned previously, decomposition of the polymer produces hydrocarbon gases that flow from the composite into the flame. When the amount of flammable volatiles at the composite/fire interface reaches a critical concentration then ignition and flaming combustion will occur. The time duration between the composite being exposed to a fire and the onset of flaming combustion is taken to be the time-to-ignition. The time-to-ignition is determined using fire testing techniques such as the International Organization for Standardization (ISO) ignitability test[7] and the cone calorimeter.[8]

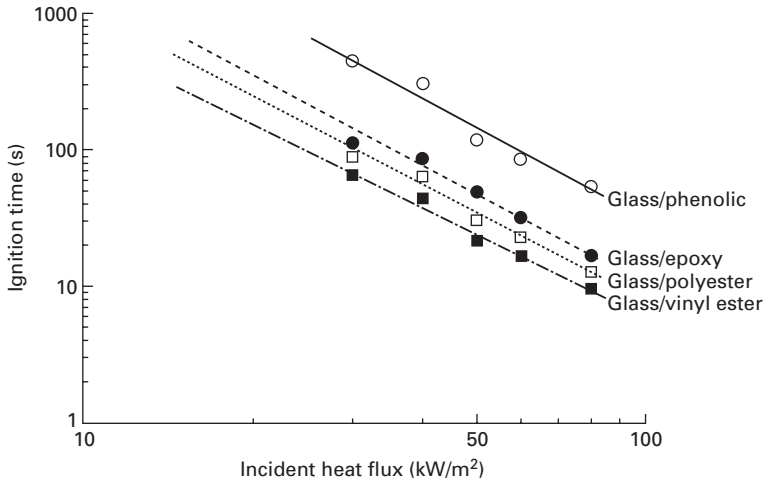
The ignition properties of a large number of composites have been published in the scientific literature, including the materials used in civil construction.[9–30] The fire reaction properties of several types of composites, including those used in civil engineering, are given in Table 6.1. These values were measured at an incident heat flux of 50 kW/m^2, which is about the radiant heat intensity of a room fire prior to flashover. The ignition times are short for polyester, vinyl ester and epoxy matrix composites, and these materials will ignite within 1–2 min when exposed to the heat flux of 50 kW/m^2. These composites are the most flammable listed in Table 6.1, and there are other materials with better ignition resistance.

Phenolic composites are being used increasingly in civil structures because of their long ignition times, excellent flame resistance and low cost. However, there is a concern about their low strength and poor durability in moist environments.[19,31] There are many thermoset polymer composites with long ignition times, most notably laminates with a bismaleimide, polyimide and phthalonitrile matrix, as well as numerous thermoplastic matrix composites, including polyphenylene sulfide (PPS), polyether ether ketone (PEEK) and polyether ketone ketone (PEKK) laminates. Most of these composites also have good mechanical properties, durability and, in the case of the thermoplastic laminates, impact damage tolerance. However, these composites are expensive and can be difficult to process into large civil structures.

The ignition time of composite materials is dependent on the heat flux (or temperature) of a fire. Figure 6.4 shows the relationship between incident heat flux and ignition time for four fibreglass laminates used in civil construction. The critical heat flux below which ignition does not occur for the polyester, vinyl ester and epoxy composites is ~15 kW/m^2 and for phenolic laminate is ~25 kW/m^2. Ignition cannot occur because the heat flux is too low to heat the composite to the pyrolysis temperature of the matrix. Above the critical value, the ignition times decrease rapidly with increasing heat flux due to the acceleration of the pyrolysis reaction rate. An increase in heat flux increases the production rate of hydrocarbon volatiles in a composite

Table 6.1 Fire reaction properties of thermoset and thermoplastic matrix laminates determined at a heat flux of 50 kW/m^2

Composite	Ignition time (s)	LOI	Peak HRR (kW/m^2)	Average HRR (kW/m^2)	Flame spread index	Smoke specific extinction area (m^2/kg)
Civil engineering composites:						
Glass/polyester	52 ± 12	23	299 ± 72	135 ± 7	–	1107 ± 57
Glass/vinyl ester	66 ± 11	–	272 ± 40	168 ± 12	27	1259 ± 151
Glass/epoxy	70 ± 16	38	352 ± 82	155 ± 14	11	1277
Carbon/epoxy	79 ± 7	41	240 ± 24	139 ± 18	11	1232
Glass/phenolic	146 ± 27	54	73 ± 15	63 ± 4	5.5	286 ± 116
Advanced thermoset composites:						
Glass/bismaleimide	141	60	176	161	18	546
Glass/cyanate ester	58	–	71	71	–	898
Glass/polyimide	175	–	40	27	2.5	170
Glass/phthalonitrile	530	–	34	32	–	–
Advanced thermoplastic composites:						
Glass/PPS (polyphenylene sulfide)	244	52	48	28	7	690
Carbon/PEEK (polyether ether ketone)	307	–	14	8	3	69
Carbon/PEKK (polyether ketone ketone)	233	–	21	10	–	274



6.4 Log–log plot of heat flux against time-to-ignition for four composite materials used in civil construction.

that provide the fuel for ignition. The thermal decomposition of the polyester, vinyl ester and epoxy composites produces a large amount of volatiles that are a plentiful fuel source. Figure 6.4 shows that the ignition times for the phenolic composite are much longer than for the other materials, and this is because of the high aromatic content of the phenolic matrix that promotes char formation. When a phenolic resin decomposes a significant amount of its mass (40–70%) is converted to solid char resulting in a relatively low yield of flammable volatiles and this delays ignition. Many of the advanced thermoset and thermoplastic composites given in Table 6.1 also have long ignition times because they produce low amounts of hydrocarbon volatiles.

Other factors that influence the ignition time are the polymer content and thickness of the composite. The time-to-ignition value of a composite material increases when the mass fraction of polymer is reduced, and this is obviously because less organic material is available to generate flammable volatiles.[32] Therefore, the ignition resistance of composites used in civil engineering can be improved by using materials with a high fibre content, which will also provide higher load-bearing properties. The ignition resistance can also be improved by increasing the thickness of a composite structure. Thick materials act as a 'heat sink' by drawing heat from the fire-exposed surface, and this increases the time taken to reach the pyrolysis temperature of the matrix.[11,12]

6.3.2 Limiting oxygen index of polymer composites

The LOI is a fire reaction property used to quantify the flammability of organic polymers and composite materials. The LOI is defined as the minimum

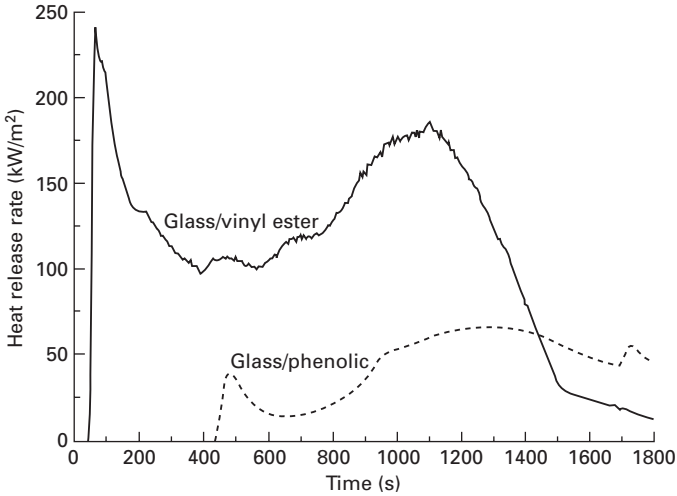
percentage of oxygen needed to sustain flaming combustion.[33] The LOI test involves exposing a composite material to a flame in atmospheres having different oxygen levels, and from this determining the minimum oxygen content that allows the sample to burn with a candle-like flame.[34] Unfortunately the method does not test the sample in a realistic fire environment, and therefore the LOI index cannot be used to quantify accurately the flammability of a material. Despite this limitation, the oxygen index value is used to rank the relative flammability of different polymer composite materials.[32,35–41]

The LOI values for a variety of composite materials are given in Table 6.1. It can be seen that the LOI values for polyester-, vinyl ester- and epoxy-based composites used in civil construction are below about 40. The LOI value for a composite will increase with the char yield of the polymer matrix. This is because the formation of char occurs at the expense of hydrocarbon volatiles, which in turn increases the oxygen level required to sustain flaming combustion. Composites containing aromatic polymers have high index values, including phenolic, high-temperature thermoset and many thermoplastic matrix laminates.[40,42–44]

6.3.3 Heat release rate of polymer composites

The HRR is considered the single most important fire reaction property because the heat released by a burning material can contribute to the growth and spread of fire.[45,46] No other reaction property has such a dominant influence on the fire behaviour of composites. Furthermore, several other reaction properties, such as surface spread of flame, smoke density and carbon monoxide emission, are dependent on or related to the HRR.[47,48] The heat release rate is determined by several combustion processes, with the most important being combustion of hydrocarbon volatiles released from a decomposing composite. These volatiles migrate from the decomposing matrix into the flame where they generate heat via exothermic combustion reactions described earlier. Composites that release large amounts of organic volatiles into the flame usually exhibit high HRR properties. The HRR of composites is measured using the cone calorimeter technique (ASTM E1354-04a).[8]

The HRR of composite materials changes continuously during the combustion process, as shown in Fig. 6.5. Due to the variation in HRR with time, several parameters are used to describe the rate behaviour. The peak HRR defines the maximum release rate of heat during the combustion process. The peak HRR occurs when the decomposition process is occurring at its fastest rate; and the peak value is considered a reliable measure of the maximum flammability and flashover potential of a material. The average HRR is the total heat released averaged over a specified period of time, which is usually taken to be 180 s, 300 s or the entire combustion period. Figure 6.5 compares the heat release rate behaviour of glass/vinyl ester and glass/phenolic composites



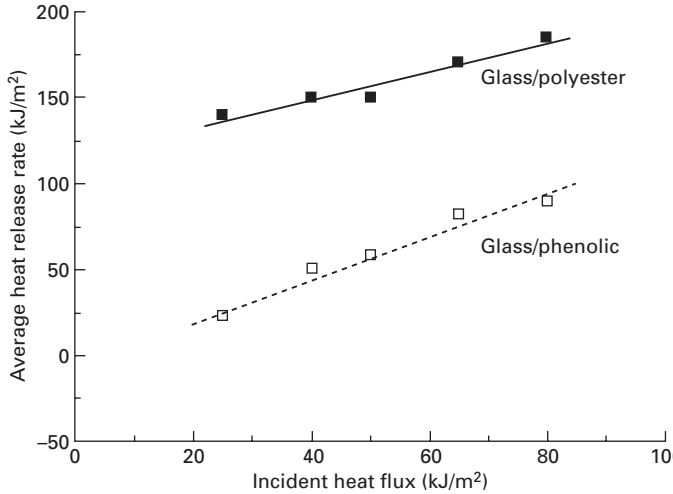
6.5 Heat release rate curves for glass/vinyl ester and glass/phenolic composites tested at a heat flux of 50 kW/m^2.

used in civil construction. The peak and average HRR values are much higher for the vinyl ester composite, and this is because the matrix releases a greater amount of hydrocarbon volatiles into the flame than the phenolic laminate. The HRR properties of polyester and epoxy composites used in civil infrastructure are also high (Table 6.1), again due to the release of a large amount of volatiles. The lower HRR properties of phenolic composites make them more suitable for use in fire-safe civil structures. Table 6.1 shows that advanced thermoset and thermoplastic composites also have heat release properties that are much lower than the polyester, vinyl ester and epoxy laminates used in civil construction.

The temperature of a fire has a significant influence on the HRR of a composite material.[12,16,18,21,30,36] Figure 6.6 shows the effect of increasing heat flux on the average HRR for polyester and phenolic composites. The heat released by these materials rises with heat flux due to an increase in the decomposition reaction rate and, as a result, yield rate of combustible volatiles. The HRR properties of advanced thermoset and high-temperature thermoplastic composites usually increase at a slower rate with heat flux due to their higher decomposition reaction temperature and, more importantly, lower yield of hydrocarbon gases.

6.3.4 Flame spread rate of polymer composites

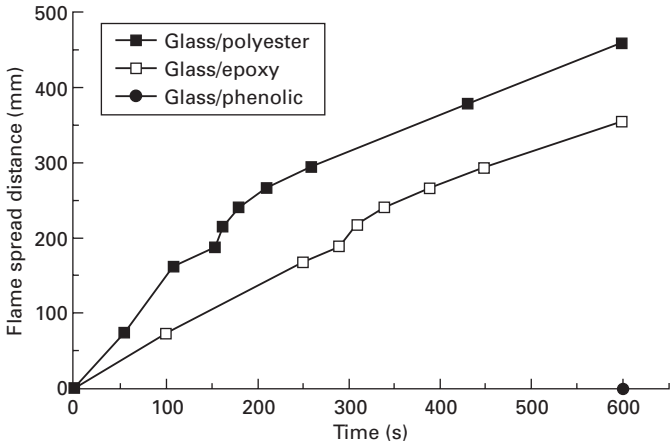
The speed at which flames can spread over the surface of a composite material is a critical factor in the growth and spread of fire. Due to the high-flammability of most types of composites used in civil infrastructure, there is the risk that



6.6 Effect of heat flux on the average heat release rates of glass/polyester and glass/phenolic composites. Data from Egglestone and Turley.[16]

flames will quickly spread and thereby increase the difficulty in containing and extinguishing a fire. This is one of the key concerns of fire safety authorities with the use of composites in high-fire-risk applications such as buildings, and for this reason there has been an effort over many years to characterise their flame spread properties. There are several methods used to measure the flame spread rate,[49–51] although the most common for testing composite materials is the radiant panel flame spread technique specified in ASTM E162.[52]

The flame spread rates for composites used in civil construction have been determined, and typical flame speeds for several of these materials are shown in Fig. 6.7.[12,13,15,19,20,24,53,54] This figure shows the time taken for a flame to travel down the inclined surface of a flat composite panel. It is seen that the flame propagates rapidly down the surface of glass/polyester and glass/epoxy laminates, and this is due to the high flammability of the resins. However, the flame is unable to spread down the glass/phenolic laminate. Phenolic laminates have excellent resistance to flame spread, and this is another outstanding fire reaction property of these materials that makes them suited for high-fire-risk applications. The flame spread index values for several composite materials are given in Table 6.1. The index value is a measure of the resistance of a material against downward flame spread. In addition to phenolic composites, it is seen that high-temperature thermoset and thermoplastic composites have a high resistance against flame spread.



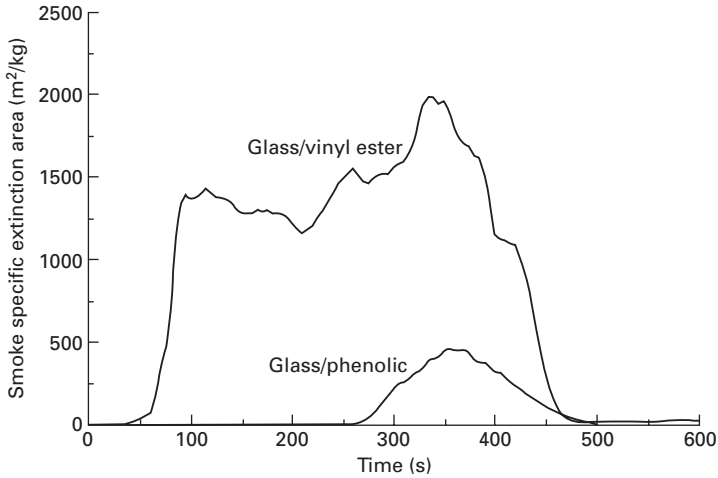
6.7 Surface spread of flame versus time.[18]

6.3.5 Smoke properties of polymer composites

One of the main safety concerns with polymer composites is the generation of thick, blinding smoke in the event of fire. The smoke can be extremely dense and thereby reduce visibility, cause disorientation for people attempting to escape and make it difficult for fire-fighters to locate the source of the fire. For these safety reasons the smoke properties of many types of composites have been determined, including those materials used in civil construction.[12–14,18,20,23,37,38,55] The smoke produced by highly flammable polymer composites (e.g. polyesters, vinyl esters, epoxies) is often dense, and much thicker than smoke from phenolic laminates. Figure 6.8 compares the specific extinction area (SEA) for glass/vinyl ester and glass/phenolic composites when exposed to the same heat flux. The SEA is a measure of how effectively a given mass of material is converted into smoke, and is often used to quantitatively define the smoke density. The SEA of the vinyl ester laminate increases rapidly at the onset of combustion, and then remains high until the matrix is completely consumed. The phenolic composite produces much less smoke, which is another reason for their use in high-fire-risk applications. The SEA values for various types of composite materials are given in Table 6.1. In addition to phenolic resins, other highly aromatic thermoset polymers and many high-temperature thermoplastics release relatively low amounts of smoke. Examples include aromatic thermosets such as polyimides, cyanate esters and phthalonitriles as well as thermoplastics such as PPS and PEEK.

6.3.6 Smoke toxicity of polymer composites

People can experience various health problems when exposed to a burning composite, which vary in severity from skin and eye irritations through to



6.8 Smoke density (specific extinction area) versus time for glass/vinyl ester and glass/phenolic composites tested at a heat flux of 50 kW/m^2.

severe coughing and respiratory problems that require hospitalisation. As yet, no human deaths or long-term health problems have been attributed to smoke inhalation from composites, although much remains unknown about the toxic potency of the combustion gases, fibre fragments and soot particles present in the smoke. The greatest hazard to people exposed to fire is toxic gas rather than flames and heat. A greater percentage of fatalities in house fires are caused by inhalation of smoke fumes rather than burns. A variety of toxic gases are released when a composite material decomposes in fire, although the gas that is usually the greatest hazard is carbon monoxide (CO).

The amount of CO produced by a burning composite depends on the composition of the organic matrix, temperature and oxygen availability. The CO level is often high for thermoset laminates, and even aromatic polymers such as phenolic and polyimide produce a high amount of CO. Certain types of advanced thermoset resins (e.g. phthalonitrile, phenolic/siloxane) and thermoplastics yield lower amounts of CO and CO_2 due to their exceptionally high char yield that retains most of the carbon as solid char. In addition to CO and CO_2, composites release a large number of other volatiles, several of which are highly toxic or corrosive. For example, more than 90 compounds have been detected in the smoke of a burning carbon/bismaleimide composite.[56]

Composite materials used in high-fire-risk applications may have a polymer matrix that is chemically modified (e.g. halogenated) or blended with flame-retardant additives (e.g. antimony trioxide) to delay ignition and reduce the HRR and smoke density, as described in section 6.4. The yield of toxic gases

from flame-retardant composites can be much less than the untreated material, particularly when the additive promotes char formation or resists pyrolysis. However, some flame-retardants increase the smoke toxicity of the polymer matrix. For example, brominated polymers release dioxins and dibenzofurans while chlorinated polymers produce hydrogen chloride, dibenzo-*p*-dioxins and related dioxin compounds that are extremely hazardous.[57] The dioxins, hydrogen chloride and other toxic gases released from halogenated polymers have led to these materials being banned in many countries. A mathematical approach called the 'N-gas model' has been developed to predict the toxic potency of smoke.[58]

Another health hazard of burning composites is the release of airborne fibre particles that can cause skin irritation, sore eyes and breathing problems.[59] While the long-term health effects of inhaling fibres are not fully known, toxicity studies on laboratory animals indicate that fibres are not hazardous for short-term and low-dose exposures. Because the toxicity of the carbon and glass fibres is not understood and the polymer matrix may release toxic, corrosive and other hazardous gases, it is recommended that fire-fighters wear self-contained breathing apparatus, sealed goggle-type eye protection, puncture-resistant gloves, neoprene overalls, hard-soled boots and chemical protective clothing – including aluminised proximity suits.

6.4 Fire-resistant polymer composites

Due to the high flammability of many polymer composites, it may be necessary to increase the flame-retardant properties of the matrix when there is a high risk of fire. There are many ways of reducing the flammability of polymers, and the most common are the addition of flame-retardant filler particles to the matrix or the chemical modification of the matrix by the addition of halogen or phosphorus compounds. This section gives an overview of the application of these methods to composites. In addition, there are several methods under development to further improve the flame-retardant properties of composites, such as inorganic polymers and nanoparticle-filler organic polymers, and these are described separately in section 6.8.

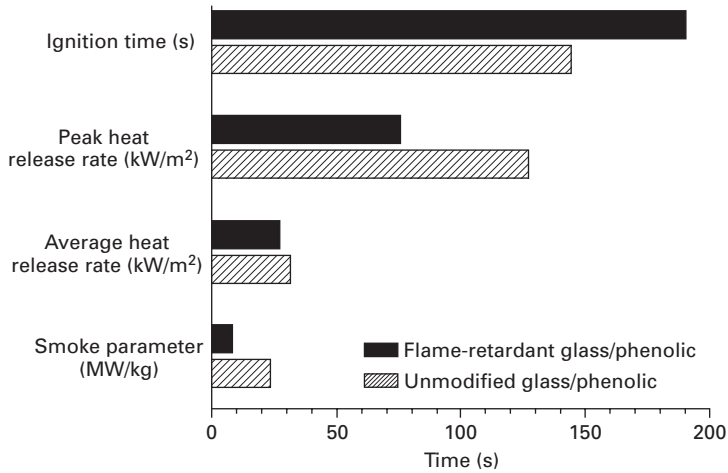
6.4.1 Flame-retardant filled composites

The simplest and (usually) most cost-effective way of reducing the flammability of polymers is the addition of flame-retardant fillers. The filler particles are blended into the liquid resin during the final stages of processing, and must be uniformly dispersed to ensure consistent flame-retardant properties throughout the polymer. Most polymers require a high loading of filler to show a substantial reduction in their flammability, and the average content in most resins is 50–60%.

There are two classes of fillers – 'inert' and 'active' flame retardants – and they are distinguished by their mode of action. Inert fillers reduce the flammability and smoke yield of polymer composites by several mechanisms. The dominant mechanism is a reduction in the fuel load of a composite by diluting the mass fraction of polymer with a non-combustible filler. Flame retardation and smoke suppression by this mechanism can only be achieved when the polymer content is reduced by a large amount, and for this reason inert filler loadings of 50–60% are often required. Another important mechanism is the absorption of heat by the filler particles to reduce the burning rate of the polymer matrix. The inert fillers most commonly used in polymers and polymer composites are silica, calcium carbonate and carbon black. In a few cases, simple hydrated clay silicates such as pumice, talc, gypsum and calcium sulphate dihydrate are used.

Active fillers are more effective than inert fillers at reducing the flammability of polymer composites.[13,16,60–62] Like inert fillers, active fillers operate as a heat sink and by diluting the mass fraction of organic matrix material in a composite. The unique feature of active fillers is that they decompose at elevated temperature via an endothermic reaction that absorbs heat. This has a cooling effect that slows the decomposition rate of the polymer matrix. The decomposition reaction of the filler also yields a large amount of inert gases, such as water vapour and carbon dioxide, which diffuse into the flame where they dilute the concentration of flammable volatiles, $H^{\bullet}$ and $OH^{\bullet}$ radicals. The dilution reduces the flame temperature, which in turn lowers the decomposition rate of a composite material. A variety of metal oxides and metal hydroxides are used as active fillers, although by far the most common is aluminium trihydroxide, $Al(OH)_3$, because of its low cost and high flame-retardant properties. Other types of aluminium oxide compounds are also used, as well as oxide compounds containing antimony (Sb_2O_3, Sb_2O_5), iron (e.g. ferrocene, FeOOH, FeOCl), molybdenum (MoO_3), magnesium ($Mg(OH)_2$), zinc and tin. Figure 6.9 shows the effect of aluminium trihydroxide particles on the fire properties of a glass/phenolic composite. The filler increased the time-to-ignition and reduced the peak HRR, average HRR and smoke density.

The efficacy of active fillers as flame-retardants depends on their composition and the composition of the host polymer. As with inert fillers, high loading levels (up to 60%) are often needed to achieve a substantial reduction in flammability. Active intumescent fillers are a novel way of improving the flame resistance of certain types of composite materials.[63,64] Intumescent fillers swell and char when heated, and this produces a protective insulating layer in a composite that slows heat conduction. However, these fillers can only be used in certain types of polymers, and their use as a flame-retardant in composite materials is low.



6.9 Effect of aluminium trihydroxide filler on the fire reaction properties of a glass/phenolic composite tested at an incident heat flux of 50 kW/m^2. Data from Scudamore.[13]

The selection of a flame-retardant filler is determined by several factors, including cost, its chemical compatibility with the host polymer, its decomposition temperature, and weight. Many fillers reduce the mechanical properties of polymers, and this is a problem when used in structural composites. Some fillers, while decreasing flammability, increase the amount of smoke and toxic fumes. For these reasons, it is common practice to use a combination of flame-retardants in polymer composites to maximise the flammability resistance while minimising the adverse effects on the mechanical properties, smoke and toxicity. It is important to note that fillers are rarely used alone, but instead are used with other flame-retardants (such as organohalogen or organophosphorus compounds) to achieve a high level of flammability resistance.

6.4.2 Flame-retardant polymer composites

Chemical modification of polymers using halogen compounds containing bromine or chlorine is one of the more common and effective methods for reducing the flammability of composite materials.[65–67] The matrix is modified by polymerising the resin with an organohalogen compound to incorporate bromine or chlorine atoms in the molecular network structure. In the event of fire, reactive halogen species are released from the matrix into the flame where they terminate the combustion reactions. This lowers the flame temperature and thereby slows decomposition of the composite material. A large improvement in the fire reaction properties of composite materials can be achieved using halogenated polymers. For example, Table 6.2 compares

Table 6.2 Comparison of the fire reaction properties of a non-brominated and brominated glass/polyester composite. Data from Scudamore[13]

Property	Heat flux (kW/m^2)	Non-brominated composite	Brominated composite	Percentage improvement (%)
Ignition time	35	41 s	93 s	127
	50	25 s	62 s	148
	75	13 s	31 s	139
Peak heat release rate	35	327 kW/m^2	112 kW/m^2	292
	50	374 kW/m^2	159 kW/m^2	235
	75	471 kW/m^2	174 kW/m^2	271
Average heat release rate	35	78 kW/m^2	38 kW/m^2	205
	50	115 kW/m^2	49 kW/m^2	235
	75	109 kW/m^2	83 kW/m^2	131
Smoke parameter	35	338 MW/kg	94 MW/kg	360
	50	374 MW/kg	155 MW/kg	241
	75	457 MW/kg	175 MW/kg	261

the fire reaction properties of a glass-reinforced laminate containing general-purpose polyester or brominated polyester. The ignition times of the brominated composite are more than double the times of the non-brominated material. Furthermore, the peak HRR, average HRR and smoke values for the brominated composite are less than half the values for the non-brominated laminate. As mentioned, however, halogenated polymers can release smoke containing corrosive, acidic and toxic gases that are serious health and environmental hazards.

The flammability resistance of polymer composites can also be improved by phosphorus.[68,69] The most common method for adding phosphorus is blending an inorganic or organic-based phosphorous filler compound into a polymer during processing. Virtually any phosphorus compound can provide some degree of fire resistance, and the most common types are elemental phosphorus, ammonium polyphosphates and trialylphosphates. Phosphorus can also be incorporated into the molecular structure by copolymerisation of the resin with a reactive organophosphorous monomer or halogenated phosphate. Phosphorus acts as a fire retardant in the flame and/or in the composite, depending on the chemical nature and thermal stability of the host polymer. When phosphorus is present in non-oxygenated polymers it releases volatiles (e.g. HPO_2, P_2) and gaseous radicals (e.g. $P^{\bullet}$, $PO^{\bullet}$) at elevated temperature. These gases diffuse into the flame where they terminate the combustion reactions. When phosphorus compounds are used in oxygenated and hydroxylated organic polymers they act mainly by promoting the formation of char, and this reduces the amount of flammable hydrocarbon gases released into the flame.

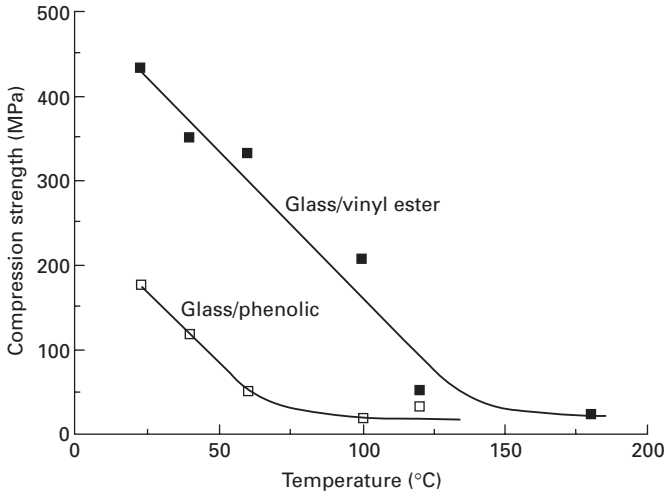
Graft copolymerisation is an emerging technique for the production of flame-retardant polymers.[70] This technique basically involves attaching a monomer, which is a strong char former, onto the polymer chain. Several types of inorganic salts are suitable monomers that can be grafted to the molecules of thermoplastics. These salts include alkaline earth salts, alkali metal salts and salts of methacrylic and acrylic acids. When grafted to a thermoplastic, these monomers decompose at elevated temperature to produce an insulating and adherent char on the polymer surface that provides fire protection. In addition, the decomposition reaction of the salts produces carbon dioxide that serves to quench the flame. While graft polymerisation is not currently used to reduce the flammability of polymers used in civil composite materials, it is possible that it will be used in future structural applications.

6.5 Structural properties of polymer composites in fire

An important consideration in the use of composites in load-bearing civil structures is the distortion, softening and failure of the material that can occur in the event of fire. While all structural materials will weaken at high temperature, it can be a greater problem for composites because their structural properties are reduced at lower temperatures than is the case for many engineering alloys, such as steels. Weakening of composites in a fire is due to several factors, with the most important being visco-elastic softening and pyrolysis of the polymer matrix, heat-induced delamination cracking, and weakening of the fibres. The modulus and strength of glass fibres are reduced by visco-plastic softening whereas the properties of carbon fibres are reduced by surface oxidation.

The mechanical properties of composite materials can be severely degraded when heated to moderate temperatures that are well below the pyrolysis temperature of the matrix. Composite materials will begin to warp under load when heated above the heat distortion temperature of the matrix, which is typically in the range of 80–120°C for many of the polymer systems used in civil structures. The stiffness and strength of composites are severely degraded when heated to about the glass transition temperature (T_g) of the matrix. This temperature is dependent on the chemical composition and degree of cure of the polymer, although it is usually a value between 90 and 180°C for the resins used in civil construction.

Figure 6.10 shows the effect of temperature on the compression strength of a glass/vinyl ester and glass/phenolic composite. The glass transition temperature of both materials is about 120°C. It is seen that the strength drops rapidly with temperature, and above 100–150°C the residual strength is very low. Pyrolysis of these composites does not occur until the temperature

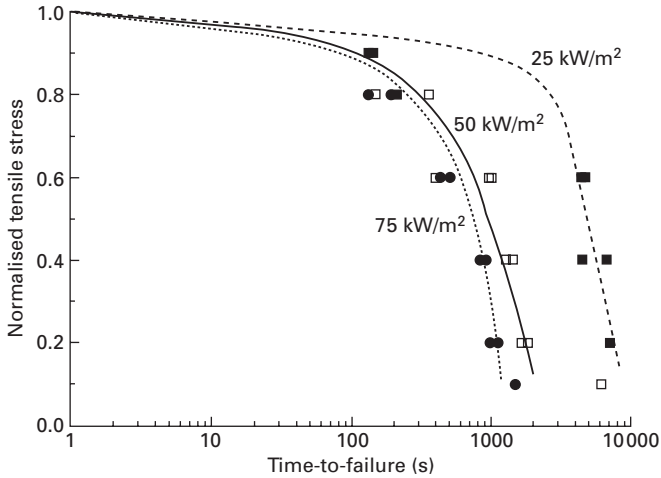


6.10 Effect of temperature on the compressive strength of glass/vinyl ester and glass/phenolic composites.

exceeds ~250–350°C, and therefore these materials are severely weakened under compression loading before the matrix begins to thermally decompose. The tension properties of composites are also reduced at temperatures below the pyrolysis temperature. However, the tension properties decrease more gradually than the compression properties with increasing temperature.[71]

It is important to note that the bulk stiffness and strength of a composite structure will not drop immediately when the surface exceeds the glass transition temperature. The low thermal conductivity of composites means that the rate of heat transfer through the material is slow (compared with metals), and therefore it may take a long time to heat a thick structure above the glass transition temperature. When softening of the hot surface region occurs in a fire, the 'cooler' region of the material supports the applied load. Failure of a structure will only occur when the load capacity of the cooler material drops below the applied load.

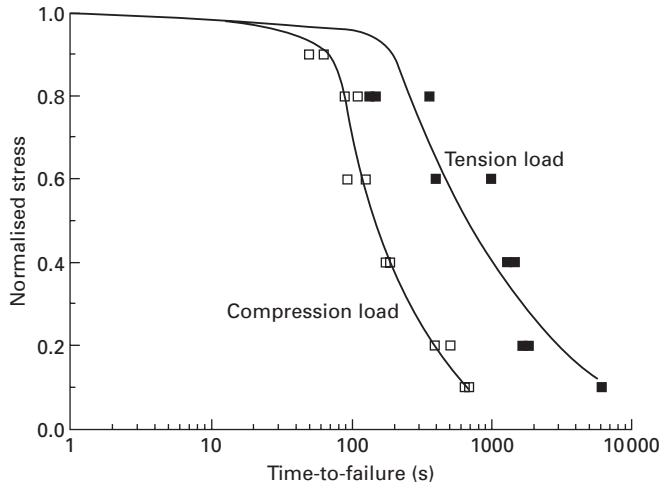
Thick composite materials are capable of supporting an externally applied load for a considerable period of time after the hot surface begins to thermally decompose and burn. For example, Fig. 6.11 shows the effect of incident heat flux on the time-to-failure of a glass/vinyl ester composite under tensile loading. The normalised stress is defined as the applied tensile stress divided by the tensile strength of the composite at room temperature. Time-to-failure is the period that the composite can support the load without breaking. It is seen that the failure times increase with decreasing heat flux and applied load. At low stress levels it is possible for a composite to continue carrying an applied tensile load after the polymer matrix has completely decomposed, with the residual strength provided by the hot glass fibres. The time-to-



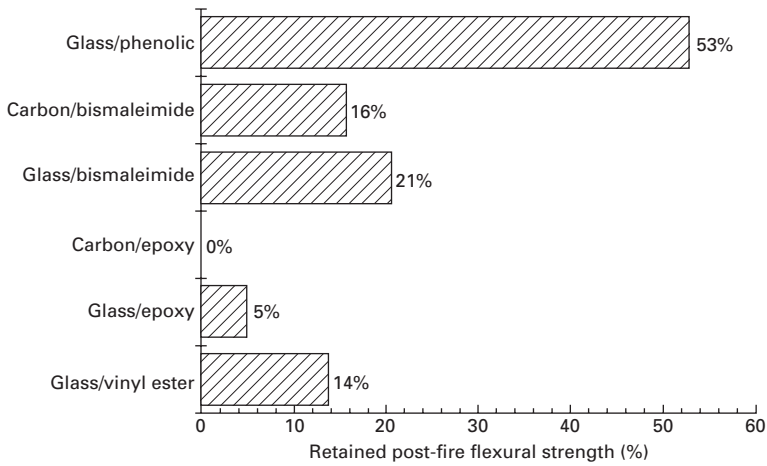
6.11 Effect of applied tensile stress on the time-to-failure of a glass/vinyl ester composite exposed to different heat fluxes.

failure values for composite materials are shorter when subjected to a compressive load. As an example, Fig. 6.12 compares the time-to-failure curves for a glass/vinyl ester laminate under tension or compression loading at a heat flux of 50 kW/m^2. Failure occurs earlier under compression loading because the compressive properties are more dependent on the matrix properties, which soften at low temperature. The load-bearing properties of civil engineering composite materials subjected to simultaneous loading and heating have been experimentally determined, and models for predicting the time-to-failure in a fire are being developed.[71–74] These models will aid in the fire-safe design of civil composite structures.

After a burning composite material has been extinguished and cooled to room temperature the loss in stiffness and strength will recover to some extent. The mechanical properties of a variety of fire-damaged composites have been measured at room temperature, including the materials used in civil construction.[28,75–77] Figure 6.13 compares the post-fire flexural strength of several composites after being exposed to a moderate heat flux (25 kW/m^2) for 20 min. All of the materials experienced a large loss in strength, and the epoxy composites had little or no retained strength. The phenolic composite experienced the smallest loss in strength, and this is because the polymer matrix yields a high amount of char which provides some strength. The post-fire properties are dependent on the amount of char damage to the load-bearing region of a composite. That is, the residual stiffness and strength decrease with an increase in the amount of char damage. Mechanics-based models have been formulated for predicting the retained tension, compression and bending properties of composites after being damaged by fire.[28,76,77]



6.12 Comparison of the time-to-failure of a glass/vinyl ester composite under tension or compression loading. The loaded composite was exposed to a heat flux of 50 kW/m^2.



6.13 Retained flexural strengths of various thermoset laminates following fire testing at the heat flux of 25 kW/m^2 for 20 min. Data from Sorathia.[12]

6.6 Fire protection coatings for polymer composites

A common method for protecting composites from fire is to apply a flame-resistant coating. There are three major classes of coatings: flame-retardant polymer, thermal barrier and intumescent coatings. Flame-retardant polymer

coatings are inherently fire-resistant organic resins (e.g. brominated polymers) or inorganic materials (e.g. geopolymers) that are applied as a film over the composite substrate.[78–80] Organic polymer coatings protect the substrate by generating volatiles at elevated temperature, such as halogen radicals or phosphorus gases. These volatiles are released into the flame where they remove the $H^{\bullet}$ and $OH^{\bullet}$ radicals that drive the combustion process. Inorganic coatings are thermally stable to very high temperatures (>1000°C) and have low thermal conductivity. These coatings protect a composite by slowing heat conduction and acting as a barrier against the egress of flammable volatiles from the matrix into the flame, thereby slowing the combustion process.

Thermal barrier coatings are ceramic-based materials that are non-flammable and have low heat-conducting properties. Examples of these coatings include ceramic (e.g. silica, rockwool) fibrous mats and ceramic (e.g. zirconia, alumina) plasma-sprayed films. Intumescent coatings provide fire protection by swelling and foaming at elevated temperature into a highly porous, thick and thermally stable char on the composite substrate.[81,82] The high void content and thickness of the coating allows it to act as an insulation barrier to the underlying composite against flame and heat. Intumescent coatings can be extremely effective in delaying combustion, suppressing flame spread, reducing the HRR and lowering the smoke density of composite materials. However, a problem with many intumescent coating systems is their poor adhesion strength to a composite substrate. This can cause the coating to fall off, thereby exposing the underlying composite directly to the flame. This is a common occurrence when a coating is applied to vertical (e.g. walls) or overhead (e.g. ceiling) structures. Furthermore, intumescent coatings are not suited to many civil applications because of poor wear resistance and environmental durability.

6.7 Fire safety regulations

The development and enforcement of fire safety regulations is a critical issue in the use of composite materials in civil infrastructure. There is no international fire safety standard for infrastructure, and many nations lack any sort of fire safety regulations for composites used in civil applications. When regulations do exist they are often unique to a single country, and are not consistent between nations. For example, the regulations applied to the use of composites in civil infrastructure differ considerably among the United States, Europe, Australasia, Japan and many other countries. As a result, certain types of composite may fulfil the fire safety requirements in one or several nations but fail in other countries. This difference arises because international civil engineering organisations do not coordinate fire safety standards. However, the European Union recently established fire safety

regulations on composite materials used in construction products for buildings, including multi-occupancy dwellings, hospitals, schools, shops, clubs, leisure centres, stadiums, factories, stations, airports, tunnels and docks.[83,84] The following properties are evaluated in the European system: ignitability to a small flame, lateral flame spread, heat release, smoke, generation of flaming droplets and fire resistance. It is hoped that the European standard will provide the direction and incentive for other countries to develop fire safety regulations on the use of composites.

6.8 Future fire-resistant composite materials

The safe use of composite materials in civil engineering structures is dependent on the polymer matrix having high fire resistance. Fire resistance is not a single material property, but is defined by a number of fire reaction properties such as time-to-ignition, HRR, LOI, flame spread rate, smoke density and smoke toxicity as well as fire-resistive properties such as burn-through resistance and structural integrity retention. All of these properties must be considered in the selection of fire-safe composites for civil applications. The selection of fire-safe materials is also dependent on well-defined fire safety regulations for the use of composites in civil infrastructure, which is lacking in most countries.

The polymer matrix to the composites used in civil applications is often unmodified polyester, vinyl ester or general-purpose epoxy resins; these are flammable, produce large amounts of heat and smoke, and can rapidly lose stiffness and strength when exposed to fire. Phenolic composites have much better flammability resistance, but have inferior mechanical properties and environmental durability that make them unsuitable in heavily loaded civil structures. The fire resistance of composites can be improved by using flame-protective coatings and/or flame-retardant polymers. Conventional methods for reducing the flammability of polymers involve the use of flame-retardant fillers or halogenated or phosphorus-containing resins. A variety of new flame-retardant polymers have the potential to improve the fire performance of civil engineering composites. Polymers containing nano-sized filler particles such as montmorillonite and carbon nanotubes can possess fire reaction properties that are superior to unmodified resins, while also having better mechanical properties. A great amount of effort is currently being devoted to the development of low-cost flame-retardant polymer nanocomposites, and it is possible these materials will be used in future civil composite structures.[85] The use of specialty inorganic polymers in composites is another emerging flame-retardant technology. Several inorganic polymers – most notably geopolymers, POSS® (polyhedral oligometric silsesquioxanes) and FyreRoc® (inorganic metallosilicates) – have outstanding flammability resistance and may eventually be used in civil infrastructure.[86,87] The development of polymers

with excellent flame retardancy together with the enforcement of safety regulations will ensure that the fire hazard is minimised for future civil composite applications.

6.9 Acknowledgements

The preparation for this chapter was performed as part of a research project (P2.1.1) within the Cooperative Research Centre for Advanced Composite Structures (CRC-ACS). The study was partially funded by the United States Office of Naval Research (grant N00014-04-10026) under the direction of Dr L. Couchman.

6.10 References

1 D. Drysdale. *An Introduction to Fire Dynamics*, John Wiley & Sons, Chichester, 1985.
2 J.G. Quintiere. *Principles of Fire Behavior*, Delmar Publishers, Albany, NY, 1998.
3 C.F. Cullis and M.M. Hirschler. *The Combustion of Organic Polymers*, Oxford University Press, Oxford, UK, 1981.
4 S.L. Madorsky. *Thermal Degradation of Polymers*, Robert E. Kreiger, New York, 1985.
5 N. Grassie and G. Scott. *Polymer Degradation and Stabilisation*, Cambridge University Press, Cambridge, UK, 1985.
6 V. Babrauskas. *Ignition Handbook*, Fire Science Publishers, Issaquah, WA, 2004.
7 ISO 11925-2: 2002. Reaction to fire tests – Ignitability of building products subjected to direct impingement of flame – Part 2: Single-flame source test, International Organization, for Standardization, Geneva, Switzerland, 2002.
8 ASTM E1354-04a Standard test method for heat and visible smoke release rates for materials and products using an oxygen consumption calorimeter, American Society for Testing and Materials, Philadelphia, PA, 2004.
9 J.E. Brown, E. Braun and W.H. Twilley. Cone calorimetry evaluation of the flammability of composite materials, NBS Report NBSIR 88-3733, 1988.
10 U. Sorathia, T. Dapp and J. Kerr. Flammability characteristics of composites for shipboard and submarine internal applications. *Proceedings of the 36th International SAMPE Symposium*, San Diego, CA, 15–18 April 1991, pp. 1868–1878.
11 J. Hume. Assessing the fire performance characteristics of GRP composites. *Proceedings of the International Conference on Materials and Design Against Fire*, London, 1992, pp. 11–15.
12 U. Sorathia. Flammability and fire safety of composite materials. *Proceedings of the 1st International Workshop on Composite Materials for Offshore Operations*, Houston, Texas, 26–28 October 1993, pp. 309–317.
13 M.J. Scudamore. Fire performance studies on glass-reinforced plastic laminates. *Fire and Materials*, **18**, (1994), 313–325.
14 A.P. Mouritz and A.G. Gibson. *Fire Properties of Polymer Composite Materials*, Springer, AA Dordrecht, The Netherlands, 2006.
15 J.R. Brown, P.D. Fawell and Z. Mathys. Fire-hazard assessment of extended-chain polyethylene and aramid composites by cone calorimetry. *Fire and Materials*, **18**, (1994), 167–172.

16 G.T. Egglestone and D.M. Turley. Flammability of GRP for use in ship superstructures. *Fire and Materials*, **18**, (1994), 255–260.
17 U. Sorathia, H. Telegadas and M. Bergen. Mechanical and flammability characteristics of phenolic composites for naval applications. *Proceedings of the 39th International SAMPE Symposium*, Anaheim, CA, 11–14 April 1994, pp. 2991–3002.
18 A.G. Gibson and J. Hume. Fire performance of composite panels for large marine structures. *Plastics, Rubbers and Composites Processing and Applications*, **23**, (1995), 175–183.
19 J.R. Brown and N.A. St John. Fire-retardant low-temperature-cured phenolic resins and composites. *TRIP*, **4**, (1996), 416–420.
20 S.B. Sastri, J.P. Armistead and T.M. Keller. Phthalonitrile-carbon fiber composites. *Polymer Composites*, **17**, (1996), 816–822.
21 J.R. Brown and Z. Mathys. Reinforcement and matrix effects on the combustion properties of glass reinforced polymer composites. *Composites*, **28A**, (1997), 675–681.
22 F.-Y. Hshieh and H.D. Beeson. Flammability testing of flame-retarded epoxy composites and phenolic composites. *Fire and Materials*, **21**, (1997), 41–49.
23 S.B. Sastri, J.P. Armistead, T.M. Keller and U. Sorathia. Flammability characteristics of phthalonitrile composites. *Proceedings of the 42nd International SAMPE Symposium*, Anaheim, CA, 4–8 May 1997, pp. 1032–1038.
24 A.P. Mouritz and Z. Mathys. Post-fire mechanical properties of marine polymer composites. *Composite Structures*, **47**, (1999), 643–653.
25 P. Van Dine and M.D. Smith. The effect of manufacturing method on the fire performance of composites. *Proceedings of the 31st International SAMPE Technical Conference*, Chicago, IL, 26–30 October, 1999, pp. 177–187.
26 A.P. Mouritz and Z. Mathys. Mechanical properties of fire-damaged glass-reinforced phenolic composites. *Fire and Materials*, **24**, (2000), 67–75.
27 U. Sorathia, T. Gracik, J. Ness, M. Blum, A. Le, B. Scholl and G. Long. Fire safety of marine composites. *Proceedings of the 8th International Conference on Marine Applications of Composite Materials*, Florida, 14–16 March, 2000.
28 A.P. Mouritz. Post-fire flexural properties of fibre-reinforced polyester, epoxy and phenolic composites. *Journal of Materials Science*, **37**, (2002), 1377–1386.
29 J.E. Brown. Combustion characteristics of fiber reinforced resin panels, NBS Report FR3970, 1987.
30 J.H. Koo, B. Muskopf, S. Venumbaka, R. Van Dine, B. Spencer and U. Sorathia. Flammability properties of polymer composites for marine applications. *Proceedings of the 32nd International SAMPE Technical Conference*, Boston, MA, 5–9 November 2000, Paper 136.
31 A. Knop and L.A. Pilato. *Phenolic Resins*, Springer-Verlag, Berlin, 1985.
32 M. Le Bras, S. Bourbigot, B. Mortaigne and G. Cordellier. Comparative study of the fire behaviour of glass-fibre reinforced unsaturated polyesters using a cone calorimeter. *Polymers and Polymer Composites*, **6**, (1998), 535–539.
33 E.D. Weil, M.M. Hirschler, N.G. Patel, M.M. Said and S. Shakir. Oxygen index: correlations to other fire tests. *Fire and Materials*, **16**, (1992), 159–167.
34 ASTM D2863-06a, Vol 08.01. Standard test method for measuring the minimum oxygen concentration to support candle-like combustion of plastics (oxygen index), American Society for Testing and Materials, Philadelphia, PA, 2006.
35 A. Tewarson and D.P. Macaione. Polymers and composites – an examination of fire spread and generation of heat and fire products. *Journal of Fire Sciences*, **11**, (1993), 421–441.

36 D.A. Kourtides, W.J. Gilwee and J.A. Parker. Thermal response of composite panels. *Polymer Engineering and Science*, **19**, (1979), 226–231.
37 D.A. Kourtides, W.J. Gilwee and J.A. Parker. Thermochemical characterisation of some thermally stable thermoplastic and thermoset polymers. *Polymer Engineering and Science*, **19**, (1979), 24–29.
38 D.M. Allison, A.J. Marchand and R.M. Morchat. Fire performance of composite materials in ships and offshore structures. *Marine Structures*, **4**, (1991), 129–140.
39 D.P. Macaione, R.P. Downing and P.R. Berguist. Summary Report AMMRC TR 83-53, Army Materials and Mechanics Research Laboratory, Watertown, MA, 1983.
40 D.A. Kourtides. Processing and flammability parameters of bismaleimide and some other thermally stable resin matrices for composites. *Polymer Composites*, **5**, (1984), 143–150.
41 S.C. Bates and P.R. Soloman. Elevated temperature oxygen index apparatus and measurements. *Journal of Fire Sciences*, **11**, (1993), 271–284.
42 B.K. Kandola and A.R. Horrocks. Composites. In: *Fire Retardant Materials*, eds A.R. Horrocks and D. Price, Woodhead Publishing Ltd, Cambridge, UK, 2002, pp. 182–203.
43 D.W. Van Krevelan. Some basic aspects of flame resistance of polymeric materials. *Polymer*, **16**, (1975), 615–620.
44 W.J. Gilwee, J.A. Parker and D.A. Kourtides. Oxygen index tests of thermosetting resins. *Journal of Fire and Flammability*, **11**, (1980), 22–31.
45 V. Babrauskas and R.D. Peacock. Heat release rate: the single most important variable in fire hazard. *Fire Safety Journal*, **18**, (1992), 255–272.
46 V. Babrauskas. Why was the fire so big? HHR: the role of heat release rate in described fires. *Fire and Arson Investigator*, **47**, (1997), 54–57.
47 U. Sorathia, R. Lyon, T. Ohlemiller and A. Grenier. A review of fire test methods and criteria for composites. *SAMPE Journal*, **33**, (July/August 1997), 23–31.
48 A.P. Mouritz, Z. Mathys and A.G. Gibson. Heat release of polymer composites in fire. *Composites A*, **37**, (2006), 1040–1054.
49 V. Babrauskas, J.A. White and J. Urbas. Testing for surface spread of flame: new tests to come into use. *Building Standards*, (March/April 1997), 13–18.
50 ASTM E1321-97a(2002)el, Vol. 04.07. Standard test method for determining material ignition and flame spread properties, American Society for Testing and Materials, Philadelphia, PA, 1997.
51 ASTM E84-07, Vol. 04.07. Standard test method for surface burning characteristics of building materials, American Society for Testing and Materials, Philadelphia, PA, 2007.
52 ASTM E162-06, Vol. 04.07. Standard test method for surface flammability of materials using a radiant heat energy source, American Society for Testing and Materials, Philadelphia, PA, 2006.
53 T.J. Ohlemiller and T.G. Cleary. Upward flame spread on composite materials. In: *Fire and Polymers II*: *Materials and Tests for Hazard Preventioin*, ed. G.L. Nelson, American Chemical Society, Washington, DC, 1995, pp. 422–434.
54 M.M. Hirschler. Fire hazard and toxic potency of the smoke from burning materials. *Journal of Fire Sciences*, **5**, (1987), 289–307.
55 J. Hunter and K.L. Forsdyke. Phenolic glass fiber-reinforced plastic and its recent applications. *Polymer Composites*, **2**, (1989), 169–185.
56 J.C. Lipscomb, K.J. Kuhlmann, J.M. Cline, R.E. Larcomb, R.D. Peterson and D.L. Courson. Combustion products from advanced composite materials. *Drug Chemistry and Toxicology*, **20**, (1997), 281–292.

57 D. Purser. Toxicity of fire retardants in relation to life safety and environmental hazards. In: *Fire Retardant Materials*, eds A.R. Horrocks and D. Price, Woodhead Publishing Ltd, Cambridge, UK, 2003, pp. 69–127.
58 B.C. Levin. A new approach for predicting the toxic potency of complex combustion mixtures. *Proceedings of the American Chemical Society Division of Polymeric Materials, Science and Engineering*, **71**, (1994), 173–174.
59 S. Gandhi, R. Lyon and L. Speitel. Potential health hazards from burning aircraft composites. *Journal of Fire Sciences*, **17**, (1999), 20–41.
60 R.M. Morchat and J.A. Hiltz. Fire-safe composites for marine applications. *Proceedings of the 24th SAMPE International Technical Conference*, Toronto, Canada, 1992, pp. T153–T164.
61 A. Casu, G. Camino, M.P. Luda and M. de Giorgi. Mechanisms of fire retardance in glass fibre polymer composites. *Makromolecular Chemistry Macromolecular Symposium*, **74**, (1993), 307–310.
62 A. Casu, G. Camino, M. De Giorgi, D. Flath, A. Laudi and V. Morone. Effect of glass fibres and fire retardant on combustion behaviour of composites, glass fibres-poly(butylene terephthalate). *Fire and Materials*, **22**, (1998), 7–14.
63 R.F. Kovar and D.E. Bullock. Multifunctional intumescent composite firebarriers, *Proceedings of the 4th Annual Conference on Recent Advances in Flame Retardancy of Polymeric Materials*, May 1993, pp. 87–98.
64 B.K. Kandola, A.R. Horrocks, P. Myler and D. Blair. The effect of intumescents on the burning behaviour of polyester-resin-containing composites. *Composites*, **33A**, (2002), 805–817.
65 J.R. Ebdon and M.S. Jones. Flame retardants (overview). In: *Polymeric Materials Encyclopaedia*, ed. J.C. Salamore, CRC Press, Boca Raton, FL, 1995, pp. 2397–2411.
66 M. Lewin and E.D. Weil. Mechanisms and modes of action in flame retardancy of polymers. In: *Fire Retardant Materials*, eds A.R. Horrocks and D. Price, Woodhead Publishing Ltd, Cambridge, UK, 2001, pp. 31–68.
67 P. Georlette. Applications of halogen flame retardants. In: *Fire Retardant Materials*, eds A.R. Horrocks and D. Price, Woodhead Publishing Ltd, Cambridge, UK, 2001, pp. 264–292.
68 A. Granzow. Flame retardation by phosphorus compounds. *Accounts of Chemical Research*, **11**, (1978), 177–183.
69 M. Bannister, P. Andrews, R. Rosu, R. Varley and W. Tian. Improved fire performance of carbon/epoxy composites through resin modification. *Proceedings of the 24th European SAMPE Conference*, Paris, 1–3 April 2003.
70 C.A. Wilkie. Graft copolymerisation as a tool for flame retardancy. In: *Fire Retardant Materials*, eds A.R. Horrocks and D. Price, Woodhead Publishing Ltd, Cambridge, UK, 2001, pp. 337–354.
71 S. Feih, Z. Mathys, A.G. Gibson and A.P. Mouritz. Property degradation of fibreglass composites in fire. *Proceedings of the 4th Conference on Composites in Fire*, Newcastle-upon-Tyne, UK, September 2005, Paper 1.
72 M. Dao and R.J. Asaro. A study on failure prediction and design criteria for fiber composites under fire degradation. *Composites*, **30**, (1999), 123–131.
73 J. Bausano, S. Boyd, J. Lesko and S. Case. Composite life under sustained compression and one-sided simulated fire exposure: characterization and prediction. *Proceedings of the SAMPE Exhibition and Symposium*, Long Beach, CA, 16–20 May 2004.
74 A.G. Gibson, P.N.H. Wright, Y.-S. Wu, A.P. Mouritz, Z. Mathys and C.P. Gardiner.

The integrity of polymer composites during and after fire. *Journal of Composite Materials*, **38**, (2004), 1283–1307.

75 G.A. Pering, P.V. Farrell and G.S. Springer. Degradation of tensile and shear properties of composites exposed to fire or high temperature. *Journal of Composite Materials*, **14**, (1989), 54–66.

76 A.P. Mouritz and Z. Mathys. Post-fire mechanical properties of glass-reinforced polyester composites. *Composite Science and Technology*, **61**, (2001), 475–490.

77 A.P. Mouritz. Simple models for determining the mechanical properties of burnt FRP composites. *Materials Science and Engineering A*, **359**, (2003), 237–246.

78 J.R. Brown, Z. Mathys, S.Z. Riddell and L.V. Wake. Fire-retardant performance of some surface coatings for naval ship interior applications. *Fire and Materials*, **19**, (1995), 109–118.

79 U. Sorathia and C. Beck. Fire protection of glass/vinyl ester composites for structural applications. *Proceedings of the 41st International SAMPE Symposium*, Anaheim, CA, March 1996, pp. 687–697.

80 J. Giancaspro, P. Balaguru and R. Lyon. Fire protection of flammable materials utilizing geopolymer. *SAMPE Journal*, **40**, (2004), 42–49.

81 U. Sorathia, T. Gracik, J. Ness, A. Durkin, F. Williams, M. Hunstad and F. Berry. Evaluation of intumescent coatings for shipboard fire protection. *Journal of Fire Sciences*, **21**, (2003), 423–450.

82 B.K. Kandola and A.R. Horrocks, Flame retardant composites, a review: the potential for use of intumescents. In: *Fire Retardancy of Polymers – The Use of Intumescence*, ed. R. Delobel, The Royal Society of Chemistry, London, 1998, pp. 395–417.

83 J. Murrell and P. Briggs. Developments in European and international fire test methods for composites used in building and transport applications. *Proceedings of the 2nd Conference on Composites in Fire*, Newcastle, UK, September 2001.

84 P. Briggs. Fire performance of composites in European construction applications. *Proceedings of the 3rd Conference on Composites in Fire*, Newcastle, UK, September 2003.

85 D. Wang and C.A. Wilkie. Fire properties of polymer nanocomposites. In: *Fire Properties of Polymer Composite Materials*, eds A.P. Mouritz and A.G. Gibson, Springer, AA Dordrecht, The Netherlands, 2006.

86 U. Sorathia. Improving the fire performance characteristics of composite materials for naval applications. *AMPTIAC Quarterly*, **7**, (2004), 49–54.

87 R.E. Lyon, P. Balaguru, A.J. Foden, U. Sorathia and J. Davidovits, Fire resistant aluminosilicate composites. *Fire and Materials*, **21**, (1997), 61–73.

7

Durability of composites under fatigue loads

A. ZHOU, N. POST, R. PINGRY, J. CAIN,
J. J. LESKO and S. W. CASE,
Virginia Polytechnic Institute and State University, USA

7.1 Introduction

Fatigue is generally defined as the physical phenomena that cause damage and failure of material or a structural component after the application of an applied condition or conditions (cycles), even though the level of that condition is not high enough to cause failure on the first cycle of application. Fatigue 'life' is usually measured as the number of cycles to failure for a given applied load level. In a general sense, applied loads include mechanical and environmental loads. The degradation and failure of civil infrastructure – such as bridges, highways, and civil service piping – is nearly always associated with dynamic cyclic loading. The loading may be mechanical (due to vehicle traffic, for example), hygrothermal (from variations in temperature and moisture), or chemical (from seasonal road treatments, oxidation, solvents, etc.).

Methods for studying fatigue of materials and structures include the stress-life method, the strain-life method, methods using damage mechanics concepts (such as damage accumulation or strength and stiffness degradation), and methods using fracture mechanics concepts (such as crack initiation and propagation). The above-mentioned methods may be used in conjunction with each other, such as using damage accumulation models in conjunction with crack propagation models to form progressive damage modeling and using the stress-life method together with damage accumulation models.

The fatigue of fiber-reinforced polymer (FRP) composites has been the subject of experimental and theoretical investigation for several decades. Typical reinforcing fibers include carbon fibers, glass fibers, and aramid fibers; and typical matrix materials include epoxy, vinyl ester, polyester, and phenolic resins. Under fatigue load, the composites may experience microcracking, delamination, fiber fracture, fiber/matrix decoupling, and microbuckling (under compressive load). These damage modes will accumulate and interact under fatigue load, and the material will lose resistance capability, or will eventually lead to fracture (or separation) of the material (Reifsnider 1991).

Many factors affect the fatigue performance of composite materials, including the properties of constitutive materials (fibers and matrix), the fiber/matrix interface or the interphase region, the manufacturing process, loading parameters (such as frequency, stress range, and stress ratio), and in-service environmental conditions (such as hygrothermal, chemical and thermal-mechanical effects). Much of the previous research on fatigue of composite materials has focused on applications on aircraft structures and epoxy composites. For civil engineering applications, polyester, vinyl ester, and epoxy resins have become the dominant matrix materials. Although there are applications of carbon/epoxy composites for repairing or strengthening of concrete or steel structures, these are not the subjects of this chapter. The main purpose of this chapter is to address the fatigue behavior of glass fiber-reinforced polymer (GFRP) composites, especially E-glass fiber-reinforced polymer composites for civil structural applications in bridges, buildings, and marine structures.

The chapter first addresses the fatigue behavior of GFRP civil engineering composites by discussing the factors that influence the fatigue performance. A review is then given of predictive and descriptive modeling of fatigue of FRP composites. A variability- and reliability-based approach to fatigue-life prediction is discussed in detail. Design for fatigue is addressed by presenting recent achievements in reliability-based design and the load and resistance factor design (LRFD) approach for FRP composites. Material resistance knockdown factors and a reliability-based framework for composite life prediction and design are also presented.

7.2 Fatigue behavior of civil engineering composites

7.2.1 Fiber effects

The fatigue performance of FRP laminate is significantly affected by the fiber type, fiber orientation, and the fiber lay-up scheme. The mechanical properties of fibers play the most important role in fatigue performance. In general, composites made from fibers with higher modulus have higher fatigue resistance. Composites with high modulus graphite have very slow strength and stiffness reduction. E-glass fiber composites have a more gradual fatigue strength reduction of 8–12% per decade of life (Demers 1998; Mandell 1982; McBagonluri *et al*. 2000), although slow strength reduction of 3–5% per decade of life has been observed (Keller *et al*. 2005). Most available data support the fiber-dominated fatigue damage mechanism in GFRP composites. Under tensile fatigue load, the fatigue failure of continuous unidirectional glass fiber composites is a fiber or strand property, independent of matrix and interface. Exceptions to the fiber-dominated fatigue behavior exist when

more severe fatigue mechanisms are involved, such as woven fabric reinforcement or short fibers in ductile matrixes.

Fiber orientation has been shown to affect the fatigue performance. Fatigue tests on unidirectional composites containing off-axis fibers showed that increasing fiber orientation angle deteriorates the fatigue resistance (Hashin and Rotem 1973). Fatigue tests on angled-ply, E-glass/epoxy composites showed that laminates with greater than ±45° off-axis angles have nearly flat peak stress (S) – life cycles (N) curves while laminates with off-axis angles below ±45° have increasing slope with decreasing ply angle (Rotem and Hashin 1976). These flat S–N curves for laminates greater than ±45° are a result of the brittle-type nature of tensile matrix properties where the tensile and shear matrix properties are the main contributor in off-axis laminate strength. Experimental data on tensile axial fatigue of GFRP composites with various fiber reinforcements show that a conservative lower bound to the test data for fatigue life less than 10 000 cycles (high load range, >50% ultimate tensile strength (UTS)) is provided by the unidirectional continuous fiber reinforcement composites (Demers 1998). For low loading levels (30–50% UTS, fatigue life between 10 000 and 1 000 000 cycles), a conservative lower bound is provided by the short fiber reinforcement composites and ±45° continuous fiber reinforcement composites, while composites with continuous unidirectional fibers interspersed with mat layers are within or near the lower bound at low loading levels. A summary of various experimental results suggests that the fatigue limit (or endurance limit) is not evident for E-glass composites (Demers 1998).

The fiber lay-up scheme can also influence the fatigue resistance. A laminate containing alternate layers of ±5° fibers has higher fatigue strength than a unidirectional laminate (Hashin and Rotem 1973). The fatigue performance of unidirectional laminates can be improved by adding a small percentage of 90° cross plies to reduce the tendency of splitting. However, the fatigue strength is reduced as the percentage of cross-angle plies increases past a certain level. Laminates containing woven fabrics or randomly oriented fibers have been shown to have lower fatigue resistance than unidirectional or non-woven cross-ply laminates with similar composition. Fiber undulation in the through-thickness direction plays an important role in the fatigue performance of pultruded E-glass non-woven laminates. The out-of-plane fiber undulation increases the local stress state and decreases the fatigue resistance (Phifer 1998).

7.2.2 Resin effects

The matrix affects not only transverse and shear properties but also affects axial loaded unidirectional fatigue properties. For unidirectional laminates, the effect of the matrix (brittle or ductile) is reflected in the failure mode. If

the matrix has higher ductility than the fiber, the fiber fractures multiple times along its length shedding the over-load through shear of the matrix to adjacent fibers. If the matrix has lower ductility than the fiber, the matrix cracks cause bridging by the fiber, eventually leading to fiber fracture or delamination along the fiber–matrix interface.

There is a lack of systematic studies of the effects of matrix type and coupling agents on the fatigue performances of FRP composites. An evaluation of the effect of resin on fatigue life from tension–tension axial fatigue of E-glass FRP composites did not show significant difference in fatigue performance of the composites with epoxy, polyester, or vinyl ester resins (Demers 1998). The evaluation also suggests that modifying resins with flexibilizer or rubber does not significantly affect fatigue life as compared with the unmodified resins for E-glass composites.

7.2.3 Interphase effects

The role of the fiber/matrix interphase is to ensure load transfer between fibers and the adjacent matrix; it affects the way damage propagates in the composite system. The term 'interphase' refers to the region near the fiber surface where the chemical composition and mechanical properties are distinct from those of the fibers and of the bulk matrix; while an 'interface' is the interlaminar region between two polymer surfaces of two adjacent plies.

The performance of the interphase is usually quantified by fiber/matrix adhesion. A good fiber/matrix adhesion increases compressive strength, flexural strength, and off-axis strength. A strong fiber/matrix interphase is preferred since it would promote crack propagation across the fibers or matrix; while a poor fiber/matrix bonding would promote failure by fiber/matrix debonding and fiber pull out. For normal composites that have strong interphase adhesion, the initiation of fatigue damage is associated with matrix cracking or fiber breaking. These microcracks then couple and lead to debonding in the matrix/fiber interphase. The growth of the debonding contributes to the separation of fibers and the matrix, and the delamination of the ply interface. The subsequent development of fiber breaking, matrix cracking, debonding, and delamination leads to final fracture of the laminate (Reifsnider 1991).

Sizing, a thin coating applied to the surface of the fiber, has been shown to affect the mechanical performance of FRP composites significantly (Broyles *et al*. 2005; Salvia *et al*. 1997; Verghese *et al*. 2005). It was shown that thermoplastic sizings can improve static mechanical performance compared with the traditionally utilized oligomeric epoxy sizing (Broyles *et al*. 2005). Further studies indicate that thermoplastic sizings, in addition to superior quasi-static properties, also result in improved hygrothermal durability (Verghese *et al*. 2005). The interphase was found to have a profound impact on the moisture uptake characteristics and residual strength of the composites.

Strong hydrogen bonds formed between the sizing polymer and the matrix proved to be extremely useful in protecting an otherwise hydrophilic sizing polymer from water.

7.2.4 Processing effects

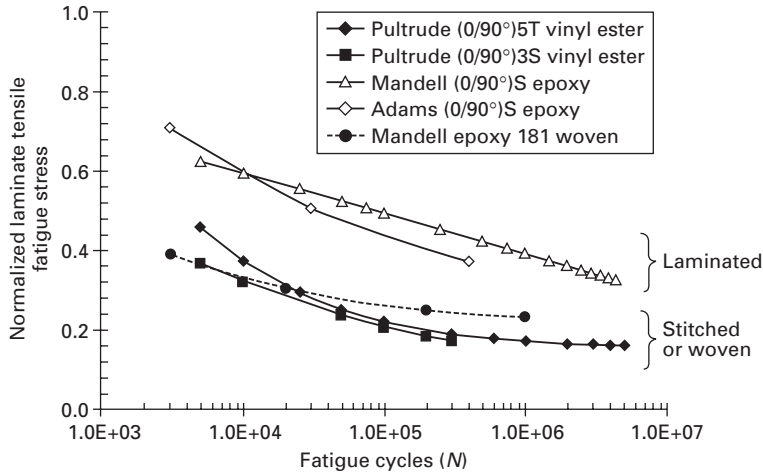
The behavior of GFRP composites depends strongly on the manufacturing process and processing defects. The most commonly used manufacturing techniques for FRP structural components used in civil engineering are pultrusion, vacuum-assisted resin transfer molding (VARTM), and filament winding. Through comparing the flexural fatigue behavior of unidirectional GFRP composites, Salvia *et al*. (1997) showed that filament winding is slightly better than molding, and much better than pultrusion. However, pultrusion is the most economically efficient technology for making GFRP structural members for civil engineering applications.

Fiber undulation is a key parameter characterizing the fatigue of FRP composites when different manufacturing techniques are used. Factors contributing to fiber undulation during the manufacturing process include laminate thickness, fiber waviness, cavities between fiber bundles, stitch stress risers, and flaws (such as microcracking and slight delamination) in the as-processed state. As shown in Fig. 7.1, pultruded E-glass/epoxy laminates with fiber undulation were shown to have lower *S–N* curves than those of unidirectional and cross-ply laminates manufactured from pre-impregnated E-glass/epoxy tape which has very little fiber undulation (Phifer 1998).

The degree of cure of polymer resin is another key processing factor that influences the fatigue and durability of FRP composites. The composite's glass transition temperature (T_g) and microstructure have been shown to correlate with the degree of cure of its polymer resin. For pultruded composites, the cure of polymer resins is usually high due to the heating of pultrusion die during the manufacturing process; thus less post-curing effects can be observed for pultruded composites. For composites made through the VARTM process at room temperature, the post-curing can have significant effects on the mechanical and fatigue properties. Examination of ambient cured VARTM E-glass/vinyl-ester resin composites by Cain *et al*. (2006) showed that their mechanical properties are significantly affected by the degree of cure. Their studies suggest that, in practice, the need for VARTMed structural composites to have stable and predictable mechanical properties necessitates the use of a post-cure regime.

7.2.5 Loading effects

The fatigue behavior of composites has been shown to be highly dependent on the stress ratio (R), the frequency of applied cyclic load (f), and loading sequence.



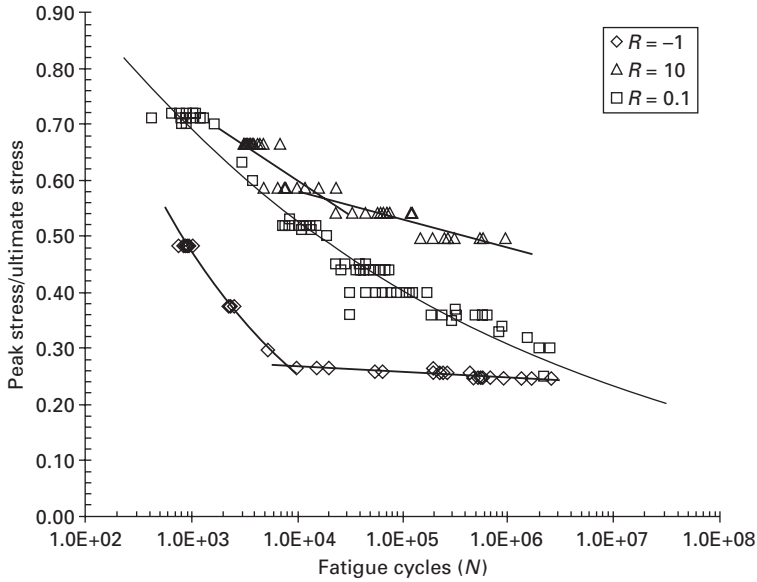
7.1 Effect of processing on fatigue.

Effects of R on fatigue

Studies on the effects of R on the fatigue life of composites have shown that for a given maximum stress in a tension–tension case, the fatigue life of the composite increases with increasing magnitude of R; in compression–compression loading, increasing the magnitude of R reduces the fatigue life of the composite (El Kadi and Ellyin 1994; Mandell and Meier 1982). Figure 7.2 shows the S–N curves for an E-glass/vinyl ester composite tested at different R values. It is clear that there are qualitative differences in the fatigue behavior for each loading ratio. While the $R = 0.1$ data are fitted well by a single power-law curve, the $R = 10$ and $R = -1$ data each exhibit a 'knee' where a transition in the fatigue sensitivity occurs. This transition is largest and especially abrupt for the case of $R = -1$, where at an applied stress of approximately 30% of the ultimate compressive strength, and a projected lifetime of approximately 10 000 cycles, the material behavior changes drastically. At higher applied stresses, the material shows a relatively high fatigue resistance, which is to say that for relatively small changes in applied stress the predicted lifetimes change by a small amount. At lower applied stresses, however, the material is very sensitive to fatigue, i.e. for small changes in applied stress the lifetimes vary drastically because of the low slope of the S–N curve in this region.

Effects of loading frequency on fatigue

The main mechanism for the effect of loading frequency on fatigue life is the internal heating of the composite during fatigue (Demers 1998). A general observation is that, as the frequency of the fatigue load increases, internal

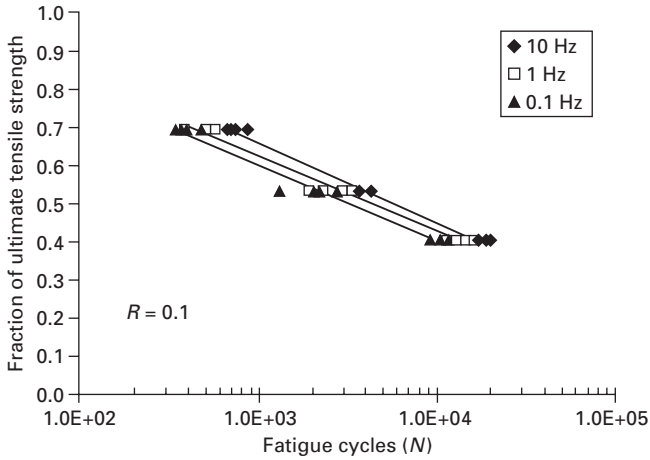


7.2 S–N curves for an E-glass/vinyl ester composite tested at different *R* values ([0/45/90/–45/0]s laminates manufactured by VARTM, straight-sided, un-tabbed samples were cut to a nominal size of 6″ × 1″, samples were post-cured at 180°F for 4 hours and slow-cooled before testing. Tests were stress-controlled at a frequency of 10 Hz.)

heating of the composite increases and the fatigue life of a composite decreases. From various published data, frequencies below 5 Hz have been shown to produce negligible internal heating in GFRP composites. A study on the fatigue of an E-glass/vinyl ester composite tested at frequencies of 0.1, 1, and 10 Hz is summarized in Fig. 7.3. It is seen that the strength decaying rates are similar at all frequency levels. The influence of the frequency on fatigue is within the range of statistical variation. However, other data suggest greater fatigue life at frequencies of 0–2 Hz than at 5 Hz, and the difference decreases as fatigue life increases (Demers 1998). A conservative lower bound to available fatigue test data is observed at 5 Hz over all fatigue life, as presented in Demers (1998); thus, 5 Hz is recommended as a test frequency limit for most civil engineering applications.

Effects of loading sequence on fatigue

A review on the topic of load sequence effects on the fatigue of composite materials showed that the published results of different authors are inconsistent in determining what type of loading is most damaging (Van Paepegem and Degrieck 2002). In some loading cases and with some materials, high amplitude followed by low amplitude is shown to be more damaging than low followed



7.3 S–N curves for an E-glass/vinyl ester composite tested at different loading frequencies (same laminates as in Fig. 7.2).

by high, while in other cases the reverse is true. Although numerical simulations showed that the transitions from low to high stress levels are the most damaging, and that the number of transitions and their relative importance in particular determine which block loading sequence (low-high or high-low) is the most devastating (Van Paepegem and Degrieck 2002), very few experimental data are actually available to verify damage models or to form generalizations. Fatigue testing of cross-ply E-glass/epoxy specimens indicated that low stress followed by high stress was the more damaging case (Broutman and Sahu 1972). These data have been used by several authors to validate their models. Other studies have found that the reverse effect can be true, i.e. high stress followed by low stress amplitude was more damaging (Hwang and Han 1986).

Recently, Post (2005) studied the effect of loading sequence on the residual strength of E-glass/vinyl ester composites manufactured by the VARTM process. The spectrum was applied in three ways: first as block loads in ascending order from lowest stress to highest, then as block loads in descending order from highest stress to lowest, and finally, the entire spectrum was randomized so that each individual cycle had an equal probability of occurring at any point during the fatigue. The results are summarized in Table 7.1. The residual strengths for the ascending and descending order loading tests were statistically identical and none of the specimens failed prior to the end of the test. This suggested to us that loading order was not very significant in determining the residual strength. However, when the randomized spectrum was applied, every specimen experienced premature failure (Post 2005). Results from this study also suggest that the strength under random loading decreases much more drastically than under either an ascending or descending block loading scheme, which indicates additional damage occurring from the frequent changes of stress levels.

Table 7.1 Summary of the residual strength and life of an E-glass/vinyl ester composite subjected to various fatigue sequence spectra

Loading sequence	Number of successful tests	Number of premature failures	Median fatigue cycles	Median remaining strength (MPa)	Median remaining life (F_r)
High to low	11	0	735 641	285	0.85
Low to high	13	0	735 641	289	0.87
Random	0	12	280 149[a]	163[b]	0.49[b]

[a]Median number of random cycles to failure.
[b]Based on results from 10 tests where fatigue failure load was recorded.

7.2.6 Synergistic effects

Environmental synergistic effects will degrade the properties and shorten the fatigue life of GFRP composites. The environmental fatigue performance of GFRP is influenced by all of its constituents: fiber, matrix, and fiber/matrix interface regions. This section concentrates on thermal–mechanical and hygrothermal effects.

Thermal–mechanical effects

In FRP composites, the fiber reinforcements are used to control stiffness and strength and to limit time-dependent behavior of the material. Glass fibers exhibit excellent resistance against temperatures well above (>650°C) the decomposition temperature of the polymer resin (typically ranges from 250–350°C). However, even though the fiber reinforcements are not directly affected by temperature, the fiber direction stiffness, strength, and fatigue life of a composite can be strongly dependent on temperature, especially in the temperature range above the glass transition temperature (T_g) of the polymer matrix. This is mainly due to the contribution of strong temperature-dependent behavior of the polymer matrix above its T_g.

Polymers exhibit increased viscoelastic behavior at elevated temperatures. With increasing temperature, the local energy in the macromolecules is increased, and thus the mobility of macromolecules is changed at the local level. When the fibers are combined with the viscoelastic polymer matrix, they produce a lamina that exhibits viscoelastic behaviors such as creep and stress relaxation (Dillard 1991). The degradation of stiffness, strength, and life of the composite is the result of the complex internal and local processes that control degradation and the strong interactions between fibers and the viscoelastic matrix.

The degradation of instantaneous stiffness and remaining strength with temperature for GFRP composites is evolved in stages, mainly due to the transitions in macromolecular mobility in the polymer resin at different

temperatures. The typical variation in instantaneous stiffness and remaining strength of GFRP composites can be described in the form of

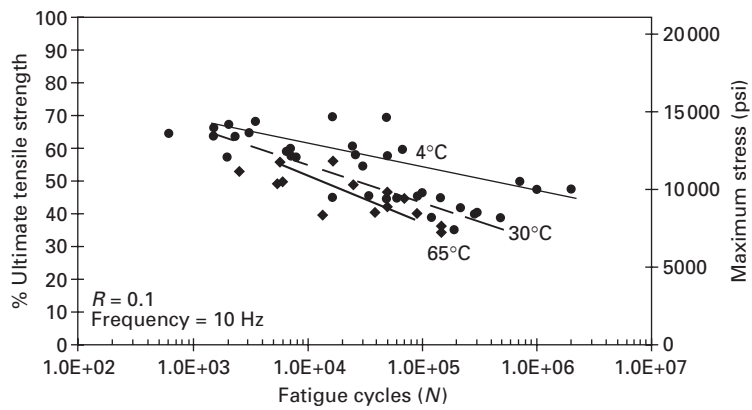
$$F(t) = \sum_{i=1}^{N} \left\{ \Delta F_i \exp \left[- \left(\frac{T}{T_i} \right)^{m_i} \right] \right\} \qquad [7.1]$$

where $F(t)$ is the instantaneous stiffness or remaining strength, T is the instantaneous temperature, ΔF_i is the stiffness or strength reduction for the ith transition process, T_i is the temperature at each transition, and m_i is the coefficient associated with the ith transition (Reifsnider and Case 2002). The number of stages in equation [7.1] may vary depending on the matrix and the thermal load. At temperatures in the vicinity of T_g, viscoelastic creep effects have the most influence on the stiffness and strength of the material. This effect is more significant when the material is under compressive load than when it is under tensile load (Bausano *et al*. 2006; Budiansky and Fleck 1993).

Temperature has a significant effect on the fatigue of GFRP composites. A study on the fatigue of a pultruded E-glass/vinyl ester composite is shown in Fig. 7.4. It can be seen that the strength decaying ratio (fatigue slope) increases as temperature increases (but below the T_g of the matrix). For civil engineering structures such as bridges and buildings, the highest application temperature of the designed FRP materials should be well below the T_g. It is recommended that GFRP materials chosen should have a T_g at least 30°C above the maximum expected use temperature (Karbhari *et al*. 2003).

Hygrothermal effects

Hygrothermal effects refer to the combined effects of environmental solvent (mainly moisture or water vapor) and temperature. Common environmental



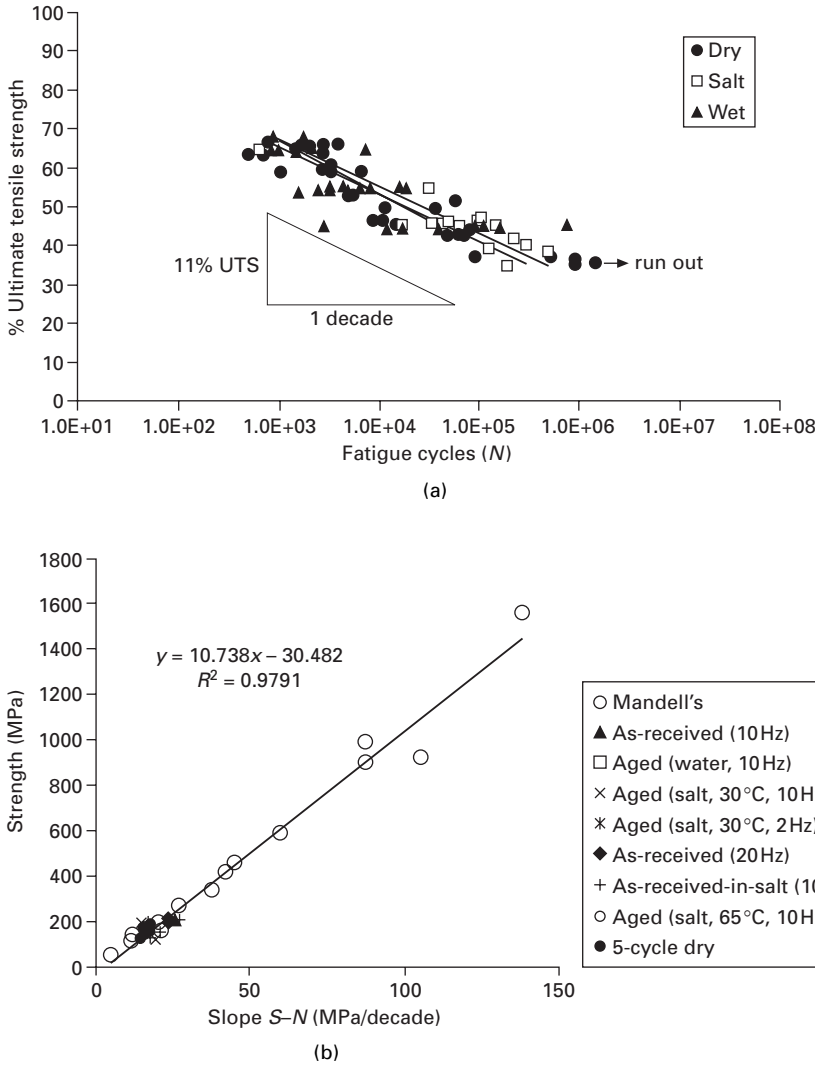
7.4 Thermal–mechanical effects on the fatigue of a pultruded E-glass/vinyl ester composite.

degradative agents in water or moisture include acids, alkalis, salts, organic solvents, and fuels/oils. Experiments showed that a moisture saturation level exists in a composite; this level depends on the resin type, the manufacturing process, and the relative humidity; while temperature can increase the moisture absorption rate, as moisture diffusivity is highly sensitive to temperature. Moisture can enhance the viscoelastic behavior (such as creep) of the composite and induce swelling strains. Environmental solvents such as moisture can lower the T_g of the material substantially and significantly alter the quasi-static stiffness and strength of FRP composites. Very limited data are available for the long-term fatigue performance of GFRP composites in environmental solvents. Studies on the fatigue of a pultruded E-glass/vinyl ester composite under dry, wet and simulated sea-water environments showed that the mechanism responsible for fatigue failure is fiber dominated for all three environments (McBagonluri *et al*. 2000). The aged material, in either fresh or salt water, experiences a one-time drop in strength with moisture ingress. When the data for each material are normalized with respect to their respective UTS, the curves collapse on top of each other, as shown in Fig. 7.5a. Statistical analysis indicated that the slopes of the lines were similar. This similarity in slope is independent of prior solvent exposure, solvent content, or type of solvent environment. The slopes of the *S–N* curves for all test conditions range from 9.9 to 12.7% per decade.

As discussed in the previous section, the composite will lose stiffness and strength at elevated temperatures above T_g. The combination of elevated temperature and moisture content is worse than either of the two environments alone. The relationship between tensile strength and slope of the *S–N* curve for different GFRP materials tested under different temperature and solvent environments is compared in Fig. 7.5b (McBagonluri *et al*. 2000). It can be seen that the effect of temperature did not depend on the presence or absence of the ambient fluid. Furthermore, fatigue damage evolution and subsequent failure of GFRP composites have been found to be independent of moisture content or moisture regime in the short term, although long-term aging and moisture ingress appear to affect the fatigue performance of the material. The combined hygrothermal effects impose severe restrictions on the use of specific composite in hot, wet environments. Composites with vinyl ester and epoxy matrixes are usually used when environmental solvent and hot weather are concerns in the service life.

7.3 Predictive/descriptive modeling of fatigue

Predictive methods for modeling the fatigue of materials include the stress-life approach, the strain-life approach, the damage accumulation (or damage mechanics) approach (such as residual strength or stiffness), the crack propagation (or fracture mechanics) approach, and combinations of these



7.5 Effect of solutions on the fatigue of a pultruded E-glass/vinyl ester composite. (a) *S–N* curves for a pultruded E-glass/vinyl ester composite under dry (open air), wet (fresh water), and salt (simulated sea-water) environments. (b) Relationship between tensile strength and slope of the *S–N* curve for different materials tested under different temperature and solvent environments (reprinted from McBagonluri *et al.* (2000), with permission from Elsevier).

methods. These methods are briefly summarized in this section. We then specifically address a methodology for a variability-based residual strength approach to life prediction. This approach incorporates composite material variability, mechanical and environmental loading effects, and reliability.

7.3.1 Fatigue-life prediction approaches

Many fatigue-life prediction approaches have the general form of

$$F_R(\tau) = A + Bf(\tau) \quad [7.2]$$

where A and B are material constants, $F_R(\tau)$ is the remaining life (or remaining stiffness and strength), $f(\tau)$ is a function related to life reduction, and τ is time or fatigue cycles. Failure is taken to occur when $F_R(\tau)$ reaches zero or a value that is predefined for a specific application. Equation [7.2] can have many variations depending on the methodologies used in fatigue-life prediction.

In the stress-life or strain-life approaches, equation [7.2] takes the form of

$$F_R(\tau) = A + B\{\log[N(\tau)]\}^C \quad [7.3]$$

where A, B, and C are constants (C is usually set to be 1), $N(\tau)$ denotes time (or cycles) to failure. Equation [7.3] can be obtained by curve-fitting using fatigue testing data on specimens. The assumption for these approaches is that the time to failure is uniquely related to the principal material strength or stiffness, and the fatigue behavior is represented in terms of material rupture or fracture.

In the stress-life approach, the life of a structural component is estimated based upon the magnitude of the alternating stress.The stress-life approach ignores the actual material response and treats all behavior as elastic and, therefore, results in an overestimation of the fatigue life when the plastic strain contribution is significant. The strain-life approach estimates fatigue life using the total strain amplitude of both plastic and elastic strains. Both the stress-life and the strain-life models do not take into account the actual degradation mechanisms, but use stress-life or strain-life curves or Goodman-type diagrams and introduce some fatigue failure criteria in the model.

Many methods using the damage mechanics concept for fatigue-life prediction of FRP composites also take the general form of equation [7.2]. The 'Palmgren–Miner's rule' (or P–M rule) is a linear model relating to the linear addition of the damage contributions of each cycle. Each cycle is considered to contribute damage in the amount of the fractional amount of life expended at that cycle. The simple P–M rule has several limitations and many researchers have proposed modifications to the simple rule and developed other models for cumulative fatigue damage prediction (Degrieck and Van Paepegem 2001; Reifsnider and Case 2002; Senne *et al*. 2000). Models based upon the change in stiffness or strength of a material undergoing fatigue have been developed. The residual stiffness and residual strength models are referred to as phenomenological models since these models propose an evolution law to describe the gradual deterioration of the stiffness or strength of the specimen in terms of macroscopically observable properties. The residual strength model in Broutman and Sahu (1972), and the residual

stiffness models in Senne *et al*. (2000) and Yang *et al*. (1990), take a similar form to

$$F_R = F_0 - (F_0 - F_i)(n/N)^j \quad [7.4]$$

where F_R is the residual strength or stiffness, F_0 is the initial strength or stiffness, F_i is the maximum applied stress at the ith cycle (in the residual strength model) or the stiffness at the ith cycle (in the residual stiffness model), N is the number of cycles to failure at a load level of F_i, n is the number of cycles experienced, and j is the strength degradation parameter. A j value greater than one indicates that materials exhibit little loss of strength or stiffness throughout most of their life and suffer a sudden failure at the end of life. A j parameter less than one represents materials that suffer the greater damage in their early life. The residual phenomenological models can have more sophisticated forms to consider the progressive damage growth and other issues, which will be discussed in detail later in this section.

Linear elastic fracture mechanics (LEFM) has been successfully applied for fatigue crack growth lifetime predictions. In this method, the crack growth rate is approximated as a function of the stress intensity factor using the 'Paris law'

$$\mathrm{d}a/\mathrm{d}N = C\Delta K^m \quad [7.5]$$

where a is the crack size, N is the number of cycles of loading, $\Delta K \equiv K_{max} - K_{min}$ is the stress intensity factor range (K_{min} and K_{max} referring to the minimum and maximum values of the stress intensity factor, respectively) and C and m are material-dependent constants that depend upon load frequency, mean load, and environment. The stress intensity factor K can be replaced by another parameter, the strain energy release rate G. The cycle to failure N_f can be obtained by integrating equation [7.5]. A full log ($\mathrm{d}a/\mathrm{d}N$) vs. log (ΔK) curve is usually S-shaped. Equation [7.5] is valid over a portion of the lifetime or crack growth history, i.e. the middle range of the overall S-shaped curve. An extension to equation [7.5] for considering the S-shaped curve can be written as (Kanninen and Popelar 1985)

$$\mathrm{d}a/\mathrm{d}N = [\mathrm{C}(\Delta K)^m]/[(1 - R)(K_{lc} - K_{max})] \quad [7.6]$$

where $R = K_{min}/K_{max}$, K_{lc} is plane strain fracture toughness. At low stress intensity factors, crack growth is extremely slow, leading to the postulate that crack growth does not occur below the threshold value, K_{th}. A major portion of the crack growth is modeled as the Paris law in equation [7.5]. Rapid crack growth occurs as the maximum stress intensity factor approaches the critical stress intensity factor K_c and leads to ultimate fracture of the material. A conservative criterion for FRP composites using the fracture mechanics concept is to only allow the designed structure to operate

below the threshold value K_{th}. In service, an examination based on fracture mechanics analysis and non-destructive evaluation of the structure can ensure safety.

7.3.2 Variability- and reliability-based approach to fatigue-life prediction

Among the fatigue-life prediction methods discussed in the previous section, the stress-life (or *S–N* curve) method is the simplest to implement. This method is straightforward to use and does not need detailed information about actual damage mechanisms. However, this method requires large amounts of experimental input for each material, loading, and environmental condition. Although methods based on crack propagation have been developed and applied to FRP composites, many issues need to be rectified in order to obtain a robust predictive method. The effects of mixed-mode stress states and creep at elevated temperature bring challenges for these methods. The most questionable point is whether crack propagation data should be used to predict fatigue life when microdamage initiation and accumulation is the dominant concern in FRP composites.

The damage of FRP composites during fatigue is a progressive process. Models considering progressive damage growth would be the reasonable tool for fatigue-life prediction because they quantitatively account for the progression of damage in the composites. A mechanically realistic method would be using progressive damage modeling considering progressive damage accumulation, crack initiation, and crack propagation during the whole fatigue process. However, this field is not well developed either in theory or in experimental techniques. At present, semi-empirical approaches based on simplified analyses such as the stress-life methods combined with residual phenomenological methods are the practical approaches available to the designers. In the following, we will present such a practical methodology; this methodology considers life evolution and residual strength development as well as the issues of variability of composite properties and reliability involved in fatigue-resistant design.

The residual phenomenological model presented here is based on previous fatigue modeling work from Reifsnider and Case (2002) to track fatigue damage in fiber-controlled composites using a generalized rate equation. By setting $F_0 = 1$ and $F_i = F_a$ in equation [7.4], taking the derivative of F_r with respect to n, and rearranging terms, we have $[(1 - F_r)^{1/j-1}]\, \mathrm{d}F_r = -(1 - F_a)^{1/j}\, (j/N)\, \mathrm{d}n$. By integrating both sides of this equation, we have

$$\int_1^{F_r} (1 - F_r)^{1/j-1}\, \mathrm{d}F_r = -\int_0^n (1 - F_d)^{1/j}\, \frac{j}{N}\, \mathrm{d}n \qquad [7.7]$$

As F_r, F_a, and N are functions of fatigue cycles n, we have

$$F_r(n) = 1 - \left\{ \int_0^n \frac{[1 - F_a(n)]^{1/j}}{N[F_a(n)]} \, \mathrm{d}n \right\} \quad [7.8]$$

In equation [7.8], $N[F_a(n)]$ is the number of cycles to failure at a loading $F_a(n)$, and j is a residual strength fitting parameter, $F_a(n)$ is the normalized applied peak stress based on the initial strength X_t of the specimen, i.e. $F_a(n) = \sigma_{applied}/X_t$, and $F_r(n)$ is the normalized residual strength, i.e. $F_r(n) = X_{residual}/X_t$. The number of cycles to failure $N[F_a(n)]$ is determined based on fatigue testing data. Most experimental data fit well to a linear log–log relationship with two parameters, $\log(N) = P$, $\log[F_a(n)] + Q$, where P and Q are fit to the S–N curve data for the material. Thus, this model has three experimentally determined parameters P, Q, and j, which can be obtained by fitting experimental fatigue data.

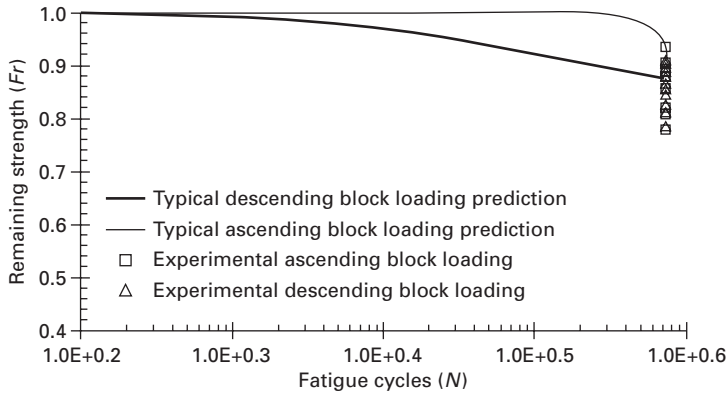
While the above model is used to predict residual strength, it also provides a fatigue failure criterion: failure to occur when the residual strength becomes less than the applied stress, i.e. $F_r(n) \leq F_a(n)$. This prediction is independent of loading history order and only depends on the total number of cycles at each applied peak stress. When applied to constant amplitude loading, i.e. $F_a(n) = \text{const.}$ for all loading cycles, equation [7.8] reduces to a formula by setting $F_0 = 1$ and $F_i = F_a$ in equation [7.4]. For variable amplitude loads, equation [7.8] should be integrated numerically with a step size of one cycle for each peak stress

$$F_r(n) = 1 - \left\{ \sum_{i=1}^{n} \frac{[1 - F_a(i)]^{1/j}}{N[F_a(n)]} \right\}^j \quad [7.9]$$

In practice, it is desirable to not only model the mean or median residual strength of a material, but also to understand the statistical distribution of strength and how that might change during the fatigue life. To do this, we can take the experimentally measured initial strength or stiffness distribution and model the residual strength response of specimens from this distribution, finally recalculating the strength distribution resulting in the end (Post 2005). For each initial strength case, equation [7.8] can be solved numerically for each cycle applied to calculate the final residual strength or time to failure. The statistical variation in strength can be modeled using a two-parameter Weibull distribution

$$F(x) = 1 - \exp[(x/\beta)^{\alpha}] \quad [7.10]$$

where $F(x)$ is the cumulative density function, β is the location parameter, and α is the shape parameter. Due to the limited number of experimental samples, there will be some uncertainty in the calculated α and β values (Post 2005).



7.6 Predicted residual strength curves compared with experimental data (E-glass/vinyl ester laminates made through the VARTM process).

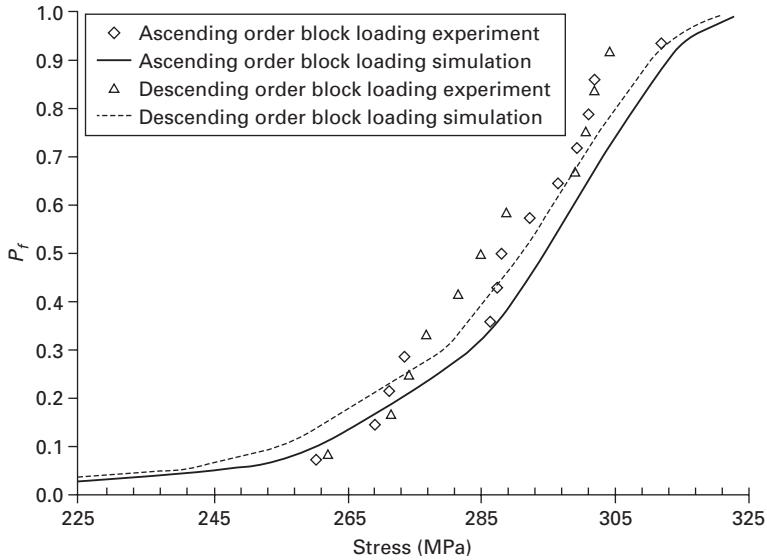
Predictions using equation [7.9] for remaining strength (F_r) as a function of typical ascending and descending block loading fatigue cycles are compared with experimental data in Fig. 7.6. The possibility of failure (P_f) for different block loading sequences is provided in Fig. 7.7. The remaining strength and possibility of failure predictions compare well with ascending/descending block loading experimental data for E-glass/vinyl ester laminates.

7.4 Reliability-based design for fatigue

7.4.1 Load and resistance factor design for polymer composites

Reliability-based design enables engineers to select structural components based on the desired reliability of the structure under its operational conditions over its lifespan. One scheme for reliability-based design is the load and resistance factor design (LRFD). The LRFD procedure uses a limit state defined by the probability distributions of the material strength and applied loads to achieve a design optimized for the desired reliability (Ellingwood 2003). In the LRFD approach, the area where the probability distribution of the loads overlaps the resistance distribution is related to the risk of failure in the design. Direct calculation of the probability of failure for each design situation would require design engineers to have a high level of understanding of the statistics and probability calculations involved. It would also be computationally impractical in many situations. In simple form, LRFD is represented as

$$\phi R_n > \sum \gamma_i Q_i \qquad [7.11]$$



7.7 Residual strength cumulative probability distribution function comparison for block ordered spectrum experimental and model results.

where R_n is the nominal resistance of the material (typically strength or stiffness) and Q_i are the nominal loads applied to the material. The uncertainties in the applied loads are incorporated for a desired reliability using the load factors γ_i. The uncertainty of the resistance is described using a resistance 'knockdown' factor ϕ. By using the LRFD through equation [7.11], the designers need not consider probabilities explicitly, and the design problem is reduced to a simple inequality involving nominal material properties, loads, and factors that can be tabulated for a series of scenarios and probabilities of failure. During a design, engineers can find load factors for specific situations from design manuals or codes (AASHTO 2005; ASCE 2002; Ellingwood 2003). The material resistance knockdown factor depends on the particular limit state of interest, the material property distribution, and failure mode, and requires prudent examination.

7.4.2 Material resistance and knockdown factor

It is desirable that the reduction factor takes into account the changes in material properties with time so that the nominal resistance can be defined as the initial material strength or stiffness. The initial material resistance should incorporate the material property distribution. A long history of data and testing over time are available for steel and concrete structures; therefore, design standards provide LRFD reduction factors for these traditional

construction materials. Unfortunately, this is not the case for the application of new materials such as FRP composites. The method presented in the previous section is used to model the resistance distributions in these materials, with the specific fatigue and environmental degradation resulting from the design conditions, so that the resistance factors may be calculated and tabulated.

The nominal resistance, R_n, is expressed in terms of a deterministic strength, R_0, and a set of factors C_i, in the form (Ellingwood 2003)

$$R_n = C_1 C_2 \ldots C_k R_0 \qquad [7.12]$$

where R_0 is determined from standardized laboratory tests, and the factors C_i account for moisture, temperature, and size effects, composite action, and similar effects, and serve to transform R_0 to the end-use nominal strength, R_n. The strength R_0 should be based on a certian percentile (5% or other agreed percentile) of the distribution of strength determined from the standard laboratory testing procedure. The parameters C_i depend on factors known to affect strength in the end-use condition, but generally are independent of the limit state considered. The European composite design code and handbook suggests three main parameters considering effects of material testing, fabrication, and methods of analysis or calculation (Clarke 1996).

The resistance knockdown factors depend on the limit state, and can be approximated by (Ellingwood 2003)

$$\phi = (\mu_R/R_n) \exp(-\alpha_R \beta_R V_R) \qquad [7.13]$$

where μ_R is the mean of R_n, V_R is the coefficient of variation in R_n, β_R is the reliability index related to the limit state probability, and α_R is the sensitivity coefficient that depends on the probability distribution function of R_n. The resistance knockdown factor ϕ takes into account the mode and consequence of failure through the reliability index. By deducing the experience with other construction materials, Ellingwood (2003) suggests that the resistance factors for limit states in pultruded FRP structural members might be: 0.70–0.80 for limit states involving tension, compression, and shear; 0.80–0.90 for the flexure limit state; and 0.60–0.70 for joints using mechanical fastening or adhesive bonding. It should be noted that these factors are based on experience from traditional construction materials. Further investigation on FRP composite structures and systems is necessary to validate these values.

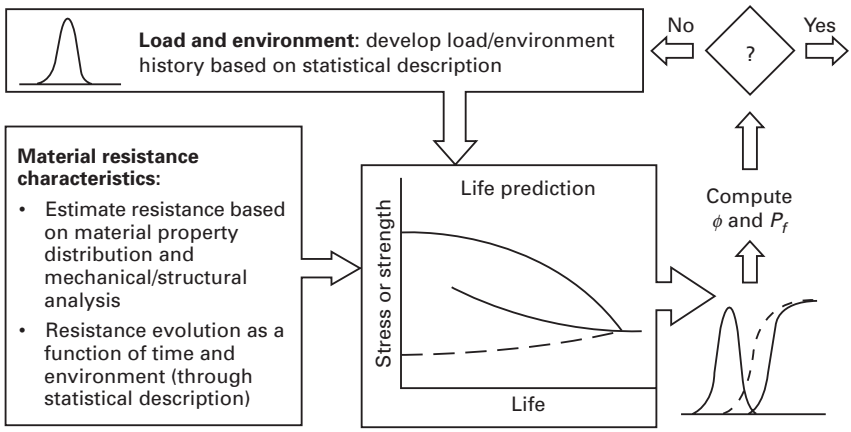
7.4.3 A reliability-based framework for composite life prediction and design

There is a reasonable amount of data regarding the fatigue and durability of glass/vinyl ester, polyester, and epoxy composites produced from low-cost fabrication methods (Demers 1998; Schutte 1994). However, these data are

available for a limited set of 'fatigue' conditions, most notably constant amplitude fatigue at frequencies ranging from 1 to 10 Hz. The slope of the *S–N* curve for most planar glass/polymer composites can be expected to range from 8–12% UTS per decade of life. This includes both fatigue of dry and moisture-saturated materials under short-term exposure. Thus, under well-defined conditions, with an intended limited service life, the longevity of the system may be estimated with some degree of confidence. However, as the complexity of the service condition (combination of stress and environment, and variation in severity) and the length of intended service life increase, the likelihood of reliably estimating service life is questioned.

The uncertainty in estimating life for structures that are designed for extended service conditions (e.g. 30–100 years) arises from a lack of understanding of degradation processes that act on the constituents alone or in combination with other enviro-mechanical conditions. Most of the available data for fatigue and durability of FRP composites have been obtained from accelerated laboratory testing. There are questions concerning whether the aging mechanisms scale properly from the accelerated laboratory test to the prototype in real service conditions. Although equations [7.11] to [7.13] provide necessary formulae for the implementation of LRFD for polymer matrix composites, the lack of field history data contributes an additional source of uncertainty that must be considered. Here we propose a refined reliability-based methodology as a framework considering statistical distributions of load/environment history as well as material resistance and its evolution to reduce the uncertainty due to the lack of field history data.

The framework is illustrated schematically in Fig. 7.8. The core of the methodology is the life prediction, i.e. residual material resistance (stiffness or strength) as a function of time or fatigue cycles (life). The life prediction uses a statistical approach considering the statistical characteristics of the load and environment history, and the material resistance, simultaneously. Limited data from laboratory testing and field histories are used in conjunction with statistical simulation and this will help us to build the confidence level and reduce uncertainty. The outputs of the life prediction and statistical simulation are resistance and its knockdown factor, as well as the possibility of failure. The obtained resistance and the knockdown factor are then used in equation [7.10] to compare to its right-hand side. The main advantage of this methodology is to use the limited data to their maximum potential for designing polymer matrix composites with consideration of fatigue and durability issues. The implementation of this framework is demonstrated in equations [7.7] to [7.10] and the results are shown in Figs 7.6 and 7.7. Efforts are under way to incorporate random block loading and synergistic effects into this framework. Using this framework, structural health monitoring



7.8 Schematic of a design approach considering fatigue and durability within a reliability-based approach.

techniques can be implemented to provide real-time feedback information to revise predictions of material resistance, load/environment effects, and remaining life (with a certain level of confidence).

7.5 Conclusions

To understand and predict the life of polymer matrix composites under fatigue load is critical in civil structural applications. Although the damage mechanism is fiber-dominated, the fatigue life of the composites is influenced by many factors, including constitutive materials, interphase, manufacturing process, as well as load history and service environment. Over the past several decades, the ability to select constitutive materials, and design and affordably construct large composite parts has improved significantly, assisted particularly by advances in high-quality manufacturing technologies such as automatic pultrusion and machine-assisted resin-infusion processing. It appears that loading history and service environment are the most uncertain factors that require further examination. Loading history such as loading ration, and loading frequency and sequence are critical parameters that affect the fatigue of FRP composites, although the mechanisms of the effects have not been well understood and the predictions have relied heavily on empirical curve fitting methods and extensive laboratory testing. The understanding of synergistic effects such as thermal–mechanical and hygro-thermal/mechanical effects on the fatigue of FRP composites has made some progress in the past decades but reliable prediction is still beyond our capability. In fact, semi-empirical approaches such as *S–N* curves and residual phenomenological methods are the only practical and somewhat 'reliable' approaches available to designers for assessing fatigue performance and life prediction, as these

methods use experimental data from extensive specimen and structural prototype testing.

Reliability-based design opens a door to consider the complexity of the fatigue damage process – as well as the influences of variations in material resistance, loading history, and environmental conditions – during the design process. By implementing the LRFD methodology, relatively new FRP composites can be treated in a similar way to traditional construction materials, and the complex fatigue damage phenomena can be represented by several key knockdown factors. These knockdown factors can be obtained from a few well-designed experiments assisted by statistical simulations as outlined in the text. The proposed reliability-based framework for life prediction and structural design of FRP composites shows potential for developing a refined method to determine material resistance knockdown factors and to understand the characteristics of loading and environment. The framework also shows potential for the incorporation of structural health monitoring and prognosis technologies to develop smart material systems for civil structural applications.

7.6 References

AASHTO (American Association of State Highway and Transportation Officials) (2005). *AASHTO LRFD Bridge Design Specifications*, 3rd Edition, Metric–2005 Interim Revisions, AASHTO, Washington, D.C.

ASCE (American Society of Civil Engineers) (2002). 'Minimum design loads for buildings and other structures.' ASCE Standard 7-02, ASCE, Reston, Virginia.

Bausano, J. V., Lesko, J. J. and Case, S. W. (2006). 'Composite life under sustained compression and one sided simulated fire exposure: Characterization and prediction.' *Composites Part A: Applied Science and Manufacturing*, **37**(7), 1092–1100.

Broutman, L. J. and Sahu, S. (1972). 'A new theory to predict cumulative fatigue damage in fiberglass reinforced plastics.' Composite Materials: Testing and Design, 2nd Conference, ASTM STP 497, American Society for Testing and Materials, Philadelphia, Pennsylvania pp. 170–188.

Broyles, N. S., Verghese, K. N. E., Davis, R. M., Lesko, J. J. and Riffle, J. S. (2005). 'Pultruded carbon fiber vinyl ester composites processed with different fiber sizing agents. Part I: Processing and static mechanical performance.' *Journal of Materials in Civil Engineering*, **17**(3), 320–333.

Budiansky, B. and Fleck, N. A. (1993). 'Compressive failure of fibre composites.' *Journal of the Mechanics and Physics of Solids*, **41**(1), 183–211.

Cain, J.J., Post, N.L., Lesko, J.J., Case, S.W., Lin, Y.N., Riffle, J.S., Hess, P.E. (2006). 'Post-curing effects on marine VARTM FRP composite material properties for test and implementation.' *Journal of Engineering Materials and Technology*, **128**(1): 34–40.

Clarke, J. L. (1996). *Structural Design of Polymer Composites: Eurocomp Design Code and Handbook*, E & FN Spon, London, UK.

Degrieck, J. and Van Paepegem, W. (2001). 'Fatigue damage modeling of fibre-reinforced composite materials: Review.' *Applied Mechanics Reviews*, **54**(4), 279–300.

Demers, C. E. (1998). 'Tension-tension axial fatigue of E-glass fiber-reinforced polymeric composites: fatigue life diagram.' *Construction and Building Materials*, **12**(5), 303–310.

Dillard, D. A. (1991). 'Viscoelastic behavior of laminated composite materials.' *Fatigue of Composite Materials*, K. L. Reifsnider, ed., Elsevier Science, New York, pp. 339–384.

El Kadi, H. and Ellyin, F. (1994). 'Effect of stress ratio on the fatigue of unidirectional glass fibre/epoxy composite laminae.' *Composites*, **25**(10), 917–924.

Ellingwood, B. R. (2003). 'Toward load and resistance factor design for fiber-reinforced polymer composite structures.'*ASCE Journal of Structural Engineering*, **129**(4), 449–458.

Hashin, Z. and Rotem, A. (1973). 'A fatigue failure criterion for fiber reinforced materials.' *Journal of Composite Materials*, **7**, 448–464.

Hwang, W. and Han, K. S. (1986). 'Cumulative damage models and multi-stress fatigue life prediction.' *Journal of Composite Materials*, **20**(2), 125–153.

Kanninen, M. F. and Popelar, C. H. (1985). *Advanced Fracture Mechanics*, Oxford University Press, New York.

Karbhari, V. M., Chin, J. W., Hunston, D., Benmokrane, B., Juska, T., Morgan, R., Lesko, J. J., Sorathia, U. and Reynaud, D. (2003). 'Durability gap analysis for fiber-reinforced polymer composites in civil infrastructure.' *Journal of Composites for Construction*, **7**(3), 238–247.

Keller, T., Tirelli, T. and Zhou, A. (2005). 'Tensile fatigue performance of pultruded glass fiber reinforced polymer profiles.' *Composite Structures*, **68**(2), 235–245.

Mandell, J. F. (1982). 'Fatigue behavior of fiber-resin composites.' *Developments in Reinforced Plastics–2*, G. Pritchard, ed., Applied Science Publishers, London, pp. 67–107.

Mandell, J. F. and Meier, U. (1982). 'Effect of stress ratio, frequency and loading time on the tensile fatigue of glass-reinforced epoxy.' *Long Term Behavior of Composites*, T. K. O'Brien, ed., American Society for Testing out Materials, Philadelphia, Pennsylvania, pp. 55–77.

McBagonluri, F., Garcia, K., Hayes, M., Verghese, K. N. E. and Lesko, J. J. (2000). 'Characterization of fatigue and combined environment on durability performance of glass/vinyl ester composite for infrastructure applications.' *International Journal of Fatigue*, **22**(1), 53–64.

Phifer, S. P. (1998). 'Quasi-static and fatigue evaluation of pultruded vinyl ester/E-glass composites,' Master's Thesis, Virginia Polytechnic Institute and State University, Blacksburg, Virginia.

Post, N. L. (2005). 'Modeling the residual strength distribution of structural composite materials subjected to constant and variable amplitude tension-tension fatigue loading,' Master's Thesis, Virginia Polytechnic Institute and State University, Blacksburg, Virginia.

Reifsnider, K. L. (1991). 'Damage and damage mechanics.' *Fatigue of Composite Materials*, K. L. Reifsnider, ed., Elsevier Science, New York, pp. 11–77.

Reifsnider, K. L. and Case, S. W. (2002). *Damage Tolerance and Durability of Material Systems*, John Wiley and Sons, Inc., New York.

Rotem, A. and Hashin, Z. (1976). 'Fatigue failure of angle-ply laminates.' *AIAA Journal*, **14**(7), 868–872.

Salvia, M., Fiore, L., Fournier, P. and Vincent, L. (1997). 'Flexural fatigue behaviour of UDGFRP experimental approach.' *International Journal of Fatigue*, **19**(3), 253–262.

Schutte, C. L. (1994). 'Environmental durability of glass-fiber composites.' *Materials Science and Engineering: R: Reports*, **13**(7), 265–323.

Senne, J., Lesko, J. J. and Case, S. W. (2000). 'A life prediction methodology for thick section composites used in civil infrastructure.' *Journal of Composites Technology and Research*, **22**(4), 241–248.

Van Paepegem, W. and Degrieck, J. (2002). 'Effects of load sequence and block loading on the fatigue response of fiber-reinforced composites.' *Mechanics of Advanced Materials and Structures*, **9**(1), 19–35.

Verghese, K. N. E., Broyles, N. S., Lesko, J. J., Davis, R. M. and Riffle, J. S. (2005). 'Pultruded carbon fiber vinyl ester composites processed with different fiber sizing agents. Part II: Enviro-mechanical durability.' *Journal of Materials in Civil Engineering*, **17**(3), 334–342.

Yang, J. N., Jones, D. L., Yang, S. H. and Meskini, A. (1990). 'A stiffness degradation model for graphite epoxy laminates.' *Journal of Composite Materials*, **24**(7), 753–769.

8

Creep and time-dependent response of composites

L. S. LEE, Louisiana Tech University, USA

8.1 Introduction

Fibre-reinforced polymer (FRP) composite materials were first associated with structural applications for the aerospace industry with specific environmental exposure conditions. More recently, the increasing prevalence of FRP composites in civil structural applications such as rebar, rehabilitation/strengthening, seismic retrofit, pipelines, beams, columns, walls, and in some cases all-FRP structures such as bridges, has required an increased understanding of the durability of these materials when subject to harsh, changing environmental conditions. Durability is typically associated with the prediction of the long-term properties of a material in order to assess the time-dependent performance of structures where service lives of 50 years or more are often required.

The time-dependent response of a material is generally associated with creep and relaxation. Creep is the time-dependent and permanent deformation of materials when subjected to an externally applied load over an extended period of time (Liao *et al*., 1998; Callister, 2003). Creep is normally an undesired phenomenon that is often the limiting factor in the lifetime of a material. Stress relaxation is the inverse of creep where a material is subject to a constant strain and a reduction in stress occurs over time (Menard, 1999).

FRP composites are typically built up of a polymeric matrix (e.g. vinylester, polyester, or epoxy resins) reinforced with glass, carbon, or aramid fibres. The creep behaviour of a unidirectional composite under a constant load assumes that fibre behaves elastically while the matrix behaves in a viscoelastic manner. The creep behaviour is characterized by a transfer of matrix stress to the fibre stress and makes the fibre strain increase equal to the composite strain (Kawada *et al*., 2005).

Creep behaviour of FRP composites depends on fibre orientation, fibre volume fraction, and structure of the material; however, creep of FRP composites is predominantly a result of creep in the polymer matrix (Liao *et*

al., 1998). Creep behaviour of civil infrastructure composites will be dominated by the matrix-dependent properties as opposed to the fibre or interfacial properties (Morgan *et al*., 2001). The resin systems and adhesives used in infrastructure applications are polymeric materials, which are by definition viscoelastic. Viscoelastic materials exhibit characteristics of both viscous fluids and elastic solids. Viscoelastic behaviour is highly dependent on time and temperature, thus making time-dependent behaviour of composite materials one of the most important factors in design (Scott *et al*., 1995). However, the occurrence of creep in composites can be attributed to a combination of bulk material strain and microflaw initiation such as fibre–matrix debond and cracking in the resin, with both of the mechanisms being time dependent due to the viscoelastic nature of the polymer matrix (Barnes and Garden, 1999). Microscopic damage in the form of microcracking in composite materials can be a result of a number of factors which include loading cycles and environmental conditions that can alter the creep strain behaviour and shorten the life of a structural component. This observation points to the need for understanding the influence of synergistic conditions on the time-dependent behaviour of composites. Long-term integrity of FRP composite structural systems requires the establishment of design procedures that avoid the occurrence of excessive creep and significantly reduce the possibility of creep-induced failures throughout the service life of a structure (Barnes and Garden, 1999).

Unlike conventional infrastructure materials such as steel and concrete, FRP composites are more susceptible to creep due to the resins and adhesives used during manufacturing and construction (Liao *et al*., 1998). Prediction of the time-dependent response of composite materials has been the focus of a number of researchers, as can be seen in the reference list provided. Liao *et al*. (1998) and Scott *et al*. (1995) provide a comprehensive review of research in creep behaviour of FRP composites and studies that discuss the influence of various environmental conditions on time-dependent behaviour. The environmental and service conditions to which FRP composites will be exposed are likely to include an interaction of all or of some of the following aspects: (a) variable mechanical loading (e.g. magnitude, direction, and frequency of loading); (b) time requirements (e.g. varying life cycles depending on structure and application); (c) temperature cycles (e.g. desert climates, freeze–thaw); (d) moisture diffusion; (e) radiation (i.e. fire, ultraviolet light); (f) aggressive solutions (i.e. salt, fuel, alkali solutions). An understanding of the time-dependent behaviour of FRP composites under synergistic conditions is an important consideration for the design and performance of composites in infrastructure applications.

Creep and the time-dependent response of polymer matrix composites are described in this chapter. First, an overview of creep and stress relaxation in FRP composites is provided followed by a description of methods and

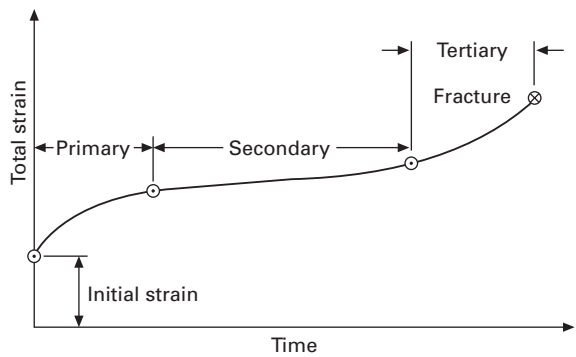
procedures used to predict the long-term response of composites including accelerated aging. Next, the effects of temperature, moisture, physical aging, and creep–fatigue interaction on the time-dependent response of composite materials are discussed. Then, the influence of creep on the time-dependent structural behaviour of all composite structures, structures rehabilitated with externally bonded FRP composites, and FRP composite reinforced concrete beam structures is reviewed to illustrate the effect of creep at the structural level. The chapter concludes with an assessment of future trends in characterizing creep behaviour and the time-dependent response of composites in civil infrastructure applications.

8.2 Creep and relaxation

8.2.1 Creep

Creep is the time-dependent change in strain due to a constant applied stress. Creep behaviour of a composite is highly dependent on the fibre orientation of the system. The time-dependent response of the composite is most affected when off-axis loading is applied and is less affected when load is applied in the fibre direction (Scott *et al*., 1995; Morgan *et al*., 2001). For an idealized creep strain curve as shown in Fig. 8.1, the primary or transient state of creep is characterized by a rapidly decreasing creep rate. In secondary creep, the creep strain rate reaches a steady-state value and is followed by the tertiary creep, where a rapid increase in creep strain rate occurs until fracture or rupture of the material (ASTM D2990, 2001).

In applications where long-term structural integrity is necessary the creep resistance of the composite is a critical property. Creep data is used in the design for FRP composite structural applications in order to ensure that structures do not fail or deform excessively during their service life due to



8.1 Typical creep strain response of a material with constant applied load (ASTM D2990, 2001).

rupture, yield, meshing of microcracks, or large deformation in the FRP composite material.

In cases where environmental exposure is not a concern, it is typically assumed that the microstructure of the composite remains intact during the creep response, such that fibre and the matrix deform together as the matrix transfers stresses between fibres (Barnes and Garden, 1999). When a fibre is oriented off the axis of loading in a unidirectional composite, especially in the transverse direction, microdamage will generally take place in the form of cracks. The observed creep behaviour, stress rupture, and stress relaxation of the composite can be attributed to the time-dependent growth of fibre matrix debonds and increasing density of microcracks in the matrix (Barnes and Garden, 1999). Consequently, the creep deformation in composites is typically associated with the viscoelastic behaviour of the polymer matrix.

The viscoelastic behaviour of polymers is well documented and a number of texts are readily available (Ferry, 1980; Ward and Sweeney, 2004; Gerdeen *et al.*, 2006). Viscoelastic deformation of polymers varies with temperature. At low temperatures a polymer behaves like a glass; at temperatures greater than the glass transition temperature, T_g, a polymer behaves like a rubbery solid; and at high temperatures, a polymer behaves like a viscous liquid.

If the stress applied is less than the yield value of the polymer, thus resulting in zero plastic strain, the total, time-dependent strain in a composite, $\varepsilon(t)$, can be represented by

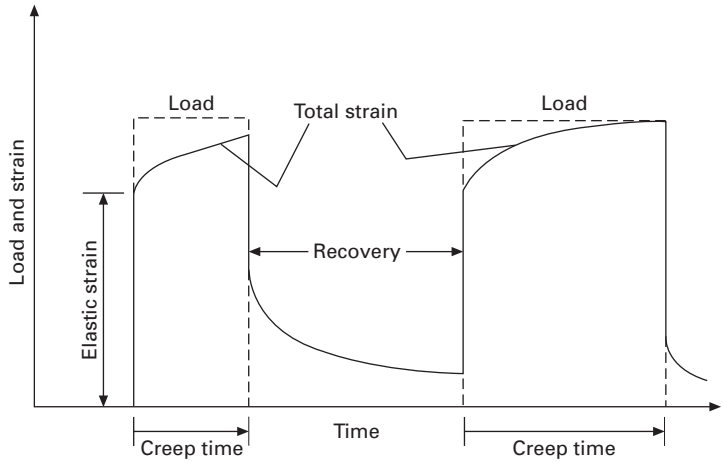
$$\varepsilon(t) = \varepsilon_0 + \varepsilon_c(t) \qquad [8.1]$$

where $\varepsilon_0 = \sigma_0/E$ is the initial strain response and $\varepsilon_c(t)$ is the creep response of the material. The initial elastic strain exhibits an instantaneous response to the applied load and can be identified in experimental measurements as the location on the total strain curve where step changes occur.

Unlike creep in metals, creep in polymers is recoverable at low strains when the applied load is removed. The period for which the load is removed and the strain approaches zero is known as the recovery period. Figure 8.2 shows the strain versus time response of a viscoelastic material for a given load history. The recovery period is shown in the figure as the time when the applied load is removed and the strain in the material dissipates and returns to its initial state.

Many polymers are susceptible to viscoelastic creep, which is primarily influenced by time, temperature, and applied load. Creep test results for viscoelastic materials in accordance with standards such as ASTM D2990 for tension, compression, and flexural loading are represented as a time-dependent creep compliance, $J_c(t)$. The following equation shows creep compliance for a linear viscoelastic material (Gerdeen *et al.*, 2006):

$$J_c(t) = \frac{\varepsilon_c(t)}{\sigma_0} \qquad [8.2]$$



8.2 Creep response of a viscoelastic material for a given load history (Hu and Sun, 2003).

where σ_0 is a constant applied stress. As indicated in equation [8.2], the creep compliance is studied as a function of the creep strain of the material. The creep strain response is determined from the total time dependent strain of the composite minus the initial elastic response, as shown in equation [8.1] (Hu and Sun, 2003).

For a nonlinear material, creep compliance depends on both time and stress as shown in the equation below,

$$J_c(t, \sigma) = \frac{\varepsilon(t, \sigma)}{\sigma} \qquad [8.3]$$

Irrespective of the linear or nonlinear viscoelastic behaviour of the material, the creep compliance is the primary parameter of interest in experimental creep tests where strain is measured with respect to a constant applied load. As shown in both equations [8.2] and [8.3], the creep compliance is normalized with respect to the stress and, thus, provides the ability to compare creep data from tests at various stress levels (Goertzen and Kessler, 2006).

In terms of durability, creep evaluation of composite materials typically involves the use of isothermal, short-term creep tests where a constant load is applied for a specified duration of time for a range of temperatures. The loading period is followed by a recovery period where the load is removed and the material returns to its initial state assuming damage has not taken place, as shown in Fig. 8.2. The creep strain is modelled using a constitutive law relating time, temperature, and stress to the time-dependent strain response of the material. Combining the short-term response of materials under load, the time–temperature superposition principle (TTSP) is used to predict the long-term creep response for a reference temperature. (TTSP will be discussed in further detail in the context of accelerated aging of composites in section 8.4.)

8.2.2 Relaxation

Stress relaxation is the time-dependent stress exhibited by a material while a constant strain is applied. The equation for relaxation modulus, $Y(t)$, for a linear, viscoelastic material is given below (Gerdeen *et al.*, 2006):

$$Y(t) = \frac{\sigma(t)}{\varepsilon_0} \qquad [8.4]$$

where $\sigma(t)$ is the time-dependent stress in the material and ε_0 is the applied constant strain. In a relaxation test a composite is quickly deformed to a set length and the decrease in stress is measured. The relaxation tests are difficult to perform since the composite must be strained very quickly (Menard, 1999) and there is the potential contribution of machine compliance where the test fixture may relax during the test thus distorting the results (Al-Haik and Garmestani, 2001). In addition, the duration of tests is limited in the relaxation tests, which are conducted typically for a period of 1 hour up to a maximum time of 1 month (Al-Haik and Garmestani, 2001).

Stress relaxation data in a polymer have been related to creep data with the following reciprocal equation (Menard, 1999):

$$\left(\frac{\varepsilon(t)}{\varepsilon_0}\right)_{\text{creep}} \approx \left(\frac{\sigma_0}{\sigma(t)}\right)_{\text{relaxation}} \qquad [8.5]$$

where ε_0 and σ_0 are the initial strain and initial stress response of the material, respectively. While the analysis of the stress relaxation curve is similar to creep analysis, the applicabillty of the above relationship for composites exposed to synergistic environmental conditions is not known.

8.3 Modelling long-term behaviour

One of the major necessities for characterizing time-dependent behaviour of FRP composites, thereby characterizing their durability, is the development of mathematical models to predict the creep behaviour of FRP composite materials. In particular, the development of mathematical models to account for the effects of varying stress and temperature ranges, as well as moisture and physical aging, on creep and relaxation behaviour is paramount to predicting the long-term responses of composite materials. The development of a predictive model for the life of an FRP composite could potentially enable extrapolation to the life of the structure.

The time-dependent behaviour of FRP composites, specifically stiffness and strength, is a function of loading history, environmental changes, and the interface conditions in a lamina and between lamina. The ability to predict the evolution of these characteristics over the lifetime of a structural component is critical at the design stage (Cardon *et al.*, 2000).

A number of analytical models have been developed to model and predict the creep strain response of polymer and composites under the individual and combined influences of stress, temperature, and moisture. These constitutive models have been typically based on fundamental concepts such as energy methods, damage mechanics, and the critical element concept with residual stress (Guedes *et al.*, 2000). The most popular analytical models used in the literature to predict long-term creep response are Findley's power law and the Boltzmann superposition principle (BSP). These models are described briefly here. Detailed explanations can be found in Scott *et al.* (1995), Gerdeen *et al.* (2006), and Ward and Sweeney (2004).

8.3.1 Findley's power law

Findley's power law is a curve-fit procedure for creep data given in the general form of a power law equation (Scott *et al.*, 1995):

$$\varepsilon(t) = \varepsilon_0' + \varepsilon_t' t^n \qquad [8.6]$$

where $\varepsilon(t)$ is the total creep strain, ε_0' is the stress-dependent and temperature-dependent initial elastic strain, ε_t' is the stress-dependent and temperature-dependent coefficient, n is a stress-independent material constant, and t is the time after loading. Findley's power law has also been developed for a longitudinal viscoelastic modulus, $E_v(t)$ and viscoelastic shear modulus, $G_v(t)$ (Scott *et al.*, 1995 – from Bank and Mosallam, 1990; Shao, 2006 – from ASCE, 1984, *Structural*, *Plastics Design Manual*):

$$E_v(t) = \frac{E_0 E_t}{E_t + E_0\left(\frac{t}{t_0}\right)^n} \qquad [8.7]$$

$$G_v(t) = \frac{G_0 G_t}{G_t + G_0\left(\frac{t}{t_0}\right)^n} \qquad [8.8]$$

where E_0 is the time-independent elastic modulus, E_t is the modulus that characterizes only time-dependent behaviour; G_0 is the time-independent initial tensile, G_t is the shear modulus which characterizes time-dependent behaviour, n is the stress-independent material constant related to tensile creep in equation [8.7] and to shear creep in equation [8.8].

While simple in its application and use, Findley's power law has been proven to be fairly accurate with researchers showing predicted strain responses within 3% at 30 000 min for temperatures up to 85°C for glass/polyester composites (Scott *et al.*, 1995, from Yen *et al.*, 1985). However, Findley's power law has been shown to be valid as long as the material undergoes

primary creep and it has been recommended that the sustained stress level for creep tests should not exceed 33% of ultimate strength in order to ensure that Findley's model provides a valid description of creep behaviour (Scott and Zureick, 1999).

8.3.2 Boltzmann superposition principle (BSP) and Schapery's integral

Typically a structural component will not be subject to a constant stress as in a creep test, rather it is more likely that a structure will have some level of stress variation throughout its service life. The BSP describes the total creep strain, $e(t)$, accumulated at any time, t, for an arbitrary stress history (Gerdeen *et al*., 2006). The single integral form of the BSP is as follows:

$$\varepsilon(t) = J_0\sigma_0 + \int_0^t J(t - t_i)\,\frac{\mathrm{d}\sigma_i}{\mathrm{d}t_i}\,\mathrm{d}t_i \qquad [8.9]$$

where J_0, is the initial time-independent compliance and t_i represents times where incremental stresses are applied. The BSP treats the composite as a linear viscoelastic material and does not apply for nonlinear behaviour (ASTM D2990, 2001; Scott *et al*., 1995; Gerdeen *et al*., 2006). The principle also indicates that the deformation of the specimen is directly proportional to the applied stress, when all deformations are compared at equivalent times (ASTM D2990, 2001). The advantage of the BSP is that an approximation of the displacement response can be obtained from a stress history analytically (Gerdeen *et al*., 2006).

Since the assumption of linear viscoelasticity for FRP composites may not hold, researchers (Ward and Sweeny, 2004 – from Leaderman, 1943 and Findley and Lai, 1967) developed a modified superposition principle for nonlinear viscoelastic behaviour. However, the modification by Schapery, by the thermodynamics of irreversible processes, to replace stress by a function of stress in the BSP integral and to replace time by a function of time, the reduced time ψ, has seen some recent progress in modelling the synergistic effects and long-term durability of FRP composites (Haj-Ali and Muliana, 2004; Muliana *et al*., 2006). The Schapery nonlinear equation has also been observed in research to have a better agreement with experimental data than the modified superposition principle (Scott *et al*., 1995).

The one-dimensional Schapery equation can be considered as a generalized non-linear standard model for viscoelastic solids (Cardon *et al*., 2000). The Schapery integral gives the strain in terms of stress history as shown:

$$\varepsilon(t) = g_0 D_0\sigma_0 + g_1 \int_0^t \Delta D(\psi - \psi_i)\,\frac{\mathrm{d}g_2\sigma_i}{\mathrm{d}t_i}\,\mathrm{d}t_i \qquad [8.10]$$

The reduced times are defined by

$$\psi = \int_0^t \frac{\mathrm{d}t'}{a_\sigma} \qquad [8.11]$$

$$\psi = \int_0^t \frac{\mathrm{d}t_i'}{a_\sigma} \qquad [8.12]$$

where g_0, g_1, and g_2 and a_σ are four nonlinearizing stress-dependent material parameters; D_0 and ΔD are the instantaneous elastic and transient compliances, which are stress and time independent. The Schapery equation is versatile since it is able to include the effects of multiple accelerators including temperature and varying stress levels (Cardon *et al.*, 2000). When the stress levels are sufficiently small, all four stress parameters are equal to one and the linear Boltzmann integral returns. The time–temperature–stress-dependent material parameters can be evaluated by creep-recovery tests (Muliana *et al.*, 2006).

There is a need to include additional nonlinear mechanisms such as the moisture, aging effects, and the mechanical degradation in FRP composites. Few studies are available for the prediction of long-term durability of composites based on the coupled effects of all these nonlinear mechanisms. Scott *et al.* (1995) (from Dillard *et al.*, 1987) compared the time–temperature–stress superposition principle (TTSSP), Findley's power law, and Schapery's single integral procedure on carbon/epoxy composites and found that the power law, while effective, could lead to instabilities in the numerical solution procedure. The Schapery equation has advantages for prediction because of its generality and easy adaptation for a numerical procedure.

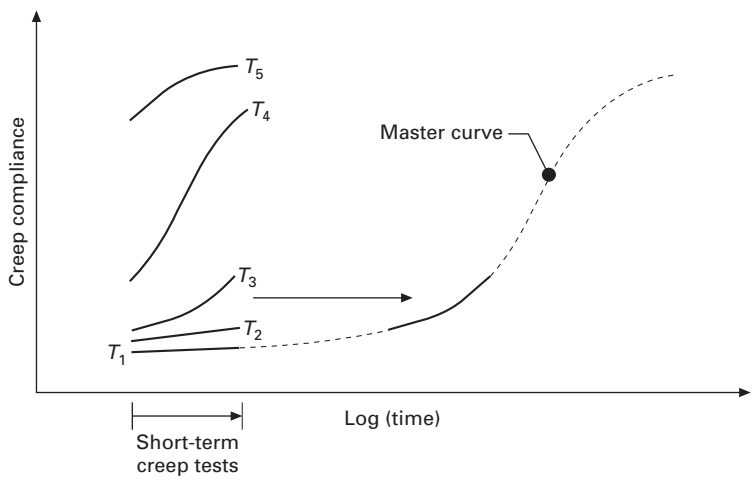
8.4 Accelerated aging

Characterizing long-term performance of materials is a critical aspect of understanding the reliability of structures. Testing a material in a specific load condition and environment for 50 or even 5 years can be expensive, labour intensive, and time-consuming – and is thus impractical. Consequently, the investigation of accelerated aging procedures for the long-term viscoelastic characterization of composite systems has seen tremendous growth amongst researchers. Because of the strong dependence of viscoelastic properties on temperature, the TTSP was developed by Williams, Landel, and Ferry (WLF) (ASTM D2990, 2001). Later, the influence of stress was included to develop the TTSSP.

8.4.1 The time–temperature superposition principle and the time–temperature–stress superposition principle

The TTSP is based on the observation that the short-term behaviour of viscoelastic materials at higher temperatures is similar to the long-term behaviour at some lower reference temperature (Cardon *et al.*, 2000). The TTSP assumes that the effect of increasing temperature is equal to expanding the time of the creep response by a shift factor, such that creep curves made at different temperatures are superposed by horizontal shifts along a logarithmic time scale to give a single curve that describes the creep response over a larger range of time or the master curve (ASTM D2990, 2001; Goertzen and Kessler, 2006). If validated for a given polymer composite, the WLF principle can be the basis of a prediction methodology for the long-term behaviour of composites based on short-term tests at different temperatures.

The TTSP allows for short-term creep tests at a range of temperatures to be used to generate a creep compliance master curve that is much longer than the short-term creep curves (Goertzen and Kessler, 2006). With this method, the short-term creep curves at each isotherm are plotted on a log scale. A reference temperature is chosen and the curves are shifted one-by-one on a log time scale until they superimpose. Curves for temperatures above the reference temperature are shifted to the right. Curves for temperatures below the reference temperature are shifted to the left (ASTM D2990, 2001). The approach is illustrated in Fig. 8.3. The shift factor, $\log a_T$, can be estimated by determining the activation energy of the glass transition relaxation from



8.3 Schematic illustrating the development of a master curve from isothermal short-term creep tests for several temperatures (Goertzen and Kessler, 2006).

the frequency dependence of T_g's measured through dynamic mechanical analysis (Goertzen and Kessler, 2006).

A similar superposition can be applied to short-term creep tests of varying stress and temperature. In the TTSSP procedure, short-term creep tests are conducted for a single reference stress level at varying temperatures. Short-term creep curves are also generated for a single reference temperature at varying stress levels. Master curves are then generated for the varying stress levels at the reference temperature and similarly for varying temperatures at the references stress level. Then the master curves are imposed for the reference temperature and reference stress level.

TTSP and TTSSP procedures can be used with short-term experimental predictions using Findley's power law or Schapery's integral to determine long-term creep response of the composite. While TTSP and TTSSP procedures have been shown to include the effects of temperature, stress, and moisture through appropriate determination of shift factors, the methodology has been difficult to automate because of the subjective nature of the graphical shift techniques (Scott *et al*., 1995). Also, some researchers have expressed caution in using elevated temperatures for accelerated aging because of the possible physical aging of the material due to the aggressive environmental conditions.

Specifically, the impact of physical aging on the accuracy of the TTSP and TTSSP methods must be considered by limiting the duration of a short-term creep test to $t_a/10$ where t_a is the time since the material was quenched to a temperature below T_g, (i.e. the time since physical aging began) (Sullivan *et al*., 1993). In general, long-term creep is not a fundamental response from a composite since significant aging can occur while the system is responding to load. Because of the simultaneous aging and response to load, the notion of a long-term creep master curve may be rendered invalid (Sullivant *et al*., 1993). The effects of physical aging and other conditions are discussed in the following section.

8.5 Synergistic effects on the time-dependent response

The time-dependent response of composite materials is a result of complex interactions between the creep behaviour of the composite and the environmental conditions affecting the application. The effect on the composite material is a stiffness degradation due to time-dependent creep and changes in strength of the composite can be attributed to damage in the composite from varying environmental factors (Cardon *et al*., 2000).

8.5.1 Effect of temperature

It is widely known that FRP composites are sensitive to temperature. In particular, composites exposed to temperatures above the T_g of the matrix

begin to degrade significantly (Goertzen and Kessler, 2006). An increase in the environmental temperature causes an increase in the creep compliance of the composite over time (Liao *et al*., 1998), due to the softening of the matrix. The increase in creep compliance becomes more pronounced for specimens loaded in the off-axis direction with 90° fibre-oriented composites showing the greatest increases in creep compliance (Hu and Sun, 2003). Even moderate temperature increases can have an order of magnitude effect on the viscous properties of polymer composites (Gerdeen *et al*., 2006).

Besides increasing the creep compliance of the material, increases in temperature have been observed to have the following effects on time-dependent behaviour (Scott *et al*., 1995):

- reduce the strength of the composite if the composite is under significant stress at the time of exposure;
- reduce the buckling strength, especially in thermoplastics;
- accelerate the time-to-failure of the composite;
- cause a departure from linear viscoelastic behaviour of composites for bidirectional and unidirectional composites;
- increase nonrecoverable flow in the matrix causing increases in creep and creep damage, with crazing at relatively low stresses.

8.5.2 Effect of moisture

FRP composites exposed to moisture are known to experience the physical effects of plasticization and swelling in the matrix. In addition, moisture can cause post-cure reactions, hydrolysis, and leaching of low molecular weight species (Guedes *et al*., 2000; Hu and Sun, 2003). While swelling and plasticizing are reversible, an excess amount of moisture can lead to microcracking and fibre debond which are irreversible processes (Ellyin and Rohrbacher, 2003).

Moisture absorption in the matrix causes an increase in the creep compliance of the composite, much like the effect of temperature, and lowers the T_g of the polymer (Hu and Sun, 2003). In addition it has been shown that moisture can have the following effects on the creep behaviour of a composite (Scott *et al*., 1995):

- moisture greatly effects the nonlinearizing parameters in the Schapery equation and has a significant impact on nonlinear viscoelastic behaviour;
- initial and steady-state creep levels can occur at lower stress levels;
- the rupture strength of a glass/polyester composite was observed to reduce by approximately 50%.

8.5.3 Effect of creep and fatigue

In the field, structures are exposed to multiple environmental conditions. Similarly, the mechanical loads on a structural member vary in terms of frequency and magnitude (Kharbari *et al.*, 2003). Consequently, the interaction of fatigue and creep is an important consideration that may significantly shorten the life of FRP composites in infrastructure applications due to degradation in strength of the composite from cyclic mechanical loading (Cardon *et al.*, 2000).

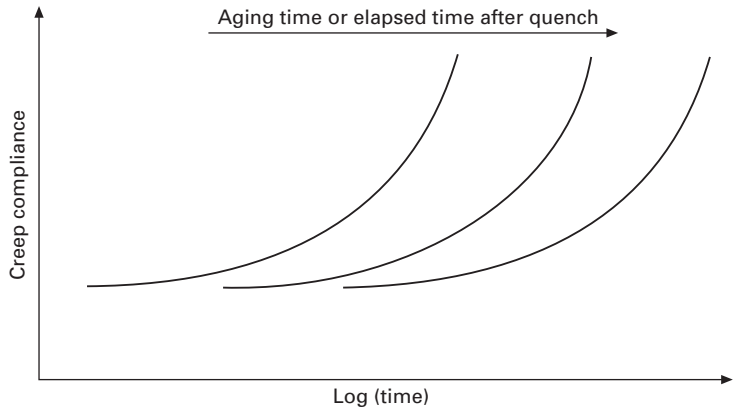
At elevated temperatures, fatigue damage due to cyclic loading and creep damage due to the loading direction can also interact (Mahadevan and Mao, 2004). Creep and fatigue damage models can be integrated by assuming creep and fatigue damage are additive. The presence of fatigue damage increases the rate of creep damage and vice versa (Mahadevan and Mao, 2004). Mahadevan and Mao (2004) proposed to account for creep and fatigue interaction by addition. For a given load history, creep damage is evaluated over each cycle time (or the duration of applied load) and the damage expected due to creep is superimposed, and the actual fatigue damage accumulated for the loading history is added to the damage ratio.

Ellyin and Rohrbacher (2003) investigated the effect of aqueous environment, temperature, and cyclic loading on glass fibre-reinforced polymer (GFRP) composites. Cross-ply, multi-ply, and angle-ply specimens were exposed to distilled water and temperature followed by cyclic loading. The accumulated cyclic creep strain of the specimens was characterized by a steep increase in the early life of the material, followed by a secondary creep with a small slope and a final increase prior to failure. The creep strain in the composite was greater for materials immersed in water at 90°C versus ambient-exposed specimens.

8.5.4 Effect of physical aging

When a polymer has been cooled to a temperature below its T_g, it is no longer in thermodynamic equilibrium and a slow gradual approach to equilibrium takes place. This approach to equilibrium is known as physical aging (Struik, 1977; Liao *et al.*, 1998; Bradshaw and Brinson, 1999; Harvey, 2005) and is associated with an internal rearrangement of molecules leading to a decrease in mobility and a decrease in the free volume of the polymer.

During physical aging, composite materials become glassier with increased stiffness and brittleness, while their creep and stress relaxation rates decrease (Struik, 1977). This may be observed as a positive phenomenon as short-term creep compliance curves are shifted to longer times as the aging time increases (Sullivan *et al.*, 1993). Figure 8.4 illustrates the change in creep compliance curves with respect to physical aging.



8.4 Schematic of creep compliance curves with increasing aging times (Liao *et al.,* 1998).

While physical aging may appear to have a 'positive' effect on creep behaviour, the aging process may be affected by many parameters including temperature, moisture, and stress (Hu and Sun, 2003). Hu and Sun (2003) investigated the equivalence between moisture and temperature in physical aging, so that the knowledge of one effect might be used to predict the other. Carbon-epoxy composites were exposed to one of two conditions where: (a) specimens were kept dry and tested under several isothermal conditions and (b) specimens were wet with a constant moisture level under room temperature at 23°C. Elastic compliances of 90° and 45° fibre-oriented specimens were observed to decrease as aging times increased for specimens with constant moisture and constant temperature. Similarly, the creep compliance under a constant moisture content or temperature content was also observed to decrease as aging time increased. Hu and Sun (2003) established a relationship for creep and elastic compliance between equivalent moisture effects and temperature effects. However, it must be noted that the relationship is not valid if the environmental temperature exceeds T_g, since aging is a thermoreversible process; and it is also not valid if moisture in the composites causes any irreversible damage such as fibre matrix debond or microcracking in the resin.

Studies are needed to evaluate the long-term effects of physical aging and moisture in order to examine how irreversible damage due to moisture uptake influences the aging process or possibly offsets the damage in terms of creep compliance.

8.6 Effects at the structural level

The durability of an FRP composite corresponds to the loading conditions in the civil structural application. There is no universal solution for durability

problems (Cardon *et al*., 2000). Depending on the application, load conditions will vary from quasi-static to fatigue loadings. In some applications, temperature and moisture diffusion must also be taken into account. In this section, the effect of creep is discussed for some recent studies on civil structural applications pertaining to all composite structural systems, FRP-strengthened structures, and FRP-reinforced concrete structures in order to illustrate the effects of creep at the structural level.

8.6.1 Creep of pultruded FRP profiles

Shao (2006) examined the flexural stiffness, shear stiffness, moment capacity, water absorption behaviour, freeze–thaw resistance, and creep response of a pultruded FRP sheet pile profile for waterfront retaining-wall applications. The author utilizes Findley's power law model for tensile and shear creep along with time-dependent viscoelastic longitudinal modulus, $E_v(t)$, and a viscoelastic shear modulus, $G(t)$, to predict the long-term deflection of the sheet piles. The design requires the sheet pile to sustain lateral pressure loads in a severe waterfront environment for 30 years. The sheet pile specimens were tested in a four-point bend configuration at one-third spacing with sustained loads of 50% and 25% of the maximum loads, corresponding to design safety factors of 2 and 4, respectively. Creep tests were conducted for a 1-year period with experimental creep deflections ranging from 13% to 19% of the initial static deflection. Predictions for creep deflection utilizing Timoshenko beam theory and Findley's power law estimate viscoelastic creep deflection exceeding 70% of the static deflection at 30 years. The author concludes that a deflection-based approach is essential and a corresponding deflection limit criterion for waterfront retaining structures needs to be established.

8.6.2 Creep of FRP-strengthened structures

Stierwalt and Hamilton (2005) investigated the creep out of concrete masonry walls strengthened with carbon/epoxy and glass/epoxy composites manufactured by the wet lay-up process. Creep is a concern for basement and retaining walls since these structures are required to sustain lateral loads from soil and groundwater pressure. The authors compared the out-of-plane flexural creep behaviour of steel-reinforced concrete masonry walls with equivalent externally bonded FRP-strengthened walls. The sustained stress on the FRP composites was approximately 40% of the ultimate strength. Creep tests were conducted outdoors to include the environmental effects of temperature and moisture variation on deflection, stiffness, and load. The steel-reinforced walls showed considerably less long-term deflection than those specimens strengthened with FRP composites. The FRP-strengthened

specimens showed a rapid increase in deflection over the first 50 days due to the creep in the resin. After the first 50 days of loading, the creep rate of the FRP-strengthened walls became linear and approached that of steel. The use of two different epoxy systems during tests indicated that the matrix type strongly influenced the creep in the FRP-strengthened structures. In general, the creep in FRP-reinforced walls was approximately 22%–56% higher than that in steel-reinforced walls. Capacity tests on FRP-strengthened walls after creep testing showed that ultimate loads were approximately 35%–71% of the design moment capacity with varying failure modes; however, it is difficult to decipher whether the degradation in capacity was due to environmental exposure and creep or to manufacturing quality since no control tests prior to long-term testing were conducted.

Tan and Saha (2006) conducted 2-year creep behaviour studies of 2-m-long reinforced concrete (RC) beams externally bonded with glass/epoxy composites. The test variables included the FRP reinforcement ratios (0%, 0.64%, 1.92%) and varying sustained load levels with a service level defined as 59% of the ultimate. As load levels increased, the creep rate and deflections were also observed to increase. As FRP ratios were increased the long-term deflections decreased, with long-term deflections being 33% lower than conventional RC beams. An effective modulus approach for concrete and steel was used to predict long-term deflections, where the creep of FRP composites was accounted for utilizing a power law.

8.6.3 Creep of FRP-reinforced concrete beams

Singhvi and Mirmiran (2002) evaluated the performance of FRP-RC beams and their components under the simultaneous effects of accelerated environmental conditions and sustained loads, and tested the suitability of fibre optic sensors for long-term monitoring of FRP-RC beams. The experimental procedure involved immersing GFRP-RC beams under sustained loads for 6 months in accelerated environmental conditions of moisture, seawater, and deicing salt solutions, as well as air for control. The sustained load was approximately 15% of the flexural capacity of the beams and was large enough to initiate cracking. Creep in the FRP rebar in the control air was lower than that in the moisture-exposed beams. The authors noted that the FRP bars and/or their bond with concrete deteriorated over time in harsh environments; however, the presence of salt in the solution did not adversely affect the creep behaviour of beams in either compression or tension. Following the sustained loading for 6 months, beams were unloaded and creep recovery was measured for 10 days until experimentally loading to failure. Not all creep strains could be recovered due to cracking of the beams. The major impact of the saltwater solutions was to lower the post-cracking stiffness of the beams more than the moisture environment. The authors developed an

analytical model based on the age-adjusted effective modulus method for concrete and Findley's power law accompanied by a stress-relaxation technique to predict the creep behaviour of FRP-RC beams.

Naguib and Mirmiran (2002) investigated the flexural creep behaviour of concrete-filled fibre-reinforced polymer tubes (CFFTs). CFFT tubes have been proposed as replacements for RC columns and prestressed columns. Creep tests were conducted on 0.152-m-diameter, 2.134-m-long CFFT specimens for 6 months in three-point bending at 40% and 25% of the static capacity of the beams followed by a 3-week creep recovery period, and were finally tested to failure to measure reserve strength. An additional specimen was subject to a slow strain rate and short-term creep rupture at 70% of the load capacity. The FRP tubes were made of 40 plies of E-glass/epoxy in a symmetric lay-up of $[0°/0°/+45°/-45°]_{10}$. The creep rate was observed to be load dependent, with the higher load corresponding to a higher creep rate in the structure. The authors utilized a creep prediction model that accounts for a general combination of axial and flexural creep when the specimen is subject to eccentric, sustained axial loads. Findley's power law was used to model viscoelastic behaviour and the double power law for creep of concrete was used for each layer of the CFFT cross-section. Within each time interval, stresses associated with creep strain are summed following BSP. It was found that the creep effect reduces the flexural stiffness of CFFT specimens; however, the ultimate strength is not significantly affected. In addition, creep of CFFT beams–columns is much less than that of CFFT beams, since axial loads retard the cracking of concrete and tensile creep of the FRP. The creep rupture life expectancy of CFFT beam-columns with diameter-to-thickness ratios of 10, 20, and 40 is greater than 50 years for a sustained load of 60% of the capacity.

8.6.4 Discussion

While the structural-level effects of the creep of an FRP structure were typically accounted for by integrating Findley's power law to determine a time-dependent viscoelastic modulus, the use of long-term creep predictions showed that creep response can be a critical design parameter (i.e. can govern the design of the structure), as in the pultruded retaining wall; or, at a minimum, the time-dependent response of the composite is useful in evaluating design options that will satisfy a specified structural service life requirement, as in the 50 years of the CFFT beam-columns. The impact of composite creep deformation on a structure can be minimized by appropriate selection and processing of resins, and the placement of fibres, with the understanding that creep effects will occur in the matrix (Morgan *et al.*, 2001). In light of environmental factors and varying load cycles in structures, the time-dependent response of composite materials will ultimately have an impact on the service

life of a structure. While widely accepted methodologies for long-term response prediction of composites are available with Findley's power law or Schapery's formula combined with TTSP methods, the interaction of creep behaviour with other types of structure response must still be taken into account; specifically, the interaction of creep and fatigue still remains unclear. Similarly, the long-term effects of moisture – which will induce chemical aging – combined with physical aging are relatively unknown.

Although there is no universal creep–durability solution for all structures, elucidating the influence of the time-dependent behaviour of the composite on the safety of the structural system is the ultimate goal. Understanding the complex interaction of creep, fatigue, moisture, aging, and other factors of all materials (e.g. steel corrosion, concrete cracking, etc.) within the structural system can potentially lead to the development of analytical models to predict the remaining service life of structures.

8.7 Future trends

Research efforts related to creep and the time-dependent response of FRP composites have typically focused on the development of analytical models to determine the long-term response at the material level. In particular, the effects of moisture, temperature, and physical aging have garnered much interest. Materials should be required to be assessed based on the intact properties of the composite and after the material has been subject to a standardized sequence of mechanical, physical, chemical, and thermal aging factors (Morgan *et al*., 2001). The lack of established testing and acceptance criteria for long-term creep responses tends to lead towards overly conservative design. In addition, as materials evolve (i.e. nanocomposites, fillers, etc.) and are introduced into infrastructure applications, the time-dependent behaviour of those materials will need to be understood.

The manufacturing of civil infrastructure composites for rehabilitation or strengthening typically includes a hand lay-up technique. Often the composite is bonded to a structure and subject to load before the matrix has fully cured. The issue of the effect of uncured resins on the creep response of composites is important for construction quality and long-term response (Morgan *et al*., 2001). The creep effect of uncured resins specifically addresses the impact that polymer cross-link density has on the creep performance of composite materials.

Using the time-dependent response of composite materials at the coupon level to predict the long-term response of a structural system needs to be verified. In particular, the impact of scale effects on the creep behaviour of composites is not fully understood.

8.8 References

Al-Haik M S and Garmestani H (2001), 'Durability Study of a Polymeric Composite Material for Structural Applications', *Polymer Composites*, **22**(6), 779–792.

ASCE (American Society of Civil Engineers) (1984), *Structural Plastics Design Manual*, Reston, Virginia, ASCE Publications.

ASTM D2990 (2001), 'Standard Test Methods for Tensile, Compressive, and Flexural Creep and Creep-Rupture of Plastics', Pennsylvania, American Society for Testing and Materials.

Bank L C and Mosallam A S (1990), 'Creep and Failure of a Full Size Fiber Reinforced Plastic Pultruded Frame', *Composite Material Technology*, **1**, 49–56.

Barnes R and Garden H N (1995), 'Time-Dependent Behaviour and Fatigue', in Holloway L C and Leeming M B Eds, *Strengthening of Reinforced Concrete Structures – Using Externally-Bonded FRP Composites in Structural and Civil Engineering*, Cambridge, Woodhead, pp. 183–221.

Bradshaw R D and Brinson L C (1999), 'A Continuous Test Data Method to Determine a Reference Curve and Shift Rate for Isothermal Physical Aging', *Polymer Engineering and Science*, **39**(2), 211–235.

Callister W D (2003), *Materials Science and Engineering: An Introduction*, Hoboken, John Wiley and Sons.

Cardon A H, Qin Y, Van Vossole C and Bouquet, P (2000), 'Prediction of the Residual Structural Integrity of a Polymer Matrix Composite Construction Element', *Mechanics of Time-Dependent Materials*, **4**, 155–167.

Dillard D A, Straight M R and Brinson H F (1987), 'The Nonlinear Viscoelastic Characterization of Graphite/Epoxy Composites,' *Polymer Engineering and Science*, **1**, 116–123.

Ellyin F and Rohrbacher C (2003), 'The Influence of Aqueous Environment, Temperature, and Cyclic Loading on Glass-Fibre/Epoxy Composite Laminates', *Journal of Reinforced Plastics and Composites*, **22**(7), 615–636.

Ferry J D (1980), *Viscoelastic Properties of Polymers*, New York, John Wiley and Sons.

Findley W N and Lai J S (1967), 'A Modified Superposition Principle Applied to Creep of Nonlinear Viscoelastic Material under Abrupt Changes in State of Combined Stress', *Transactions of the Society of Rheology*, **11**(3), 361–380.

Gerdeen J C, Lord H W and Rorrer R A L (2006), *Engineering Design with Polymers and Composites*, Boca Raton, CRC Press.

Goertzen W K and Kessler M R (2006), 'Creep Behavior of Carbon Fiber/Epoxy Matrix Composites', *Materials Science and Engineering A*, **421**, 217–225.

Guedes R M, Morais J J L, Marques A T and Cardon A H (2000), 'Prediction of Long-Term Behaviour of Composite Materials', *Computers and Structures*, **76**, 183–194.

Haj-Ali R M and Muliana A H (2004), 'A Multi-Scale Constitutive Formulation for the Nonlinear Viscoelastic Analysis of Laminated Composite Materials and Structures', *International Journal of Solids and Structures*, **41**, 3461–3490.

Harvey J (2005), 'Chemical and Physical Aging of Plastics', in Kutz M Ed., *Handbook of Environmental Degradation of Materials*, New York, Williams Andrew Publishing.

Hu, H and Sun C T (2003), 'The Equivalence of Moisture and Temperature in Physical Aging of Polymeric Composites', *Journal of Composite Materials*, **37**(10), 913–928.

Karbhari V M, Chin J W, Hunston D L, Benmokrane B, Juska T, Morgan R, Lesko J J, Sorathia U and Reynaud D (2003), 'Durability Gap Analysis for Fiber-Reinforced Polymer Composites in Civil Infrastructure', *Journal of Composites for Construction*, **7**(3), 238–247.

Kawada H, Kobiki A, Koyanagi J and Hosoi A (2005), 'Long-term Durability of Polymer Matrix Composites Under Hostile Environments', *Materials Science and Engineering A*, **412**, 159–164.

Leaderman H (1943), *Elastic and Creep Properties of Filamentous Materials and Other High Polymers*, Washington DC, Textile Foundation.

Liao K, Schultheisz C R, Hunston D L and Brinson L C (1998), 'Long-term Durability of Fiber-Reinforced Polymer-Matrix Composite Materials for Infrastructure Applications: A Review', *Journal of Advanced Materials*, **30**(4), 3–40.

Mahadevan S and Mao H (2004), 'Probabilistic Fatigue-Creep Life Prediction of Composites', *Journal of Reinforced Plastics and Composites*, **23**(4), 361–371.

Menard K P (1999), *Dynamic Mechanical Analysis*, Boca Raton, CRC Press.

Morgan R, Dunn C and Edwards C (2001), 'Effects of Creep and Relaxation', in CERF Report 40578, *Gap Analysis for Durability of Fiber Reinforced Polymer Composites in Civil Infrastructure*, Reston, Virginia, Civil Engineering Research Foundation, pp. 52–59.

Muliana A, Nair A, Khan K A and Wagner S (2006), 'Characterization of Thermo-Mechanical and Long-Term Behaviors of Multi-layered Composite Materials,' *Composite Science and Technology*, **66**, 2907–2924.

Naguib W and Mirmiran A (2002), 'Flexural Creep Tests and Modeling of Concrete-Filled Fiber Reinforced Polymer Tubes', *Journal of Composites for Construction*, **6**(4), 272–279.

Scott D W and Zureick A-H (1999), 'Compression creep of a pultruded e-glass vinylester composite', *Composites Science and Technology*, **58**, 1361–1369.

Scott D W, Lai J S and Zureick A-H (1995), 'Creep Behavior of Fiber-Reinforced Polymeric Composites: A Review of Technical Literature', *Journal of Reinforced Plastics and Composites*, **14**, 588–617.

Shao Y (2006), 'Characterization of a Pultruded FRP Sheet Pile for Waterfront Retaining Structures', *Journal of Materials in Civil Engineering*, **18**(5), 626–633.

Stierwalt D D and Hamilton H R (2005), 'Creep of Concrete Masonry Walls Strengthened with FRP Composites', *Construction and Building Materials*, **19**, 181–187.

Singhvi, A and Mirmiran, A (2002), 'Creep and Durability of Environmentally Conditioned FRP-RC Beams Using Fiber Optic Sensors', *Journal of Reinforced Plastics and Composites*, **21**(4), 351–373.

Struik L C E (1977), 'Physical Aging in Plastics and Other Glassy Materials', *Polymer Engineering and Science*, **17**(3), 165–173.

Sullivan J L, Blais E J and Houston D (1993), 'Physical Aging in the Creep Behavior of Thermosetting and Thermoplastic Composites', *Composite Science and Technology*, **47**, 389–403.

Tan K H and Saha M K (2006), 'Long-Term Deflections of Reinforced Concrete Beams Externally Bonded with FRP System', *Journal of Composites for Construction*, **10**(6), 474–482.

Ward I M and Sweeney J (2004), *The Mechanical Properties of Solid Polymers*, West Sussex, John Wiley and Sons.

Yen S C, Hiel C and Morris D H (1985), 'Viscoelastic Response of SMC-R50 Under Different Thermomechanical Conditions', in Wilson D W Ed., *High Modulus Fiber Composites in Ground Transportation and High Volume Applications,* ASTM STP 873, Pennsylvania, American Society for Testing and Materials, pp. 131–143.

9

Durability of composites in relation to wear and erosion

A. P. MOURITZ,
Royal Melbourne Institute of Technology, Australia

9.1 Introduction

The wear of fibre–polymer composites is an important durability issue in the design and materials selection of civil infrastructure. Wear is usually not considered important in civil engineering structures built from traditional construction materials such as steel and concrete because of their good wear resistance. However, composites are more susceptible to wear and therefore wear performance must be a key consideration in the design of new structures. Civil structures can experience one or many types of wear during their life, with the most common being gouging, abrasion and erosion. Gouging occurs when a large, hard object scrapes against a surface removing up to several millimetres of material. Abrasion is a similar wear process to gouging, but occurs on a smaller scale. Abrasion occurs by small grit particles sliding over a surface with the removal of a small amount of material by wear processes that occur at the microstructural level. The scratches caused by abrasion are only a few microns deep, but when this wear process is repeated many times a large amount of material is eventually worn away. Erosion occurs by hard grit particles striking a surface at high speed with the removal of material. The impact craters are often less than a few microns deep, but as with abrasion when the erosion process is repeated many times the surface gradually erodes away. In some civil structures, another wear process known as sliding wear can occur; this involves material being worn by sliding against a hard metal counter-face. There are many other forms of wear – such as cavitation wear, fretting wear and adhesive wear – but civil infrastructure is unlikely to experience these types.

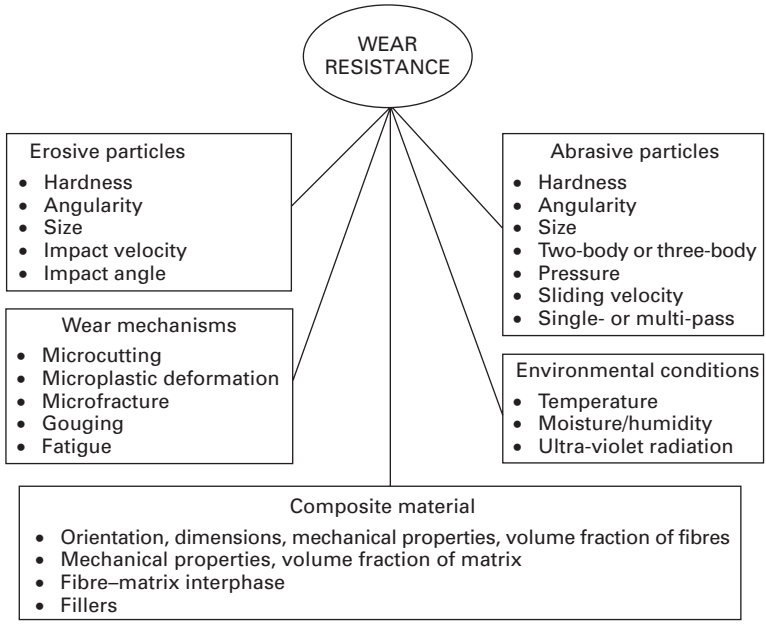
Examples of excessive wear to civil composite structures are rare because polymer composites are not often used in components prone to gouging, abrasion or erosion. The current applications of composites – such as deck foundations to small bridges, reinforcement of pylons, strengthening of ageing concrete structures – are situations where wear is not usually a problem. However, with the expanding uses for composites it is not difficult to imagine

a multitude of wear scenarios, particularly after these materials have been in service for many years, when the accumulation of wear damage becomes noticeable. For example, composites used in bridge deck surfaces are exposed to wear from road vehicles. Composites used below the waterline in pylons to bridges and wharves can be eroded by water-borne grit particles and be gouged by large moving objects and debris in the water. Composites used in semi-arid and desert environments can be eroded by sand particles in a dust storm. The wear rate is often accelerated when the wear event occurs in combination with other environmental factors, such as degradation of the polymer matrix from ultra-violet radiation, moisture absorption or thermal ageing.

The main types of polymer composites in civil infrastructure – namely glass/thermoset and carbon/thermoset laminates – are used for their high specific strength, long fatigue life, toughness and corrosion resistance, but not their wear resistance. In fact, the wear performance of these composites is poor compared with conventional construction materials such as steel, aluminium alloy and concrete. Depending on the wear scenario, composites may be worn at a similar rate to steel and concrete, but it is more likely that they will wear at rates many tens to hundreds of times faster. While many composite materials have better wear resistance than the glass/thermoset and carbon/thermoset laminates used in civil infrastructure, very few composite systems have the wear durability to match steel or concrete. For this reason, civil engineers need a good understanding of the wear properties of composite materials to ensure long-term durability.

A major challenge in determining the durability of composites is that their wear resistance is not a simple or intrinsic material property, like elastic modulus, strength and fracture toughness. Instead, wear resistance is dependent on many factors, including the mechanical and physical properties of the composite, the contact conditions between the composite and mating material, the relative movements between the mating materials, the environmental conditions and the wear mechanisms. The complex relationship between wear resistance and these factors is shown in Fig. 9.1.

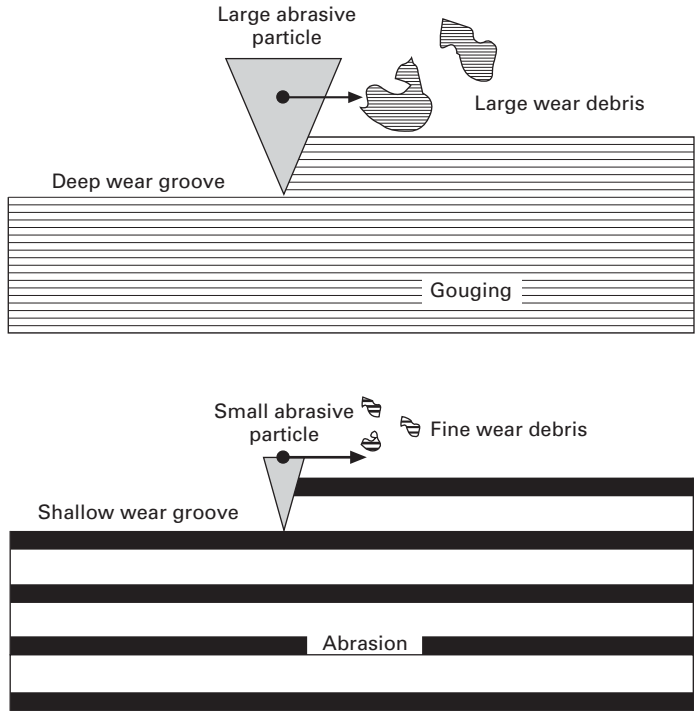
This chapter gives an overview of the gouging, abrasion and erosion wear properties of fibre–polymer composites for civil infrastructure. The wear mechanisms involved with gouging, abrasion and erosion are described, and the effect of the hardness, shape and size of the abrasive particles on these wear processes is discussed. The effect of the physical and mechanical properties of composites on their wear resistance is examined, including the influence of the polymer matrix and the type, size, volume content and orientation of the fibre reinforcement. The chapter concludes with a description of recent developments in wear-resistant composite materials that may be used in future civil infrastructure to improve their durability.



9.1 The factors controlling the abrasive and erosive wear performance of polymer composites.

9.2 Gouging and abrasion wear

Gouging and abrasive wear of polymer composites are examined in this section. The abrasion properties of composites have been investigated in great detail,[1–16] but much less is known about their gouging wear resistance. As mentioned previously, gouging occurs when a coarse, hard abrasive particle scrapes across a composite with the removal of a large volume of material in a single pass. The scratch can be several millimetres deep, and the damage is clearly visible. Abrasion occurs on a smaller scale to gouging, and involves fine grit particles rubbing against the surface with the removal of a small amount of material. The scratch depth is usually less than a few microns, but the process is often repeated many times resulting in the removal of a large volume of material. The difference between gouging and abrasion is somewhat arbitrary and ill-defined, although the scale of the scratches relative to the microstructure is a useful metric for distinction (Fig. 9.2). The scratch depth due to gouging is many times larger than the dimensions of the microstructure (e.g. fibre diameter). For this reason, gouging can be considered an abrasive wear process where the bulk properties (e.g. hardness, fracture toughness) of the material control the wear resistance. Abrasion, on the other hand, is a wear process at the same scale as the microstructure. For this reason, the abrasion rate and wear mechanisms are sensitive to microstructural details of the material, such as the fibre diameter and fibre–matrix interface.



9.2 The relative scale of gouging and abrasive wear of composites. Each horizontal line approximates the fibre dimensions.

Gouging wear is expected to be an infrequent event for civil infrastructure because there should be few incidents when large particles or objects scrape against a surface. Abrasion is a more common event, and the focus of this section is the abrasive wear properties of polymer laminates. The abrasion process can occur by 'two-body' or 'three-body' wear. The definition of two-body abrasion is wear by the sliding of hard asperities or rigid grit particles over the surface. A classic example of two-body wear is the rubbing of sandpaper over a surface. Three-body abrasion occurs when grit particles are free to roll and slide between two surfaces. It is possible that composite materials used in civil infrastructure would be exposed to both two- and three-body abrasion. However, there is greater concern with two-body abrasion because the wear rates are much higher. Comparisons between the two- and three-body wear rates of composites are not well known, although for metals the two-body wear rate is typically ten times higher than the three-body rate. Other terms used to describe abrasion are 'low-stress' and 'high-stress' wear. Low-stress wear occurs when the abrasive particles do not experience any damage when sliding across the surface. High-stress abrasion occurs when the pressure acting on the grit particle exceeds its crushing strength, and it is broken into small fragments during the wear process.

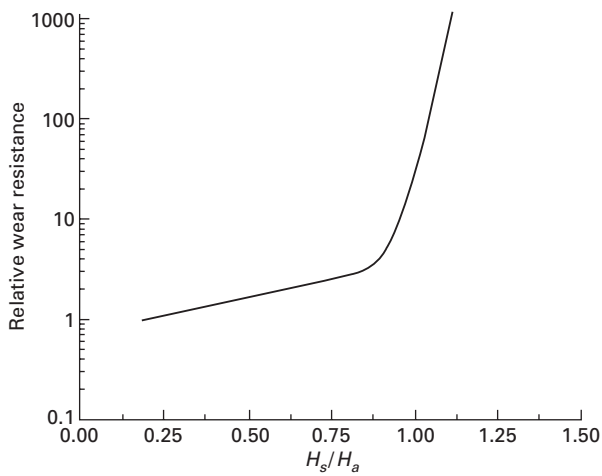
The abrasion of composites does not usually occur by a single wear process, and instead several wear mechanisms occur simultaneously. The main mechanisms are microcutting, microploughing, microcracking and microfatigue by repeated deformations. Microcutting is analogous to machining, but occurs on a smaller scale, and involves a sharp abrasive particle shaving off the surface material as small chips of debris. Microploughing occurs when an abrasive particle plastically deforms the surface material in its path. The deformed material is displaced to the sides and ahead of the wear groove, although no material is lost from the surface. Microploughing occurs when the leading face of the abrasive particle is relatively blunt, and lacks the sharpness needed to remove material by microcutting. Wear by microcracking involves fine-scale fracture of a brittle surface under the stress applied by the abrasive particles, with the formation of wear debris. Microfatigue wear occurs when the processes of microplouging or microcracking are repeated many times by a large number of grit particles sliding over the surface. This causes the formation and growth of fatigue cracks that eventually cause the loss of surface material.

Ideally, the abrasive wear resistance of composites used in civil infrastructure should be determined in their end-use condition in the actual service environment. In reality, however, this is often not practical due to the long duration and high cost of field tests. Instead, the abrasion properties of composites are usually determined using laboratory wear test rigs. Several wear tests are used, with the most common being the pin-on-disc and pin-on-drum tests for two-body abrasion and the dry sand rubber wheel test for three-body abrasion.[14] The pin-on-disc method (see standards ASTM G99, DIN 50324, and ISO/DIS 7148-2) is the most common abrasion test, and it basically involves pressing the end face of a cylindrical pin specimen made of the test material against abrasive paper bonded to a rotating flat disc. The pin-on-drum test is similar, but rather than sliding against a flat disc, the pin is pressed against a rotating drum covered with abrasive paper. In both the pin-on-disc and pin-on-drum tests, the pin is abraded for a fixed sliding distance or time, and then the wear rate is measured by the mass (or volume) loss. The dry sand rubber wheel test (ASTM G65) involves pressing a flat specimen block against the curved surface of a rotating rubber wheel. Sand or any other abrasive medium is gravity fed into the contact zone between the specimen and wheel. The abrasive particles roll and slide through the contact zone, which is usually less than 5–10 mm long, to create three-body wear conditions. The specimen is tested for a fixed time, and the resulting mass (or volume) loss is measured to determine the wear rate.

The hardness of the abrasive has a major influence on the wear rate of composites and other engineering materials. The basis of abrasive wear resistance of materials is hardness; grit particles with a higher hardness than the material cause greater wear than softer particles. The effect of abrasive

hardness on the wear resistance of isotropic ductile materials, such as most metals and polymers, is shown in Fig. 9.3. When the ratio of the surface hardness of the material (H_s) to the abrasive hardness (H_a) is less than about 0.8, then the wear resistance is low. The wear resistance increases rapidly when H_s/H_a approaches unity because the wear mechanisms of microcutting and microploughing are suppressed. The relationship between the wear resistance and hardness ratio shown in Fig. 9.3 for isotropic materials is more complicated for composite materials. The hardness of composites is a complex property because it is dependent on the hardness, volume fraction and packing density of the fibres and the hardness of the matrix. Fine-scale abrasion processes can occur that involve only a single fibre or a small region of the resin matrix, and then the hardness of the individual material is important. More often, however, abrasion involves the combined wear of both the fibres and matrix. The wear rate is also dependent on more properties than just hardness, including the adhesion strength between the fibres and matrix, fracture toughness of the fibres and matrix,[6,7,13,15] and fibre orientation. The influence of these properties on the wear rate will be described shortly. Despite the complexity, it is generally observed that the wear rate of composite materials increases with the hardness of the abrasive.[3]

The shape and size of the abrasive particles also affect the wear rate. The wear rate increases with the angularity of the grit particles. Angularity defines the amount of the particle surface that consists of sharp edges. Common examples of different degrees of angularity are grit particles on sandpaper, beach sand and glass beads, which have high, intermediate and low angularity, respectively. Materials are worn more rapidly by angular hard particles because

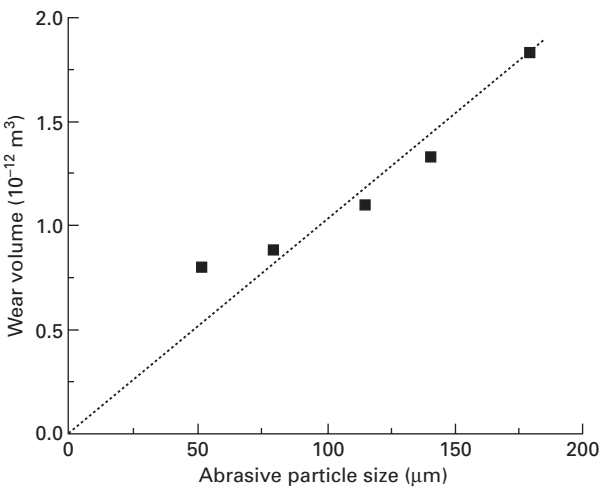


9.3 Relationship between hardness ratio and wear resistance for isotropic materials.

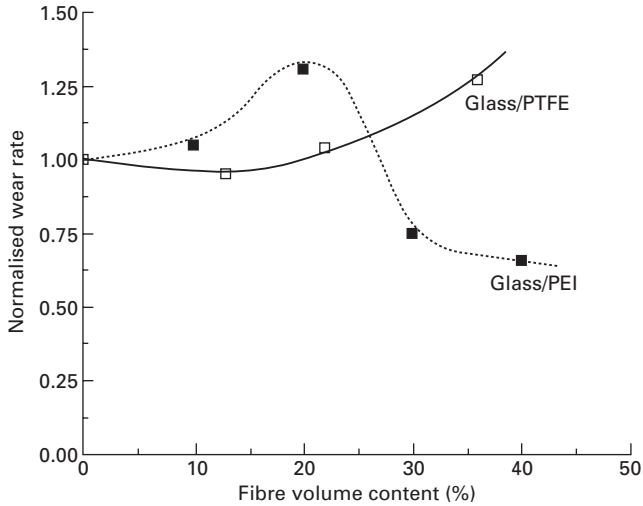
their sharp edges can machine chips from the surface. The wear rate of composites also increases with the abrasive particle size.[5–7,12,17] For example, Fig. 9.4 shows the effect of grit size on the abrasion rate of a polyetherimide (PEI) composite containing short glass fibres. This figure shows a linear increase in wear rate with grit size, although this may not always be the case for composite materials. Depending on the microstructure, applied pressure and particle hardness, the relationship between wear rate and particle size can be linear, quasi-linear or non-linear, and this can only be determined by abrasion testing over a wide range of grit sizes. The increase in wear rate with particle size is due to several factors, with the most important being that larger particles can penetrate deeper into the surface to remove material. Beyond a certain size, however, the wear rate is independent of the grit size.

The microstructural properties of a composite material have a major influence on its abrasive wear resistance. The volume content, orientation, length and type of fibres; the volume content and mechanical properties of the polymer matrix; and the adhesion strength between the fibres and matrix each affect the wear rate to a greater or lesser extent. Understanding the relationship between these properties and wear rate provides the opportunity for the design of composite materials with maximum abrasion resistance.

The abrasive wear resistance of composites is sensitive to their fibre content.[4,7,10,12,13,17] Figure 9.5 shows the relationship between wear rate and fibre volume content for two types of fibreglass composites. The wear rates of the composites have been normalised to the wear rate of the neat resin. It is obvious that the dependence of wear rate on the fibre content is considerably



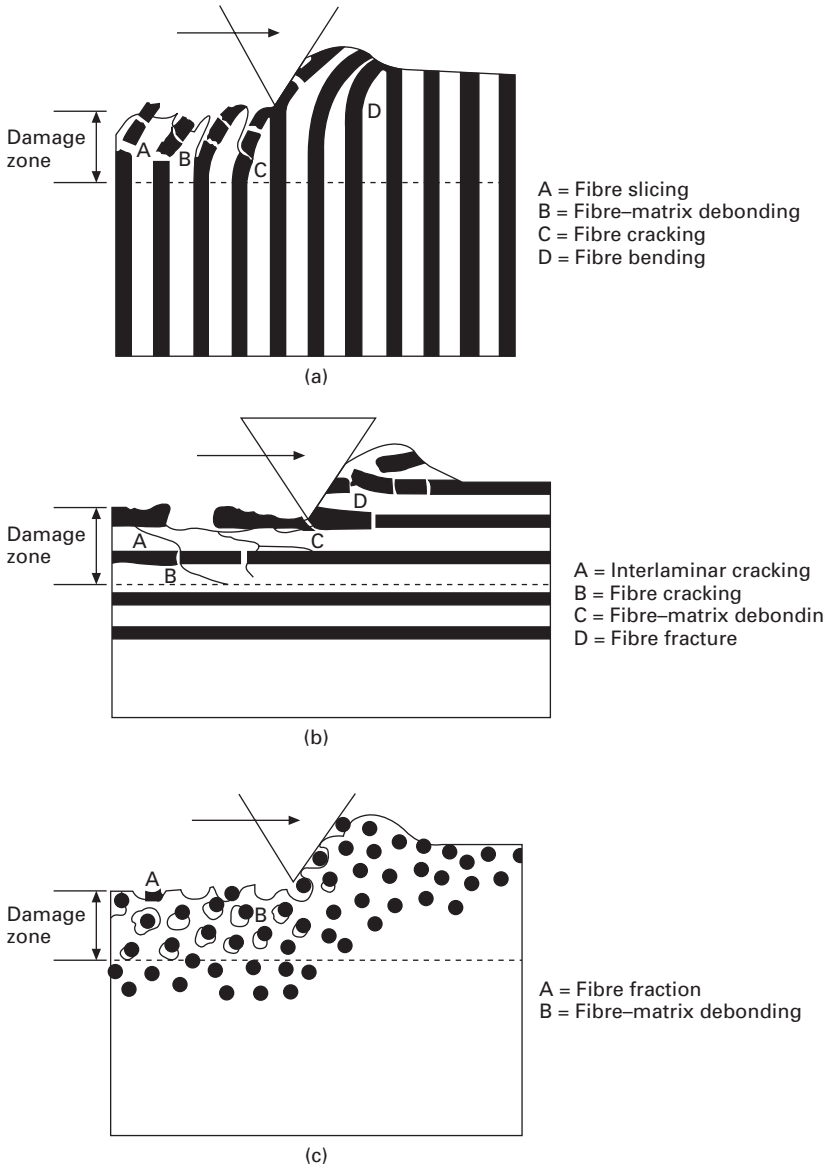
9.4 Effect of abrasive particle size on the wear rate of short glass fibre/PEI. The abrasive was silicon carbide. Data from Bijwe *et al.*[12]



9.5 Effect of fibre content on the abrasive wear rate. Data for the glass/PTFE are from Voss and Friedrich,[18] and those for the glass/PEI are from Bijwe *et al.*[12]

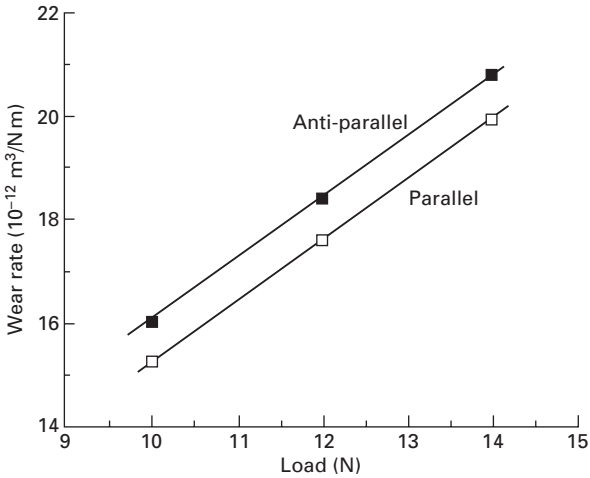
different for the two materials. This is typical of composites, and it is not possible to describe a general relationship between wear rate and fibre content. The wear rate of the PEI laminate increases with the glass content up to a maximum at 20% by volume, and then drops rapidly at higher fibre contents. The PTFE shows the opposite behaviour with the lowest wear rate occurring at a fibre content of 20%. The wear rate under dry sliding conditions, which basically involves rubbing between a composite and steel counter-face, is also lowest at a fibre volume content of 10–20%, and increases at higher fibre contents.[18–23]

The orientation of the fibres relative to the sliding direction of the abrasive particles is another important factor controlling wear resistance. Several studies have investigated the wear rates of composites with the fibres aligned in the parallel, anti-parallel and normal directions relative to sliding.[5–7,12,15] Figure 9.6 presents a schematic of the wear mechanisms for the different fibre directions.[6] The lowest wear rate occurs when the fibres are normal to the sliding direction, when abrasion occurs by cutting or fracturing of the fibre ends. However, engineering structures are rarely, if ever, designed with the fibre ends exposed to the surface. Instead, the fibres are aligned in the parallel and anti-parallel directions to the surface of composites structures. Wear studies have shown that the abrasion rate is highest when the fibres are in the anti-parallel direction. For example, Fig. 9.7 compares the abrasion rates measured over a range of applied loads for a unidirectional glass/PEI laminate with the fibres in the parallel or anti-parallel directions. The wear rate is slightly higher in the anti-parallel direction, and this is because the



9.6 The abrasive wear mechanism of brittle fibre composites with the fibres (a) normal, (b) parallel and (c) anti-parallel to the sliding direction. Reproduced (with permission from Springer) from Cirino *et al.*,[6] their reference 12.

fibres are more easily broken and the fragments gouged out by the abrasive. The wear rate of composites sliding against steel also decreases in the following order: normal, parallel, anti-parallel.[24,25]



9.7 Comparison of the wear rates of a PEI laminate with the glass fibres aligned parallel and anti-parallel to the sliding direction. The wear rate (m^3/N m) is the volume of material removed per unit applied force and sliding distance. Data from Bijwe *et al.*[12]

In some cases, the type of fibre reinforcement can influence the abrasion resistance.[7,15] As mentioned, the composites used in civil structures usually contain brittle glass or carbon fibres. Both fibres are broken under high-stress wear and their fragments dug from the wear surface, and for this reason the wear resistance of glass and carbon fibre composites is usually similar. The situation is different for dry sliding wear, with carbon fibres providing better wear resistance than glass fibres. This is due to the graphite crystals shearing along the fibre length by a fibre thinning process that provides self-lubricating properties at the composite surface.[26–29] However, such an effect is not observed in the abrasion of carbon fibre composites. The abrasion and sliding wear resistance are higher for composites with ductile fibres, such as aramid, which resist fracture and instead are worn by microcutting and microploughing processes.[6,20,24,30] However, aramid composites are not well suited to many civil applications because of their low compressive strength and poor durability in moist environments.

The abrasion rate is also controlled by the microstructure and mechanical properties of the polymer matrix. The wear resistance is usually better for composites with a tough matrix (e.g. toughened thermoset, thermoplastic) than a quasi-brittle matrix with low ductility (e.g. epoxy). This is because a tough matrix is more resistant to wear by microcracking. Many of the polymers used in civil composite materials contain fillers, such as pigments and ultra-violet stabilisers, which also affect the wear rate. It is not possible to make a general statement about the influence of fillers on wear rate because it is dependent on the type, size and loading of the filler particles, the type of

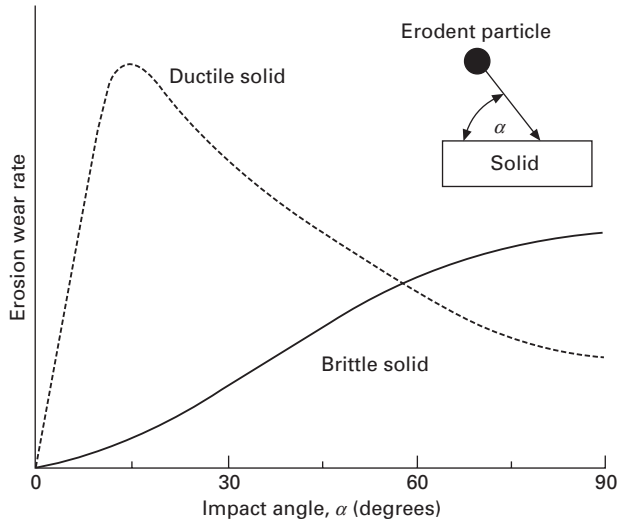
polymer and the adhesion between the filler and matrix. However, many fillers reduce the yield strength and toughness of polymers which results in poor wear resistance.[31]

Many attempts have been made to correlate the mechanical properties of composite materials with their abrasive wear resistance. Individual wear studies have found that abrasion resistance increases with a factor ($\sigma\varepsilon_f$) combining tensile strength (σ) and failure strain (ε_f);[1,2] or ε_f alone.[11] However, many other wear studies report no strong relationship between bulk properties and abrasion resistance. This matter remains unresolved, and therefore the design of abrasion-resistant composites for civil engineering applications cannot be reliably based on the intrinsic properties of the composites used.

9.3 Erosive wear

Erosion is caused by the impact of solid hard particles or liquid against the surface of an object. Erosion of civil composite materials by liquid impact is unlikely to occur because very high impact speeds are required to cause appreciable wear. For this reason, liquid erosion will not be considered, and this section will focus on erosion of composites by solid particle impact. Erosion can occur by several mechanisms which are controlled by the type, size, shape, velocity and impact angle of the particles and the microstructural properties of the composite. The four most common types of erosion are microcutting, microploughing, microcracking and fatigue. Erosion involving microcutting and microploughing processes occurs when ductile materials are impacted at a shallow angle. Plastic deformation of ductile materials and fracture of brittle materials occurs in high-angle impact. Fatigue-induced erosion of ductile and brittle materials can also occur in high-angle impact when the kinetic energy of the particles is low. Other types of solid particle erosion can also occur, such as local melting and vapourisation under extremely high impact speeds, although these events will not occur with civil structures.

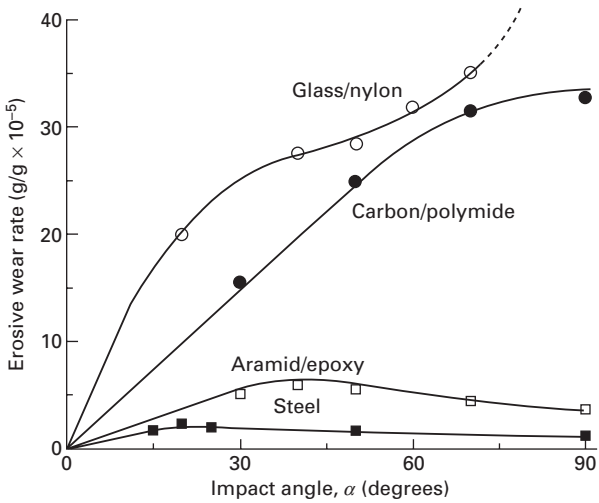
The erosion rate of engineering materials, including composites, is strongly dependent on the impingement angle (α), which is the angle between the substrate surface and the particle trajectory. The erosion wear rate is defined as the mass (or volume) loss of material per unit mass of impacting particles. The wear rate is usually measured using a laboratory erosion test machine that fires a continuous stream of abrasive particles travelling at a constant speed at the flat surface of a test specimen. The wear rate is simply determined by measuring the mass or volume loss of the test piece after being impacted by a specific mass of particles. Further information on erosion tests is given by Hutching.[14] The effect of impingement angle on wear rate is determined by increasing the angle between the particle stream and the specimen surface from 0° to 90°. Figure 9.8 shows the effect of impingement angle on the



9.8 Effect of impingement angle on the erosive wear rates of ductile and brittle materials. The erosion rate is measured as mass loss of material per unit mass of impacting particles.

erosion rates of ductile and brittle materials. The wear rate of ductile materials at $\alpha = 0°$ is negligible because the eroding particles do not impact the surface. The erosion rate rises rapidly with the impingement angle up to about 30° due to the increasing severity of microcutting wear. The wear rate then drops from 30° to 90° as microplastic deformation becomes more prevalent and the incidence of microcutting diminishes. Examples of polymers that experience the ductile mode of erosive wear are highly ductile thermoplastics such as nylon, polyvinylchloride and polypropylene. The wear rate of brittle materials increases progressively with impingement angle and reaches a maximum at 90° due to the increasing incidence of brittle fracture. Materials that show this behaviour include polymers with low ductility (e.g. epoxies) and reinforcing fibres (e.g. carbon, glass). In some circumstances, most notably when erosion is caused by very small particles, brittle materials wear by a combination of microfracture and microplastic deformation, and therefore the relationship between wear rate and impingement angle is a hybrid of the ductile and brittle modes shown in Fig. 9.8.

Several erosion studies have examined the effect of impingement angle on the wear rates of composite materials.[32–36] Composites containing glass or carbon fibres usually show the brittle mode of wear, as shown in Fig. 9.9. The erosion rate is expressed as mass loss from the composite per unit mass of impacting particles. The erosion process begins with the local removal of the surface resin from between the fibres which leaves them unsupported. The impacting particles cause the exposed fibres to break into small fragments

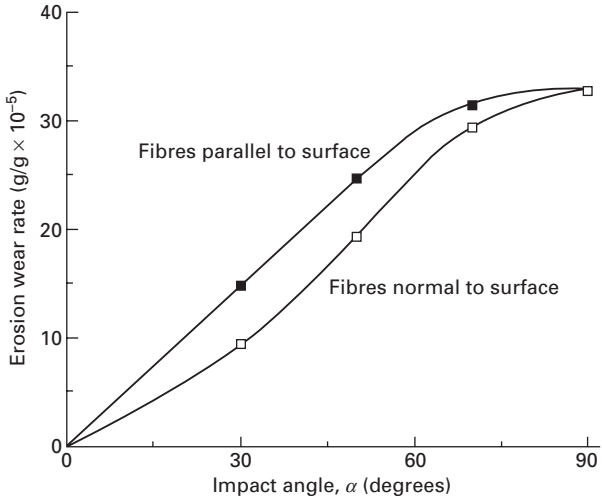


9.9 Effect of impingement angle on erosive wear of composites. Data for glass/nylon are from Tilley[33] and all other data are from Pool *et al.*[32]

that become detached from the surface. In some composite systems, the presence of brittle fibres greatly accelerates the wear rate. For example, Zahavi and Schmitt[34] measured a four-fold increase in the erosion rate when nylon was reinforced with carbon or glass. Composites containing ductile fibres (e.g. aramid, polyethylene) usually exhibit the ductile mode of erosion. For example, Fig. 9.9 shows that the wear rate of an aramid/epoxy laminate increases with impact angle up to 30°–40° and then decreases at higher angles. The aramid fibres do not suffer brittle-type fracture, and instead are gradually eroded along with the matrix by microcutting and microploughing processes.

The erosion rate is also dependent on the orientation of the fibres relative to the impact angle.[32,35,36] Figure 9.10 compares the wear rates of a unidirectional carbon/polyimide composite with the fibres aligned normal and parallel to the surface. The composite shows the brittle mode of erosion in both fibre orientations, although the wear rate at most impact angles is higher for the parallel direction. This is because it is easier for the erosive particles to fracture the fibres in the length-wise direction.

Based on published erosion studies, it is clear that the design of erosion-resistant composite materials is dependent on fibre orientation, fibre toughness and matrix ductility. However, the effect of other microstructural properties on erosion rate is not well understood, such as fibre content and fibre–matrix bond strength. The lack of a complete understanding of the relationship between erosion rate and the particle impact conditions, microstructure and mechanical properties has meant that reliable models to predict the wear rate



9.10 Effect of fibre orientation on the erosive wear rate of a carbon/polyimide laminate with the fibres aligned parallel and normal to the impact surface. Data from Pool *et al.*[32]

of composites are not available. The lack of accurate models means that the erosion properties of candidate materials for civil structures must be determined by laboratory and field testing. Despite the inability to model the erosion process, it is apparent from laboratory erosion tests that the wear rate of composite materials can be 30 times or more higher than that of mild steel,[32] and therefore an erosion-resistant surface layer to protect civil composite structures in highly erosive environments is essential.

9.4 Conclusions and future trends

Wear will become an increasingly important durability issue for certain types of composite infrastructure, particularly after many years of service in harsh environments. Many civil composite structures located in high-wear environments have only been in service for a few years, and the long-term effects of wear damage over many decades are not yet known. It also means that a large database of information on the wear performance of civil composite materials is not available. Such a database is needed for the design and materials selection of wear-resistant structures, and it is important that civil engineers carefully monitor, record and report the wear rates and wear mechanisms of composites in service. Until this time, it is necessary to rely on wear studies performed in the laboratory using small-scale apparatus. However, interpreting the wear performance of civil composite structures based on laboratory wear tests is fraught with danger because the test material is not in the end-use condition and the wear test conditions are

often different to the actual operating environment. Laboratory tests are useful for ranking the relative performance of different composite materials for a specific wear condition, but should not be used to estimate the wear life of civil structures.

Most of the current knowledge on wear is based on experimental testing of composite materials that are not regularly used in civil infrastructure, such as thermoplastic laminates and thermoset materials with low fibre contents. It is risky to interpret the wear performance of glass/thermoset and carbon/thermoset laminates using empirical wear data for thermoplastic materials. While several wear tests have been performed on glass/thermoset and carbon/thermoset laminates, they are not identical to the materials used in civil infrastructure, so again it is difficult to predict wear performance using published data. A further problem is that most wear studies on composites have been performed for wear conditions unlikely to be experienced by civil infrastructure. A large amount of information is available on the sliding wear of composites against steel counterparts because of their use in bearing applications such as gears, cams and impellers. However, sliding wear of civil composite materials against steel is unlikely to occur, and therefore such wear data have limited value for civil engineers.

It is possible to apply a few simple rules in the selection of composite materials with increased resistance against abrasion and erosion. Research has shown that the wear resistance improves with the toughness and ductility of the polymer matrix and fibres. Abrasion resistance is also dependent on the fibre orientation, with fibres normal to the sliding direction having the best wear resistance and fibres in the anti-parallel direction having the poorest resistance. Likewise, the erosion resistance is highest when the fibres are parallel to the impact direction. However, the fibre orientations that provide the best wear resistance may not necessarily give the highest load-bearing properties.

While the microstructural and mechanical properties of composites can be tailored to maximise wear resistance, the wear performance will still probably be inferior to conventional construction materials such as steel and concrete. Therefore, in high-wear applications it is recommended that the composite structure is protected with a wear-resistant coating. There are many coating systems that are commercially available, with the most common being polyurethane and elastomer-based films. An emerging class of wear-resistant materials are polymer nanocomposites.[31,37–40] The materials contain nanoscopic-sized particles that improve the wear properties at low filler contents (only 1–5 vol%). Improvements in the wear resistance of more than four orders of magnitude have been reported;[37] however, more research and development of these materials is required before they can be considered a viable wear-resistant material for civil infrastructure.

9.5 References

1 S.B. Ratner, I.I. Faberova, O.V. Radyakewich and E.G. Lure, *Soviet Plastics*, **12**, (1964).
2 J.K. Lancaster, 'Friction and wear', In: *Polymer Science: A Material Science Handbook*, ed. A.D. Jenkins, North Holland, Amsterdam, 1972, pp. 159–207.
3 E. Hornbogen and K. Schafer, In: *Fundamentals of Friction and Wear of Materials*, ed. D.A. Ridney, American Society of Metals, Ohio, 1981, p. 409.
4 K. Friedrich and J.C. Malzahn, In: *Wear of Materials 1983*, ed. K.C. Ludema, ASME, New York, 1983, p. 604.
5 C. Lhymn, K.E. Tempelmeyer and P.K. Davis, 'The abrasive wear of short fibre composites', *Composites*, **2**, (1985), 127.
6 M. Cirino, R.B. Pipes and K. Friedrich, 'The abrasive wear behaviour of continuous fibre polymer composites', *Journal of Materials Science*, **22**, (1987), 2481–2492.
7 H. Voss and K. Friedrich, 'On the wear behaviour of short-fibre-reinforced PEEK composites', *Wear*, **116**, (1987), 1–18.
8 M. Vaziri, R.T. Spurr and F.H. Stott, 'An investigation of the wear of polymeric materials', *Wear*, **122**, (1988), 329–342.
9 K.H. Zum Gahr, *Microstructure and Wear of Materials*, Elsevier, Amsterdam, 1987.
10 A.P. Mouritz and D.H. St John, 'The wear of some commercial epoxy resin/ceramic particle composites by sliding and impact abrasion', *Materials Forum*, **16**, (1992), 9–18.
11 B.M. Sole and A. Ball, 'On the abrasive wear behaviour of mineral filled polypropylene', *Tribology International*, **29**, (1996), 457–465.
12 J. Bijwe, J. Indumathi and A.K. Ghosh, 'Evaluation of engineering polymeric composites for abrasive wear performance', *Journal of Reinforced Plastics and Composites*, **18**, (1999), 1573–1591.
13 G.W. Stachowiak and A.W. Batchelor, *Engineering Tribology*, Butterworth-Heinemann, Boston, 2001.
14 I.M. Hutching, *Tribology: Friction and Wear of Engineering Materials*, Edward Arnold, London, 1992.
15 J. Bijwe, J. Indumathi and A.K. Ghosh, 'On the abrasive wear behaviour of fabric-reinforced polyetherimide composites', *Wear*, **253**, (2002), 768–777.
16 K. Friedrich, 'Wear of reinforced polymers by different abrasive counterparts', In: *Friction and Wear of Polymer Composites*, ed. K. Friedrich, Elsevier, Amsterdam, 1986, pp. 233–287.
17 A.P. Harsha and U.S. Tewari, 'Tribological studies on glass fiber reinforced polyetherketone composites', *Journal of Reinforced Plastics and Composites*, **23**, (2004), 65–82.
18 H. Voss and K. Friedrich, 'Sliding and abrasive wear of short glass-fibre reinforced PTFE-composites', *Journal of Materials Science Letters*, **5**, (1986), 1111–1114.
19 B. Arkles, S. Gerakaris and R. Goodhue, 'Wear characteristics of fluoropolymer composites', In: *Advances in Polymer Friction and Wear*, ed. L.H. Lee, Plenum Press, New York, 1974, pp. 663–688.
20 S. Bahadur, 'Mechanical and tribological behaviour of polyester reinforced with short fibers of carbon and aramid', *Journal of the Society of Tribologists and Lubrication Engineers*, (August 1991), 661–667.
21 K. Friedrich, Z. Lu and A.M. Hager, 'Overview on polymer composites for friction and wear application', *Theoretical and Applied Fracture Mechanics*, **19**, (1993),1–11.

22 H. Pihili and N. Tosun, 'Investigation of the wear behaviour of a glass-fibre-reinforced composite and plain polyester resin', *Composites Science and Technology*, **62**, (2002), 367–370.
23 Z. Zhang, C. Breidt, L. Chang, F. Haupert and K. Friedrich, 'Enhancement of the wear resistance of epoxy: short carbon fibre, graphite, PTFE and nano-TiO_2', *Composites*, **35A**, (2004), 1385–1392.
24 N.-K. Sung and N.P. Suh, 'Effect of fiber orientation on friction and wear of fiber reinforced polymeric composites', *Wear*, **53**, (1979), 129–141.
25 A.C. McGee, C.K.H. Dharan and I. Finnie, 'Abrasive wear of graphite fiber-reinforced polymer composite materials', *Wear*, **114**, (1986), 97–107.
26 K. Tanaka, 'Friction and wear of glass and carbon fiber-filled thermoplastic polymers', In: *Wear of Materials*, eds. W.A. Gleaser, K.C. Ludema and S.K. Rhee, ASME, New York, 1977, pp. 510–517.
27 O. Jacobs, 'Scanning electron microscopy observation of the mechanical decomposition of carbon fibres under wear loading', *Journal of Materials Science Letters*, **10**, (1991), 838–839.
28 K. Friedrich, Z. Lu and A.M. Hager, 'Overview on polymer composites for friction and wear application', *Theoretical and Applied Fracture Mechanics*, **19**, (1993), 1–11.
29 K. Friedrich, Z. Lu and A.M. Hager, 'Recent advances in polymer composites' tribology', *Wear*, **190**, (1995), 139–144.
30 A. Bolvari, S. Glenn, R. Janssen and C. Ellis, 'Wear and friction of aramid fiber and polytetrafloroethylene filled composites', *Wear*, **203/204**, (1997), 697–702.
31 Kishore, P. Sampathkumaran, S. Seetharamu, S. Vynatheya, A. Murali and R.K. Kumar, 'SEM observations of the effects of velocity and load on the sliding wear characteristics of glass fabric-epoxy composites with different fillers', *Wear*, **237**, (2000), 20–27.
32 K.V. Pool, C.K.H. Dharan and I. Finnie, 'Erosive wear of composite materials', *Wear*, **107**, (1986), 1–12.
33 G.P. Tilly, 'Erosion caused by airborne particles', *Wear*, **14**, (1969), 63–79.
34 J. Zahavi and G.F. Schmitt, 'Solid particle erosion of reinforced composite materials', *Wear*, **71**, (1981), 179–180.
35 A.M. Latifi, 'Solid particle erosion in composite materials', Masters Thesis, Wichita State University, December 1987.
36 P.J. Mathias, W. Wu, K.C. Goretta, J.L. Routbort, D.P. Groppi and K.R. Karasek, 'Solid particle erosion of a graphite-fibre-reinforced bismaleimide polymer composite', *Wear*, **135**, (1989), 161–169.
37 B. Wetzel, F. Haupert, K. Friedrich, M.Q. Zhang and M.Z. Rong, 'Impact and wear resistance of polymer nanocomposites at low filler content', *Polymer Engineering and Science*, **42**, (2002), 1919–1927.
38 F. Li, K. Hu, J. Li and B. Zhao, 'The friction and wear characteristics of nanometer ZnO filled polytetrafluoroethylene', *Wear*, **249**, (2002), 877–882.
39 W.G. Sawyer, K.D. Freudenberg, P. Bhimaraj and L.S. Schadler, 'A study of the friction and wear behaviour of PTFE filled with alumina nanoparticles', *Wear*, **254**, (2003), 573–580.
40 G. Shi, M.Q. Zhang, M.Z. Rong, B. Wetzel and K. Friedrich, 'Friction and wear of low nanometer Si_3N_4 filled epoxy composites', *Wear*, **254**, (2003), 784–796.

Part II

Applications and monitoring of composites in civil engineering

10

Fibre-reinforced polymer composite structures and structural components: current applications and durability issues

L. C. HOLLAWAY,
University of Surrey, UK

10.1 Introduction

The structural fibre-reinforced polymer (FRP) composite material is a relatively recent addition to the civil engineering industry with one of the first all-composite cable stay footbridge structures erected in 1991, at Aberfeldy, Scotland, UK. Before this time, non- and semi-load-bearing cladding panels, in conjunction with the more conventional civil engineering materials, were first employed in the building industry some 35 years ago. The polymer materials that were used to manufacture and fabricate these panels have been improved over the intervening years and it can be expected that the durability properties of present day polymers will have been considerably enhanced. When considering new materials for structural use their mechanical properties are of paramount importance to the structural designers contemplating their use. These properties would be determined from tests undertaken in a laboratory or would be derived from the manufacturer's data and would, in both cases, be obtained using pristine material. However, of equal importance in the examination of potential materials and systems for use in civil infrastructure applications are the environmental, durability and external loading conditions and a consideration of the duration of the applied loads. Exposure to a variety of adverse and sometimes harsh environmental conditions in construction could degrade the FRP composite material and thus this degradation would alter the mechanical performance. Exposure to high and low temperatures, moisture and salt solution ingress, ultra-violet rays from the sun, and fire will all lead to reduced mechanical performance. A further concern is the durability of ambient-cured systems as these have a relatively low glass transition temperature and may not reach their full polymerisation if they have not been post-cured before use, thereby making them more susceptible to degradation.

It should be remembered, however, that all engineering materials are sensitive to environmental changes in different ways and those adverse factors mentioned above will not be unique to the FRP materials. Indeed, composite

materials do offer some significant durability advantages over the more conventional construction materials.

One of the problems in acquiring data relating to the durability properties of any material and in particular those of FRP composites is the length of time involved in gathering the relevant information. This is particularly difficult with respect to polymer composites as there are many different polymers on the market and the majority will have additives that have been incorporated to enhance curing or to improve some specific mechanical or physical property. Furthermore, polymers have been chemically upgraded over the years to further improve these properties and as a consequence their durability performance.

In order to obtain durability properties of the polymer composite system in a reasonable time frame, accelerated tests are sometimes undertaken on the material or structural unit whereby the test specimens are exposed to an accelerated test environment. This generally involves the specimen or structural unit being subjected to some form of an environment many times more severe than that which would be experienced in practice. This extreme method, although allowing information to be obtained very rapidly from that one known environmental situation, will generally not be equivalent or relevant to the more gradual degradation effect had the environment been applied in a less rigorous manner. Accelerated testing sometimes involves applying an elevated temperature to the polymer; this method should be used with caution. Temperatures above 60°C are not relevant in the context of making service life predictions for most engineering structures that operate in normal conditions, as the degradation mechanisms in FRP materials are different under the lower temperatures found in practical situations. As the temperature rises towards the glass transition temperature the polymer will lose some of its stiffness and strength, with the result that the investigation will not be analysing the original material. Furthermore, materials used in construction would normally be exposed to many different environments acting simultaneously but in a less harsh way, and each possibly having an effect upon the other.

With the increase in the number of FRP composite structural members being constructed currently, and the sparse knowledge of the long-term property characteristics of composite materials, it is advantageous to monitor the performance of such structures with time. This procedure might involve: (a) test loading the structural system at certain periods of time after construction to obtain stress and deflection values against time under specified external loading – such tests would characterise the overall behaviour of the structural system; (b) visual inspections of the structure, at specified times, for any signs of distress or deterioration of the material from the point of view of environmental degradation or from exposure to long-term application of loads that might influence the creep rate of the polymer component of the

composite; (c) mechanical and physical/chemical material tests on specific areas of the exposed FRP structure to investigate any possible degradation effects between the component parts of the FRP material.

There are various instrumentation systems that could be used to detect structural behaviour and response to external loads and/or environmental effects. Typically, the response is measured continuously at predetermined sampling times. Long-term monitoring is intended to predict where and how failure might occur during a designed environmental time limit. As the instrumentation costs are high, long-term monitoring is justified only on a few structures of reasonable importance or interest. The instrumentation systems would generally be an integral part of the structure, incorporated during its fabrication and construction and embedded into its structural components. Vibrating wire sensors are probably the strain instruments most commonly used for monitoring flexural and axial strains and, independently, temperature values of the environmental surrounds. The vibrating wire gauges do drift over long periods of monitoring but generally this does not present too much of a problem. The Bragg grating and Fabry–Perot fibre optic sensors is another monitoring system that has been used in the field; these gauges do require annual calibration by the manufacturers and this can cause a problem over periods of monitoring greater than 1 year. All sensors are permanently connected to a data logger stationed at the side of the structure in a protection cabinet. The data logger would be remotely accessed and programmed via a telephone wire.

In many structural rehabilitation scenarios and in the fabrication of 'all-composite' structural systems that are manufactured from precast FRP units, the structural components are joined on site using adhesives. Structural adhesives can be both cold cured and hot cured, but on-site adhesive bonding would invariably be cold cured. Consequently, these polymers will cure at site temperatures and, therefore, ideally should be post-cured at a temperature of 50°C. Most cold-cured/post-cured epoxy polymer resins will have a glass transition temperature of between 45 and 60°C and therefore will have reduced mechanical characteristics when exposed to temperatures above these values.

This chapter will analyse field applications of FRP composite structures and structural components, from the point of view of any reductions in their mechanical or physical characteristics with time as a result of degradation due to the environment or external loading. An understanding of the behaviour of existing infrastructure applications of composites is fundamental to the development of optimum design concepts, manufacturing methods and installation procedures.

The utilisation of FRP composites in construction can be divided into two categories:

(a) the 'all-composite' FRP structure used independently of other engineering materials;

(b) the FRP structural unit used in conjunction with other engineering materials to form a composite material structure.

This chapter will concentrate on the durability of structural composites under two categories:

Category 1

(a) 'All-composite' FRP building systems, structures and infill panels.

Category 2

(a) External strengthening.
(b) Tendons and rebars (internal strengthening of concrete).
(c) Bridge decks.
(d) FRP girders and profiles.

The above examples, illustrating specific durability properties of FRP composites exposed to particular civil engineering environments, have been obtained from researchers or from published papers. In either case acknowledgements have been made.

10.2 'All-composite' structures

10.2.1 Introduction

In the early period of utilising FRP composites in construction, structures tended to be architecturally orientated to building systems using only FRP composite materials specifically shaped to provide strength and stiffness to that structure. In addition, FRP composite infill panels to the conventional steel or reinforced concrete skeletal beam and column structural units were also manufactured. These constructions now provide a reasonable time span in which to study any degradation of the FRP composite material. At the time of manufacturing these components, the matrix component was generally the polyester but this material has now been superseded by the vinylester or epoxy polymers. Nevertheless, these early polymers can give a good indication of what can be expected from the materials used currently; these latter materials should have more robust durability properties than the early materials.

10.2.2 Building systems

The early 'all-composite' building systems and load-bearing infill panels, and this includes the majority of the examples mentioned in the following case studies, were generally constructed from E-glass fibres and polyester resins. Since the 1970s polyester resins have been improved in quality and

in most instances, in civil engineering, have been replaced by the vinylester or epoxy polymers. Consequently, the durability of those former resins will not be as robust as that of the current resins.

Classroom of Primary School, Thornton Cleveleys, Lancashire, UK

The shape of this classroom is in the form of a geometrically modified icoshedron and is made up of 35 self-supported tetrahedral panels; 28 panels have a solid single skin glass fibre-reinforced polymer (GFRP) composite skin and in 5 of these panels circular apertures have been constructed to contain ventilation fans. In the remaining 7 panels, non-opening triangular windows have been inserted. The GFRP composite skins were manufactured by the hand lay-up method (the technique has been modified and is now known as wet lay-up) using a chopped-strand E-glass fibre/polyester composite The inside of the panels have a 50 mm thick integral skin phenolic foam core acting as a non-load-bearing fire protection lining to the GFRP composite skins. The icoshedron structure is separated from the concrete base by a ring of hardwood. The FRP panels were manufactured by the hand lay-up technique using a mould lining of perspex with an appropriate profile to give a fluted finish to the flat surfaces of the panels. The edges of the panels were specially shaped to provide a flanged joint which formed the connection with the adjacent panels. Sandwiched between two adjacent flanges is a shaped hardwood batten to give the correct geometric angle between the panels; the whole is bolted together using galvanised steel bolts placed at 450 mm intervals. The external joint surfaces between the adjacent panels were sealed with polysulphide mastic. The glass windows were fixed in position on site by means of neoprene gaskets.

Dirt accumulation has been the main problem with the external surfaces of the structure, and after 25 years in service there is evidence of chalking on some panels and some surface cracks. However, there have been no leakage problems associated with the structure. The lead flashing at the base of the structure between the GFRP composite and hardwood timber base has been damaged in several places and the timber base itself is rotting.

It is interesting to note that when the classroom structure was under construction a fire test at the Buildings Research Establishment (BRE) Fire Research Station at Thornton Cleveleys, Lancashire, UK was undertaken on four connected panels, with the integral skin phenolic foam in place. At the same time, tests were also undertaken on an identical geometrically shaped school system used at that time. The results demonstrated that the GFRP classroom had over 30 minutes fire rating whereas the existing school system had only 20 minutes.

Severn Bridge Visitor's Centre

To house the Government's agency team during the Second Severn Crossing project in the early 1990s, a two-storey building (rectangular in plan) was constructed using the Advanced Composite Construction System (ACCS) Maunsell planks.[1] The planks were constructed from E-glass fibres and isophthalic polyester resin. The requirement of the construction was to provide thermal insulation and fire resistance to Class O fire regulation specifications with a fire resistance of at least 30 minutes when tested to BS 476: Part 21. The erection of the building was rapid, in an area with difficult access, and it was cost effective. A feature of this structure was that the first floor planks and roof system were interlocked with the walls and bonded without any additional framework to form a membrane structure with complete structural integrity.

The structure was inspected by an engineer from the BRE, Garston, UK, 9 years after it was erected and the panels were in fairly good condition with no visible deterioration. The building had been jet-washed once during this period and 6 months prior to the BRE inspection had been hosed down. There were some faults found, these were:

1 The building was stained by algal growth.
2 The roof leaked although it had roofing felt in place, some attempt had been made to remedy this using mastic to the ceiling joints internally. It was not possible to inspect the roof to discover the cause of the leakage.
3 In winter the internal temperature of the structure reached equilibrium very quickly. However, during the summer period the structure became very hot.
4 During the inspection the engineer reported that one panel was found to have shed its fibres, this panel appeared to have been produced without a veil coating.

The long-term durability information in this example has been derived from the inspection undertaken by the BRE at Garston, UK and is gratefully acknowledged.

10.2.3 Load-bearing and infill panels

Infill panels were first introduced into the construction industry in the late 1960s, they were generally made from thermoplastic materials but in the early 1970s semi- and full-load-bearing composite panels were manufactured from E-glass fibre-reinforced polyester polymers.

Mondial House, London, UK

One of the earliest types of semi-load-bearing GFRP composite panel structures was Mondial House, erected on the banks of the River Thames in 1974. It

stands at 45 metres high and the main structural part of the building is constructed from reinforced concrete, with each floor except the second being slightly smaller than the floor beneath and each storey has a GFRP composite semi-load-bearing cladding system. The main panels have a white fluted edge and are 3 metres high by 1.8 metres wide and 1.2 metres deep, except for the panels on the eighth floor which are 6.7 metres high. The panels are stiffened by means of top hat sections of GFRP ribbing. They also have complicated side ribbing which allows for a degree of flexibility of support and fixing. The rear casing is 1 metre by 0.6 metres white pigmented single-skin GFRP laminate. Thermal insulation is provided behind these panels by polyurethane rigid foam attached to the panels by soft metal tags. The main panels were constructed using E-glass fibre and polyester resin, with a gel coat of isophthalic resin pigmented white with an ultraviolet stabiliser. The face of the external GFRP composite is reeded on the vertical surfaces to mask any minor undulations and to provide channels for surface water run-off. The units were manufactured by the hand lay-up method; the rear casings were hot-press moulded units. The joints between the panels were designed to accommodate thermal movement between panels and fixing tolerances, and also to prevent the ingress of water and air into voids formed by the panels.

The 20 years and 25 years service inspection, the former being undertaken by the author in conjunction with Scott Bader (resin manufacturer), Wallingford, UK, and the latter by an engineer from the BRE, Garston, UK, showed that the GFRP composite material was in almost pristine condition. The surface of the panel had the normal build up of city dirt but when this was removed and the exposed surface was polished it revealed no sign of any degradation. No repairs had been undertaken on the structure. The maintenance house is the only part of the construction that is constructed using a brown pigment in the GFRP composite. The colour had faded and chalked with some signs of crazing. The information derived from the two industrial firms is gratefully acknowledged.

Bridge enclosures on the Second Severn Crossing approach

Three motorways approach the second Severn Bridge across the River Severn at an interchange situated at the main estuary crossing. The total length of the crossing is 15 km and there are 24 structures, 7 of which incorporate advanced polymer composite enclosure systems for improved maintenance life. These enclosures are aesthetically very pleasing. The structure was erected in 1993. An inspection of the enclosures by staff from the BRE, Garston, UK was made in 2001 and the interior of the enclosures was found to be dry and clean with no ingress of water, damp, build up of debris or corrosion. An important aspect of the system is that ventilation is allowed

and any condensation that might have formed is removed. There were no visible signs of deterioration of the panels, but one ring seal to a bridge column was adrift and one or two panels appeared to have been marked by site mortar or concrete. However, apart from this the exterior surfaces of the composite were clean, in spite of the dirt and spray from passing traffic.

10.3 'All-composite' bridges

The first highway bridge to be manufactured entirely out of GFRP is believed to be the 10 metre span bridge constructed in Bulgaria in 1981/1982 using hand lay-up techniques. The bridge was built, rather like Ironbridge 200 years earlier, to show what could be achieved with the material. The second 'all-GFRP' bridge is the Miyun Bridge in Beijing, China. This prototype structure was completed in October 1982.[2] The cable-stayed advanced composite Aberfeldy bridge over the River Tay in Scotland was designed and built in 1991 for the Aberfeldy Golf Course. It was a fundamental advance not only in the main span length but in the technology of the pultruded ACCS planks (the Maunsell planks).[1] Over the past few years there have been a number of 'all-composite' bridge structures constructed and instrumented for load testing and for long-term health monitoring; some of these may be found in reference 3.

Aberfeldy Footbridge, Aberfeldy, Scotland

The Aberfeldy Footbridge (built in 1991) spans 63 metres and has a width of 2.12 metres, an overall length of 113 metres, a design capacity of 10 kN m and weighs 14.5 tonnes. The cable stays were manufactured from aramid fibres and the ACCS polymer components, which form the deck and towers of the bridge, were manufactured from GFRP composites; the component parts of the composites were made from E-glass fibre and isophthalic polyester resin. Three planks and four connectors were joined alternately in a single thickness, to form the width of the deck. A GFRP handrail and a wear-resistant deck finish were connected to the main ACCS panels.

Within the first year of the bridge being built it was exposed to hurricane-force winds, unprecedented snowfall and flooding to above deck level. During this hostile weather no damage was done to the bridge. Visual examinations only have been carried out on the bridge, although small-scale specimens were manufactured at the time of the bridge construction and tested over the early years of its life. In 1997 the deck was strengthened with GFRP pultruded plates due to bridge overloading, which caused cracks to form on the deck surface. The primary structure is generally performing well; however, there have been some superficial weathering effects on non-ACCS sections, but this does not affect the structural performance of the bridge. The ACCS

GFRP panels are showing no significant degradation. The connections between the parapet rails and posts and many post-to-deck connections have worked loose. This is due to the movement cycles from external influences of the deck and could be avoided by reducing the deck displacement by introducing a stiffer cable system.

Both the parapets and the primary structure have been affected by mould and moss growth due to standing surface moisture; these effects can also be observed on masonry structures in the damp climatic area. It is suggested that in order to minimise the visual impact of the mould growth, a mould-inhibiting additive is used in the resin formulations to avoid water traps, and that the maintenance regime ensures that drainage paths are kept clear of leaves and other debris.

Bonds Mill Bridge, Stonehouse/Bonds Mill, Gloucester, UK

The Bonds Mill Bridge was constructed in 1994 to link Stonehouse and Bonds Mill across the Thames–Severn canal by a single bascule lift bridge. The work required the replacement of a fixed bridge which carried the access road for all types of vehicles into a busy industrial estate. The bridge is 8.2 metres long and 4.3 metres wide and carries a single lane of traffic. It was designed to carry full UK highway loading (1993) including a 38 tonne truck. The bridge consisted of an epoxy-bonded interconnected multi-celled box beam fabricated from ten pultruded ACCS planks (Maunsell planks). The planks were manufactured from E-glass fibre/polyester (mainly unidirectional fibre weight fraction of 68%). Epoxy foam of density 90 kg/m^3 was foamed in-place in the compressive flange cells and the web cells of the ACCS modules; the box beams and foam were fabricated in a factory and transported to site. Transverse ACCS planks were bonded to the compressive flange of the box beam and were also filled with foam. All the GFRP panels were bonded together using an epoxy adhesive and ultraviolet inhibitors were added to the resin to increase resistance to environmental exposure. The running surface of the polymer composite bridge used the Cicol™ Acmegrip system manufactured by Rocol, Leeds, UK. The system is a combined anti-slip wearing course and waterproof membrane and is used when a lightweight, anti-slip surface is required. The proprietary system was bolted to the transverse ACCS planks. On the outside surfaces of the webs and soffit of the box beam a thick epoxy coat was applied to reduce to a minimum any degradation of those surfaces in close proximity to the water in the canal.

A detailed condition survey was carried out by the author on the bridge 2 months after it had been erected at Bonds Mill and again 1 year after it had been erected. There was a transverse crack on the ACME board at the south end of the bridge, at the position of the steel angle encapsulating the end of

the ACME board. Vehicles coming from the industrial estate approach the essentially level bridge from a rising hill and consequently tend to impact the bridge at this position. This constant load impact damaged the ACME board, rain entered the crack and penetrated the ACCS transverse plank; both the ACME board and the first transverse ACCS plank were replaced shortly after this survey. A second detailed survey, carried out some 5 years later by Maunsell Structural Plastics (now FaberMaunsell) showed the bridge to be in excellent condition apart from the same problem at the south side of the bridge. Bolts holding the metal angle that encapsulates the end of the ACME board had become loose and the angle moved as vehicles passed over it. At this position of the bridge further changes were made to the design and these were incorporated into the bridge structure. In addition, deflections of the bridge with a 38 tonne load stationed on the bridge were taken and the maximum value was well within the design limit. The ACCS planks that were directly exposed to the environment were in a satisfactory condition with no apparent damage or degradation. The pultruded handrails were in good condition.

After 8 years service, a visual survey only was undertaken by the author, this indicated that again there was no significant degradation to the GFRP construction. However, at the south end of the bridge, again, the wearing surface showed signs of breakdown. This is undoubtedly due to the constant impact from lorries mounting the bridge deck from a steep slope running to and from the industrial estate. This would indicate that there is a fault in the design of the bridge at this point and cannot be associated with a normal degradation of the FRP composite material. No exposed coupon samples were taken from the bridge to estimate any possible serviceability reduction, but from visual examinations the material of the bridge had not suffered any surface damage.

Smith Road Bridge, Hamilton, Butler County, Ohio, USA (Tech 21)

An ‘all-composite’ bridge, which has been monitored for the past 4 years, will be used to demonstrate the performance of an FRP composite structure. Field-monitored information is being studied to evaluate the behaviour and durability of composite components bonded to each other and then exposed to a harsh infrastructure environment. A brief description of the construction of the bridge is given to enable an understanding of the structural system and its function; this information has been derived from reference 3.

The bridge consists of a structural sandwich configuration, the centre core is constructed from 171 mm pultruded glass fibre/polyester tubes and these are aligned with the span of the bridge and mounted between two face materials. The three trapezoidal beams supporting the deck were fabricated from quasi-isotropic E-glass fibre/polyester resin laminates with additional

unidirectional reinforcing layers added where the tensile stresses are the highest. Each beam was fabricated as an integral unit to the deck to facilitate transportation to site, erection and construction. A vinylester polymer adhesive was used to bond each separate beam to a section of the deck construction. The final bonding of the separate beam/deck units was carried out on site with an epoxy resin. The site installation process was completed within 3 hours. An ultraviolet protection coat was applied to the exposed surfaces at the factory. The design engineer states that the components of the composites forming the face and core materials of the deck, the deck and structural beams, and the adhesives were tested under laboratory conditions, including effects of sustained and cyclic loading and exposure to moisture, salt solution, ultraviolet light, and high and low temperatures. The types of sensors and their locations were designed to monitor and detect small long-term changes in performance of the bridge in terms of durability of the materials, the structural integrity of the components and the environmental stability.

After 4 years of continuous monitoring of the structure, there appear to have been no adverse effects while being subjected to climatic cycles. The structural results appear to coincide with the daily and yearly temperature cycles. The bridge has performed well in terms of the durability of the materials, the integrity of the structural components and the environmental stability. In addition, the long-term structural response was observed to be consistent and was well within acceptable strength and serviceability design limits. Based on these results, the bridge has demonstrated performance reliability during the monitored years and thus can be considered to be satisfactory. It was reported that all vibrating-wire strain gauges had positive strain drifts; these drifts were attributed to non-stationary behaviour of the reference index due to the time and temperature dependence of the sensors and/or signal conditioning and processing system. In addition, the particular Bragg grating fibre optic sensors used reported large and accumulating drift.

10.4 External strengthening

10.4.1 Introduction

The repair of deteriorated, damaged and substandard civil infrastructure has become one of the important issues for the civil engineer worldwide. The rehabilitation of existing structures is fast growing especially in developed countries, which completed most of their infrastructure in the middle period of the last century. Furthermore, structures that were built after the Second World War had little attention paid to durability issues. Externally bonded FRP strengthening is particularly attractive where there are severe access constraints or high cost associated with installation time. In addition, the

capacity of FRP strengthening to extend the life of historic structures with minimum disruption to users makes for genuinely sustainable engineering solutions.

Canada and certain northern regions of the United States experience severe winter conditions and this, combined with the extensive use of de-icing salts, causes serious deterioration in a large number of structures. Furthermore, the traffic loads often exceed the original design expectations. These hostile environments have in the past put a limit on the use of FRP composites for structural repair and strengthening. However, in recent years, researchers at the University of Sherbrooke, Quebec have assessed the reality of composite retrofitting technologies in severe environments and field applications have been undertaken on various structural elements such as buildings, highway columns, partially submerged bridge piers, beams and beam/column elements of a major car-park structure. As the initial projects were of an innovative character, comprehensive analytical programmes and laboratory tests were undertaken at the University's laboratory before actual field implementation; the field investigations commenced in 1995.

Tables 10.1 and 10.2 provide examples of the durability of FRP composites utilised on some 10-year-old projects that have provided and are still providing useful information on the rehabilitation of structural units in very hostile environments. The first examples, called the early projects, concentrated upon the instrumentation procedures for an FRP composite system on a practical structure. The second group of examples, called the demonstration projects, verified the feasibility of using FRP materials in harsh environmental conditions.

Tables 10.1 and 10.2 demonstrate the excellent durability of FRP composites used for the rehabilitation of structures that have been and are still exposed to both cold harsh environments and warm temperate climates. However, it should be remembered that these tests have been undertaken on composite systems that have been exposed for only 10 years, on structures that have a possible further life expectation of some 30 years. Furthermore, thin FRP composite sheets used in the rehabilitation of highway structures are vulnerable to surface damage from vehicle impact and consequently should be protected against such damage.

A detailed discussion will be given below of the retrofitting of a structure that was built in 1951 and required upgrading in 1998. The discussion will concentrate upon the work that was required to instigate a monitoring system for such an investigation, and the immense amount of preparation, mounting of measuring devices and logging of data that were undertaken.

Bridge over the Rivière Noire, Canada

The first major bridge to be selected by the Ministère des Transports du Québec (MTQ) to use FRP composites rehabilitation was that over the Rivière

Table 10.1 Examples of the durability of fibre-reinforced polymer composites utilised on some early projects (the information given has been extracted from reference 4)

Year of upgrate	Structural units	Site location and damage	Objectives of investigation	Material used and method of construction	Remarks on condition of composite construction
Early project, 1996	RC concrete columns.	Université de Sherbrooke; columns badly corroded.	To test installation procedure.	(a) GFRP fabric.	After 10 years of inspection, no degradation of the GFRP composite has been revealed.
Early project, 1996	Highly exposed RC columns on highway overpass – 9 No. 6 m high × 760 mm diameter columns.	Saint-Étienne-de-Bolton, Québec, Canada; corrosion damage, occasional strike by snowploughs.	(a) Repair corrosion damage. (b) Provide column protection against salt infiltration. (c) Comparison with conventional repair.	FRP repair; 2 layers used, 1 vertical followed by 1 horizontal. Four different FRP systems used.	Several inspections were made: (a) conventional repair suffered from cracks and started to delaminate in 1998; (b) 2005 inspection, no visible degradation on FRP except that caused by impact.
Early project, 1996	7 No. 460 mm wide beams, 17 No. 460 mm diameter.	Municipal Webster multi-level parking garage. (a) Wide crack just below slab level on whole length of a main beam. (b) Corrosion and delamination of column.	(a) To increase strength and ductility of columns. (b) To protect selected columns top and bottom. (c) Flexural strengthening of beams. (d) Shear enhancement of some slab/beam connections.	CFRP and GFRP composites used from 3 different suppliers.	(a) Soon after installation numerous scars from vehicles observed on column base including damage to a 0.3-mm-thick CFRP sheet. (b) In 1998, damage to low clearance beams discovered. (c) In 2005, many impacts and scars from vehicles, no additional damage to the thin CFRP sheet on column.

RC, reinforced concrete.

Table 10.2 Examples of the durability of fibre-reinforced polymer composites utilised on some demonstration projects (information given has been extracted from reference 4)

Year of upgrade	Structural units	Site location and damage	Objectives of investigation	Material used and method of construction	Remarks on condition of composite
Demonstration project, 1998	Precast roof unit.	School roof. Shear cracking occurred in roof panel due to record ice storm.	To carry out repairs and strengthen.	(a) GFRP composite material. (b) Bonding 200 mm depth × 1 m long fabric at supports.	Visual inspection undertaken in February revealed no damage to GFRP strengthening system.
Demonstration project, 1999	RC column and slab. Dimensions of columns: 4.7 m high × 360 mm diameter.	Université de Sherbrooke campus in a basement. (a) No damage to column was found – strength increase required. (b) To restore strength after opening had been created.	(a) To increase column to support 40% more axial load. (b) To restore strength of a waffle slab after openings had been created for ventilation ducts.	(a) 3 vertical layers and 3 horizontal layers of GFRP material wrapped around column. (b) CFRP plates bonded to the top of the slab.	(a) No degradation of the FRP composite has been observed. (b) No need to install protection to the FRP wrap. (c) As CFRP plates have been bonded on the top of the slab, inspection is not possible.
Demonstration project, 2001	Containment structure for a decommissioned nuclear reactor. Dimensions of ring beam are 40 m diameter, 3.4 m high and 2.1 m thick.	Gentilly, Canada. Extension of service life of the containment structure by 75 years.	To replace the secondary concrete filling of the ring-beam, where a considerable number of pre-stressing wires are anchored.	GFRP sheets were placed horizontally on the cold joint. Vertical sheets were placed to hold the concrete in place.	The repairs continue to be in good form.

Noire on route 131 near the village of Sainte-Émélie-de-l'Énergie in the Laurentides-Lanaudière region, about 130 km northeast of Montréal. The bridge is single span and serves a secondary road; the traffic on it is not excessive, but the bridge is required to carry heavy loads. Bridges in Canada are characterised by the live load rating factor (LLRF) defined in the standard CAN/CSA-S6-88, 'Design of Highway Bridges' (CSA 1998); these two publications have been combined into the standard CAN/CSA-S6–00. For demonstration projects involving new technologies the MTQ prefer that the LLRF > 0.85. The bridge has an LLRF of 0.94 and, therefore, its replacement was not considered. However, upgrading the load-carrying capacity to the current standards was deemed necessary.

The bridge was built in 1951 to the standard requirement of a 20 tonne truckload applied through two axles. It has a span of 21.3 metres and four longitudinal parallel reinforced concrete beams with an integrated slab forming a series of T-sections. The flexural capacity of the bridge was required to be increased by 35% and the shear strength to be improved by 20%. The general condition of the bridge indicated neither significant spalling of the concrete nor degradation of the steel rebars through corrosion; these favourable conditions made the bridge ideal for experimental full-scale examination.

Experimental work was sponsored by the MTQ at the Université de Sherbrooke to evaluate the potential for FRP strengthening; the tests were undertaken on a series of 1:3 scale models.[5] In general the work undertaken confirmed the potential for reinforcing T-beams with carbon fibre composite materials. There were two design options for the rehabilitation; the option eventually chosen had three longitudinal strips of Sika Carbodur SI214 of width 120 mm and thickness 1.4 mm, no anchorage was required at the free end of the strips. U-shaped GFRP external stirrups and Sikawrap Hex 100G were selected for the shear reinforcement and were wrapped around the section with the fibres in the vertical direction. The width of the stirrups in the vicinity of the supports was 686 mm with spacing of 102 mm, the width and spacing of these stirrups were decreased and increased respectively towards the centre of the beam. During the installation, there were practical difficulties in eliminating the formation of voids between the concrete and the FRP near the supports. Eventually, epoxy polymer was injected into the voids to expel the air. A layer of protection paint was finally applied to the upgraded beams. Due to the cold weather, the repair took place in a heated enclosure in order to cure the epoxy polymer. The bridge strengthening was completed in the autumn of 1998.

Since 1998, the bridge has been monitored to evaluate the reliability and durability of the reinforcement. Various sensors were installed on the structure while the repair was completed and since their activation the sensors have been interrogated on a specific schedule to assess the performance of the bridge rehabilitation. The instruments that were installed for continuous

structural monitoring consist of fibre optic strain sensors, conventional resistive strain gauges and thermocouples. Loading tests were also performed using the mobile testing laboratory of the MTQ. These tests were performed immediately before and after the strengthening of the bridge, they were then repeated 1 year and 6 years later. The loading tests conducted together with the instrumentation programme on the Sainte-Émélie-de-l'Énergie Bridge have provided a thorough evaluation of the reliability and durability of the technology of strengthening existing structures with composite materials. The study has shown that this particular structure has maintained its integrity since it was strengthened and that the FRP strengthening scheme has performed as designed. Up to the present time there has been no sign of deterioration of the composite material used or the rehabilitation overall.

During construction, electrical resistance strain gauges and innovative fibre optic sensors were incorporated into the bridge; loading tests, under the direction of the MTQ, were undertaken immediately after the completion of the rehabilitation procedure. Three four-axle trucks of 33 tonnes weight were used to apply simulated traffic loading to the bridge before and after rehabilitation. These tests confirmed that the behaviour of the bridge was consistent with the design hypothesis for the FRP reinforcement. The total cost of the rehabilitation of the structure was $108 500 in 1998; the MTQ estimated that this sum was 50% of the total cost if the structure was completely replaced. They suggested that this type of repair would be economically viable if it could be reduced to about 33% of the replacement cost.

Information and descriptions of the upgrading of this bridge, and the tests undertaken before and after its rehabilitation, have been taken from references 6 and 7; further information was obtained from Professor K. W. Neale at the Université de Sherbrooke.

10.5 Seismic retrofit

10.5.1 Introduction

When a structure is built in a seismic region it is vital to evaluate its seismic behaviour and performance. Ideally the three main approaches would be as follows.

1 Laboratory testing. Sub-systems, components and possibly scaled models of the complete system would be tested under static, quasi-static or dynamic loading, and if possible under controlled simulated environments – thus contributing to knowledge and understanding of dynamic soil properties and soil/structure interaction.
2 Computer analysis. Using dynamic software to analyse prescribed loads on the structure, these loads would be determined from codes or postulated site-specific ground motions.

3 Natural laboratory of the Earth. Observing and studying the performance and, if possible, damage to structures following earthquakes. Following these investigations it would be necessary to determine why specific designs lack earthquake resistance.

Bridges are among the most vulnerable components of the surface transportation system. For instance, approximately 70% of all bridges in the United States were constructed before 1970 and these bridges had little or no consideration given to seismic resistance. The recent damaging earthquakes in Loma Prieta (1989) and Northridge (1994) in the United States – and in other countries such as Kobe, Japan (1995), Chichi, Taiwan (1999) and Kocaeli, Turkey (1999) – demonstrate the need to provide new and improved procedures and specifications for designing and constructing earthquake-resistant bridges and highway systems.

Currently, many authorities with structures built in seismic areas are taking steps to strengthen them and to undertake structural health monitoring by remote sensing. One such bridge structure is situated in British Columbia, Canada, where the columns have been retrofitted with GFRP composites to prevent collapse during a design seismic event; the columns have, to date, been fully instrumented and any malfunctioning has been eliminated. The bridge is being continuously monitored in real time (www.isiscanada.ca) for any possible seismic event. A short description of the methods used will be given here.

Portage Creek Bridge concrete columns

ISIS Canada and the British Columbia Ministry of Transport[8] have discussed an innovative means of seismic strengthening and remote structural health monitoring of the Portage Creep Bridge, City of Victoria, British Columbia, Canada. This is one of 36 demonstration bridges across Canada sponsored by ISIS Canada to assess the performance of bridges being strengthened with FRP composites. One of the objectives of these projects is to evaluate the performance of FRP composites under various loading conditions and in hostile environments. The Portage Creek Bridge was designed by the Ministry of Transport, British Columbia, and was built in 1982. The design was undertaken prior to the introduction of current bridge seismic design codes and construction practices. However, there was consideration given to seismic aspects but the bridge was not designed to resist the earthquake forces as required by current standards. The bridge is classified as a Disaster Route bridge and was retrofitted to prevent collapse during a design seismic event, with a return period of 475 years. The bridge is of reinforced concrete construction and has three spans. It is 125 metres long with a roadway width of 16 metres and two 1.78 metre sidewalks.

It was predicted by dynamic analysis that the two tall columns of pier number 1 would develop plastic hinges under an earthquake. When this happens the short columns of pier number 2 would be required to take additional shear. It was estimated from a non-linear static pushover analysis that the short columns will not be able to form plastic hinges prior to failure in shear. Consequently, these columns were strengthened in shear but without increasing their moment capacity; the strengthening was undertaken by wrapping 5 mm GFRP composites on to the column. The composites used for the GFRP composite wraps were thickened Tyfo® S or Tyfo® WS and the glass fibre was Tyfo® SHE, products of Fyfe Co. LLC, San Diego, USA. During the wrapping fabrication, the bridge was instrumented with intelligent sensing equipment to enable its structural performance to be monitored in an earthquake situation; bidirectional electrical resistance strain gauges and long-gauge fibre optic sensors were attached to the outer layer of the GFRP wrap composite. In addition, three-dimensional crossbow accelerometers were installed to the pier cap immediately above the column and the National Instrument data acquisition system facilitated the internet-based transfer of data, via cable, to the engineer's office.

The numerical work undertaken in this research project has enabled an assessment to be made of the possible earthquake damage and the retrofit requirements. With the retrofit in position, a partial health monitoring system completed and the initial problems associated with the instrumentation overcome, the next phase is the installation of the remaining data loggers. The bridge will then be a smart bridge for continuous remote monitoring.

The durability of the GFRP composite wraps in this example – situated in a harsh environment equivalent to that in the examples given in Section 10.4 concerned with the static strengthening of structural elements – will behave in a similar way with no degradation of the GFRP composite. However, during a seismic event the installed health monitoring system of the bridge would indicate the extent of any possible damage that might be inflicted on the bridge structure and on the FRP composite. A site visit and a judgement by the engineer responsible for the structure would enable a decision to be made as to whether such structural or material damage was detrimental to the strength of the structural system.

10.6 Tendons

Hythe Bridge, Oxford, UK (strengthening cast-iron beams with prestressed carbon fibre-reinforced polymer composite)

Hythe Bridge carries a busy city centre road above a tributary of the River Thames, and a means of strengthening was required that did not cause traffic disruption. The two-span (each span 7.8 metres), cast-iron Hythe Bridge at

Oxford was constructed circa 1861 and is a simply supported structure with ten cast-iron longitudinal beams at approximately 1.1 metre centres. Brickwork jack-arches span transversely between the cast-iron beams. At the end of the 1990s the bridge capacity was required to be raised from Group 2 fire engines to 40 tonne vehicles. Under this load the bridge was weak in mid-span bending, but was able to support the full 40 tonnes assessment in shear. In 1999 the internal cast-iron beams were strengthened with pre-stressed carbon fibre-reinforced polymer (CFRP) plates to the bottom flanges; this was the first known application of the pre-stressing technique for flexural upgrading of bridges. The following description of the technique applied to the bridge, and the inspection of the bridge after strengthening, have been obtained from the consulting engineer to the scheme, Mouchel Parkman (West Byfleet, UK), and from references 9–11.

A feasibility study was carried out and this showed that it was theoretically possible to strengthen the structure with either steel plate bonding, unstressed composite plates or stressed composite plates. Each of the three options involved a degree of uncertainty as all extended previous practical limits. It was eventually concluded that the stressed CFRP composite technique offered the most satisfactory solution. Trials were carried out by Concrete Repairs Ltd in May 1998 on a site in Oxfordshire, to demonstrate the newly developed Mouchel Parkman pre-stressing device and its applicability to cast iron before approval was given to go ahead with the actual strengthening contract. The trials proved successful, and the strengthening of both spans of the bridge was completed by Balvac Whitly Moran Ltd, in April 1999. A total of 500 metres of CFRP plates 76 mm wide by 4 mm thick, manufactured by Fibreforce Ltd, were used for this contract; the adhesive was supplied by Exchem Ltd. The scheme costs of around £160 000 were estimated to be approximately £100 000 cheaper than any other strengthening alternative. Re-construction was ruled out early on due to the busy nature of the road and the level of service diversions that would have been required; suffice to say that this would have been by far the most expensive option.

The proprietary technique required anchorages at the extremities of the plate to be fixed by bonding, friction or mechanical means or a combination of all methods. End tab plates were bonded to each end of the carbon fibre-reinforced composite tendons and provided a means of attaching jacking equipment and anchoring the tendon when extended to the final working strain. The tendons are stressed by a hydraulic jack, which reacts against a jacking frame temporarily fixed to the anchorage. The stressed tendon is secured after extension by a shear pin that transfers load from a keyway in the end tab to the anchorage. The tendons are bonded to the beam by epoxy resin in addition to the end anchorages. The anchorage itself is surrounded by a protective casing and is fully grouted to assist in long-term durability.

The first 6 year principal inspection of the entire bridge including the

strengthened cast-iron beams was undertaken on 1st and 2nd September 2004. The objective of the inspection was to observe, identify and record the condition of the bridge and any defects in the following areas:

- the brickwork abutments and jack-arches;
- cast-iron beams and jack-arches;
- pre-stressed CFRP plates and anchorages;
- scour protection;
- parapets, verges and carriageway.

Only the condition of the CFRP composite upgrading of the cast-iron beams will be reported here. However, this will draw attention to the environment to which the CFRP composite material was exposed. The painted cast-iron beams were generally in good condition with minor pitting and spots of surface corrosion. The pre-stressed CFRP plates were generally in good condition with no evidence of surface damage, indentations, discolouration, splitting or delamination within the plate. A number of voids were found in the adhesive bond between the CFRP plates and the cast-iron beams; however, this has no effect on the pre-stressing as the anchorages fully transfer the pre-stress force to the cast-iron beams. The adhesive just gives an additional factor of safety. The CFRP composite plate anchorages were generally in good condition, with no evidence of movement, rotation or slippage. Nevertheless, a small number of the cover-plate bolt fixings were rusted and were not tightened against the cover plate.

The long-term durability information in this example has been derived from the inspection undertaken by Mouchel Parkman, West Byfleet, UK and is gratefully acknowledged.

10.7 Rebars – exposure to concrete environments

10.7.1 Introduction

In Canada and North America the preferred material for reinforcing concrete has been the GFRP rebar for a number of mechanical and physical reasons, including: (a) competitive advantage; (b) resistance to corrosion; (c) electromagnetic immunity; (d) excellent fatigue performance; and (e) potentially good durability in a concrete environment.

As mentioned in the Introduction to this chapter, when degradation of material properties is being investigated caution should be used when studying changes given by accelerated tests using concentrated environments. Some very contradictory conclusions have been reached and published concerning the results of research into the durability of GFRP in alkaline concrete environments. Accelerated laboratory test results of GFRP in a simulated concrete pore water solution of high pH values and at elevated temperatures

up to 80°C have indicated that there is a decrease in the tensile, shear and bond strengths;[12–14] these results would suggest that there is a case for not using GFRP rebars in concrete.[15] However, Tomosawa and Nakatsuji[16] showed that after 12 months exposure to alkaline solutions at temperatures between 20 and 30°C there had been no material or physical deterioration to the GFRP composite. Similar results were reported by Clarke and Sheard[17], for GFRP composite after 2 years exposure to a tropical climate on a test platform off the Japanese coast. Furthermore, Sheard *et al.*[18] reported that the overall conclusions of the work of the EUROCRETE project were that GFRP is suitable in a concrete environment.

It is important that a good bond between the glass fibre and the matrix polymer is maintained throughout the life span of the structure. Any degradation at the fibre/matrix interface would lead to partial separation which would impede the transfer of load between the two components. Moisture and alkali solutions would migrate into the separated areas and degradation of the glass fibre would result. Consequently, when investigating durability problems, interface areas should be examined for any signs of separation between the fibre and matrix.

In 2004, ISIS, Canada Research Network of Centres of Excellence and Mufti *et al.*[19–21] investigated five GFRP reinforced concrete structures to provide information on the reliability of GFRP materials, which had been incorporated into a concrete situated in the natural environment for 5–8 years. To undertake this task, core specimens of the GFRP reinforcement were removed from the structures; the structures were located across Canada from east to west, giving a wide coverage of varying natural environmental conditions. The specimens were analysed to determine any degradation of the GFRP in concrete structures. The GFRP composites were manufactured from E-glass fibre and vinylester polymer.

The methods used by ISIS to examine the interfaces between the GFRP reinforcement and the concrete, and to evaluate the pH value of field samples of the concrete, included optical microscope (OM), scanning electron microscope (SEM), energy dispersive X-ray (EDX), differential scanning calorimetry (DSC) and the Fourier-transformed infrared spectroscopy (FTIS). The evolution of the pH values of concrete/solution systems was determined by leaching tests; these used a Beckman 170 pH meter with glass electrode calibrated against standard buffers. Table 10.3 gives the examinations performed by ISIS at the interface between the GFRP reinforcement and the concrete. The names and location of the structures, construction details, the structural environments and the analytical methods used to evaluate the various properties of the material are given in Table 10.4.

The conclusions from the various tests undertaken on the GFRP rebars exposure to a concrete environment are as follows.

1 There was good quality, consistency and integrity in the results – as

shown by OM, FTIS and DSC analyses – for GFRP composites and the concrete component materials exposed to wet/dry cycles, salt water, freeze–thaw cycles and de-icing salts.

2 The results from the DSC analysis indicated that there were no significant changes in the glass transition temperature during the period of exposure.

3 Due to the alkaline environment in the concrete a possible degradation mechanism of the resin is alkali hydrolysis of the ester bonds in the structure of the polymer and it is possible that some alkali hydrolysis might have taken place. However, the FTIS showed that almost no change in the spectra of the specimens occurred and therefore no significant hydrolysis took place. In addition, the EDX analysis indicated that no alkali ingress into the GFRP reinforcement had taken place. Furthermore as the reduction in pH values of concrete pore solution reduces over the years, this form of attack is likely to reduce in magnitude.

4 The results of the SEM and EDX analyses showed that there was no visible degradation of the GFRP reinforcement used in rebar or grid form when embedded in concrete and exposed to the various external environmental conditions over the 5 to 8 year exposure period.

The overall conclusions of the ISIS researchers were that GFRP flexural tension reinforcement is durable and compatible with concrete.

The long-term durability information in these examples has been derived with the help of Professor A. Mufti, ISIS, Canada and the advice of Professor K. Neale, Université de Sherbrooke; both sources are gratefully acknowledged.

Table 10.3 Examinations performed by ISIS during the investigations and the analysis methods used (Mufti *et al.*[19])

Examinations performed	Analytical method
To examine the interface between GFRP and concrete (entire surface examined and photographed)	OM
To examine the glass fibre and polymer interface	SEM
To detect chemical changes in the matrix and glass fibres in order to detect alkali ingress from the concrete pore solution	EDX
To characterise chemical changes/degradation of the resin matrix	FTIS
To observe changes in glass transition temperature of the resin matrix due to exposure to concrete environment	DSC
To determine evolution of pH values of concrete	Beckman 170 ph meter

For analytical method abbreviations see text.

Table 10.4 Names, locations, construction details and analytical methods used in examination of the structures (Mufti *et al.*[20])

Name and location of structure used in ISIS investigations	Construction details	Age in 2004 (years)	Environment	Analytical methods used to evaluate degradation of GFRP material
Hall's harbour wharf, Bay of Fundy, Nova Scotia.	Hybrid construction of 16-mm GFRP-ISOROD™ and steel bars. Concrete strength, 45 MPa.	5	Temperature range, +35°C to –20°C. Freeze–thaw cycles. Wet and dry cycles (splash and tidal). Salt/water solution.	OM, SEM, EDX and DSC.
Joffre Bridge (over St-François river), Sherbrooke, Quebec, Canada.	Ribbed deformed 16-mm GFRP C-Bar. Concrete strength, 45 MPa.	7	Temperature range, +35°C to –20°C. Freeze–thaw cycle. Wet and dry cycles. De-icing salts.	OM, SEM, EDX and DSC.
Chatham Bridge, Chatham, Ontario. Two outer spans, steel-free deck barrier. Barrier wall is deck supported.	GFRP reinforced in two outer spans of deck with steel-free deck. Concrete strength, 35 MPa, reinforced with NEFMAC™ glass fibre G13 grid-pitch (100 × 100 mm).	8	Temperature range, 30°C to –24°C. Freeze–thaw cycle. Wet–dry cycle. De-icing salts.	OM, SEM, EDX and DSC.
Crowchild Trail Bridge, Calgary, Alberta. Barrier wall is deck supported.	Ribbed-deformed GFRP C-bar rods used as reinforcement in the barrier walls and bridge deck. Concrete strength, 35 MPa.	8	Temperature range, +23°C to –15°C. Freeze–thaw cycle. De-icing salts.	OM, SEM, EDX and DSC.
Waterloo Creek Bridge, Vancover Island, British Columbia.	GFRP reinforced concrete barrier walls and deck slab. NEFMAC™ glass fibre G6/G13 grid used in construction of traffic barriers. Concrete strength, 35 MPa.	6	Temperature range, +23°C to –0°C. Freeze–thaw cycles. De-icing salts.	OM, SEM, EDX and DSC.

All GFRP reinforcement rods or grids in all structures were manufactured using E-glass and vinylester polymer. For analytical method abbreviations see text.

10.8 Bridge decks

10.8.1 Introduction

The FRP composite material is a viable alternative material for replacing short-span reinforced concrete bridge decks. The main advantage of using FRP composite deck construction is its use as a replacement for a traditional concrete slab in order to reduce the weight of the deck and to minimise repairs to other bridge components. Furthermore, it allows the life span of an old bridge to be extended cost-effectively and will possibly remove any existing load restriction on the bridge.

FRP bridge over the River Cole, West Mill, Oxfordshire, UK

The first all-FRP composite bridge on a public highway network in Western Europe was opened in October 2002; it was a complete replacement of the existing bridge deck and the abutments over the River Cole, at West Mill, Oxfordshire, UK. The bridge spans 10 metres and has a width of 6.8 metres to carry a single carriageway and footpath. The upgraded bridge now comprises reinforced concrete spread footings and abutments with brickwork facing, supporting four GFRP composite box beams with unidirectional CFRP composite flanges bonded to the GFRP beams. The deck system consists of a series of adhesively bonded GFRP advanced composite ASSET profiles spanning transversely, on to which a polymer concrete surfacing and epoxy-based wearing course for the carriageway are mounted; the bridge is detailed in reference 22. In addition, reinforced concrete parapet edge beams hold the parapets in place and are in turn anchored through the ASSET deck. The ASSET deck was one of the key deliverables of a Mouchel Parkman-led 4 year EU-funded project to develop a lightweight deck system for bridges and other structures. West Mill Bridge experiences 500–1000 vehicles per day, of all types varying from cars to 40 tonne articulated lorries. The maximum/minimum environmental temperatures at the bridge over the past 3 years have been 30°C to –5°C.

To determine the in-service structural behaviour of the bridge, dial gauges, electrical resistance strain gauges and optical fibre sensors were installed at strategic positions on the bridge during the bridge fabrication and installation. Table 10.5 shows the location and type of each instrumentation point. A 28 tonne and a 30 tonne lorry were used to undertake an initial and 3-year load tests respectively. A complete description of the bridge behaviour was obtained by the lorry traversing three times across the bridge in incremental distances, the first along the centre of the bridge and then flush with each of the eastern and western edges of the carriageway. A dynamic load test was also undertaken at the 3 year inspection with the lorry travelling at speed. A complete description of these tests is given in Canning and Luke.[24]

Table 10.5 Location and type of instrumentation on West Mill Bridge (Canning and Luke[23])

Reference	Location/type
FBG1	FBG sensor at bottom of web of internal beam, mid-span (longitudinal)
FBG2	FBG sensor at middle of web of internal beam, mid-span (longitudinal)
FBG3	FBG sensor at top of web of internal beam, mid-span (longitudinal)
FBG4	FBG sensor at internal beam top flange/ASSET beam bottom flange bonded interface, mid-span (longitudinal)
FBG5	FBG sensor at bottom of web of external beam, mid-span (longitudinal)
FBG6	FBG sensor at middle of web of external beam, mid-span (longitudinal)
FBG7	FBG sensor at top of web of external beam, mid-span (longitudinal)
FBG8	FBG sensor at external beam top flange/ASSET beam bottom flange bonded interface, mid-span (longitudinal)
FBG9–FBG15	FBG sensors at top flange of ASSET deck, mid-span (transverse)
FBG16–FBG22	FBG sensors at bottom flange of ASSET deck, mid-span (transverse)
FBG23–FBG26	FBG rosette sensors at bonded ASSET deck web interface over beams 1–4, mid-span (transverse)
ERSG1–ERSG4	ERSG sensors at soffit of beams 1–4, mid-span (longitudinal)
ERSG5–ERSG7	ERSG sensors at soffit of ASSET deck between beams 1–4, mid-span (longitudinal)
ERSG8–ERSG11	ERSG sensors at outer surface of top flange of ASSET deck above beams 1–4, mid-span (longitudinal)
DG1–DG5	Dial gauges at soffit of beam 1, at bearings, $^1/_4$ span, mid-span and $^3/_4$ span
DG6	Dial gauge at soffit of ASSET deck between beams 1 and 2, mid-span
DG7–DG11	Dial gauges at soffit of beam 2, at bearings, $^1/_4$ span, mid-span and $^3/_4$ span

FBG, fibre-optic Bragg grating; ERSG, electrical resistance strain gauge.

Some of the results of the test procedure are given in Table 10.6 for the main beams. The strain profiles through the depth of the FRP deck were linear. It was shown, from a comparison of the results of the field test data with theoretical data, that there remains a high level of composite action between the GFRP deck, GFRP/CFRP hybrid main beams and parapet beams.

The neutral axis level below the deck of the bridge, after 3 years in service, had decreased in value by 36%; consequently, composite action between the surface and the ASSET deck appears to have reduced, although composite action between the ASSET deck and the main beams is still fully intact. Therefore, the potential advantageous effect of this action between the FRP deck and the epoxy-based surfacing cannot be relied upon. However,

Table 10.6 Comparison of longitudinal behaviour of West Mill Bridge (Canning and Luke[23])

Parameter	Flexural rigidity (assuming 1.75 m width of GFRP deck and half-axle loading) (kN/m^2)	Neutral axis level above soffit of beam (mm)
Theory (main beams only)	2.1×10^5	260
Theory (main beams and GFRP deck)	3.2×10^5	335
Theory (main beams, GFRP deck and parapet beams)	8.5×10^5	535
Initial load test (beam 2)	$\sim 6 \times 10^5$	~500
Initial load test (beam 1)	$\sim 9 \times 10^5$	~600
3-year load test (beam 2)	$\sim 6 \times 10^5$	~410
3-year load test (beam 1)	$\sim 8 \times 10^5$	~600

the results of the test seem to imply that composite action between the FRP deck and the main beams can be relied upon. The maximum shear strains in the FRP deck at time zero and at 3 years was approximately 80 micro-strain. Furthermore, it was reported by Canning and Luke[21] that there was a significant difference, amounting to 18%, in the behaviour of the FRP deck under a dynamic load compared with that under a static one. This was measured by electrical resistance strain gauges on the bottom flange of the FRP deck.

The investigators concluded that, after the 3 year period in which the bridge had been in operation, the adhesive bond between the GFRP deck and the GFRP/CFRP hybrid main beam remained in full contact and thus complete composite action exists in the longitudinal direction and a high level of composite action exists between the parapet beam, GFRP deck and the main beam. The main beams were designed assuming that there was no transverse composite action. The GFRP deck was designed assuming no transverse composite action with the deck surfacing material or the main structural beams of the bridge.

From the results of the test, the authors have recommended that for design purposes the composite action between the surfacing and the GFRP deck should not be assumed, although load dispersion through the surfacing may be. In addition, composite action between the bonded GFRP deck and the main beams may be assumed. A possible design method has been proposed by Guertler.[25] It specifically notes that the authors have stressed the importance of adhesive monitoring.

Bridge over Bennetts' Creek, Rexville, New York, USA

The first FRP superstructure in the United States on a Federal Highway Administration (FHWA), a Recognised State Highway, was built in 1998;

since this time ten decks/superstructures have been built. As there was a dearth of information on FRP durability and to enable appropriate guidelines to be developed for future decks/superstructures, in-service performance of this first structure was monitored for 4 years via strain and deflection measurements and visual examinations. In addition, modal tests were undertaken to characterise its dynamic properties and to calibrate theoretical analysis. Furthermore, the bridge was required to undergo the mandatory bridge inspection by the National Bridge Inspection Standards (NBIS) for all bridges carrying public highway traffic. Due to the experimental nature of the bridge further supplementary inspections were required. Alampalli[26] discusses the testing arrangements, field monitoring systems and results of the field performance of this structure over 4 years. Alampalli *et al*.[27] have described the FRP slab design, fabrication, installation and cost-benefit details for this structure.

The superstructure was fabricated from E-glass-stitched bonded fabric and vinylester resin using a cell core system which provided stiffness in two directions. The top and bottom surfaces are 12.8 mm thick plates and comprise seven composite plies. The webs are made with two composite plies and foam core, and the whole is wrapped by an outer shell to form the integral unit. The deck is 7.8 metres long, 10 metres wide and has a 30° skew. The FRP slab is 621 mm deep with a 10 mm thick polymer–concrete wearing surface and was fabricated in two skewed units, each 5.036 metres wide and 7.807 metres long. The two deck units are joined throughout the longitudinal length by a shear-key which is designed to carry the shear force that develops along the longitudinal plane resulting from the differential deflection of the two superstructure panels.

The bridge was loaded in four increments closely resembling the American Association of State Highways and Transportation Officials (AASHTO) M-18 truck configuration.[28] The target proof load could not be reached due to truck size and load limitations, but MS loadings were reached. Alampalli[26] reported that the strain data from the load cases were generally consistent. The maximum strain recorded was considerably less than the 600 micro-strain predicted by a numerical analysis. This indicated a significantly higher load capacity than that originally assumed.[29] The maximum deflection at mid-span under the maximum load applied to the superstructure was 3.5 mm which is considerably less than the Span (L)/800 design limitation of 8.8 mm. These low strains and deflections in the field compared with those predicted were attributed to assumptions made regarding the boundary conditions during the design. The performance of the shear-key was examined during the initial proof-loading test and at intervals during the 4 year test period and it was concluded that the loads were being effectively transferred across the longitudinal centreline of the superstructure. The visual inspection and non-destructive test results are given in Table 10.7. It will be noted that

Table 10.7 Notable observations from the visual inspection reports (Alampalli[26])

Inspection date	Observations
11/24/98	Three areas of debonding amounting to about 0.15 m^2 were observed under side slab at mid-span.
06/24/99	Top of deck was observed to be breaking up at the junction of the transverse and longitudinal joint. A large portion under the right slab ($^1/_4$ to $^1/_3$) had delaminated from mid-span to near the end section of the slab.
01/13/00	Wearing surface has been reworked but still has a longitudinal crack at the centreline. Delaminations in the face skin were repaired by epoxy injection. The slab now sounds solid when tapped with a hammer or stone.
10/22/01	Inspection report shows bottom west side slab showing delaminations in face skin again. The repairs to this section of the slab are sound. The delaminations noted appear to be new and require further investigation.
11/13/02	40% of the bottom west side slab seems delaminated in face skin when sounded. Repairs to the section of the slab are still sound.

several delaminations were found during the visual inspections and it is clear that for future applicability of FRP materials for bridge decks these issues affecting the long-term durability should be resolved.

The Gills Creep Bridge, Franklin County, Virginia, USA

The next field survey relating to bridge decks is associated with the monitoring of GFRP rebars in the deck.[30] The Gills Creep Bridge is a river crossing with three spans A, B and C of lengths 13.7, 24.4 and 13.7 metres, respectively. The girders are rolled steel sections and are simply supported. Spans A and C are symmetrical about the bridge plan. On span A the concrete bridge deck is reinforced with GFRP rebars as the top mat and epoxy-coated steel as bottom mat; on span C the deck is reinforced with epoxy-coated steel rebars only.

Electrical resistance strain gauges and vibrating wire strain gauges were installed in the deck and also on the bottom flanges of all girders in both spans and mid-span. The latter gauges were used to determine common bridge design against theoretical predicted values. Deflections of the girders were monitored by deflectometers in order to determine bridge design parameters such as girder redistribution factors and dynamic load allowance. The loading was in accordance with the Virginia Department of Transport.

The preliminary conclusions after the first year of monitoring are that: (a) the GFRP/epoxy-coated steel rebars of span A are behaving in a similar way to that of the epoxy-coated steel rebars of span C as regards deflections, girder strains and girder distribution factors; (b) the yearly fluctuations in

strain values of the top layer GFRP rebars of span A are temperature dominated; (c) the current method for the determination of the effective widths for deck design is conservative for this deck. The monitoring of this bridge is continuing.

The information for this bridge deck has been obtained from Phillips *et al.*[30] (contact Dr C. Roberts-Wollman at the Department of Civil and Environmental Engineering, Virginia Tech. 200 Patton Hall, Blacksburg, VA 24061, USA for further details).

10.9 Girders and profiles

Pontresina Bridge over the Fiaz Creek in Pontresina, Switzerland

Keller *et al.*[31] discuss the long-term performance of Pontresina Bridge, which is a two-span bridge centrally supported; each span is 12.5 metres long and the truss girders are 1.48 metres deep on the lateral sides of the walkway. The bridge crosses Fiaz Creek in Pontresina, Swiss Alps, at an altitude of 1790 metres. The bridge was built in 1997 and is classified as temporary as it is used mainly during the winter months for ski touring access. During the summer period it is removed, due to the high water level in the creek, and stored on site. Since 1997 it has been removed and replaced eight times. During this time it has been exposed to environments typical of alpine climates with temperature variations from –20°C to 25°C. The annual hours of sunshine are approximately 1700 and the average rainfall is 1000 mm. The alpine location exposes the structure to a high ultraviolet radiation and a dense layer of snow normally covers the walkway during winter.

The pultruded composite material is constructed from unidirectional rovings of E-glass fibre. In addition, depending upon the thickness of the pultruded profile, there are either one or two layers of stitched chopped-strand/(0°/90°) woven mats on the external surfaces of the sections. The GFRP materials are manufactured from E-glass fibre embedded in an isophthalic polyester resin. The structure is fabricated from five different GFRP pultruded profiles; on one of the spans the members are connected at nodes by bonding and on the other span they are connected by bolting; a GFRP deck grating connects the two lateral sides of the walkway. The structure was designed for pedestrian loads according to the Swiss Structural Standard SIA 161[32] and, at serviceability, a uniformly distributed load of 4 kN/m^2 and a 10 kN knife edge were assumed. In addition, a snow load of 9 kN/m^2 had to be assumed but this was reduced to 1.2 kN/m^2 for the design as the snow is normally removed to make the bridge passable.

Immediately after the bridge was constructed the two spans were test loaded to serviceability limit state. Likewise, in 2005 the full-scale serviceability load tests were repeated and, in addition, a numerical analysis was performed on both spans containing the two different joint types. Table 10.8 provides a

Table 10.8 Comparison of the test results from the 1997 and 2005 field loading experiments after Keller *et al.*[31]

Measured parameter	Bolted span			Bonded span		
	Measured 1997	Measured 2005	Difference (%)	Measured 1997	Measured 2005	Difference (%)
Total load (kN)	83.9	87.0	3.7	84.0	86.2	2.6
Mid-span deflection left/right girder (mm)	17.6–17.6	19.0–18.7	8.0–6.3	14.2–14.2	17.5–16.4	23.2–15.5
Load corrected average value (%)	17.6–17.6	18.3–18.0	4.0–2.3	14.2–14.2	17.1–16.0	20.0–12.5

comparison of the test results from the 1997 and 2005 field loading experiments. A detailed inspection of the two structures was undertaken in 2005. Table 10.9 gives an indication of the damage to some of the members of the bridge. Some of the main observations made are detailed here. Local damage was

Table 10.9 Overview of bridge components, damage categories and causes (Keller *et al.*[31])

Components	Shapes	Dimensions	Damage	Causes
Upper chord	Channel	160 × 48 × 8 mm	(a Fibre blooming top surface. (b) Longitudinal cracks in flanges.	(a) Missing surface veil. (b) Local impact on flange.
Lower chord	Channel	160 × 48 × 8 mm	(a) Crushed lower flange. (b) Longitudinal cracks in flange.	(a) Impact on flange. (b) Local impact on flange.
Diagonals in compression	Tube	100 × 100 × 8 mm	(a) Longitudinal cracks at joints. (b) Spot damages.	(a) Over-tightening of bolts. (b) Vandalism.
Vertical posts	Tube	100 × 100 × 8 mm	(a) Spot damage.	(a) Vandalism.
Diagonals in tension	Flat sections	100 × 100 mm	(a) Degraded surfaces of upper cut ends.	(a) Loss of sealing of cut sections.
Spacer plates	Flat sections	10 (depth) mm	(a) Degraded surfaces of upper cut ends.	(a) Loss of sealing of cut sections.
Transverse beams at joints	Channel sections	160 × 48 × 8 mm	(a) Crushed flanges at end beams. (b) Fibre blooming top surface. (c) Longitudinal cracks in upperflanges of webs.	(a) Impact on flanges. (b) Missing surface veil. (c) Transverse bending in flanges below grating.
Transverse beams between joints	I-sections	160 × 80 × 8 mm	(a) Fibre blooming top surfaces. (b) Longitudinal cracks in upper flanges over webs.	(a) Missing surface veil. (b) Transverse bending flanges below grating.
Wind bracing	I-sections	80 × 80 × 8 mm	No damage	—

observed, caused by different local defects including: impact damage and inappropriate storage during movement of bridge; fibre blooming due to misalignment of surface veils; degradation of cut surfaces that were unprotected; and damage due to vandalism. The FRP units used were open section. It was felt that a more appropriate section would have been a closed one. A microscopic material examination suggested that structural safety and serviceability of the bridge were not significantly affected.

The researchers concluded that the durability of the material of the bridge was primarily affected by inappropriate choice of pultruded section, construction detailing and manufacturing. They point out that there was a slight decrease in material strength and if this result were to be extrapolated to 60–80 years from the 8 years in a linear relationship the structural safety of the bridge would become critical. Currently the bridge is being repaired and will be returned to site for a further 8 years of testing.

The information in this example has been derived with the help of Professor T. Keller (Ecole Polytechnique Fédérale de Lausanne), Switzerland and is gratefully acknowledged.

10.10 Observations

It has been demonstrated in the various field surveys illustrated in this chapter that provided the various FRP structural components have been correctly designed, manufactured, fabricated and applied appropriately on site, the material offers acceptable and in many cases advantageous long-term durability performance over the more conventional construction materials. The current automated GFRP, CFRP and aramid FRP composite materials that are utilised in the fabrication of structural members are superior, both physically and mechanically, and have been improved in quality over the years compared with those manufactured by the hand lay-up system utilising glass fibre chopped-strand mat/polyester composite materials for the 'all-composite' buildings of some 30 years ago. However, these early GFRP composites have indicated good performance in normal atmospheric environments. As more information becomes available from the various monitored structures currently being studied and future surveys of new structural systems, a greater understanding of the long-term structural characteristics of the material in a civil engineering environment will be developed and, hopefully, further confidence in its ability to provide resistance against degradation will be gained.

The examples given in Section 10.4 have shown that the use of FRP composites has been driven by their excellent durability and their economic advantages when exposed to the harsh environment of Québec, Canada. However, it was also pointed out that the material must be protected from severe impacts when these forces are likely to occur from, say, vehicles colliding with components of bridge structures.

The results of field tests of FRP composite rebars, which were exposed to general civil engineering limits of temperature, moisture and salt solutions, were examined after 8 years in service; these have been discussed in Section 10.7. Observations from these examinations have been made at the end of Section 10.7, where it was concluded that GFRP flexural tension reinforcement is durable and compatible with concrete. Monitoring of the rebars is continuing and it is likely that they will perform as well over the longer time interval.

From the visual inspections of structures, which have been mentioned in the various surveys, a variety of different local defects and damage have been noted:

(a) local crushing damage of the material by impact, mainly caused by the original inadequate design considerations, or inappropriate use of the structural material;
(b) degradation caused by non-protection of cut surfaces during fabrication, omitted surface veils, damage due to vandalism, colour change of exposed surfaces of the composite due to omission of ultraviolet, stabilisers, etc.
(c) bridge construction damage to the material has been noted such as scratch marks from cars and lorries passing under low bridges, etc.

In order to overcome these problems, it will be necessary, in future, to design out these areas and provide physical protection for the structure and a greater supervisory control during manufacture and site erection of the product.

Planned instrumentation of engineered structures to monitor their responses to long-term loading and to earthquake motion is very much in its infancy with currently only a few structures being instrumented. However, this type of monitoring is very important for the establishment of a better understanding of the structural performance when developing building codes and specifications and, in addition, to achieve improved earthquake resistance in both new constructions and retrofitted structures.

The estimation of long-term durability performances from accelerated test studies requires considerable understanding. Many such studies have been undertaken and conclusions have been drawn that have completely misrepresented the situation. An example has been mentioned in this chapter concerning the ingress of salt solutions into GFRP composite rebars which, from accelerated tests using concentrated salt solutions, have indicated a serious alkali attack on the glass fibre; in practice, however, it was shown that no such attack took place.

The fungal growth on FRP composite structures can be a problem from a visual point of view, but the indications from long-term visual monitoring are that it is unlikely to cause any lasting degradation of the structure. It is always advisable to jet-wash the structure every 6 months to eliminate the fungal growth.

10.11 Acknowledgements

The author wishes to acknowledge the valuable help and assistance freely given by the many researchers undertaking investigative work into the monitoring of the durability of civil/structural systems exposed to the civil engineering environments. Without their helpful assistance this chapter would not have been written. It is hoped that all researchers and/or firms who have helped in the production of this chapter have been named; if any names have inadvertently been omitted the author extends his sincere apologies.

10.12 References

1 Hollaway, L. C. and Head, P. (2001). *Advanced Polymer Composites and Polymers in the Civil Infrastructure*. Elsevier, Oxford.
2 Shu, Y. (1983). 'Chinese crossing first for plastics pioneers'. *New Civil Engineer*, 14 April.
3 Farhey, D. N. (2005). 'Long-term performance monitoring of the Tech 21 all-composite bridge'. *Journal of Composites for Construction*, **9** (3), 255–262.
4 Demers, M., Labossière, P. and Neale, K. (2005). 'Ten years of structural rehabilitation with FRPs – a review of Quebec applications'. Proceedings of Composites in Construction 2005 – 3rd International Conference, edited by Hamelin *et al*., Lyon, France, 11–13 July 2005.
5 Lapierre, P., Labossière, P. and Neale, K.W. (1998). 'Modélisation de pouters en Ten béton armé renforcées avec des matériaux composites'. Proceedings of the Canadian Society for Civil Engineering Annual Conference, Halifax, Nova Scotia, edited by J. P. Newhook and L. G. Jaeger, 613–622.
6 Labossière, P., Neale, K. W., Rochette, P., Demers, M., Lamothe, P., Lapierre, P. and Desgagné, G. (2000). 'Fibre reinforced polymer strengthening of the Sainte-Émélie-de-l'Énergie bridge: design, instrumentation and field-testing'. *Canadian Journal of Civil Engineering*, **27**, 916–927.
7 Rochette, P., Labossière, P., Neale, K. W., Demers, M., Savard, M. and Desgagné, G. 'Long-term behaviour of a FRP-strengthened structure: The case of the Sainte-Émélie-de-l'Énergie Bridge'. *Canadian Journal of Civil Engineering* (submitted).
8 Sargent, D., Mufti, A. A. and Neale, K. W. (2002). 'GFRP seismic strengthening of Portage Creek Bridge columns'. Developments in Short and Medium Span Bridge Engineering, Vol. 1, pp. 281–288, Vancouver, British Columbia, Canada, 31 July–2 August 2002.
9 Luke, S. (2001). 'Strengthening structures with carbon fibre plates. Case histories for Hythe Bridge, Oxford and Qafco Prill Tower'. NGCC First Annual Conference and AGM – Composites in Construction through Life Performance, Watford, UK, 30–31 October 2001.
10 Luke, S. (2001). 'Strengthening of existing structures using advanced composite materials'. Network group for composites in construction. Fibre composites – structural materials for the 21st century. NGCC course run through the Institution of Structural Engineers, 18 September 2001.
11 Luke, S. (2001). The use of carbon fibre plates for the strengthening of two metallic bridges of an historic nature in the UK. Proceedings of CICE 2001, FRP Composites in Civil Engineering, edited by J.-G. Teng, Elsevier, London, pp. 975–983.

12 Bank, L. C. and Gentry, R. T. (1995). Accelerated test methods to determine the long-term behaviour of FRP composite structures: Environmental effects'. *Journal of Reinforced Plastics and Composites*, **14**, 559–587.
13 Sen, R., Mullins, G. and Salem, T. (2002). 'Durability of E-glass/vinylester reinforcement in alkaline solution'. *ASI Structural Journal*, **99**, 369–375.
14 Bank, L. C., Gentry, R. T., Barkatt, A., Prian, L., Wang, F. and Mangla, S. R. (1998). 'Accelerated aging of pultruded glass/vinylester rods'. Proceedings of 2nd International Conference on Fibre Composites in Infrastructure (ICCI), Vol. 2, pp. 423–437.
15 Uomoto, T. (2000). 'Durability of FRP as reinforcement for concrete structures'. Advanced Composite Materials in Building and Structures, 3rd International Conference, Ottawa, Ontario, Canada, pp. 3–17.
16 Tomosawa, F. and Nakatsuji, T. (1997). 'Evaluation of ACM reinforcement durability by exposure tests'. Non-Metallic (FRP) Reinforcement for Concrete Structures, Proceedings of the 3rd International Symposium, Sapporo, Vol. 2, pp. 139–146.
17 Clarke, J. L. and Sheard P. (1998). 'Designing durable FRP reinforced concrete structures'. Proceedings of the 1st International Conference on Durability of Fibre Reinforced Polymer (FRP) Composite for Construction (CDCC 1998), Sherbrooke, Quebec, Canada, pp. 13–24.
18 Sheard, P., Clarke, J. L., Dill, M., Hammersley, G. and Richardson, D. (1997). 'EUROCRETE – Taking account of durability for design of FRP reinforced concrete structures'. Non-Metallic (FRP) Reinforcement, for Concrete Structures, Proceedings of the 3rd International Symposium, Sapporo, Vol. 2, pp. 75–82.
19 Mufti, A., Onofrei, M., Benmokrane, B., Banthia, N., Boulfiza, M., Newhook, J., Bakht, B., Tadros, G. and Brett, P. (2005). 'Durability of GFRP reinforced concrete in field structures'. Proceedings of the 7th International Symposium on Fiber Reinforcement for Reinforced Concrete Structures (FRPRCS-7), New Orleans, Lousiana, USA, 7–10 November 2005.
20 Mufti, A., Benmokrane, B., Boulfiza, M., Bakht, B. and Breyy, P. (2005). 'Field study on durability of GFRP Reinforcement'. International Bridge Deck Workshop, Winnipeg, Manitoba, Canada, 14–15 April 2005.
21 Mufti, A., Onofrei, M., Benmokrane, B., Banthia, N., Boulfiza, M., Newhook, J., Bakht, B., Tadros. G. and Brett, P. (2005). 'Report on the studies of GFRP durability in concrete from field demonstration structures'. Proceedings of Composites in Construction 2005 – 3rd International Conference, edited by Hamelin *et al*., Lyon, France, 11–13 July 2005.
22 Luke, S., Canning, L., Collins, S., Brown, P., Knudsen, E. and Olofsson, I. (2002). 'The Development of an Advanced Composite Bridge Decking System – Project ASSET'. *Structural Engineering International*, **12** (2), 76–79.
23 Canning, L. and Luke, S. (2006). 'West Mill Bridge – comparison of initial and long-term structural behaviour'. Proceedings of Symposium IABMAS 2006, Porto, Portugal, 16–19 July 2006.
24 Canning, L. and Luke, S. (2005). 'West Mill Bridge 3-Year Monitoring Report'. Internal Report to Mouchel Parkman, West Byfleet, Surrey, UK.
25 Guertler, H. (2004). 'Composite action of FRP bridge decks adhesively bonded to steel main girder'. PhD Thesis, Ecole Polytechnique Federale De Lausanne (EPFL).
26 Alampalli, S. (2006). 'Field performance of an FRP slab bridge'. *Composite Structures*, **72** (4), 494–502.
27 Alampalli, S., O'Connor J. and Yannotti, A. (2002). 'Fiber reinforced polymer composites for the superstructure of a short-span rural bridge'. *Composite Structures*, **58**, 21–27.

28 AASHTO American Association for Highway and Transportation Officials, (1994). *Standard Specification for Highway Bridges*, 15th edition AASHTO, Washington, DC.
29 'Level 1 Load Rating-BIN 104315022' (1999). Report submitted to New York State Department of Transportation Officials, New York.
30 Phillips, K., Hartan, M., Mejias, M., Roberts-Wollmann, C., Cousins, T., Lesko, J. and Case, S. (2005). 'Field performance of a bridge deck with GFRP as top mat reinforcement'. Proceedings of Composites in Construction 2005 – 3rd International Conference, edited by Hamelin *et al*., Lyon, France, 11–13 July 2005.
31 Keller, T., Bai, Y. and Vallée, T. (2007) 'Long-term performance of a glass fiber reinforced polymer truss bridge'. *Journal of Composites for Construction*, **11** (1), 97–108.
32 Swiss Code SIA 161 (1990). Stahlbauten, Schweizerischer Ingenieur- und Architektenverein (SIA), Zürich, Switzerland.

11

Reinforcement of concrete using fibre-reinforced polymer composites

B. BENMOKRANE, M. ROBERT and T. YOUSSEF
University of Sherbrooke, Canada

11.1 Introduction

The corrosion of steel in concrete has been identified as one of the most important causes of deterioration and structural deficiency. It is estimated that the required repair cost for parking garages in Canada is approximately $6 billion (Benmokrane and Wang, 2001) and in the United States the rehabilitation cost for all concrete structures is estimated to exceed $250 billion per year (Chin, 1996). Different remedy techniques including concrete patching and the use of epoxy-coated or galvanized steel have proven to be inefficient for long-term applications. A relatively recent solution that is receiving global attention is the use of fiber-reinforced polymer (FRP) composites as a cost-effective alternative to traditional construction materials and techniques. FRP internal reinforcements, such as bars and pre- or post-tensioned tendons, are promising solutions due to their attractive properties, including their excellent mechanical properties, light weight, damage tolerance, resistance to electrochemical corrosion, magnetic neutrality and real-time monitoring capabilities (Nkurunziza *et al*., 2004). The most commonly available FRPs, which can be used for internal reinforcement, are glass (GFRP), carbon (CFRP) and aramid (AFRP). Therefore, GFRP bars are gaining popularity as reinforcement for concrete bridge deck slabs and other concrete structures due to their low cost compared with CFRPs (El-Salakawy *et al*., 2003; Huckelbridge and Eitel 2003). Even if FRP reinforcement seems to be a promising solution for corrosion problems, the principal problems confronted by designers and engineers in using FRP composite materials are their durability qualities and long-term behavior in general, and in particular in severe civil infrastructure environmental conditions. In fact, upon certifying the structural integrity of the composite bars, the industry is still in need of long-term durability data for the material in order to gain wider acceptance of FRPs in infrastructure applications (Benmokrane and El-Salakawy 2002; Harries *et al*., 2003). Compared with the large amount of work originating from the aerospace, chemical and military industries on the durability of FRP composites,

there is only a small, but growing, amount of research concerned with the durability of FRP composites in civil infrastructure applications. This review summarizes recent research on various aspects of the durability of FRP composites when used as internal reinforcement for concrete structures. The main topics of this chapter are related to the effects of environmental conditions on FRP internal reinforcement. In particular, the effects of moisture, alkaline environment, freeze and freeze–thaw cycle, high temperature, fatigue, and creep and relaxation are of interest.

11.2 Durability concerns

Even if FRPs are resistant to electrochemical corrosion, which affects steel, their performance may deteriorate due to several types of environments and conditions. The reported literature (Benmokrane *et al*., 1998; Saadatmenesh and Ehsani 1998; Burgoyne, 2001; Chin *et al*., 2001; Benmokrane and EL-Salakawy, 2002; Masmoudi *et al*., 2003; Al-Zahrani, 2005; Nkurunziza *et al*., 2005) has indicated that properties of FRPs could deteriorate due to certain physical (loading, moisture, temperatures) or chemical (alkaline solution, acid) exposures.

The degree of damage/deterioration depends on a multitude of factors such as the type and volume of fibers, the resin matrix, the exposure environments and the process of molding. E-glass fibers are the most susceptible to degradation due to moisture and alkalinity, while carbon fibers are relatively inert to the environment. On the other hand, aramid fibers are resistant to abrasion and impact, but are sensitive to creep, absorb moisture and degrade under ultraviolet exposure. To show an appropriate performance, the fibers must be protected by the resin. The durability of the resin system is dependent on several factors including the resin components and their proportions, as well as curing time and conditions. The composites industry has many resin systems that are designed for specific applications and they must be chosen based on their mechanical, physical, chemical and electrical properties, but also on durability considerations. The findings from investigations thus far indicate that the resin used in the reinforcing bar and manufacturing parameters play an important role in the durability of GFRP internal reinforcements. Studies by Vijay and Gangarao (1999) indicated that reinforcing bars with urethane-modified biphenol vinylester exhibited the lowest vulnerability to different harsh environments. Among unsaturated polyesters, medium reactivity polyesters exhibited least vulnerability to different conditioning schemes. Reinforcing bars with isocyanurate vinylester (IVE) resins exhibited superior strength and stiffness in unconditioned, salt-conditioned and freeze–thaw salt-conditioned environments; however, severe strength and stiffness reductions of 76.5% and 31.6%, respectively were observed in alkaline environments.

11.3 Principal environments affecting fiber-reinforced polymer internal reinforcement durability

11.3.1 Fluids and moisture

Concrete containing internal FRP reinforcement will generally be exposed to alternating wet/dry cycles, natural weathering and sometimes corrosive media. Even if concrete provides an excellent first line of defence, the permeability is significant enough to eventually transmit moisture and other corrosive elements to the internal reinforcement.

The effect of fluids on the performance of FRP composites has, over the past decades, been one of the most studied subjects related to the durability of composites. The majority of the theoretical investigations have been focused on sorption processes and reporting gain in weight by using linear and non-linear Fickian law. In general, the sorption behavior of fluid into FRPs depends on the type of fluid (water, acid, base), fluid concentration, temperature, external applied stress, type of fiber and resin, interphase, the process of molding and the state of the material (damage, curing condition). Weitsman and Elahi (2000) give a comprehensive review of this topic. The authors identified five different types of fluid sorption behavior based on weight gain versus fluid sorption time plot: (1) linear Fickian behavior; (2) 'pseudo-Fickian' behavior, where material never attains equilibrium moisture content; (3) 'two-stage diffusion' behavior, related to change of environmental conditions or parameters such as temperature, loading or relative humidity; (4) the rapid gain in weight due to moisture resulting from large deformation or damage of the material, fiber/matrix rebounding and matrix cracking which is often irreversible; and finally, (5) an irreversible process as a result of leaching out of the material from the bulk by chemical or physical breakdown. More recently, Shao and Kouadio (2002) showed that the process by which moisture diffusion occured in pultruded composites was typically non-Fickian; it was a combination of Fickian diffusion and polymeric relaxation of the composite.

It has been proved that the rate of sorption is controlled by the chemical structure of the matrix (degree and type of cross-linking, presence of void), the interface/interphase and the manufacturing process. Consequently, researchers have attempted to control the diffusion process by using resin matrices with lower permeability (Benmokrane, 2000), modifying the interphase region by using suitable sizing chemistry or selecting appropriate molding processes to reduce void content. In addition, moisture ingress can degrade the resin by chemical attack (hydrolysis) or by a drop in the glass transition temperature (Chin *et al.*, 2001). For this reason, fluids affect matrix-dominant properties such as the transverse and shear strengths of FRP composites, and decreases in these properties become more important with increased exposure time and temperature (Liao *et al.*, 1998).

Glass fibers are particularly sensitive to fluids ingress, since glass fibers are sensitive to chemical and physical attack. The level of degradation depends on the composition of the fibers, the fluid type and concentration, and the temperature to which fibers are exposed. Extensive studies have been conducted in this research area (Chin *et al*., 2001; Masmoudi *et al*., 2003; Al-Zahrani, 2005). Typically, the tensile strength of E-glass/vinylester composites would decrease by 40% in a 100% relative humidity environment at 93°C. The flexural and tensile modulus decreased by approximately 10% at 93°C and 100% relative humidity after 200 days exposure (Springer *et al*., 1980). In general, Al-Zahrani (2005) has showed that the modulus of elasticity was less affected by all the exposure conditions than the tensile strength. Moreover, fiber orientation was reported to significantly affect the ultimate tensile strength (UTS) and Young's modulus of composites after moisture exposure (Gopalan *et al*., 1989). The authors (Gopalan *et al*., 1989) investigated E-glass/epoxy composites with different fiber orientation and architecture specimens in water at 70°C for 20 days, and reported a decrease in UTS of 33.3, 8.0, 13.7 and 20.4% for resin, unidirectional, bidirectional and chopped-strand mat, respectively. For the same specimens, the Young's modulus decreased by 45.2, 5.0, 14.6 and 24%, respectively.

Carbon fibers are not affected by fluids ingress, but the resin matrix is usually affected. Consequently, the performance of composites is also affected in the case of CFRPs. For unidirectional carbon composites, this usually leads to a reduction in the compressive strength and shear strength, but only a small effect on the tensile strength since this property is especially dominated by fibers, which are not affected by fluids (Dejke, 1998). Hancox and Mayer (1994) reported minimal weight gain and strength loss when carbon/epoxy specimens were exposed to 65% humidity for over 4 months and to boiling water for over 3 weeks. Rege and Lakkad (1983) tested compressive, flexural and interlaminar shear strengths of CFRP laminates immersed in salt water and distilled water for over 120 hours at several temperatures. The data showed a decrease in strength with increasing temperature for both solutions. In addition specimens immersed in distilled water and salt solution at the same temperature showed greater decreases in strength and higher equilibrium uptake with the salt water. Water was also found to accumulate at the fiber/matrix interface.

Aramid fibers are affected by fluids, mostly at higher temperatures. AFRP composites saturated in water have been reported to lose 35% of their flexural strength at room temperature (Allred, 1984), and up to 55% if stressed and under wet/dry thermal cycles (Sen *et al*., 1996). On the other hand, Technora and Kevlar fibers, which are categorzed as aramid fibers, show different behavior under the combined effects of fluids and temperatures. For Technora fibers, no degradation was observed in distilled water at any temperature, the decreases in strength were reported for specimens immersed in acid and

alkali solutions. This reduction increased with time and temperature. For Kevlar fibers, degradation was observed for samples immersed in distilled water and acid and alkali solutions at high temperatures (Uomoto, 2001).

In terms of the effect of fluids on fracture and toughness of FRP composites, a detailed review is given by Weitsman (1998). In general, the reported literature is contradictory. On the one hand, due to an increase in compliance through plasticization processes, increases in fracture energy and fracture toughness are observed. On the other hand, due to degradation in the fiber/matrix interphase region, reductions in fracture energy and toughness are reported.

11.3.2 Alkaline environments

The reaction of FRP composites in an alkaline environment, like concrete, is one of the major durability concerns for design engineers. Typically, a concrete environment has high alkalinity, with a pH between 12 and 13 depending on the design mixture of the concrete, and the type of cement used. This alkaline environment damages glass fibers through loss in toughness and strength, and embrittlement. Glass fibers are damaged due to the combination of two processes: (a) chemical attack on the glass fibers by the alkaline cement environment; and (b) concentration and growth of hydration products between individual filaments (Murphy *et al*., 1999). The embrittlement of fibers is due to the nucleation of calcium hydroxide on the fiber surface. The hydroxylation can cause fiber surface pitting and roughness, which act as flaws that severely reduce fiber properties in the presence of moisture. In addition, calcium, sodium and potassium ions found in the concrete pore solution are highly aggressive towards glass fibers. Therefore, the degradation of glass fibers not only depends on the high pH level, but is also a result of the combination of alkali salts, pH and moisture.

Vijay and Gangarao (1999) compared moisture absorption by GFRPs for tap water, salt water and alkaline conditioning. An increase in moisture content was noted with increasing temperature. Tests were conducted at different temperatures of 32°C, 49°C and 66°C, and freeze–thaw temperatures of –29°C to 49°C. Alkaline conditioning resulted in maximum moisture absorption as compared with other solutions. A maximum moisture content of about 0.6% by weight or less was observed after 543 days of conditioning under room and freeze–thaw temperatures for tap water, salt water and alkaline solution. On average, alkaline conditioning produced about twice the percentage moisture content by weight as compared with tap-water and salt-water conditioning. The authors concluded that the higher absorption of alkaline solution in relation to other solutions is an indication of a high degradation in tensile strength of GFRP reinforcing bars under accelerated aging.

Aramid fibers show strength degradation in an alkaline environment. Kevlar

29 exposed to 10% NaOH solution for 1000 hours loses 74% of its strength. High modulus aramids such as Kevlar 49 demonstrate better alkaline resistance (Malvar, 1998). A 3% strength loss has been reported for Kevlar 49 after 100 hours immersion in 40% NaOH solution (DuPont De Nemours & Co., 1992). Carbon fibers are commonly believed not to be affected by alkaline environment; Judd (1971) reported that carbon fibers were resistant to alkaline solutions at all concentrations and all temperatures up to boiling. Carbon tows immersed for 257 days in a very basic 50% HaOH solution showed variations in strength and elastic modulus of around only 15%.

For the use of resin matrices in FRP composites, researchers (Malvar, 1998; Benmokrane, 2000) have suggested that the resin must provide enough toughness to prevent the development of microcracks, and hence ensure minimal diffusion through the resin matrix. Among the resin matrices commonly used for construction – i.e. vinylester, epoxy and polyester – vinyl/ester resin was reported to be more suitable for this purpose. The reason is that, in the vinyl/ester resin, the weakest ester linkage is partly replaced by the stronger ether linkage that is highly resistant to alkali. Furthermore, vinylester resin is tough because of a longer distance between crosslinks. Thus, if flaws/microcracks pre-exist in a specimen, their growth under stress would be at lower rate in vinylester (Benmokrane, 2000). Additionally, vinylester resins are resistant to a wide range of acids (sulfuric, hydrochloric, hydrofluoric, phosphoric, nitric) as well as to chlorine (Malvar, 1998).

Although an appropriate resin matrix (vinylester, epoxy) provides fibers with a certain level of protection from alkaline degradation, migration of high pH solutions and alkali salts through the resin (or through voids, cracks or the interface between fiber and matrix) to the fiber surface is possible. Katsuki and Uomoto (1995) used electron probe microscopy to track the ingress of alkali ions (sodium ions) into aramid-, carbon- and glass-reinforced vinylester rods. Sodium ions penetrated into the GFRP in the radial direction with time. No degradation was noticed in AFRP or CFRP rods immersed for 60 days. Chin *et al*. (2001) observed by energy dispersive X-ray analysis that appreciable amounts of sodium, potassium and calcium were found in the interior of isopolyester specimens exposed to a 60°C pore solution for 60 days. However, the authors also noticed that no evidence for the ingress of ions was found for the vinylester specimen. Hojo *et al*. (1991) studied the corrosion behavior of resins in aqueous solutions, and compared it with that of the metal. Three forms of corrosion mechanism were found, namely, surface reaction, corrosion layer forming and penetration. By using corrosion depth, with immersion time, the authors found that the concept of corrosion rate could be applied even in polymeric materials. The corrosion rates were dependent on chemical structure and the reactivity between the resin and the environment.

Aqueous solutions with high pH are known to degrade the tensile strength and stiffness of GFRP bars (Porter and Barnes, 1998), although particular

results vary tremendously according to differences in test methods. Higher temperatures and long exposure times exacerbate the problem. Most of the data were generated using temperatures as low as slightly sub-freezing and as high as a few degrees below the glass transition temperature of the resin. Tensile strength reductions in GFRP bars ranging from 0 to 75% of initial values have been reported in the literature. In many cases, tensile stiffness reductions in GFRP bars range between 0 and 20%. Tensile strength and stiffness of AFRP rods in elevated temperature alkaline solutions, with and without applied tensile stress, have been reported to decrease by between 10–50% (Rostasy, 1997) and 0 – 20% (Sen *et al*., 1998) of initial values respectively. In the case of CFRPs, strength and stiffness have been reported to decrease by between 0 and 20% (Takewaka and Khin, 1996).

In order to evaluate the long-term durability performance of FRPs in alkaline environments, extensive studies have been conducted to develop accelerated aging procedures and predictive models for long-term strength estimates, especially for GFRP bars. Several models are being developed such as: the model developed at Iowa State University (Porter *et al*., 1995), which is based on an Arrhenius-type model proposed by Litherland and colleagues (Litherland *et al*., 1981); a durability test protocol model being developed at the University of Sherbrooke (Benmokrane, 2000); and diffusion models developed at West Virginia University and the University of Southern Florida (Faza *et al*., 1994). Researches on the effects of temperature on the durability of FRP bars in concrete alkaline environments indicate that an accelerated factor for each temperature difference can be defined by using Arrhenius laws. These factors differ for each product, depending on type of fiber, type of resin and bar size. In addition, the factors are affected by the environmental conditions, such as surrounding solution media, temperature, pH, moisture, and freeze–thaw conditions (Benmokrane and Rahman, 1998). Gerritse (1998) indicated that at least three elevated temperatures are necessary to perform an accurate Arrhenius-type prediction, and the measured data should be in continuous time intervals. The immersion temperatures were chosen in order to accelerate the degradation effect of aging; however they were not too high to avoid producing any thermal degradation mechanisms.

11.3.3 Freeze and freeze–thaw cycles

In general, freeze and freeze–thaw exposures do not affect fibers, although they can affect the resin and the fiber/resin interface. The majority of studies on this subject have concerned aerospace materials. The reported literature on the effect of freeze–thaw on pultruded FRP composites is very limited. In terms of material degradation due to low temperatures and freeze–thaw cycles, Lord and Dutta (1988) gave an extensive review on this subject. In general, at low temperatures, complex residual stress arises within the FRP composites

as a result of matrix stiffening and mismatch of thermal expansion coefficients of the matrix and resin, as well as FRP and concrete. Residual stresses can cause microcracks in the matrix and the fiber/matrix interface, which can grow under low-temperature thermal cycling and coalesce to form transverse matrix cracks and cause fiber/matrix debonding, leading to degradation of FRP composites. The severity of cracking is directly related to the amount of resin shrinkage during curing. The authors (Lord and Dutta (1988)) also found that even if the composites were produced in a state free of stress, the subsequent thermal cycling usually produced microcracks. Transverse matrix cracking can affect laminate stiffness, strength, dimensional stability and fatigue resistance. Freeze–thaw effects can be more severe due to moisture-initiated effects causing microcrack growth and coalescence because of the temperature cycling. In addition, the presence of deicing salt in wet conditions with subsequent freeze–thaw cycling can cause microcrack formation and gradual degradation due to crystal formation and increased salt concentration, in addition to effects of moisture – including swelling and drying (Karbhari *et al*., 2003).

In general, the reported literature shows that unidirectional tensile strengths decrease in the –10 to –40°C range, whereas the off-axis and transverse strengths may increase due to matrix hardening; increasing freeze–thaw cycles have been shown to accentuate residual stresses resulting in increased severity and density of cracks. An apparent increase in matrix brittleness and decrease in tensile strength was also reported (Lord and Dutta, 1988; Benmokrane *et al*., 1998; Burgoyne, 2001). On the other hand, Shao and Kouadio (2002) have shown that samples from pultruded GFRP sheets saturated in water have an excellent resistance to freeze–thaw cycles. The authors observed nearly no changes in the tensile properties of FRP composites after 564 cycles between 4.4 and –17.2°C, even if samples were saturated with water.

Mashima and Iwamoto (1993) studied the change in bond characteristics due to freeze–thaw action on non-metallic reinforcement made up of synthetic fibers such as carbon, aramid and vinylon fibers. The bond strength was measured by the pullout test after 200 freezing and thawing cycles. The freeze–thaw cycle testing of the $10 \times 10 \times 10$ cm cube specimens began after 14 days curing in water at 20°C. Four types of FRP rods – CFRP, GFRP, AFRP, and vinylon FRP (VFRP) – and steel reinforcing bars were used in the study. It was determined that the bond strength of GFRP, VFRP and CFRP rods was not influenced by freeze–thaw, but AFRP (both braided and coiled types) rods showed a gradual reduction of bond strength up to about 20% as freezing and thawing progressed.

11.3.4 Effect of thermal expansion

As is the case for freeze–thaw cycling, the effect of thermal expansion of composite materials and concrete is of great interest. In fact, civil engineering

structures experience temperatures in the range of –30°C to +80°C during their service life. Reinforced concrete itself is a composite material, where the reinforcement acts as the strengthening medium and the concrete as the matrix. Therefore, it is imperative that under thermal stresses the behavior of the two materials is similar, so that differential deformation of the concrete and the reinforcement is minimized. For FRP–concrete systems, the different mechanical/thermal properties of the constituents will lead to thermal restraint stresses when subjected to temperature changes. The resultant axial and radial stresses in the FRP element itself may not be significant; however, its radial thermal expansion may cause a considerable stress field in the surrounding concrete. In the cases of CFRP and GFRP reinforcing bars, the resin matrix controls the mechanical properties that depend on temperature. The glass transition temperature of the resin, T_g, has to exceed the maximum service temperature.

In conventional steel-reinforced concrete structures, the coefficient of thermal expansion for a steel reinforcing bar and the concrete is almost similar. On the other hand, the coefficients of thermal expansion for FRP reinforcing bars vary in the longitudinal and transverse directions depending on the types of fiber and resin, the volume fraction of fiber and the orientation of the fibers. Moreover, the resin as a binding material has a very large expansion coefficient. Therefore, thermal stresses are developed at the interfaces between the FRP reinforcing bar and the concrete. FRP reinforcing bars generally consist of unidirectional fibers, except when the surface configuration is modified through the use of veils or different fiber types. Absence of transverse fibers results in the transverse coefficient of thermal expansion being higher than the longitudinal one; the transverse coefficient is then 5 times larger than the coefficient of concrete, which causes an important mismatch. The longitudinal thermal expansion of an FRP reinforcing bar is relatively low, since it is mainly due to the fiber. However as stated above, the transverse expansion coefficient of FRP reinforcing bars is mainly due to the resin and is 3–5 times larger than that of concrete. The coefficient of thermal expansion of GFRP reinforcing bars is 9.9×10^{-6} mm/mm/°C. In addition, the expansion coefficient of other FRP reinforcing bars is different from that of concrete and steel, and even becomes negative in the case of AFRP rods. As a consequence, due to the difference in expansion and contraction between the FRP reinforcing bar and the concrete, forces develop in a concrete member subjected to temperature variation. The presence of moisture or other chemicals in the FRP reinforcing bars contributes to further degradation.

11.3.5 Creep and relaxation

Polymer resins generally exhibit creep and relaxation behavior. Since glass and carbon fibers are linear elastic to failure, the addition of these fibers

increases the creep resistance of the resins. Moreover, the creep behavior of FRP composites strongly depends on the structure of the material (especially fiber orientation) and the load condition of the material. Consequently, creep and relaxation behavior are more pronounced when a load is applied transversely to the fibers or when the composite has a low fiber volume fraction. For these reasons, for unidirectional FRP composites, the creep compliance is less affected by the creep behavior of the polymer matrix when the material is loaded along the fiber direction. For off-axis loading, the creep behavior is strongly dependent on the creep of the matrix. For FRP composites reinforced with discontinuous randomly orientated fibers or with continuous bi-directional woven fibers, the properties of the material are matrix dominated, therefore creep of the polymer matrix is the main reason for the creep behavior of FRP composites. Typically, thermosetting resins (unsaturated polyesters, vinylesters, epoxies and phenolics) are more resistant to creep than are thermoplastics (polypropylene, nylon, polycarbonates, etc.). Under-cured resins are susceptible to creep during the early stages of service, but this susceptibility diminishes with time.

In addition, physical aging, temperature, moisture and stress levels could affect the creep behavior of FRP composites; some data related to these parameters can be found from recent reviews (Scott *et al*., 1995; Liao *et al*., 1998; Weitsman and Elahi, 2000), although data on the effect of moisture absorption on creep behavior are rare. Fluids and time can often affect the creep behavior of FRP composites in a manner similar to the effect of temperature and time. Fluid absorption in FRP composites will lead to the development of residual stress and plasticizing of the resin, which can accelerate time-dependent behavior of FRP composites. Liao *et al*. (1998) schematically described the effect of time, temperature and fluids on the creep behavior of FRP composites; the authors concluded that creep compliance was increased with the increase in fluid content and temperature over time.

In terms of test results, most of the published literature concerns results from uniaxial tension tests. Relatively little work has been conducted on compression and bending tests; this is mainly due to the difficulties in setting up the tests and accurately controlling the test data (Liao *et al*., 1998). There is also less literature available concerning creep relaxation and cure kinetics in natural service environments of ambient-cured vinylesters, polyester and epoxies (Morgan *et al*., 1999). In general, the creep behavior of carbon fiber-reinforced composites is well documented. However, only limited data exist for pultruded GFRP composites and their structural members. Yamaguchi *et al*. (1997) performed experiments to investigate the creep properties of 6 mm diameter AFRP, CFRP and GFRP bars in a 1000 hour creep test. Creep tests were performed at various load levels for 1000 hour duration while strain measurements were made. The findings indicated a linear relationship between the loading level for the FRP rods and the logarithm of the time to

rupture. Each type of FRP rod has a unique creep failure behavior depending on the degree of loading and the fiber's characteristics.

Creep-rupture (stress-rupture) is another important concern when FRP composites are subjected to long-term loading. Creep-rupture is the tensile fracture of a material subjected to sustained high stress levels over a period of time and occurs when a material strain capacity is reached. As the ratio of the sustained tensile stress to the short-term strength of the FRP bars increases, endurance time decreases. The creep-rupture endurance time can irreversibly decrease under sufficiently adverse environmental conditions – such as high temperature, ultraviolet radiation exposure, high alkalinity, wet and dry cycles, or freeze–thaw cycles. Creep-rupture is particularly important for prestressed and reinforced concrete structures with high permanent load.

In general, carbon fibers are the least susceptible to creep-rupture, aramid fibers are moderately susceptible and glass fibers are the most susceptible to creep-rupture. Creep-rupture tests have been conducted on GFRP, CFRP and AFRP bars with 0.25 in (6.25 m) diameter. The bars were tested at different load levels at room temperature, the results indicated that a linear relationship exists between creep-rupture strength and the logarithm of time for all load levels. Extrapolation of short-term creep data to longer service lifetimes in room temperature air suggested rupture strengths of 29–55%, 47–66% and 79–93% of the initial strength for essentially unidirectional GFRP, AFRP and CFRP bars, respectively (Yamaguchi *et al.*, 1997; Greenwood, 2002).

In another study, the ratio of the stress at creep-rupture to the ultimate strength after 50 years calculated using a linear relationship was found to be 0.66 for AFRP and 0.79 for CFRP (Ando *et al.*, 1997). Tests were also conducted to study the environmental effects on the creep-rupture strength and to evaluate the creep-rupture strength of GFRP (Dolan *et al.*, 1999). Short-term (48 hours) and long-term (1 year) sustained loads corresponding to 50% of the initial ultimate strength were applied to GFRP and CFRP bars at room temperature.

Benmokrane (2000) studied the stress-rupture mechanism of GFRP bars in various alkaline environments (NaOH, simulated pore water, moist concrete) under different stress levels (22–68% of ultimate strength). The results obtained indicate that the stress-rupture mechanism of GFRP bars depends on the environment and the stress level. Under a stress level of about 20–30% of the ultimate strength, in NaOH solution, the stress-rupture mechanism mainly involves the damage of fibers; while in simulated pore water solution and in a concrete environment, the stress-rupture is caused by interface damage. At high stress levels, above 55%, matrix and fiber cracking are the most dominant mechanisms.

Nkurunziza *et al.* (2005) conducted stress-rupture tests on GFRP bars. Two test series, with 9.5 mm diameter sand-coated bars were investigated under two different stress corrosion environmental conditions. The first series

consisted of ten specimens immersed in deionized water, stressed to 30% of ultimate strength, and subjected to a temperature range of 65.5 to 75.5°C. The other series consisted of ten specimens immersed in alkaline solution (pH = 13.11 at room temperature), stressed to 40% of ultimate, and subjected to the same temperature range. After 60 days of exposure, the loss of tensile strength was 4% and 11% for the first and the second series, respectively.

Almusallam *et al*. (2002) also conducted stress-rupture tests, but on GRFP bars embedded in concrete beams. Twenty-four concrete beams of 100 × 100 × 2000 mm with a single 10 mm diameter GFRP bar were loaded to create stress levels in the bar of 20–25% of the UTS. The maximum reductions in tensile strength for unstressed specimens submerged in tap water and sea water were about 5% and 2%, respectively. For stressed GFRP bars, the maximum reduction in tensile strength in sea water, and sea water under wet and dry conditions, was 30 and 28%, respectively.

Different models have been proposed to predict the stress-rupture behavior of FRP bars; Gerritse (1998) developed a linear relationship between stress-rupture strength and logarithm time. This can be written as follows:

$$\frac{\delta_{sus}}{f_t} = A + B \log t$$

where, δ_{sus} is the sustained applied stress, f_t is the short-term tensile strength, t is the time in hours, and A and B are constants.

Yamaguchi *et al*. (1999) proposed a model to calculate the creep-rupture time based on failure statistics of both resin and fibers.

11.3.6 Fatigue

Over the last several decades, extensive fatigue data for FRP composites have been generated for other industrial applications (Liao *et al*., 1998; Weitsman and Elahi, 2000). However, limited studies have been conducted on the fatigue performance of pultruded FRP composites (bars, tendons, sheets, plates and FRP structural shapes) for civil infrastructure applications. The fatigue performance of FRP composite materials depends on the matrix composition and on the type of fiber. Liao *et al*. (1998) demonstrated that the matrix composition has a greater effect on the fatigue performance than the type of fiber used. Cyclic loading promotes the creation and development of flaws and microcracks in FRP materials. In addition, as frequency of loading increases, the stress difference between fiber and resin increases, resulting in interfacial damage. The cyclic loading category in bridges is called high-cycle or fatigue loading, where the load history contains in the range of 2 million cycles at a low bond stress range. Such high-cycle loading is considered a problem at service load levels. The most significant effect of high-level repeated loads is the reduction of bond at failure. Moreover, since bridge

decks are subjected to excessive cyclical loads and degradation in properties under long-term environmental exposure, endurance limits for FRP reinforcement in tension-fatigue should be established. In addition, endurance limits under varying temperatures (–28 to 60°C) have to be established to arrive at threshold limits for designing structures with FRP reinforcement.

The bond mechanism of FRP reinforcing bars in concrete was studied by Katz (2000) in order to evaluate the effect of cyclic loading. Five different types of reinforcing bars were tested. The FRP rods were embedded in concrete blocks and subjected to up to 450 000 cycles at service stress levels. During loading the specimens were kept immersed in water at 60 and 20ºC to accelerate deterioration effects. The results indicated a reduction in the bond strength after loading. Three mechanisms of failure were identified: (a) abrasion of the surface of the rod which may lead to a reduction of 20–30% in the bond strength; (2) delamination of the outer layer of the resin at the surface of the rod which may lead to a reduction of up to 60% in the bond strength; and (c) abrasion of the cement particles entrapped between the rod and the concrete. There was no significant change in the effect of curing temperature on the loss of bond.

From the reported literature (Benmokrane and Rahman, 1998; Burgoyne, 2001), some general tendencies can be observed on unidirectional FRP coupons with 60% fiber volume fraction, under tension-tension fatigue testing in an ambient laboratory environment. Of all the types of FRP composites for civil infrastructure applications, the CFRP composite is generally reported to be least prone to fatigue loading. At 1 million cycles, the fatigue strength is generally between 50 and 70% of the initial static strength and is relatively unaffected by realistic moisture and temperature exposure of concrete structures unless constituent materials are substantially degraded by the environment.

Based on the fatigue tests of up to 2.25 million cycles conducted at frequencies under 4.25 Hz by Vijay and Gangarao (1999), it is concluded that beams reinforced with GFRP reinforcing bars and designed for compression failure have a better fatigue life as compared with those designed for tension failure. This is due to the larger depth of compression block available in the case of beams designed for compression failure. It is suggested that, due to fatigue considerations, the maximum concrete strains at working loads should be limited to well below 750×10^{-6} (25% of ε_{cu}, where ε_{cu} is the ultimate strain of concrete) for GFRP-reinforced concrete beams designed for compression failure.

Although aramid fibers show poor durability in compression, the tension-tension fatigue behavior of an impregnated aramid fiber bar is excellent. Two-million-cycle endurance limits for commercial AFRP bars in concrete applications have been reported as being in the range of 54–73% of the initial tensile strength (Odagiri *et al.*, 1997). Based on these observations,

Odagiri *et al.* (1997) suggested that the maximum stress should be set at between 0.54 and 0.73 times the tensile strength.

Studies on the fatigue behavior of FRP tendons indicated that the fatigue life of FRP tendons in prestressed concrete beams is shorter than that of tendons tested in air. For loaded post-tensioned beams, curvature of the tendon profile causes the tendon to rub against the teeth of the given crack instigating premature failure. Special attention needs to be given to the fatigue resistance of the anchorage. Such devices can usually develop the full tendon strength under monotonic load conditions, but develop less than this value when a cyclic load is applied. Rostasy and Budelmann (1991) evaluated the Wöhler curves for GFRP tendons. The authors reported that the fatigue strength of GFRP tendons is influenced by anchorage properties. However, the fatigue strength of GFRPs is markedly below that of wedge-anchored prestressing wire. Rahman *et al.* (1996) have conducted tensile fatigue tests on 65% fiber volume fraction carbon-epoxy CFRP reinforcing bars encased in concrete at a stress ratio of 0.1 and a cycling rate of 4 Hz. The reinforcing bars were found to have a fatigue life of 4 million cycles, if the maximum stress is below 38% of the tensile strength.

Saadatmanesh and Tannous (1999) studied the relaxation, creep and fatigue behavior of commercially available CFRP tendons (Leadline PC-D8 with 8 mm diameter and CFCC (Carbon Fiber composite concrete) with 7.5 mm diameter). For the fatigue tests, the investigators used ambient laboratory conditions with sinusoidal load control at 3–5 Hz; there were seven different minimum loads corresponding to 30, 40, 50, 60, 70, 80 and 90% of ultimate strength and three different stress ranges corresponding to about 5, 10 and 20% of ultimate strength. The results indicated that the residual strength of Leadline and CFCC decreased by less than 10% of virgin ultimate strength. There was little change in the modulus of both tendons at the lower stress ranges, but some increase was noted at higher stress ranges. No change in Poisson's ratio was noted in the Leadline tendon.

Exposure environments (elevated temperatures, humidity and corrosive fluids) reduce the fatigue life of FRP composites. These effects depend on the fiber and matrix types, laminate lay-up, pre-conditioning methods, solution content, and the environmental conditions during fatigue, especially the interface between the fiber and the matrix. In general, the effects of environmental conditions on tensile fatigue behavior are well documented for aerospace composite materials, but there is a lack of the data for effect of exposure environments on the flexural and compression fatigue behavior for pultruded FRP composites. There is very limited long-term fatigue data, especially beyond 10 million cycles (Liao *et al.*, 1998).

Other parameters – such as alkalinity, salinity of concrete, temperature, surface deformation, ratio of maximum to minimum cyclic stress and loading frequency – were also found to affect the fatigue life of FRP composites

(Rahman *et al*., 1997). The fatigue strength of CFRP bars encased in concrete has been observed to decrease when the environment temperature increased from 20°C to 40°C (Adimi *et al*., 1998). In the same investigation, the endurance limit was found to be inversely proportional to the loading frequency. It has also been found with CFRP bars that the endurance limit also depends on the ratio of maximum to minimum cyclic stress. Higher mean stress or lower stress ratio (minimum divided by maximum) will cause a reduction in the endurance limit (Saadatmanesh and Tannous, 1999). The addition of ribs, wraps and other types of deformations are commonly used to improve the bond behavior of FRP bars. Such deformations, however, have been shown to induce local stress concentrations that significantly affect the performance of CFRP bars under fatigue loading (Katz, 1998). Local stress concentrations degrade fatigue performance by imposing multiaxial stresses that serve to increase matrix-dominated damage mechanisms.

11.3.7 High temperature

It is well known that organic matrix-based, fiber-reinforced materials exhibit viscoelastic transitions followed by reversible and irreversible thermal degradation when exposed to elevated temperature, especially at temperatures close to or above the glass transition temperature. Above the glass transition temperature, the elastic modulus of a polymer will be significantly reduced due to change in its molecular structure. The value of the glass transition temperature depends on the type of resin, and is normally in the range of 90–150°C in a composite material. The fibers, which exhibit better thermal properties than the resin, can continue to support some load in the longitudinal direction until the temperature threshold of the fibers is reached. This occurs at temperatures near 980°C for glass fibers and 175°C for aramid fibers. Carbon fibers are capable of resisting temperatures in excess of 1650°C. However, the tensile properties of the composites are reduced due to a reduction in force transfer between fibers through the bond to the resin. Test results have indicated that a temperature of 250°C (much higher than the glass transition temperature) reduced the tensile strength of GFRP and CFRP composites by more than 20% (Kumahara *et al*., 1993). Other properties more directly affected by the shear transfer through the resin, such as bending strength, reduce significantly at higher temperature.

Using the available literature, Kodur and Baingo (1999) compared the behavior of FRP composites with that of traditional building materials at elevated temperature; the rate of strength loss was much greater for FRPs than for concrete and steel. FRP composites lost little strength when the temperature was below 100°C. After that temperature, the strength degradation became much faster, resulting in 50% strength loss at 200°C. In the case of concrete, a 50% strength loss did not occur until about 700°C, whereas for

steel the corresponding temperature was 500°C, the critical temperature for FRP composites was much lower than that for steel. In the same way, Katz *et al*. (1999) determined that FRP reinforcing bars showed a reduction of between 80 and 90% in bond strength as the temperature increased from 20 to 250°C, compared with only 38% reduction for steel reinforcing bars in the same temperature range. The effects of high temperature on the properties of FRP bars were studied by Kumahara *et al*. (1993), who found a reduction of 20% in the tensile strength of glass and carbon fiber FRP bars at a temperature of 250°C. The reduction in the tensile strength of aramid fiber bars was 60% at 250°C. However, prolonged thermal aging at a high temperature combined with sustained loading can cause deterioration in the properties of the matrix (Chin *et al*., 1988; Uomoto, 2004). Research is still ongoing in different research groups around the world to improve the performance of FRP composites at high temperatures.

The fire endurance of FRP internal reinforcement is also one of the major safety requirements in the design of structures and buildings. Parametric studies were carried out to investigate the effect of a range of parameters on the fire performance of FRP-reinforced concrete slabs (Kodur *et al.*, 2005). The results of the parametric studies show that FRP-reinforced concrete slabs have lower fire resistance than slabs reinforced with conventional reinforcing steel, when fire endurance is defined in terms of the critical temperature of the reinforcement. In this context the main factors that influence the fire resistance of FRP-reinforced concrete slabs are: the concrete cover thickness, the type of reinforcement and the type of aggregate in the concrete. Kodur *et al.* (2005) conclude that the reinforcement type has a significant effect on the predicted fire resistance of reinforced concrete slabs, with FRP-reinforced concrete slabs having much lower fire resistance compared with those reinforced with steel. This conclusion is based on the assumed critical temperatures for FRP rebars as compared with conventional steel reinforcement, and does not account for thermally induced bond degradation, which may be severe at temperatures well below the critical temperature of the FRP reinforcement. The critical temperature for tensile reinforcement has been defined as the temperature at which it loses much of its strength (50% loss of room temperature yield strength) and can no longer support the applied load (Lie, 1992). The critical temperatures for CFRP, GFRP and conventional reinforcing steel have been defined as 250, 325 and 593°C.

11.4 Design and application recommendations

For design purposes, it is clear that the design engineer must take into consideration the durability parameter. Therefore, civil engineers, contractors and designers must take care about the long-term behavior of FRP composites in different environmental conditions and then design structures with this

behavior in mind. For these reasons, a relatively large safety factor is commonly proposed to allow for the uncertainty.

For field applications, it is vital to determine the optimum combination of resin matrix and fiber, sizing chemistry and manufacturing process for maximum durability. Several studies (Benmokrane *et al.*, 1998; Chin *et al.*, 2001; Al-Zahrani, 2005) have been conducted on the effects of the reinforcing bar constituents on performance and durability. The constituents of new generation GFRP reinforcing bars have been modified based on the results of the studies in this field of research.

FRP reinforcing bars with modified fiber architecture have to be evaluated for the long-term serviceability of a deck system. Thermal creep, thermal fatigue and thermal stress build-up in concrete environments have to be established and the long-term durability of FRP reinforced concrete bridge decks properly accounted for.

The extensive research performed has paved the way for the publication of codes and handbooks on the use of FRP reinforcing bars and prestressing tendons in the reinforcement and rehabilitation of new and existing bridges and structures. Design codes in North America and Japan (Japanese Society of Civil Engineers, 1997; CAN/CSA-S6-00, 2000; ISIS-M03-01, 2001; CAN/CSA-S806-02, 2002; ACI 440.1R-03, 2003; ACI 440.3R-04, 2004; ACI 440.4R-04, 2004) provide factors for the reduction of resistance to account for the effects of environmental conditions, creep from sustained loads and fatigue from repeated loads.

11.5 Conclusions and future trends

Karbhari *et al*. (2003) conducted a durability gap analysis for FRPs for civil engineering applications. Based on this study, it appears that there is a substantial commonality of needs, which provides for the selection of a set of data/research requirements that is critical to the generic implementation of FRP composites in civil infrastructures (Karbhari *et al*., 2003). The recommendations are summarized below.

- Collection, assessment and appropriate documentation of available data in a form useable by the civil engineer/designer.
- Testing over extended (more than 18 months) time periods. Tests conducted over short time periods (less than 18 months) can yield misleading results due to effects of post-cure and slow interphase- and fiber-level degradation, and can provide an erroneous level of comfort in some cases.
- Testing under combined conditions (stress, moisture, solution, temperature and/or other regimes) at both the material and structural levels is critical.
- Assessment and characterization of the effects of incomplete cure and undercure, especially for ambient-temperature cure systems, are essential.

- Development of standardized solutions and conditions for laboratory studies that closely simulate actual field conditions.
- Development of appropriate resin systems, gel coats and coatings that would serve as protective layers for the bulk composite against external influences – including environmental conditions, and intended and accidental damage.

Furthermore, due to the introduction of FRP composites in concrete structures, the durability performance of FRP-reinforced concrete structures becomes more complex due to the combined effects of FRP composites, the interface, the concrete and various environmental and mechanical conditions. Therefore, the complete process of assessing the durability of FRPs in association with concrete structures is a very complex task. For these reasons, the necessity for a wide-ranging assessment of the durability of FRP composites in association with concrete, and as an individual material, cannot be overemphasized.

11.6 References

ACI (American Concrete Institute) (2003) ACI 440.1R-03, *Guide for the Design and Construction of Concrete Reinforced with FRP Bars*, Farmington Hills, Michigan: American Concrete Institute.

ACI (American Concrete Institute) (2004) ACI 440.3R–04, *Guide Test Methods for Fiber Reinforced Polymers (FRP) for Reinforcing or Strengthening Concrete Structures*, Farmington Hills, Michigan: American Concrete Institute.

ACI (American Concrete Institute) (2004) ACI 440.4R–04, *Prestressing Concrete Structures with FRP Tendons*, Farmington Hills, Michigan: American Concrete Institute.

Adimi, R., Rahman, H., Benmokrane, B., Kobayashi, K. (1998) Effect of temperature and loading frequency on the fatigue life of a CFRP reinforcing bar in concrete, Proceedings of the 2nd International Conference on Composites in Infrastructure (ICCI'98), Tucson, Arizona eds Saadatmanesh, H. and Ehsani, M. vol. 2, pp. 203–210.

Allred, R. E. (1984) The effects of temperature and moisture content on the flexural response of Kevlar/epoxy laminates: Part II [45/0/90] filament orientation, *Environmental Effects on Composite Materials*, vol. 2, ed. Springer, G., Lancaster, Pennsylvania: Technomic Publishing Company Inc.

Almusallam, T. H., Al-Salloum, Y. A., Alsayed, Y. H., Albozaimy, A. M. (2002) Tensile strength of GRFP bar in concrete beams under sustained loads at different environments, Proceedings of the 2nd International Conference on Durability of FRP Composites for Construction, (CDCC 2002), Montreal, Quebec, eds Benmokrane, B., El-Salakawy, E., pp. 523–534.

Al-Zahrani, M. (2005) Effect of accelerated laboratory conditions on tensile strength and moisture absorption of two GRFP bars, Proceedings of Composites in Construction 2005 – 3rd International Conference, Lyon, France, pp. 775–782.

Ando, N., Matsukawa, H., Hatorri, A., Mashima, A. (1997) Experimental studies on the long-term tensile properties of FRP tendons, Proceedings of the 3rd International Symposium on Non-Metallic (FRP) Reinforcement for Concrete Structures, (FRPRCS-3), Japan Concrete Institute, Tokyo, Japan, vol. 2, pp. 203–210.

Benmokrane, B. (2000) Improvement of the durability performance of glass fiber reinforced polymer (GFRP) reinforcements for concrete structures, Technical Report, Civil Engineering Department, University of Sherbrooke.

Benmokrane, B., El-Salakawy, E., eds (2002) *Durability of Fiber Reinforced Polymer (FRP) Composites for Construction:*, proceedings of the 2nd International Conference (CDCC 02), Montreal, Quebec, Canada, May 28–31.

Benmokrane, B., Rahman, H., eds (1998) *Durability of Fiber Reinforced Polymer (FRP) Composites for Construction*, Proceedings of CDCC'98, Sherbrooke, Québec, Canada.

Benmokrane, B., Wang, P. (2001) Durability of FRP composites for civil infrastructure applications, Civil Engineering Department, University of Sherbrooke.

Benmokrane, B., Rahman, H., Ton-That, M. T., Robert, J. F. (1998) Improvement of the durability performance of FRP reinforcement for concrete structures, Proceedings of the 1st International Conference on Durability of FRP Composites for Construction, CDCC '98, Sherbrooke, Quebec, Canada, pp. 571–586.

Burgoyne, C. J. (2001) Proceedings of Fiber-Reinforced Plastics for Reinforced Concrete Structures, FRPRCS-5, Cambridge UK, vol. 1–2, 1152 p.

CAN/CSA (Canadian Standards Association) (2000) CAN/CSA-S6-00, *Canadian Highway Bridge Design Code*, Rexdale, Ontario, Canada: CSA International.

CAN/CSA (Canadian Standards Association) (2002) CAN/CSA-S806-02, *Design and Construction of Building Components with Fiber Reinforced Polymers*, Rexdale, Ontario, Canada: Canadian Standards Association.

Chin, J. (1996) Materials aspects of fiber reinforced polymer composites in infrastructure, NISTIR 5888, Galthersburg, MD: National Institute of Standard and Technology.

Chin J., Haight M. R., Hughes W. L., Nguyen T. (1988) Environmental effects on composites matrix resins used in construction. Proceedings of the 1st International Conference on Durability of Fibre Reinforced Polymer (FRP) Composites for Construction (CDCC'98), Sherbrooke, Quebec, Canada, eds Benmokrane, B. and Rahman, H., pp. 229–241.

Chin, J., Aouadi, K., Haight, M. R., Hughes, W. L., Nguyen, T. (2001) Effects of water, salt solution and simulated concrete pore solution on the properties of composite matrix resins used in civil engineering applications, *Polymer Composites*, **22**(2), 282–297.

Dejke, V. (1998) Durability of fiber reinforced polymers (FRP) as reinforcements in concrete structures – An update of knowledge and an overview of current research activities, Technical report, Department of Building Materials, Chalmers University of Technology, pp. 98–108.

Dolan, C.W., Rizkalla, S., Nanni, A. eds (1997) *Fiber Reinforced Polymer Reinforcement for Reinforced Concrete Structures*, Proceedings of the 4th International Symposium, ACI SP-188 Farmington Hills, MI: American Concrete Institute.

DuPont De Nemours & Co. (1992) *Kevlar Data Sheet*, Wilmington, Delaware.

El-Salakawy, E., Benmokrane, B., Desgagné, G. (2003) FRP composites bars for the concrete deck slab of Wotton Bridge, *Canadian Journal of Civil Engineering*, **30**(5), 861–876.

Faza, S., Gangarao, H., Ajjarapu, S. (1994) Strength and stiffness degradation of glass reinforced polyester and vinyl ester structural plates, West Virginia University, Constructed Facilities Centre, Morgantown, West Virginia.

Gerritse, A. (1998) Assessment of long term performance of FRP bars in concrete structures, Proceedings of the 1st International Conference on Durability of FRP Composites for Construction (CDDC '98), Sherbooke, Quebec, eds Benmokrane, B. and Rahman, H., pp. 285–297.

Gopalan, R., Somashekar, B. R., Dattaguru, B. (1989) Polym. Degrad. Stability, vol. 24, p. 361–371.

Greenwood, M. (2002) Creep-rupture testing to predict long-term performance, Proceedings of the 2nd International Conference on Durability of Fiber Reinforced Polymer (FRP) Composites for Construction (CDD C'02), eds Benmokrane, B. and El-Salakawy, E. Québec, Canada.

Hancox, N. L., Mayer, R. M. (1994) Design data for reinforced plastics, New York: Chapman and Hall, pp. 202–204.

Harries, K. A., Porter, M. L., Busel, J. P. (2003) FRP materials and concrete-research needs, *ACI Concrete International*, **25**(10), 69–74.

Hojo, H., Tsuda, K., Ogasawara, K. (1991) Form and rate of corrosion–resistance FRP resins, *Advanced Composite Materials*, **1**(3), 55–67.

Huckelbridge, A., Eitel, A. K. (2003) Preliminary performance observations for FRP reinforced concrete bridge deck, American Concrete Institute (ACI) Special Publication, *Field Applications of FRP Reinforcement: Case Studies*, SP-215-7 Farmington Hills, Michigan: American Concrete Institute, pp. 121–138.

ISIS (Intelligent Sensing For Innovative Structures) (2001) ISIS-M03-01, *Reinforcing Concrete Structures with Fiber Reinforced Polymers*, University of Manitoba, Winnipeg, Manitoba, Canada: The Canadian Network of Centres of Excellence, ISIS Canada.

Japanese Society of Civil Engineers (1997) *Recommendations for Design and Construction of Concrete Structures using Continuous Fiber Reinforced Materials*, Tokyo, Japan: Japanese Society of Civil Engineering.

Judd, N. C. W. (1971) The chemical resistance of carbon fibers and a carbon fiber/polyester composite, First International Conference of Carbon Fibers, Plastics Institute, pp. 1–8.

Karbhari, V. M., Chin, J. W., Hunston, D., Benmokrane, B., Juska, T., Morgan, R., Lesko, J. J., Sorathia, U., Reynaud, D. (2003) Durability gap analysis for fiber-reinforced polymer composites in civil infrastructure, *Journal of Composites for Construction*, **7**(3), 238–247.

Katsuki, F., Uomoto, T. (1995) Prediction of deterioration of FRP rods due to alkali attack, (FRPRCS-2), ed. Taerwe, L., London: E & F Spon pp. 108–115.

Katz, A. (1998) Effect of helical wrapping on fatigue resistance of GFRP. *Journal of Composites for Construction*, **2**(3), 121–125.

Katz, A. (2000) Bond to concrete of FRP reinforcing bars after cyclic loading, *Journal of Composites for Construction*, **4**(3), 137–144.

Katz, A., Berman, N., Bank, L. C. (1999) Effect of high temperature on bond strength of FRP reinforcing bars, *Journal of Composite for Construction*, **3**(2), 73–81.

Kodur, V. K. R., Baingo, D. (1999) Fire resistance of FRP reinforced concrete slabs, IRC Internal Report (758) National Research Council. Ottawa, Canada, 37.

Kodur, V. K. R., ASCE, M., Bisby, L. A. (2005) Evaluation of fire endurance of concrete slabs reinforced with fiber-reinforced polymer bars, *Journal of Structural Engineering*, **131**(1), 34–43.

Kumahara, S., Masuda, Y., Tanano, Y. (1993) Tensile strength of continuous fiber reinforcing bar under high temperature, ACI SP-138, *Fiber-Reinforced-Plastic Reinforcement for concrete Structures - International Symposium*, eds Nanni, A., Dolan, C.W., Farmington Hills, Michigan: American Concrete Institute, pp 731–742.

Liao, K., Schultheisz, C. R., Hunston, D. L., Brinson, L. C. (1998) Long-term durability of fiber-reinforced polymer-matrix composite materials for infrastructures application: a review, *Journal of Advanced Materials*, **30**(4), 3–40.

Lie, T. T., ed. (1992) Structural Fire Protection. Manuals and Reports on Engineering Practice No. 78, New York: American Society of Civil Engineers.

Litherland, K. L., Okley, D. R., Proctor, B. A. (1981) The use of accelerated aging procedures to predict the long term strength of GRC composites, *Cement and Concrete Research*, **11**, 455–466.

Lord, H. W., Dutta, P. K. (1988) On the design of polymeric composite structure for cold regions application, *Journal of Reinforced Plastics and Composites*, **7**, 435–459.

Malvar, L. J. (1998) Durability of composites in reinforced concrete, Proceedings of the 1st International conference on Durability of FRP Composites for Construction (CDDC '98), eds Benmokrane, B. and Rahman, H., Sherbrooke, Quebec, Canada, pp. 361–365.

Mashima, M., Iwamoto, K. (1993) Bond characteristics of FRP rods and concrete after freezing and thawing deterioration, ACI SP-138, *Fiber-Reinforced-Plastic Reinforcement for Concrete Structures - International Symposium*, eds Nanni, A., Dolan, C.W., Farmington Hills, Michigan: American Concrete Institute, pp. 51–69.

Masmoudi, R., Nkurunziza, G., Benmokrane, B., Cousin, P. (2003) Durability of glass FRP composite bars for concrete structure reinforcement under tensile sustained load in wet and alkaline environments, Annual Conference of the Canadian Society for Civil Engineering, Moncton, New Brunswick.

Morgan, R. J., Dunn, C., Edwards, C. (1999) Research panel report: creep and relaxation, Civil Engineering Research Foundation Manufacturing Development Association Study on Durability of Composites in Civil Engineering.

Murphy, K., Zhang, S. and Karbhari, V. M. (1999) Effect of concrete based alkaline solutions on short term response of composites, Proceeding of 44th Int. SAMPE Symposium and Exhibition, Society for the Advancement of Material and Process Engineering, Long Beach, Calif., 2222–2230.

Nkurunziza, G., Benmokrane, B., Debaiky, A. S., Masmoudi, R. (2005) Effect of sustained load and environment on long-term tensile properties of glass FRP reinforcing bars, *ACI Stuctural Journal*, **102**(4), 615–621.

Odagiri, T., Matsumoto, K., Nakai, H. (1997) Fatigue and relaxation characteristics of continuous aramid fiber reinforced plastic rods, Proceedings of the 3rd International Symposium on Non-Metallic (FRP) Reinforcement for Concretes Structures (FRPRCS-3), Japan Concrete Institute, Tokyo, Japan, vol. 2, pp. 227–234.

Porter, M. L., Barnes, B. A. (1998) Accelerated aging degradation of glass fiber composites, Proceedings of the 2nd International Conference on Composites in Infrastructure (ICC I–98), Tucson, Arizona, eds Saadatmanesh. H., Ehsani, M. R., vol 2, pp. 446–459.

Porter, M., Mehus, J., Young, K. (1995) Aging degradation's of fiber composites reinforcement for structural concrete, Iowa State University, Engineering Research Institute, Ames, Iowa.

Rahman, A. H., Adimi, M. R. Benmokrane, B. (1996) Fatigue Behavior of FRP Reinforcements Encased in Concrete, Proceedings of Advanced Composite Materials in Bridges and Structures (ACMBS-II), ed. M. M. El Badry, Canadian Society for Civil Engineering, Montreal, Canada, pp. 691–698.

Rahman, H., Adimi, R., Crim, J. (1997) Fatigue behavior of carbon FRP grid encased in concrete, Proceedings of the 3rd International Symposium on Non-Metallic (FRP) Reinforcement for Concrete Structures (FRPRCS-3), Japan Concrete Institute, Tokyo, Japan, vol. 2, pp. 219–226.

Rege, S. K., Lakkad, S. C. (1983) Effect of salt water on mechanical properties of fiber reinforced plastics, *Fiber Science and Technology*, **19**, 317–328.

Rostasy, F. S. (1997) Durability of FRP in aggressive environments, Proceedings of the 3rd International Conference on Non-Metallic (FRP) Reinforcement for Concrete Structures (FRPRCS-3), Japan Concrete Institute, Tokyo, Japan, vol. 2, pp. 113–128.

Rostasy, F. S., Budelmann, H. (1991) FRP-tendons for the post-tensioning of concrete structures, Advanced Composite Materials in Civil Engineering Structures, Proceedings of the Specialty Conference, ASCE, Las Vegas, February, pp. 156–166.

Saadatmanesh, H., Ehsani, M. R. (1998) International Conference on Composites for Infrastructure, Proceedings of ICCI'98, Tucson, Arizona, vols 1 and 2.

Saadatmanesh, H. Tannous, F. E. (1999) Long-term behavior of aramid fiber reinforced plastic tendons, *ACI Materials Journal*, **96**(3) 297–305.

Scott, D.W, Lai, J. S., Zureick, A. H. (1995) Creep behavior of fiber-reinforced polymeric composites: a review of the technical literature, *Journal of Reinforced Plastics and Composites*, **14**, 588–617.

Sen, R., Ross, J., Sukamar, S., Snyler, D. (1996) Durability and bond of AFRP pretensioned piles, Research Report, Department of Civil Environmental Engineering, University of South Florida.

Sen, R., Shahawy, M., Sukumar, S., Rosas, J. (1998) Durability of carbon pretensioned elements in a marine environment, *ACI Structural Journal*, **95**(6) 716–724

Shao, Y., Kouadio, S. (2002) Durability of fiberglass composite sheet piles in water, *Journal of Composites for Construction*, **6**(4), 280–287.

Springer, G. S., Sanders, B. A., Tung, R. W. (1980) Environmental effects on glass fiber reinforced polyester and vinylester composites, *Journal of Composite Materials*, **14**, 213–232.

Takewaka, K., Khin, M. (1996) Deterioration of stress-rupture of FRP rods in alkaline solution simulating a concrete environment, Proceedings of Advanced Composite Materials in Bridges and Structures (ACMBS-II), ed. M. M., El-Badry, Canadian Society for Civil Engineering, Montreal, Canada, pp. 649–664.

Uomoto, T. (2001) Durability considerations for FRP reinforcements, Proceedings of Fibre-Reinforced Plastics for Reinforced Concrete Structures (FRPRCS-5) ed. C.J. Burgoyne, London: Thomas Telford. pp. 17–32.

Uomoto, T. (2004) Development of new GFRP with high alkali resistivity, Proceedings of the 4th International Conference on Advanced Composite Materials in Bridges and Structures (ACMBS-IV), Calgary, Alberta (on CD-Rom).

Vijay, P. V., Gangarao, H. V. S. (1999) Development of fiber reinforced plastics for highway application: aging behavior of concrete beams reinforced with GFRP bars, CFC-WVU Report No. 99-265 (WVDOH RP #T-699-FRP1).

Weitsman Y. J. (1998) Effect of fluids on polymer composites–a review. Report MAES 95-1.0 CM. University of Tennessee, Knoxville, USA.

Weitsman, Y. J., Elahi, M. (2000) Effects of fluids on deformation, strength and durability of polymeric composites – an overview, *Mechanics of Time-Dependent Materials*, **4**(2) 107–126.

Yamaguchi, T., Kato, Y., Nishimura, T., Uomoto, T. (1997) Creep rupture of FRP rods made of aramid, carbon, and glass fibers, Proceedings of the 3rd International Symposium on Non-Metallic (FRP) Reinforcement for Concrete Structures (FRPRCS-3), Japan Concrete Institute, Tokyo, Japan, vol 2, pp. 179–186.

Yamaguchi, T., Nishimura, T., Uomoto, T., Takewaka (1999) Simulation for creep rupture of FRP rods based on statistical theory of fracture of fibers, *Transactions of the Japan Concrete Institute*, **21**, 227–234.

12

Durability of external fiber-reinforced polymer strengthening systems

J. J. MYERS,
University of Missouri-Rolla, USA

12.1 Introduction

Composites in construction offer many advantages such as higher strength, lighter weight, corrosion resistance, and design flexibility. Other factors that strengthen the case for using fiber-reinforced polymer (FRP) composites in the rehabilitation and construction of structures are time and tailorability; strengthening techniques using FRP composites allow for cost-efficient retrofit options although in many cases the initial cost of FRP composites is higher then conventional materials. The alarming deterioration of the world's infrastructure and the susceptibility of steel to corrosion have caused engineers to seek out FRP composites as a retrofitting option, especially in structures like buildings, bridges, marine and water front constructions, and chemical plants.

Although impressive inroads have been made into infrastructure applications, there are still barriers that need to be overcome to achieve the full potential of these materials in construction. Currently, the issue of most importance is durability. Of particular concern are such issues as performance degradation in severe operating environments such as marine environments and conditions of extreme temperature, high relative humidity (RH), freeze–thaw (F–T) cycles, ultraviolet radiation, and long-term exposure to de-icing salts.

While a large number of experimental studies have demonstrated the effectiveness of externally FRP-strengthened reinforced concrete (RC) structures, important questions related to long-term behavior and durability still remain. When a concrete structure is strengthened with an externally bonded FRP fabric or pre-cured plate, the most critical aspect of its behavior is that the composite action in the system must be preserved during the designed service life of the structure. To date few studies have considered the long-term durability performance of FRP-strengthened RC structures under combined environmental exposures and stress. The majority of available research studies have focused on the durability performance of the FRP alone rather than the durability performance of concrete members externally

strengthened with FRP as a system under stress. The durability performance of the parent material, including the interfacial bond between the FRP and the substrate, plays a very important role in the overall durability performance of a strengthened member. The cognizance of the long-term behavior of FRP under various environmental exposures is of importance as it directly affects the correlation of durability data of the externally strengthened FRP concrete members with the durability of FRP alone. Furthermore, long-term durability performance data from *in-situ* case studies of structures externally strengthened with FRP systems are lacking.

12.2 Definition and types of environments

Definitions of the types of environments and exposure conditions are given in detail in Chapters 1 and 2 of this book.

12.3 Retrofit and external strengthening of flexural members

External strengthening systems are most often adhesively bonded to the concrete substrate to add additional flexural capacity or shear capacity. External systems may also be pre-cured plates that are mechanically fastened to the RC parent material. Degradation in the external FRP-strengthening system may occur due to deterioration in the FRP material, deterioration in the bond at the FRP–concrete interface, or deterioration in the parent material(s). The following discussion will focus on the state-of-the-art as it relates to deterioration in the FRP material alone, and degradation in the bond between the FRP and the concrete. It is assumed that prior to the installation of an external FRP retrofit, proper care will be taken to replace or repair any existing damage to the parent material(s) and this is not therefore discussed herein.

12.3.1 Durability of fiber-reinforced polymer material alone

Moisture/solution

Significant work has been conducted on the effects of moisture and salt solution on the performance of FRP composites. In general, moisture and salt solution effects primarily have an effect on the strength properties, rather than the modulus, of the composite system. It is also well documented that aramid fibers absorb moisture and this can result in fibrillation. Glass fibers are degraded when exposed to moisture; moisture extracts ions thereby altering the composite fiber structure. Moisture and salt solutions can also adversely

affect the bond behavior of the FRP and the parent material, as further discussed in Section 12.3.2, Moisture/solution.

Alkaline environment

The performance of an FRP system over time in an alkaline or acidic environment depends on the matrix material and the reinforcing fiber. Dry, unsaturated, bare, or unprotected carbon fiber is resistant to both alkaline and acidic environments, while bare glass fiber can degrade over time in these environments. A properly applied resin matrix, however, should isolate and protect the fiber from the alkaline/acidic environment and retard deterioration. The FRP system selected should include a resin matrix resistant to alkaline and acidic environments (ACI Committee, 2002 (440.2R-02)).

Extreme temperature and thermal cycling

The primary effects of temperature at the composite level are related to the viscoelastic response of the resin. As temperature increases, the modulus of the resin will decrease. If the temperature exceeds the glass transition temperature (T_g), FRP composite performance will decrease substantially. Thermal cycling in general does not cause harmful effects, although extended thermal cycling of brittle resin systems can result in microcrack formation. Issues related to the coefficient of thermal expansion (CTE) of the composite and parent material(s) are discussed in Section 12.3.2, Extreme temperature and thermal cycling.

Freezing and thawing

In general, low temperature and freezing and thawing exposures do not affect fibers, although they can affect the resin and the fiber–resin interface. Polymeric resin systems are known to embrittle, resulting in increased strength and stiffness under sub-zero (but non-cryogenic) conditions. Freezing and thawing effects can be more severe due to moisture-initiated effects causing microcrack growth and coalescence because of cycling. The presence of road salts in wet conditions with subsequent freezing and thawing can cause microcrack formation and gradual degradation due to crystal formation and increased salt concentration (ACI Committee, 2006 (440.R-06)).

Creep

Most externally bonded FRP systems are intended to strengthen or restore an existing structure to the original design capacity that has been lost due to deterioration, steel corrosion for example. In these cases, the level of sustained

load carried by the FRP will probably be low. As long as the sustained load is kept below the limits prescribed in ACI 440.2R-02 (ACI Committee, 2002), the remaining capacity of the FRP system will still be available to resist live load. If, however, a change of use is proposed for a structure previously strengthened with FRP, then creep rupture limits should be re-examined as a potential limiting factor.

Fatigue

In continuous fiber-reinforced composites the fatigue process is characterized by the initiation and multiplication of cracks, rather than initiation and propagation. Crack initiation occurs early in the fatigue life, and coincides with cracking of the weakest ply (Pritchard, 1999). However, fibers in unidirectional composites have relatively few defects, and any crack that forms does not travel across the matrix easily, which contributes to the fatigue resistance of FRPs (Barnes and Mays, 1999). In a research study conducted by Curtis (1989), the fatigue life or endurance limit of unidirectional carbon fiber/epoxy strips at 2 million cycles was found to be 1.5 GPa. Curtis claimed that the fatigue resistance of unidirectional composites might be expected to depend solely on fibers. Hence, carbon fiber composites are believed to have higher resistance to fatigue as compared with metals.

Ultraviolet exposure

The effects of ultraviolet exposure on externally bonded FRP materials by itself causes minor changes in the mechanical properties of composite systems (Karbhari *et al*., 2003). Degradation of the surface (top few microns) provides the potential for ingress of moisture and other agents, causing further degradation. In general, an appropriate admixture in the resin or barrier coating may be specified to prevent harmful ultraviolet effects.

12.3.2 Durability of fiber-reinforced polymer-reinforced concrete members including bond

Moisture/solution

Prolonged exposure of FRP composites to moisture can cause problems, particularly if matrix microcracking occurs in the composite. This will result in increased uptake of moisture or solution into the composite and accelerated damage. It can be noted that moisture can gain access to the resin and fibers from the exposed face or via cracks and diffusion/capillary action in the underlying concrete. Thus, both faces of externally applied composites may be exposed to moisture and salt solution including at the critical bonded interface.

Karbhari and Howie (1997) studied the effect of water, seawater, and freezing and thawing on bonded FRP systems using a peel test. They found that the nature of the bond changed and reduced in strength when exposed to water. Wan *et al*. (2003) and Wan (2002) found similar results even though the FRP was not directly exposed to moisture. In the same study, the presence of moisture on the FRP substrate during FRP application was also investigated. Once again, bond behavior deteriorated with increased moisture present during application. Myers and Ekenel (2005) reported that environmental effects during installation can also have a negative effect on the bond performance. In their work it was noted that very high levels of pore structure moisture in the concrete near the surface of the concrete during installation can have significant detrimental effects on the bond performance. Chajes *et al*. (1995) found similar results for small-scale beams strengthened with glass, aramid, or carbon fiber composites that were subjected to wetting and drying, or freezing and thawing, and then tested in flexure. The beams strengthened with carbon fibers maintained their strength better than glass or aramid fiber composites. They also found that the wetting and drying caused slightly greater degradation than the freezing and thawing. The exposure to moisture also resulted in a debonding failure mode indicating a loss in adhesion due to exposure. Moisture damage can occur either in the adhesive at the bond line or just below the bond line in the concrete and masonry substrate (cracking). Beaudoin *et al*. (1998) tested beams that had been strengthened with carbon FRP (CFRP) laminates and then subjected to moisture cycling. Although there was strength reduction noted in one series, the loss of capacity was attributed to the adhesive and not to failure of the substrate.

Research studies indicate that long-term exposure of externally bonded FRP composites to moisture can cause deterioration of the adhesion between the composite and the concrete substrate.

Alkaline environment

Thus far there is limited reported research work that has focused on the effects of alkaline environment on the critical bonded region/specific adhesive types. Alkaline environment can affect the resin and fibers as noted in Section 12.3.1, Alkaline environment. In operating situations where high alkaline environments are expected, high-grade adhesive epoxies may be used to retard such effects.

Extreme temperature and thermal cycling

Extreme temperatures can not only affect the FRP reinforcement, as noted in Section 12.3.1, Extreme temperature and thermal cycling, but also the bond between the reinforcement and the concrete. Care should be taken in the

design of adhesively bonded systems to ensure that adhesives do not soften excessively, since they tend to lose shear capacity with increased temperature. For bonded systems, both the laminate and adhesive T_g must be controlled to provide adequate performance under service temperatures. Care must be taken to ensure that service temperatures are below the T_g. ACI 440.2R-02 (ACI Committee, 2002) recommends that maximum service temperature should never rise above T_g. The FIB report (Fib, 2001) suggests that T_g should be 20°C above the maximum air temperature (in shade), but not less than 45°C.

Freezing and thawing

Chajes *et al*. (1995) tested FRP-strengthened concrete beams exposed to 100 freezing and thawing cycles. They found strength losses of 21% for CFRP and 27% for glass FRP (GFRP). In similar tests, Bisby and Green (2002) found little strength loss and no noticeable bond deterioration with FRP-strengthened beams exposed to up to 200 cycles of freezing and thawing. Green *et al*. (2003) examined the effects of F–T cycling on the bond between CFRP sheets and concrete. Higher strains were observed along the bonded length for specimens exposed to 300 F–T cycles compared with control specimens. It was also noticed that the failure shifted from the concrete substrate region in control specimens to the adhesive region as F–T cycles increased. The results suggested some level of degradation in the FRP–concrete bond due to F–T cycles. Other studies have reported similar findings. Myers and Ekenel (2005) reported that low temperatures (<4°C) during installation can also have a negative effect on the bond performance.

From these studies it may generally be concluded that F–T cycles affect the bond performance of externally bonded systems to a degree, but as discussed in Section 12.3.2, Synergistic effects, the presence of moisture and sustained load in combination with F–T cycles appears to accelerate the bond degradation.

Creep

Most externally bonded FRP systems are intended to strengthen or restore an existing structure to the original design capacity lost due to deterioration, for example steel corrosion. In these cases, the level of sustained load carried by the FRP will probably be low. As long as the sustained load is kept below the limits prescribed in ACI 440.2R-02 (ACI Committee, 2002), for example, the remaining capacity of the FRP system will still be available to resist live load. If, however, a change of use is proposed for a structure previously strengthened with FRP, then creep rupture limits should be re-examined as a potential limiting factor.

Fatigue

The initial studies on the fatigue resistance of externally FRP-bonded RC beams began in the early 1990s. Meier *et al*. (1993), Heffernan (1997), Barnes and Mays (1999), Shahawy and Beitelman (1999), Papakonstantinou *et al*. (2001); Masoud *et al*. (2001), Aidoo *et al*. (2004), and Quattlebaum *et al*. (2005) all reported on fatigue testing of concrete beams with bonded FRP: the eventual failure was fatigue fracture of the longitudinal steel reinforcement, as was the case for the unstrengthened companion specimens. It has been reported by many researchers that the fatigue resistance of RC beams is significantly improved after being strengthened by externally bonded FRP laminates because the applied FRP reduces the stress range in the existing steel reinforcement (Barnes and Mays, 1999; El-Tawil *et al*., 2001; Senthilnath *et al.*, 2001; Breña *et al*., 2002). Researchers have also reported increases in fatigue life of as high as 3 times that of the non-strengthened beam under the same load range (Muszynski and Sierakowski, 1996; Papakonstantinou *et al.*, 2001; Toutanji *et al*. 2006). Shahawy and Beitelman (1999) noted a significant improvement in fatigue life even when the RC beams were severely damaged before rehabilitation. An improvement in fatigue life after strengthening with FRP laminates is expected, since the increase in stiffness and strength reduces the crack propagation, causing a reduction in the stresses in the reinforcing steel. However, a reduction of ductility was also reported (Shahawy and Beitelman 1999). Ekenel *et al*. (2006) and Grace (2004) applied fatigue loading on CFRP plate- and laminate-strengthened RC beams under service loading, and noted that there was no significant effect on the load-carrying capacity of such beams. According to Inoue *et al.* (1994), Barnes and Mays (1999), Papakonstantinou *et al.* (2001) and Heffernan and Erki (2004), who applied higher loads, failure of RC beams strengthened with FRP laminates under fatigue loading was primarily caused and initiated by failure of the steel reinforcement, followed by FRP debonding as a secondary failure mode. Inoue *et al.* (1994) have also reported that the fatigue strength at 2 million cycles of load repetition for an RC beam bonded with a CFRP plate was 57% of the static strength of the same beam. Other fatigue-related work which includes environmental conditioning is discussed in the next section.

Synergistic effects

Of the exposure conditions studied, synergistic effects and their effects under sustained load are active areas of on-going study. A limited number of studies have been completed to date and these are highlighted below. Mukhopadhyaya *et al*. (1998) studied the influence of F–T cycling and wet–dry cycling on the behavior of epoxy adhesive-bonded concrete–GFRP joints. The three test regimes adopted for this study consisted of alternate wet–dry cycles in 5% NaCl solution, cyclic F–T, and a combination of wet–dry cycles in salt water

and F–T cycles in air. Wet–dry cycling is known to inflict more degradation on GFRP-bonded specimens than F–T cycling. The study also showed that the F–T cycles and the combined chloride immersion/F–T cycle exposure regime created the largest differential movements between FRP and concrete, more than wet–dry cycles alone. Therefore, F–T cycles were more likely to be harmful in the long run to the integrity of the joints.

Chajes *et al*. (1995) conducted environmental durability studies by subjecting small-scale strengthened beams to aggressive environments including F–T cycling, wet–dry cycling, and exposure to chlorides. Of the 60 beams studied, 45 were reinforced with aramid, E-glass, and graphite composite fabrics (15 with each type), and 15 had no external reinforcement. The durability of the externally reinforced beams was assessed by varying the time of exposure to the different conditions and loading the beams to failure after environmental exposure. A total of 48 beams were exposed to F–T or wet–dry cycling in a calcium chloride solution, and the additional beams were left in a control environment. After the environmental cycling, the beams were loaded to failure under four-point bending. Among CFRPs, GFRPs, and aramid FRPs (AFRPs), CFRPs proved to be the most durable. Study results indicated that chloride exposure in both wet–dry and F–T environments caused degradation to beam strength. While there was a strength reduction of 21% in CFRP-wrapped beams compared with control specimens after the F–T exposure, strength reduction in GFRP-wrapped beams was 27% and AFRP-wrapped beam strength reduced by 9%. Of the three fabrics tested, strength reduction in the E-glass fabrics after environmental exposure was approximately 50%. Again, the wet–dry environment was found to cause slightly greater degradation. The reduction in strengthened specimens after the environmental exposure is mainly due to the effect of the exposure on concrete itself rather than the FRP (Toutanji and Balaguru, 1999). This study was conducted on FRP-strengthened beams exposed to F–T and wet–dry cycles under no stress.

Arockiasamy and Thayer (1998) and Lopez *et al*. (2003) considered fatigue loading of CFRP-strengthened beams at low temperature and found no observable difference in fatigue behavior caused by the exposure to low temperature. Sen *et al*. (1999) studied the damage resistance of high-strength concrete under the action of load and F–T cycles. The damage depended on the strength of the concrete: the lower the strength, the greater the damage. Lopez *et al*. (1999) tested small-scale beams strengthened with two types of CFRP and subsequently exposed to up to 300 freezing and thawing cycles. Their results showed, for one type of FRP, that pre-cracking of the beams before strengthening could result in significant deterioration (up to 40% loss in strength) due to freezing and thawing. This result indicates that the combination of load and cold regions exposure may be more severe than cold regions exposure alone.

Murthy *et al.* (2002) conducted laboratory tests on externally strengthened concrete beams subjected to environmental conditioning with sustained loading. Tests were conducted on beams that had been strengthened with aramid, glass and carbon fibers using wet lay-up. They introduced a bond retention factor as the stiffness of the bond between the FRP sheet and the concrete and defined it as the ratio of load to strain. The study noted significant decreases in the bond capacity of the FRP–concrete, particularly for the conditioned specimens with sustained load. The ultimate capacity of the specimens was also affected by conditioning and the sustained loading, yielding reduced ultimate capacity. CFRP specimens exhibited 7.2% degradation in strength under the most severe conditioning and sustained loading case, while AFRP and GFRP specimens degraded by 15% and 21%, respectively. All specimens exhibited a peeling or debonding failure.

Lopez *et al.* (2003) carried out fatigue tests under low temperatures (–29°C). They reported the sequence of failure as failure induced by debonding between the CFRP laminate and the concrete. They concluded that the fatigue at low temperatures decreases the strength of the FRP–concrete interface and increases the stiffness of the concrete. Masoud *et al.* (2001) also performed a series of fatigue tests on CFRP-strengthened corroded specimens. They found that the fatigue life was increased 2.5–6.0 times over non-strengthened samples but that it was lower than the uncorroded specimens. Grace (2004) noted that the load-carrying capacity of CFRP-strengthened RC beams was reduced after long-term exposure to 100% humidity (up to 10 000 hours), dry heat, freezing and thawing (up to 700 cycles), and thermal expansion environmental conditions (48.9°C and 26.7°C).

M. Ekenel and J.J. Myers (unpublished observations, 2006) studied the effect of fatigue and severe environmental conditions (F–T, high RH, high temperature with sustained load during conditioning) on CFRP-strengthened RC beams in the presence of defects, namely interfacial delaminations. After 2 million fatigue cycles, they reported a stiffness loss of about 25% for the most severely exposed specimens without significant growth in the defects. All CFRP-strengthened beams survived fatigue testing of 2 million cycles.

K. Ghosh *et al.*, Q. Yang, and V. M. Karbhari (unpublished observations, 2006) studied the bond of FRP to concrete under immersion in water, salt water, ponding at various RH values, and freezing conditions. Results for ten systems considered clearly showed the effects of environmental exposure on deterioration of bond strength with the maximum level of overall deterioration being over 40% due to exposure to a sub-zero environment due to increased brittleness of the resin/adhesive systems. With the exception of two systems, immersion in salt water caused a higher level of degradation in bond strength in all systems than that due to immersion in deionized water, possibly due to ingress of NaCl into the bond-line resulting in straining and rupture of

intermolecular bonds in the bulk. While conditions of continuous immersion of the entire system could be considered as a severe, and hence accelerated, environment, study of the effects of ponding also indicates significant deterioration in bond strength in some systems with half the systems showing over 40% loss in pull-off strength over the 2 year period of investigation.

12.4 Seismic retrofit and external strengthening of columns

Compression members constitute the most critical elements of a building or bridge system. Column confinement is the most common and effective method used to enhance the capacity and ductility of vertical RC or masonry members. Due to construction errors or antiquated design codes in seismic regions, many column elements are in need of retrofit to satisfy the latest design codes. Traditional techniques use steel plates and ties externally mounted in order to guarantee passive or active confinement, and several real cases were successfully studied and solved using traditional materials such as steel or wood.

In the last decade, FRP composites have been successfully used for confinement of RC and masonry columns. Their high mechanical properties, light weight, and low installation costs contribute to make wet lay-up wrapping one of the most affordable techniques for column confinement. Seismic retrofits and load-capacity upgrades using FRP composites can be found in field applications all over the world.

Previous experimental studies showed that the effectiveness of FRP wrapping in increasing the strength and ductility of columns is strictly related to: type of loading and associate failure modes; duration of expected loads; column geometry and substrate material properties; types of FRP system used; and environmental effects. FRP-confined concrete analytical models were developed and compared with available experimental data for circular cross-section columns, in order to predict the confinement action of FRP. Design codes based on experimental results were drawn in order to make designers more confident with the use of this innovative technique.

Although previous studies have shown the high performance of FRP strengthening systems in terms of significant increases in strength and ductility of column elements, several concerns remain related to the long-term behavior of wrapped columns. Environmental effects – such as F–T cycles, wet–dry cycles, ultraviolet exposure, and de-icing salt solutions – may affect the material properties, and therefore the structural response, of the wrapped elements. For example, it must be investigated if the FRP-confinement analytical models can be used to model the stress–strain behavior in cold or marine regions. Safety coefficients are needed in order to prevent undesired

premature failures due to FRP degradation or further embrittlement of the strengthened systems that may lead to catastrophic failures.

Although several experimental studies (FRPRCS-4, 1999; CCC, 2001; ICCI, 2002; FRPRCS-6, 2003) have demonstrated the effectiveness of repairing damaged or inadequate vertical members with FRP confinement, important questions related to long-term behavior and durability were not addressed. Knock-down factors to address environmental conditioning are an important design consideration for long-term performance, thus research efforts are needed in this field. Since in most cases the cure of the resin happens *in situ*, all the information related to the durability of the industrial cured FRP composites used in the aerospace and naval industries could not help in the study of the durability of FRP-confined systems.

Two major issues generate concerns related to the use of FRPs in construction, and especially for confinement applications: fire and environmental agents. Fire is a major question especially for applications in civil and historical buildings, and in galleries. Environmental agents reduce the durability in infrastructure applications, such as bridges and marine structures. Earlier studies demonstrated that external agents can significantly reduce the effects of confinement, due to material degradations, embrittlement of the resin and fibers, and chemical attack which reduce the original amount of reinforcement (Toutanji and Rey 1997; Toutanji, 1998a and b; Toutanji and Balaguru, 1999).

In particular it was observed that different resin systems and wet–dry cycling affect the ductility of GFRP confinement, reducing the ultimate capacity by 18% (Toutanji, 1999). F–T cycles combined with moisture have been shown to reduce ductility by more than 30% for GFRPs, and resulted in a more catastrophic failure for exposed CFRP-confined columns (Kharbari and Eckel 1994). The only effect of temperature in F–T cycling was found to be very low in a dry environment; only the radial strain was affected, resulting in more brittle failure modes (Kharbari *et al*., 2000). Combined effects, including moisture and F–T cycling, in different pH environments were also investigated. A reduction in compressive strength and axial strain of greater than 20% was reported, while a reduction in hoop strain of 50% was found (Kshirsagar *et al*., 2000). In Table 12.1, results related to previous experimental tests of FRP-wrapped concrete cylinders subjected to accelerated conditioning are reported.

All these results clearly highlight that further investigations are needed in order to furnish design guidelines and safety coefficients for long-term behavior. Technological parameters such as type of resin and fibers, external coatings required in aggressive environments, geometry and amount of reinforcement should be optimized in order to guarantee the desired safety in the long-term. Section 12.5.2 discusses proposed reduction factors for manual wet lay-up wrapped columns subjected to synergistic exposure (Micelli *et al*., 2001).

Table 12.1 Retained mechanical properties of fiber-reinforced polymer-wrapped concrete cylinders after conditioning – state of the art (Micelli *et al.*, 2001)

Conditioning	FRP	f'_{cc} (%)	ε_{axial}(%)	ε_{hoop}(%)	Reference
pH = 9.4, 23°C, 1000 h	E-glass 0°	100.0	100.0	100.0	Kshirsagar
pH= 12.4, 23°C, 1000 h	E-glass 90°	100.0	100.0	100.0	*et al.* (2000)
pH = 12.4, 66°C, 1000 h	Kevlar 49™ 90°	74.4	50.8	51.1	
pH = 7, 66°C, 1000 h		73.7	68.2	51.7	
Dry, 66°C, 1000 h		97.7	100.0	93.6	
F–T cycles, 1000 h		97.4	91.9	82.7	
pH = 9.4, 23°C, 3000 h	E-glass 0°	97.1	89.3	96.1	Kshirsagar
pH = 12.4, 23°C, 3000 h	E-glass 90°	97.5	100.0	93.7	*et al.* (2000)
pH = 12.4, 66°C, 3000 h	Kevlar 49™ 90°	68.1	70	37.1	
pH = 7, 66°C, 3000 h		66.1	56.8	30.4	
Dry, 66°C, 3000 h		89.2	100.0	81.6	
F–T cycles, 3000 h		78.4	78.5	47.3	
Wet–dry cycles (salt water)	E-glass 0° Epoxy A	90.5	100.0	82.9	Toutanji (1999)
	E-glass 0° Epoxy B	83.4	68.4	40.0	
	Carbon 0° Epoxy A	95.8	70.0	72.4	
	Carbon 0° Epoxy B	95.6	77.5	89.4	
F–T (–17.8°C)	E-glass 0°	100.0	67.0	NA	Karbhari
	Carbon 0°	121.2	105.1	NA	and Eckel
	Aramid 0°	100.0	132.8	NA	(1994)
Dry F–T (–20°C)	E-glass 0°	94.5	114.0	114.8	Karbhari
	Carbon 0°	98.8	105.4	0.97	*et al.* (2000)
	Carbon 0°/90°	102.7	104.0	87.4	
Synergistic exposure	E-glass 0° Carbon 0°/45°/90°	See Section 12.5.2			Micelli *et al.* (2001)

For notation see Section 12.5.5.

Another important question is also related to the fact that for repair purposes the strengthening system is installed on a substrate that in most cases has been subjected to external agents. Therefore, an accurate knowledge of the properties of the core materials is required in order to predict the desired performance of the confined system. Recent research has suggested that, under the right conditions, FRP wraps can slow or even stop steel reinforcement corrosion in chloride-contaminated concrete columns (Chauvin *et al.*, 2000; Pantazopoulou *et al.*, 2001; Debaiky, 2002; Debaiky *et al.*, 2002; Sen, 2003; Teng *et al.*, 2003). Pantazopoulou *et al.* (2001) subjected small concrete columns containing steel reinforcement to accelerated corrosion conditions and then strengthened them with GFRP wraps. The retrofitted specimens

were then subjected to continued accelerated corrosion conditions and there appeared to be some reduction in the corrosion rates with the application of the wraps.

Debaiky *et al*. (2002) conducted similar tests on small concrete cylinders with half-cell potential and linear polarization. They found that under strict control and monitoring, CFRP wraps reduced the corrosion activity in the reinforcing steel. This protection did not vary with the number of plies so it was concluded that the resin provided the protection rather than the fibers. It was also observed that partial wrapping led to macrocell corrosion in the steel reinforcement at the extremities of the wrap. The authors indicated that further research was needed into the effect of partial coverage on full-scale columns. These results were also confirmed with tests on larger-scale columns (Debaiky, 2002). Teng *et al*. (2003) found similar results. Section 12.5.3 discusses proposed reduction factors for manual wet lay-up wrapped columns with and without core material degradation.

12.5 Design and use recommendations

The use of FRPs as reinforcement started in the 1950s. In the 1990s this material was used for the repair and rehabilitation of infrastructure and bridges in countries including the USA, Japan, Canada, and European nations. As the use of FRPs increased in different countries, different codes and design guidelines developed. The reduction factors that are recommended for FRPs in various guidelines have often differed in their values. One reason for this could be the varying climatic conditions prevailing in the different countries because the durability of FRPs depends on the environmental condition that it is being exposed to. Another contributing factor may be the lack of standardized testing methods and their correlation with *in-situ* field-conditioned specimens and structures. In the following section, code reduction factors are summarized followed by a discussion on laboratory-collected data correlation. While structures have been retrofitted and strengthened with external FRP systems for over two decades now, *in-situ* durability performance data to corroborate or refute laboratory durability data are very limited.

12.5.1 Material resistance factors and/or load reduction factors

It is important to distinguish between material resistance factors and/or load reduction factors and environmental reduction factors. The environmental reduction factors or so-called ‘knock-down factors’ consider degradation in the FRP material. Table 12.2 contains summary of prescribed material resistance factors and/or a load reduction factors recommended by various organizations

Table 12.2 Reduction factors and durability considerations provided by design guides for externally bonded fiber-reinforced polymer reinforcement (ACI Committee 440R, 2006)

Document	Material resistance factors and/or load reduction factors for flexural strengthening			Document addresses:			
	CFRP	GFRP	AFRP	Creep and fatigue	Environmental exposure	Delamination and debonding	Strengthening limits
ACI 440.2R-02, Chapter 9	0.90 for $\varepsilon_s > 0.005$ 0.70 for $\varepsilon_s < \varepsilon_{sy}$			FRP stress limit	Environmental reduction factors	FRP strain limits	Capacity without FRP exceeds: 1.2DL + 0.85LL
CAN/CSA S806-02, Chapter 11	0.75			Reference to CAN/CSA S478		Refer to 'currently available information'	Capacity without FRP exceeds: 1.0DL + 1.0LL
ISIS Design Manual 4	Reference to others including ACI 440.2R			No specific recommendations, typically reference is made to ACI 440.2R			
Fib Bulletin 14				Effect discussed but no clear guidance provided		Direct calculation of bond stresses	Reference to 'accidental design situation' of EC1
Prefab	1/1.20	1/1.30	1/1.25				
Wet layup	1/1.35	1/1.45	1/1.45				

For notation see Section 12.5.5. DL, dead load; LL, live load.

and summarizes the philosophy that each document follows regarding durability concerns. It may be noted that the load factors differ in the case of the Canadian Code and those of the American Concrete Institute (ACI). Thus, direct comparisons of reduction factors between the different codes do not necessarily indicate the relative conservatism of the codes.

Beyond simply providing the required capacity, three significant design issues, associated with applications of external FRPs for repair and strengthening, are (ACI Committee, 2006):

1. Assuring quality of bond (and/or anchorage) between FRP and concrete substrate.
2. The durability and long-term performance of FRP materials.
3. Strengthening limits.

Each design guide concurs that each of these issues requires further study.

Code summary

The following summarizes how each organization has chosen to address environmental durability.

ACI 440.2R-02 *Design and Construction of Externally Bonded FRP Systems for Strengthening Concrete Structures* (ACI Committee, 2002) provides strength reduction factors based on ductility of the expected failure mode (as measured by reinforcing steel strain) consistent with ACI 318-99 (1999). ACI 440.2R specifically addresses environmental exposure with environmental reduction factors associated with various typical exposures. Values for environmental reduction factor, C_E, were developed at the point of writing the initial ACI Committee 440 design guide document (ACI Committee, 2002) based on available information regarding durability, with the expectation that with continued research the values would be modified to better reflect the advancing state of knowledge regarding the actual effects of the environment. The current ACI 440.2R-02 environmental reduction factors for external FRP systems are reported in Table 12.3. The design ultimate tensile strength and rupture strain are determined using the environmental reduction factor shown in Table 12.3 and equations [12.1] and [12.2], whereby the guaranteed performance characteristic is modified by an environmental reduction factor, C_E, to account for environmental conditions.

$$f_{fu} = C_E f^*_{fu} \quad [12.1]$$

$$\varepsilon_{fu} = C_E \varepsilon^*_{fu} \quad [12.2]$$

(Reported properties are based on a population of 20 or more coupons tested in accordance with ASTM D3039.) In addition, in order to prevent failure due to creep rupture and cyclic loads, stress limits were defined for the three primary material types, as listed in Table 12.4.

Table 12.3 Environmental reduction factor for various fiber-reinforced polymer systems and exposure conditions (ACI Committee, 2002; ACI 440.2R-02)

Exposure conditions	Fiber and resin type	Environmental reduction factor C_E
Interior exposure	Carbon/epoxy	0.95
	Glass/epoxy	0.75
	Aramid/epoxy	0.85
Exterior exposure (bridges, piers, and unenclosed parking structures)	Carbon/epoxy	0.85
	Glass/epoxy	0.65
	Aramid/epoxy	0.75
Aggressive environments (chemical plants and waste water treatment plants)	Carbon/epoxy	0.85
	Glass/epoxy	0.50
	Aramid/epoxy	0.70

Table 12.4 Sustained plus cyclic service load stress limits in fiber-reinforced polymer reinforcement (ACI Committee, 2002; ACI 440.2R-02)

FRP type	GFRP	AFRP	CFRP
Sustained plus cyclic stress limits	$0.20f_{fu}$	$0.30f_{fu}$	$0.55f_{fu}$

f_{fu}, design ultimate tensile strength of FRP.

The durability of externally bonded FRP reinforcement for concrete in the Canadian CAN/CSA S806-02 *Design and Construction of Building Components with Fibre-Reinforced Polymers* (CAN/CSA, 2002) is addressed through reference to CAN/CSA S478-95 *Guideline of Durability in Buildings* (CAN/CSA, 1995). Although a single limiting FRP tensile strain (0.007) is provided, delamination and debonding are addressed by directing the designer to 'currently available information appropriate to the combination of sheets and adhesive'.

For durability of externally bonded FRPs, the *ISIS Design Manual 4 – Strengthening Reinforced Concrete Structures with Externally-Bonded Fibre Reinforced Polymers* (ISIS Canada, 2001) references the recommendations of others, rather than making its own clear design or durability recommendations.

The European Federation Internationale de Beton (Fib) *Bulletin 14 Externally Bonded FRP Reinforcement for RC Structures* (Fib, 2001) produced by fib Task Group 9.3 discusses durability effects, but no clear design guidance is provided. Fib *Bulletin 14* recognizes the difference in expected performance between FRP material types and FRP systems in the form of different material safety factors.

The Concrete Society in Great Britain has published *Technical Report 55 – Design Guidance for Strengthening Concrete Structures Using Fibre*

Composite Materials (Concrete Society, 2000). This document is similar to *ISIS Design Manual 4* (ISIS Canada, 2001) and Fib *Bulletin 14* (Fib, 2001) in its approach and scope. Importantly, *Technical Report 55* has been followed by *Technical Report 57 – Strengthening Concrete Structures with Fibre Composite Materials: Acceptance, Inspection and Monitoring* (Concrete Society, 2003). This report addresses more practical construction issues associated with externally bonded FRP materials.

The Japanese *JSCE Recommendations for the Upgrading of Concrete Structures with use of Continuous Fiber Sheets* (JSCE, 2001) adopts a performance-based approach to the design of externally bonded FRP materials (ACI Committee, 2006).

The Egyptian FRP code (2005) uses the *limit states* design approach for externally bonded FRP reinforcement for concrete and prescribes a material resistance factors approach related to the ductility of the failure mode considered in addition to all durability-related criteria with the exception of fire resistance.

Future code directions relating to environmental durability

Based on current knowledge it is increasingly being recognized by the civil engineering community that for FRP products the variability in properties is not only affected by the environmental conditioning, but is also affected by the manufacturing method (Concrete Society, 2000; Karbhari, 2000; Taljsten, 2002; Atadero *et al*., 2005). Processing method and conditions also have a significant effect on the durability of FRP materials. FRP materials commonly used in civil infrastructure may be divided into three classes, namely: those fabricated using pultrusion, those fabricated by wet lay-up, and those made by other factory-controlled processes. Currently, ACI Committee 440L, Durability of FRP Structures, is considering durability factors based on both method of manufacture and materials-based environmental factors, with their product determining the actual factor to be used for determining the design value. These factors under development will thereby acknowledge that manufacturing quality affects long-term durability.

12.5.2 Correlation of laboratory-reported durability data with code-reported reduction factors

Myers and Viswanath (2006) conducted a worldwide survey of environmental reduction factors for FRPs. The reduction factors for FRPs proposed by various guidelines from countries including the USA, Japan, Canada, Great Britain, Norway, and Europe were obtained to assemble a database of current environmental reduction factors and review their appropriateness. A literature review was conducted in conjunction that summarized recent durability investigations conducted worldwide on various FRP materials under

different exposure conditions. These FRP materials included carbon, aramid, glass, and hybrid FRPs. The reduction factors obtained from the results of the recent laboratory studies were compared with those provided by various codes on FRPs around the world and results are discussed in the following sub-sections. In this study the environmental reduction factors were not re-calibrated for any material resistance or load factor differences in the codes.

Appropriateness

The scarcity of the data opened a window to examine the appropriateness of the environmental reduction factors used in the FRP-strengthened structures. The available data regarding the durability performance of FRPs exposed to the actual environment (i.e. field data) are still very limited and in many cases inaccessible. Therefore, in this survey a database was developed by obtaining laboratory-based durability data. This was used for comparing the reported code reduction factors used in practice and the values obtained through the results of experiments performed by researchers.

Collection of data

The environmental reduction factors reported in this summary were collected from ACI 440.2R-02 (ACI Committee, 2002), ACI 440.1R-03 (ACI Committee, 2003), a Task Group Report on the Environmental Reduction Factors for Internal and External FRP by ACI Sub-Committee 440L (Myers *et al*., 2004), and other worldwide codes. A literature survey was performed in order to obtain information regarding the durability of FRPs. Technical papers published in various books and journals were reviewed to retrieve the required information.

Reporting of data

Table 12.5 was developed to obtain the range of values used for environmental reduction factors in the various guidelines. The information collected from the literature survey was compiled using data sheets (Myers and Viswanath, 2005). The collected data were classified based on the different applications of FRPs in concrete. The classification was based on internally bonded, externally bonded, material alone, and hybrid FRPs. Table 12.6 was prepared to compare the values obtained for reduction factors through various research results and the code-specified values. Both experimentally reported values and code reduction factors are presented to contrast and compare. The limitations of this study include the following: the manufacturing technique of the FRP was not delineated in many of the code reduction factors; some code values did not delineate the application (i.e. external or internal FRP);

Table 12.5 Summary comparison of the existing environmental reduction factors

Criteria	Type of fibers used	Highest value used	Median	Lowest value used
Reduction for environmental degradation	CFRP	1.00	0.88	0.60
	GFRP	0.80	0.70	0.14
	AFRP	0.90	0.85	0.31
Reduction for sustained stress	CFRP	1.00	0.95	0.90
	GFRP	1.00	0.90	0.80
	AFRP	1.00	0.85	0.70
Total strength reduction for environmental exposure	CFRP	1.00	0.86	0.60
	GFRP	0.80	0.55	0.30
	AFRP	0.90	0.74	0.42
Creep rupture limits	CFRP	0.55	0.55	0.55
	GFRP	0.22	0.22	0.22
	AFRP	0.30	0.30	0.30
Stress limits for permanent load	CFRP	0.85	0.76	0.44
	GFRP	0.75	0.70	0.14
	AFRP	0.85	0.70	0.16

the factors were not tied directly to a service life estimate or detailed exposure condition; and a direct comparison of the reduction factors between the different codes is not possible due to variations in local circumstances. The literature survey assisted in the compilation of data regarding the strength degradation in FRP materials used for concrete systems.

Figure 12.1 shows that strength degradation varies from 4% to 19% for concrete members reinforced with externally bonded carbon fibers under various exposures, except for exposure to fresh water and humidity. Under freshwater and 100% humidity exposures, strength degradation was about 23% and 33%, respectively. Similarly, for concrete members with externally bonded glass fibers as reinforcement, strength degradation was from 10 to 28% under various exposures. No data were obtained for aramid fibers.

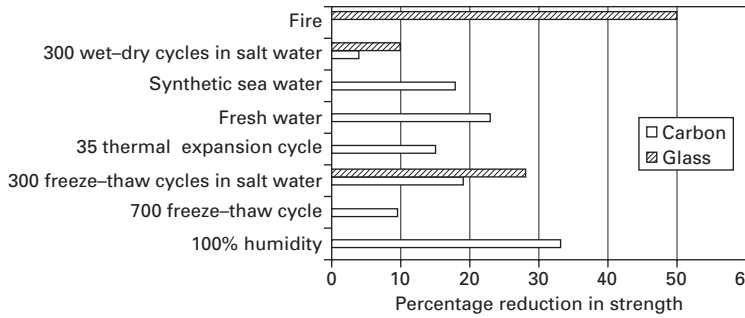
As illustrated in Fig. 12.2, it was observed that for aramid fibers the strength degradation is different in acidic exposure at different temperatures. In alkaline solution, AFRP bars retained more strength than aramid fibers. Maximum degradation for CFRP bars was due to ultraviolet exposure according to the available data collected and this percentage degradation was reported to be 23%.

The percentage reduction in strength was reported to be about 85% for glass fibers exposed to alkaline solution at 40°C, but was 71% for glass bars when exposed to the same environment. The reduction in strength of glass fibers and bars under other exposure conditions is shown in Fig. 12.3.

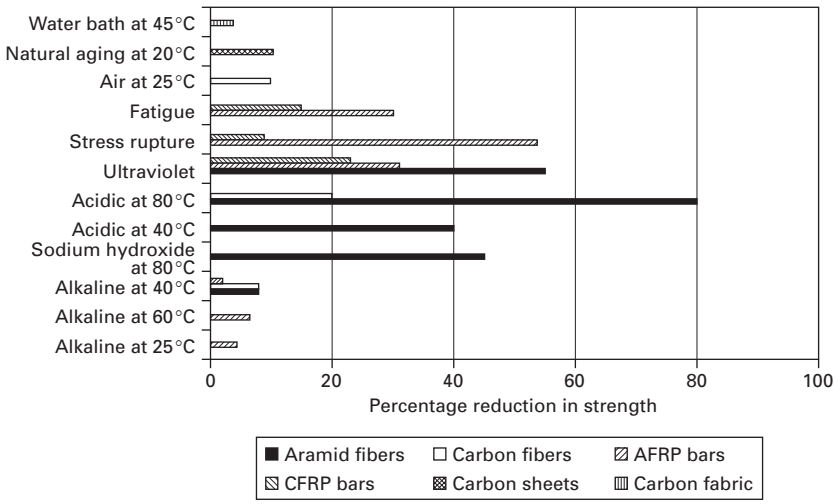
It should be noted that among the data collected and presented in Figs 12.1 to 12.3, very little information was available on synergistic effects (the

Table 12.6 Comparison of the environmental reduction factors specified by existing codes and experimentally determined reduction factors

Criteria		Highest value used		Median		Lowest value used	
	Type of fibers used	Code specified	Experimentally determined	Code specified	Experimentally determined	Code specified	Experimentally determined
Reduction for environmental degradation	CFRP	1.00	1.00	0.88	0.90	0.60	0.67
	GFRP	0.80	0.97	0.70	0.81	0.14	0.15
	AFRP	0.90	0.98	0.85	0.69	0.31	0.20



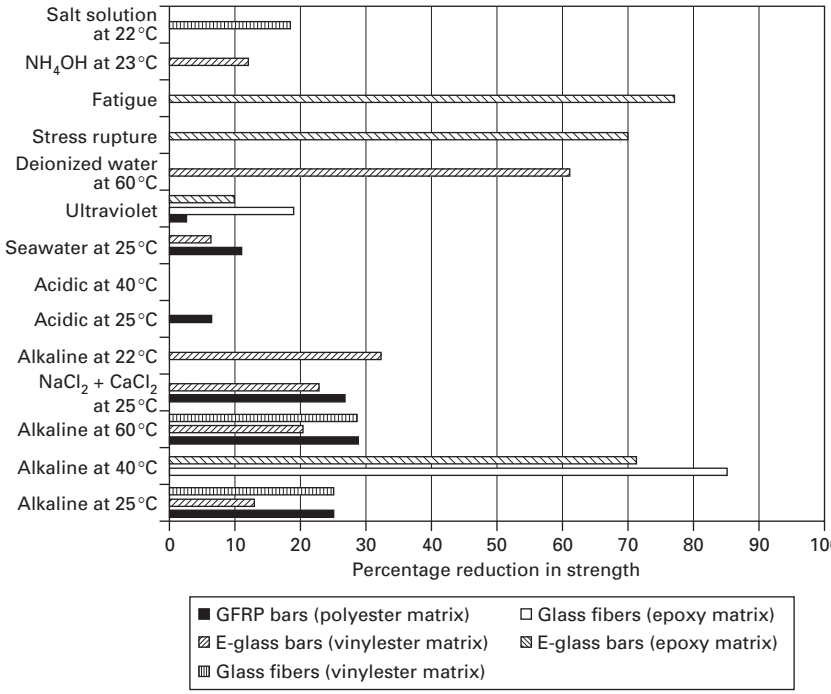
12.1 Strength degradation in externally bonded fiber-reinforced polymers.



12.2 Strength degradation of fiber-reinforced polymer material alone.

effects of combined environmental conditioning), including those associated with sustained loading or cycled (fatigue) loading. These synergistic or combined effects may result in a faster or higher rate of degradation, and this is currently an area of on-going research by many leading researchers in the durability area.

Some of the values obtained from reported experimental work were similar to the values proposed by various guidelines; however, none of the experimental results obtained provided the strength degradation due to the synergistic effect under sustained load for the different exposures presented. Therefore, in the author's opinion more field data need to be compiled and compared with the laboratory studies that consider synergistic and system behavior to see if these code reduction factors should be eliminated, reduced or increased.



12.3 Strength degradation in glass fiber-reinforced polymers alone.

12.5.3 Environmental reduction factors for columns

In the previous discussion, it was noted that the lack of data regarding synergistic effects, particularly for specimens subjected to stress or sustained load during cycling, indicates an area where more research is warranted. In the case of an FRP-wrapped column system, the presence of sustained axial load during durability evaluation may be considered less of a concern as the stress in the FRP jacket is negligible under service conditions. It would only be significant during overload conditions that are temporary in nature. The primary durability issues for wrapped columns revolve around how the degradation in the jacket affects the confinement of the column, and thereby the strength and ductility of the column. Another issue, which will be discussed in Section 12.5.4, is how the jacket affects the potential for corrosion of the reinforcing steel in the column concurrent with FRP jacket degradation.

To investigate the initial issue, Micelli *et al*. (2002) studied the behavior of glass–epoxy and carbon–epoxy FRP fabric systems used to wrap low-scale concrete cylinders that were subjected to environmental cycles and immersion in aggressive aqueous solutions. FRP-confined specimens were subjected to three different environments: a controlled laboratory environment at a constant temperature of 22°C and RH ≈ 40%; a combined environmental

regime, including F–T cycles, moisture cycles, and high-temperature cycles; and immersion in saturated NaCl aqueous solution (15% by weight). The first environment was used to preserve virgin specimens that were used as reference; the second environment simulated seasonal changes; the third environment simulated the presence of de-icing salts in infrastructures.

FRP-wrapped specimens were immersed in NaCl solution for a total of 2880 hours. The immersion in saline solution simulated an accelerated exposure to the de-icing salt solutions that constitute the usual service conditions of many infrastructure systems around the world. These very aggressive conditions could result when the mechanical properties of the resin are significantly affected by diffusive phenomena of aggressive fluids. In fact, resin damage and defects generated by fluid absorption may open a dangerous path for chemical attack of the fibers as a result of fibers being directly exposed to the external agents. A degradation of the fibers may reduce the FRP properties and therefore the confinement pressure would be less than assumed under ideal conditions.

Environmental aging consisted of four complete combined cycles plus one additional series of F–T cycles. One complete combined cycle consisted of 50 F–T cycles (non-saturated state), 120 temperature cycles, and 120 high-RH cycles. Ultraviolet radiation was applied in correspondence with high-temperature cycles. High and low temperatures were related to the weather conditions typical of central United States and the cycling represented the seasonal changes. F–T cycles were considered as a simulation of winter effects where the temperature varied from –18°C to 4°C in accordance with the ASTM C666-92 standard F–T test for concrete.

High-temperature cycles simulated the summer season effects. The temperature cycle was chosen to vary between 16°C and 49°C. The temperature cycles alternated with high-RH cycles. The first RH cycles started after 50 temperature cycles to simulate rain or high moisture content in the air. In the first series of cycles RH varies between 60% and 100% at a constant temperature of 16°C to simulate the humidity and rain during the night time. In the second series of cycles RH varies between 60% and 100% at a constant temperature of 27°C to simulate humidity and rain during the day time. In the third cycle, it was assumed that on bridge decks as soon as it starts raining the heat from the concrete bridge deck might escape, causing the nearby air temperature to actually rise to a higher level, so RH is varied from 60% to 100% at a constant temperature of 38°C.

The specimens were exposed in total to 250 F–T cycles, 480 humidity cycles and 480 temperature cycles. After environmental and saline solution exposure, conditioned specimens were kept for 2 days in a chamber at 30°C to provide full drying. It must be noted that in all cases the conditioning regime of cylinders in this laboratory study did not take place in the presence of axial stress (i.e. sustained loading), which may vary from the typical field

application where low levels of axial load cycling may be experienced. However, it may also be noted that in real RC columns it is well known that under service loads microcracking should not occur and the transverse strain in the concrete should remain below its cracking strain. Therefore, the stress in the FRP jacket is negligible under service conditions, and it should be significant only during overloads that are temporary in nature.

The concept that should be clear is that the positive outcome of a strengthening project depends on important issues such as knowledge of the status of the structure; use of proper design equations developed by adequate structural modeling; use of proper coefficients that can assure safety in the long term, especially when the structure is exposed to an aggressive environment. This third issue was highlighted in this research study.

The authors noted that the epoxy resin used as the polymer matrix showed water retention of about 2.5% in weight after immersion in water at 40°C for 2000 hours. The CFRP-confined cylinders were affected to a lesser degree than the GFRP specimens as would be expected, but the failure mode of the CFRP-confined cylinders was more explosive without a significant loss in ductility. The GFRP specimens exhibited a loss in ductility of more than 40%. The external agents, such as saline fluids and environmental cycles, affected the mechanical properties of the FRP-confined systems; therefore design recommendations should take into account the durability effects that may compromise structural safety. Micelli *et al*. (2001) reported the reduction factors shown in Table 12.7. Further work was suggested to evaluate specimen size effects in order to validate these trends on large-scale specimens.

12.5.4 Area reduction factors for columns

Bae *et al*. (2005) studied the effects of environmental degradation for column elements wrapped with CFRP composite in the presence of steel corrosion and environmental conditioning. The study aimed to investigate the effects of various environmental conditions on the long-term behavior of RC columns

Table 12.7 Proposed environmental reduction factors for various wet-layup fiber-reinforced polymer systems and exposure conditions (Micelli *et al*., 2001)

FRP jacket	f'_{cc}	ε_{axial}	ε_{hoop}	Environment
CFRP	0.75	0.70	0.70	Exposed to thermal cycles, humidity cycles, fluid penetration, chemical agents
GFRP	0.60	0.50	0.50	Exposed to thermal cycles, humidity cycles, fluid penetration, chemical agents
CFRP	0.90	0.70	0.85	Protected or placed inside a building
GFRP	0.80	0.80	0.75	Protected or placed inside a building

For notation see Section 12.5.5.

wrapped with FRPs. The experimental program comprised two parts: ambient environmental effects and corrosion tests. The environmental conditions considered F–T cycles, high-temperature cycles, high-humidity cycles, ultraviolet radiation, and 5% saline solution; while the corrosion tests investigated the corrosion of steel reinforcing embedded in RC columns wrapped with FRP fabrics.

A total of 36 small-scale and 6 mid-scale RC columns were conditioned under the accelerated environmental and/or corrosion process and then tested under uni-axial compression up to failure. Some of the columns were wrapped with CFRP fabrics prior to the beginning of the accelerated corrosion process to simulate newly constructed RC columns wrapped with CFRP sheets. The others were strengthened with CFRP sheets after a certain period of the accelerated corrosion process to duplicate the corrosion-damaged RC columns being repaired by wrapping with CFRP sheets. During the accelerated corrosion process, the corrosion rate was monitored. The test results showed that although CFRP-sheet wrapping decreased the corrosion rate, the corrosion of the steel reinforcement could continue to occur.

Based on the small-scale RC column tests, design guidelines were proposed and these were validated through the test results of 6 mid-scale RC columns. The proposed design guidelines introduced a concept of equivalent area to account for the corrosion damage – such as internal cracking and cross-sectional loss of steel reinforcement – along with strength reduction factors to account for the environmental degradation in the FRP wrap due to environmental conditioning. This concept differs slightly from the ACI 'knock-down' or environmental reduction factors presented previously in Section 12.5.1 since this approach also considered the long-term degradation in the system by considering corrosion in the column reinforcing steel.

For an FRP-wrapped column, Bae (2004) proposed that the axial compressive capacity of RC spiral columns wrapped with CFRP sheets under a corrosive environment could be determined as follows:

$$\phi P_n = 0.85\phi[0.85\psi_f\phi_{env} f'_{cc}A_{eqv} + f_y(A_{st})_{cor}] \quad [12.3]$$

where: ϕ is code reduction factor; P_n is the nominal axial strength of cross-section; ψ_f is a strength reduction factor proposed by ACI 440.2R-02 to account for the uncertainty of new technology, taken as 0.95; ϕ_{env} is the strength reduction factor associated with the FRP jacket; and f'_{cc} is strength of concrete confined with FRP sheets. The equivalent area, A_{eqv}, and reduced area of steel reinforcement, $(A_{st})_{cor}$, can be determined using the area reduction factors ϕ_{cor1} and ϕ_{cor2}, as shown in equations [12.4] and [12.5].

$$A_{eqv} = \phi_{cor2}[A_g - (A_{st})_{cor2}] = \phi_{cor2}(A_g - \phi_{cor1}A_{st}) \quad [12.4]$$

$$(A_{st})_{cor} = \phi_{cor1}A_{st} \quad [12.5]$$

where A_{eqv} is equivalent area, A_g is gross area, A_{st} is area of steel reinforcement, $(A_{st})_{cor}$ is reduced area of steel reinforcement due to corrosion, ϕ_{cor1} is an area reduction factor to account for the steel loss due to corrosion, and ϕ_{cor2} is an area reduction factor to account for the degradation of concrete due to cracking caused by corrosion of steel reinforcement.

In order to determine the area reduction factors ϕ_{cor1} and ϕ_{cor2}, the area reduction factor ϕ_{cor2} of small-scale RC columns was determined and the corresponding experimental results are summarized in Table 12.8. In some cases the corrosion cell was initiated before while others after the FRP jacket was installed. Based on the results shown in Table 12.8, area reduction factors, ϕ_{cor1} and ϕ_{cor2}, for four RC columns exposed to four different categories of environmental conditions were proposed for use in equation [12.3]; these are summarized in Table 12.9. In Table 12.9, area reduction factors, ϕ_{cor1}, were calculated using the relationship between ϕ_{cor1} and ϕ_{cor2} and correlated for larger-scale columns, as reported by Bae (2004).

Table 12.8 Area reduction factors, ϕ_{cor2}, of small-scale reinforced concrete columns (Bae *et al.*, 2005)

Specimen	ϕ_{cor2}	Testing scheme
Control	1.00	Control
CFRP1	0.93	CFRP sheets were applied before the accelerated corrosion process
CFRP2	0.86	CFRP sheets were applied as a repair method after the columns were severely damaged by corrosion
CFRP3	0.89	Same as CFRP1 but conditioned under F–T cycles after CFRP wrapping
CFRP4	0.76	Same as CFRP2 but conditioned under F–T cycles after CFRP wrapping

Table 12.9 Proposed area reduction factors, ϕ_{cor1} and ϕ_{cor2} (Bae *et al.*, 2005)

ϕ_{cor1}	ϕ_{cor2}	Environmental conditions
0.75	0.95	[Case 1] Newly constructed RC columns wrapped with CFRP sheet
0.65	0.85	[Case 2] Corrosion-damaged RC columns repaired by CFRP wrapping
0.70	0.90	[Case 3] Newly constructed RC columns wrapped with CFRP sheet and placed where possible non-moist F–T damages are anticipated
0.55	0.75	[Case 4] Corrosion-damaged RC columns repaired by CFRP wrapping, and placed where possible non-moist F–T cycles are anticipated

Table 12.10 Strength reduction factor, ϕ_{env} (Bae, 2004)

FRP sheet type/ adhesive type	Strength reduction factor, $\phi_{env} = \phi_{FT}\phi_H\phi_{Na}$			Remark
	ϕ_{FT}	ϕ_H	ϕ_{Na}	
CFRP/epoxy	1.00*	0.95	0.95	If one of the environmental conditions can be ignored, the strength reduction factor for the environmental condition can be taken as unity.
GFRP/epoxy	1.00*	0.85	0.85	

* Reduction factor based on non-moist F–T cycles. For notation see Section 12.5.5.

Currently, many analytical models are available to determine strength of concrete confined with FRP sheets, f'_{cc}. The models have been proven to be reasonably accurate for estimating the strength of concrete confined by FRP sheets to within less than 10% prediction error. The performances of the proposed design guidelines were validated through comparison with the test results of mid-scale RC columns where the size, material properties, and confinement level were different from the small-scale RC columns used for the development of the proposed design guidelines.

Equations to calculate the axial compressive capacity of FRP-wrapped RC columns exposed to various environmental conditions were also proposed. The equations utilized a strength reduction factor, ϕ_{env}, accounting for the effects of various ambient environmental conditions (see Table 12.10), and the area reduction factors for corrosion, ϕ_{cor1} and ϕ_{cor2}, accounting for the effects of corrosion of reinforcement.

While this work clearly advanced the understanding and provides recommendations for FRP-RC columns with steel corrosion coupled with considerations for environmental exposure of the jacketed FRP, limitations remain: the study examined a single CFRP–epoxy and GFRP–epoxy system; moist F–T cycles were not studied; and the exposure and conditioning were not linked to a specific climate location or service life exposure duration. These limitations constitute part of the difficulty in addressing the very complex issue of design and use recommendations for a wide variety of systems and constituent materials. This is not to diminish the very impressive inroads in the development of external strengthening systems and codification that has occurred over the past two decades. This is just to highlight that further work remains, as discussed and highlighted in the next section.

12.5.5 Notation

A_{eqv} = equivalent cross-sectional area
A_g = gross area

A_{st} = area of steel reinforcement
$(A_{st})_{cor}$ = reduced cross-sectional area of steel reinforcement
C_e = environmental reduction factor
f'_{cc} = compressive strength of FRP-confined concrete
f'_c = concrete compressive strength (MPa)
f_{fu} = design ultimate tensile strength of FRP (MPa)
T_g = glass transition temperature (°C)
$\varepsilon_{acc} = \varepsilon_{axial}$ = ultimate axial strain of confined concrete
$\varepsilon_{hoop} = \varepsilon_{radial}$ = ultimate hoop strain of confined concrete
ε_{fu} = design ultimate strain of FRP (mm/mm)
ε_s = strain in the reinforcing steel (mm/mm)
ε_{sy} = yield strain of the reinforcing steel (mm/mm)
ϕ = code reduction factor
ϕ_{cor1} = area reduction factor for longitudinal reinforcing steel
ϕ_{cor2} = area reduction factor for area of concrete
ϕ_{env} = strength reduction factor
ϕ_{FT} = reduction factor for freeze–thaw
ϕ_H = reduction factor for relative humidity
ϕ_{Na} = reduction factor for salt solution/immersion
P_n = nominal axial strength of cross-section
ψ = strength reduction factor = 0.95 proposed by ACI 440.2R-02
$\psi_f = 0.85$ = 'partial' resistance factor applied only to the FRP reinforcement

12.6 Future trends and research needs for the durability of external fiber-reinforced polymer strengthening systems

As new and innovative external FRP systems develop and continue to evolve – whether they consist of traditional adhesively bonded fabrics or pre-cured plates composed of carbon, glass, or aramid fibers, mechanically fastened pre-cured plates, or include the use of non-traditional systems such as steel reinforced polymers (SRPs) – the obvious challenge on the durability side will be to characterize their long-term performance and implement appropriate reduction factors in the design codes. The continued growth in the variety of external FRP strengthening systems, composed of various materials that constitute the composite matrix, continues to challenge the development of appropriate environmental reduction factors for such a wide variety of systems and composite materials.

Research needs impeding the widespread implementation of external FRP systems in this author's opinion revolve around several key issues, namely: developing standardized durability test methods that accurately correspond to appropriate *in-situ* exposure; being able to develop accurate service life models to predict accurately the long-term performance of externally

strengthened systems; and to standardize or develop a performance-based approach for mechanical and material properties that FRP materials and systems must satisfy, similar to standards developed for other construction materials.

12.6.1 Workshop on Research in FRP Composites in Concrete Construction

In October 2004, the National Science Foundation (NSF), USA, sponsored a workshop (Porter and Harries, 2005). The primary objective was to identify critical research needs affecting the implementation of FRP composites in construction applications and to develop a consensus on the priority of these needs. This workshop was developed out of a 2002 survey of research needs (Harries *et al*., 2003). The consensus of the workshop is presented below.

> To address the immediate needs of the use of FRPs in concrete construction, the following research topics are *highly recommended* for investigation as they relate to external reinforcing and their long-term durability performance. These topics address needs based on widely accepted applications of FRP in civil infrastructure.
>
> *Identification of appropriate environments for durability testing*
>
> Considerable disagreement exists among researchers and practitioners as to exactly what environmental parameters need to be considered when using FRP materials. Additionally, the intended use, regional climates, and maintenance practices will significantly impact which parameters affect a particular application. Such research studies must include participation from all primary climatic regions.
>
> *Development of standardized durability/environmental exposure test methods*
>
> Coupled to the previous topic, a consensus on accelerated environmental conditioning techniques and subsequent durability test methods is required. Methods are required for both external FRP applications and internal FRP-reinforcement applications.
>
> *Durability studies of external bonded FRP repair or retrofit measures*
>
> Time-dependent effects and factors affecting the durability of concrete structures with FRP (including fatigue) need to be identified. Clearly, the durability of the adhesive bond or interface between the FRP and the substrate is of primary concern.

Service life prediction of structures using FRP

Models need to be developed to extrapolate short-term test results to long-term service life predictions. This topic also deals primarily with parameters related to durability and should involve models of degradation processes. Fatigue life of bonded FRP has been shown to be of particular concern and predictive models of this behavior are required.

Fire resistance and protection of FRP

The behavior of FRP materials, whether imbedded in concrete or externally applied, when subject to fire loading is largely unknown. Modeling techniques must be developed and verified for predicting the performance of structures in fire.

12.6.2 Other trends and research needs in external FRP composites in concrete construction

In addition to the areas noted by the NSF-sponsored workshop and discussed previously, further study on the long-term performance of structural stay-in-place forms (concrete-filled composite tubes or pipes) is warranted.

12.7 Sources of further information and advice

The following codes and guides may be consulted for further discussion on external FRP strengthening systems and their related durability performance. Recent specialty conferences related to FRP and their durability performance are also cited.

12.7.1 Documents published by the American Concrete Institute (www.concrete.org)

- ACI 440-L (In Committee Ballot): Durability of Fiber Reinforced Polymer (FRP) Composites Used with Concrete.
- 440.2R-02: Design and Construction of Externally Bonded FRP Systems for Strengthening Concrete Structures.
- 440.3R-04: Guide Test Methods for Fiber-Reinforced Polymers (FRPs) for Reinforcing or Strengthening Concrete Structures.
- SP-215: Field Applications of FRP Reinforcement: Case Studies.
- SP-230: 7th International Symposium on Fiber-Reinforced (FRP) Polymer Reinforcement for Concrete Structures.
- SP-230CD: (CD-ROM) FRPRCS-7 – Proceedings of the 7th International Symposium on Fiber-Reinforced Polymer (FRP) Reinforcement for Concrete Structures, Kansas City, Missouri, USA, 2005.

- SP-188: FRPRCS-4 – Proceedings of the 4th International Symposium on Fiber-Reinforced Polymer (FRP) Reinforcement for Concrete Structures, Baltimore, Maryland, USA, 1999.

12.7.2 Fiber-reinforced polymer-reinforced concrete design codes

- BSI 1997, BS8110 Structural Use of Concrete, British Standards Institute, London, UK.
- CAN/CSA, 2000, CAN/CSA S6-00: Canadian Highway Bridge Design Code, Canadian Standards Association, Ottawa, Canada.
- CAN/CSA, 2000, CAN/CSA S806-02: Design and Construction of Building Components with Fibre Reinforced Polymers, Canadian Standards Association, Ottawa, Canada.
- JSCE, 1986, JSCE Standard Specifications for Concrete Structures, Japanese Society of Civil Engineers, Tokyo.
- JSCE, 1993, JSCE State of the Art Report on Continuous Fiber Reinforcing Materials, Research Committee on Continuous Fiber Reinforcing Material: Concrete Engineering Series, No.3, Ed. A. Machida, Japanese Society of Civil Engineers, Tokyo.
- JSCE, 1997, Recommendations for Design and Construction of Concrete Structures Using Continuous Fiber Reinforcing Materials: Concrete Engineering Series, No. 23, Japanese Society of Civil Engineers, Tokyo.
- JSCE, 2001, JSCE Recommendations for the Upgrading of Concrete Structures with the use of Continuous Fiber Sheets: Concrete Engineering Series, No. 41, Japanese Society of Civil Engineers, Tokyo.
- Fib, 2001, Bulletin 14 Externally Bonded FRP Reinforcement for RC Structures, Fédération Internationale du Béton.
- Norwegian Council for Building Standardization, 1998, NS 3473 Concrete Structures – Design Rules, Oslo, Norway.
- Egyptian FRP Code, 2005, Egyptian Code for the Use of Fiber Reinforced Polymers (FRP) in the Construction Fields, Egyptian Housing and Building National Research Center, Egyptian Ministry of Housing, Utilities, and Urban Development.

12.7.3 Recent fiber-reinforced polymer conferences/ proceedings

- FRPRCS-8, 2007, Proceedings of the 8th International Symposium on Fiber-Reinforced (FRP) Polymer Reinforcement for Concrete Structures, Patras, Greece, July 16 to 18, 2007.
- CDCC 2007, Proceedings of the 3rd International Conference on Durability and Field Applications of Fibre Reinforced Polymer (FRP)

Composites for Construction, Quebec City, Quebec, Canada, May 22 to 24, 2007.
- ACIC 2007, Proceedings of the 3rd International Conference on Advanced Composites in Construction, University of Bath, Bath, UK, April 2 to 4, 2007.
- ACIC 2006, Proceedings of the 2nd International Conference on Advanced Composites in Construction, University of Cambridge, Cambridge, UK, March 21 to 23, 2006.
- FRPRCS-7, 2005, Proceedings of the 7th International Symposium on Fiber-Reinforced Polymer (FRP) Reinforcement for Concrete Structures, Kansas City, Missouri, USA, November 6 to 9, 2005.
- CCC 2005, Proceedings of the 3rd International Conference on Composites in Construction, Lyon, France, July 11 to 13, 2005.
- ACIC 2004, Proceedings of the 2nd International Conference on Advanced Composites in Construction, University of Surrey, Surrey, UK, April 20 to 22, 2004.
- FRPRCS-6, 2003, Proceedings of the 6th International Symposium on Fiber-Reinforced Polymer (FRP) Reinforcement for Concrete Structures, Singapore, July 8 to 10, 2003.
- CDCC 2002, Proceedings of the 2nd International Conference on Durability of Fibre Reinforced Polymer (FRP) Composites for Construction, Montréal, Québec, May 29 to 31, 2002.
- ACIC 2002, Proceedings of the 1st International Conference on Advanced Composites in Construction, University of Southampton, Southampton, UK, April 15 to 17 2002.
- CCC 2001, Proceedings of the 2nd International Conference on Composites in Construction, Porto, Portugal, October 10 to 12, 2001.
- FRPRCS-5, 2001, Proceedings of the 5th International Symposium on Fiber-Reinforced Polymer (FRP) Reinforcement for Concrete Structures, Cambridge, UK, July 16 to 18, 2001.

12.7.4 Manufacturers' design manuals for fiber-reinforced polymer strengthening systems

- MBrace, 1998, MBrace Composite Strengthening System: Engineering Design Guidelines, Master Builders, OH, USA. Current edition at www.mbrace.com.
- Replark, 1999, Replark System: Technical Manual, Mitsubishi Chemical Corporation, Sumitomo Corporation of America, New York, USA. Current edition at www.sumitomocorp.com.
- Sika, 1997, Sika Carbodur: Engineering Guidelines for the use of Sika Carbodur (CFRP) Laminates for Structural Strengthening of Concrete Structures, Sika Corporation, Lyndhurst, NJ, USA. Current edition at www.sikaconstruction.com.

- S&P, 1998, Clever Reinforcement Company, Schere & Partners, Brunnen, Switzerland. Current edition at www.sp-reinforcement.ch.
- Tonen, 1996, Forca Towsheet Technical Manual, Rev. 5.0, Tonen Corporation, Tokyo, Japan.
- Tyfo, 1998, Design Manual for the Tyfo Fibrwrap System, Fyfe Co. LLC, San Diego, CA, USA. Current edition at www.fyfeco.com.

12.8 References

ACI Committee (1999), 318-99: *Building Code Requirements for Structural Concrete and Commentary* (*ACI 318R-02*), American Concrete Institute, Farmington Hills, MI, USA.

ACI Committee (2002), 440.2R-02: *Design and Construction of Externally Bonded FRP Systems for Strengthening Concrete Structures*, American Concrete Institute, Farmington Hills, MI, USA.

ACI Committee (2003), 440.1R-03: *Guide for the Design and Construction of Concrete Reinforced with FRP Bars*, American Concrete Institute, Farmington Hills, MI, USA.

ACI Committee (2006), 440.R-06: *Report on Fiber Reinforced Polymer (FRP) Reinforcement for Concrete Structures*, American Concrete Institute, Farmington Hills, MI, USA, Submitted, Under TAC Review.

Aidoo, J., Harries, K. A. and Petrou, M. F. (2004), 'Fatigue Behavior of CFRP-Strengthened Reinforced Concrete Bridge Girders,' *ASCE Journal of Composites for Construction*, **8**(6), 501–509.

Arockiasamy, M. and Thayer, C. C. (1998), 'Damage Process of CFRP Composite-Concrete Interface Under Fatigue Loading at Low Temperatures,' Proceedings of the Eighth International Offshore and Polar Engineering Conference, Vol. 4, Montreal, Canada, pp. 211–218.

Atadero, R., Lee L. and Karbhari, V. M. (2005), 'Consideration of Material Variability in Reliability Analysis of FRP Strengthened Bridge Decks,' *Composite Structures*, **70**, 430–443.

Bae, S. W. (2004), 'Evaluation of the Effects of Various Environmental Conditions on Reinforced Concrete Columns Wrapped with FRP Sheets,' PhD Dissertation, Department of Civil, Architectural, and Environmental Engineering, University of Missouri-Rolla, Rolla, MO.

Bae, S., Belarbi, A. and Myers, J. J. (2005), 'Performance of Corrosion-Damaged RC Columns Repaired by CFRP Sheets,' American Concrete Institute Special Publication-230, FRPRC-7, eds C. Shield, J. Busel, S. Walkup and D. Gremel, pp. 1571–1592.

Barnes, R. A. and Mays, G. C. (1999), 'Fatigue Performance of Concrete Beams Strengthened with CFRP Plates,' *Journal of Composites for Construction*, **3**(2), 63–72.

Beaudoin, Y., Labossiere, P. and Neale, K. W. (1998), 'Wet-Dry Action on the Bond Between Composite Materials and Reinforced Concrete Beams,' Proceedings of CDCC 1998, Sherbrooke, Canada, eds. B. Benmokrane and H. Rahman, pp. 537–546.

Bisby, L. A. and Green, M. F. (2002), 'Resistance to Freezing and Thawing of Fiber-Reinforced Polymer-Concrete Bond,' *ACI Structural Journal*, **99**(2), 215–223.

Breña, S. F., Wood, S. L. and Kreger, M. E. (2002), 'Fatigue Tests of Reinforced Concrete Beams Strengthened Using Carbon Fiber Reinforced Polymer Composites,' Proceedings of the Second International Conference on Durability of FRP Composites for Construction, Montreal, Canada, pp. 575–586.

CAN/CSA (1995), CAN/CSA S478-95: *Guideline of Durability in Buildings*, Canadian Standards Association, Ottawa, Canada.

CAN/CSA (2002), CAN/CSA S806-02: *Design and Construction of Building Components with Fiber-Reinforced Polymers*, Canadian Standards Association, Ottawa, Carada.

CCC (2001), Proceedings of the Second International Conference of Composites in Construction – CCC 2001, Porto, Portugal, October 10 to 12, 2001.

Chajes, M. J., Thomson, T. A. and Farshman, C. A. (1995), 'Durability of Concrete Beams Externally Reinforced with Composite Fabrics,' *Construction and Building Materials*, **9**(3), 141–148.

Chauvin, M., Shield, C., French, C. and Smyrl, W. (2000), 'Evaluation of Electrochemical Chloride Extraction (ECE) and Fibre-Reinforced Polymer (FRP) Wrap Technology,' Final Report 2000-24, Minnesota Department of Transportation.

Concrete Society (2000), 'Design Guidance for Strengthening Concrete Structures Using Fibre Composite Materials,' Technical Report 55, The Concrete Society, Camberley, Surrey, UK.

Concrete Society (2003), 'Strengthening Concrete Structures with Fibre Composites Materials: Acceptance, Inspection and Monitoring,' Technical Report 57, The Concrete Society, Camberley, Surrey, UK.

Curtis, P. T. (1989), 'The Fatigue Behavior of Fibrous Materials,' *Journal of Strain Analysis*, **24**(4), 235–244.

Debaiky, A. S. (2002), 'Rehabilitation of Corrosion-Damaged Reinforced Concrete Columns Using Carbon Fibre Reinforced Polymer (CFRP) Wraps,' PhD Thesis, Queen's University, Kingston, Ontario, Canada.

Debaiky, A. S., Green, M. F. and Hope, B. B. (2002), 'Carbon Fiber-Reinforced Polymer Wraps for Corrosion Control and Rehabilitation of Reinforced Concrete Columns,' *ACI Materials Journal*, **99**(2), 129–137.

Egyptian FRP Code (2005), *Egyptian Code for the Use of Fiber Reinforced Polymers (FRP) in the Construction Fields*, The Egyptian Housing and Building National Research Center, Egyptian Ministry of Housing, Utilities and Urban Development.

Ekenel, M., Rizzo, A., Myers, J. J. and Nanni, A. (2006), 'Flexural Fatigue Behavior of Reinforced Concrete Beams Strengthened with FRP Fabric and Pre-Cured Laminate Systems,' *Journal of Composites in Construction*, **7**(5), 433–442.

El-Tawil, S., Ogunc, C., Okeil, A. and Shahawy, M. (2001), 'Static and Fatigue Analyses of RC Beams Strengthened with CFRP Laminates,' *Journal of Composites for Construction*, **5**(4), 258–267.

Fib (2001), *Bulletin 14 External Bonded FRP Reinforcement for RC Structures*, Fédération Internationale du Béton.

FRPRCS-4 (1999), Proceedings of the Fourth International Symposium on Fiber Reinforced Polymer (FRP) Reinforcement for Reinforced Concrete Structures (FRPRCS-4), American Concrete Institute SP-188.

FRPRCS-6 (2003), Proceedings of the Sixth International Symposium on Fiber Reinforced Polymer (FRP) Reinforcement for Reinforced Concrete Structures (FRPRCS-6), Singapore, July 8 to 10, 2003.

Grace, N. F. (2004), 'Concrete Repair with CFRP,' *Concrete International*, **26**(5), 45–52.

Green, M. F., Dent, A. and Bisby, L. A. (2003), 'Effect of Freeze-Thaw Cycling on the Behaviour of Reinforced Concrete Beams Strengthened in Flexure with FRP Sheets,' *Canadian Journal of Civil Engineering*, **30**(6), 1081–1088.

Harries, K. A., Porter, M. and Busel, J. (2003), 'FRP Materials and Concrete – Research Needs,' *Concrete International*, **l25**(10), 69–74.

Heffernan, P. J. (1997), 'Fatigue Behavior of Reinforced Concrete Beams Strengthened with CFRP Laminates,' PhD Dissertation, Department of Civil Engineering, Royal Military College of Canada, Kingston, Ontario.

Heffernan, P. J. and Erki, M. A. (2004), 'Fatigue Behavior of Reinforced Concrete Beams Strengthened with Carbon Fiber Reinforced Plastic Laminates,' *Journal of Composites for Construction*, **8**(2), 132–140.

ICCI (2002), Proceedings of the Third International Conference on Composites in Infrastructure – ICCI–02, San Francisco, June 10 to 12, 2002.

ISIS Canada (2001), *Design Manual 4 – Strengthening Reinforced Concrete Structures with Externally-Bonded Fibre Reinforced Polymers*, ISIS Canada, Winnipeg.

Inoue, S., Nishibayashi, S., Yoshino, A. and Omata, F. (1994), 'Strength and Deformation Characteristics of Reinforced Concrete Beam Strengthened with CFRP Plate under Static and Fatigue Loading,' *Journal of Society of Materials Science, Japan*, **43**(491), 1004–1009.

JSCE (2001), 'Recommendations for the Upgrading of Concrete Structures with the use of Continuous Fiber Sheets,' Concrete Engineering Series, No. 41, Japanese Society of Civil Engineers, Tokyo.

Karbhari, V. M. (2000), 'Determination of Materials Design Values for the Use of Fibre-Reinforced Polymer Composites in Civil Infrastructure,' *Proceedings of the Institution of Mechanical Engineers, Part L, Materials: Design and Applications*, **214**L, 163–171.

Karbhari, V. M. and Eckel, D. A. (1994), 'Effect of Cold Regions Climate on Composite Jacketed Concrete Columns,' *Journal of Cold Regions Engineering*, **8**(3), 73–86.

Karbhari, V. M. and Howie, I. (1997), 'Effect of Composite Wrap Architecture on Strengthening of Concrete Due to Confinement: II – Strain and Damage Effects,' *Journal of Reinforced Plastics and Composites*, **16**(11), 1039–1063.

Karbhari, V. M., Rivera, J. and Dutta, P. K. (2000), 'Effect of Short-term Freeze-thaw Cycling on Composite Confined Concrete,' *Journal of Composites for Construction* **4**(4), 191–197.

Karbhari, V. M., Chin, J. W., Hunston, D., Benmokrane, B., Juska, T., Morgan, R., Lesko, J., Sorathia, U. and Reynaud, D. (2003), 'Durability Gap Analysis for Fiber-Reinforced Polymer Composites in Civil Infrastructure,' *Journal of Composites for Construction*, **7**(3), 238–247.

Kshirsagar, S., Lopez, R. A. and Gupta, R. K. (2000), 'Environmental Ageing of Fiber-Reinforced Polymer Wrapped Concrete Cylinders,' *ACI Materials Journal*, **97**(6), 703–712.

Lopez, M. M., Naaman, A. E. and Till, R. D. (1999), 'Bending Behavior of RC Beams Strengthened with CFRP Laminates and Subjected to Freeze–Thaw Cycles,' Proceedings of the Fourth International Symposium on Fiber Reinforced Polymer (FRP) for Reinforced Concrete Structures (FRPRCS-4), Baltimore, MD, pp. 559–576.

Lopez, M. M., Naaman, A. E., Pinkerton, L., and Till, R. D. (2003), 'Behavior of RC Beams Strengthened with FRP Laminates and Tested under Cyclic Loading at Low Temperatures,' *International Journal of Materials and Product Technology*, **19**(1–2), 108–117.

Masoud, S., Soudki, K. and Topper, T. (2001), 'CFRP-Strengthened and Corroded RC Beams under Monotonic and Fatigue Loads,' *Journal of Composites for Construction*, **5**(4), 228–236.

Meier, U., Deuring, M., Meier, H. and Schwegler, G. (1993), 'Strengthening of Structures with Advanced Composites,' *Alternate Materials for the Reinforcement and Prestressing of Concrete*, ed. J. L. Clarke, Blackie Academic and Professional, Glasgow.

Micelli, F., Myers, J. J. and Murthy, S. (2001), 'Durability of Concrete Cylinders Wrapped with GFRP and CFRP,' Center for Infrastructure Engineering Studies, Report Number 00-23.

Micelli, F., Myers, J. J. and Murthy, S. (2002), 'Performance of FRP Confined Concrete Subjected To Accelerated Environmental Conditioning,' Proceedings of the Second International Conference (CDCC 02) on Durability of Fiber Reinforced Polymer (FRP) Composites for Construction, eds B. Benmokrane and E. El-Salakawy, Montreal, Quebec, Canada, May 29 to 31, pp. 87–98.

Mukhopadhyaya, P., Swamy, R. N., and Lynsdale, C. J. (1998), 'Influence of Aggressive Exposure Conditions on the Behavior of Adhesive Bonded Concrete–GFRP Joints,' *Construction and Building Materials*, **12**, 427–446.

Murthy, S., Myers, J. J. and Micelli, F. (2002), 'Environmental Effects on Concrete-FRP Bond under Various Degrees of Sustained Loading,' Proceedings of the Second International Conference (CDCC 02) on Durability of Fiber Reinforced Polymer (FRP) Composites for Construction,' eds B. Benmokrane and E. El-Salakawy, Montreal, Quebec, Canada, May 29 to 31, pp. 333–346.

Muszynski, L. C. and Sierakowski, R. L. (1996), 'Fatigue Strength of Externally Reinforced Concrete Beams,' Materials for the New Millennium: Proceedings of the Fourth Materials Engineering Conference, Washington, DC, pp. 648–656.

Myers, J. J. and Ekenel, M. (2005), 'Performance of FRP-Concrete Bond Subjected to Environmental Conditioning during Installation Process', American Concrete Institute Special Publication-230, FRPRC-7, eds C. Shield, J. Busel, S. Walkup and D. Gremel, pp. 1447–1464.

Myers, J. J. and Viswanath, T. (2005), 'Appropriate Environmental Factors for FRP,' CIES Report 05-59, University of Missouri-Rolla, MO, USA.

Myers, J. J. and Viswanath, T. (2006), 'A Worldwide Survey of Environmental Reduction Factors for Fiber Reinforced Polymers (FRP),' Proceedings of the ASCE 2006 Structures Congress, St Louis, MO, Published on CD Rom.

Myers, J. J., Harries, K., Karbhari V. M. and Ziehl, P. (2004), 'Task Group Report on the Environmental Reduction Factors for Internal and External FRP by ACI Sub-Committee 440L.'

Pantazopoulou, S. J., Bonacci, J. F., Sheikh, S., Thomas, M. D. A. and Hearn, N. (2001), 'Repair of Corrosion-Damaged Columns with FRP Wraps,' *Journal of Composites for Construction*, **5**(1), pp. 3–11.

Papakonstantinou, C. G., Petrou, M. F. and Harries, K. A. (2001), 'Fatigue Behavior of RC Beams Strengthened with GFRP Sheets,' *Journal of Composites for Construction*, **5**(4), 246–253.

Porter, M. L. and Harries, K. A. (2005), Workshop on Research in FRP Composites in Concrete Construction – Final Report, Submitted to the National Science Foundation.

Pritchard, G. (1999), *Reinforced Plastics Durability*, Woodhead Publishing Limited, Cambridge, UK.

Quattlebaum, J., Harries, K. A. and Petrou, M. F. (2005), 'Comparison of Three CFRP Flexural Retrofit Systems under Monotonic and Fatigue Loads,' *Journal of Bridge Engineering*, **10**(6), 731–740.

Sen, R. (2003), 'Advances in the Application of FRP for Repairing Corrosion Damage,' *Progress in Structural Engineering Materials*, **5**, 99–113.

Sen, R., Shahawy, M., Mullins, G. and Spain, J. (1999), 'Durability of Carbon Fiber-Reinforced Polymer/Epoxy/Concrete Bond in Marine Environment,' *ACI Materials Journal*, **96**(6), 906–914.

Senthilnath, P. S., Belarbi, A. J. and Myers, J. J. (2001), 'Performance of CFRP Strengthened RC Beams in the Presence of Delaminations and Lap Splices under Fatigue Loading,' Proceedings of Composites in Construction: 2001 International Conference, Porto, Portugal.

Shahawy, M. and Beitelman, T. E. (1999), 'Static and Fatigue Performance of RC Beams Strengthened with CFRP Laminates,' *Journal of Structural Engineering*, **125**(6), 613–621.

Taljsten, B. (2002), 'FRP Strengthening of Existing Concrete Structures,' Lulea University of Technology.

Teng, M. H., Sotelino, E. D. and Chen, W. F. (2003), 'Performance Evaluation of Reinforced Concrete Bridge Columns Wrapped with Fiber Reinforced Polymers,' *Journal of Composites for Construction*, **7**(2), 83–92.

Toutanji, H. (1998a), 'Assessment of Long-Term Performance of Concrete Columns Strengthened with Fiber Advanced Fiber Composites,' Proceedings of the Young Faculty Research Symposium, University of Alabama in Huntsville, Huntsville, AL, USA.

Toutanji, H. (1998b), 'Durability Evaluation of Concrete Columns Strengthened with Advanced Composites,' Proceedings of the First International Conference on Durability of Composites for Construction (CDCC '98),' Sherbrooke, Canada.

Toutanji, H. A. (1999), 'Durability Characteristics of Concrete Columns Confined with Advanced Composite Materials,' *Composite Structures*, **44**, 155–161.

Toutanji, H. and Rey, F. (1997), 'Durability Characteristics of Concrete Columns Wrapped with FRP Tow Sheets,' Proceedings of the Third International Symposium on Non-Metallic (FRP) Reinforcement for Concrete Structures, Sapporo, Japan, Japan Concrete Institute (JCI).

Toutanji, H. and Balaguru, P. (1999), 'Effects of Freeze-Thaw Exposure on Performance of Concrete Columns Strengthened with Advanced Composites,' *ACI Materials Journal*, **96**(5), 605–611.

Toutanji, H., Zhao, L., Deng, Y., Zhang, Y. and Balaguru, P. (2006), 'Cyclic Behavior of RC Beams Strengthened with Carbon-Fiber Sheets Bonded with an Inorganic Matrix,' *Journal of Materials in Civil Engineering*, **18**(1), 28–35.

Wan, B. (2002), 'Study of the Bond Between FRP Composites and Concrete,' PhD Dissertation, University of South Carolina, Department of Civil and Environmental Engineering.

Wan, B., Harries, K. A., Petrou, M. F., Sutton, M. A. and Li, N., (2003) 'Experimental Investigation of Bond between FRP and Concrete,' Proceedings of the 2003 SEM Annual Conference, Charlotte.

13

Rehabilitation of concrete structures using fibre-reinforced polymer composites: identifying potential defects

H. KAISER and V. M. KARBHARI,
University of California San Diego, USA; and
C. SIKORSKY, California Department of Transportation, USA

13.1 Introduction

Fiber-reinforced polymer (FRP) composites are increasingly being considered for the rehabilitation of deteriorating and/or under-strength concrete structural components and assemblies through the external bonding of these materials to concrete. Applications range from the seismic retrofit of columns, piers, and walls, to the strengthening of slabs and girders. While strength and stiffness of the composite material are important to the systems' overall efficiency, the composite–substrate adhesive layer must provide adequate stress transfer capabilities. Unless the adhesive material is specifically designed for the purposes of adhesion to the specific substrate in question, stress transfer between the substrate and the composite, and resistance to the harsh outdoor environment, the rehabilitation will lack performance and will eventually undergo rapid deterioration.

If the composite element is bonded onto a concrete substrate, the efficacy of the method depends on the combined action of the entire system with emphasis on the integrity of the bond and the interface layers. The composite–adhesive/resin–concrete system must be considered as a complete system and materials aspects of each of the constituents, and interactions thereof between themselves and with the external environment, could have a significant effect on overall efficiency, renewal capacity, and durability. The external reinforcement can be applied in three generic ways, namely: adhesive bonding of prefabricated elements, wet layup of fabric, or resin infusion. Of these, the pre-manufactured alternative shows the highest degree of uniformity and quality control, since processing is done under controlled conditions. The composite strip/panel/plate is prefabricated manually or by an automated means (e.g. pultrusion) and is then bonded onto the concrete substrate using an adhesive under pressure. Application is rapid, but the efficiency is predicated by the use of an appropriate adhesive and through the achievement of a good bond between the concrete substrate and the composite adherend. Care must be taken to ensure that the adhesive is chosen to match as closely as possible

both the concrete and composite *vis-à-vis* their elastic moduli and coefficients of thermal expansion, while providing an interlayer to reduce mismatch-induced stresses. Commercially available strips are currently fabricated using unidirectional carbon fiber reinforcement, which is pultruded to preset thicknesses and widths. While this ensures uniformity of the material, preset dimensions often restrict the use of prefabricated material on structures with a more complex geometry.

As in other industries, the wet layup process is perhaps the most used currently and gives the maximum flexibility for field application. Moreover, it is probably the least costly alternative. However, it presents the most variability and necessitates the use of excessive resin and could result in wrinkling or shear deformation of the fabric used, decreasing its designed efficiency. The process entails application of resin to the concrete substrate followed by the impregnation of layers of fabric, which are bonded onto the substrate using the resin itself. Both the composite and the bond are formed at the same time in the field. The process affords the maximum flexibility in the field but has the disadvantage of field mixing and fabrication along with a high potential for absorption of moisture and/or inclusions and impurities. Once applied, the composite is left to cure under ambient conditions. At present, both plain weave and unidirectional fabrics are commercially available for rehabilitation means.

The *in-situ* resin infusion method is a fairly new variant and is capable of achieving uniformity and good fabric compaction, while making it easier for the reinforcement to be placed without excessive unintended deformation. However, this scheme is difficult to apply over large areas and necessitates application of vacuum. In the infusion process, the reinforcing fabric is first formed into a preform, which is attached to the substrate using a vacuum bag. Resin is infused into the fibrous assembly under vacuum to form the composite. As in wet layup, the composite and bond are formed at the same time.

To date, a reasonable level of effort has been expended on developing an understanding of materials choices (Hawkins *et al*., 1998; Karbhari, 2001; Seim *et al*, 2001), design and analysis considerations (Seible and Karbhari, 1997; Ali *et al*., 2000; Triantafillou *et al*., 2000), and to a lesser extent design detailing. Despite the potential of these materials for rapid and cost-effective rehabilitation, two major challenges still need to be addressed. The first relates to the development of a sufficient level of knowledge about lifetime durability, whereas the second is related to the identification of potential defects that may occur at each step of the life cycle. The latter is critical since without it civil engineers in the field, who generically have very little specialized knowledge of FRP composites, will be hesitant to use these new techniques for lack of a basis for inspection and field acceptance of rehabilitated systems.

13.2 Defects in composite materials

The performance of composite materials depends on the successful incorporation of high-strength and -stiffness fibers in a surrounding matrix material. While fibers are the main contributors to strength and stiffness, the matrix serves as a medium for transferring stresses between adjacent fibers. Thus, an ideal unidirectional fiber-reinforced composite material would have straight fibers running exactly parallel to each other, with fibers completely embedded in a strongly adhering, uniform matrix material. However, due to several factors, which will be addressed in the following, uniformity of the material may be disturbed. Such imperfections can occur in the fiber material and in the matrix, as well as at the interface between both materials. If two materials are bonded together to form a composite (e.g. two composite strips), high quality of the interface is crucial, since it ensures stress transfer between layers. Bonding can be achieved using a resin system identical to that used for fiber infiltration or by application of special adhesives. These materials are preferably high-viscosity polymeric systems, particularly in cases where one material shows a significant amount of surface irregularities (i.e. when bonding composites to concrete).

Apart from knowledge of the common defect types encountered in composite materials, their initiating factors (why and when a defect is introduced) must be studied. For most applications, two distinct stages can be identified, namely defects produced during manufacture and in-service damage. A large body of research has already been conducted by the aerospace industry, a sector where high material uniformity and performance are an absolute necessity (Bishop, 1981; Farioli *et al*., 1983; Parslow 1983; Potter, 1983; Purslow, 1983; Cawley and Adams, 1989; Davies and Brunelliere, 1993). In this chapter, results of the extensive knowledge from the aerospace and marine industries are used to provide a basis for defect identification and assessment for the specific application under consideration in this book. Due care is however taken to assure applicability and appropriateness for the materials set and to use processing conditions that would be used in a civil engineering context.

Depending on size, defects can be classified as either microscopic or macroscopic. The former includes material flaws such as hollow, cracked, or otherwise damaged or degraded fibers, and variation in fiber diameter, as well as fiber–matrix debonds and/or non-uniform and poor fiber wet-out; the latter is mostly related to matrix voids, misorientation, wrinkling or shearing of fabric, as well as delamination or separation of reinforcing fabric layers. It has been shown that microscopic defects in the form of existing defects on fibers occur even in the best laminates and that their effect on material performance is mostly negligible. Consequently, it has been suggested that, whilst causing slight reductions in material strength, microdefects should be

regarded as a material property (Purslow, 1983). However, effects of environmental exposure-induced fiber degradation, fiber–matrix bond non-uniformity, and non-uniformity in wet-out can be significant and cannot be neglected. However, most of these effects can be avoided through the judicious and appropriate selection of constituent materials (fiber and resin) and adherence to rigid processing standards. The use of prefabricated components is one means of ensuring a reasonable level of quality control and assurance. Classification of defects in wet layup systems is, however, more complicated. Here, the ratio of defective material over good material seems more deterministic towards defect criticality than the actual type of flaw encountered. As such the isolated local existence of microscopic traces of contaminants such as moisture may be less significant than the larger agglomerations of inclusions or global uptake of aqueous media.

Generally, it may be assumed that the manufacturer controls the quality of constituent materials (fibers, resin system components) to a sufficient degree. Nevertheless, poor manufacturing, handling, or storage of the material during production/transportation can result in fiber damage, distorted alignment of fibers within the fabric, contaminations, or surface moisture accumulation. Small debris, dirt, or other objects that adhere to single fiber bundles typically contaminate fibrous reinforcement (Cawley and Adams, 1989). While resin systems are less susceptible to physical damage, the vast majority of systems can be degraded by impurities. Contaminations in resins occur in the form of foreign chemicals, moisture, or fine particles, altering its chemical consistency and reactivity. Furthermore, their limited shelf life provides the chance of using over-aged material that has lower reactivity along with an increase in viscosity to a point where processing becomes virtually impossible. Also, fiber–matrix bond is substantially lower if the resin system lacks reactivity or if contaminations are deposited on the fiber surface.

Prefabricated material designed for installation in the field typically possesses a higher degree of material uniformity. Since cutting of fabric and/or tensioning of individual tows in unidirectional pultruded elements, infiltration, and cure of the part are performed by automated processes as well as in a controlled environment, most of the previously addressed material flaws can be ruled out in this form of material. It can thus be assumed that these materials possess a relatively low amount of internal defects. Nevertheless, handling damage remains as a potential initiator for material flaws.

Another important aspect in material quality is related to moisture accumulation. Resin systems are capable of moisture absorption, generally resulting in inferior material properties, including loss in shear strength, reduction in modulus, and depression in the level of the glass transition temperature. Furthermore, moisture absorption can cause significant physical and chemical changes in the resin leading to irreversible changes through hydrolysis, saponification, and other such phenomena. While the strength

and modulus of carbon fibers is not influenced by moisture, a significant decrease in bond strength in the composite can occur if moisture is accumulated on their surface. However, both glass and aramid fibers can be severely degraded by the presence of moisture next to the bare fiber. Material properties can further be influenced by storage conditions. Resins and fibrous material should therefore be stored in a cool and dry environment, to prevent moisture accumulation and unintended gelling.

One of the main reasons for variations in material properties is the manufacturing process, i.e. the procedure used to develop the desired combination of resin and fibers to form the composite material. Since a small degree of human involvement always remains, even the most automated processes are susceptible to human errors. Naturally, composite material defects occur more frequently in parts manufactured by hand layup than in most other automatically processed components. Common types of defects include: porosity, voids (air pockets), incorrect fiber orientation, resin richness/poorness, poor mixing, incorrect cure, inclusions and dirt, as well as wrong stacking sequences and delaminations (Bishop, 1981; Parslow, 1983; Purslow, 1983; Cawley and Adams, 1989; Davies and Brunelliere, 1993). Air pockets typically become entrapped when stacking multiple sheets of lamina and must be removed via use of rollers. Although this provides a means to remove most of the entrapped air, small amounts always remain inside the matrix. Porosity, a microscopic defect, can also be caused by volatiles given off during the curing cycle. In regions where porosity shows a high occurrence, these microscopic defects may join together to form a large void (Cawley and Adams, 1989).

High localized loading, such as from the impact of an object, causes one of the most common in-service defects. The exposure to runway debris often induces subsurface delaminations that are not visible on the surface yet significantly reduce material performance. Material defects induced during manufacturing, such as voids or excess resin, often weaken the plane between two layers of fibrous reinforcement. Under high-loading conditions, interlaminar cracks can form. Furthermore, moisture penetration remains critical even in the cured state. Over time, water and other liquids can penetrate the material and accumulate in porous matrix regions.

Similar to the composite material itself, quality and performance of adhesive bonds can be influenced by a number of material flaws. Depending on the substrate material, adhesives must be chosen to match the surface structure. The two main phases involved in adhesive bonding are the adhesive and the adhesive–adherent interface.

Similar to the matrix in composite materials, porosity, voids, incorrect or incomplete curing, and application of incorrect amounts of constituents of the adhesive can be found in the application of polymeric adhesives. Moreover, the adhesive–adherent interfaces can experience weak bonding due to chemical

deposits or material inclusions. Here, adherent refers to both prefabricated as well as substrate material. Sufficient abrasion followed by cleaning and, in the case of a concrete substrate, application of adequate surface primers, often results in a high-quality bond. During service, moisture penetration can lower the material properties and cause the loss of bond, resulting in separation of the bonded materials.

13.3 Defects occurring during rehabilitation

During rehabilitation of structural elements, defects may be induced at one or more of four phases, namely: in the incoming raw materials, during site preparation stages, during field installation, and/or during the service life of the rehabilitated component/system. It is important, however, to note that not all inconsistencies in materials, form, or process should be considered as critical defects. A structurally significant defect can be defined as a material flaw that, within the lifetime of a structure, reduces its load-carrying capabilities to a level less than or equal to the level of desired performance. Although it may be impossible in some cases to eliminate defects once they occur, criticality can vary significantly based on defect type, location, size, and density. The following sections describe the classes of defects most likely to be encountered during structural renewal of concrete structures using FRP composites. It is emphasized that while most defects can be related to a specific stage of the rehabilitation process, some may be induced at several, if not all, stages of the rehabilitation process.

13.3.1 Incoming raw or constituent materials

Generally, any variation from the manufacturer's specifications should be reported and considered carefully. While a large number of resin systems are commercially available, they generally cannot be used interchangeably. If the resin system is not suitable for the desired purpose, it must not be used. Material variations caused by improper storage or production, such as chemical inconsistency or impurities, are typically inspected visually on a pass/no-pass basis, typically through viscosity tests. More sophisticated techniques of material testing are mostly unavailable in the field since they generally require laboratory equipment. Consequently, control has to be performed in compliance with a specification sheet, as commonly supplied with most resin systems. While this may be used for some aspects, such as shelf life, it does not provide any information on impurities or moisture absorption during storage.

Resin, hardener, catalyst, or additives may be beyond their specified shelf life and thus classified as over-aged material. Most cans bear a label showing the date of expiration of the contents. Typically, resin shelf life ranges between

3 and 8 months. If stored in warm environments, resin tends to polymerize inside the container, thus decreasing shelf life. Although reactive agents have not been introduced to the resin, the constituents slowly cure, as the material is stored. If expired, resins should not be used. An over-aged resin system shows lower reactivity, resulting in lower strength and elastic modulus. Also, viscosity increases with time, leading to difficulties during fiber infiltration. These properties can be checked through the use of viscosity tests and differential scanning calorimetry (DSC).

Resin inclusions may be present in the form of small particles, such as dirt, sand, etc. If worked into the fabric, fibers may be damaged. In addition, chemical consistency may be altered, depending on the type of inclusion. If oils or silicones are mixed within the resin, they may serve as potential initiators for debonding or delamination. These material flaws can be detected through viscosity tests since additions cause an increase in viscosity. Moisture can be detected through DSC or dynamic mechanical thermal analysis (DMTA) of cured materials, and in extreme cases, Fourier transform infrared (FTIR) spectroscopy can be used to assess the state of the resin system itself.

Improper storage of sealed containers over extended periods of time may induce moisture to the resin, leading to poor reactivity and incomplete cure. In addition, resealing of containers may result in moisture contamination of the remaining resin. If large quantities of resin have been stored in a humid environment, a DSC or FTIR test may be used to check for increased moisture content. Although time consuming due to additional off-field laboratory time, it can ascertain the quality of the resin and prevent long-term effects. The introduction of moisture into resin can lead to premature gelation, degradation through saponification, hydrolysis, or other chemical reactions.

Fibers are supplied in different forms with varying fibrous assembly geometries (unidirectional and multidirectional) to provide strength in one or multiple directions. For most rehabilitation applications, a unidirectional or a woven fabric is preferable. As the fabrics are usually supplied on rolls, damage to fibers may not be detected until immediately prior to installation. Prior to installation, fiber type, structure, and weave geometry has to be inspected. The material must meet the design specifications (type, strength and stiffness properties) in all aspects. If the material appears different in geometry, it most probably possesses strength and stiffness properties that vary from those required. Although this control process is visual and rather unsophisticated, it requires the installer to have basic knowledge of fiber geometry and the appearance of different fiber types.

Fibers inside a fabric may be kinked or wavy due to handling. If kinked, fibers may easily break during handling or installation. Wavy fiber bundles do not run in the principal loading direction, hence they are not capable of resisting equally high loads along this direction. As a result, adjacent, straight fiber bundles have to account for higher stresses (stress concentrations). In

addition, a loss in stiffness is likely to be encountered. While a single broken fiber is difficult to detect, broken fiber strands are more critical and should be noted. Although each fiber bundle contains a large number of fiber discontinuities (due to the manufacturing process), these discontinuities differ in location throughout a bundle. Therefore, stress concentrations from one broken fiber may be easily adopted by adjacent fibers. In the case of a ruptured bundle, however, stress concentrations are significantly higher and weaken the fabric to an enormous extent. The fiber surface may contain impurities in the form of chemicals or small objects, which can harm both fiber and bond strength. While carbon fibers are rather inert to chemicals, glass fibers are highly susceptible to alkali attack. Sizing chemistry, a measure for resin–fabric bond capability, can be affected by certain chemicals and thus reduce bond strength. Small objects are likely to be trapped near the fiber surface to form a void and serve as a potential debond. In the case of sharp-edged inclusions, fibers may be severely damaged upon infiltration.

During handling, impregnation, and placement of fabric layers, as part of the rehabilitation process, the architecture itself may be changed, resulting in movement and/or wrinkling of the path of individual or groups of tows. Often this results in the formation of kinks and wrinkles in the fabric itself, causing the fabric to be non-planar. It is essential that these non-uniformities be straightened as far as is feasible without further deterioration of the fabric, prior to impregnation, or at least before resin gelation. If a fabric has a wrinkle running along its entire width, strength and stiffness reduction may be a concern, especially if the wrinkle is not smoothed out during fabrication of the composite resulting in air entrapment, fiber misalignment, and local zones of weakness and points of crack/delamination initiation.

If woven fabrics are exposed to shear forces during handling, fiber alignment can change to an undesirable off-axis direction, due to which the full strength and stiffness may not be realized. During handling of fabric rolls, damage to free edges is likely to occur. Because a fabric structure does not exhibit the same integrity around the edges as inside the woven area, edges are also more likely to decompose during resin infiltration. Materials often utilize additional rows of stitching along the material edges that are effective in preventing such decomposition. However, if the stitching is damaged or missing, the affected portion must be discarded. In the case of multiaxial fabrics, the removal or damage of tows can cause change in the local reinforcement ratio.

Pull-out of single fibers or fiber bundles may occur during processing, as well as during handling in the field. Loose material does not exhibit the same intermediate contact to nearby fibers and is more likely to be sheared during resin infiltration. Furthermore, resin-rich areas tend to form in these regions, resulting in low stress transfer capabilities between adjacent fiber strands. Separation of fiber tows within a woven fabric or unidirectional tape can be

experienced in the form of gaps. Such gaps will disturb fiber integrity, lower strength and stiffness, promote resin richness, and serve as locations of low crack propagation resistance.

Similar to resins, fibers may accumulate surface moisture if exposed to humidity for an extended period. Overnight storage should be performed under stable temperatures and in a moisture-controlled environment. If moisture is apparent, fabric should be discarded. Most fibers do not absorb moisture. However, surface moisture will lower bond strength to the resin matrix and present the risk of large area delamination.

For some applications, prefabricated composite strips are preferred over wet layup of fabric. Manufactured under controlled conditions, prefabricated material is less likely to experience material strength degradation due to voids, non-uniform impregnation, or moisture entrapment. A special adhesive is chosen to bond the reinforcement to the prepared concrete substrate. In most cases, long uniform strips are used to serve as additional flexural or shear reinforcement. These are commonly made via the pultrusion process. On more complex members, such as T-girders, the use of prefabricated material is likely to be limited due to the requirement of exact conformance with specific geometric configurations. Although L- and U-shaped sections are commercially available, their suitability must be confirmed for each individual member prior to attempting installation. A slight deviation in chamfer or web dimensions along the girder length may therefore not allow the use of identically prefabricated parts. Nevertheless, prefabricated material has been used successfully in concrete rehabilitation. Since prefabricated material is manufactured under controlled conditions, void content may be considered low. In most cases, the quality control of the supplier determines whether a part is acceptable or should be discarded. In addition, specification sheets of prefabricated material are based on average results and account for a typical void content.

Damage to prefabricated material may be induced during storage, transportation, or handling. Typical defects include splitting, delamination, matrix cracking, scratched surfaces, etc. Once the material has left the processing facility, the installer must determine whether it has experienced additional damage and make assessments towards the suitability for installation. It must be emphasized, however, that these forms of material damage are not a common occurrence.

13.3.2 Site preparation and on-site processing

Any successful rehabilitation measure demands proper preparation of the structural element. This includes surface preparation, such as sandblasting, of the concrete to a desired degree, storage of fiber and resin constituent materials, as well as mixing of the resin system. On-site processing, if performed

incorrectly, contains a high potential for flaw introduction. It further necessitates assessments with regards to the integrity and bond capability of the concrete substrate. In some cases, cracked or split concrete sections may contain wide cracks that must be injected with resin prior to application of the composite-strengthening system. Defects induced by preparation and site processing are listed below.

Improper storage of the resin system, as well as the hardener/catalyst, can lead to significant moisture absorption. If stored under inappropriate conditions – such as extreme cold, heat, or humidity – resin properties may change dramatically with time. In addition, as discussed previously, shelf life must be monitored to assure sufficient reactivity and viscosity.

Difficulties may arise with systems that show inadequate stoichiometry. Resin and hardener/catalyst must be compatible and of adequate mechanical and chemical properties for the job at stake. For all resin systems, the hardener/catalyst ratio must be determined very carefully to prevent premature gelling or loss of matrix strength.

During mixing, several defects may be introduced to the system, and consequently to the laminate itself. Firstly, if using rotary mixers, air can be drawn into the resin and remain as small air bubbles, leading to laminate porosity. In some cases, this porosity may later result in the formation of air bubbles of much larger diameter (millimeter range). A high number of roller passes are thus required to remove porosity from laminates that have been infiltrated with air-rich resin systems, since it is known that in the range from zero to 5%, each 1% increase in void content decreases interlaminar shear strength by about 10% (Ghiorse, 1993). Consequently, mixing must be performed at a slow rate and without drawing an excessive amount of air into the matrix. In contrast, a low degree of mixing can result in chemical inconsistency, meaning that some regions contain high percentages of reactant, while others may contain no reactant at all. Secondly, the efficacy of the resin system depends on the appropriate use of mix ratio. Errors in mix ratio can result in under cure, extreme lack of even gel and vitrification, premature gelation, or local hot spots and runaway exotherms resulting in degradation.

Like resin, fibers are susceptible to moisture accumulation; however, accumulated moisture does not alter the performance of individual fiber tows. Instead, the bond to the surrounding matrix is severely weakened. Since fibers can be directly exposed to the environment, conditions must be monitored more closely than in the case of a sealed resin container. If visual detection shows a significant amount of moisture accumulation on the fiber surface, they must be discarded. When a moist fabric is infiltrated, it will experience a weak bond to the surrounding matrix. Debonding and subsequent delamination are likely to result.

To obtain adequate force transfer between the retrofit material and the concrete substrate, concrete preparation is essential. This includes thorough surface preparation to a specified degree and filling of concrete cracks. Large, deep cracks propagating into the concrete may contain water that can destroy the composite–concrete interface bond and should therefore be injected prior to rehabilitation. Cracks propagating at shallow depth can promote failure in the substrate. As such, the retrofit becomes ineffective.

Concrete is a porous material and hence absorbs liquids. Moreover, due to abrasion of cement paste during sandblasting, a large number of small to medium diameter voids become exposed on the concrete surface. Prior to application of the composite overlay, regardless of type, a compatible primer coat should be applied. The role of this primer is to fill voids and quench the absorption so that the surface is prepared for the subsequently applied composite material. If primer coatings are omitted, the saturating resin would be to an extent absorbed. In addition, the primer presents a 'bondable' surface. To ensure an intimate bond between composite and concrete, the thickness of the coating should be kept as thin as possible. If excessive amounts of primer are used, low stress transfer capabilities and resin dripping can result.

Marking of areas that require strengthening is generally done using a chalk line. However, care must be taken not to cause separation between the layup and base material by applying a material that cannot be penetrated by the resin/adhesive, or that could cause edge debonding, which not only serves as a weak zone but also a potential initiator for bond degradation.

If the concrete substrate displays a high degree of microcracking at its surface, the composite overlay must bond to an initially weak base material. In extreme cases the degraded cover material may need to be completely removed and replaced by appropriate fillers, prior to rehabilitation.

Naturally, many structures in need of rehabilitation already show a large number of cracks, which may have opened to a significant degree and thus accumulated moisture, dirt, or other foreign material over time. By applying a primer coating, inclusions may become permanently encapsulated within the surface to serve as weak spots for future crack initiating and propagation at the interface level. As a preventive measure, cracks should be cleaned and injected with appropriate filler materials, depending on the depth and diameter of the crack.

To provide a smooth surface for bonding, any irregularities such as form lines or protruding aggregate should be ground down. If a composite laminate is applied to concrete surfaces that contain high spots, the laminate will tend to form an air pocket. Similarly, large, hollow regions, which may result from high spots in the formwork, must be filled prior to composite application.

Carbon fibers, when in direct contact with steel, cause the formation of a galvanic cell, which results in the accelerated corrosion of steel and degradation of the matrix in the composite (Woo *et al*., 1993). In spalled, or otherwise

substantially degraded concrete components the loss of cover concrete can result in this interaction. Thus appropriate levels of concrete rebuilding are essential prior to the placement of the fiber.

13.3.3 Field installation

Among the four main stages of rehabilitation, field installation may be considered the most critical step with regards to quality assurance. A wide range of defects, classifiable from benign to severe, can be introduced at this stage. Numerous research studies have been conducted that quantify the possible defects in composite materials. However, most research has been focused on aerospace applications (Farioli *et al.*, 1983; Potter, 1983). Environmental conditions and material preparation are key elements to a successful installation of the material. For instance, many resin formulations do not cure at low ambient temperatures (≈5°C) and develop significantly lower glass transition temperatures. In addition, a hot environment will cause premature gelling and make handling virtually impossible. Thus, installation should not be undertaken when temperatures, both ambient and on the concrete surface, are either below or above specific temperature levels and humidity conditions. The levels must be set based on the specific requirements of the resin/adhesive system being used. Furthermore, surface preparation and application procedures have to be followed closely to ensure proper interfacial bond strength as well as complete infiltration of the fibers. In the following paragraphs the defects most likely to be encountered during retrofit installation are addressed.

Until the resin has developed adequate tackiness, i.e. turns into a gel, the infiltrated material tends to separate from the concrete (sagging), especially in vertical and overhead regions. To prevent large-scale debonding, the most susceptible areas must be rolled repeatedly until resin tack can be confirmed. If the material sags there is no bond or intimate contact between the composite and the substrate, thus stress transfer capabilities are severely reduced. Moreover, air pockets promote the accumulation of moisture as a long-term effect. Insufficient amounts of resin/adhesive can lead to a weak interfacial bond. While resin-rich regions experience low stress transfer, resin-starved areas tend to favor disbonding of the composite material from the concrete substrate.

Any air bubbles contained in the resin system will probably appear as porosity on the substrate or the composite as it is laid up. Porosity is termed as the presence of a large number of microscopic air voids, typically in the range of 10 μm. It may be caused by volatiles and entrained gasses (air and water vapor) inside the resin/adhesive. While porosity can be considered an expected phenomena, it serves as a depository for diffused moisture. In certain areas, microvoids may combine to form a large void.

Voids are typically caused by air entrapment during the layup process. Other factors contributing to void formation are entrapped air from mixing, volatiles/gasses, an insufficient amount of resin applied, and inclusion of foreign particles. In addition, if laminate is placed over high spots, which can occur as a result of formwork irregularities, air is likely to become entrapped around it. Thus, careful grinding of irregularities after sandblasting is advisable. Both porosity and voids cause internal stress concentrations.

If multiple layers of fabric are placed on top of each other, air usually becomes entrapped between them. Rollers can be used to 'work out' most of the air. In addition, overlapping of layers promotes the formation of voids, since additional resin is needed to fill the gap formed at the overlap. For instance, voids in unidirectional composites exist as tubular pores, which run along adjacent fiber directions, almost exclusively at the fiber–matrix interface.

In the case of moisture accumulation on the fiber surface, deficiencies in bond strength between fibers and the surrounding matrix may occur. Depending on the amount and location of moisture accumulation, this can mean lack of bond formation during cure or debonding of the fibers from the matrix at a later stage. Generally, debonding results in loss of composite strength in transverse tension, interlaminar shear, and impact. Unlike delamination, debonding occurs in localized areas.

Wrinkles, in which air is entrapped between layers, inclusions of non-adherent foreign objects, or an inadvertent use of moist material may cause a delamination. In most cases, delamination is present over a fairly large area and severely reduces shear transfer capacity.

Just as the intrinsic properties of a composite are affected by the alignment or orientation of fibers, waviness or wrinkling introduced in the fabric during placement can cause significant reduction in performance. The waviness can originate either from handling damage prior to or during impregnation, or during placement and rolling on the composite layer after placement in contact with the concrete substrate. Often this happens when rollers are used in an arbitrary fashion in an attempt to remove voids.

Resin-rich areas result from the use of excessive amounts of resin during fiber infiltration. Proper rolling/squeezing of the fibers may contribute to lower void volume, higher uniformity, and removal of resin-rich areas. Resin-starved areas (resin poorness) are caused by an insufficient amount of resin. Consequently, no interlaminar bond will be present in those areas. In addition, resin-poor areas serve as a potential initiator for delamination.

Damage to edges mostly occurs in regions where fibers have already been pulled out of the fabric in the dry state. Upon infiltration, the weave loosens and allows fibers to be pulled from the fabric, causing a reduction in performance attributes and increasing the potential for eventual separation of the material from the concrete substrate along the bond line.

The high susceptibility of structural renewal measures to human error allows for the omission of entire layers within a stacking sequence, particularly in more complex applications, where multiple layers are used. Consequently, the occurrence of such a defect will result in strength/stiffness properties of the laminate that will most probably be entirely different from the design values.

The use of prefabricated material involves two distinct interfaces, the concrete–adhesive interface and the adhesive–adherent interface. The strength of each individual interfacial zone is dependent on different factors, including surface preparation as well as preparation of the adherent. Adequate preparation of the prefabricated composite material is essential in obtaining a strong bond. Similar to concrete, surface preparation of prefabricated material is performed to abrade its surface and, ideally, expose some fibers to the surface. However, care must be taken so that the fibers will not be severely damaged, i.e. abraded or cut. Bead blasting (Chajes *et al.*, 1996) and solvent wipe have proven to be suitable methods for enhancing mechanical interlock between adhesive and the adherent surface. On certain systems, strips are pre-sanded as part of the manufacturing process, leaving a smooth outer surface and one with a more pronounced fiber texture. Apart from preconditioning of the adherent, the adhesive used must be suitable for the composite material, i.e. it must allow for stress transfer and remain functional at a wide temperature range.

Given the fact that prefabricated strips are applied in a cured state, they are less flexible than wet fabric and do not conform to surface irregularities as well. To obtain high uniformity of the adhesive prior to joining, strips are commonly passed through special resin applicators. If this operation is performed at a highly inconsistent rate, it can lead to non-uniform application including regions having no adhesive. These must later be filled in by hand to reduce the risk of air entrapment. Due to a natural tendency of composite strips to retain their straight orientation, regions of overlapping are usually critical. This includes utilization of grid patterns, which often result in excessive bondline thicknesses, which result in a higher load being borne by the adhesive layer causing its premature failure. If strips are rolled in an attempt to reduce bondline thickness, much of the resin becomes removed from underneath the strip, resulting in resin-poor areas once the composite has returned to its natural orientation. In other applications the ends can sag downwards due to the viscoelastic nature of the adhesive prior to cure, resulting in increased adhesive thickness in these regions of sag. Since the ends generically face the highest level of shear this can cause premature peeling or cracking within the adhesive layer itself under load.

While these characteristics are unique to the application of prefabricated strips, other defects include non-uniform concrete/composite interfacial thickness, porosity, and voids, as discussed earlier.

13.3.4 In-service defects

Most in-service defects found in rehabilitated structures may be considered to have long-term effects only, assuming that no significant defects have been induced during the installation process. These include the propagation of existing flaws at the concrete–composite interface or inside the composite. Service loading, fatigue, or environmental effects – such as moisture or heat – can cause growth of defects. Damage initially caused during service includes moisture diffusion, both from outside as well as inside the concrete, and impact of objects. Although impact is a rare occurrence, vehicle impact or road debris can induce subsurface delaminations that are often barely visible on the surface. Instead, damage increases with depth and can therefore cause substantial damage to the concrete–composite interface.

Penetration of moisture and chemicals over time can degrade the interfacial properties by plasticization of the resin/adhesive. This change in material properties results in reduced stiffness of the resin and increases the likeliness of delamination. In general, bonded joints are especially susceptible to damage from aggressive chemicals and moisture.

The glass transition temperature, T_g, of each individual resin system, depending on resin type and cure conditions, predetermines maximum service temperatures at which the resin will start to severely degrade. Exposure to high temperatures influences the mechanical properties of most adhesive/resin systems. Under elevated temperatures, polymers may soften and lose their ability to transfer stresses efficiently. Under extreme conditions such as exposure to fire, the material completely degrades.

Moisture can be absorbed from the air or can diffuse through the concrete to the concrete–composite interface and ultimately into the composite itself. These phenomenona are promoted by either inadequate or damaged surface coatings, which are designed to protect the material from any form of diffusion, or a high degree of concrete moisture. To allow evaporation of entrapped moisture inside the concrete, placement of composite sheets over excessively large areas must be avoided. Those regions already containing delaminations, voids, or other forms of air entrainment attract moisture and serve as a depository.

Most matrix cracking occurs in the form of interlaminar cracks (delamination), as opposed to translaminar (perpendicular to the layer direction) or transfibrous (perpendicular to the fiber direction) cracks. Initiating factors can be entrapped air and excess resin, causing sudden changes in direction of load transfer and local stress concentration. Since the transverse stress of a typical carbon composite is about 30 times lower than its tensile strength, such cracks may easily grow under sustained loading.

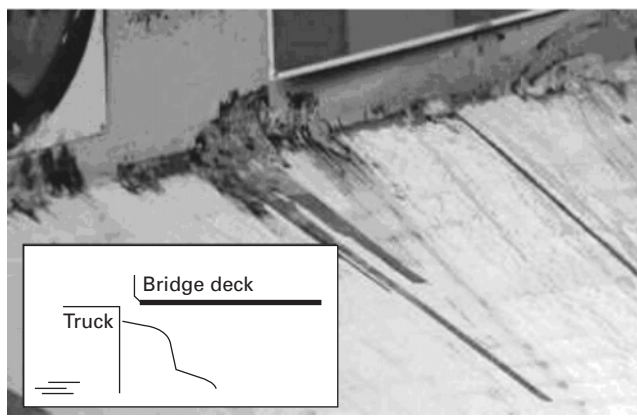
Unless they propagate deep into the fibers, scratches and surface abrasion can be considered largely a form of benign flaw that has a negligible influence

on strength and stiffness. However, if scratches are caused by the impact of an object, internal damage in the form of subsurface delamination can result. Figure 13.1 displays a severe form of surface damage as found on an FRP-rehabilitated bridge girder subject to local abrasion and impact from a vehicle. Barely visible impact damage (BVID) is considered one of the most critical material flaws that may occur during service of a composite member (Potter, 1983). If a hard, slow-moving object impacts the surface of a composite laminate it may cause only slight damage to the surface, while severe subsurface matrix cracking is likely to occur.

Other service defects include matrix brittleness due to ultraviolet radiation, exposure to freeze/thaw cycles, as well as growth of any existing defect due to service loading or environmental effects. Unprotected composite surfaces lacking adequate protective coatings are especially susceptible to ultraviolet radiation which causes a steady level of surface degradation. This can result in a more brittle matrix behavior and unfavorable mechanical properties. Growth of existing defects is one of the critical aspects in servicing of rehabilitated structures, since it demands continuous monitoring of composite and concrete–composite interface quality. While many defects may remain constant in size and, to some respect, criticality, others may grow quite rapidly under service loading or environmental influences to form flaws that call for immediate repair measures.

13.4 Effect of defects

The performance and expected lifetime of rehabilitation measures greatly depend on quality of workmanship and are jeopardized by a wide range of material defects. Prior to installation, potential defects must be known and



13.1 Severe form of surface abrasion caused by trucks.

evaluated for their likelihood of occurrence during the individual project. Special attention should be paid to storage, handling, and preparation of incoming materials as well as site preparation. Apart from a well-coordinated installation process, a suitable environment for work with composite materials must be provided. Although a successfully performed installation procedure with low defect occurrence would yield a fairly long service life, harsh environmental conditions can cause rapid deterioration of most composite strengthening systems. Hence, quality monitoring must be performed beyond the installation stage and should continue throughout the lifetime of a rehabilitated structure. Tables 13.1 to 13.4 summarize all previously discussed defects by their initiating phase. Furthermore, possible potential effects are also listed.

While the types of defects likely to be encountered are mostly known, information on defect criticality and their effect on short-/long-term structural performance remain widely unknown. Nevertheless, previous research has shown that defects such as localized porosity, surface scratches, or single broken fibers do not have a significant effect on material performance. Instead, they should be considered a material property that must be accounted for, especially if processing of composites is performed manually. Assessment of criticality of such 'normal' defects can therefore be done on the basis of previous research results, whereas different techniques must be employed to characterize and quantify the effect of defects such as severe debonding, delamination, large voids, tow breakage or moisture accumulation, to name only a few. Thus, the need for further investigation in this field arises.

Since most rehabilitations are expected to provide significant periods of service it is important that the effect of defects be clearly determined so as to provide the engineer with guidance as to whether a defect found during inspection has to be immediately treated, or can be monitored for a period of time before repair/replacement becomes necessary, or merely neglected as being non-critical and aesthetic in nature. In addition, it is important that the effect of environmental exposure on the system be assessed since this could have an accelerative effect on the progression of growth of the defect, and hence on its criticality. In effect, what is needed is the development of an 'effect of defects' methodology such as has been developed for the use of FRP composites in aircraft following a damage tolerance-based design/inspection methodology (as shown schematically in Fig. 13.2). Research in this area is still critically needed. However, some results pertaining to defects, with special emphasis on the effects under conditions of environmental exposure, have been investigated at the University of California San Diego (Kaiser, 2002; Navada, 2004).

Table 13.1 Defects in raw and constituent materials

Defect type	Cause/description	Potential effect
Resin		
Over-aged resin	Expired shelf-life	Low strength and modulus; potential for incomplete cure and non-uniform impregnation
Resin inclusions	Dirt and/or chemicals	Change in chemical consistency, voids; potential effect on cure
Resin moisture	Inadequate storage/ environmental exposure	Change in chemical consistency, voids due to evaporation; resin degradation
Fabric		
Incorrect fiber/fabric type	Fiber/resin mismatch, human error	Change in strength and modulus, low fiber/ matrix bond (sizing)
Kinked or wavy fibers	Handling/manufacturing flaw	Fiber breakage, loss in composite properties
Broken fiber tows	Handling/manufacturing flaw	Stress concentrations
Fabric contaminations	Environmental exposure/ storage	Initiator for debonding and crack propagation
Fabric wrinkles	Handling/manufacturing flaw	Lower modulus, higher strain at failure; resin-rich encapsulated areas
Sheared fabric	Handling/manufacturing flaw	Off-axis alignment, lower strength and modulus; resin-rich regions
Damage to free edges	Handling/manufacturing flaw	Loss of integrity, stress concentrations
Pull-out of fiber tows	Handling/manufacturing flaw	Resin richness, localized low strength and stiffness
Fiber gaps	Handling/manufacturing flaw	Resin richness, low crack arresting capability
Fabric moisture	Inadequate storage/ environmental exposure	Reduced fiber–matrix bond; effect on composite performance and durability

Table 13.2 Defects from site and material preparation

Defect type	Cause/description	Potential effect
Resin system		
Moisture absorption	Inadequate storage/ environmental exposure	Change in chemical consistency, voids due to evaporation; potential for incomplete cure and decreased performance levels
Incorrect stoichiometry	Type or proportions of resin and hardener/ catalyst	Inadequate matrix strength/modulus, incomplete and/or non-uniform cure
Incorrect mixing	Low degree mixing, drawing of air	Partial cure, porosity, non-uniform rheology
Substrate		
Inadequate primer coating	Over-, under-saturation of substrate	Low stress transfer capability, potential for poor bond
Lamination on top of 'marked-out' regions	Placement on duct tape, crayon layer, etc.	Weak or no bond to substrate
Degraded substrate	Microcracks, spalled concrete	Lower or no composite action
Inclusions at imperfections	Dirt, moisture or chemicals in concrete cavities	Low bond of primer/putty to substrate
Galvanic corrosion	Intimate contact of fibers with steel reinforcement	Deterioration of matrix/ steel

13.5 Use of non-destructive evaluation/non-destructive testing

For centuries, relevant material properties such as ultimate strength, yield point, or impact resistance have been determined through a number of destructive test methods in order to provide comprehensive information on material behavior. Unarguably, the advantage of a destructive test is the fact that materials can be exposed to a variety of load conditions without the necessity to remain functional upon completion of a test. While this methodology has long served in the optimal design of structures, it can rarely be applied to evaluation of civil structures.

Today, the continuously rising demands on civil and transportation infrastructure has led to the need for finding alternative testing techniques, which allow the inspection of existing structures without damaging or dismantling individual components. The impetus for such action is largely based on the need to ensure continuous safety and provide means of monitoring their overall 'health'. While much information on a structures' physical

Table 13.3 Installation defects

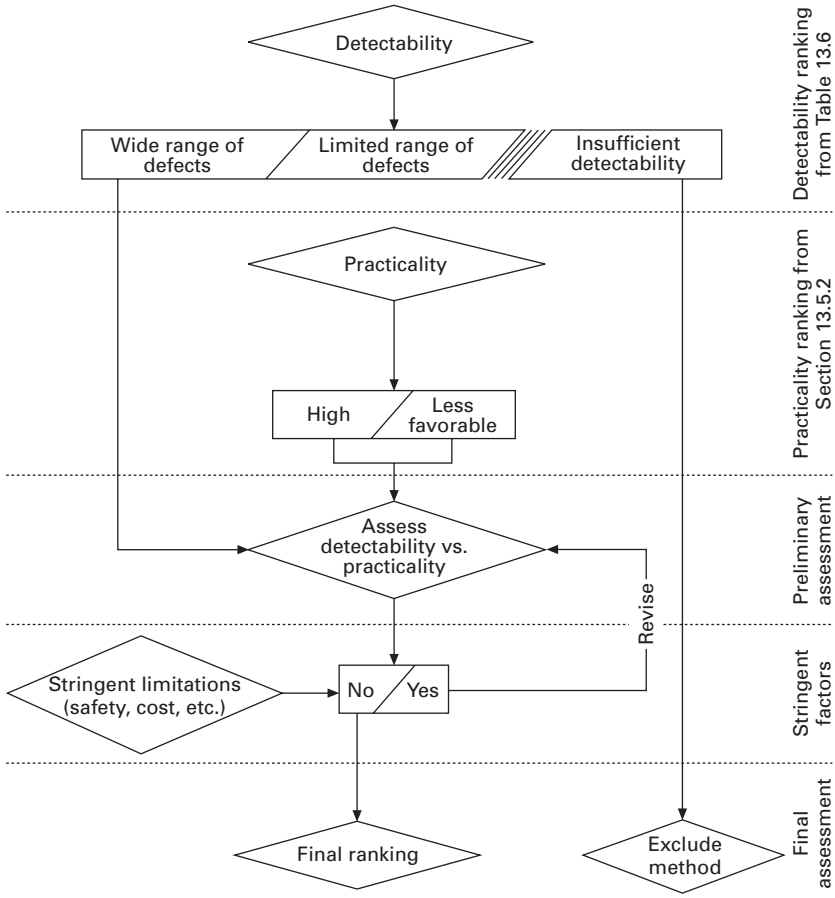
Defect type	Cause/description	Potential effect
Wet layup		
Composite-concrete interphase		
Concrete cavities	In current practice, concrete cavities are not always filled with putty	Stress concentrations
Sagging of infiltrated fabric	Critical in overhead regions	No composite action, potential for moisture entrapment at concrete/composite interface
Resin-rich/poor concrete/ composite interface	Non-uniform primer coating and over-, under-saturation during layup	Low stress transfer efficiency
Porosity and voids	Porous primer, entrapment of air pockets during layup	Low stress transfer, stress concentrations, debond and crack initiation sites
Highly uneven concrete surface	High degree of sandblasting	Voids or air pockets
Inside composite		
Porosity and voids	Air entrainment in resin, entrapment of air pockets during layup	Low stress transfer, stress concentrations, decreased performance attributes
Delamination	Moisture, inclusions	Low or no stress transfer
Debonding	Fiber contamination, tubular voids	Low stress transfer (localized), sites for wicking of moisture
Incorrect stacking sequence	Misplaced fabric, human error	Alteration of strength and stiffness
Resin richness/ poorness	Non-uniform infiltration	Low crack arresting capability, decreased stress transfer capabilities, locally weak zones
Indentations	Handling damage	Damaged fibers, stress concentrations
Missing layers	Human error	Entirely different (and reduced) laminate properties
Damaged edges	Fiber pull-out during infiltration	Stress concentrations, site for crack initiation
Prefabricated material		
Voids at concrete–adhesive interface	Adhesive applied to highly porous concrete substrate	Stress concentrations, moisture accumulation, local zones of weakness
Disbonding at adhesive–composite interface	Smooth surface of prefabricated strip	Low stress transfer/inadequate bond strength

Table 13.4 In-service defects

Defect type	Cause/description	Potential effect
Concrete–composite interface		
Penetration of moisture and chemicals	Exposure to aggressive environments	Degradation of adherent layer, plasticization, reduced stiffness, potential for premature failure through peel and/or delamination
Heat damage	Exposure to sun or fire damage	Softening/degradation of matrix, peel and/or separation from substrate
Composite		
Penetration of moisture and chemicals	Exposure to aggressive environments	Plasticization, reduced stiffness, degradation of composite
Heat damage	Exposure to sun or fire damage	Softening/degradation of matrix
Matrix cracking	Interlaminar crack formation	Initiator for delamination and/or splitting
Surface scratches	Traffic, hail, etc.	Fiber breakage, and initiator for premature local failure
Impact damage	Traffic, hail, etc.	Delamination

condition can be extracted from visual inspections, most internal damage – namely cracking, corrosion, the presence or formation of voids, as well as moisture accumulation – can rarely be identified *per se* and thus demands more sophisticated methodologies.

In theory, non-destructive testing (NDT) should provide information on material properties while neither influencing the material in its current state, nor requiring disassembly or any form of modification that would cause extensive service disruptions, possibly restricting serviceability over extended periods of time. While the term ‘destructive’ can be of broad context, its onset can be defined as the instant a component undergoes initial forms of permanent, non-reversible modification. These include changes in chemical or molecular structure as well as stages at which it experiences severe degradation and can no longer serve the original purpose it has been designed for. This implies that a component that is tested non-destructively shall retain its original strength, stiffness, chemical consistency, and appearance throughout the entire procedure as well as for a substantial period thereafter. Although the literature offers a seemingly endless array of definitions for NDT, the following was found to provide a suitable foundation for the subsequent discussion: ‘A process that does not result in any damage or change to the material or part under examination and through which the



13.2 Flowchart for ranking assessment.

presence of conditions or discontinuities can be detected' (Hellier, 2001). Similar to the multitude of definitions for non-destructive inspection, several abbreviations are commonly used by field inspectors and the NDT industry. These include non-destructive testing (NDT), non-destructive evaluation (NDE), and non-destructive inspection (NDI). While this terminology is often used interchangeably, distinct differences exist. Both NDT and NDI refer to the inspection process itself, i.e. testing of a part in a non-destructive fashion, leading to identification of defects/discontinuities with possible findings on defect type, location, size, and shape. However, NDT and NDI generally do not assess the severity of damage on either a local or global scale. Instead, the effect of damage on system behavior is mostly accomplished through a subsequent evaluation process, implied by the term NDE. Here, data collected through testing/inspection are evaluated and interpreted to

assess the impact on integrity and performance of the inspected object. Consequently, apart from a systematic methodology for localization and dimensioning of eventual material discontinuities, NDE necessitates an understanding of the significance and structural impact of found defects. As the presence of material discontinuities – introduced during erection, rehabilitation, or service of a structure – does not imply a reduction of the structure's performance or safety, NDE represents the most challenging task.

To perform a non-destructive test, the object is typically exposed to a single form of external media (radiation, stress, temperature, etc.) emitted from the testing equipment, which must be capable of partially or completely penetrating the material. However, some forms of NDT techniques do not require penetration of the test object to reveal anomalies, such as optical methods. Others utilize sensors that are embedded inside the structure, and hence make use of yet another alternative testing methodology. Techniques that employ sources that cannot be interpreted by human perception (ultrasound, x-ray, etc.) must employ a suitable detection media coupled to an output device such as a monitor/screen in order to display the recorded information. Finally, the recorded information can be displayed in a form that is detectable for the inspector. This is imperative, since incorrect interpretation of images can lead to erroneous conclusions about the composition of a material. Hence, apart from choice of method, success of NDT depends largely on the experience and expertise of the inspector.

Whilst serving strongly in assessing the suitability of a few established NDT techniques, most traditional methods cannot dispose of such background and must thus be classified on an alternative basis. Primarily, techniques that have proven to be applicable for investigating FRP rehabilitation must be rated higher than those having little or no history in NDE of composites. As mentioned earlier, a suitable method must satisfy two preconditions, namely:

- It must possess characteristics that strongly encourage its use on FRP rehabilitation systems, i.e. provide adequate detectability, preferably supported by previous research conducted in the composites sector.
- It must utilize equipment that meets the practical necessities imposed by *in-situ* NDT, i.e. be suitable for inspecting a variety of geometric configurations and be operable in a number of different field environments.

Most importantly, NDT techniques must allow the inspector to obtain information from inside the composite material or concrete–composite interfacial regions to such detail that predictions on the overall integrity of the composite–concrete system can be made. While this does not imply a global assessment on structural safety, defect type, location, and size should be obtainable from a potential technique. Although practical aspects can have a profound effect on efficiency and safety, as well as on equipment and

labor expenses, only systems yielding high detectability can be considered feasible. Undoubtedly, methods not capable of providing the desired level of sensitivity and comprehensiveness are to be disregarded, irrespective of their practical merits. Hence, compared with practical aspects, defect detectability will generally be assigned a higher level of importance. Nonetheless, if stringent safety requirements or unjustifiably high cost imply practical limitations, the former ranking scheme shall be revised and adjusted accordingly. However, stringent practical limitations will not result in immediate exclusion of the method, as would be the case for insufficient detectability. Figure 13.2 depicts the individual steps of the previous ranking rationale in more detail. Although adherence to the ranking procedure should not be considered stringent in every aspect, it provides insight to the general rationale.

As may be seen, Fig. 13.2 entails information given in Table 13.5 to enable an assessment on detectability and practicality, respectively. In the following, the rationale for obtaining this information will be presented. Because detectability and practicality each encompass a number of subcomponents, which can be of considerable relevance for an individual technique, these will be discussed in further detail. Components of the classification scheme include the following:

1 Defect detectability:
   - range of detectable defect types;
   - minimum detectable defect size;
   - range of detection depth;
2 Practicality:
   - system type (near-field/full-field/global);
   - system portability;
   - coupling requirements;
   - real-time data acquisition;
   - ease of interpretation;
   - possible service inflictions;
   - initial and servicing cost of equipment;
   - level of sophistication.

Ideally, it would be preferable to obtain defect detectability from a number of field or laboratory experiments. However, for most techniques, such information has not yet been made available. Moreover, the presence of a concrete substrate can cause substantial signal interference in the form of scattering or absorption. Due to this limited knowledge, the classification matrix shown in Table 13.5 must, at present, be considered mostly qualitative. Although minimum detectable size and depth penetration will later be of profound importance, it is extremely difficult to assess at this point.

Table 13.5 Detectability classification matrix

NDE methods	Defect types							
	Delamination	Voids	Moisture	Resin thickness irregularities	Fiber waviness	Fiber breakage	Porosity	Matrix cracking
Visual testing (VT)	⇨$_{L}$	⇩	⇩	⇩	⇨$_{L,S}$	⇩	⇩	⇩
Acoustic impact testing (AIT)	⇧$_{L}$	⇨$_{L}$	⇩	⇩	⇨$_{L}$	⇨$_{L}$	⇩	⇩
Penetrant testing (PT)	⇩	⇩	⇩	⇩	⇩	⇨$_{L,S}$	⇩	⇨$_{L,S}$
Ultrasonics (UT)	⇧$_{L,S}$	⇨$_{L}$	⇨$_{L}$	–	–	⇩	⇩	⇩
Radiographic testing (RT)	⇧$_{L,S}$	⇧$_{L,S}$	⇨$_{L,S}$	⇧$_{L,S}$	⇧$_{L,S}$	⇧$_{L,S}$	⇧$_{L,S}$	⇧$_{L,S}$
Thermographic testing (TIR)	⇧$_{L,S}$	⇨$_{L,S}$	⇨$_{L}$	–	–	–	–	⇩
Eddy current testing (ET)	⇩	⇩	–	⇩	⇧$_{L}$	⇧$_{L}$	⇩	⇩
Optical methods (shearography)	⇧$_{L,S}$	⇧$_{L,S}$	–	–	⇧$_{L,S}$	⇧$_{L,S}$	–	–
Acoustic emission (AE)	⇨	⇩	⇩	⇩	⇩	⇧	⇩	⇧
Ground-penetrating radar (GPR)	–	–	–	–	–	–	–	–
Strain measurement techniques (optical fibers)	⇨$_{L}$	⇩	⇩	⇨$_{L}$	⇨$_{L}$	⇩	⇩	⇩
Modal analysis	–	–	–	⇩	⇩	–	⇩	⇩
Rapid load testing	–	–	–	⇩	–	–	⇩	⇩

Arrows: ⇧, generally detectable; ⇨ limited detectability; ⇩, not detectable – detectability unknown. Indices: L, allows localization; S, allows accurate sizing.

13.5.1 Detectability matrix

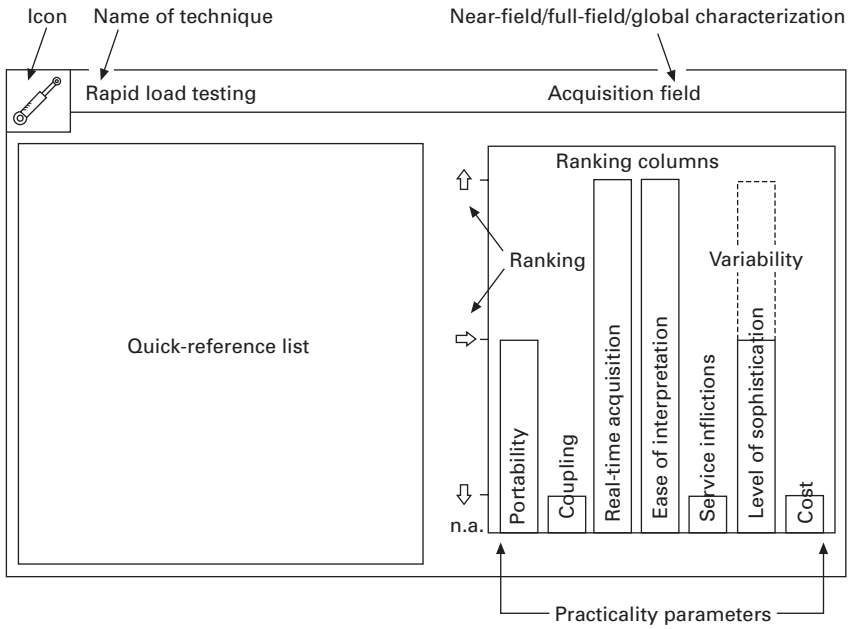
The detectability matrix (DM) is given in Table 13.5. Only a limited number of defects were chosen for assessment purposes, Furthermore, the reader should differentiate sharply between defects that cannot be identified (⇩) and those for which detectability is currently unknown (—). The DM differentiates between *unknown* and *unidentifiable* in such a manner that the former does not necessarily imply the unsuitability of a method for the specific type of defect. Rather, the method has not yet been investigated upon its sensitivity to this type of defect, hence no assessment can be given. In contrast, unidentifiable defects are those for which insensitivity has already been proven. Furthermore, the capability of localizing and sizing a specific form of defect is addressed.

As may be noted, the capability of techniques to detect the presence of defects does not necessarily imply the abilities of localization and sizing. Excellent examples of this are acoustic emission as well as optical fiber measurements. Although signals of internal material fracture and/or friction can be sensed by both methods, exact localization and sizing, the former being especially critical for acoustic emission, pose extreme difficulties. As was discussed, the material anisotropy of CFRP causes localization via acoustic emission measurements to be inconclusive. Hence, only methods bearing indices 'L' and 'S' show adequate means of defect characterization.

13.5.2 Practicality matrix

Irrespective of previous application to CFRP-rehabilitated structural components, most of the above methods have found use in one or multiple fields of engineering. Hence, much information can be given on equipment and overall system complexity, as well as the detection methodology of each individual technique. Although practicality entails a number of individual aspects, experience gained through past applications often provides solutions to difficulties in system setup, data acquisition, interpretation, portability issues, etc. Such background knowledge thus builds the basis for subsequent practicality assessment.

A template for the practicality matrix (PM) is shown in Fig. 13.3. To aid the reader in comparing individual methods, the matrix displays information in graphical format. As may be seen, individual aspects are assigned columns of various heights, with longer columns representing a more preferable situation while implicit limitations are indicated by a short column height. This appears particularly helpful since the overall practicality must be considered a combination of its individual components. Hence, by comparing the overall column heights, one may quickly distinguish unsuitable methods from those showing high practicality.



13.3 Schema used in the practicality matrix.

In addition, the PM includes a short list of some of the most outstanding advantages and/or disadvantages of each individual method. Similar to the DM, three distinct levels of practicality are used in the ranking scheme. It should be noted that certain parameters cannot be ranked and are thus classified as 'not applicable'. In cases where one method may be applied in different forms (e.g. A-scan versus C-scan) dotted lines are used to indicate a range of practicality variation. In such cases, a footnote will provide further information of why such variability must be granted. In the following, a brief introduction to each of the individual practicality parameters is given.

System type

Foremost, NDE systems can be assigned to one of three general system types, namely near-field, full-field, and global. The profound difference between these system types is given by their field-of-view. As such, a global system is preferably used to obtain information on a structural level, while near- and full-field techniques provide a more localized and detailed analysis in regions where the presence of defects is known or expected to be of particularly high occurrence. While global methods can provide rapid insight into large discontinuities and overall structural deficiency, they typically lack sensitivity to localized defects. Conversely, local systems are given preference once defects have already been located on a global level, as they provide enhanced

sensitivity to minute anomalies. As discussed, a suitable combination of the two can provide means for rapid inspection on the structural level with subsequent near-field capabilities for a more detailed inspection.

Portability

As for all field inspection, portability and ease of handling of test equipment and related tooling are of paramount importance. During local inspection, equipment must be easily transportable from one location to the next, preferably by a single person. Quite often, bulky equipment restricts applicability of a technique simply because inspectors cannot handle, adjust, or even assemble the individual components in the field. For global methods, which may allow users to inspect entire parts of a structure from a single location, portability, as outlined above, will be of less significance. Nevertheless, global methods must be portable insofar as equipment must be of manageable size and weight to be transported to and from the site. Generally, portability of global testing equipment entails any factors restricting the removal from a laboratory environment, such as high power source, environmental sensitivity, etc.

Coupling

Intimate contact requirements can impose great limitations on the overall efficiency of an NDE method. The necessity to provide permanent coupling between the part and the inspection tool often results in a slow and sometimes messy inspection procedure, especially in cases where gels or chemicals are applied to the test surface. Furthermore, immediate and long-term effects of couplants and chemicals on the integrity of CFRP laminates have not yet been established. Thus, to ensure a more efficient scanning process, it is preferable to operate all equipment in a non-coupled arrangement, i.e. data can be acquired without intimate contact to the structure.

Real-time acquisition

To allow *in-situ* interpretation, data acquisition shall be realizable in real-time, i.e. the inspection technique must extract all information during or directly following completion of a testing cycle. Herein, difficulties typically arise in cases where a method requires massive computational effort or development of exposed films in a laboratory environment. In most cases, the use of digital systems in combination with modern laptop computers can facilitate faster acquisition times as well as a more efficient computation process.

Ease of interpretation

Upon completion of the acquisition process, the user is typically presented with a plot or image, showing a systematic representation of the collected data in a tabular, graphical, or other suitable format. Ideally, graphical images show the inspected part in two-dimensional view with information superimposed in the desired format (e.g. temperature contours in infrared testing, strain profiles in shearography, etc.). These 'mapped' images are most convenient to interpret as the observer can best correlate between the displayed image and the test part. In contrast, information provided in x–y coordinate systems (e.g. A-scan, acoustic impact testing force–time history plot) is more difficult to interpret and requires a more fundamental knowledge of the technique.

Service inflictions

During inspection, serviceability of the structure should not be influenced to a significant degree, i.e. inspection teams should not be required to disrupt traffic or shut down entire lanes of a bridge. Typically, disruption of traffic is required for one of two reasons. Firstly, the test setup may require simultaneous access to one or multiple traffic lanes, such that inspectors would be exposed to a significant safety hazard if traffic was not disrupted. Secondly, ongoing traffic may induce vibration to the structure that, while preferable for passive methods, may result in background noise and/or erroneous readings for a number of active methods. Hence, methods that are immune to either of the two formerly mentioned conditions are most preferable.

Level of sophistication

Sophistication is mainly dictated by the amount of previous research and practical work conducted in a specific area. Although a method can be rather simplistic, a long history of industrial and experimental application ensures familiarity, reproducibility, and higher efficiency during inspection. Furthermore, equipment is likely to be more readily available and obtainable at lower cost. As such, sophistication is profoundly different from the level of complexity, which mostly relates to how exhaustive and detailed the given information is. However, high complexity does not necessarily imply that the technique is highly established in the particular industry.

Cost

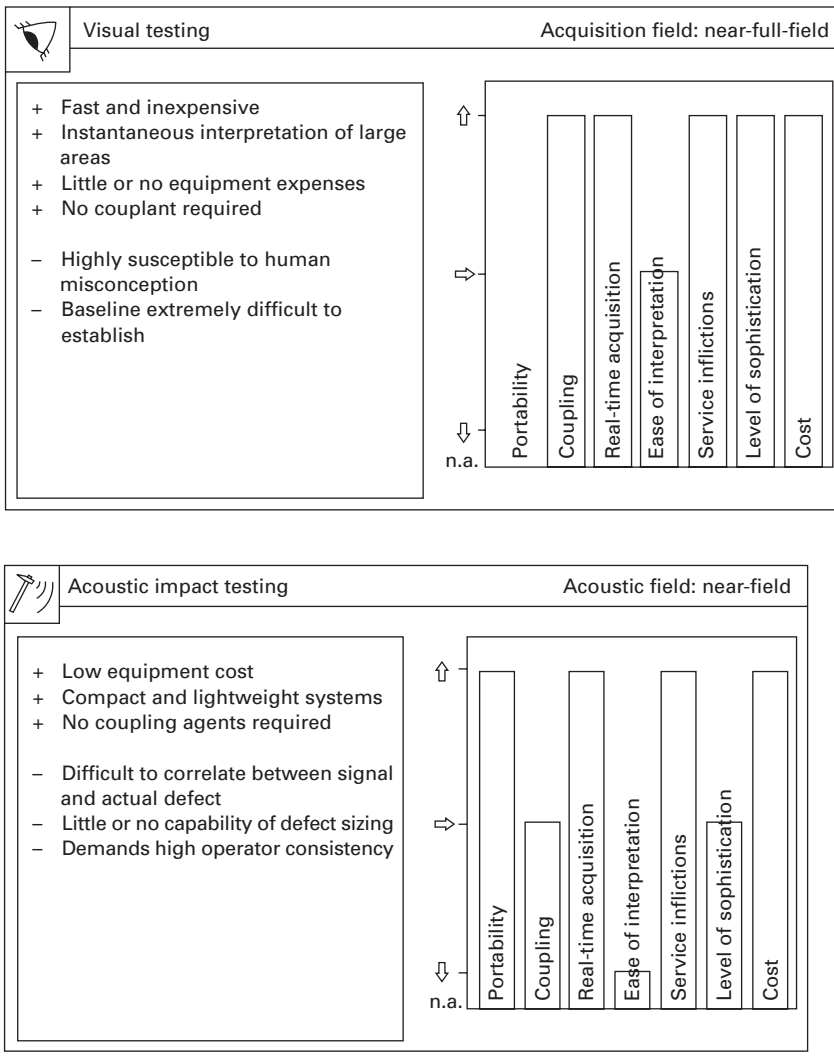
Equipment cost is mostly regulated by two factors, namely complexity and how widespread the use of the technique is in the industry. In most

instances, complexity may be assumed to be the governing factor; however, high industrial demand often leads to a significant reduction in equipment and instrumentation costs.

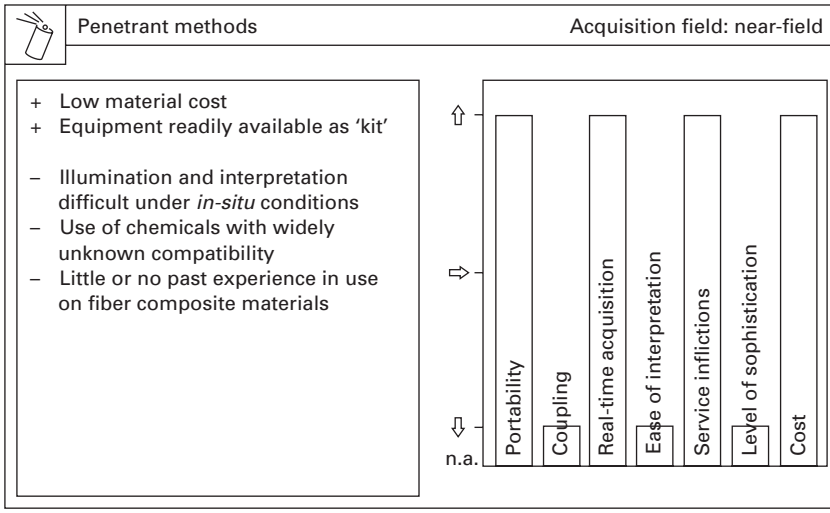
The results for a range of methods are shown in Fig. 13.4.

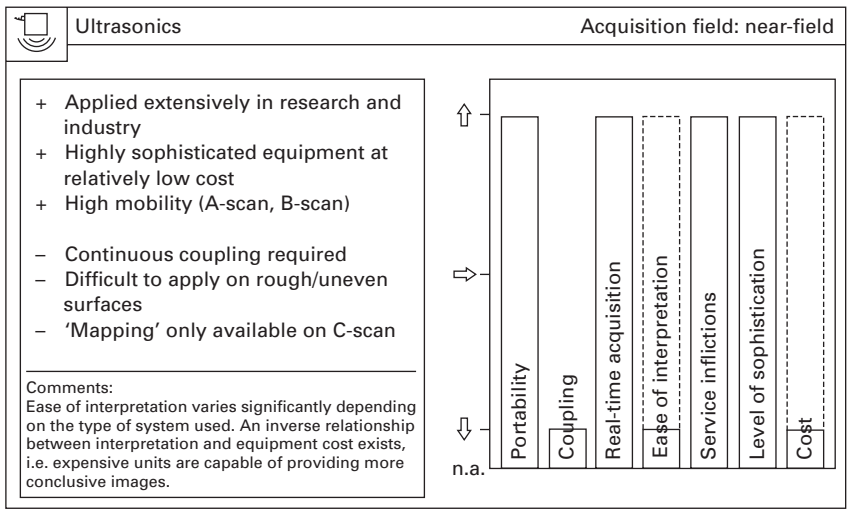
13.5.3 Ranking matrix

Taking into account the previous discussion, the final ranking matrix (RM) can now be assembled as in Table 13.6. As outlined, it entails all of the



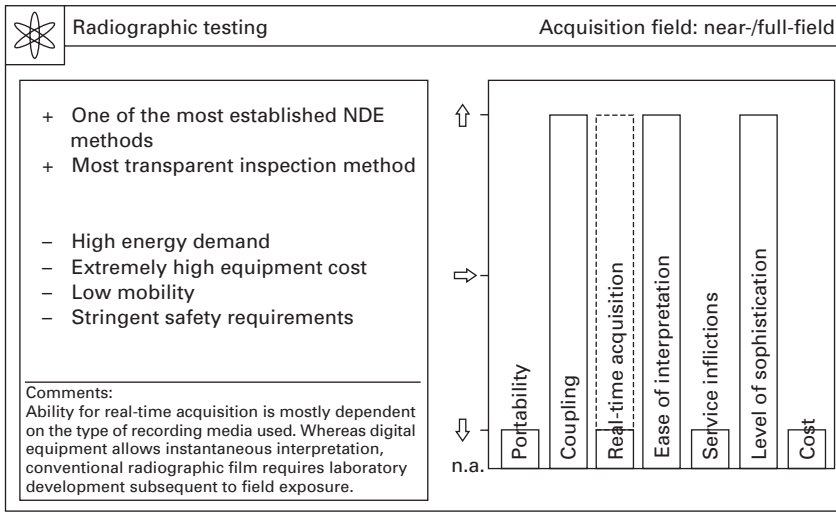
13.4 Practicality matrices.

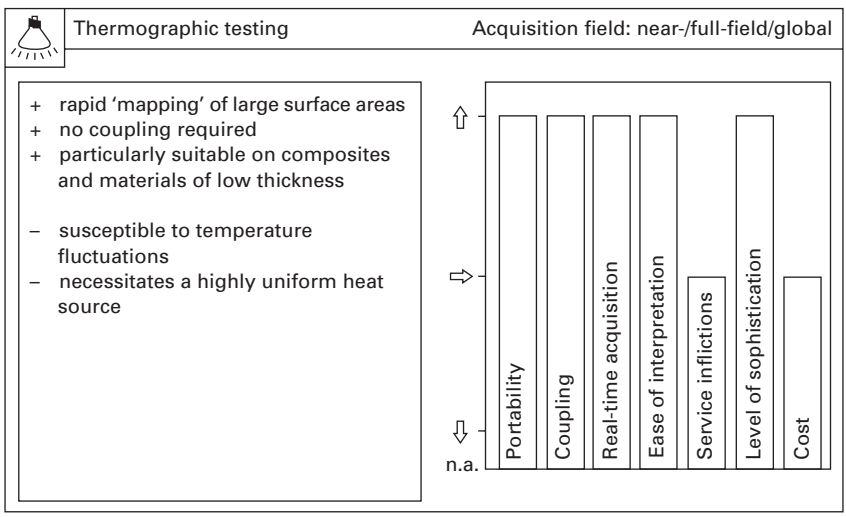




13.4 Continued

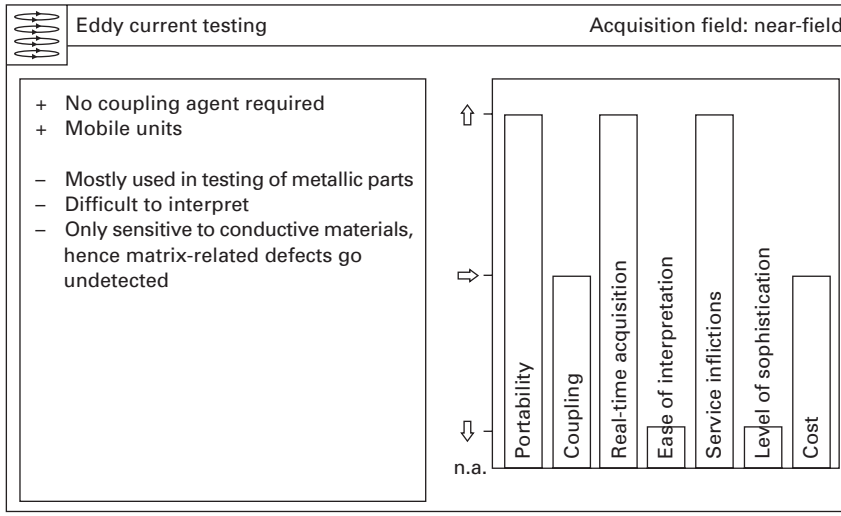
discussed methods, ranked according to a combination of detectability, practicality, and eventual stringent requirements. Herein, selected methods will be classified as *primary* choices, as they show superior applicability over the remaining field. This superiority is mostly expressed in terms of defect detectability but can extend significantly into the practicality regime. As formerly mentioned, the primary category will include techniques applicable in both full-field and near-field inspection. Again, the basic methodology proposed by the authors is to first inspect a structure for defects on a full-field scale with subsequent detailed analysis of any discontinuous regions.

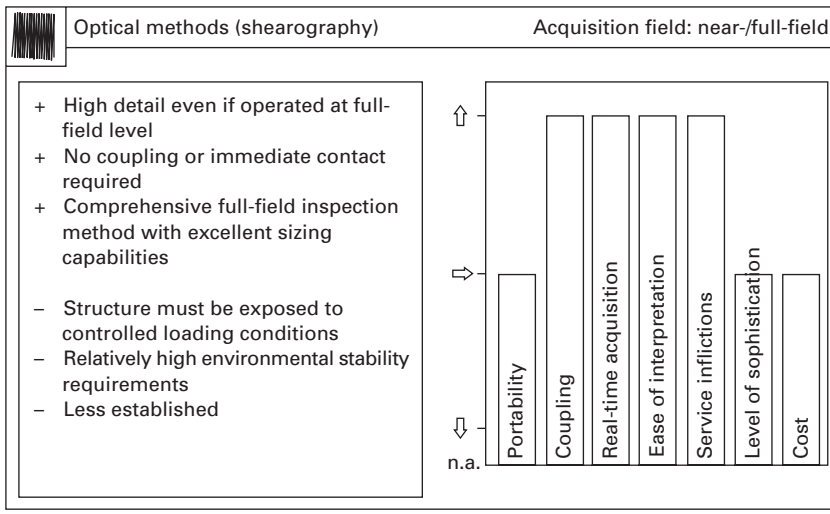




13.4 Continued

Secondly, a subset of *conditional* choices will be given. Their applicability largely depends on the specific inspection objective and/or site conditions. A majority of defects found in FRPs used for rehabilitation are of relatively small dimensions and thus give preference to near- and full-field inspection techniques. However, if a global assessment on structural integrity is to be established, near- and full-field methods are mostly inappropriate choices. Furthermore, in well-controlled environments, practical drawbacks may be less pronounced and will enable the use of methods that require a more complex test setup.

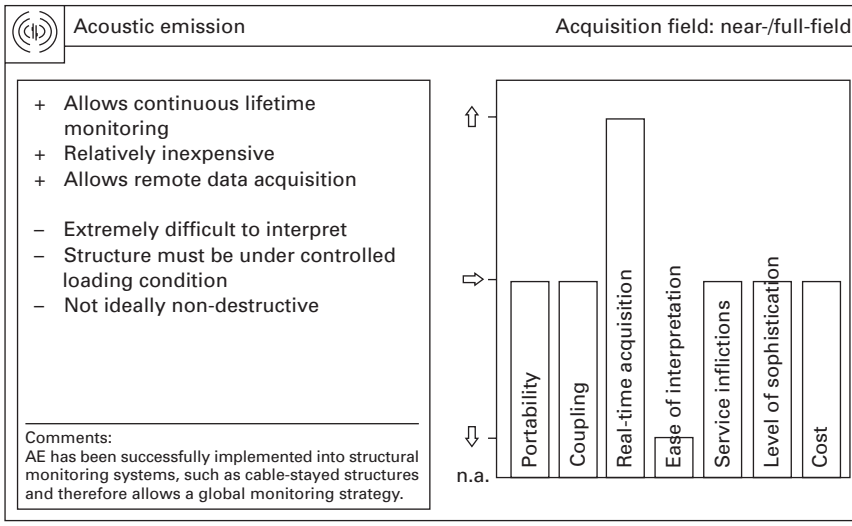


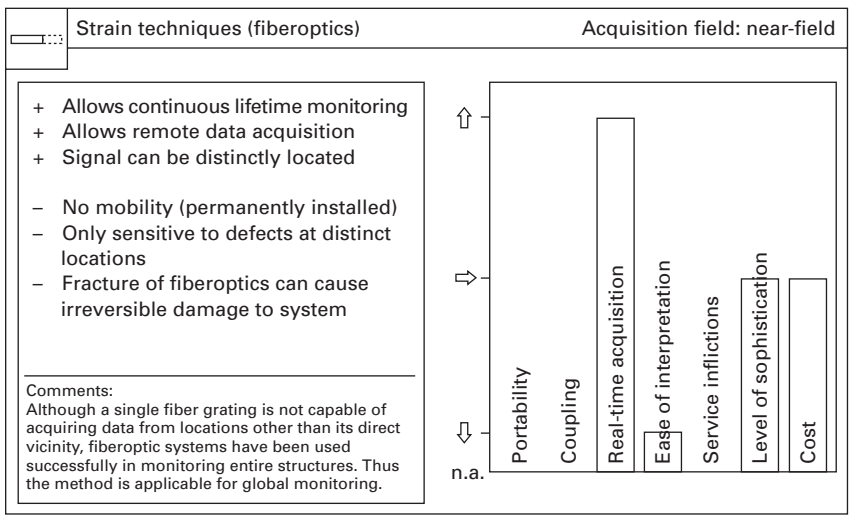


13.4 Continued

Thirdly, a number of methods will be classified as *supplementary* to the primary choices. Supplementary methods should be applicable in the near- to full-field range, portable, and inexpensive, yet provide information on material properties that cannot be extracted from the two primary methods.

Lastly, the RM will address methods that were shown to have significantly lower applicability and should hence be *excluded* from the list of viable methodologies. Such inapplicability is implied by either the high uncertainty and/or profound insensitivity towards a large number of defects, significant



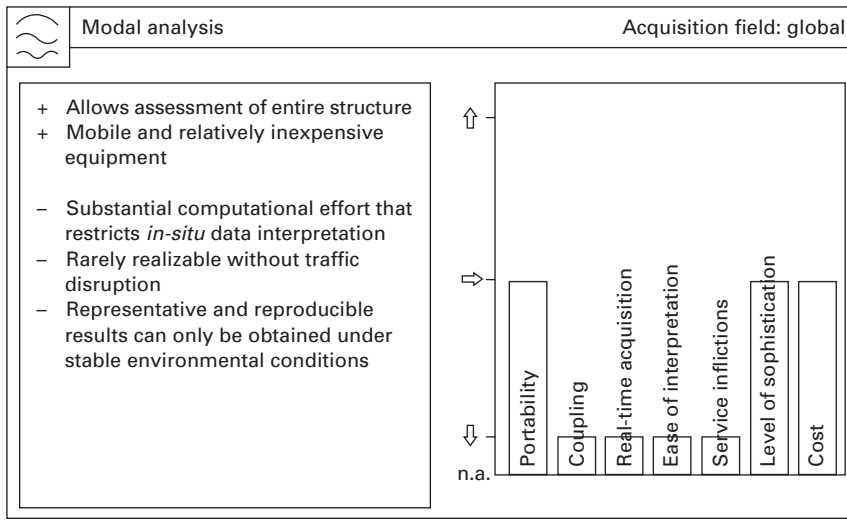


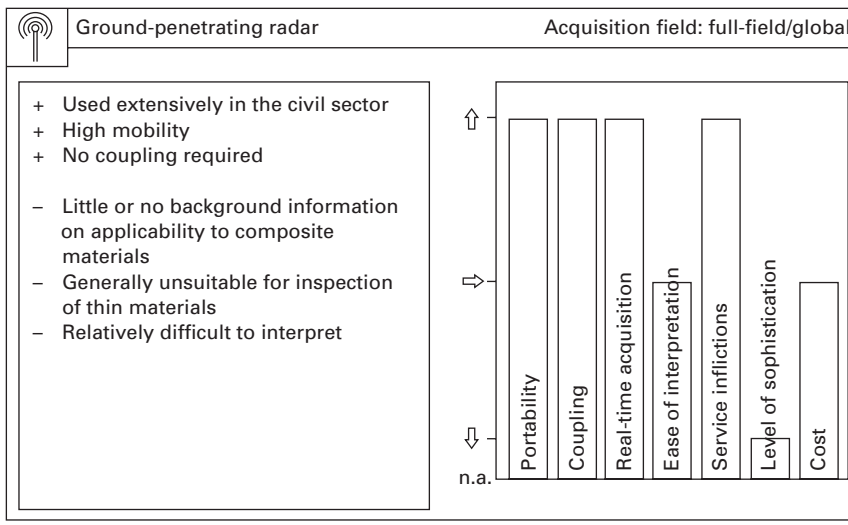
13.4 Continued

restrictions in practicality, or certain stringent requirements that extend past the issues addressed by the DM and PM. Prior to presentation of the RM, the rationale will again be outlined in a systematic manner, so as to provide the reader with conclusive information on why certain decisions were made.

Primary methods

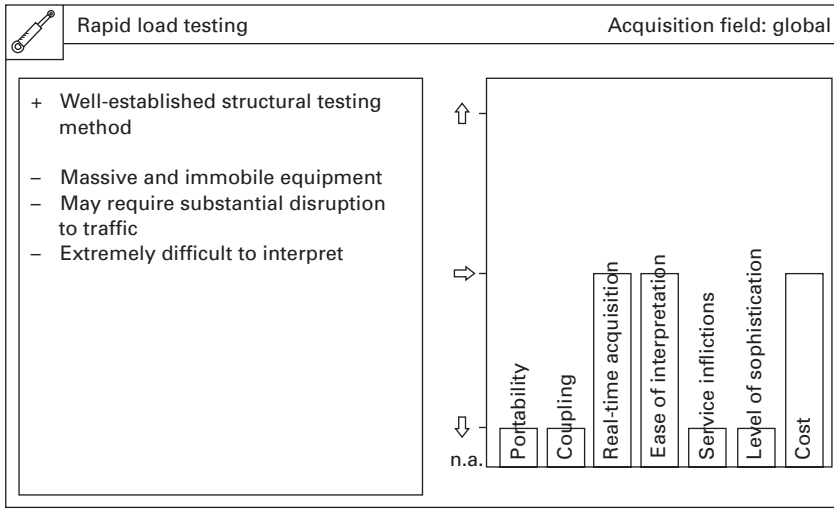
Primary methods will combine a generally high defect sensitivity with capabilities of locating and, ideally, sizing of each individual defect. As may





13.4 Continued

be seen from Table 13.5, this precondition is satisfied, within limitations, by ultrasonics, thermography, shearography, as well as radiographic imaging. While the latter is undoubtedly the most transparent of all the methods, its stringent safety requirements, implied by the utilization of aggressive x- or γ-radiation, may often restrict its flexible use in field environments. Hence, thermography, optical methods, and ultrasonics remain as possible methods, where it should be pointed out that the latter is largely restricted to localized inspection, while thermography and optical methods can be applied in both a near- and full-field manner.



13.4 Continued

While the stringent requirement of external loading in optical testing appears to add to the complexity of the inspection procedure, it should be considered that service load levels might often be of sufficient magnitude to expose a majority of the internal deficient regions. In contrast, defects located in regions of negligible strain levels are likely to go undetected. Nevertheless, optical methods have been shown to provide strain patterns of excellent geometric clarity.

Presently, the sensitivity of thermography and optical methods to a variety of defects remains largely unknown. This is in part conditioned by the fact that the majority of past research work has been focused on inspection of a very limited range of defects, most of which involved delamination, impact-related damage, or voids of rather significant magnitude. Hence, both methods are given equal potential and must be subject to future investigation.

Conditional methods

Considering the characteristics of radiographic testing and modal analysis discussed in previous sections, their drawbacks for safe, economical, and, in the latter case, detailed analysis of defects have become apparent. Nevertheless, if site conditions allow use of radiographic equipment – i.e. supply a source capable of providing the several kilovolts required for operation and further allow its safe use – the high transparency can most certainly be of considerable advantage.

Alternatively, as supported by numerous reports, the impact of material degradation on the global structural response can most successfully be

Table 13.6 Ranking matrix

Ranking	Method	Comments
Primary methods	Thermography (TIR)[†] Shearography[†] Ultrasonics (UT)[††]	[†]Both methods are proposed for near- and full-field monitoring; however, one may yield higher applicability over the other, which must be confirmed through future experimental investigation. [††]Ultrasonics must be considered applicable for near-field inspection, exclusively. Its extensive background and range of instrumentation makes it especially favorable.
Conditional methods	Radiographic testing (RT) Modal analysis	Applicability of these methods is largely dependent on site conditions and detail of inspection. For highly detailed inspection in controlled environments (i.e. access to adequate power supply, no concern of safety) RT remains a favorable technique. In contrast, for changes in structural response through material degradation, modal analysis provides most conclusive results.
Supplementary methods	Visual testing (VT) Acoustic impact testing (AIT)	These methods are proposed as supplementary, mostly due to their general ease of use and extremely high flexibility. Moreover, they can be applied in simplistic form and do not necessitate extensive background knowledge in theory and/or application of the technique. The reader should be reminded, however, that neither method is of such transparency or level of sophistication that it could be considered solely for comprehensive *in-situ* inspection.
Excluded methods	Penetrant testing[1] Eddy current testing (ET)[2] Acoustic emission (AE)[3] Strain measurement techniques (fiberoptics)[4] Ground-penetrating radar (GPR)[5] Rapid load testing[6]	*Quick-reference list*: • Low detectability [1,2,4,5,6] • Presumed inadequate for defect localization[3,5,6] • Presumed inadequate for defect sizing [3,4,5,6]

monitored using modal data. As the evaluation of global behavior remains one of the primary objectives in structural testing, modal analysis must be considered a viable, though in view of the present report, conditional method.

Supplementary methods

Traditionally, visual and acoustic impact testing have been the methods of choice to perform fast and preliminary inspections on composite materials. To date, similar methodology has been followed for rapid *in-situ* quality assessment of CFRP overlays. This was mostly dictated by the fact that neither method demands extensive background knowledge of material properties, operation of equipment, or signal interpretation. As such, visual inspection precedes virtually all automated test procedures. Hence, instead of treating visual testing as a separate NDE technique, it should rather be considered a precondition for all further inspection, simply due to its simplicity and extreme flexibility.

Moreover, visual testing and acoustic impact testing are both inexpensive and have been proven to detect the defects that are often of primary interest, namely medium to large delamination, considerable moisture accumulation, and severe fiber misalignment. Hence, both methods are proposed to serve as additional tools in assessing the quality of CFRP overlays. Nevertheless, it should be emphasized that neither method possesses the detectability required for a comprehensive quality assessment.

Excluded methods

The remaining techniques have been excluded due to their typically low detectability. These include penetrant and eddy current techniques. Although fiberoptic sensors and acoustic emission systems have been proven to be suitable as lifetime monitoring systems for new and existing structures, the data from such systems often lacks sufficient interpretability. As such, localization and sizing of defects through mere detection of stress concentrations or acoustic activity at a fracture surface remains difficult. In existing structures, sensors cannot be situated at the concrete–composite interface or at interlaminar locations, which are the regions of high interest.

13.6 Future trends

While the areas of defect identification, defect criticality assessment, and damage tolerance are fairly well developed in the aerospace industry, they are still not well developed as related to FRP composite materials used in civil infrastructure. There is, however, a critical need for the development of this area, especially as related to assessment of the effect of defects, both at

a specific point of inspection and over the service life of the rehabilitated structure. The development of defect maps with probable effects and rates of progression, as a function of period and type of exposure, is extremely important and it is likely that these will be needed before the use of FRP as a method of rehabilitation is widely accepted on par with conventional methods.

In the future, it is likely that methods such as infrared-thermography, microwave detection, and forms of non-contact ultrasonics will be developed to provide both rapid post-installation inspections, and autonomous inspections over the structures intended service life. One could imagine these being linked to a structural health monitoring (SHM) system that provides routine periodic data to a centralized station, thereby providing up to date information on the health of a rehabilitated system. This would also provide the impetus for shifting from a time-based inspection methodology to a condition-based inspection methodology for civil structures, which is intrinsically more in line with the enhanced durability of FRP materials as compared with conventional construction materials.

13.7 References

Ali, M. S. M., Oehlers, D. J., and Bradford, M. A., 'Shear Peeling of Steel Plates Adhesively Bonded to the Sides of Reinforced Concrete Beams,' *Proceedings of the Institution of Civil Engineers – Structures and Buildings*, **140**(3), 2000, 249–259.

Bishop, S. M., 'The Significance of Defects on the Failure of Fibre Composites,' Neuilly-sur-Seine, France: North Atlantic Treaty Organization, Advisory Group for Aerospace Research and Development (AGARD), 1981, iv.

Cawley, P., and Adams, R. D., 'Defect Types and Non-Destructive Testing Techniques for Composites and Bonded Joints,' *Materials Science and Technology*, **5**, 1989, 413–425.

Chajes, M. J., Finch, W. W., Januszka, T. F., and Thomson, T. A., 'Bond and Force Transfer of Composite Material Plates Bonded to Concrete,' *ACI Structural Journal*, **93**(2), 1996, 208–217.

Davies, P., and Brunelliere, O., 'Effect of Defects on Interlaminar Fracture of Glass Fibre-Reinforced Polyester Composites,' *Journal of Material Science Letter*s, **12**(6), 1993, 427–429.

Farioli, M., Porro, F., Samanni, G., and Wagner, V., 'Advanced Techniques for Composite Primary Structures,' in *Characterization, Analysis and Significance of Defects in Composite Materials*, AGARD Conference Proceedings, no. 355, 1983.

Ghiorse, S. R., 'Effect of Void Content on the Mechanical Properties of Carbon/Epoxy Laminates,' *SAMPE Quarterly*, January 1993, 54–59.

Hawkins, G. F., Johnson, E., and Nokes, J., 'Typical Manufacturing Flaws in FRP Retrofit Applications,' *Concrete Repair Bulletin*, July/August 1998, 14–17.

Hellier, C. J., *Handbook of Nondestructive Evaluation*, 2001, New York: McGraw-Hill.

Kaiser, H., Assessment of Defect Criticality and Non-destructive Monitoring in CFRP-Rehabilitated Civil Structures, Masters Thesis, Department of Structural Engineering, University of California San Diego, La Jolla, California, 2002, p. 264.

Karbhari, V. M., 'Materials Considerations in FRP Rehabilitation of Concrete Structures,' *ASCE Journal of Materials in Civil Engineering*, **13**(2), 2001, 90–97.

Navada, R. A., Fracture Mechanics Approach to Assessment of Defect Criticality in FRP Rehabilitated Concrete, Masters Thesis, Department of Structural Engineering, University of California San Diego, La Jolla, California, 2004, p. 256.

Parslow, N., 'An Empirical Appraisal of Defects in Composites,' in *Characterization, Analysis and Significance of Defects in Composite Materials*, AGARD Conference Proceedings, no. 355, 1983.

Potter, R. T., 'The Significance of Defects and Damage in Composite Structures,' in *Characterization, Analysis and Significance of Defects in Composite Materials*, AGARD Conference Proceedings, no. 355, 1983.

Purslow, D., 'Fractographic Analysis of Failures in CFRP,' in *Characterization, Analysis and Significance of Defects in Composite Materials*, AGARD Conference Proceedings, no. 355, 1983.

Seible, F., and Karbhari, V. M., 'Seismic Retrofit of Bridge Columns Using Advanced Composite Materials,' *Proceedings of the National Seminar on Advanced Composite Material Bridges*, Washington, DC, May 1997.

Seim, W., Horman, M., Karbhari, V., and Seible, F., 'External FRP Poststrengthening of Scaled Concrete Slabs,' *ASCE Journal of Composites for Construction*, **5**(2), 2001, 67–75.

Triantafillou, T. C., and Antonopoulos, C. P., 'Design of Concrete Flexural Members Strengthened in Shear with FRP,' *ASCE Journal of Composites for Construction*, **4**(4), 2000, 198–205.

Woo, E. M., Chen, J. S., and Carter, C. S., 'Mechanism of Degradation of Polymer Composites by Galvanic Reactions Between Metals and Carbon Fiber,' *Polymer Composites*, **14**(5), 1993, 395–401.

14

Structural health monitoring and field evaluation of composite durability

A. A. M U F T I, University of Manitoba, Canada; and
L. A. B I S B Y, Queen's University, Canada

14.1 Introduction

For many years, engineers have been searching for methods to assist them in obtaining information on how a structure is behaving in service by incorporating, at the time of construction or subsequently, sensing devices that can provide information about conditions relating to strain, temperature, and humidity (Tennyson, 2001). The development of structurally integrated fiber optic sensors (FOSs) leading to the concept of 'smart' structures and structural health monitoring (SHM) has greatly assisted the engineering community to resolve these issues by providing them with some of the necessary tools to collect the required information over long periods of time.

The Canadian Network of Centres of Excellence on Intelligent Sensing for Innovative Structures (ISIS Canada) has been studying and implementing smart structures and SHM systems for more than 10 years. For infrastructure owners, one of the greatest values of ISIS Canada research lies in its practical application. Recently, there have been many new opportunities for applying ISIS Canada technologies, as is evidenced by the growing number of field demonstration projects currently underway. These projects range from a concrete steel-free bridge deck for the Salmon River Bridge in Nova Scotia (Newhook and Mufti, 2000), to the strengthening of a decommissioned nuclear containment structure in Quebec (Demers *et al*., 2003). Government agencies as well as other infrastructure owners have made conscious decisions to monitor these structures for health due to the benefits derived from this practice including innovation, improved economics, and critical information on long-term durability.

This chapter presents a summary of current thinking with respect to SHM of infrastructure along with a number of case studies of FOSs and SHM applications used to elucidate the long-term durability of innovative structures that incorporate fiber-reinforced polymer (FRP) materials.

14.1.1 Basic concepts of structural health monitoring

Structural health monitoring (SHM) is a relatively new idea in civil engineering applications, and a single widely recognized definition has yet to be standardized. For the purposes of this chapter, SHM will be defined both by its objectives and by the physical system and sensors required to achieve these objectives. This chapter focuses mainly on SHM as applied to bridges, but the concepts are equally applicable to virtually all civil engineering structures.

The objective of SHM is to monitor the *in-situ* behavior of a structure accurately and efficiently, to assess its performance under various service loads, to detect damage or deterioration, and to determine the health or condition of the structure. The SHM system should be able to provide, on demand, reliable information pertaining to the safety and integrity of a structure. This information can subsequently be incorporated into bridge maintenance and management strategies, and improved design guidelines. The immediacy and sensitivity of modern SHM systems can allow for short-term verification of innovative designs, early detection of assorted problems, avoidance of catastrophic failures, more effective allocation of scarce resources, and reduced service disruptions and maintenance costs. The physical diagnostic tool of SHM is a comprehensive integration of various sensing devices and ancillary systems, including:

- a sensory system;
- a data acquisition system;
- a data processing system;
- a communication system;
- a damage detection and modeling system.

Although SHM is relatively new in civil engineering, the use of instruments to assess the health (i.e. integrity and condition) of structures is not new. Bridge field testing using various measuring instruments is, in fact, an old activity.

Similarly, the basic instruments that comprise a SHM system have been in use for many years in structural engineering laboratories around the world. Furthermore, bridge codes of practice and bridge owners have established evaluation and inspection guidelines that have been in practice for decades. Indeed, the objectives of SHM are consistent with the objectives of many of these long-standing structural evaluation practices. SHM is, in many ways, an augmentation of current practice, not only through the use of leading-edge technology in sensing, instrumentation, communications, and modeling, but also through effective integration of these technologies into an intelligent monitoring system.

The driving force behind implementing SHM comes from recognizing the limitations of conventional visual inspections and evaluations using conservative codes of practice. Conventional means are not always sufficient to determine the structural adequacy of many older bridges and buildings, for example those constructed in earthquake-prone areas (Chase, 1999). The development of an integrated SHM system is also justified in many cases by the fact that North American infrastructure currently includes a very large number of aged bridges, with a sometimes questionable capacity for sustaining modern traffic loads.

Just as consumers demand state-of-the-art technology in products and services, bridge owners and users are increasingly demanding advanced technologies, such as SHM systems, in civil engineering infrastructure management. The intention, therefore, is to provide a framework for consolidating various basic instruments and technologies into an integrated system that can be utilized to advantage for the maintenance of bridges, buildings, power plants, offshore platforms, and other significant infrastructure.

14.1.2 Analogy

One way of gaining an appreciation for SHM is to draw an analogy with the human body. Just as doctors check the health of patients, today's engineers must to be able to check on the prevailing condition of in-service bridges and structures. Doctors use specialized equipment to check a patient's blood pressure, pulse, cholesterol, and other parameters when monitoring a patient's health. In much the same way, an engineer can utilize specialized sensors imbedded in a structure to take readings and gain an insight into its structural health. If a patient's blood pressure is too high, the doctor prescribes corrective medicine. Similarly, in SHM, if the data flowing from the sensors indicate excessive stresses on the structure, an engineer can take appropriate measures to correct the situation. In both cases, immediate preventative action guards against catastrophic consequences.

Annual check-ups by a doctor are a routine form of preventative maintenance for the human body. Similarly, SHM of infrastructure to provide continuous or periodic check-ups as preventative maintenance is becoming more commonplace. SHM is a rapidly emerging technology destined to be of great value to those responsible for the safety and well being of civil engineering structures.

14.2 The need for structural health monitoring

To remain competitive in the current global economic environment, it is necessary to minimize service disruptions to civil engineering structures because of routine maintenance or repairs due to excessive deterioration, the

need for upgrade, or following extreme events – such as earthquakes, hurricanes, tornadoes, and man-made events.

By providing instant, on-demand information on issues relating to the serviceability, safety, and durability of structures, an SHM system can help civil engineers cope with disruptions; and when events that negatively impact a structure do occur, SHM can provide engineers with the information needed to design future structures that are safer, more durable, and constructed as economically conservative as conditions allow so that these structures become better able to withstand environmental and man-made problems.

Monitoring and evaluating the integrity of large civil structures, which are in service, also optimizes resources for repair and rehabilitation, or may point out the need for the replacement of a structure. SHM is also useful in evaluating the life-cycle costs of structural components, a rapidly expanding consideration in the construction and maintenance of bridges.

The direct potential benefits of an SHM system are numerous, including:

- real-time monitoring and reporting;
- reductions in down time during maintenance and repair;
- improved safety and reliability, in combination with reduced maintenance costs.

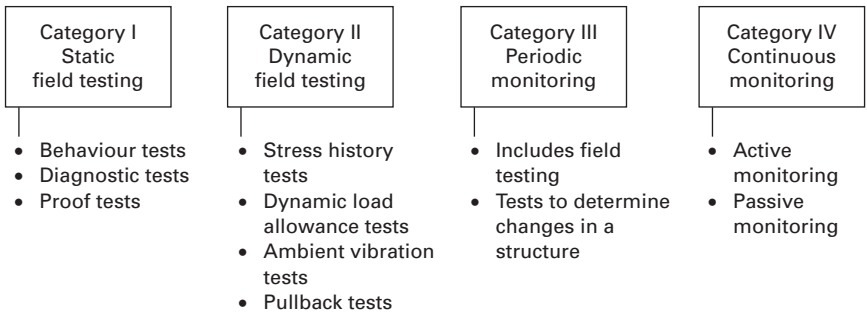
As noted by Chang (1999) and Aktan *et al*. (1999), reduction of down time and improvement in reliability enhances the productivity of structures. Finally, the results of SHM provide information about the in-service behavior of structures and can thus be used to improve the design of future structures.

14.2.1 Subsystems and classification of structural health monitoring

For ease of description, a typical SHM system has been divided into the following four categories, which have been modified and enhanced from the levels originally described by Sikorsky (1999); these are subdivided further in Fig. 14.1:

- static field testing;
- dynamic field testing;
- periodic monitoring;
- continuous monitoring.

The main difference between the SHM under consideration in this chapter and other kinds of structural monitoring is that modern SHM systems, in addition to detecting damage in a structure, can in some cases also provide information on the location and severity of damage, and on the safety of the structure. The damage-detection capabilities of SHM systems can be classified



14.1 Categories of structural health monitoring systems.

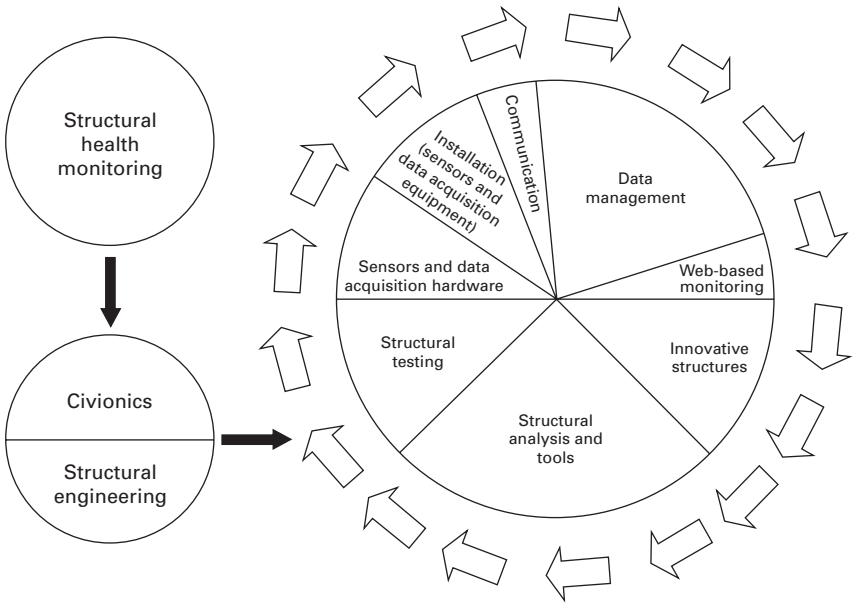
into the four categories previously noted, which are described in ascending order of complexity: in Category I, SHM can detect only the presence of damage; in Category II, the capabilities of the monitoring system are expanded to provide information on the location of damage; in Category III, the severity of damage is quantified; and in Category IV, the most comprehensive SHM system, evaluation of the safety of the structure is also included.

Several other classification systems for SHM have been suggested in the literature on the subject, with no precisely defined demarcation. This can be attributed to the tremendous variety of sensors and systems that have been utilized and the variety of structures monitored. Indeed, most classification systems overlap in some way.

14.3 Civionics

Civionics (Mufti, 2003) is a new term coined from the integration of civil and electronics engineering, and is derived from the application of electronics to civil structures. It is similar to the term 'avionics' used in the aerospace industry to denote the detailed in-service monitoring of aircraft. For SHM to become an integral part of civil structural engineering, it must include the new discipline of civionics, which requires the development of formal definitions and widely accepted guidelines so as to encourage its inclusion in the curricula of universities and colleges around the world. Civionics is an integral part of the overall SHM process shown schematically in Fig. 14.2. This figure highlights the interdependencies created in the civionics process, which begins with the SHM of infrastructure. In showing how each discipline is dependent upon the other, Fig. 14.2 shows the synergy created within the disciplines of structural engineering, electrical engineering, computer engineering, and photonics engineering.

The discipline of structural engineering is well established. Its various components – including analysis, design, computer programs, and laboratory testing – having been extensively developed over several centuries. However,



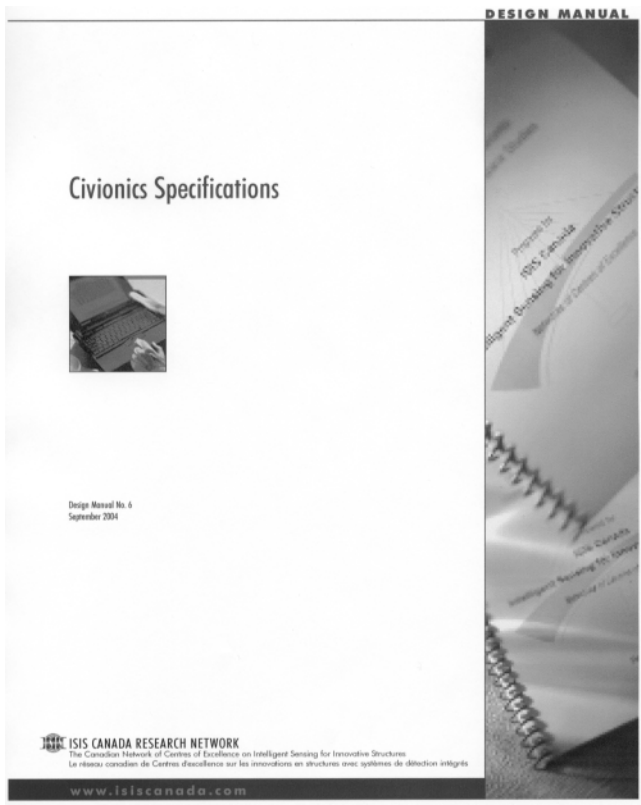
14.2 Various components of structural engineering and civionics.

the development of innovative structures to include new materials such as FRPs has been slow, due in part to the absence of the discipline of civionics, which is required to provide comprehensive learning programs for future engineers to assist them in developing intelligent sensing systems for innovative structures. Many of the individual components that constitute a civionics system already exist in the fields of electronic and civil engineering. However, to meld these individual components into a system that is beneficial and necessary to the construction industry, and then integrate them into the construction process, is the interesting and demanding challenge that will be faced by civil engineers of the future. Innovation in structural engineering (such as the use of FRPs in structural applications) will increase more rapidly if the discipline of civionics becomes an integral part of civil engineering.

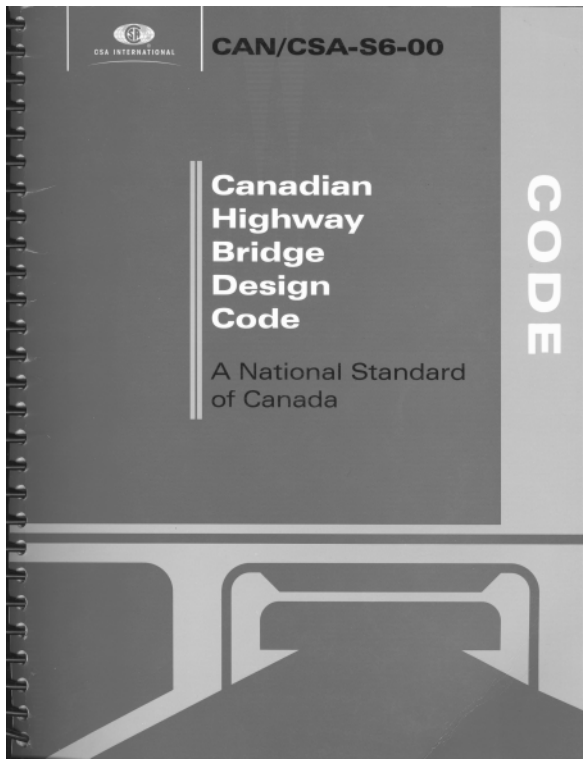
Currently, the development of new concepts and/or the use of new technologies in structural engineering requires the use of sophisticated analysis tools. When a concept cannot be formulated by existing analytical tools, it is frequently studied by physical testing in a laboratory setting. Acceptance of innovations is thus quite slow in the construction industry, due also to the conservative nature of the industry; however, if SHM systems can be used to demonstrate that innovative materials and systems are functioning as predicted, then acceptance of these innovative concepts and technologies would be greatly accelerated.

Realistically, consulting engineers and contractors will not invest widely in the development of the expertise created by graduates of the civionics

discipline until they can be assured that the prospects for business are good, and that civionics can meet the rigid economic and safety requirements demanded by the industry. The ISIS Canada experience – integrating FOSs and FRPs into innovative structures that have been built across Canada – demonstrates that these opportunities do in fact exist and that government departments and engineers are developing confidence in the viability of these systems, particularly in harsh climates. Furthermore, Canadian universities and technical colleges are actively conducting SHM and civionics research, and academic and training manuals and courses have been or are being established (Bisby and Mufti, 2005) to assist them. It is the intention of ISIS Canada that future generations of structural engineers and technologists become familiar with the requirements of industry related to civionics and that civil engineering graduates have an awareness and basic understanding of SHM systems. To that end, ISIS Canada has developed the *Civionics Specifications* manual (Rivera *et al*., 2004) for use in the training of highly qualified personnel in Canada (Fig. 14.3).



14.3 ISIS Canada *Civionics Specifications* manual.



14.4 Canadian Highway Bridge Design Code.

In addition, ISIS Canada has provided leadership and resources that have contributed to the re-drafting of the Canadian Highway Bridge Design Code (CHBDC, 2000) to provide practicing bridge engineers with confidence that FRP materials and SHM systems can be utilized safely, economically, and effectively. The Canadian Standards Association recently approved the changes to the code (Fig. 14.4) that were drafted by a national and international body of engineering experts based on their research and field experience, as well as the proven performance of FRP materials and SHM systems that are currently in service.

14.4 Field applications and service-life determination

The following sections present a series of case studies of applications of the combined use of FRPs and SHM systems in structural applications in Canada. It is intended that these case studies demonstrate the effective use of both technologies, and that the reader recognizes the links between innovative materials (such as FRPs) and the need for long-term SHM to provide assurances of adequate in-service performance and durability.

14.4.1 Case study: structural health monitoring and civionics in a second-generation steel-free bridge deck

In the spring of 2004, research engineers at the University of Manitoba constructed a full-scale, second-generation steel-free bridge deck for testing under laboratory conditions. This bridge deck was the first of its kind to fully incorporate a complete civionics SHM system, designed and implemented using ISIS Canada's *Civionics Specifications* manual, to monitor the deck's behavior during destructive testing. The steel-free deck incorporated both carbon fiber-reinforced polymer (CFRP) and glass fiber-reinforced polymer (GFRP) materials.

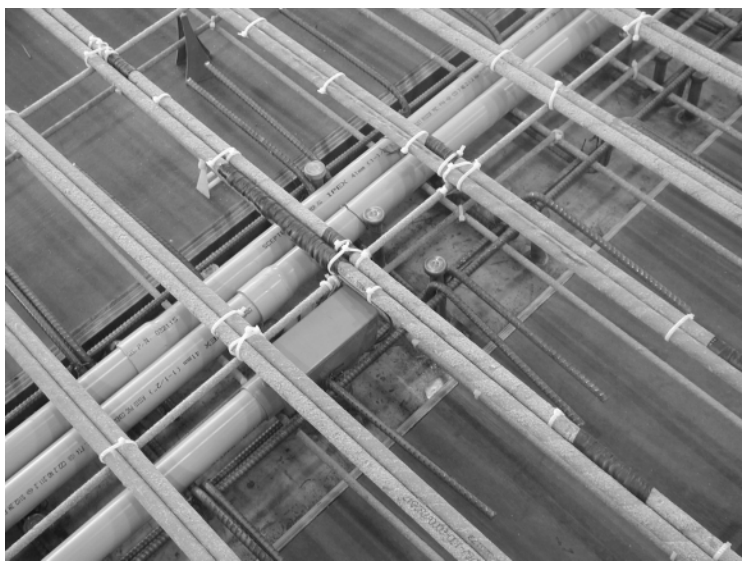
Throughout the construction of the bridge deck, the installation of the SHM system was carried out by research engineers in such a way as to simulate the actual implementation of a civionics system in a large-scale construction environment. One major concern raised by consulting engineers when contemplating the use of SHM systems is the impact that a civionics system using conduit, junction boxes, and other electrical ancillary protection could have when embedded or installed externally on full-scale infrastructure. The destructive testing of this second-generation steel-free bridge deck provided engineers with some of the information necessary to address many of these constructability and structural integrity issues (Klowak *et al*., 2006).

The SHM system for the test bridge deck at the University of Manitoba utilized rigid polyvinyl chloride (PVC) conduit and junction boxes to provide protection for the network of sensors embedded within the deck and all of the sensors installed externally on various bridge components. The placement of the system of conduits and junction boxes is critically important, as both the effects of the system on the structural integrity of the bridge deck, as well as the amount of conduit and exposed cable within the concrete deck, must be minimal. In this case, conduits were placed within the haunches of the deck (Fig. 14.5).

The sizing of the conduit was determined using the ISIS *Civionics Specifications* manual. The conduit size and junction boxes required for this project were $1^1/_2$ inches (38 mm) in diameter. For research purposes, this bridge deck was equipped with several additional sensors that would probably not be required in a true field application, and the conduit was sized accordingly. A civionics system for an actual steel-free bridge deck would contain a minimal number of embedded sensors, thus reducing the amount and size of conduit required. For a typical installation, a local electrical contractor could place the conduit and all of the necessary wires would be terminated at junction boxes. A short time before casting of the bridge deck and after all major placement of the reinforcement has been completed, qualified civionics personnel should install the sensors and make the appropriate connections at



(a)



(b)

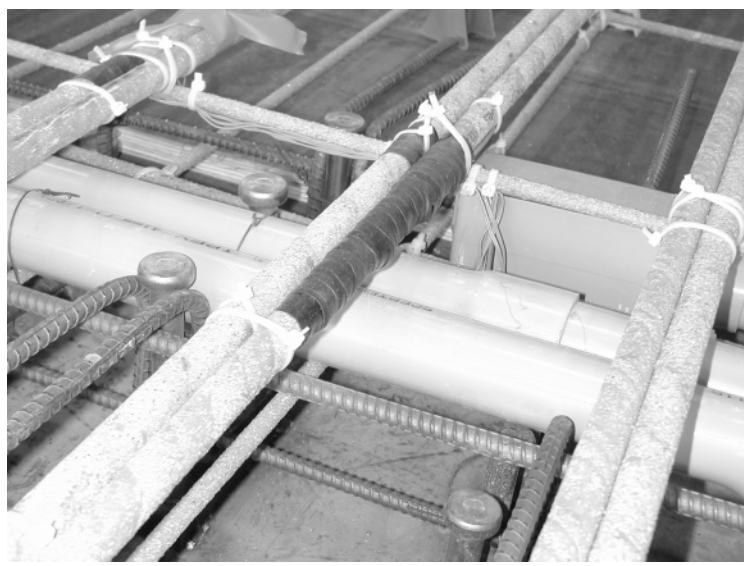
14.5 Rigid polyvinyl chloride conduit embedded with bridge-deck haunches.

the junction boxes. Field installation of sensors typically requires the application of several protective coatings, and exposed sensor lead wires should be located in such a way as to prevent damage during placement of concrete (i.e. wires should be placed on the underside of the reinforcement and properly

secured, as in Fig. 14.6). The sensors embedded within the bridge deck on the reinforcing bars allow engineers to monitor stresses both during and after construction.

Surface-mounted sensors located on external bridge elements can also provide engineers with pertinent information relating to the overall performance of a bridge. However, these sensors must also be properly protected from vandalism and environmental conditions. Therefore, a system of rigid PVC conduits and junction boxes should be permanently installed on these elements also. Under actual conditions, an electrical contractor would install the conduit and lead wires after all of the formwork has been removed. Clearly, the wires must be properly labeled to ensure that the correct locations and designations of all sensors are known. Once again, qualified civionics personnel should perform the installation of the necessary instrument gauges within the junction boxes and splice all lead wires.

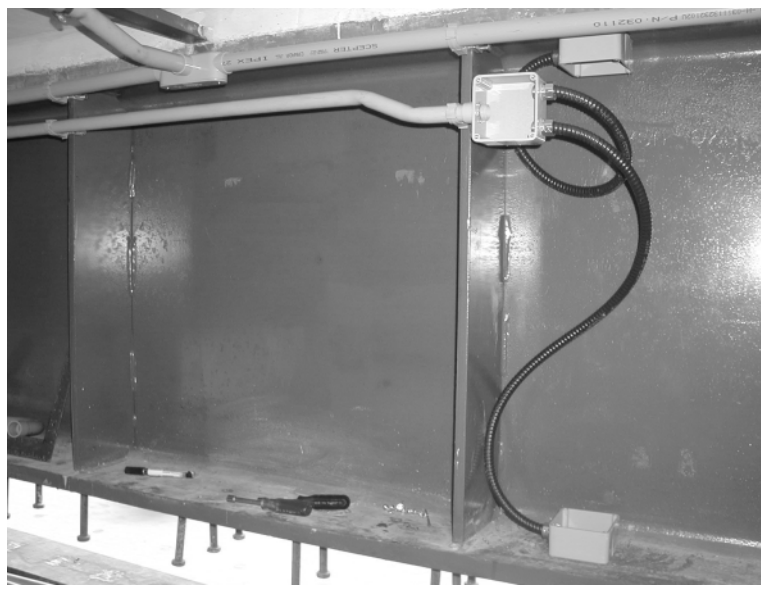
The conduit and junction boxes on the external elements of the steel-free bridge deck in this case were 1 inch in diameter to provide enough space in the junction boxes to install the sensors. The backs of the PVC junction boxes were removed to facilitate surface mounting of the sensors (Fig. 14.7). Strain gauges installed on these elements allow engineers to monitor live load stresses. Flexible conduit measuring $^{3}/_{4}$ inches (19 mm) in diameter was used with the junction boxes on the top and bottom flanges of the steel girders (Fig. 14.8). The purpose of the gauges installed on the girders was to



14.6 Protected sensors complete with properly located and secured lead wires.



14.7 Rigid polyvinyl chloride conduit and junction box for externally installed gauges.



14.8 Junction box and flexible conduit.

determine the live load stress ranges and also to determine the transverse load distribution pattern. In addition, the gauges allowed engineers at the University of Manitoba to determine if placement of the conduit within the haunches had a significant effect on the composite action between the girders and the deck.

14.4.2 Case study: Beddington Trail Bridge, Calgary, Alberta

The City of Calgary in the province of Alberta, after considering the benefits of SHM, decided to utilize this procedure in the construction of the highly

innovative, FRP prestressed Beddington Trail Bridge. The benefits considered included: the ability to respond to events, whether minor or catastrophic in a timely manner; the fact that engineers could monitor the structure from a remote site at any time and in any weather, thereby reducing the need to disrupt traffic flow for inspections and, in the process, providing a more reliable source of data; and the economics involved, which indicated that while a monitored smart structure is perhaps slightly more expensive to build than a conventional structure, cost savings can be expected through reduced maintenance requirements over the long term.

In 1992, the Beddington Trail Bridge (Rizkalla and Tadros, 1994), was the first bridge in Canada to be reinforced with FRP tendons and a system of structurally integrated optical sensors for remote SHM. The bridge opened in 1993, and although this was before the ISIS Canada Research Network was formed, it was significant to the ISIS network because it demonstrated to the initial group of researchers involved the need for an organization like ISIS Canada that could spearhead the transfer of this new technology into the construction industry.

The Beddington Trail Bridge is a two-span, continuous skew bridge of 22.83 and 19.23 m spans, each consisting of 13 bulb-Tee section, precast, prestressed concrete girders. Two different types of FRP tendons were used to pretension 6 of the precast concrete girders. Carbon fiber composite cables produced by Tokyo Rope™ of Japan were used to pretension 4 girders while the other 2 girders were pretensioned using Leadline™ rod tendons produced by Mitsubishi Kasei.

Fiber optic strain and temperature sensors (of a type known as Bragg grating) were used to monitor structural behavior during construction and under serviceability conditions. Because this was one of the first uses of FOSs in monitoring infrastructure in the world, a four-channel fiber Bragg grating (FBG) laser sensing system was developed specifically for this purpose at the University of Toronto Institute for Aerospace Studies.

Before constructing the Beddington Trail Bridge, an experimental program was conducted at the University of Manitoba's W. R. McQuade Structures Laboratory to examine the behavior of scale-model beams pretensioned by the same type, size, and anchorage of the two different FRP tendons (Leadline and Tokyo Rope) used for the Beddington Trail Bridge girders. The tests compared results using the same fibre optic sensor as that used for the bridge in addition to electric resistance strain gauges.

Prestressing of CFRP was adapted by coupling the carbon fiber composite cables and Leadline rods to conventional steel strands. Couplers helped to minimize the length of the CFRP tendons used and were staggered to allow use of the same spacing as was used for conventional steel reinforcing tendons. The Leadline rods were cut on site with two rods being used for each tendon. The Tokyo Rope carbon fiber composite cables were delivered precut to the

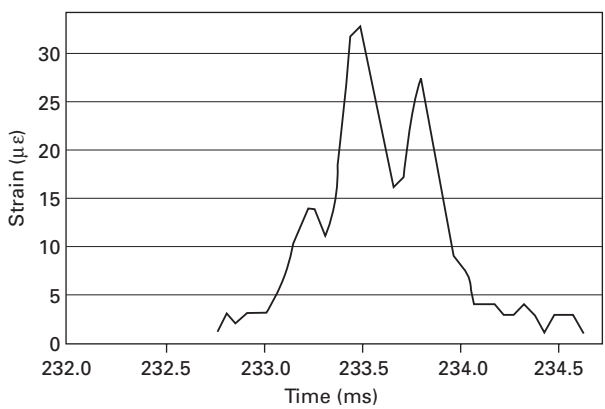
specified length with 300 mm die cast at each end to distribute the stresses in the anchoring zones. Construction of the bridge and handling of the girders at the site was typical.

A 4-channel FBG FOS system was used at different locations along the specific bridge girders that were pretensioned using CFRP. Each FOS was attached to the surface of the tendon after pretensioning. The sensors were connected, through a modular system, to a notebook computer used on the construction site to record assorted data at different stages of construction and after completion of the bridge. The FOS system measures the absolute strain rather than the strain relative to an initial calibrated value, similar to electric resistance strain gauges and mechanical gauges.

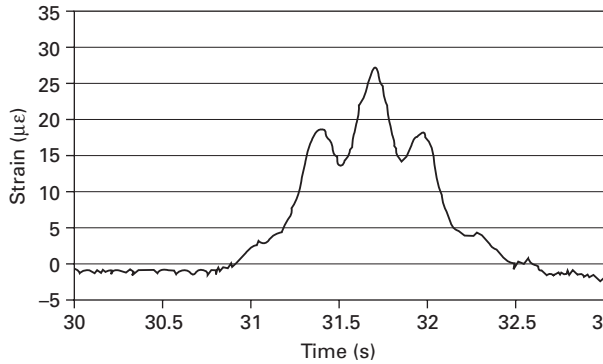
In 1999, 6 years after it opened, the bridge was tested statically and dynamically to assess the durability of its fiber optic sensors. After 6 years, all FOSs were functioning (Fig. 14.9). This finding validated the view that FOSs were durable and reliable for long-term monitoring. In November 2004, the bridge was tested again with the same vehicle and weight. The data obtained, some of which are shown in Fig. 14.10, demonstrated that the FBG sensors are durable, that they are providing accurate results, and that the CFRP is performing as originally designed in 1992.

14.4.3 Case study: Red River Bridge – second-generation steel-free bridge deck

The Red River Bridge located on the South Perimeter Highway, which encircles the City of Winnipeg, Manitoba, is a 250 m long, seven-span structure, consisting of three simply supported spans and one continuous span. During the next few years, the entire bridge deck is scheduled for replacement with



14.9 Dynamic fiber Bragg grating response to three-axle truck load, 1999.



14.10 Dynamic fiber Bragg grating response to three-axle truck load, 2004.

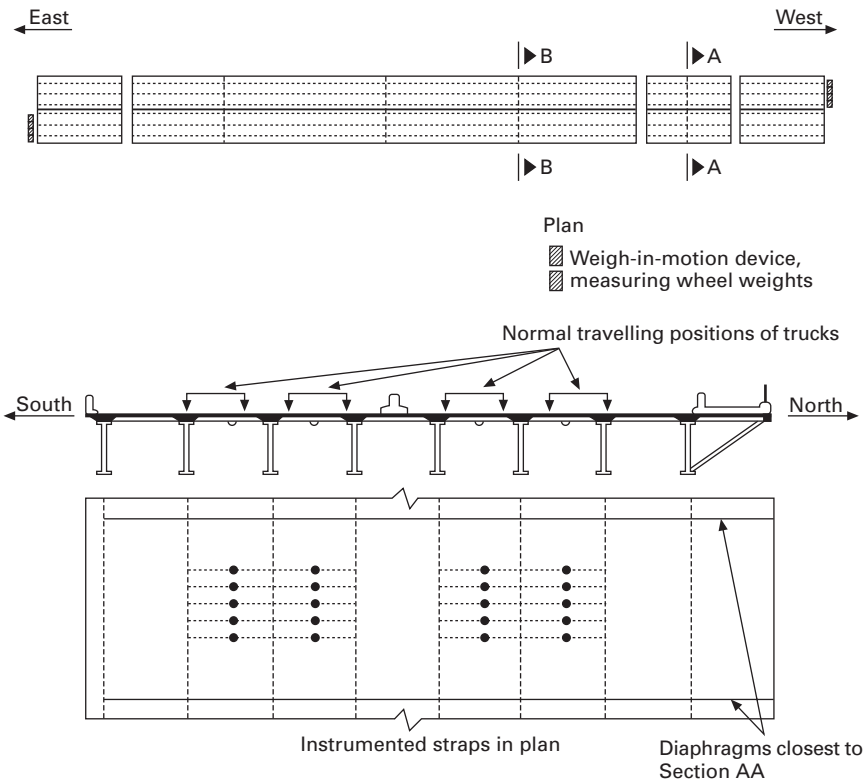
an innovative second-generation steel-free GFRP hybrid bridge deck (ISIS Canada, 2004). The installation of a civionics SHM system in this bridge is following the requirements outlined in the ISIS *Civionics Specifications* manual and was incorporated to provide information on the long-term performance of the structure in service.

Preliminary plans incorporate a minimal number of sensors including FOSs, accelerometers, conventional sensors, and weigh-in-motion sensors. These sensors will allow engineers to track the performance of the bridge and thus to study its long-term performance and, indirectly, the durability of the FRP materials that it contains. A cross-section of the bridge deck is seen in Fig. 14.11, which shows that the deck consists of an FRP-reinforced concrete slab supported on conventional steel girders. The top flanges of the girders connect by steel straps that act as tension ties to allow the development of arching action in the concrete bridge deck.

14.4.4 Case study: Portage Creek Bridge – strengthening against earthquakes and field assessment

The Portage Creek Bridge situated in Victoria, Vancouver Island, British Columbia, was designed in 1982 by the British Columbia Department of Highways Bridge Engineering Branch. It is a 125 m (410 ft) long three-span continuous steel structure with a reinforced concrete deck supported on two reinforced concrete piers with abutments on steel H-piles. The deck has a roadway width of 16 m (52 ft), with two 1.5 m (5 ft) sidewalks and aluminum railings.

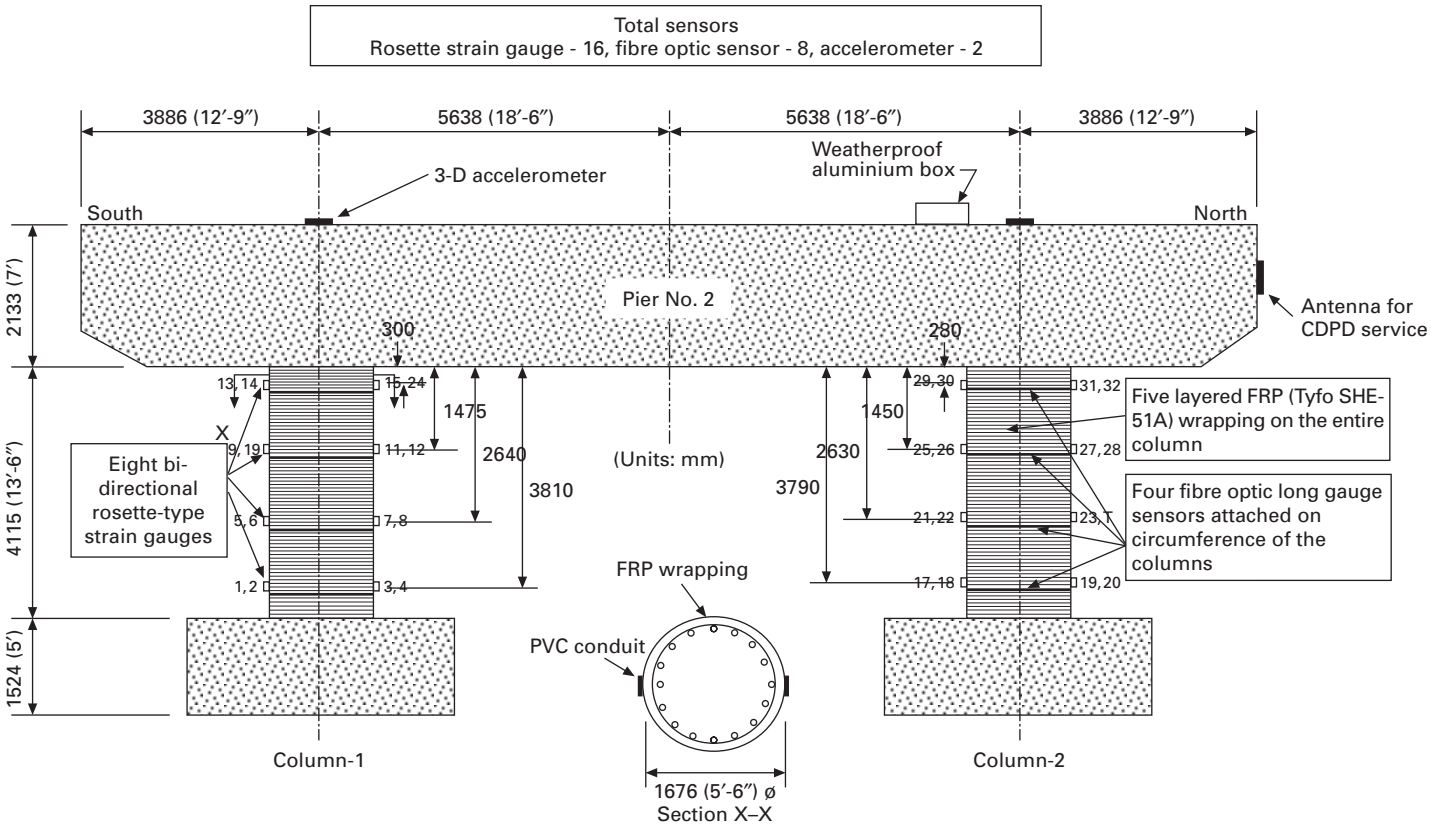
This is a high profile bridge that has been classified a Disaster Route Bridge, since Vancouver Island is located in a highly active seismic zone. However, the bridge was built prior to current seismic design codes and construction practices and was thus judged to be inadequate to resist the



14.11 Location of weigh-in-motion sensors and externally applied electronic strain gauges.

potential earthquake forces required by current standards. As such, it required retrofitting to prevent collapse during potential seismic events (Mufti *et al*., 2003).

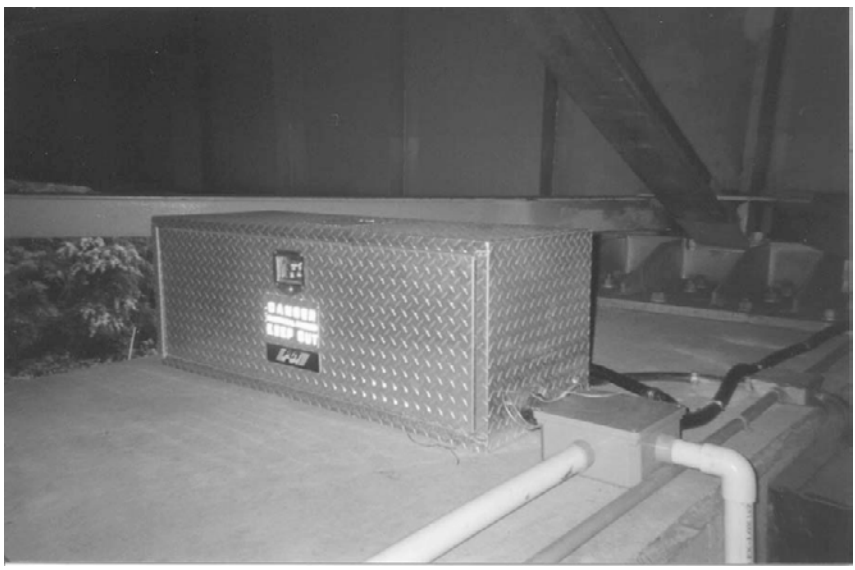
Most of the bridge was strengthened with conventional materials and methods. A dynamic analysis of the bridge predicted that the two tall columns of the first pier of the bridge would form plastic hinges during an earthquake. Once these hinges have formed, additional shear would be attracted by the shorter columns of the second pier. A nonlinear static pushover analysis indicated that the short columns would not be able to form plastic hinges before failure, and it was therefore decided that circumferential FRP wraps should be used to strengthen the short columns of the second pier for shear, without increasing their flexural capacity. The bridge was instrumented with 16 conventional foil gauge rosettes, 8 FOSs, and 2 accelerometers (Fig. 14.12). The retrofit included the installation of an SHM system through which the bridge continues to be monitored remotely (Figs 14.13 and 14.14). ISIS Canada is assisting with the SHM of this bridge, which is intended to



14.12 Portage Creek Bridge structural health monitoring sensor locations.



14.13 Datalogger installed on Portage Creek Bridge.



14.14 Monitoring system housing installed on pier cap.

provide both short- and long-term performance and durability information on the FRP system, as well as potentially important information on the seismic response of bridges in the event of an earthquake. The system that was installed has been functioning well.

14.4.5 Case study: Brookside Cemetery – long-term performance of anchor assembly for markers in concrete at veteran affairs cemetery

The rapid deterioration of markers and the supporting concrete beams at Brookside Cemetery in Manitoba, and other similar cemeteries across Canada, was and is a major issue of concern for Veterans Affairs Canada (VAC) National and International Memorials, and Heritage Conservation Services, Public Works and Government Services Canada (Mufti and Onofrei, 2004). As a result of this deterioration, VAC decided to investigate several different marker options for long-term use at cemeteries across Canada, with a view to selecting the most durable design based on budgetary and durability constraints. Researchers at the University of Manitoba were asked to test the various marker options under field conditions (i.e. weather cycles of extreme heat and cold, vandalism, etc.) and to make recommendations on which options would be the most durable. The test site selected was Brookside Cemetery in Winnipeg, Manitoba, Canada (Fig. 14.15).

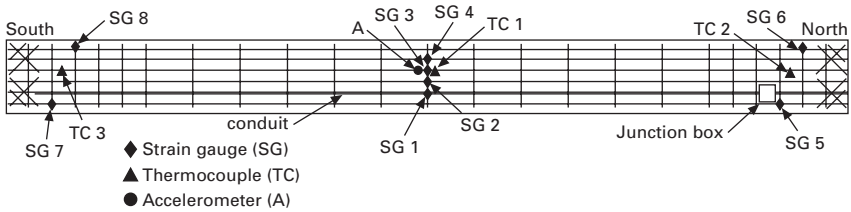
Brookside Cemetery is a very large cemetery with over 96 000 graves. A portion of the cemetery is designated for Canadian veterans from World Wars I and II, as well as from the Korean War. The rest of the cemetery is designated for civilians.



14.15 Brookside Cemetery, Winnipeg, Manitoba, Canada.

Field application of fiber-reinforced polymer-reinforced smart beam

One of the grave marker solutions investigated incorporated an FRP-reinforced concrete support beam intended to provide superior long-term durability. As part of the SHM system installed in the test beam, a total of 12 sensors were installed at various instructive locations (Fig. 14.16) (Mufti *et al*., 2004). To gain a comprehensive representation of the condition of the beam over the long term and validate the theoretical calculations of midspan deflection and natural frequency, three types of electrical sensors were selected. Each type of sensor provides information on a different aspect of the concrete beam. Electrical strain gauges (Fig. 14.17) were used to provide strain measurements from the GFRP reinforcing bars. These strain readings can be used to determine the deflection of the beam at the midspan (Fig. 14.18). Thermocouples were

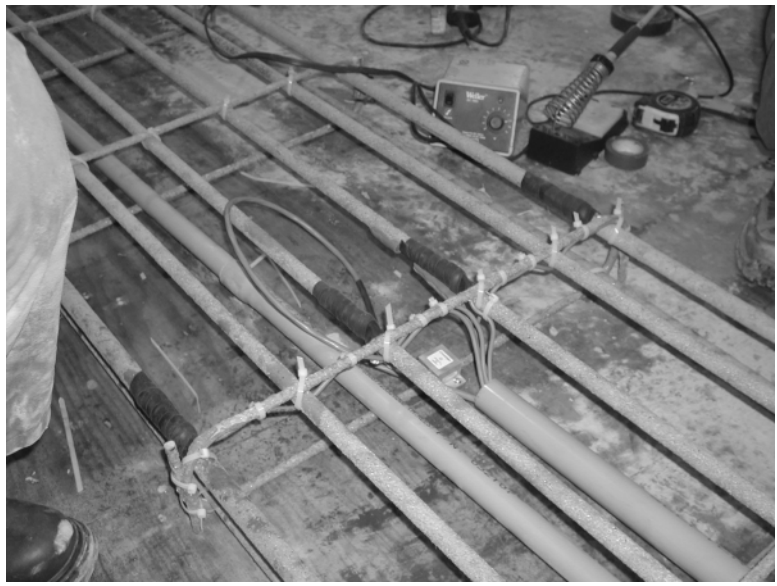


14.16 Sensor locations on a 24 ft (7.32 m) long field trial beam (plan view showing reinforcement).

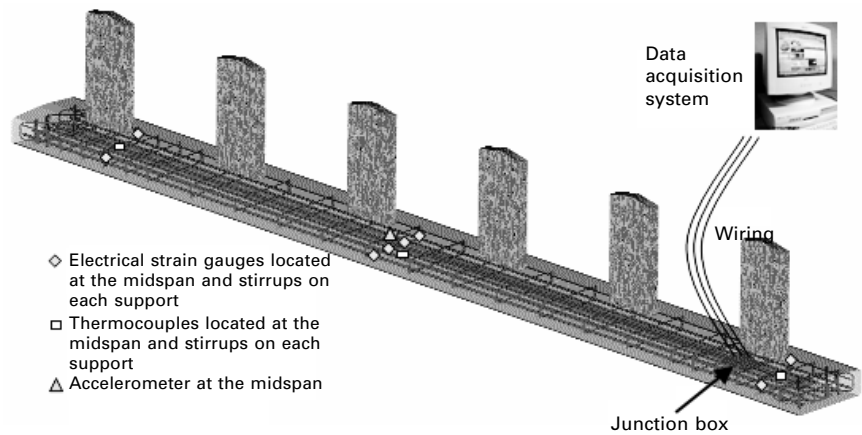


14.17 Strain gauges and thermocouple installed inside field trial beam.

installed to measure the temperature inside the beam. Finally, an accelerometer was installed in the beam to measure the frequency response of the beam to an applied load. Changes in behavior of the beam during its service life can thus be used to provide indications of satisfactory performance or of deterioration (Fig. 14.19).



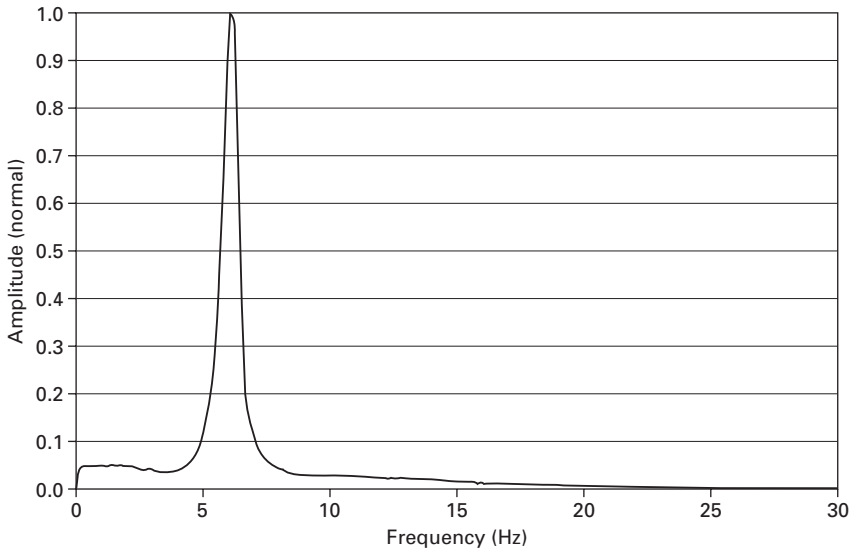
14.18 Strain gauges, accelerometer, and thermocouple installed at midspan of field trial beam.



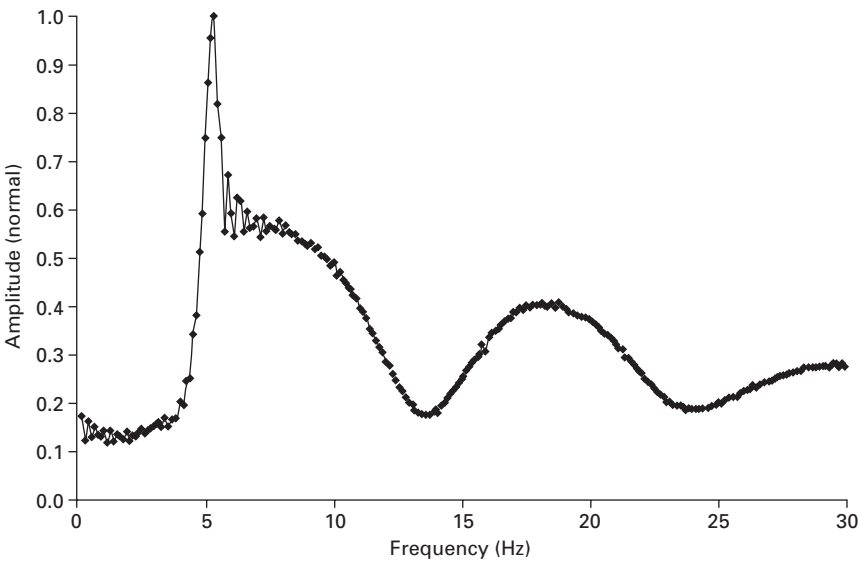
14.19 Schematic diagram of a 24 ft beam and structural health monitoring system.

Frequency response of beam

Following the successful installation of the beam at Brookside Cemetery (Mufti *et al*., 2004), the short-term static and dynamic responses of the beam were studied (Figs 14.20 and 14.21). The accelerometer embedded at midspan in the beam was used to determine the frequency of the beam. After the beam

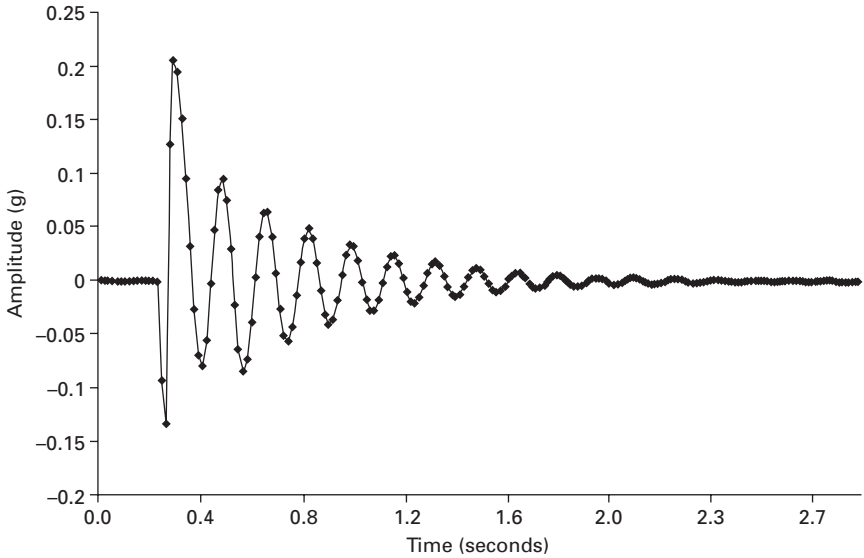


14.20 Frequency of the concrete beam before installation of markers.

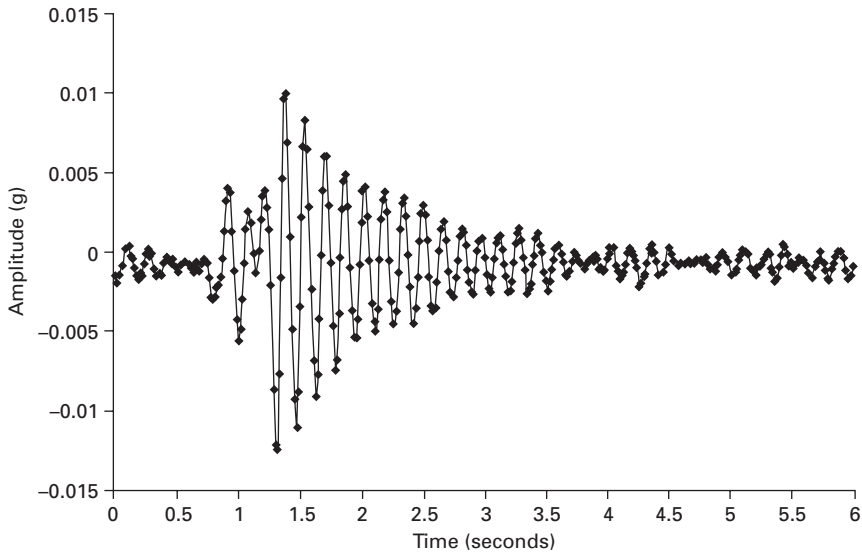


14.21 Frequency of the concrete beam after installation of markers.

was placed on the piles, the beam was excited at midspan with a 68 kg mass. The accelerometer responses of the beam before and after installation of the markers are presented in Figs 14.22 and 14.23, and demonstrate that the SHM system is functioning well. The dynamic response of the beam can be



14.22 Accelerometer response to a load applied at midspan of beam before installation of the markers.



14.23 Accelerometer response to a load applied at midspan of beam after installation of the markers.

checked periodically in the future and can thus be used to provide an indication of changes in the beam's behavior, which would then necessitate an on-site inspection to determine the exact cause for the fluctuation (i.e. damage to the beam).

14.4.6 Web-based monitoring and structural health monitoring data management

The previous sections very briefly outlined a few applications of SHM systems on structures incorporating FRP materials in Canada. For those structures instrumented with SHM systems having remote monitoring capabilities, data are constantly collected at varying frequencies. As the amount of collected data grows, so does the need for sophisticated archival data management systems. Indeed, data management becomes one of the most vital aspects of SHM. ISIS Canada is currently developing on-line archiving systems (visit www.isiscanada.com) whereby authorized researchers may submit raw data that will be accessible to other users. In a user-friendly, internet-based interface, the site will offer information on sensor characteristics and locations, as well as real-time and archived response measurements from both static and dynamic load tests. The on-line archive will enable interested parties to browse the contents, view the relevant documentation, and download data for ongoing analysis.

Several different strategies are currently being investigated for data collection (Card, 2004; Han and Newhook, 2007). In some cases, the sensors are triggered manually at selected intervals of time, with the sensor data being stored on computer disks. In other cases, sensor data are collected continuously at specified scan rates, and automatically transmitted to a remote location where they are stored on a computer. Eventually, the on-line system should provide a wealth of data on the performance of structures incorporating FRP materials. This will allow an holistic evaluation of the long-term durability of FRP-reinforced concrete structures.

14.4.7 Field evaluation of fiber-reinforced polymer durability

ISIS Canada has been involved in numerous field applications of FRP materials for both reinforcement and strengthening of concrete structures; in most cases these have involved the use of FRPs in combination with SHM systems. However, in addition to SHM applications for structures incorporating FRP materials, ISIS Canada is also conducting ongoing field investigations to monitor the durability of FRP materials in structural applications across Canada. The following section briefly describes a recent study investigating the in-service durability performance of GFRP reinforcing bars for concrete.

Field evaluation of glass fiber-reinforced polymer durability in demonstration projects

In order to investigate the in-service durability of GFRP reinforcing materials for concrete, samples of GFRP reinforcing bars were removed (by coring) from five different FRP-reinforced concrete structures that had been in service in Canada for up to 8 years. The methods used in the evaluation study (Mufti *et al.*, 2005) to investigate the degradation of GFRP-reinforced concrete were: scanning electron microscopy (SEM), energy dispersive X-ray (EDX), optical microscopy (OM), differential scanning calorimetry (DSC), and infrared spectroscopy (IS).

In order to obtain reliable information using these methods, special attention was given to sample preparation. During specimen preparation, glass fibers can be scratched, and microcracks can be induced into the matrix and concrete; also the glass fiber can be debonded, and the glass and matrix polished surfaces can be contaminated with elements from each other and with elements from the concrete.

Details of the sample preparation techniques and presentation of the results obtained from the entire set of GFRP-reinforced concrete specimens have been presented in detail elsewhere (Mufti *et al.*, 2005); the following is a brief excerpt of the main findings suggested by the results obtained to date. The analyses were performed during 2005 at the universities of British Columbia, Manitoba Saskatchewan, and Sherbrooke, on randomly selected core specimens from field demonstration projects. The cores were taken



14.24 Waterloo Creek Bridge – core sample extraction.

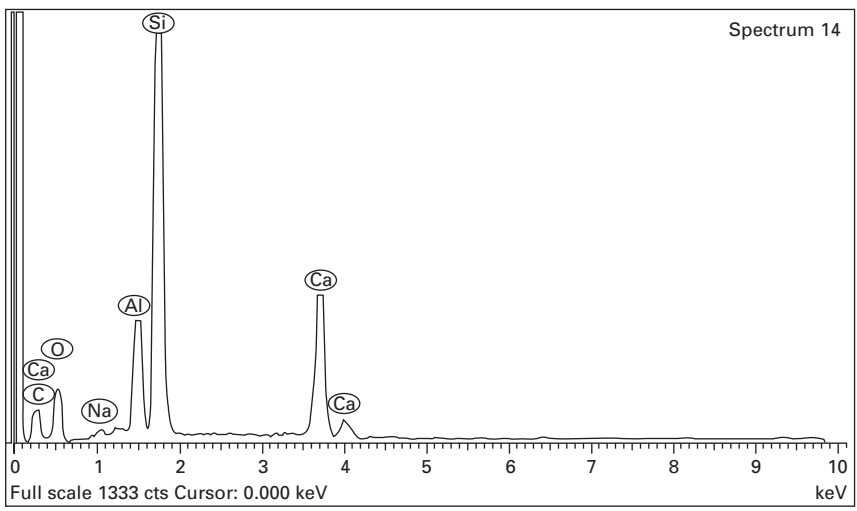
from five structures across Canada. Figure 14.24 shows the extraction of cores from a GFRP-reinforced barrier wall on one of the five bridges – the Waterloo Creek Bridge on Vancouver Island, British Columbia.

SEM was used to examine the glass fiber/polymer matrix interface within the FRP bars and to study the individual glass fibers. SEM photomicrographs can be used to study the durability of the bond between FRP materials and concrete. In the current study, SEM photomicrographs indicated no damage to the FRP-concrete bond or to the GFRP material after up to 8 years in service. Data from SEM analyses suggest that that there are no visible signs of any degradation occurring on the reinforced bars/grids. The individual fibers are intact with no gaps between the fibers and the matrix. In addition, good contact is apparent between the concrete and the matrix.

EDX techniques were used to detect the potential ingress of alkalis from the high-alkalinity concrete pore solution, which is known to be damaging to bare glass fibers. Figure 14.25 shows sample EDX data obtained from the Joffre Bridge. These data also supported the findings that there had been no significant damage to the GFRP reinforcing materials.

OM was used to study the FRP/concrete interface; IS was used to provide information on any changes in chemical composition of the FRP bars' constituents; and finally, DSC was used to check for changes in the glass transition temperature of the polymer matrix, changes that might indicate changes in the matrix properties. No significant deterioration of the GFRP reinforcing bars was indicated in any of the data collected.

The resulting conclusion is that, for the range of conditions of the field demonstration projects included in the study, there appears to be no degradation



14.25 EDX data from Joffre Bridge.

of the GFRP reinforcement. Because the alkalinity of the concrete pore water solution is expected to decrease further with time, it is likely that, for most practical applications, the degradation of GFRP in concrete can be considered as insignificant.

The results obtained in the current study do not support the results obtained in laboratory durability studies on GFRP materials. Many previous studies have reported that GFRP degrades to various degrees in simulated in-service environments. There are several reasons for this apparent disagreement. In the current study, the specimens under investigation were from in-service engineering structures, whereas in laboratory studies the conditions are typically extremely severe and may be quite different from true exposure conditions. Laboratory studies are also typically conducted in alkaline solutions maintained at constant elevated pH values and/or high temperatures where the GFRP is effectively kept in contact with infinite leachant volume. With the exception of special projects, such conditions rarely exist for actual structures.

14.5 Future trends

As mentioned at the beginning of this chapter, through the use of FRP materials and SHM systems incorporating the principles of the emerging discipline of civionics, ISIS Canada intends to significantly change the design and construction of civil engineering structures. For changes in design and construction to be accepted, it is necessary that innovative structures and materials (such as those incorporating SHM systems and FRP materials) be monitored for both their long- and short-term health so that a scientific database of performance data can be developed. This will give practicing engineers the comfort level necessary to be confident that structures incorporating these new concepts will be safe and economically viable. To assist in achieving this goal, ISIS Canada has contributed to the development of the new discipline of civionics, integrating civil engineering and electronics.

The emerging discipline of civionics must be further developed and embraced by civil structural engineers and electronics engineers to lend validity and integrity to the process. ISIS Canada researchers and others around the world are actively participating in this process to ensure the advancement of this necessary aim by educating instructors at university and college levels, as well as by providing, free of charge, educational modules for their use. In addition, ISIS researchers have created a series of design manuals to instruct practicing engineers on the proper techniques for utilizing FRPs, SHM, and civionics systems. Eventually, this will produce many engineers with the knowledge to build ‘smart’ structures containing the SHM systems that are currently needed to provide important information on the health of existing and future structures.

FRPs, SHM, and civionics will all play pivotal roles in the future development of efficient, effective, and sustainable infrastructure systems. Thoughtful application of SHM systems, in particular, has the potential to provide a wealth of information on the long-term durability of FRP materials in structural applications. In many ways, FRPs and SHM systems are complementary technologies that together have the potential to change the way infrastructure is constructed and maintained.

14.6 Sources of further information and advice

Further information and advice on the proper use of SHM systems and civionics principles for use in the building and/or rehabilitation of infrastructure can be obtained from a variety of sources, including the following.

- ISIS Canada Design Manual No. 2: Guidelines for Structural Health Monitoring (Mufti, 2001).
- ISIS Canada *Civionics Specifications* manual (Rivera *et al.*, 2004).
- ISIS Canada Educational Module No. 5: An Introduction to Structural Health Monitoring (in draft form, 2005) (El-Hacha and Campbell, 2007).
- The ISIS Canada Research Network web site at www.isiscanada.com (this site has real-time links to infrastructure projects that are currently being monitored for health through the remote monitoring systems discussed in this chapter) (ISIS Canada, 2003).
- The website of the International Society for Structural Health Monitoring of Intelligent Infrastructure (ISHMII) at www.ishmii.org (ISHMII, 2002).
- Report to Federal Highway Administration Research and Development on Development of a Model Health Monitoring Guide for Major Bridges (Drexel Intelligent Infrastructure and Transportation Safety Institute) (FHWA, 2002).
- International Organization for Standardization (ISO), ISO 18649: 2004: Mechanical Vibration – Evaluation of Measurement Results from Dynamic Tests and Investigations on Bridges (ISO, 2004).
- Fédération Internationale du Béton (fib), Monitoring and Safety Evaluation of Existing Concrete structures. Task Group 5.1 (fib, 2003).

14.7 References

Aktan, A.E., Tsikos, C.J., Catbas, F.N, Grimmelsman, K. and Barrish, R. 1999. Challenges and Opportunities in Bridge Health Monitoring. *Proceedings of the 2nd International Workshop*, Stanford University, CA, USA.

Bisby, L.A. and Mufti A.A. 2005. SHM in the Class Room: A Unique Educational Opportunity. *Proceedings of the 2nd International Conference on Structural Health Monitoring of Intelligent Infrastructure (SHMII-2)*, Shenzhen, P. R. of China.

CHBDC (Canadian Highway Bridge Design Code). 2000. Canadian Standards Association, Toronto, Ontario, Canada.

Card, L. 2004. Unsupervised Neural Computation for Event Identification in Structural Health Monitoring Systems. Master of Science Thesis, Department of Electrical and Computer Engineering, University of Manitoba, Winnipeg, Manitoba, Canada.

Chang, F.-K. 1999. Editor. *Structural Health Monitoring 2002 Workshop. Proceedings of the 2nd International Workshop*, Stanford University, CA, USA.

Chase, S.B. 1999. Dynamics and Field Testing of Bridges in the New Millennium: A Look Forward. Transportation Research Board Report A2C05, USA.

Demers, M., Popovic, A., Neale, K., Rizkalla, S. and Tadros, G. 2003. FRP Retrofit of the Ring-Beam of a Nuclear Reactor Containment Structure. *ACI Special Publication*: SP-215: 303–316.

El-Hacha, R. and Campbell, T.I. 2007. Prestressing Concrete Structures with Fibre Reinforced Polymers (FRPs). ISIS Canada Design Manual 5. Winnipeg, Manitoba, Canada (in press).

Fib (Fédération Internationale du Béton). 2003. Monitoring and Safety Evaluation of Existing Concrete Structures, Task Group 5.1, Lausanne, Switzerland.

FHWA (Federal Highway Administration). 2002. Report to Federal Highway Administration Research and Development on Development of a Model Health Monitoring Guide for Major Bridges, Drexel Intelligent Infrastructure and Transportation Safety Institute, USA.

Han, L. and Newhook, J. 2007. Centralized Web Based Structural Health Monitoring. *Canadian Journal of Civil Engineering – Special Issue* (in press).

ISO (International Organization for Standardization). 2004. ISO 18649: 2004: Mechanical Vibration – Evaluation of Measurement Results from Dynamic Tests and Investigations on Bridges.

ISHMII (International Society for Structural Health Monitoring of Intelligent Infrastructures) 2002. www.ishmii.org.

ISIS Canada. 2003. ISIS Canada Research Network web site, www.isiscanada.com, Winnipeg, Manitoba, Canada.

ISIS Canada. 2004. ISIS Canada Research Network Proposal to the Department of Transportation of the Province of Manitoba. Winnipeg, Manitoba, Canada.

Klowak, C., Memon, A. and Mufti, A.A. 2006. Static and Fatigue Investigation of Innovative Second Generation Steel Free Bridge Decks. *Canadian Journal of Civil Engineering – Special Issue* (in press).

Mufti, A., Onofrei, M., Benmokrane, B., Banthia, B., Boulfiza, M., Newhook, J., Bakht, B., Tadros, G. and Brett, P. 2005. Durability of GFRP Reinforced Concrete in Field Structures. *Proceedings of the 7th International Symposium on Fiber Reinforced Polymer Reinforcement for Reinforced Concrete Structures (FRPRCS-7)*, New Orleans, LA, USA.

Mufti, A.A. 2001. Guidelines for Structural Health Monitoring. ISIS Canada Design Manual No. 2. ISIS Canada Research Network, Winnipeg, Manitoba, Canada.

Mufti, A.A. 2003. Integration of Sensing in Civil Structures: Development of the New Discipline of Civionics. *Proceedings of the 1st International Conference on Structural Health Monitoring and Intelligent Infrastructure (SHMII-1 '2003)*, pp. 119–129. Tokyo, Japan.

Mufti, A.A. and Onofrei, M. 2004. Long-Term Performance of GFRP and Steel Anchor Assemblies for Markers in Concrete at Veteran Affairs Brookside Cemetery. ISIS Canada Technical Progress Report, Winnipeg, Manitoba, Canada.

Mufti, A.A., Neale, K., Rahman, S., Huffman, S. 2003. GFRP Seismic Strengthening and Structural Health Monitoring of Portage Creek Bridge Concrete Columns.

Proceedings of the fib2003 Symposium – Concrete Structures in Seismic Regions, Athens, Greece.

Mufti, A.A., Onofrei, M., Rivera, E., Klowak, C. and Bindiganavile, V. 2004. Structural Health Monitoring of Field Trial Beam at Veteran Affairs Brookside Cemetery. ISIS Canada Technical Progress Report, Winnipeg, Manitoba, Canada.

Newhook, J.P. and Mufti, A.A. 2000. A Reinforcing Steel Free Concrete Bridge Deck Slab for the Salmon River Bridge. *Concrete International*, **18**(6), 81–90.

Rivera, E., Mufti A.A. and Thomson, D. 2004. *Civionics Specifications*. Design Manual, ISIS Canada Research Network, Winnipeg, Manitoba, Canada.

Rizkalla, S.H. and Tadros, G. 1994. A Smart Highway Bridge in Canada. *Concrete International*, **16**(6), 42–44.

Sikorsky, J.M. 1999. Development of a Health Monitoring System for Civil Structures Using a Level IV Non-Destructive Damage Evaluation Method. *Proceedings of the 2nd International Workshop on Structural Health Monitoring 2000*, pp. 68–81, Stanford University, CA, USA.

Tennyson, R. 2001. Installation, Use and Repair of Fiber Optic Sensors. ISIS Canada Research Network, Winnipeg, Manitoba, Canada.

Index

Aberfeldy Footbridge, Scotland 196–7
abrasion 170
  surface 299
accelerated aging 158–60
accelerated testing 85, 89–90, 190, 208, 221
accelerometers 339, 344, 345–6
accidents, fire and 98
acids 115, 135
acoustic emission 317
acoustic impact testing 313
acrylic acids 115
acrylic fiber mats 94
additives 289
adhesives
  bonding 284, 288–9
  structural 191
  wear 170
  see also resin
advanced composite ASSET profiles 212–13
Advanced Composite Construction System (ACCS) 193, 196, 197–8
Advanced Composites in Construction (ACIC) conference 278
aerospace industry 6–7, 14, 257, 286, 295, 300, 328
aging
  accelerated 158–60
  physical, synergistic effects 161
air entrapment 295–7
airborne fiber particles 111
alkali metal salts 115
alkaline earth salts 115
alkaline environments 27, 229–31, 249, 251
alkalis 135
'all-composite' structures 192–6
  bridges 196–9
aluminium alloys 171
aluminium oxide compounds 112
aluminium trihydroxide ($Al(OH)_3$) 112–13
ambient-cured systems 189, 234
American Association of State Highways and Transportation Officials (AASHTO) 215
American Concrete Institute (ACI)
  environmental durability 263, 264, 271
  load factors 241, 250, 261
  publications 276–7
  temperature 252
ammonium polyphosphates 114
angularity of grit particles 175
antimony 112
antimony trioxide 110
aqueous environments 31–71
  constituent level 32–41
  mass uptake profiles 41–50
  mechanical/physical properties effects 50–8
  stress and hygrothermal effects 58–66
aramid fibers 196, 265
  internal strengthening 226, 228, 230, 235, 237, 239–40
aramid FRPs (AFRPs) 85, 179
  durability 220, 225
  strengthening
    external 251, 254–5, 265
    internal 228, 230–2, 234–5, 237
aramid/epoxy laminates 182
area reduction factors, columns 270–3

Army Corps of Engineers 88
Arrhenius analysis 53, 231
arson 98
ASME (American Society of Mechanical Engineers) standards 4, 8, 9
ASTM (American Society for Testing and Materials) standards 57, 89–91, 106, 108, 174, 261, 269
atomic force microscopy (AFM) 82
autoclave molding 21–2
axial properties, FRPs 85

Balvac Whitly Moran Ltd 207
barely visible impact damage (BVID) 299
Beckman meter 209
Beddington Trail Bridge, Alberta 335–7
  bending properties 117
Bennetts' Creek bridge, New York 214–16
inspection reports 216
bismaleimide 103
bisphenol polyester resin 51
blockers/absorbers, UV 92–3
Boiler and Pressure Vessel Code (ASME) 9
Boltzmann superposition principle (BSP) 157–8, 166
bond strength 232, 288
bonding 237, 286, 294
Bonds Mill Bridge, Gloucester 197–8
'bound water' 42
Bragg grating 191
  dynamic fiber 337–8
  fiber optic (FBG) sensors 191, 199, 213, 336–7
bridge decks 212–17
  steel-free 332–5
bridge enclosures, Second Severn Crossing 195–6
bridge field testing 325
British Columbia Ministry of Transport 205
brominated polymers 111, 119
  glass/polyester composites 114
Brookside Cemetery, Winnipeg 342–7
BSI (British Standards Institute) 4, 9, 277
Building Research Establishment (BRE) 193, 194, 195
building systems, 'all-composite' 192–4

calcium carbonate 112
calcium hydroxide 229
calcium sulphate dihydrate 112
Canada Research Network of Centres of Excellence 209, 324, 336
Canadian Highway Bridge Design Code (CHBDC) 331
Canadian Standards Institute (CAN/CSA) 203, 241, 261, 262, 277
carbon black 93, 112
carbon fiber-reinforced polymer composites (CFRPs) 85–6, 98
  /GFRP hybrids 213–14
  defects 285, 309, 311, 321
  durability 206–8, 212, 220
  strengthening
    external 251–5, 257, 259, 265, 270–1, 273
    internal 225, 228, 230–5, 237–40
  structural health monitoring (SHM) 332, 336–7
carbon fibers 111, 115, 179, 265, 288, 291, 294
  internal strengthening 226, 228, 230, 233, 235, 239
carbon monoxide (CO) 110
carbon nanotubes 120
carbon/epoxy composites 59, 75–6, 88, 163, 164
carbon/polyimide composites 182
carbon/thermoset laminates 171, 184
catalysts 289
cavitation wear 170
ceramic matrix composites (CMC) 13
chain scission reactions 83
chalking 94
chloride-contaminated concrete columns 258
chlorinated polymers 111
chopped-strand mat/isopolyester composites 63
Cicol™ Acmegrip system 197
Civil Engineering Research Foundation 4
civil infrastructure 2–3
civionics 328–31, 338
Civionics Specifications manual (ISIS) 330, 332, 338
classification
  defect detectability 307
  fabrication processes 18

structural health monitoring (SHM) 327–8
classroom, Thornton Cleveleys 193
coating systems 184
coefficient of thermal expansion (CTE) 249
cold cured adhesives 191
columns
area reduction factors 270–3
environmental reduction factors 268–70
seismic retrofit 256–9
mechanical properties 258
combustion 99–102
composite materials, rules in selection 184
compression 21, 115–16, 117, 118
concrete 151, 171
-filled fiber-reinforced polymer tubes (CFFTs) 166
columns
chloride-contaminated 258
seismic retrofit 205–6
preparation 294
rebars and 208–11
substrate 307
see also rehabilitation, concrete structures; reinforcement of concrete
Concrete Repairs Ltd 207
Concrete Society 262–3
conditional methods, of inspection 315, 319, 321
cone calorimeter 103
Conference on Composites in Construction (CCC) 257, 278
Conference on Durability and Field Applications of Fiber Reinforced Polymer Composites for Construction (CDCC) 277–8
constant tensile load/strain test 60
constituent materials 289–92
defects in 301
corrosion
electrochemical 226
steel 225, 294
costs 312–13
coupling 311
agents 54–5, 129
cracking, of matrix 298
creep 136, 140, 150–2, 249–50, 252
-rupture (stress-rupture) 62–3, 235–6
strain 60–3
creep and time-dependent response 150–69
accelerated aging 158–60
future trends 167
modeling long-term behaviour 155–8
relaxation 28, 155, 233–6
structural level effects 163–7
synergistic effects 160–3
cross-ply laminates 130
cyanate esters 109
cyclic loading 162, 236–7

damage mechanics concepts 126
damage tolerance-based design/inspection methodology 300
datalogger 341
de-icing salts 247, 269
debonding 73
decision areas, interacting 17
defects
detectability classification scheme 307
effect of 299–302
from site/material preparation 302
in FRPs 286–9
installation 303–4
occurring during rehabilitation 289–99
in raw materials 301
in service 298–9, 304
Department of Defense (DoD) 7, 15
descriptive modeling *see* predictive/descriptive modeling, fatigue
design codes/manuals 178–9, 277
detectability matrix (DM) 308, 309, 317
dial gauges 212
differential scanning calorimetry (DSC) 209–10, 290, 348–9
diffusion models 231
DIN (German Institute for Standardization) 174
dirt accumulation 193
Disaster Route classification 205, 338
dispersive x-ray analysis 230
distortion of materials 115
dithiocarbamates 93
Doolittle equation 58
Drexel Intelligent Infrastructure and

Transportation Safety Institute 351
dry sand rubber wheel test 174
durability 3–5
'all-composite' structures 192–6
bridges 196–9
bridge decks 212–17
code summary 261–3
code-reported reduction factors 263–8
external strengthening 199–204, 247–8
field evaluation of FRP/GFRPs 347–50
FPR-reinforced concrete and bond 250–6
FRP alone 248–50
FRP examples 201–2
girders and profiles 217–20
laboratory-reported data 263–8
rebars 208–11
reinforcement of concrete 226
seismic retrofit 204–6
tendons 206–8
test protocol model 231
dynamic load test 212
dynamic mechanical thermal analysis (DMTA) 47, 52, 290

E-glass
-stitched bonded fabric 215
fibers 73, 194, 196, 217, 226
resins 192, 195
filaments 39–40
non-woven laminates 128
E-glass FRP composites 127, 128, 197
E-glass/epoxy composites 54, 65, 128–30, 133, 228
E-glass/polyester composites 57, 63, 65, 129, 193–4, 197–8
E-glass/vinylester composites 129, 131–4, 142, 228
aqueous environments 46–7, 49, 52–6, 62, 65
pultruded 135, 136, 137
earthquakes 338–41
see also seismic retrofit
eddy current testing 316
'effect of defects' methodology 300
Egyptian FRP code 263, 277
elastic compliance 163
electrical resistance strain gauges (ERSG) 212–13, 339, 343–4
electrochemical corrosion 226
electron probe microscopy 230
elemental phosphorus 114
endothermic reaction 112
energy dispersive X-ray (EDX) 209–10, 348–9
environment
agents 135, 257
conditions 295
reduction factors 259, 263–8, 271
for columns 268–70
epoxies
adhesives 197, 253
ambient-cured 234
composites 50, 60, 87, 117, 136, 144, 192–3, 203
general purpose 94, 98, 101, 103, 105–6, 109
resins 44, 51, 82, 120, 191, 197, 207, 230, 253
steel rebars coating 216
epoxy-polyamide material 86
erosion
surface 83, 85, 86
tests 180, 183
see also wear/erosion
EUROCRETE project 209
European composite design code and handbook 144
European Union (EU) 119–20
-funded projects 212
Exchem Ltd 207
excited-state quenchers 93
excluded inspection methods 316, 321
exposure environments 26–9, 226
external strengthening 199–204

fabric orientation, moisture uptake 46–9
fabrication processes 16–25
autoclave molding 21–2
classification 18
compression molding 21
filament winding 22–3, 130
injection molding 20–1
liquid molding 24
pultrusion 23–4
selection of 24–5
spray up 19–20
wet lay-up 18–19, 20
Fabry-Perot fiber optic sensor 191

fatigue 28, 180, 236–9, 250, 253
  synergistic effects 161
fatigue loads 126–49
  FRP performance 127–36
  predictive/descriptive modeling 136–42
  reliability-based design 142–6
Federal Highway Administration (FHWA) 4, 214, 351
Fédération Internationale de Béton (FIB) 252, 262, 277, 351
fiber optic sensors (FOSs) 212, 324, 330, 336–7, 338, 339
  Bragg grating (FBG) 191, 199, 213, 336–7
fiber-matrix bond 182, 287
Fiber-Reinforced Polymer Reinforcement for Concrete Structures (FRPRCS) symposium 257, 277–8
fiber-reinforced polymers (FRPs) 2–3, 3–5, 5–10
fiber/matrix
  adhesion 129
  interface 40–1, 134
fiberglass 98
  composites 100–1, 103
fibers
  'blooming' 84
  content 176–7, 182
  defects 290–1
  fatigue performance 127–8
  moisture accumulation 45–6, 293
  orientation 177, 182
  undulation 130
  volume, damage and 226
Fibreforce Ltd 207
Fickian diffusion 41–4, 45–6, 59, 489
Fick's law 42, 50, 227
field evaluation 347–50
field installation 295–7
filaments 39–40
  winding 22–3, 130
filled composites, flame-retardant properties 111–13
fillers 179–80
Findley's power law 156–7, 158, 164, 166, 167
fire 29, 257
  properties 98
  protection coatings 118–19
  reaction properties 102–11, 120
  resistance 101, 240
  safety regulations 119–20
  tests 193
  see also high temperature/fire
flame spread rate 107–9
flame-retardant
  additives 110
  fillers 112, 120
  polymers 118–19, 120
  properties 111–15
    filled composites 111–13
  resins 101
flashover potential 106
flexural members 248–56
  properties 88
  strength 117–18
fluids
  creep and 234
  moisture absorption and 49–50, 227–9
foil gauge rosettes 339
Fourier-transformed infrared spectroscopy (FTIS) 47, 49, 209–10, 290
fracture mechanics 126, 140
freeze-thaw conditions 249, 252
  cycles 231–2, 247, 299
  see also sub-zero/freeze-thaw conditions
fretting wear 170
fuels/oils 136
fungal growth 221
FyreRoc® 120

galvanized steel 225
gel coats 93–4
geopolymers 119, 120
Gills Creep Bridge, Virginia 216–17
girders and profiles 217–20
glass fibers 94, 115, 134, 179, 291, 349
  moisture effects on 37–40
  reinforcement 228, 229, 233, 235, 239, 265
  toxicity 111
glass FRPs (GFRPs) 32, 85, 162
  durability 193–7, 203, 206, 208–10, 212–14, 216–17, 220–1
  fatigue *see* fatigue loads
  strengthening
    external 251–5, 257–8, 268, 270

internal 225–6, 229–35, 237–41
structural health monitoring (SHM) and 332, 338, 343, 347–50
glass/epoxy composites 74, 88, 164, 216–17, 273
aqueous environments and 47, 56–7, 60, 62, 64
ultraviolet radiation (UV) and 85–8, 93
glass/isopolyesters 87
glass/phenolic composites 106–10, 112–13, 115–16
glass/polyester composites 53–4, 56–8, 62–3, 86, 94, 108, 114, 198
glass/polyetherimide (PEI) laminates 176–7, 179
glass/polytetrafluoroethylene (PTFE) 177
glass/polyurethane composites 60
glass/thermoset laminates 171, 184
glass/vinylester composites 37, 45, 48–9, 57, 87, 144
high temperature and 106–7, 109–10, 115–18
Goodman-type diagrams 138
gouging 170
graft copolymerisation 115
graphite crystals 179
graphite/epoxy composites 86, 87
Griffith-Irwin-Orowan equation 38
ground-penetrating radar 318
gypsum 112

halogen
compounds 111
polymers 111, 113
resins 120
hand lay-up techniques 193, 196
handling damage 287
hardener 289
hardness ratio 175
heat flux 99–101, 103–5, 107, 109, 110
heat release rate 106–7, 108
'heat sink' 105, 112
Heitman and Lindstrom model 53
Heritage Conservation Services, Public Works and Government Services Canada 342
high temperature/fire 98–125, 239–40
combustion 99–102
fire protection coatings 118–19
fire reaction properties 102–11
fire safety regulations 119–20
flame-retardant properties 111–15
structural properties 115–18
synergistic effects 160–1
thermal cycling 249, 251–2
'high-stress' wear 173
hindered amine light stabilizers (HALS) 92–4
humidity 292
hydroperoxides 93
2-hydroxy-benzophenone 93–4
2-hydroxy-benzotriazole 93
hydroxylation 229
hydroxyphenylbenzotriazole 94
hydroxyphenyltriazine derivatives 93
hygrothermal effects 58–66, 75–7, 135–6
Hythe Bridge, Oxford 206–8

icosahedron structure 193
ignitability test (ISO) 103
impingement angle 180–2
in-fill panels and load-bearing 194–6
'inert' fillers 112
infrared spectroscopy (IS) 348–9
Fourier-transformed (FTIS) 47, 49, 209–10, 290
injection molding 20–1
inorganic polymers 120
inorganic salts 115
inspection
conditional methods 315, 319, 321
damage tolerance-based 300
excluded methods 316, 321
non-destructive inspection (NDI) 305
primary choices 314, 317–19
reports on visual 216
supplementary choices 316
installation, defects 303–4
instrumentation, location 213
'interface' (interlaminar region) 129
International Conference on Composites for Infrastructure (ICCI) 257
International Organization for Standardization (ISO) 89–90, 103, 174, 351
International Society for Structural Health Monitoring of Intelligent Infrastructure (ISHMII) 351
interphase

fatigue performance 129–30
moisture effects on 37–40
interpretation, ease of 312
intumescent
coatings 118–19
fillers 112
Iowa State University 231
iron 112
ISIS (Intelligent Sensing for Innovative Structures) 205, 241, 262–3
health monitoring (SHM) 324, 330–2, 336, 338–9, 347, 350–1
visual examinations 210, 211
isocyanurate vinylester (IVE) 226
isophthalic polyester 82–3
resin 51, 194, 195, 196
isopolyesters 35
isothermal short-term creep tests 159
isotropic ductile materials 175

Japanese Society of Civil Engineers 241, 263, 277
Joffre Bridge 349

Keller, Professor T. 220
Kevlar yarn 27, 31, 228–9, 230
'knock-down' factors 147, 257, 259, 271
material resistance and 143–4

laboratory tests 184
accelerated 89–90
Langmuir diffusion model 46
laser scanning confocal microscopy (LSCM) 82
Leadline™ 238, 336
limiting oxygen index (LOI) 105–6
linear elastic fracture mechanics (LEFM) 139
liquid erosion 180
liquid molding 24
live load rating factor (LLRF) 203
load reduction 259–63
load and resistance factor design (LRFD) 127, 142–3
load-bearing structures 115
infill panels and 194–6
properties 100, 117
loading
fatigue performance 130–3
history 146
test results 218
local melting 180
longitudinal behaviour (bridge project) 214
'low-stress' wear 173

magnesium 112
manufacturing process 288
marine environments 247
marine industry 286
Market Development Alliance 4
materials
preparation 295, 302
resistance 259–63
'knock-down' factors 143–4
testing 289
transformation process 16
matrix
cracking 298
phase 13
Maunsell planks 194, 196, 197
Maunsell Structural Plastics 198
mechanical properties 85, 117, 179–80, 184, 258
degradation 87–8
moisture effect on 50–8
mercaptobenzothiazoles 93
metal chelates 93
metal hydroxides 112
metal matrix composites (MMC) 13
metal oxides 112
methacryl silane 54–5
microcracking 174, 180
microcutting 174, 179, 180–2
microfatigue 174
microfracture 181
microplastic deformation 181
microploughing 174, 179, 180, 182
microstructural properties 176, 184
Ministère des Transports du Québeq (MTQ) 200–4
Mitsubishi Kasei 336
mixing 293
Miyun Bridge, China 196
modal analysis 318
models
creep and time-dependent response 155–8
fatigue 136–42
Langmuir diffusion 53

'N-gas' 111
moisture 250–1
accumulation 287–8, 293, 296
concrete structures and 227–9, 292, 298
effects 26–7, 248–9
see also aqueous environments
synergistic effects 161
molding process 226
molybdenum 112
Mondial House, London 194–5
monitoring systems 221, 341
structural performance 190–1
web-based 347
see also structural health monitoring (SHM)
monomers 115
montmorillonite 120
Mouchel Parkman 207, 212
Mufti, Professor A. 210
multiple layers 297
myths and mysteries 5–10

'N-gas model' 111
National Bridge Inspection Standards (NBIS) 215
National Instrument data acquisition system 206
National Science Foundation (NSF) 275–6
natural events, fire and 98
naval industry 257
Neale, Professor K. 203, 204, 210
New York 94
non-brominated glass/polyester composites 114
non-destructive evaluation (NDE)/testing (NDT) 302–21
detectability classification matrix 308
ranking assessment flowchart 305
system types 310–11
non-destructive inspection (NDI) 305
non-Fickian diffusion 46
Norwegian Council for Building Standardization 277
notation 273–4
nylon 181

oligomeric epoxy sizing 130
on-site processing 292–5
optical methods (shearography) 316
optical microscopy (OM) 209, 348–9
organic polymers 102
organic solvents 135–6
organohalogen 113
organophosphorus 113
orientation of fibers 177, 182
outdoor accelerated testing 89
oxide compounds 112

'Palmgren-Miner's rule' (P-M rule) 138
'Paris' law 139
particle size 176
peel test 251
penetrant methods 314
phenolic composites 101, 103, 105–6, 108–10, 117, 120, 193
phenomenological methods of fatigue-life predictions 140, 146
phosphite esters 93
phosphorus 111, 114, 120
photodegradation 82, 92–3
phthalonitriles 103, 109
physical aging 161
physical properties 50–8
pigments 179
pin-on-disc test 174
pin-on-drum test 174
plastic deformation 180
plasticization 229, 298
Poisson's ratio 238
polyaramid/epoxy composites 88
polyester composites 45, 49, 94, 144, 192, 226, 234
high temperature and 98, 101, 103, 105–6, 109
polyester resins 35–6, 44–5, 50, 82, 120, 192, 195, 230
isophthalic 51, 194
polyether ether ketone (PEEK) 103, 109
polyether ketone ketone (PEKK) 103
polyetherimide (PEI) 176, 177
polyimides 103, 109, 110
polymer matrix composites (PMC) 13, 179–80
polymer-concrete wearing surface 215
polymers
combustion cycle of organic 102
fire-resistant 101
nanocomposites 184

polyphenylene sulfide (PPS) 103, 109
polypropylene 181
polyurethane coating 86
polyvinyl chloride (PVC) 181, 332–5
  degradation of 88
polyvinylesters 36–7
Pontresina Bridge, Switzerland 217–20
  damage categories 219
  loading test results 218
porosity 295–6
portability 311
Portage Creek Bridge, British Columbia 205–6, 338–41
POSS® 120
  post-curing 61
  adhesives 191
short-term properties and 88
post-fire properties 117
practicality matrix (PM) 309–13, 313–19
predictive/descriptive modeling, fatigue 136–42
  approaches to 138–40
  variability/reliability approach 140–2
prefabricated composites 292, 297
  components 287
preparation
  material 302
  site 292–5, 302
prestressed carbon FRPs 206–8
primary methods, of inspection 314, 317–19
processing methods 16
  effect on fatigue 130, 131
proof-loading test 215
pull-out 291–2
  test 232
pultrusion 23–4, 55–6, 130, 135–7, 164, 232
pumice 112
pyrolysis 115–16

quality control 25–6

radiant panel flame spread technique 108
radical scavengers 93
radiographic testing 315, 319
ranking assessment flowchart 305
ranking matrix (RM) 313–21
rapid load testing 319
raw materials 289–92
  defects in 301
real-time acquisition 311
rebars, concrete and 208–11
Red River Bridge, Winnipeg 337–8
reduction factors
  area 270–3
  environmental 259, 263–8, 268–70, 271
rehabilitation, concrete structures 284–323
  defects in FRPs 286–9
  defects occurring during 289–99
  effect of defects 299–302
  future trends 321–2
  non-destructive evaluation/testing 302–21
reinforcement of concrete
  creep and 165–6
  design codes 277
  FRP external 247–83
  columns, seismic retrofit 256–9
  design and use 259–74
  flexural members 248–56
  further information 276–9
  future trends 274–6
FRP internal 225–46, 227–40
  design and application 240–1
  durability concerns 226
  future trends 241–2
reinforcement phase 13–14
relative humidity (RH), high 247
relaxation 28, 155, 233–6
  see also creep
reliability-based design 127, 146–7
  fatigue 140–2, 142–6
resin 289–90, 293
  fatigue performance 129
  flame-retardant 101
  infusion 24, 284–5
  matrix 226
  moisture effect 33–7, 51–2
  thermoset 110
  unstabilized 93
  see also individual resins
resin transfer molding (RTM) 24
resistance
  load and resistance factor design (LRFD) 127, 142–3
  material/knockdown factor 143–4
retrofitting technologies 200

River Cole bridge, Oxfordshire 212–14
Rivière Noire bridge, Canada 200, 203–4
Rockguard-wrapped concrete cylinders 74

safety regulations, fire 119–20
saline solution 271
Salmon River Bridge, Nova Scotia 324
salts 135
  of methacrylic 115
  solutions 248, 269
sandblasting 294, 296
scanning electron microscopy (SEM) 56, 86, 209–10, 348–9
Schapery equation 157–8, 167
Scott Bader 195
scratches 298–9
Second Severn Crossing, bridge enclosures 195–6
seismic retrofit 204–6
selection of composite materials, rules 184
sensors 333–4, 339
  Bragg grating (FBG) 191, 199, 213, 336–7
  bridge locations 340
  fiber-optic (FOSs) 212, 324, 330, 336–7, 338, 339
service inflictions 312
Severn Bridge Visitor's Centre 194
shear modulus 88
sheet-molding compound (SMC) 21
Sika Carbodur SI214 203
Sikawrap Hex 100G 203
silica 112
silicate glasses 40
site preparation 292–5
  defects 302
sizing 129–30
sliding
  dry 177, 179
  wear 170, 178, 184
smart beams 343–4
  frequency response 345–7
Smith Road Bridge, Ohio 198–9
smoke
  properties 109
  toxicity 109–11
soda lime glass rods 38
softening of materials 115–16
solid particle erosion 180
solutions
  salts 248, 269
  see also aqueous environments; moisture
sophistication, system 312
specific extinction area (SEA) 109
spray up 19–20
'spring load' test 60
stabilizers 92–3, 179, 195
static bending fatigue 64–5
static tensile fatigue 39
steel 115, 151, 171, 183–4, 294
  strengthening
    external 247, 253, 256, 258, 271
    internal 225, 240
steel reinforced polymers (SRPs) 164–5, 274
storage 293
strain gauges 199, 212–13, 334, 339, 343–4
strain techniques (fiberoptics) 317
strain-life approach 126, 138
strength
  creep and 164–5
  degradation 267, 268
  external 199–204
  internal 225–46
  reduction factors 273
  systems 278–9
stress
  /hygrothermal effects 58–66
  corrosion 39–40
  ratio 130–1
  relaxation 150
stress-life approach 126, 138, 140, 145, 146
stress-rupture behaviour 62
structural health monitoring (SHM) 322, 324–53
  basic concepts 325–6
  civionics 328–31
  data management 347
  field applications 331–50
  further information 351
  future trends 350–1
  need for 326–8
  subsystems and classification 327–8
structural properties, fire and 115–18
structural reaction injection molding (SRIM) 24

sub-zero/freeze-thaw conditions 72–9
  hygrothermal effects 75–7
  overall effects 72–5
supplementary methods, of inspection 316, 321
surface
  abrasion 299
  erosion 83, 85–6
spread of flame 109
Swiss Structural Standard, SIA 161 217
synergistic effects 253–6
  fatigue 133–6
  stress/hygrothermal exposure 58–66
  time-dependent response 160–3

talc 112
Technora fibers 228–9
temperature *see* high temperature/fire
tendons 206–8, 238
tensile
  fatigue 88, 128
  properties of PVC 88
  strength 128, 136, 137, 228, 236
  stress 116–17
tension
  -tension axial fatigue 129
  loading 118
  properties 116–17
terrorist attack, fire and 98
testing
  accelerated 85, 89–90, 190, 208, 221
  acoustic impact 313
  field 325
  methodologies 89–92
  structural performance 190–1
thermal barrier coatings 118–19
thermal effects 27–8
thermal expansion 232–3
thermal-mechanical effects, fatigue 134–5
thermocouples 343–4
thermodynamic equilibrium 162
thermographic testing 315
thermoplastic composites 86, 93, 130, 181, 184, 194
  high temperature and 103–6, 107, 108, 109, 110
thermoset composites 103–6, 107–8, 110, 118, 184
three-body abrasion 173
three-point bending 61–2, 64
time-dependent response *see* creep and time-dependent response
time-temperature superposition principle (TTSP) 154, 159–60, 167
time-temperature-stress superposition principle (TTSSP) 158, 159–60
time-to-ignition 102–5, 105, 112
titanium oxide (TiO_2) 93
Tokyo Rope™ 336
Toronto Institute for Aerospace Studies 336
toxicity, smoke 109–11
transformation process, materials 16
transverse properties 85
trialylphosphates 114
'turbulent fire' 99–100
two-body abrasion 173

ultimate tensile strength (UTS) 128, 136, 228, 236
ultimate tensile unit load (UTUL) 63
ultrasonics 314
ultraviolet radiation (UV) 29, 80–97, 299
  blockers/absorbers 92–3
  effects on FRP composites 83–8
  effects on polymers 80–3
  external strengthening and 247, 250, 269, 271
  mitigation strategies 92–4
  protection 197, 199
  stabilizers 179, 195
  testing methodologies 89–92
uniaxial tension tests 234
unidirectional materials 128–30, 177, 212, 285, 286, 290
United States of America (USA) standards *see* ASME
University of British Columbia 348
University of California 300
University of Manitoba 332, 336, 342, 348
University of Saskatchewan 348
University of Sherbrooke, Quebec 200, 203–4, 210, 231, 348
University of Southern Florida 231
urethane-modified biphenol vinylester 226

vacuum-assisted resin transfer molding (VARTM) 130, 132–3, 142
vapourisation 180
variability/reliability approach, fatigue 140–2

Veteran Affairs Canada (VAC) 342
vibrating wire
  sensors 191
  strain gauges 199
vinylester composites 45–6, 82–3, 136, 192–3, 226, 234
  high temperature and 98, 101, 103, 105–6, 109
vinylester resins 83, 120, 199, 215, 230
  in aqueous environments 33–7, 44, 48, 51, 55–6, 62
vinylon FRP (VFRP) 232
Virginia Department of Transport 216
visco-elastic softening 115
viscoelastic behaviour 134, 136, 153–4, 157, 158
visual testing 313
voids 295–6

Waterloo Creek Bridge, British Columbia 348–9
waterproofing 31
wear/erosion 170–86
  erosive wear 180–3
  future trends 183–4
  gouging and abrasion 172–80
web-based monitoring 347
weigh-in motion sensors 339
West Mill Bridge, Oxfordshire
  instrumentation 213
  longitudinal behaviour 214
West Virginia University 231
wet lay-up process 18–20, 164, 193, 256–7, 270, 284–5, 292
wet-dry cycling 257
woven fabric 290–1
W.R. McQuade Structures Laboratory 336

x-ray photoelectron spectroscopy 82

Young's modulus 54, 88, 228